

UNIVERSITY OF OKLAHOMA

GRADUATE COLLEGE

INVESTIGATION OF THE HYDROLOGY, FLUVIAL GEOMORPHOLOGY, AND  
SEDIMENT TRANSPORT IN THE LAKE THUNDERBIRD WATERSHED IN  
CENTRAL OKLAHOMA

A DISSERTATION

SUBMITTED TO THE GRADUATE FACULTY

in partial fulfillment of the requirements for the

Degree of

DOCTOR OF PHILOSOPHY

By

RUSSELL C. DUTNELL

Norman, Oklahoma

2015

INVESTIGATION OF THE HYDROLOGY, FLUVIAL GEOMORPHOLOGY, AND  
SEDIMENT TRANSPORT IN THE LAKE THUNDERBIRD WATERSHED IN  
CENTRAL OKLAHOMA

A DISSERTATION APPROVED FOR THE  
SCHOOL OF CIVIL ENGINEERING AND ENVIRONMENTAL SCIENCE

BY

---

Dr. Randall Kolar, Chair

---

Dr. Robert Nairn

---

Dr. Gerald Miller

---

Dr. Caryn Vaughn

---

Dr. Jason Julian

© Copyright by RUSSELL C. DUTNELL 2015  
All Rights Reserved.

## **DEDICATION**

To my family: Cheryl, Mom, Dad, Steve and Tammy. Your love has been the foundation of my life.

## **ACKNOWLEDGEMENTS**

Numerous individuals and entities contributed, in one way or another to this dissertation, and at the risk of forgetting somebody, I would like to acknowledge them and thank them for their support.

First, I would like to thank my committee; Dr. Randall (Randy) Kolar, Dr. Robert (Bob) Nairn, Dr. Gerald (Jerry) Miller, Dr. Caryn Vaughn, and Dr. Jason Julian. Special thanks go to Randy and Bob, who have supported me in all of my educational endeavors over these many years. They are both excellent educators and researchers, with good hearts, who have inspired not just me, but many other students as well.

Dr. Reid Coffman, deserves the credit, and is to be thanked, for setting the wheels in motion, when he asked me to co-teach a Landscape Architecture Park Design course with him, and then when I thoroughly enjoyed the experience, suggested that I look into getting a stipend. I talked to Randy, who thankfully sponsored me for a Graduate Assistance in Areas of National Need (GAANN) fellowship. Funding for my studies and research was also provided by an Oklahoma Water Resources Research Institute (OWRRI) Water Research Grant, the Chickasaw Nation, and the Grand River Dam Authority (GRDA). Without their financial support, the study presented in this dissertation could not have been conducted.

The research required field work that I could not do by myself, and I was fortunate to have several friends and colleagues volunteer their time and labor to help me. Hollis Henson and Steve Zawrotny helped with the majority of the survey work, although I also had help from Xiaodi (Sean) Yu, Chunyang Liu and Dan Butler. I was

assisted in making discharge measurements by Hollis, Steve, Sean, and Dan, as well as by my brother, Steve, Randy's youngest son Charlie, and Jason Julian. I thank them for their assistance. Most of the people previously mentioned also accompanied me on at least one HOBO downloading trip, as did my nephew, Ellis, and I am thankful that I could share the experience with them.

At the risk of forgetting somebody, others who deserve thanks include the following: Monica Deming, a Service Climatologist at the Oklahoma Climatological Survey, for providing me with the Mesonet rainfall data; Thad Pratt and Dave Perkey, with ERDC in Vicksburg, Mississippi, for allowing me to use their lab and LISST, and instructing me on the methods; Dan Murphy with Teledyne RDI, Jeroen Aardoon with Aqua Vision, and David Dana with Sequoia, for providing technical assistance with the ADCP, the ViSea PDT software, and the LISST, respectively; and Dave Dalkin with Teledyne RDI, for providing assistance and support from the outset and becoming a friend.

Finally, I would like to thank my wife for putting up with me and supporting me in whatever I do, and to my parents for the numerous sacrifices they lovingly made to give me a good life and make me a better person. I appreciate everything they have done for me over the years.

# TABLE OF CONTENTS

DEDICATION .....	iv
ACKNOWLEDGEMENTS .....	iv
TABLE OF CONTENTS .....	vi
LIST OF TABLES .....	x
LIST OF FIGURES .....	xiv
ABSTRACT .....	xxiii
I. Introduction .....	1
II. Part 1: Hydrology and Fluvial Geomorphology (FGM) of the Lake Thunderbird Watershed in Central Oklahoma .....	8
A. Lake Thunderbird Watershed .....	8
B. Objective.....	15
C. Methodology.....	16
1. Hydrology .....	16
2. Fluvial Geomorphology (FGM).....	32
D. Results .....	44
1. Hydrology .....	44
2. Fluvial Geomorphology (FGM).....	94
E. Comments and Conclusions .....	108
III. Part 2: Evaluation of an Acoustic Doppler Current Profiler (ADCP) for use in Measuring Sediment Transport in the Lake Thunderbird Watershed in Central Oklahoma .....	112
A. Basics of ADCP Operation.....	112
B. Hypothesis .....	112
C. Objectives .....	113
D. Methodology.....	113
1. ADCP Deployment Methods .....	113
2. Traditional Suspended Sediment Sampling Methods .....	116
3. Data Analysis .....	117
E. Results .....	129
1. Sediment Analysis.....	129
2. Sediment Flux Methods Analysis .....	141
3. Suspended Sediment Load to Lake Thunderbird .....	154
F. Discussion.....	161
G. Conclusion.....	164
IV. Summary of Hydrologic, Geomorphologic, and Sediment Transport Findings	165
V. Future Work.....	168

VI. References .....	171
VII. APPENDICES .....	182
A. Appendix A – Monitoring Sites Summary .....	183
A.1 Little River at 60th Ave NE .....	183
A.2 Little River at Porter.....	187
A.3 Hog Creek at SE 119 <sup>th</sup> Ave.....	190
A.4 Rock Creek at 72 <sup>nd</sup> Ave NE .....	193
A.5 Elm Creek at Indian Hills.....	196
A.6 North Fork at Franklin .....	199
A.7 Dave Blue Creek at 72 <sup>nd</sup> Ave SE .....	202
B. Appendix B – ADCP Operating Procedure.....	206
C. Appendix C – HOBO Data Plots.....	214
C.1 Ambient Conditions .....	214
C.2 Little River @ 60th Ave NE .....	214
C.3 Little River at Porter.....	216
C.4 Hog Creek at SE 119 <sup>th</sup> Ave.....	217
C.5 Rock Creek at 72 <sup>nd</sup> Ave NE .....	218
C.6 Elm Creek at Indian Hills.....	220
C.7 North Fork at Franklin .....	221
C.8 Dave Blue Creek at 72 <sup>nd</sup> Ave SE .....	223
D. Appendix D – Stage-Discharge Data Summaries and Rating Curves.....	225
D.1 Little River at 60 <sup>th</sup> Ave NE .....	225
D.2 Little River at Porter.....	227
D.3 Rock Creek at 72 <sup>nd</sup> Ave NE .....	229
D.4 Hog Creek at SE 119 <sup>th</sup> Ave.....	231
D.5 Elm Creek at Indian Hills.....	232
D.6 North Fork at Franklin .....	233
D.7 Dave Blue Creek at 72 <sup>nd</sup> Ave SE .....	234
E. Appendix E – FGM Survey Summaries .....	235
E.1 FGM Site LR-01 .....	236
E.2 FGM Site LR-02 .....	239
E.3 FGM Site LR-03 .....	242
E.4 FGM Site LR-04 .....	245
E.5 FGM Site LR-05 .....	248
E.6 FGM Site LR-06 .....	251
E.7 FGM Site LR-07 .....	254



E.8 FGM Site LR-08 .....	257
E.9 FGM Site LR-09 .....	260
E.10 FGM Site NF-01 .....	263
E.11 FGM Site NF-02 .....	266
E.12 FGM Site NF-03 .....	269
E.13 FGM Site NF-04 .....	272
E.14 FGM Site EC-01 .....	275
E.15 FGM Site EC-02 .....	278
E.16 FGM Site EC-03 .....	281
E.17 FGM Site RC-01 .....	284
E.18 FGM Site RC-02 .....	287
E.19 FGM Site RC-04 .....	290
E.20 FGM Site DBC-01 .....	293
E.21 FGM Site DBC-02 .....	296
E.22 FGM Site DBC-03 .....	299
E.23 FGM Site DBC-04 .....	302
E.24 FGM Site HC-01 .....	305
E.25 FGM Site HC-02 .....	308
F. Appendix F – FGM Site Photographs .....	311
F.1 FGM Site LR-01.....	311
F.2 FGM Site LR-02.....	312
F.3 FGM Site LR-03.....	315
F.4 FGM Site LR-04.....	318
F.5 FGM Site LR-05.....	321
F.6 FGM Site LR-06.....	324
F.7 FGM Site LR-07.....	327
F.8 FGM Site LR-08.....	330
F.9 FGM Site LR-08.....	333
F.10 FGM Site NF-01.....	336
F.11 FGM Site NF-02.....	337
F.12 FGM Site NF-03.....	339
F.13 FGM Site NF-04.....	340
F.14 FGM Site EC-01.....	341
F.15 FGM Site EC-02.....	342
F.16 FGM Site EC-03.....	343

F.17 FGM Site RC-01 .....	344
F.18 FGM Site RC-02 .....	345
F.19 FGM Site RC-04 .....	346
F.20 FGM Site DBC-01 .....	347
F.21 FGM Site DBC-02 .....	348
F.22 FGM Site DBC-03 .....	349
F.23 FGM Site DBC-04 .....	350
F.24 FGM Site HC-01 .....	351
F.25 FGM Site HC-02 .....	352
G. Appendix G: Total Suspended Material (TSM) SOP .....	353
H. Appendix H – Suspended Sediment Concentration Analyses Summary Tables	355
I. Appendix I - Suspended Particle Size Distribution Analyses Summary Tables	360
J. Appendix J – Sediment Flux Summary Tables .....	367
K. Appendix K – Personal Reflections on the Study .....	373

## LIST OF TABLES

Table 1: Reservoir capacity loss due to sedimentation. (Sources: Oklahoma Water Atlas 2007;OWRB Beneficial Use Monitoring Program Lakes Report, Lakes Sampling 2004-2005, 2005).....	4
Table 2: Lake Thunderbird watershed hydrological study sites.....	16
Table 3: Lake Thunderbird watershed fluvial geomorphology (FGM) study sites.....	34
Table 4: FGM Bank Stability Assessment Spreadsheet Categories 1 – 3.....	40
Table 5: FGM Bank Stability Assessment Spreadsheet Categories 4 -5.....	41
Table 6: FGM Bank Stability Assessment Spreadsheet Category 6. ....	42
Table 7: FGM Bank Stability Assessment Spreadsheet Category 7. ....	43
Table 8: HOBO Deployment Times.....	46
Table 9: Monthly Rainfall Data for Norman, Oklahoma; Jan2010 – Mar2015. (OCS, 2015).....	58
Table 10: Number of days that the study sites went dry, by year. ....	60
Table 11: Number of discharge measurements taken at each site.....	62
Table 12: Stage-Discharge rating curve coefficients and exponents.....	77
Table 13: FGM Assessment Results Summary.....	95
Table 14: Bank Erosion Indices Results Summary.....	100
Table 15: ADCP Deployments.....	130
Table 16: Particle Size Distribution for Little River at 60 <sup>th</sup> , April 15, 2012; Sample 1 – Left; Sample 2 – Center; Sample 3 – Right.....	137
Table 17: Sediment flux (kg/s) estimated by ViSea PDT for Little River at 60 <sup>th</sup> , April 15, 2012; Sample 1 – Left; Sample 2 – Center; Sample 3 – Right.....	137
Table 18: Effect of particle size distribution on sediment flux (kg/s) estimated by ViSea PDT for Little River at 60 <sup>th</sup> , April 15, 2012.....	139
Table 19: Difference in flux (kg/s) estimated by ViSea PDT for Little River at 60 <sup>th</sup> , April 15, 2012 using uniform distribution versus measured distribution.....	139
Table 20: Percent difference in flux estimated by ViSea PDT for Little River at 60 <sup>th</sup> , April 15, 2012 using uniform sand distribution versus measured distribution. ....	140
Table 21: Sediment Flux Rating Curve Coefficients and Exponents for Little River at 60 <sup>th</sup> ; All Data. ....	143
Table 22: Sediment Flux Rating Curve Coefficients and Exponents for Little River at 60 <sup>th</sup> ; Q > 60 cfs. ....	144
Table 23: Suspended Sediment Flux Curve Slope Comparison – Little River at 60 <sup>th</sup> ; Q > 60 cfs. ....	146
Table 24: Suspended Sediment Flux Curve Slope Comparison Using Pooled Error Variance – Little River at 60 <sup>th</sup> ; Q > 60 cfs. ....	148
As before, Excel was used to perform the required computation. Table 25 shows the results of this assessment. The first row shows the .....	149
Table 25: Suspended Sediment Flux Curve Intercept Comparison – Little River at 60 <sup>th</sup> ; Q > 60 cfs. ....	150
Table 26: Sediment Flux Rating Curve Coefficients and Exponents for Little River at Porter; All Data.....	151
Table 27: Sediment Flux Rating Curve Coefficients and Exponents for Little River at Porter; 60 cfs < Q < 1000 cfs. ....	152

Table 28: Suspended Sediment Flux Curve Slope Comparison – Little River at Porter; 60 cfs < Q < 1,000 cfs. ....	153
Table 29: Suspended Sediment Flux Curve Slope Comparison Using Pooled Error Variance – Little River at Porter; 60 cfs < Q < 1,000 cfs.....	153
Table 30: Suspended Sediment Flux Curve Intercept Comparison – Little River at Porter; 60 cfs < Q < 1,000 cfs. ....	154
Table 31: Total Annual Sediment Loads to Lake Thunderbird from the Little River Watershed (DA=55.4 mi <sup>2</sup> ); 2010-2014. ....	156
Table 32: Total Annual Sediment Loads at the Little River at Porter site (DA=20.26 mi <sup>2</sup> ); 2010-2014.....	160
Table A.1.1: Little River at 60 <sup>th</sup> Ave NE Cross-section survey data. ....	185
Table A.1.2: Little River at 60 <sup>th</sup> Ave NE initial HOBO elevation Survey data. ....	185
Table A.1.3: Little River at 60 <sup>th</sup> Ave NE HOBO replacement elevation Survey data (after July 27, 2011). ....	186
Table A.2.1: Little River at Porter Ave Cross-section survey data. ....	188
Table A.2.2: Little River at Porter Ave HOBO elevation Survey data, ....	189
Table A.3.1: Hog Creek at SE 119 <sup>th</sup> Ave cross-section survey data. ....	191
Table A.3.2: Hog Creek at SE 119 <sup>th</sup> Ave SE HOBO elevation Survey data.....	192
Table A.4.1: Rock Creek at 72 <sup>nd</sup> Ave NE Cross-section survey data. ....	194
Table A.4.2: Rock Creek at 72 <sup>nd</sup> Ave NE HOBO elevation Survey data. ....	195
Table A.5.1: Elm Creek at Indian Hills (SE179 <sup>th</sup> )cross-section survey data. ....	197
Table A.5.2: Elm Creek at Indian Hills HOBO elevation Survey data. ....	198
Table A.6.1: North Fork at Franklin Cross-section survey data.....	200
Table A.6.2: North Fork at Franklin HOBO elevation Survey data.....	201
Table A.7.1: Dave Blue Creek at 72 <sup>nd</sup> Ave SE Cross-section survey data. ....	204
Table A.7.2: Dave Blue Creek at 72 <sup>nd</sup> Ave SE HOBO elevation Survey data. ....	205
Table D.1.1: Stage-Discharge Measurements at Little River at 60 <sup>th</sup> Ave NE.....	225
Table D.1.2: Estimated Discharges for Little River at 60 <sup>th</sup> Ave NE. ....	226
Table D.2.1: Stage-Discharge Measurements at Little River at Porter. ....	227
Table D.2.2: Estimated Discharges for Little River at Porter. ....	228
Table D.3.1: Stage-Discharge Measurements at Rock Creek at 72 <sup>nd</sup> Ave NE.....	229
Table D.3.2: Estimated Discharges for Rock Creek at 72 <sup>nd</sup> Ave NE. ....	230
Table D.4.1: Stage-Discharge Measurements at Hog Creek at SE 119 <sup>th</sup> Ave.....	231
Table D.4.2: Estimated Discharges for Hog Creek at SE 119 <sup>th</sup> Ave.....	231
Table D.5.1: Stage-Discharge Measurements at Elm Creek at Indian Hills. ....	232
Table D.5.2: Estimated Discharges for Elm Creek at Indian Hills. ....	232
Table D.6.1: Stage-Discharge Measurements at North Fork at Franklin. ....	233
Table D.6.2: Estimated Discharges for North Fork at Franklin. ....	233
Table D.7.1: Stage-Discharge Measurements at Dave Blue Creek at 72 <sup>nd</sup> Ave.....	234
Table D.7.2: Estimated Discharges for Dave Blue Creek at 72 <sup>nd</sup> Ave.....	234
Table E.1.1: FGM Site LR-01 Survey Control.....	236
Table E.1.2: FGM Site LR-01 Channel Morphology Summary. ....	238
Table E.1.3: FGM Site LR-01 Stream Channel Stability Summary. ....	238
Table E.2.1: FGM Site LR-02 Survey Control.....	239
Table E.2.2: FGM Site LR-02 Channel Morphology Summary. ....	241
Table E.2.3: FGM Site LR-02 Stream Channel Stability Summary. ....	241

Table E.3.1: FGM Site LR-03 Survey Control.....	242
Table E.3.2: FGM Site LR-03 Channel Morphology Summary. ....	244
Table E.3.3: FGM Site LR-03 Stream Channel Stability Summary. ....	244
Table E.4.1: FGM Site LR-04 Survey Control.....	245
Table E.4.2: FGM Site LR-04 Channel Morphology Summary. ....	247
Table E.4.3: FGM Site LR-04 Stream Channel Stability Summary. ....	247
Table E.5.1: FGM Site LR-05 Survey Control.....	248
Table E.5.2: FGM Site LR-05 Channel Morphology Summary. ....	250
Table E.5.3: FGM Site LR-05 Stream Channel Stability Summary. ....	250
Table E.6.1: FGM Site LR-06 Survey Control.....	251
Table E.6.2: FGM Site LR-06 Channel Morphology Summary. ....	253
Table E.6.3: FGM Site LR-06 Stream Channel Stability Summary. ....	253
Table E.7.1: FGM Site LR-07 Survey Control.....	254
Table E.7.2: FGM Site LR-07 Channel Morphology Summary. ....	256
Table E.7.3: FGM Site LR-07 Stream Channel Stability Summary. ....	256
Table E.8.1: FGM Site LR-08 Survey Control.....	257
Table E.8.2: FGM Site LR-08 Channel Morphology Summary. ....	259
Table E.8.3: Site LR-08Stream Channel Stability Summary. ....	259
Table E.9.1: FGM Site LR-09 Survey Control.....	260
Table E.9.2: FGM Site LR-09 Channel Morphology Summary. ....	262
Table E.9.3: Site LR-09 Stream Channel Stability Summary. ....	262
Table E.10.1: FGM Site NF-01 Survey Control.....	263
Table E.10.2: FGM Site NF-01 Channel Morphology Summary. ....	265
Table E.10.3: Site NF-01 Stream Channel Stability Summary. ....	265
Table E.11.1: FGM Site NF-02 Survey Control.....	266
Table E.11.2: FGM Site NF-02 Channel Morphology Summary. ....	268
Table E.11.3: Site NF-02 Stream Channel Stability Summary. ....	268
Table E.12.1: FGM Site NF-03 Survey Control.....	269
Table E.12.2: FGM Site NF-03 Channel Morphology Summary. ....	271
Table E.12.3: FGM Site NF-03 Stream Channel Stability Summary. ....	271
Table E.13.1: FGM Site NF-04 Survey Control.....	272
Table E.13.2: FGM Site NF-04 Channel Morphology Summary. ....	274
Table E.13.3: FGM Site NF-04 Stream Channel Stability Summary. ....	274
Table E.14.1: FGM Site EC-01 Survey Control.....	275
Table E.14.2: FGM Site EC-01 Channel Morphology Summary. ....	277
Table E.14.3: FGM Site EC-01 Stream Channel Stability Summary. ....	277
Table E.15.1: FGM Site EC-02 Survey Control.....	278
Table E.15.2: FGM Site EC-02 Channel Morphology Summary. ....	280
Table E.15.3: FGM Site EC-02 Stream Channel Stability Summary. ....	280
Table E.16.1: FGM Site EC-03 Survey Control.....	281
Table E.16.2: FGM Site EC-03 Channel Morphology Summary. ....	283
Table E.16.3: FGM Site EC-03 Stream Channel Stability Summary. ....	283
Table E.17.1: FGM Site RC-01 Survey Control. ....	284
Table E.17.2: FGM Site RC-01 Channel Morphology Summary. ....	286
Table E.17.3: FGM Site RC-01 Stream Channel Stability Summary. ....	286
Table E.18.1: FGM Site RC-02 Survey Control. ....	287

Table E.18.2: FGM Site RC-02 Channel Morphology Summary. ....	289
Table E.18.3: FGM Site RC-02 Stream Channel Stability Summary. ....	289
Table E.19.1: FGM Site RC-04 Survey Control. ....	290
Table E.19.2: FGM Site RC-04 Channel Morphology Summary. ....	292
Table E.19.3: FGM Site RC-04 Stream Channel Stability Summary. ....	292
Table E.20.1: FGM Site DBC-01 Survey Control. ....	293
Table E.20.2: FGM Site DBC-01 Channel Morphology Summary. ....	295
Table E.20.3: FGM Site DBC-01 Stream Channel Stability Summary. ....	295
Table E.21.1: FGM Site DBC-02 Survey Control. ....	296
Table E.21.2: FGM Site DBC-02 Channel Morphology Summary. ....	298
Table E.21.3: FGM Site DBC-02 Stream Channel Stability Summary. ....	298
Table E.22.1: FGM Site DBC-03 Survey Control. ....	299
Table E.22.2: FGM Site DBC-03 Channel Morphology Summary. ....	301
Table E.22.3: FGM Site DBC-03 Stream Channel Stability Summary. ....	301
Table E.23.1: FGM Site DBC-04 Survey Control. ....	302
Table E.23.2: FGM Site DBC-04 Channel Morphology Summary. ....	304
Table E.23.3: FGM Site DBC-04 Stream Channel Stability Summary. ....	304
Table E.24.1: FGM Site HC-01 Survey Control. ....	305
Table E.24.2: FGM Site HC-01 Channel Morphology Summary. ....	307
Table E.24.3: FGM Site HC-01 Stream Channel Stability Summary. ....	307
Table E.25.1: FGM Site HC-02 Survey Control. ....	308
Table E.25.2: FGM Site HC-02 Channel Morphology Summary. ....	310
Table E.25.3: FGM Site HC-02 Stream Channel Stability Summary. ....	310
Table H.1: Suspended Sediment Concentration Analyses Summary (1 of 4). ....	356
Table H.2: Suspended Sediment Concentration Analyses Summary (2 of 4). ....	357
Table H.3: Suspended Sediment Concentration Analyses Summary (3 of 4). ....	358
Table H.4: Suspended Sediment Concentration Analyses Summary (4 of 4). ....	359
Table I.1: Suspended Particle Size Distribution Analyses Summary (1 of 6). ....	361
Table I.2: Suspended Particle Size Distribution Analyses Summary (2 of 6). ....	362
Table I.3: Suspended Particle Size Distribution Analyses Summary (3 of 6). ....	363
Table I.4: Suspended Particle Size Distribution Analyses Summary (4 of 6). ....	364
Table I.5: Suspended Particle Size Distribution Analyses Summary (5 of 6). ....	365
Table I.6: Suspended Particle Size Distribution Analyses Summary (6 of 6). ....	366
Table J.1: Grab Sample Sediment Flux Summary (1 of 2). ....	368
Table J.2: Grab Sample Sediment Flux Summary (2 of 2). ....	369
Table J.3: Depth-integrated Sample Sediment Flux Summary (1 of 2). ....	370
Table J.4: Depth-integrated Sample Sediment Flux Summary (2 of 2). ....	371
Table J.5: ADCP with ViSea PDT Sediment Flux Summary. ....	372

## LIST OF FIGURES

Figure 1: Distribution of mean annual loss of reservoir capacity in the continental United States mapped by HUC-2 units (water resource regions broadly defined by large river basins). (Graf et al., 2010) .....	3
Figure 2: Little River Watershed.....	9
Figure 3: Lake Thunderbird Watershed. ....	10
Figure 4: Indications of the Little River channel incision and widening including a) exposed high pressure gas lines and b) tributary head cuts.....	13
Figure 5: Channel Evolution Model – The Little River is currently at Stage IV, the degradation and widening stage. (Simon (1989)).....	14
Figure 6: a) Channelized versus natural meandering Wildhorse Creek channel, in Garvin County, Oklahoma (Barclay, 1980); b) Comparison of Wildhorse Creek channel dimensions in 1933. (blue line - Barclay, 1980) and 1999 (green line - Dutnell, 2000)	15
Figure 7: Location of the Lake Thunderbird watershed hydrological study sites.....	17
Figure 8: HOBO water level logger with PVC housing.....	18
Figure 9: HOBO installed to staff gauge at Hog Creek study site. ....	19
Figure 10: Discharge measurement using Marsh McBirney flow meter at the Little River at 60 <sup>th</sup> site.....	23
Figure 11: ADCP measurement instrument setup. Left) Trimaran setup; Right) Base station setup.....	26
Figure 12: Discharge measurement using Acoustic Doppler Current Profiler (ADCP) at the Little River at 60 <sup>th</sup> site. ....	30
Figure 13: Map of the Lake Thunderbird watershed showing the location of the fluvial geomorphology (FGM) study sites.....	34
Figure 14: Classification Key for Natural Rivers. (Rosgen, 1996) .....	38
Figure 15: Cross-section plot for the Little River at 60 <sup>th</sup> Ave NE monitoring site. ....	46
Figure 16: HOBO temperature and pressure plots for the Ambient Conditions site.....	48
Figure 17: Temperature and pressure plots for the Little River at 60 <sup>th</sup> Ave NE site.....	49
Figure 18: Stage plot for the Little River at 60 <sup>th</sup> Ave NE site.....	50
Figure 19: HOBO Side-By-Side Pressure Measurement Plots. ....	53
Figure 20: HOBO Side-By-Side Temperature Measurement Plots. ....	53
Figure 21: HOBO Side-By-Side Calculated Depth (Stage) Plots. ....	54
Figure 22: HOBO Side-By-Side Pressure Measurement Difference Plot.....	54
Figure 23: HOBO Side-By-Side Temperature Measurement Difference Plot. ....	55
Figure 24: HOBO Side-By-Side Depth (stage) Measurement Difference Plot.....	55
Figure 25: HOBO Side-By-Side Measurement Plots; Left-Pressure, Right- Temperature. ....	57
Figure 26: HOBO Side-By-Side Measurement Depth Plot.....	57
Figure 27: Temperature and pressure plots for the Rock Creek at 72 <sup>nd</sup> Ave NE site.....	59
Figure 28: Little River at 60 <sup>th</sup> Ave NE stage-discharge rating curve. ....	64
Figure 29: Manning’s “n” versus hydraulic radius at Little River at 60 <sup>th</sup> Ave NE. ....	66
Figure 30: Little River at Porter stage-discharge rating curve. ....	67
Figure 31: Manning’s “n” versus hydraulic radius at Little River at Porter. ....	69
Figure 32: Rock Creek at 72 <sup>nd</sup> stage-discharge rating curve.....	70
Figure 33: Hog Creek at SE119 <sup>th</sup> stage-discharge rating curve. ....	72

Figure 34: Elm Creek at Indian Hills stage-discharge rating curve. ....	73
Figure 35: North Fork at Franklin stage-discharge rating curve. ....	74
Figure 36: Dave Blue Creek at 72nd stage-discharge rating curve. ....	75
Figure 37: Little River at 60th Ave NE site discharge plot. ....	77
Figure 38: Little River at Porter site discharge plot. ....	78
Figure 39: Rock Creek at 72nd Ave NE site discharge plot. ....	78
Figure 40: Hog Creek at SE 119th Ave site discharge plot. ....	79
Figure 41: Elm Creek at Indian Hills site discharge plot. ....	79
Figure 42: North Fork at Franklin site discharge plot. ....	80
Figure 43: Dave Blue Creek at 72nd Ave SE site discharge plot. ....	80
Figure 44: Cumulative Runoff Volume - Little River at 60 <sup>th</sup> Ave, 2010-2014. ....	82
Figure 45: Cumulative Runoff Volume - Rock Creek, 2010-2014. ....	82
Figure 46: Cumulative Runoff Volume – North Fork at Franklin, 2010-2014. ....	83
Figure 47: Cumulative Runoff Volume – Dave Blue Creek, 2010-2014. ....	83
Figure 48: Cumulative Runoff Volume – Little River at Porter, 2010-2014. ....	84
Figure 49: Cumulative Runoff Volume - Elm Creek, 2010-2014. ....	84
Figure 50: Cumulative Runoff Volume – Hog Creek, 2010-2013. ....	85
Figure 51: 30-Minute Rainfall Data for Norman, Oklahoma; Mar 2010 - Mar 2015. ...	86
Figure 52: Storm Runoff Volume at Little River @ 60th vs. Rainfall Events > 1.5"; Preceding 10-day rainfall. ....	87
Figure 53: Storm Runoff Volume at Little River @ 60th vs. Rainfall Events > 1.5"; Preceding 30-day rainfall. ....	88
Figure 54: Storm Runoff Volume at Little River @ 60th vs. Rainfall Events > 1.5"; Preceding 60-day rainfall. ....	88
Figure 55: Rock Creek data used to calibrate Vflo hydrologic distributed runoff model (Sabohan, 2010). ....	90
Figure 56: Discharge at Little River at 60 <sup>th</sup> and rainfall at the Norman Mesonet station for May, 2011. ....	91
Figure 57: Cross-section Change at the Little River at 60 <sup>th</sup> site. ....	93
Figure 58: Bankfull Area (ft <sup>2</sup> ) versus Drainage Area (mi <sup>2</sup> ) Regional Curve for Lake Thunderbird watershed. ....	97
Figure 59: Bankfull Width (ft) versus Drainage Area (mi <sup>2</sup> ) Regional Curve for Lake Thunderbird watershed. ....	98
Figure 60: Bankfull Depth (ft) versus Drainage Area (mi <sup>2</sup> ) Regional Curve for Lake Thunderbird watershed. ....	98
Figure 61: Channel Stability Indices (CSI's) in the Lake Thunderbird watershed. ....	102
Figure 62: Bank Erosion Hazard Indices (BEHI's) in the Lake Thunderbird watershed. .....	103
Figure 63: Near Bank Stress (NBS) Ratings in the Lake Thunderbird watershed. ....	105
Figure 64: Pfankuch Ratings in the Lake Thunderbird watershed. ....	106
Figure 65: Ozark Eco-Region Bank Stability Indices (OEBSI's) in the Lake Thunderbird watershed. ....	107
Figure 66: Teledyne RDI 600 kHz Workhorse Rio Grande OceanScience Riverboat with RTK GPS. ....	114
Figure 67: FISP DH-76 isokinetic depth integrated sampler. ....	116
Figure 68: Diagrammatic view of the sonar parameters; from Urick (1967). ....	121



Figure 69: Environmental Processing screen in ViSea PDT.....	125
Figure 70: Sample Data screen in ViSea PDT. ....	126
Figure 71: Iteration Processing screen in ViSea PDT. ....	127
Figure 72: Correlation Processing screen in ViSea PDT. ....	128
Figure 73: Typical ViSea PDT screen display; transect of the Little River at 60th site on July 17, 2013. ....	129
Figure 74: LISST Repeatability Analysis Particle Size Distribution Plot.....	132
Figure 75: Mean Particle Size Value Comparison between the Sequoia LISST Portable XR and the Malvern Mastersizer 2000.....	133
Figure 76: Particle Size Class Distribution of the Sequoia LISST Portable XR and the Malvern Mastersizer 2000 – Sample 1 – LR@60th; 4-15-2012; grab-lt2. ....	135
Figure 77: Particle Size Class Distribution of the Sequoia LISST Portable XR and the Malvern Mastersizer 2000 – Sample 2 – LR@60th; 4-15-2012; grab-ctr2. ....	135
Figure 78: Particle Size Class Distribution of the Sequoia LISST Portable XR and the Malvern Mastersizer 2000 – Sample 3 – LR@60th; 4-15-2012; grab-rt. ....	136
Figure 79: Suspended Sediment Rating Curves for Little River at 60 <sup>th</sup> ; All Data. ....	142
Figure 80: Suspended Sediment Rating Curves for Little River at 60 <sup>th</sup> ; Q > 60 cfs. ...	144
Figure 81: Suspended Sediment Rating Curves for Little River at Porter; All Data ...	151
Figure 82: Suspended Sediment Rating Curves for Little River at Porter; 60 cfs < Q < 1000 cfs. ....	152
Figure 83: Annual Cumulative Sediment Loads to Lake Thunderbird from the Little River Watershed; 2010-2014.....	155
Figure 84: Annual Cumulative Sediment Loads at the Little River at Porter site; 2010-2014. ....	159
Figure 84: Aqua Vision ViSea PDT Suspended Sediment Concentration (Lt) and Flux (Rt) Profile Plots; Little River at Porter; May 21, 2013; Transect 5; Q = 3.26 cms (115 cfs); Flux = 1.33 kg/s (127 tons/day).....	163
Figure 85: Aqua Vision ViSea PDT Suspended Sediment Concentration (Lt) and Flux (Rt) Profile Plots; Little River at 60 <sup>th</sup> ; May 23, 2013; Transect 6; Q = 73.43 cms (2.593.2 cfs); Flux = 123.9 kg/s (11,800.2 tons/day). ....	163
Figure A.1.1: Little River at 60 <sup>th</sup> Ave NE site location map.....	183
Figure A.1.2: Little River at 60 <sup>th</sup> Ave NE HOBO initial installation.....	184
Figure A.1.3: Little River at 60 <sup>th</sup> Ave NE HOBO replaced installation. ....	184
Figure A.1.4: Little River at 60 <sup>th</sup> Ave NE - Site cross-section plot. ....	186
Figure A.2.1: Little River at Porter Ave site location map. ....	187
Figure A.2.2: Little River at Porter Ave HOBO installation.....	188
Figure A.2.3: Cross-section plot for the Little River at Porter monitoring site.....	189
Figure A.3.1: Hog Creek at SE 119 <sup>th</sup> Ave site location map.....	190
Figure A.3.2: Hog Creek at SE119th Ave site HOBO installation. ....	191
Figure A.3.3: Cross-section plot for the Hog Creek at SE 119 <sup>th</sup> Ave monitoring site. ....	192
Figure A.4.1: Rock Creek at 72 <sup>nd</sup> Ave NE site location map.....	193
Figure A.4.2: Rock Creek at 72 <sup>nd</sup> Ave NE site HOBO installation. ....	194
Figure A.4.3: Cross-section plot for the Rock Creek at 72nd Ave NE monitoring site. ....	195
Figure A.5.1: Elm Creek at Indian Hills (SE 179 <sup>th</sup> ) monitoring site location map. ....	196

Figure A.5.2: Elm Creek at Indian Hills (SE 179 <sup>th</sup> ) monitoring site HOBO installation.	197
Figure A.5.3: Cross-section plot for the Elm Creek at Indian Hills monitoring site....	198
Figure A.6.1: North Fork at Franklin monitoring site location map. ....	199
Figure A.6.2: North Fork at Franklin monitoring site HOBO installation. ....	200
Figure A.6.3: Cross-section plot for the North Fork at Franklin monitoring site. ....	201
Figure A.7.1: Dave Blue Creek at 72 <sup>nd</sup> Ave SE monitoring site location map. ....	202
Figure A.7.2: Dave Blue Creek at 72 <sup>nd</sup> Ave SE monitoring site HOBO installation. ...	203
Figure A.7.3: Cross-section plot for the Dave Blue Creek at 72 <sup>nd</sup> Ave SE monitoring site.....	205
Figure C.1.1: Ambient Conditions site HOBO data plot.....	214
Figure C.2.1: Little River at 60 <sup>th</sup> Ave NE site HOBO data plot.....	214
Figure C.2.2: Little River at 60 <sup>th</sup> Ave NE site stage plot. ....	215
Figure C.2.3: Little River at 60 <sup>th</sup> Ave NE site water surface elevation plot.....	215
Figure C.3.1: Little River at Porter site HOBO data plot. ....	216
Figure C.3.2: Little River at Porter site stage plot.....	216
Figure C.3.3: Little River at Porter site water surface elevation plot.....	217
Figure C.4.1: Hog Creek at SE 119 <sup>th</sup> Ave site HOBO data plot. ....	217
Figure C.5.1: Rock Creek at 72 <sup>nd</sup> Ave NE site HOBO data plot.....	218
Figure C.5.2: Rock Creek at 72 <sup>nd</sup> Ave NE site stage plot. ....	219
Figure C.5.3: Rock Creek at 72 <sup>nd</sup> Ave NE site water surface elevation plot. ....	219
Figure C.6.1: Elm Creek at Indian Hills site HOBO data plot. ....	220
Figure C.6.2: Elm Creek at Indian Hills site stage plot.....	220
Figure C.6.3: Elm Creek at Indian Hills site water surface elevation plot. ....	221
Figure C.7.1: North Fork at Franklin site HOBO data plot.....	221
Figure C.7.2: North Fork at Franklin site stage plot.....	222
Figure C.7.3: North Fork at Franklin site water surface elevation plot.....	222
Figure C.8.1: Dave Blue Creek at 72 <sup>nd</sup> Ave SE site HOBO data plot.....	223
Figure C.8.2: Dave Blue Creek at 72 <sup>nd</sup> Ave SE site stage plot.....	223
Figure C.8.3: Dave Blue Creek at 72 <sup>nd</sup> Ave SE site water surface elevation plot.....	224
Figure E.1.1: FGM Site LR-01 Site Map with Survey Points.....	236
Figure E.1.2: FGM Site LR-01 Cross-section Survey Plot. ....	237
Figure E.1.3: FGM Site LR-01 Longitudinal Profile Survey Plot. ....	237
Figure E.2.1: FGM Site LR-02 Site Map with Survey Points.....	239
Figure E.2.2: FGM Site LR-02 Cross-section Survey Plot. ....	240
Figure E.2.3: FGM Site LR-02 Longitudinal Profile Survey Plot. ....	240
Figure E.3.1: FGM Site LR-03 Site Map with Survey Points.....	242
Figure E.3.2: FGM Site LR-03 Cross-section Survey Plot. ....	243
Figure E.3.3: FGM Site LR-03 Longitudinal Profile Survey Plot. ....	243
Figure E.4.1: FGM Site LR-04 Site Map with Survey Points.....	245
Figure E.4.2: FGM Site LR-04 Cross-section Survey Plot. ....	246
Figure E.4.3: FGM Site LR-04 Longitudinal Profile Survey Plot. ....	246
Figure E.5.1: FGM Site LR-05 Site Map with Survey Points.....	248
Figure E.5.2: FGM Site LR-05 Cross-section Survey Plot. ....	249
Figure E.5.3: FGM Site LR-05 Longitudinal Profile Survey Plot. ....	249
Figure E.6.1: FGM Site LR-06 Site Map with Survey Points.....	251

Figure E.6.2: FGM Site LR-06 Cross-section Survey Plot. ....	252
Figure E.6.3: FGM Site LR-06 Longitudinal Profile Survey Plot. ....	252
Figure E.7.1: FGM Site LR-07 Site Map with Survey Points.....	254
Figure E.7.2: FGM Site LR-07 Cross-section Survey Plot. ....	255
Figure E.7.3: FGM Site LR-07 Longitudinal Profile Survey Plot. ....	255
Figure E.8.1: FGM Site LR-08 Site Map with Survey Points.....	257
Figure E.8.2: FGM Site LR-08 Cross-section Survey Plot. ....	258
Figure E.8.3: FGM Site LR-08 Longitudinal Profile Survey Plot. ....	258
Figure E.9.1: FGM Site LR-09 Site Map with Survey Points.....	260
Figure E.9.2: FGM Site LR-09 Cross-section Survey Plot. ....	261
Figure E.9.3: FGM Site LR-09 Longitudinal Profile Survey Plot. ....	261
Figure E.10.1: FGM Site NF-01 Site Map with Survey Points.....	263
Figure E.10.2: FGM Site NF-01 Cross-section Survey Plot. ....	264
Figure E.10.3: FGM Site NF-01 Longitudinal Profile Survey Plot. ....	264
Figure E.11.1: FGM Site NF-02 Site Map with Survey Points.....	266
Figure E.11.2: FGM Site NF-02 Cross-section Survey Plot. ....	267
Figure E.11.3: FGM Site NF-02 Longitudinal Profile Survey Plot. ....	267
Figure E.12.1: FGM Site NF-03 Site Map with Survey Points.....	269
Figure E.12.2: FGM Site NF-03 Cross-section Survey Plot. ....	270
Figure E.12.3: FGM Site NF-03 Longitudinal Profile Survey Plot. ....	270
Figure E.13.1: FGM Site NF-04 Site Map with Survey Points.....	272
Figure E.13.2: FGM Site NF-04 Cross-section Survey Plot. ....	273
Figure E.13.3: FGM Site NF-04 Longitudinal Profile Survey Plot. ....	273
Figure E.14.1: FGM Site EC-01 Site Map with Survey Points.....	275
Figure E.14.2: FGM Site EC-01 Cross-section Survey Plot. ....	276
Figure E.14.3: FGM Site EC-01 Longitudinal Profile Survey Plot. ....	276
Figure E.15.1: FGM Site EC-02 Site Map with Survey Points.....	278
Figure E.15.2: FGM Site EC-02 Cross-section Survey Plot. ....	279
Figure E.15.3: FGM Site EC-02 Longitudinal Profile Survey Plot. ....	279
Figure E.16.1: FGM Site EC-03 Site Map with Survey Points.....	281
Figure E.16.2: FGM Site EC-03 Cross-section Survey Plot. ....	282
Figure E.16.3: FGM Site EC-03 Longitudinal Profile Survey Plot. ....	282
Figure E.17.1: FGM Site RC-01 Site Map with Survey Points.....	284
Figure E.17.2: FGM Site RC-01 Cross-section Survey Plot. ....	285
Figure E.17.3: FGM Site RC-01 Longitudinal Profile Survey Plot. ....	285
Figure E.18.1: FGM Site RC-02 Site Map with Survey Points.....	287
Figure E.18.2: FGM Site RC-02 Cross-section Survey Plot. ....	288
Figure E.18.3: FGM Site RC-02 Longitudinal Profile Survey Plot. ....	288
Figure E.19.1: FGM Site RC-04 Site Map with Survey Points.....	290
Figure E.19.2: FGM Site RC-04 Cross-section Survey Plot. ....	291
Figure E.19.3: FGM Site RC-04 Longitudinal Profile Survey Plot. ....	291
Figure E.20.1: FGM Site DBC-01 Site Map with Survey Points.....	293
Figure E.20.2: FGM Site DBC-01 Cross-section Survey Plot. ....	294
Figure E.20.3: FGM Site DBC-01 Longitudinal Profile Survey Plot. ....	294
Figure E.21.1: FGM Site DBC-02 Site Map with Survey Points.....	296
Figure E.21.2: FGM Site DBC-02 Cross-section Survey Plot. ....	297

Figure E.21.3: FGM Site DBC-02 Longitudinal Profile Survey Plot. ....	297
Figure E.22.1: FGM Site DBC-03 Site Map with Survey Points.....	299
Figure E.22.2: FGM Site DBC-03 Cross-section Survey Plot. ....	300
Figure E.22.3: FGM Site DBC-03 Longitudinal Profile Survey Plot. ....	300
Figure E.23.1: FGM Site DBC-04 Site Map with Survey Points.....	302
Figure E.23.2: FGM Site DBC-04 Cross-section Survey Plot. ....	303
Figure E.23.3: FGM Site DBC-04 Longitudinal Profile Survey Plot. ....	303
Figure E.24.1: FGM Site HC-01 Site Map with Survey Points. ....	305
Figure E.24.2: FGM Site HC-01 Cross-section Survey Plot.....	306
Figure E.24.3: FGM Site HC-01 Longitudinal Profile Survey Plot. ....	306
Figure E.25.1: FGM Site HC-02 Site Map with Survey Points. ....	308
Figure E.25.2: FGM Site HC-02 Cross-section Survey Plot.....	309
Figure E.25.3: FGM Site HC-02 Longitudinal Profile Survey Plot. ....	309
Figure F.1.1: FGM Site LR-01 – Looking upstream (lt); Looking downstream (rt)....	311
Figure F.1.2: FGM Site LR-01 – Right Bank.....	311
Figure F.2.1: FGM Site LR-02 – Cross Section - Looking upstream (lt); Looking downstream (rt). ....	312
Figure F.2.2: FGM Site LR-02 – Cross Section - Left Bank (lt) – Right bank (rt).....	312
Figure F.2.3: FGM Site LR-02 – Bank 1 - Bank (lt) – Looking upstream (rt).....	312
Figure F.2.4: FGM Site LR-02 – Bank 1 - Facing downstream (lt); Bank 2 - Bank (rt). .....	313
Figure F.2.5: FGM Site LR-02 – Bank 2 - Facing upstream (lt); Facing downstream (rt). .....	313
Figure F.2.6: FGM Site LR-02 – Bank 3 - Bank (lt); Facing upstream (rt). ....	313
Figure F.2.7: FGM Site LR-02 – Bank 3 – Facing downstream (lt); Bank 4 - Bank (rt). .....	314
Figure F.2.8: FGM Site LR-02 – Bank 4 – Facing upstream (lt); Facing downstream (rt). ....	314
Figure F.3.1: FGM Site LR-03 – Cross Section - Looking upstream (lt); Looking downstream (rt). ....	315
Figure F.3.2: FGM Site LR-03 – Cross Section - Left Bank (lt) – Right bank (rt).....	315
Figure F.3.3: FGM Site LR-03 – Bank 1 - Bank (lt) – Looking upstream (rt).....	315
Figure F.3.4: FGM Site LR-03 – Bank 1-Facing downstream (lt); Bank 2-Bank (rt). 316	
Figure F.3.5: FGM Site LR-03 – Bank 2-Facing upstream (lt); Facing downstream (rt). .....	316
Figure F.3.6: FGM Site LR-03 – Bank 3 - Bank (lt); Facing upstream (rt). ....	316
Figure F.3.7: FGM Site LR-03 – Bank 3–Facing downstream (lt); Bank 4-Bank (rt). 317	
Figure F.3.8: FGM Site LR-03 – Bank 4–Facing upstream (lt); Facing downstream (rt). .....	317
Figure F.4.1: FGM Site LR-04 – Cross Section - Looking upstream (lt); Looking downstream (rt). ....	318
Figure F.4.2: FGM Site LR-04 – Cross Section - Left Bank (lt) – Right bank (rt).....	318
Figure F.4.3: FGM Site LR-04 – Bank 1 - Bank (lt) – Looking upstream (rt).....	318
Figure F.4.4: FGM Site LR-04 – Bank 1-Facing downstream (lt); Bank 2-Bank (rt). 319	
Figure F.4.5: FGM Site LR-04–Bank 2-Facing upstream (lt);Facing downstream (rt). .....	319

Figure F.4.6: FGM Site LR-04 – Bank 3 - Bank (lt); Facing upstream (rt). .....	319
Figure F.4.7: FGM Site LR-04 – Bank 3–Facing downstream (lt); Bank 4-Bank (rt). .....	320
Figure F.4.8: FGM Site LR-04-Bank 4–Facing upstream (lt);Facing downstream (rt). .....	320
Figure F.5.1: FGM Site LR-05 – Cross Section - Looking upstream (lt); Looking downstream (rt). .....	321
Figure F.5.2: FGM Site LR-05 – Cross Section - Left Bank (lt) – Right bank (rt). .....	321
Figure F.5.3: FGM Site LR-05 – Bank 1 - Bank (lt) – Looking upstream (rt). .....	321
Figure F.5.4: FGM Site LR-05 – Bank 1-Facing downstream (lt); Bank 2-Bank (rt). .....	322
Figure F.5.5: FGM Site LR-05–Bank 2-Facing upstream (lt);Facing downstream (rt). .....	322
Figure F.5.6: FGM Site LR-05 – Bank 3 - Bank (lt); Facing upstream (rt). .....	322
Figure F.5.7: FGM Site LR-05 – Bank 3–Facing downstream (lt); Bank 4-Bank (rt). .....	323
Figure F.5.8: FGM Site LR-05-Bank 4–Facing upstream (lt);Facing downstream (rt). .....	323
Figure F.6.1: FGM Site LR-06 – Cross Section - Looking upstream (lt); Looking downstream (rt). .....	324
Figure F.6.2: FGM Site LR-06 – Cross Section - Left Bank (lt) – Right bank (rt). .....	324
Figure F.6.3: FGM Site LR-06 – Bank 1 - Bank (lt) – Looking upstream (rt). .....	324
Figure F.6.4: FGM Site LR-06 – Bank 1-Facing downstream (lt); Bank 2-Bank (rt). .....	325
Figure F.6.5: FGM Site LR-06–Bank 2-Facing upstream (lt);Facing downstream (rt). .....	325
Figure F.6.6: FGM Site LR-06 – Bank 3 - Bank (lt); Facing upstream (rt). .....	325
Figure F.6.7: FGM Site LR-06 – Bank 3–Facing downstream (lt); Bank 4-Bank (rt). .....	326
Figure F.6.8: FGM Site LR-06-Bank 4–Facing upstream (lt);Facing downstream (rt). .....	326
Figure F.7.1: FGM Site LR-07 – Cross Section - Looking upstream (lt); Looking downstream (rt). .....	327
Figure F.7.2: FGM Site LR-07 – Cross Section - Left Bank (lt) – Right bank (rt). .....	327
Figure F.7.3: FGM Site LR-07 – Bank 1 - Bank (lt) – Looking upstream (rt). .....	327
Figure F.7.4: FGM Site LR-07 – Bank 1-Facing downstream (lt); Bank 2-Bank (rt). .....	328
Figure F.7.5: FGM Site LR-07–Bank 2-Facing upstream (lt);Facing downstream (rt). .....	328
Figure F.7.6: FGM Site LR-07 – Bank 3 - Bank (lt); Facing upstream (rt). .....	328
Figure F.7.7: FGM Site LR-07 – Bank 3–Facing downstream (lt); Bank 4-Bank (rt). .....	329
Figure F.7.8: FGM Site LR-07-Bank 4–Facing upstream. ....	329
Figure F.8.1: FGM Site LR-08 – Cross Section - Looking upstream (lt); Looking downstream (rt). .....	330
Figure F.8.2: FGM Site LR-08 – Cross Section - Left Bank (lt) – Right bank (rt). .....	330
Figure F.8.3: FGM Site LR-08 – Bank 1 - Bank (lt) – Looking upstream (rt). .....	330
Figure F.8.4: FGM Site LR-08 – Bank 1-Facing downstream (lt); Bank 2-Bank (rt). .....	331
Figure F.8.5: FGM Site LR-08–Bank 2-Facing upstream (lt);Facing downstream (rt). .....	331
Figure F.8.6: FGM Site LR-08 – Bank 3 - Bank (lt); Facing upstream (rt). .....	331
Figure F.8.7: FGM Site LR-08 – Bank 3–Facing downstream (lt); Bank 4-Bank (rt). .....	332

Figure F.8.8: FGM Site LR-08-Bank 4–Facing upstream (lt);Facing downstream (rt).	332
.....	
Figure F.8.9: FGM Site LR-08 – Debris jam (lt); Large Oak tree (rt).	332
Figure F.9.1: FGM Site LR-09 – Cross Section - Looking upstream (lt); Looking downstream (rt).	333
Figure F.9.2: FGM Site LR-09 – Cross Section - Left Bank (lt) – Right bank (rt).	333
Figure F.9.3: FGM Site LR-09 – Bank 1 - Bank (lt) – Looking upstream (rt).	333
Figure F.9.4: FGM Site LR-09 – Bank 1-Facing downstream (lt); Bank 2-Bank (rt).	334
Figure F.9.5: FGM Site LR-09–Bank 2-Facing upstream (lt);Facing downstream (rt).	334
.....	
Figure F.9.6: FGM Site LR-09 – Bank 3 - Bank (lt); Facing upstream (rt).	334
Figure F.9.7: FGM Site LR-09 – Bank 3–Facing downstream (lt); Bank 4-Bank (rt).	335
Figure F.9.8: FGM Site LR-09-Bank 4–Facing upstream (lt);Facing downstream (rt).	335
.....	
Figure F.10.1: FGM Site NF-01 – Cross Section - Looking upstream (lt); Looking downstream (rt).	336
Figure F.10.2: FGM Site NF-01 – Cross Section - Left Bank (lt) – Right bank (rt).	336
Figure F.11.1: FGM Site NF-02 – Cross Section - Looking upstream (lt); Looking downstream (rt).	337
Figure F.11.2: FGM Site NF-02 – Cross Section - Left Bank (lt) – Right bank (rt).	337
Figure F.11.3: FGM Site NF-02 – Bank 1 - Bank (lt) – Looking upstream (rt).	337
Figure F.11.4: FGM Site NF-02 – Bank 1 - Looking downstream (rt).	338
Figure F.12.1: FGM Site NF-03 – Cross Section - Looking upstream (lt); Looking downstream (rt).	339
Figure F.12.2: FGM Site NF-03 – Cross Section - Left Bank (lt) – Right bank (rt).	339
Figure F.13.1: FGM Site NF-04 – Cross Section - Looking upstream (lt); Looking downstream (rt).	340
Figure F.13.2: FGM Site NF-04 – Cross Section - Left Bank (lt) – Right bank (rt).	340
Figure F.14.1: FGM Site EC-01 – Cross Section - Looking upstream (lt); Looking downstream (rt).	341
Figure F.14.2: FGM Site EC-01 – Cross Section - Left Bank (lt) – Right bank (rt).	341
Figure F.15.1: FGM Site EC-02 – Cross Section - Looking upstream (lt); Looking downstream (rt).	342
Figure F.15.2: FGM Site EC-02 – Cross Section - Left Bank (lt) – Right bank (rt).	342
Figure F.16.1: FGM Site EC-03 – Cross Section - Looking upstream (lt); Looking downstream (rt).	343
Figure F.16.2: FGM Site EC-03 – Cross Section - Left Bank (lt) – Right bank (rt).	343
Figure F.17.1: FGM Site RC-01 – Cross Section - Looking upstream (lt); Looking downstream (rt).	344
Figure F.17.2: FGM Site RC-01 – Cross Section - Left Bank (lt) – Right bank (rt).	344
Figure F.18.1: FGM Site RC-02 – Cross Section - Looking upstream (lt); Looking downstream (rt).	345
Figure F.18.2: FGM Site RC-02 – Cross Section - Left Bank (lt) – Right bank (rt).	345
Figure F.19.1: FGM Site RC-04 – Cross Section - Looking upstream (lt); Looking downstream (rt).	346
Figure F.19.2: FGM Site RC-04 – Cross Section - Left Bank (lt) – Right bank (rt).	346

Figure F.20.1: FGM Site DBC-01 – Cross Section - Looking upstream (lt); Looking downstream (rt). .....	347
Figure F.20.2: FGM Site DBC-01 – Cross Section - Left Bank (lt) – Right bank (rt). .....	347
Figure F.21.1: FGM Site DBC-02 – Cross Section - Looking upstream (lt); Looking downstream (rt). .....	348
Figure F.21.2: FGM Site DBC-02 – Cross Section - Left Bank (lt) – Right bank (rt). .....	348
Figure F.22.1: FGM Site DBC-03 – Cross Section - Looking upstream (lt); Looking downstream (rt). .....	349
Figure F.22.2: FGM Site DBC-03 – Cross Section - Left Bank (lt) – Right bank (rt). .....	349
Figure F.23.1: FGM Site DBC-04 – Cross Section - Looking upstream (lt); Looking downstream (rt). .....	350
Figure F.23.2: FGM Site DBC-04 – Cross Section - Left Bank (lt) – Right bank (rt). .....	350
Figure F.24.1: FGM Site HC-01 – Cross Section - Looking upstream (lt); Looking downstream (rt). .....	351
Figure F.24.2: FGM Site HC-01 – Cross Section - Left Bank (lt) – Right bank (rt). ..	351
Figure F.25.1: FGM Site HC-02 – Cross Section - Looking upstream (lt); Looking downstream (rt). .....	352
Figure F.25.2: FGM Site HC-02 – Cross Section - Left Bank (lt) – Right bank (rt). ..	352

## **ABSTRACT**

As human population continues to rise, an ever increasing burden is being placed on earth's water resources. Between 1950 and 2010, the world's population increased from 2.6 billion to almost 7 billion, and the population of the United States increased from 150 million to 310 million, while available water resources have remained constant. The 2050 worldwide population is projected at over 9 billion and the population of the United States is projected at 400 million. The increasing demand, and the uncertainty of the impacts that climate change will have on available water resources, make it increasingly important that society more effectively manage our water resources in a sustainable fashion.

One of the many issues that must be addressed is sedimentation of reservoirs. The World Commission on Dams reports that "25% of the world's existing fresh water storage capacity may be lost in the next 25 to 50 years in the absence of measures to control sedimentation." In 2010, the Oklahoma Water Research Advisory Board (OWRAB) identified development of methods for estimating sediment yield in reservoirs as a "higher priority research topic", and others stress the need for further research on streambank and gully erosion as part of managing reservoir sedimentation.

This study initiated the process of assessing the suspended sediment transport occurring in the Little River and other tributaries to Lake Thunderbird, which is the primary source of drinking water for approximately 200,000 people residing in Norman, Midwest City, and Del City, in central Oklahoma, and provides numerous and valuable recreation benefits. The study documented the current hydrological and morphological



characteristics of the watershed and evaluated the use of an Acoustic Doppler Current Profiler (ADCP) for measuring sediment transport in small rivers.

Documentation of the hydrology within the watershed was accomplished using HOBO pressure transducers installed at seven locations, site surveys, and discharge measurements to generate discharge rating curves. Rating curves were used to estimate cumulative runoff for the watershed during the period of study, which occurred during a drought, and to assess the effects of antecedent conditions on runoff volume. The morphological characteristics of the watershed were documented by conducting fluvial geomorphological (FGM) surveys at 25 sites. Each of the sites was classified using Rosgen's classification system and Simon's Channel Evolution Model, and scored using various bank stability indices (BSIs). The channels at the sites were found to be predominantly type G5c channels, at Stage IV of the channel evolutionary process, and were mostly rated as unstable to highly unstable by all of the BSIs used in the study, although additional work is required to validate the individual BSI scores. The study provides a base-line for future studies on the hydrology and the changing morphology of the channels within the watershed, which are required to better understand the sedimentation of Lake Thunderbird.

The ADCP was evaluated by comparing sediment flux curves generated using a Teledyne RDI 600 kHz Workhorse Rio Grande ADCP, coupled with Aqua Vision's ViSea Plume Detection Toolbox (PDT) software, to curves generated using traditional grab, and depth-integrated suspended sediment sampling methods. Data from this study show no statistical difference between flux curves developed using grab samples, depth-integrated samples, or ADCP/PDT methods. Data were only obtained from two sites

however, and the number of samples was limited at one of them, so additional study is required to validate the use of ADCPs for estimating suspended sediment transport in small rivers.

## **I. Introduction**

As human populations continue to rise, an ever-increasing burden is being placed on earth's water resources. The worldwide population has increased from approximately 2.6 billion in 1950, to almost 7 billion in 2010. In the United States, the population has increased from approximately 150 million to almost 310 million over the same 60 year period (U.S. Census Bureau, 2015). Available water resources have remained constant, so that there are ever-increasing reports of water shortages. With the 2050 worldwide population projected at over 9 billion, and the population of the United States projected at 400 million, it is imperative that society more effectively manage its available water resources in a sustainable fashion.

During this time period, the world, including the United States, was meeting a considerable portion of their water demand by building dams in what has become known as "the golden age of dam building". The report by the World Commission on Dams (WCD), "Dams and Development: A New Framework for Decision Making" (2000) reports that in 1949 only "about 5,000 large dams [exceeding 50 feet (15 meters) in height] had been constructed worldwide," predominantly in industrialized countries. By the end of 2000, there were over 45,000 large dams in over 140 countries." China has led the way. In 1949 they had only 22 large dams. By 2000, that number had increased to 22,000.

According to the National Inventory of Dams (NID), maintained and published by the United States Army Corps of Engineers (USACE), in cooperation with the Association of State Dam Safety Officials (ASDSO), states and territories, and federal

dam-regulating agencies, there are currently more than 87,000 dams in the United States. Of these, 6,433 are considered large dams. Of course, not all dams are built to supply water for human consumption. In fact, only 9% of dams in the NID database were built primarily for water supply. More dams were built primarily for recreation (34%), flood control (16%), for stock use or fire protection (15%), or for irrigation (10%) than for water supply. Hydroelectric power generation is the primary purpose of just 3% of the dams in the NID inventory, but is the primary purpose for over 9% of large dams.

With the “golden age of dam building” of the second half of the twentieth century becoming further in the past, the average age of dams is rising. The average age of the dams in the NID data-base is 53 years. The average age of major dams in the United States is 43 years (USACE-NID, 2013). The U.S. Army Corps of Engineers owns 694 dams, 95 percent of which are more than 30 years old. More than half of them (52 percent) have reached or exceeded the 50-year service lives for which they were designed (USACE, 2013).

One of the primary factors limiting a dam’s service life is sedimentation of the reservoir. The WCD (2000) reports that, “An estimated 0.5–1% of the total fresh water storage capacity of existing dams is lost each year to sedimentation in both large and small reservoirs worldwide,” and that “25% of the world’s existing fresh water storage capacity may be lost in the next 25 to 50 years in the absence of measures to control sedimentation.”

The rate of storage capacity lost to sedimentation, however, varies greatly from dam to dam (Sabo et al., 2010). Qinghua and Wenhao (1989) reported that some

reservoirs on the main stream of the Yellow River, such as the Yanguoxia, the Qingtongxia, and the TianQiao Reservoirs, lost 50-87% of their storage capacities within 5-7 years of impoundment. In the United States, Graf et al., (2010) used data from the Reservoir Sedimentation Survey Information System II (RESIS II) to explore the sustainability of American reservoirs. They found that the reported sedimentation rates of reservoirs varies geographically across the United States, from less than 0.40% per year to more than 2% per year. Figure 1, taken from Graf et al. (2010), shows the annual percentage storage loss of reservoirs in the United States, mapped by Hydrologic Unit Code (HUC) 2, dividing the country into 21 hydrologic units.

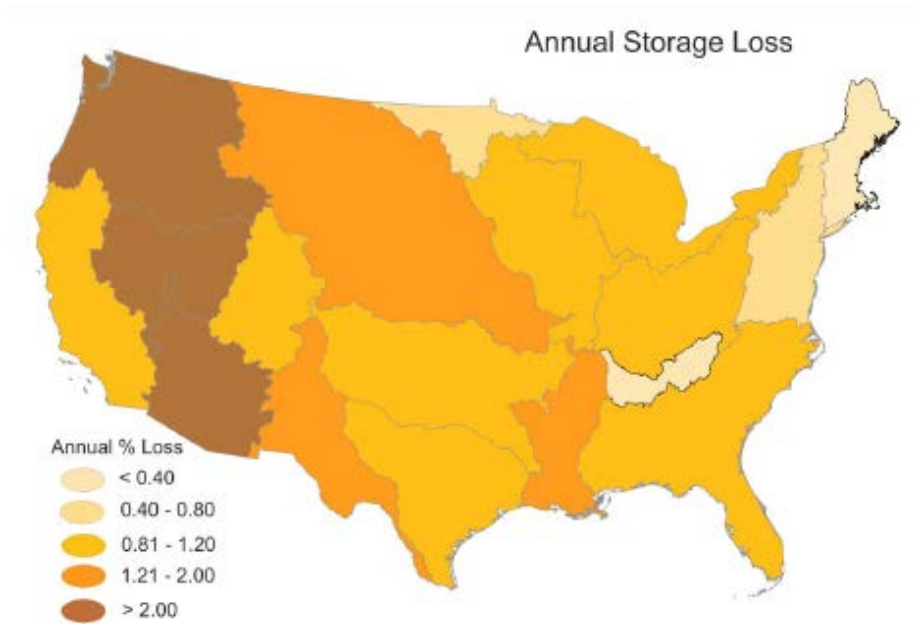


*Figure 1: Distribution of mean annual loss of reservoir capacity in the continental United States mapped by HUC-2 units (water resource regions broadly defined by large river basins). (Graf et al., 2010)*

This variability in sedimentation rates is also evident in Oklahoma reservoirs. Data obtained from the Oklahoma Water Atlas (OWRB, 2007) and the 2004 Beneficial Use Monitoring Program (BUMP) Lakes Report (OWRB, 2005) were used to estimate loss of pool capacity for several Oklahoma Reservoirs. Table 1 shows the storage capacity losses, total percent loss, and annual percent loss for all reservoirs for which bathymetry data are available. Annual capacity loss rates range from 0.09 to 0.95% per year, which is in line with the WDC report. With human populations ever increasing, there is a continuously increasing demand for fresh water. Any loss of storage as a result of sedimentation is a concern to society and water management planners. It is therefore of little surprise that in 2010, the Oklahoma Water Research Advisory Board (OWRAB) identified development of methods for estimating sediment yield in reservoirs as a “higher priority research topic.”

*Table 1: Reservoir capacity loss due to sedimentation. (Sources: Oklahoma Water Atlas 2007; OWRB Beneficial Use Monitoring Program Lakes Report, Lakes Sampling 2004-2005, 2005)*

Lake	Date Built	Capacity (Acre-ft)	Survey Date	Capacity (Acre-ft)	% Loss	% Loss/yr
Atoka	1964	125000	2000	105195	15.8%	0.44%
Eucha	1952	79600	2000	74237	6.7%	0.14%
Hefner	1947	75000	1998	68868	8.2%	0.16%
Hugo Lake	1974	157600	1999	126741	19.6%	0.78%
McGee Creek	1987	113930	2000	100146	12.1%	0.93%
Overholser	1919	15000	1999	13913	7.2%	0.09%
Sardis	1982	274330	1999	230053	16.1%	0.95%
Spavinaw	1924	38000	2000	25725	32.3%	0.43%
Stanley Draper	1962	100000	1999	87296	12.7%	0.34%
Texoma*	1942		1985		11.0%	0.26%
Thunderbird	1965	119600	2001	105644	11.7%	0.32%
Wister	1949	62360	2001	47414	24.0%	0.46%

\* Texoma data obtained from Gido et al (2000)

Reservoir capacity loss is not the only effect that sediment has on water bodies. It also impacts water quality. Sediment is the second highest cause (behind pathogens) of impairment to rivers and streams assessed and reported by the States to EPA under Section 305(b) and 303(d) of the Clean Water Act (FWPCA, 2009). Over 125,000 miles of streams are reported to be threatened or impaired due to sediment (U.S. EPA, 2013). Not only that, but many nutrients, the third highest cause of impairment, and other contaminants, such as metals, the sixth highest cause of impairment, are transported bound to sediment particles.

Sedimentation and turbidity can also negatively affect aquatic organisms. Excess sediment and turbidity degrades habitat and reduces productivity in stream systems. This in turn causes a depletion of food availability for zooplankton, insects, fresh water mussels and fish, and can result in stunted growth, reduced reproduction rates, and mortality (Ryan et al., 2006).

Even though sedimentation is depleting water supply reservoir capacity, degrading water quality and negatively impacting aquatic life, it remains one of the more poorly quantified water quality parameters. This is primarily due to the difficulty in obtaining accurate estimates of sediment transport.

New technologies for measuring suspended-sediment transport include acoustic backscatter, digital-image analysis, Laser In Situ Scattering and Transmissometry (LISST) laser diffraction, optical sediment flux, and pressure differential and bulk optics (Kuhnle and Wren, 2006). Only the LISST series of laser diffraction instruments (Sequoia Scientific, Inc., 2009), acoustic backscatter meters (single frequency acoustic Doppler current profilers from RD Instruments USA (2009), Sontek/YSI, Inc. (2009),

and Nortek AS (2009)), multi-frequency manufactured by Aquatec (2009)), and several types of bulk-optic meters (optical backscatter, nephelometry, and transmission devices), are available commercially.

Measuring bed load sediment transport in rivers is considerably more difficult than measuring suspended sediment and therefore it is not conducted as often as suspended sediment measurements. Bed load measurement techniques can be categorized as instream installations, portable/physical devices, and surrogate technologies (Gray et al., 2010).

Instream installation methods include Birkbeck samplers, vortex samplers, pit traps, net frame samplers and sediment detention basins. Portable measuring devices include pressure-difference samplers (such as the U.S. BL-84, Helley-Smith, Toutle River, and Elwha River bed load samplers), bed load traps, and instream baskets, tracer particles, scour chains and bed load collectors. Although these devices are the mainstays in measuring bed load and have provided useful data in a variety of settings, they all have deficiencies that restrict their use and prevent widespread use as the standard method for monitoring bed load. Surrogate technologies being explored include Acoustic Doppler Current Profilers (ADCPs), hydrophones, gravel impact sensors, magnetic tracers, magnetic sensors, topographic differencing, sonar-measured debris basins and underwater video cameras (Ryan et al., 2006, Gray et al., 2010).

ADCPs show the most promise in the immediate future. Rennie et al. (2002) explored exploiting the bottom tracking capability of a commercially available ADCP for measurement of bed-load velocity with the goal of developing a non-invasive technique for gauging bed-load transport. Bottom tracking is used to determine the



speed of a boat taking ADCP measurements and involves measuring the Doppler shift in the frequency of an independent echo-sounding off of the bed. If the bed is mobile, then bottom tracking is biased by the sediment motion, and the frequency shift is from both the boat speed and the sediment movement so that a stationary boat in the stream would appear to be moving upstream. The USGS “Quality-Assurance Plan for Discharge Measurements Using Acoustic Doppler Current Profilers” (Oberg et al., 2005) presents two acceptable methods for performing a moving-bed test. One requires that the “ADCP be held in a stationary position while recording ADCP data for 10 minutes, using bottom tracking as the boat-velocity reference.” If the bed is moving the ADCP will appear to have moved upstream. The other method, “the loop test”, is performed by moving the ADCP from a starting point on one bank of the stream, to the other bank and back to the same point. If the bed load is moving, the point will appear to have returned to a point upstream of the initial point. The positional errors observed in the moving-bed tests are used to correct ADCP velocity measurements, and theoretically could allow the ADCP to indirectly measure bed load.

The United States Geological Survey is routinely using ADCPs for measuring stream velocity and flow throughout the United States, and has recently released guidance on the use of ADCPs for measuring stream discharge (Mueller and Wagner, 2009). Similar protocols had previously been developed by the Water Survey of Canada (2004), and water agencies across the world are increasingly using ADCPs for measuring stream discharge in their countries.

Over the last decade, ADCPs have also been used to estimate suspended sediment concentrations in rivers (Filizola and Guyot, 2004; Kostaschuk et al., 2004;

Stephens, 2005; Wall et al., 2006) and estuaries (Kim and Voulgaris, 2003), and to quantify bedload transport (Rennie et al., 2002; Gaeuman and Jacobson, 2007). These methods show promise and warrant further attention.

The study presented here evaluated the use of ADCPs for measuring suspended sediment in small sand/silt-bed rivers in the Lake Thunderbird watershed in Central Oklahoma. Evaluation of the ADCP was conducted as part of a broader study to characterize the hydrology and morphology of the Little River and other tributaries within the watershed. The hydrological and morphological characterization of the watershed will provide the Central Oklahoma Master Conservancy District (COMCD), that operates and maintains the dam, lake, and raw water pumping and delivery system under contract with the U.S. Department of the Interior, Bureau of Reclamation (BOR), with additional data to assist with future planning. The study consisted of two parts; “Part 1: Hydrology and Morphology of the Little River Watershed in Central Oklahoma” and “Part 2: Evaluation of an Acoustic Doppler Current Profiler (ADCP) for use in Measuring Sediment Transport in the Lake Thunderbird Watershed in Central Oklahoma.”

## **II. Part 1: Hydrology and Fluvial Geomorphology (FGM) of the Lake Thunderbird Watershed in Central Oklahoma**

### **A. Lake Thunderbird Watershed**

The Little River originates in Cleveland County, in west Norman and Moore, Oklahoma and flows in an easterly direction for approximately 80 miles to its

confluence with the Canadian River, near Holdenville, in Hughes County. Figure 2 shows the Little River watershed and its location.

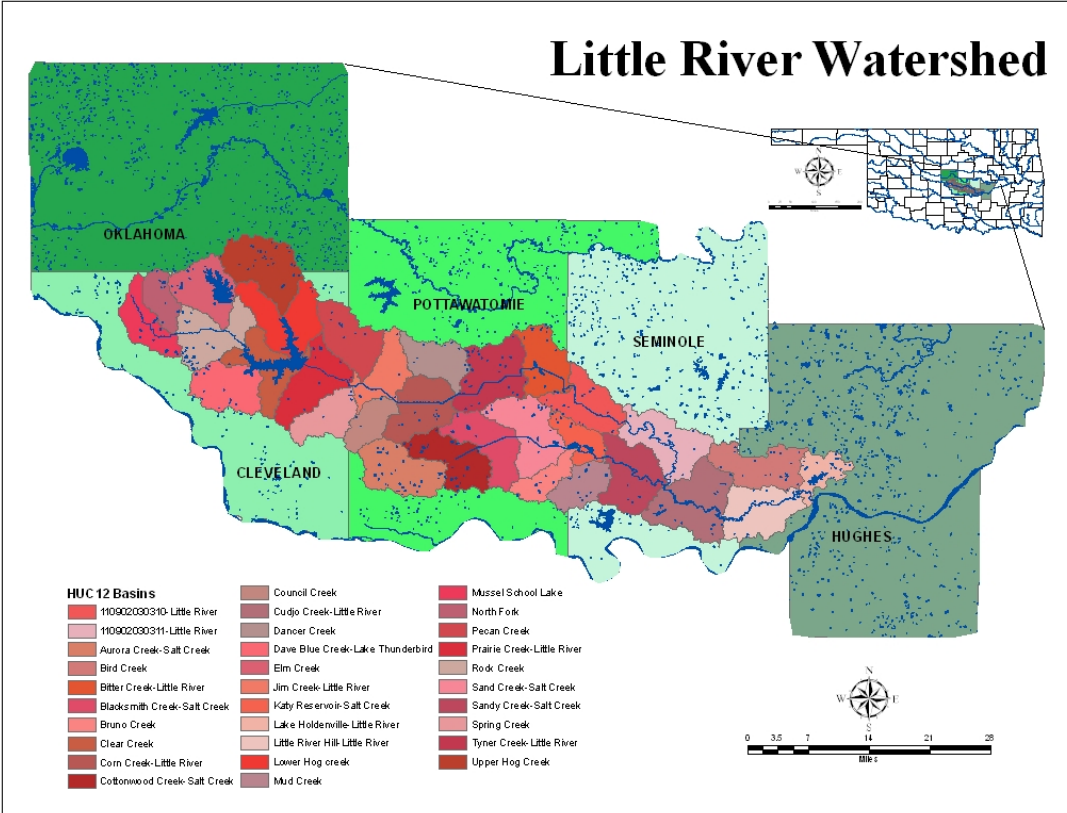
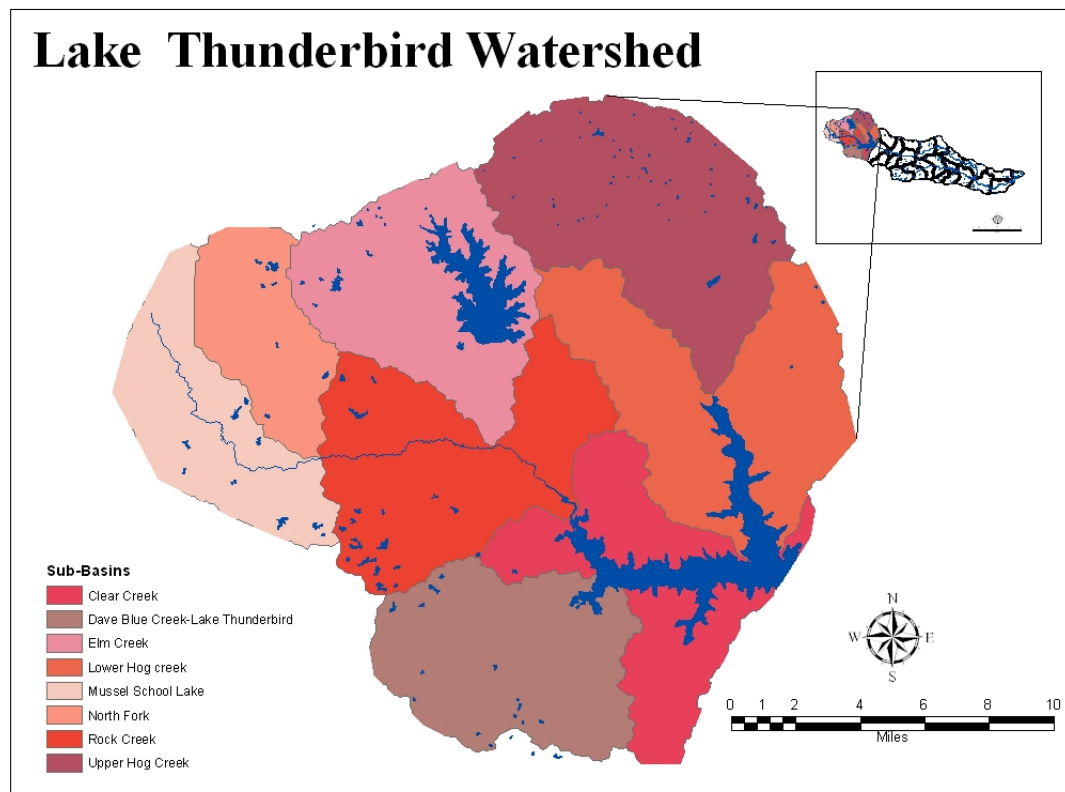


Figure 2: Little River Watershed.

In 1965, the Bureau of Reclamation (BOR) completed construction of Norman Dam at the confluence of Hog Creek and the Little River, to form Lake Thunderbird. The dam is located approximately 13 miles east of Norman, and 30 miles southeast of Oklahoma City and has a 257 square mile drainage basin or watershed. Figure 3 shows the Lake Thunderbird watershed and sub-watersheds.

Lake Thunderbird, which supplies water to the City of Norman, Midwest City, and Del City, is designated in the Oklahoma Water Quality Standards as a sensitive

public and private water supply (SWS) [OAC 785:45-5-25(c)(4)] with a nutrient limited watershed (NLW) [OAC 785:45-5-2(b)(20)]. Studies by the Oklahoma Water Resources Board (OWRB, 2005) indicate that the lake is “eutrophic, indicative of high levels of productivity and nutrient rich conditions” due to the fact that the average trophic state index (TSI), using Carlson's TSI (chlorophyll-a), was found to be 58.



*Figure 3: Lake Thunderbird Watershed.*

The Oklahoma Conservation Commission (OCC) used total phosphorous concentration as a surrogate to estimate the current chlorophyll-a concentration in the lake, finding it to average 30.8 µg/L, three times the State Water Quality Standard of 10 µg/L (Vieux & Associates, 2007). Chlorophyll-a concentrations in excess of 20 µg/L

result in hyper-eutrophic water conditions with excessive algae growth (OWRB, 2004). OWRB also determined that the turbidity was sufficiently high so that the Fish and Wildlife Propagation beneficial use was deemed to be only partially supported (OWRB, 2005). Data from 2006 indicates that Lake Thunderbird is impaired due to excessive turbidity and low dissolved oxygen.

In 2001, OWRB conducted a bathymetric study of Lake Thunderbird and determined that the pool capacity of the lake had been reduced from 119,600 acre-feet in 1966 to 105,838 acre-feet in 2001 for a loss of capacity of 13,762 acre-feet, or 11.5% in 35 years (OWRB, 2002). This amounts to a loss rate of 393 acre-feet/year, which is only slightly higher than the 350 acre-feet/year reportedly estimated by BOR in correspondence to OWRB back in 1965 (Flaigg, 1959). Most of the sedimentation has reportedly “occurred in the shallower to medium-depth parts of the lake,” which is attributed, without support, to “larger grained sediment washed in from the watershed” (OWRB, 2002).

In 2011, a bathymetric study was conducted of the lower Little River arm of Lake Thunderbird, north of the Alameda Bridge (Henson, 2011). Comparing the results of that survey with the OWRB survey conducted in 2001, he found “an average loss of capacity of 1.88 ac-ft per year (0.20% loss per year) between 2001 and 2011 within the Study Area.” This is slightly less than the 0.33% loss per year reported by OWRB in 2001, which could indicate that the sedimentation rate has slowed over the last decade, but is more likely due to the sediment being delivered to the lake from Little River passing through the study area into the remaining un-surveyed portion of the lake.

The OCC study addressed sediment loading to the lake, modeling it as a function of imperviousness, but did not directly measure it. To date, there has never been a comprehensive study of the sediment transport characteristics of the Little River or its tributaries and the morphological processes that both drive them and are driven by them. However, there is evidence, upon cursory examination, that the Little River is highly unstable and undergoing an evolutionary process of morphological change, in response to increasing urbanization and “channel improvements” made in the past. This instability is resulting in increased stream bank and bed erosion and is potentially a significant source of sediment loading to the lake, a source of sediment that is not accounted for in the OCC study.

In September 2007 a reconnaissance of the Little River was conducted following a fairly significant storm event. The reconnaissance revealed clear indications of significant channel incision and widening, including exposed bridge abutments, exposed high pressure gas lines (Fig 4a), slumping banks, exposed tree roots, fallen trees and tributary head cuts (Fig 4b). The importance of this cannot be overstated as the ramifications to infrastructure, lost property, and increasing sedimentation rates to the lake are potentially substantial.

Lane (1955) described that the morphology of a channel is the result of several factors, including the sediment load and size transported through the channel, the discharge in the channel and the slope of the channel. The size and load of sediment transported through a channel is balanced by the stream slope and discharge. If the balance is altered, the channel morphology adjusts to accommodate the change.

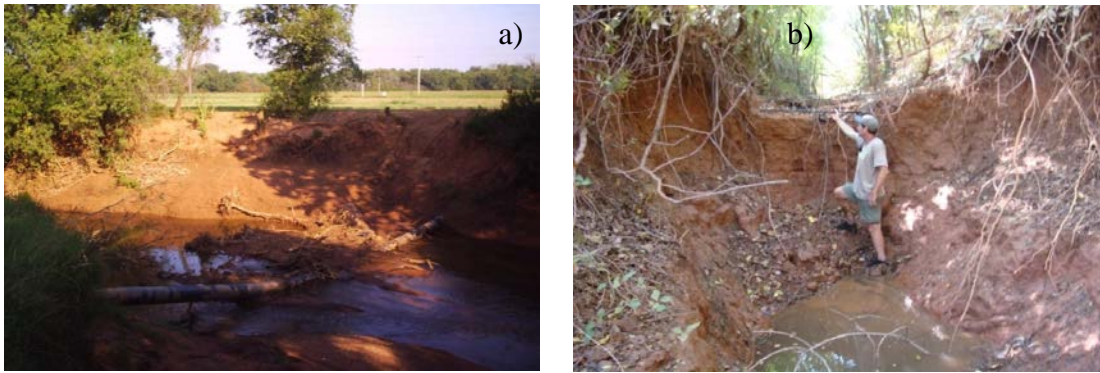


*Figure 4: Indications of the Little River channel incision and widening including a) exposed high pressure gas lines and b) tributary head cuts.*

Schumm et al. (1984), and later Simon (Simon, 1989, 1994) developed a process-based classification scheme that describes a natural channel's adaptation to straightening. As shown in Figure 5, the Channel Evolution Model, describes a complete “cycle” of bank-slope development from the pre-modified conditions through stages of adjustment to the eventual reestablishment of stable bank conditions. The Little River channel bed, in the reach reconnoitered in the vicinity of 12th Avenue NE, appears to have just entered Stage IV of the evolutionary cycle, the degradation and widening phase, and appears to have incised at least 6-8 feet at the time.

To fully understand the significance of this process, consider Wildhorse Creek, near Hoover, in Garvin County, Oklahoma. Between 1922 and 1933 the channel was “improved” over a length of 20 miles by constructing a straight 10 feet deep trapezoidal channel with a top width of 25 feet and 2:1 side slopes, as seen in Figure 6 (Barclay, 1980). In 1999, Dutnell (2000) found the channel to be 193 feet wide and approximately 25 feet deep. The channel has thus incised approximately 15 feet and experienced a 20-fold increase in area (Figure 6b). As a result, almost 50 million cubic yards of sediment has eroded and been transported to Lake Texoma since the “channel improvements”

were completed. Wildhorse Creek appeared to be at Stage V (see Figure 5), the aggradation and widening phase, in 1999, as there was evidence of deposition on inside bends and point bars were beginning to form.

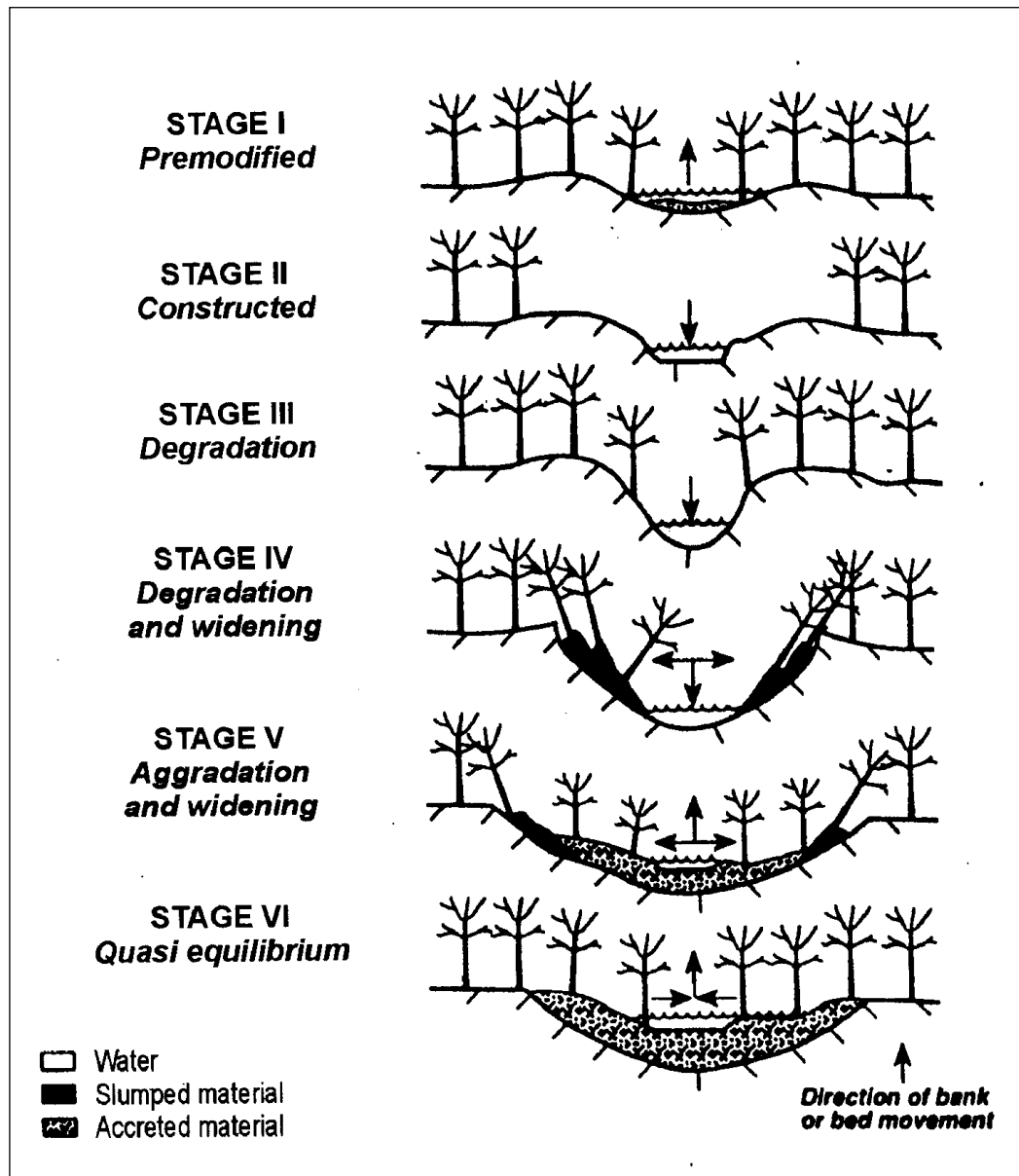


Figure 5: Channel Evolution Model – The Little River is currently at Stage IV, the degradation and widening stage. (Simon (1989))



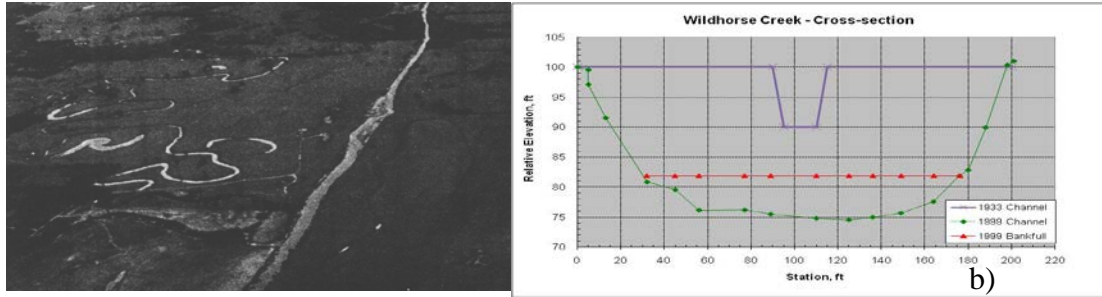


Figure 6: a) Channelized versus natural meandering Wildhorse Creek channel, in Garvin County, Oklahoma (Barclay, 1980); b) Comparison of Wildhorse Creek channel dimensions in 1933. (blue line - Barclay, 1980) and 1999 (green line - Dutnell, 2000)

The Little River may, or may not experience the same level of degradation and widening as Wildhorse Creek, but the process is certainly ongoing and the degradation and widening occurring in the Little River channel already appears to be significant. It should be noted that the Little River and Wildhorse Creek are not the only streams in Oklahoma that are undergoing this process of change. A large number of the creeks and rivers in the central and western portions of the State have been observed by the author to be undergoing the exact process described here. They have been straightened or are receiving more flow due to urbanization and thus they are incising and widening. The proposed project will implement a methodology in the Lake Thunderbird watershed that may be used for assessing and documenting this channel evolution process in all of the State's streams.

## B. Objective

The primary objective of Part 1 of the study was to investigate and document the current hydrological and morphological characteristics of the Lake Thunderbird

watershed. The data collected to accomplish this objective also provide baseline information that will be beneficial for future research in the watershed.

## C. Methodology

### 1. Hydrology

The hydrological investigation portion of this study was conducted by establishing seven discharge monitoring sites on the main tributaries of Lake Thunderbird. The sites, listed in Table 2, include two sites on the Little River, and one site each on the North Fork, Elm Creek, Hog Creek, Rock Creek and Dave Blue Creek. The table also shows the geographic location and the drainage area for the sites. An aerial photograph showing the locations of the hydrological study sites is provided in Figure 7.

*Table 2: Lake Thunderbird watershed hydrological study sites.*

Site	Geographic Location		Drainage Area	
	Latitude	Longitude	mi <sup>2</sup>	KM <sup>2</sup>
Little River @ 60th Ave NE	35°16'41"	97°21'10"	55.4	143.5
Little River @ Porter Ave	35°16'08"	97°26'28"	20.3	52.6
Hog Creek @ SE 119th	35°20'54"	97°15'29"	35.7	92.5
Rock Creek @ 72nd Ave NE	35°15'41"	97°20'08"	11.4	29.6
Elm Creek @ Indian Hills (179th SE)	35°17'27"	97°20'55"	20.9	54.2
North Fork @ Franklin	35°16'34"	97°25'48"	16.5	42.7
Dave Blue Creek @ 72nd Ave SE	35°11'42"	97°20'08"	13.2	34.3

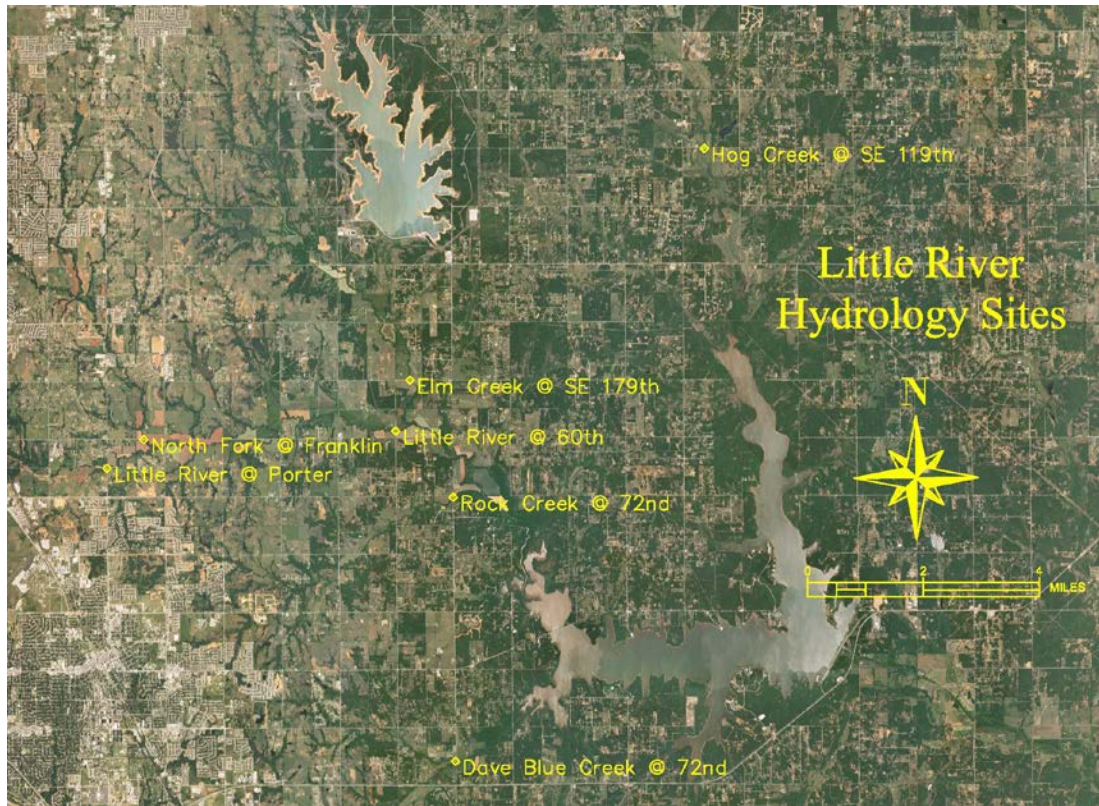


*Figure 7: Location of the Lake Thunderbird watershed hydrological study sites.*

At each of the hydrology sites, reference markers in the form of 18” long x ¾” rebar pins, with plastic caps, were placed on either side of the channel. Cross-section surveys were conducted between the markers using a total station, and the position and elevation of the markers were determined, with respect to the Oklahoma State Plane-South (NAD83) and North American Vertical Datum of 1983 (NAVD83), respectively, using either traditional survey methods or GPS. All surveying was conducted using U.S. surveying units (feet).

HOBO U20 Water Level Data Loggers were installed at each of the sites and were set to measure temperature (°F) and pressure (psi) every 30 minutes. The HOBOS,

with reported accuracies of  $\pm 0.03$  psi, were each protected with a PVC housing, as shown in Figure 8.



*Figure 8: HOBOTM water level logger with PVC housing.*

Installing the HOBOTMs and their housings in the channel was accomplished in various ways, depending on the site. The primary concern in installing them was insuring that they would be submerged at all flows, while protecting them from being washed out in large storm events. A secondary concern was vandalism. Where feasible, either a T-post or a 4 foot long piece of rebar was hammered into the bed, and the PVC housings were then attached to them, at as low a depth as practical, using plastic zip ties. At the Hog Creek and Little River at 60<sup>th</sup> Ave NE sites, the PVC housing was attached to staff gauges maintained by the OCC. At the North Fork site, the HOBOTM and housing were suspended underneath a rock from a cable wrapped around the rock and secured with c-clamps.

After installation, the elevations of the HOBOS were surveyed relative to the site reference markers on the left side of the channel. Figure 9 shows the HOBOS installation at the Hog Creek site. Photographs of the HOBOS installations at all of the sites are provided in the monitoring site summaries in Appendix A.



*Figure 9: HOBOS installed to staff gauge at Hog Creek study site.*

An additional HOBOS logger was installed in the shade at a convenient location and was used to measure the ambient temperature ( $^{\circ}\text{F}$ ) and pressure (psi) at the same 30 minute intervals as the HOBOS installed at the monitoring sites. Data from the HOBOS pressure transducers were downloaded to a laptop computer on an interval ranging from 30 to 60 days. A typical download event, including driving time, walking to and from the HOBOS, removing them from their housings, downloading the data, and replacing them took between two and three hours.

A spreadsheet was made using Excel and the Date-Time, temperature (in °F), and pressure (in psi) data were added to the spreadsheet after each download. Data from each station, including the ambient station, were placed on separate worksheets.

Columns on the “Ambient” worksheet include the Date-Time, temperature (in °F), pressure (in psi), pressure (in N/m<sup>2</sup>), and temperature (in °C). Columns on the monitoring station site worksheets include the Date-Time, temperature (in °F), total pressure (in psi and N/m<sup>2</sup>), temperature (in °C), water density (in kg/m<sup>3</sup>), the ambient pressure (in psi and Pa), the hydrostatic pressure ( $\Delta P$  in Pa), the depth (in m and ft), the staff gauge reading where applicable (in feet), the water surface elevation above MSL (in ft), the discharge (in cfs), the time increment discharge volume (in Mgal), and the cumulative annual volume.

The ambient pressure on the monitoring station site worksheets is copied from the “Ambient” worksheet. The water density ( $\rho$ ) is calculated using the relationship developed by McCutchen et al (1993) that relates the water density as a function of water temperature only, for non-saline water:

$$\rho = 1000 \left[ 1 - \frac{T+288.9414}{508929.2*(T+6812963)*(T-3.9863)^2} \right] \quad (1)$$

$\rho$  = Water density (kg/m<sup>3</sup>)

$T$  = Temperature (°C)

The hydrostatic pressure ( $P$ ) is determined by subtracting the ambient pressure from the total pressure. The depth is determined using the fact that the hydrostatic pressure is a function of depth, as given by:

$$P = \rho g H. \quad (2)$$

with,

$P$  = Hydrostatic pressure (Pa)

$\rho$  = Water density ( $\text{kg/m}^3$ )

$g$  = Acceleration due to gravity ( $9.8 \text{ m/s}^2$ )

$H$  = Depth (m)

Estimating the discharge required the development of rating curves for each site. To accomplish this, multiple discharge measurements were taken at each site over a range of flows. Low flow measurements were conducted using traditional wading methods and a Marsh McBirney Flo-Mate Model 2000 flow meter.

Traditional wading methods are described by Harrelson et al. (1994), and in more detail by the U.S. Geological Survey (1977), and, briefly, involve measuring the velocity at equally spaced intervals across the channel using a velocity meter attached to a calibrated wading rod. Initially, so called “pygmy meters”, requiring the operator to wear head phones and “count clicks” over a specified time, were used to measure velocity. The clicks represented the number of revolutions of a little cup fitted propeller, which was then converted to obtain the water velocity. Later, the audible signal was replaced by an electrical one that allowed the operator to directly read the revolutions per minute, but the water velocity still had to be calculated at a later time.

The Marsh McBirney Flo-Mate used in this study measures velocity using Faraday’s law of induction. A sensor containing an electromagnetic coil and a pair of carbon electrodes is placed in the water, so that the sensor is pointing upstream. The electrodes measure the voltage generated by the water (a conductor) passing by the

magnetic field generated by the coil. This voltage, which is proportional to the velocity of the water, is processed by the meter and the water velocity is directly displayed, so that no post processing is required. The accuracy of the Flo-Mate is reported to be  $\pm 2\%$  of reading + zero stability ( $\pm 0.05$  ft/sec), and the instrument range is -0.5 to +19.99 ft/sec.

Figure 10 shows flow measurements being taken at the Little River at 60th Ave NW site using a Marsh McBirney flow meter. For each measurement, a measuring tape was first stretched across the channel, and the station (in feet) of the water surface edge on each side was recorded in a spreadsheet on a hand held computer. The spreadsheet was designed to divide the channel into 20 segments, and thus displayed the stations where the velocity measurements were taken. All measurements were taken using a calibrated wading rod, calibrated for English units, so that the magnetic sensor was suspended at two-thirds depth, the location of the average velocity for depths of 3 feet or less. At each station, the depth (feet) was measured, and recorded in the spreadsheet, and the wading rod was set to the proper height. Once the rod was stationary, the velocity measurement was taken (in ft/sec), using the averaging function set at 30 seconds, and recorded in the spreadsheet.

The advantages of using the spreadsheet on a hand held computer included quick and easy identification of the 20 evenly spaced measuring stations, rapid entry of data, and the fact that the discharge was known as soon as the last velocity measurement was recorded. The only disadvantage was the risk of dunking the computer in the water when doing a measurement solo, as it had to be carefully balanced on top of the Marsh McBirney. This disadvantage may easily be eliminated by using two people to take



discharge measurements, so that the advantages of using a hand held computer easily outweigh the disadvantages.



*Figure 10: Discharge measurement using Marsh McBirney flow meter at the Little River at 60<sup>th</sup> site.*

Where possible, high flow measurements were conducted using a Teledyne RDI 600kHz Workhorse Rio Grande Acoustic Doppler Current Profiler (ADCP) mounted on a trimaran Riverboat from Ocean Science. The Riverboat was outfitted with Hydrolink ML2 radios and GPS-ready wiring for a GPS-RTK system provided by Hemisphere.

The use of ADCP technology for water resource applications is relatively new. Using them for measuring sediment transport is even newer. When this study was

initiated, there were only two manufacturers producing ADCPs: Sontek and Teledyne RDI. Each company offers, and continues to offer, several models of ADCPs, although, at the time, only a couple of them were suitable for use in the current study, the RiverSurveyor made by Sontek and the Rio Grande made by Teledyne RDI.

When the decision was being made on what system to purchase for the study, the RiverSurveyor was listed at \$24,700 and the Rio Grande was listed at \$35,900. However, the RiverSurveyor is a Narrow Band (NB) system and the Rio Grande is a Broad Band (BB) system. Although either one would be suitable for discharge measurement, Broad Band systems are preferred for sediment transport applications.

Another factor in determining what system to purchase was that a GPS-RTK system was desired for identifying the ADCP's position. Sontek's quote for the RiverSurveyor with the GPS option was \$43,650. Teledyne RDI's quote for the Rio Grande with a Hemisphere R130 GPS system was \$48,960. However, by purchasing the GPS system directly from Hemisphere, the University received a 35% reduction in price through Hemisphere's "Educational & Research Sponsorship Program," which lowered the cost of the Rio Grande system to \$44,255.

Spending the extra \$605 was more than justified by the fact that software was available from Aqua Vision, developed specifically for use with the Teledyne RDI Rio Grande ADCP, which uses the backscatter data collected by the ADCP to estimate sediment size and concentration in the water column. Because there was not, and still is not, any similar software available for the Sontek Narrow Band systems, selecting the Teledyne RDI Rio Grande saved countless hours of software code development.

Having decided on the Teledyne RDI Rio Grande, the next decision to be made was whether to purchase the 600kHz system, or the 1200 kHz system. The 1200kHz system can be operated at slightly shallower depths than the 600kHz system, but personnel with the Teledyne staff were concerned that the 1200 kHz system might not have the ability to penetrate the very turbid suspended sediment load expected at high flows, and recommended the 600 kHz system.

Procedures and guidance for conducting discharge measurements with the ADCP are provided in numerous Teledyne RDI publications, including, but not limited to, the “Workhorse Rio Grande ADCP User’s Guide” (Teledyne RDI, 2007a), the “Work Horse Rio Grande Acoustic Doppler Current Profiler Technical Manual” (Teledyne RDI, 2007b), and several “Application Notes” (Teledyne RDI, 1999a, 1999b, 2002a and 2002b). Guidance may also be found in publications distributed by the United States Geological Survey (USGS), with one in particular from Mueller and Wagner (2009) that provides techniques to be used for taking ADCP measurements from moving boats. An updated, Version 2.0 was released in December, 2013 (Mueller et al, 2013), although it was not used during the course of the current research, because it was not released until after the discharge data had already been collected.

Additional instruction on using ADCPs was obtained in a five-day course, “Measurement of Streamflow Using Acoustic Doppler Current Profilers”, conducted by the USGS Office of Surface Water (OSW) Hydroacoustics, in Houston, Texas, January 24-28, 2011. The course was extremely informative, providing hands on training in taking discharge measurements using ADCPs, and the knowledge obtained was

invaluable in the collection of the ADCP discharge data conducted in the research presented here.

Taking discharge measurements with the ADCP required first setting up the system. The mobile GPS station, two radios, and two batteries had to be carefully, and properly, arranged in the aft cavity of the trimaran. The various components were connected to provide communication and power to the trimaran. Next, the base station, including the base GPS station, GPS antenna, two radios, two antennas, and a battery had to be set up and connected to a laptop computer. Figure 11 shows all of the components except the mobile GPS station positioned in the trimaran (left) and the various components of the base station (right). A detailed step-by step procedure for setting up and operating the ADCP is provided in Appendix B. A condensed version of the procedure is presented below.

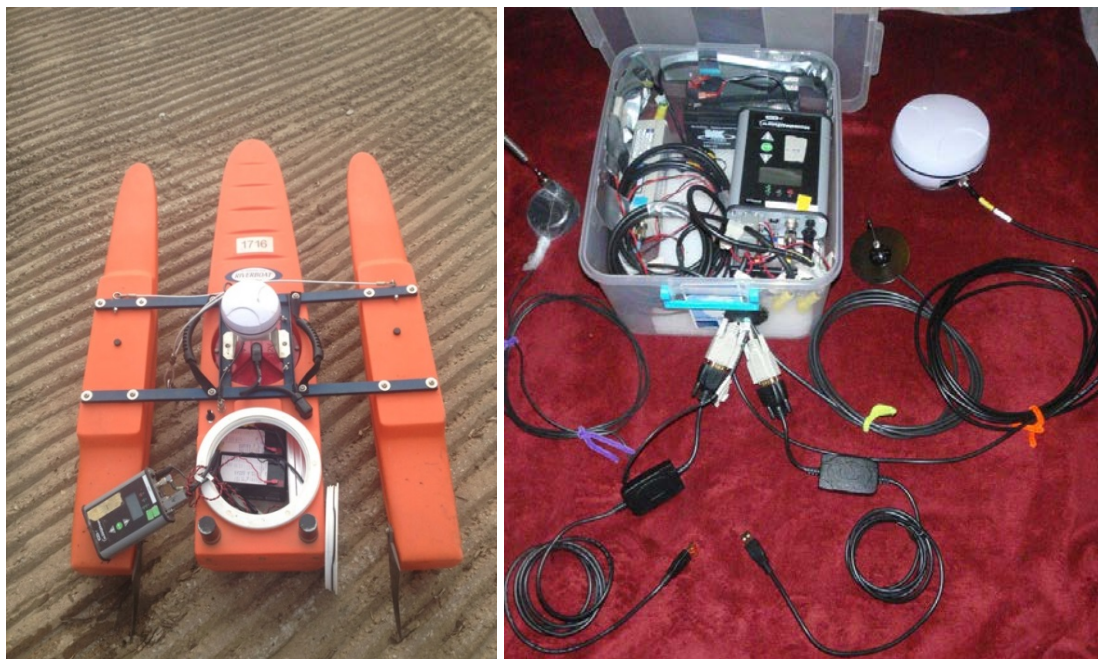


*Figure 11: ADCP measurement instrument setup. Left) Trimaran setup; Right) Base station setup.*

At this point, a new measurement was started in WinRiver II, Teledyne RDI's real-time data collection software that came with the ADCP, and the ADCP was configured for the site being measured. After it was confirmed that the ADCP was recognized and the GPS signal was being received, information specific to the conditions at the site, including the transducer depth (0.3 ft), the magnetic variation (4 in the study area), estimates of maximum water depth (ft), secondary (minimum) depth (ft), maximum water speed (ft/sec) and maximum boat speed (ft/sec), and the streambed material were entered in the program. Initial estimates of channel depths and velocities did not need to be accurate, as they could be modified later.

The next step was to calibrate the compass, which involved rotating the ADCP 360 degrees, at a constant rate, while keeping pitch and roll to a minimum. The calibration was performed with the trimaran as close to the measurement section as possible, typically on the bank, away from electro-magnetic objects.

With the compass calibration completed, the ADCP was started, which is easily detected by the tell-tale sonar "pinging" and the boat was lowered to the water. In some locations, putting the boat on the water is a simple process, but at the sites monitored in this study, it was somewhat difficult, as the trimaran had to be lowered on a rope over the side of a bridge down to the water, and then had to be raised back up after the measurements had been taken. This was done on two occasions using manual labor, at which point a "crane" was fashioned out of angle iron and a boat winch.

The ad-hoc crane was designed to be attached to the bridge railing using come-along straps. The crane made the task of raising and lowering the boat somewhat less strenuous, but the trimaran still had to be lifted over the bridge rail and lowered

carefully until the winch cable could take the weight. On more than one occasion this process resulted in the battery being disconnected, requiring restarting the entire setup procedure. That is why starting the ADCP before lowering it to the water is a good idea. It is an audible indicator of power problems.

Although the crane reduced the back strain involved in the process, it introduced another problem. Because there was no way to disconnect the cable from the trimaran after it was safely on the water, the cable had to be extended far enough so that the trimaran could freely traverse from bank to bank. This meant that there was slack in the cable throughout much of the traverse, especially in the middle of the channel. This slack was not a particular issue at the lower flows measured, although care had to be taken to prevent it from interfering with the motion of the trimaran. At higher flows, however, extra care had to be taken to control the cable and trimaran so as to avoid large debris and partially submerged trees moving down the channel.

With the trimaran safely on the water, one person slowly pulled the boat from side to side across the channel, while another person monitored the computer screen, and noted the water depths and velocities. It should be noted that at high flows, it is good to have a third person present to watch for on-coming trees and detritus. At this point the measurement was stopped, a new measurement was started, entering the observed depths and velocities on the startup screen, and a loop moving bed test was conducted. The trimaran was positioned as close to the left bank (facing downstream) as possible, maintaining sufficient depth for the ADCP to function, which is approximately 3 feet. The test was initiated, and the trimaran was pulled slowly, at a constant speed, to

the other side of the channel, again getting as close to the bank as possible without losing the ADCP signal, and then back to the initial starting point.

If the bed was not moving, the traverse plot would appear to return to the initial point, and bottom tracking, the preferred navigation reference because it minimizes the potential error sources, was used. If there was movement of the bed, the plot would show that the trimaran had returned to a point upstream of the start point, and the GPS position data were used for the navigation reference.

At this point the actual discharge measurements were taken. The boat was positioned near the left bank as before, recording was started, and the distance from the bank entered in the program. Measurements were collected over at least 10 so-called “ensembles.” The trimaran was then pulled slowly across the channel to the other bank location, where it was held steady for 10 ensembles or more, and the recording was stopped. The process was repeated going back and forth across the channel, with each pass being referred to as a “transect”. USGS guidance on the recommended number of transects that should be performed for an accurate measurement is evolving. The most recent guidance is based on time of measurement, rather than number of transects, but when the study was initiated, it was recommended that 10 transects be done for each measurement, so that was the target which was adhered to in this study, unless extenuating conditions dictated otherwise.

After the measurements were completed, the boat was pulled back up, and the system was disassembled sufficient for transport. Figure 12 shows the ADCP being used to collect discharge data at the Little River at 60<sup>th</sup> Ave NE site. Note the boat winch “crane” attached to the guard rail, and base station setup behind the researcher.



*Figure 12: Discharge measurement using Acoustic Doppler Current Profiler (ADCP) at the Little River at 60<sup>th</sup> site.*

The discharge measurements taken using both the Marsh McBirney and the ADCP, together with the HOBO data, allowed for the development of stage-discharge rating curves for three of the seven sites, including both Little River sites and the Rock Creek site. At the other four sites - Dave Blue Creek, Elm Creek, Hog Creek, and North Fork - discharge measurements were conducted at low and medium flows, but were not obtained at high flows, so it was not possible to develop full rating curves using measured data. In order to develop rating curves for these sites, it was necessary to use Manning's equation to estimate the stage-discharge relationships at high flows.



Manning's equation, an empirical equation for estimating the average velocity of a liquid flowing in an open channel, is given by:

$$V = \frac{1.49}{n} R_h^{2/3} S^{1/2} \quad (3)$$

where

$V$  = Cross-sectional average velocity (ft/sec)

$n$  = Manning's coefficient (sec/ft<sup>1/3</sup>)

$R_h$  = Hydraulic Radius =  $A/P$  (ft)

$A$  = Cross-sectional area (ft<sup>2</sup>)

$P$  = Wetted perimeter (ft)

$S$  = Slope

Since the discharge,  $Q = AV$ , Manning's equation may be used to estimate discharge (ft<sup>3</sup>/sec), if the channel cross-section dimensions and slope are known, and an appropriate value for Manning's coefficient is used. The channel cross-section dimensions and slope can be easily measured. Determining an appropriate Manning's "n" is not so straightforward in natural channels. Factors affecting Manning's "n" include the surface roughness, vegetation, channel irregularity, channel alignment, silting and scouring, obstruction, size and shape of the channel, and stage (or discharge).

Chow (1959) presents a method developed by Cowan (1956) for estimating "n" based on the channel material, degree of irregularity, variations of channel cross section, relative effect of obstructions, vegetation, and degree of meandering, and also

provides tables of “n” values for numerous channels, including natural channels. Barnes (1967) and Hicks and Mason (1991) provide pictures of numerous channels for which “n” is known, that may be used as a visual references for selecting “n” for a given channel. Rosgen (1996) used these sources to develop “n” based on stream type. Each of these methods provides a single estimate of “n” however, and do not account for variation of “n” with stage (or discharge). Strum (2001) presents curves for estimating “n” based on vegetative cover (or vegetal retardance class), hydraulic radius and slope that do account for variable stage. The curves, developed for grass-lined channels by Chen and Cotton (1998), differentiate channels based on the type and condition of grasses within the channel. These sources, combined with stream surveys and measured discharges, were used to evaluate and estimate Manning’s “n” for the sites.

The rating curves were used to estimate the cumulative runoff volumes for the sites during the study period, and the data for the Little River at 60<sup>th</sup> site were used to evaluate the effects of antecedent moisture conditions on runoff volume. This was accomplished by looking at the volume of runoff at the Little River at 60<sup>th</sup> site generated by various storm events, to see if preceding rainfall affected the amount of runoff. The lag time between rainfall and runoff at the Little River at 60<sup>th</sup> site was also evaluated using data from May, 2011.

## **2. Fluvial Geomorphology (FGM)**

To complete the morphological investigation portion of this study, fluvial geomorphological (FGM) surveys were conducted at 25 sites within the Lake Thunderbird watershed. The FGM sites were initially selected using aerial photography to assure adequate spatial coverage of the watershed, so that the sites

would be representative of the stream reaches located in the watershed. However, due to the fact that the vast majority of sites were located on private property, and in a few cases access to the site was denied, a few of the sites initially chosen were moved to a location as close as possible to where access was granted. Table 3 shows the FGM sites established for this portion of the study, and an aerial photograph showing the locations of the FGM study sites is provided in Figure 13.

At each FGM site, reference markers in the form of 18" long x 3/4" rebar pins, with plastic caps, were established on both sides of the channel, as was done at the hydrology sites. A survey was then conducted at the site using a total station and U.S. surveying units (feet).

How the survey was performed depended on the availability of survey control at the site. At a few sites, sufficient survey control was located so that Easting, Northing and Elevation coordinates with respect to the Oklahoma State Plane-South (NAD83) and North American Vertical Datum of 1983 (NAVD83) could be determined. At these sites, the survey was conducted using "real" Easting, Northing, and Elevation coordinates.

More often than not, however, existing survey control was not available at the site. For these sites, one of the pins, typically the left pin, was assigned reference coordinates such as 5000.00, 5000.00, 100.00, or something similar, and the other pin was used as a back sight to assign the "zero" line. During the survey, the MAP and GPS applications on an iPhone or a hand held GPS unit, were used to identify the location of the base pin.

Table 3: Lake Thunderbird watershed fluvial geomorphology (FGM) study sites.

Site No.	Site Name	Latitude	Longitude	Site No.	Site Name	Latitude	Longitude
LR01	Little River 01	35° 16' 1" N	97° 19' 54" W	EC01	Elm Creek-01	35° 16' 55" N	97° 21' 01" W
LR02	Little River 02	35° 16' 45" N	97° 22' 01" W	EC02	Elm Creek-02	35° 18' 14" N	97° 21' 26" W
LR03	Little River 03	35° 16' 52" N	97° 23' 45" W	EC03	Elm Creek-03	35° 19' 23" N	97° 22' 35" W
LR04	Little River 04	35° 16' 30" N	97° 23' 56" W	RC01	Rock Creek 01	35° 15' 47" N	97° 19' 56" W
LR05	Little River 05	35° 16' 29" N	97° 25' 42" W	RC02	Rock Creek 02	35° 18' 14" N	97° 21' 26" W
LR06	Little River 06	35° 16' 23" N	97° 25' 50" W	RC04	Rock Creek 04	35° 14' 28" N	97° 22' 32" W
LR07	Little River 07	35° 16' 09" N	97° 27' 14" W	DB01	Dave Blue Creek 01	35° 12' 17" N	97° 19' 03" W
LR08	Little River 08	35° 16' 43" N	97° 27' 59" W	DB02	Dave Blue Creek 02	35° 11' 47" N	97° 19' 51" W
LR09	Little River 09	35° 17' 11" N	97° 28' 20" W	DB03	Dave Blue Creek 03	35° 11' 38" N	97° 20' 20" W
NF01	North Fork 01	35° 16' 31" N	97° 25' 45" W	DB04	Dave Blue Creek 04	35° 11' 12" N	97° 21' 2" W
NF02	North Fork 02	35° 17' 29" N	97° 26' 04" W	HC01	Hog Creek 01	35° 19' 15" N	97° 15' 01" W
NF03	North Fork 03	35° 18' 24" N	97° 26' 39" W	HC02	Hog Creek 02	35° 20' 14" N	97° 15' 17" W
NF04	North Fork 04	35° 20' 24" N	97° 27' 13" W				



Figure 13: Map of the Lake Thunderbird watershed showing the location of the fluvial geomorphology (FGM) study sites.

A survey of the cross-section between the pins, and of the longitudinal profile of the channel, was conducted at each site using a total station. The longitudinal profile at each site extended a minimum distance of between 10 and 20 times the width of the channel. Key features, including the thalweg, water surface (if present), bankfull indicators, and the tops of the banks, were identified and surveyed. Indicators of the bankfull level included vegetation lines, and flat depositional features. It should be noted that the bankfull level is not the same as the top of the bank in incised systems that are no longer in connection with their floodplain. Other commonly used terms that are synonymous with bankfull discharge include effective discharge, dominant discharge, and active discharge. The bankfull level in this study refers to the level associated with the effective or dominant discharge, and not the top of the bank.

The data for all surveys were collected using a TDS Recon handheld computer and SurveyPro software. When the survey was completed, the survey job was exported to a CSV file. This CSV file was then opened in Excel for processing.

Prior to conducting the surveys, base maps had been created in AutoCad Civil3D (ACAD) and ArcMap using NAIP 2010 Statewide imagery from the National Agriculture Imagery Program (NAIP), obtained from the OKMaps website (OKMaps, 2010). At sites where the state plane coordinates were known for both pins, the CSV file from the survey required no processing and could simply be imported into the ACAD basemap.

At sites where there was insufficient survey control data to establish the state plane coordinates for the reference markers, the exported CSV files required processing to determine the “true” location of the surveyed points. This process involved first using

the location of the base pin as provided by the iPhone or GPS unit, together with aerial photographs to determine the Easting and Northing coordinates for the left reference marker. Although this approach may not provide as much accuracy as traditional methods, it is sufficient to locate the control pins with relative ease, especially with the use of a metal detector.

At this point, a large circle was drawn on the ACAD base map using the Easting and Northing coordinates for the left pin as the center point. The survey CSV file was imported into ACAD, and the points were moved as a group, moving them from the survey coordinates of the left pin (e.g., 5000.00, 5000.00, 100.00) to the center of the circle. The points were then rotated using the surveyed points so that the points matched the aerial photography on the base map. The rotation angle had to be fairly precise for all of the points surveyed in the longitudinal profile to line up properly with the aerial photograph of the channel. In some cases, easily identifiable features, such as fence lines, or corners of buildings, were surveyed to aid in alignment. When the alignment was deemed correct, the points were exported to a CSV file.

Again, while this approach does not provide as much accuracy as traditional methods, it does allow for a fairly accurate depiction of the survey points on the base map. Nor does this method provide a means of determining the true elevations of the surveyed points. However, because all of the FGM assessment information is relative to the site, and the surveys are accurate with respect to the reference markers, this has no effect on the interpretation of the results of this study. If future studies require true elevations, and more accurate positioning, all that would be required is to determine the

coordinates of the reference markers. The survey data itself could then be reprocessed to provide more accurate positioning data for the site.

The FGM survey data were used to determine the morphological parameters required to classify the stream reach using the “classification of natural rivers” scheme developed by Rosgen (1994, 1996), as shown in Figure 14. These parameters include the entrenchment ratio, the bankfull width to bankfull depth ratio, the channel sinuosity, and the slope. Methodologies for conducting the geomorphic surveys proposed for use in this study may be found in Rosgen (1996) and in Harrelson et al (1996). Each FGM site was also classified using Simon’s Channel Evolution Model (Figure 5).

The bed and bank material of the majority of the channels was clearly identifiable as sand. Where there was doubt, a bed material analysis was conducted to determine the dominant bed material type. The bed material analysis consisted of conducting a “pebble count” in which the bed material size is determined at 100 randomly chosen points in the study reach, and the mean particle size (D50) is calculated. A sieve analysis of the bed and bank material was also conducted at a few of the sites.

Additional data were collected at each site, as needed to determine bank stability indices for the site. Bank stability indices evaluate various features of the bed, banks, and riparian vegetation to give the site a numerical index that is theoretically related to the amount of erosion expected to occur at the site. Various stability indices have been developed by researchers, including Pfankuch (1975), Rosgen (1996, 2001), Simon and Downs (1995), and Storm et al (2010).

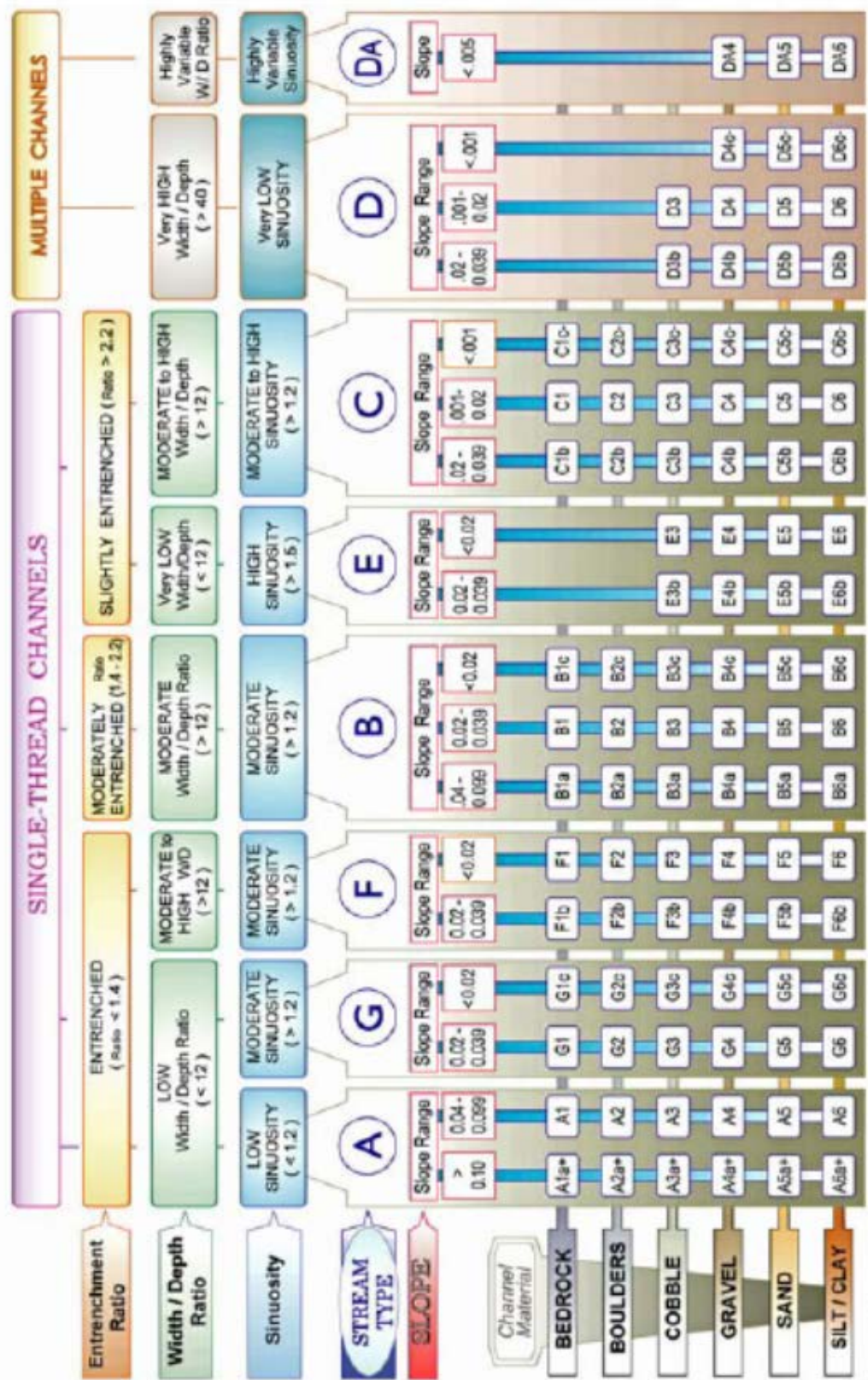


Figure 14: Classification Key for Natural Rivers. (Rosen, 1996)



The latter of these indices was developed specifically for the Ozark ecoregion, and although the Little River watershed is located in the Central Great Plains ecoregion and the stream beds are dominated by sand and not gravel, they were included simply because little additional effort was required to evaluate their use outside the ecoregion where they were developed. It is not known if any of these indices are applicable in the watershed, but the data collected for the various indices are similar, so data were collected at all of the FGM sites, in order to allow calculation of the indices using all four of the methods cited.

To aid in collection of the bank stability index data, and to eliminate duplication of effort, a spreadsheet was developed for use in the TDS Recon handheld computer. The raw data were divided into seven categories, including 1) Site Information, 2) General Description, 3) Reach Morphology, 4) Reach Characteristics, 5) Site Characteristics, 6) Study Bank Characteristics, and 7) Pfankuch Data.

Table 4 shows the information included in the Site Information, General Description and Reach Morphology categories of the spreadsheet. Site Information includes the site number, site name, bank number (if more than one bank was assessed at the site), the date of the assessment, the location of the bank being assessed (latitude and longitude), and whether or not pictures were taken of the site.

Table 4: FGM Bank Stability Assessment Spreadsheet Categories 1 – 3.

1. SITE INFORMATION
Site No
Site Name
Bank No.
Date
Bank Location, Lat Long
Pictures (Mark with X if taken):
Upstream
Downstream
Bank
2. GENERAL DESCRIPTION
Valley Type:
Pattern (Meander/ Shallow Curve/Straight)
Dominant Bed Material (Bedrock, Boulder, Cobble, Gravel, Sand, Silt, Clay)
3. REACH MORPHOLOGY
Bankfull Width Wbkf (ft)
Mean Bankfull Depth, dbkf (ft)
Maximum Bankfull Depth, dmax (ft)
Width of Flood Prone Area, (ft)
Entrenchment Ratio
Stream Slope:
Sinuosity
Existing Stream Type:
Potential Stream Type:
Stage of channel evolution (I-VI)

Table 5 shows the information included in the Reach Characteristics and Site Characteristics categories of the spreadsheet. Reach Characteristics include the presence or absence of bed protection (yes/no), the number of banks protected (0, 1 or 2), the presence or absence of transverse/central bars (yes/no), the presence or absence of extensive deposition (yes/no), and the presence or absence of chute cutoffs, down-valley meander migration, or converging flows (yes/no). Site Characteristics include the upstream and downstream reach lengths, upstream width, channel width at the bank being assessed, degree of constriction, the presence or absence of streambank erosion on the left and right banks (none/fluvial/failure), the percentage of each bank failing on the left and right banks, the percentage of riparian woody-vegetative cover on the left

and right banks, the percentage of fluvial deposition on the left and right banks, and the most unstable bank (left or right).

*Table 5: FGM Bank Stability Assessment Spreadsheet Categories 4 -5.*

4. REACH CHARACTERISTICS
Bed Protection (Yes/No)
Bank Protection (1 Bank/2 Banks)
Transverse/central bars (Yes/No)
Extensive deposition (Yes/No)
Chute cutoffs, down-valley meander migration, converging flows (Yes/No)
5. SITE CHARACTERISTICS
Upstream Reach Length, Lu (ft):
Downstream Reach Length, Ld (ft):
Upstream width, Wu (ft)
Channel width, W (ft)
Degree of Constriction, %
Streambank Erosion (None/Fluvial/Failure) - Left and Right
Streambank Instability (% each bank failing) - Left and Right
Riparian woody-vegetative cover (% each bank) - Left and Right
Bank accretion (% of each bank with fluvial deposition) - Left and Right
Most Unstable Bank (Right/Left):

Information included in the Study Banks Characteristics category of the spreadsheet is shown in Table 6. Study Bank Characteristics include the bank height, bank face length, the presence or absence of undercut banks, (yes/no), the bank height ratio (bank height/maximum bankfull depth), the bank height to bank face length ratio, the percent of the bank with a bank angle greater than 80°, the bank material (if composite, the percentage that is sand), stratification of bank materials (low/med/high), the rooting depth and density, percentage of bank protection, percentage of bank experiencing mass wasting, the percentage of the bank with unconsolidated material, the percentage of the bank with riparian woody vegetation cover, degree of incision (mean bankfull depth/bank height), the chord length, arc height and radius of curvature

of the bend, the near-bank maximum depth, the ratio of the radius of curvature versus the bankfull width, and the ratio of the near-bank maximum depth, versus mean bankfull depth.

*Table 6: FGM Bank Stability Assessment Spreadsheet Category 6.*

6. STUDY BANK CHARACTERISTICS
Bank Height, BH (ft)
Bank Face Length, BFL (ft):
Undercut Bank (Yes/No):
Bank Height Ratio (Bank Height/Bankfull Depth)
BH/BFL:
Bank Angle, Deg (H)
Percentage of Bank Angle > 80o:
Bank Material
(If comp, % sand)
Stratification (Low/Med/High)
Root Depth, ft (D)
Root Densiy, % (F)
Bank Protection (% of bank)
Mass Wasting (% of Bank):
Unconsolidated Matl (% of Bank)
Riparian Woody-Veg. Cover (%):
Degree of Incision, %
Chord Length, Lc (ft):
Arc Height, Harc (ft):
Near-Bank Max Depth dnb (ft)
Radius of Curvature Rc (ft)
Ratio Rc/Wbkf
Ratio dnb/dbkf

Table 7 shows the information included in the Pfankuck Data category of the spreadsheet. Unlike the other categories, information in the Pfankuck Data category is applicable to only the Pfankuck Stream Stability Index. Pfankuck Data information includes metrics for the upper bank, including bank slope, mass erosion, debris jam

potential, and vegetative bank protection; the lower bank, including channel capacity, bank rock content, obstructions to flow, and cutting and deposition; and the channel bottom, including rock angularity, rock brightness, consolidation of particles, bottom size distribution, scouring and deposition, and aquatic vegetation.

*Table 7: FGM Bank Stability Assessment Spreadsheet Category 7.*

7. PFANKUCH DATA
Upper Banks
Bank slope (<30%=2; 30-40%=4; 40-60%=6; >60%=8)
Mass erosion (None=3; Infreq.=6; Freq.=9; Very Freq.=12)
Debris jam potential (None=2; Small=4; Med-Lrg=6; Large=8)
Vegetative bank protection(>90%-Hi Variety=3; 70-90%-Less Variety=6; 50-70%-Fewer species=9; <50%-Sparse=12)
Lower Banks
Channel capacity (BHR≤1.0=1; BHR=1.0-1.1=2; BHR=1.1-1.3=3; BHR>1.3=4)
Bank rock content (Boulder-12"=2; Bldrs/Cobbles-6-12"=4; Grvl/Cobble-3-6"=6; <gravel-<3"=8)
Obstructions to flow (None-Stable Bed=2; Some-minor pool filling=4; Moderate-cutting & pool filling=6; Frequent-erosion yearlong=8)
Cutting (Little or None-<6'=4; Some-6-12'=6; Significant-12-24'=12; Extreme->24'=16)
Deposition (Little or None=4; Some bar increase-crse gravel=8; Moderate deposition-gravel & sand=12; Extensive-fines=16)
Bottom
Rock angularity (Well rounded/smooth=1; Corners & edges rounded=2; Rounded corners and edges/surfaces smooth=3; Sharp Edges/rough faces=4)
Brightness (Dull=1; <35% bright surfaces=2; 35-65% bright surfces=3; >65% bright surfaces=4)
Consolidation of particles (Tightly packed=2; Moderately packed=4; Mostly loose=6; No packing/loose=8)
Bottom size distribution (Stable matl.- 80-100%= 4; Stable matl.- 50-80%=8; Stable matls.- 20-50%=12; Stable matls.-0-20%=16)
Scouring and deposition (<5% of bottom effected=6; 5-30% effected=12; 30-50% effected=18; > 50 % effected=24)
Aquatic vegetation (Abundant-Moss like=1; Common-Algal+Moss=2; Present-Seasonal algal=3; Scarce or absent=4)

The raw data from the TDS Recon handheld computer was then copied into a “RawData” sheet on a more extensive spreadsheet that uses these raw data to calculate the various metrics that form the basis of the stability indices. In addition to the RawData sheet, the spreadsheet had another sheet named Data, where many of the metric calculations were made from the raw data. Additional sheets, BEHI, NBS, CSI, OEBSI, and Pfankuch, compile the metrics and generate the indices for the various assessment methods. Finally, a Summary sheet was included that summarizes the results.

A rigorous interpretation of the bank stability indices for use in a given site requires that multiple surveys be conducted over time, so that the bank erosion rate can

be related to the index. Because only one survey was conducted at each site, it was not possible to determine bank erosion rates in the current study. However, the surveys conducted will provide a base line for future research in the watershed, as well as provide a qualitative assessment of current conditions based on the indices relative value to other study sites

With the FGM surveys and bank stability assessments completed, the drainage area for each site was determined using the hydrology spatial analysis tool, within ArcMap, which generates a drainage basin for any so-called “pour point.” Using the coordinates determined from the survey as pour points, drainage areas were defined for each of the survey sites. This information, together with the channel morphology obtained from the surveys, was used to develop a “regional curve” for the watershed that relates bankfull dimensions (width, depth and area) to drainage area.

## **D. Results**

### **1. Hydrology**

The results of the investigation of the hydrological characteristics of the Lake Thunderbird Watershed include the monitoring site survey results, the HOBO pressure transducer results, the discharge measurement results and the resulting stage-discharge rating curves. Applications of the rating curves are also presented.

#### *i. Monitoring Site Surveys*

The monitoring site surveys were conducted in March and April of 2010. Summaries of the monitoring site surveys are provided in Appendix A. Information

provided in the appendix for each site includes the date of the survey, the time that the HOBOS were deployed and started, the elevation of the installed HOBOS, the coordinates of the control pins in NAD83 state plane coordinates, a site location map showing the location of the site, the HOBOS, the surveyed cross-section, the cross-section survey data, the HOBOS elevation survey data, information for the staff gauge, if applicable, and the cross-section plot.

For the two sites with staff gauges present, Hog Creek and Little River at 60<sup>th</sup>, the information provided for the staff gauge includes the staff gauge reading at the time of the survey and the 0-datum elevation of the staff gauge. This additional information on the staff gauges may perhaps prove more beneficial now than it might have otherwise been, because both staff gauges were removed, without any record of their datum elevations.

Figure 15 shows the cross-section plot for the Little River at 60<sup>th</sup> Avenue NE site. The figure is typical of the plots developed for each monitoring site, and includes the ground surface elevation (green) and the water surface elevation at the time of the survey (blue). The elevation of the HOBOS is also provided. Cross-section plots for all seven monitoring sites are provided in Appendix A.

## *ii. HOBOS Pressure Transducer Results*

Installation of the HOBOS was conducted in conjunction with the site surveys, with the HOBOS being installed prior to the survey. In some cases, the survey was conducted the day after installation. Table 8 provides the date and time each HOBOS was started and the elevation that it was installed. Note that the table also includes a site

called “Ambient Conditions.” This site provides the baseline ambient temperature and pressure for the study.

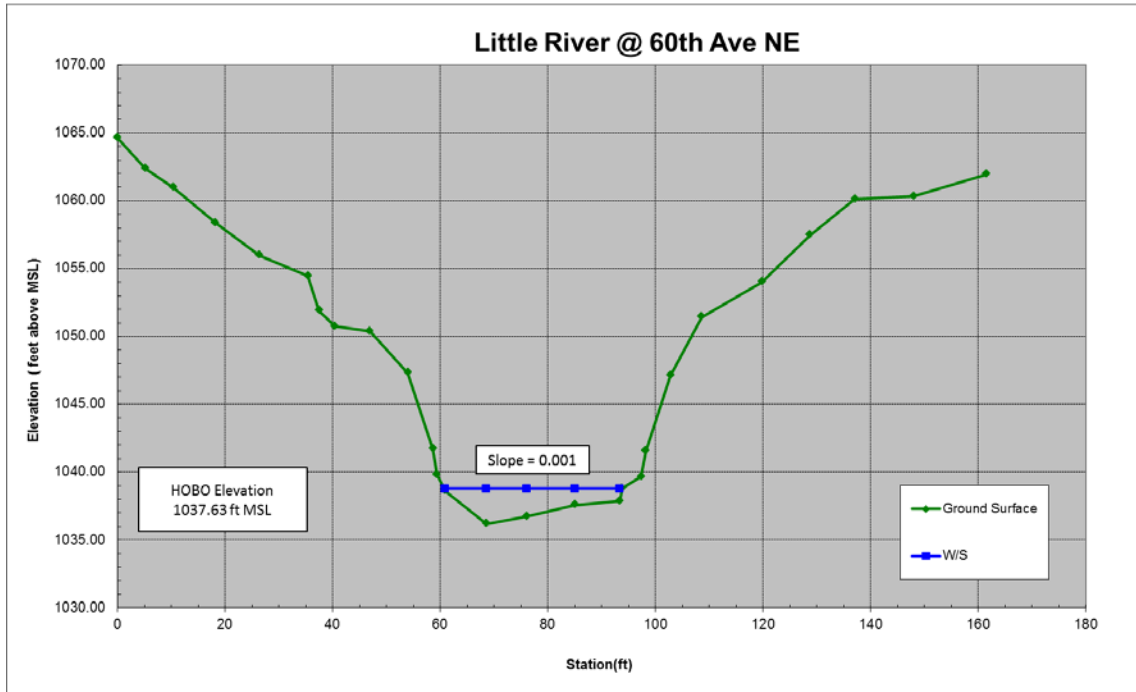


Figure 15: Cross-section plot for the Little River at 60<sup>th</sup> Ave NE monitoring site.

Table 8: HOBO Deployment Times.

Site	HOBO Deployment Time	
	(GMT-0600)	
Little River @ 60th Ave NE	March 6, 2010	14:30
Little River @ Porter Ave	April 16, 2010	11:30
Hog Creek @ SE 119th	March 29, 2010	13:30
Rock Creek @ 72nd Ave NE	March 29, 2010	14:30
Elm Creek @ Indian Hills (179th SE)	March 26, 2010	14:00
North Fork @ Franklin	March 29, 2010	12:00
Dave Blue Creek @ 72nd Ave SE	April 16, 2010	12:00
Ambient Conditions	March 6, 2010	14:30



Data from the HOBO pressure transducers were downloaded on an interval ranging from 30 to 60 days. This phase of the study took the most long-term commitment, requiring repeated trips to the field to download data.

With data being collected for over four years at 30 minute intervals, there were a lot of data points to manage. As of the latest data download on March 24, 2015, there are over 88,000 data lines for the Ambient Conditions site, and just under 84,000 data lines at the Dave Blue Creek site, the active site with the fewest recorded observations. With each site being placed on a separate sheet within the same Excel spreadsheet, the spreadsheet is quite large, with the current file size at over 252 MB. Due to the large amount of data, it is not feasible to include it as text in this dissertation, even as an Appendix. The raw data files and spreadsheets used in the study may be obtained from the author, Dr. Kolar, or Dr. Nairn upon request. Plots of the HOBO data for all of the sites are provided in Appendix C.

Figure 16 shows the temperature and pressure plots for the Ambient Conditions site for the period of record beginning on March 6, 2010 through the last data download on March 24, 2015. As expected, there is a wide swing in temperature, both diurnally and seasonally. The diurnal variation is evident by the wide “band width” of the plot, and the seasonal variation is seen in the sinusoidal pattern. Smaller variation may also be seen in the pressure plot with the variation being only slightly variable from season to season and less variable diurnally.

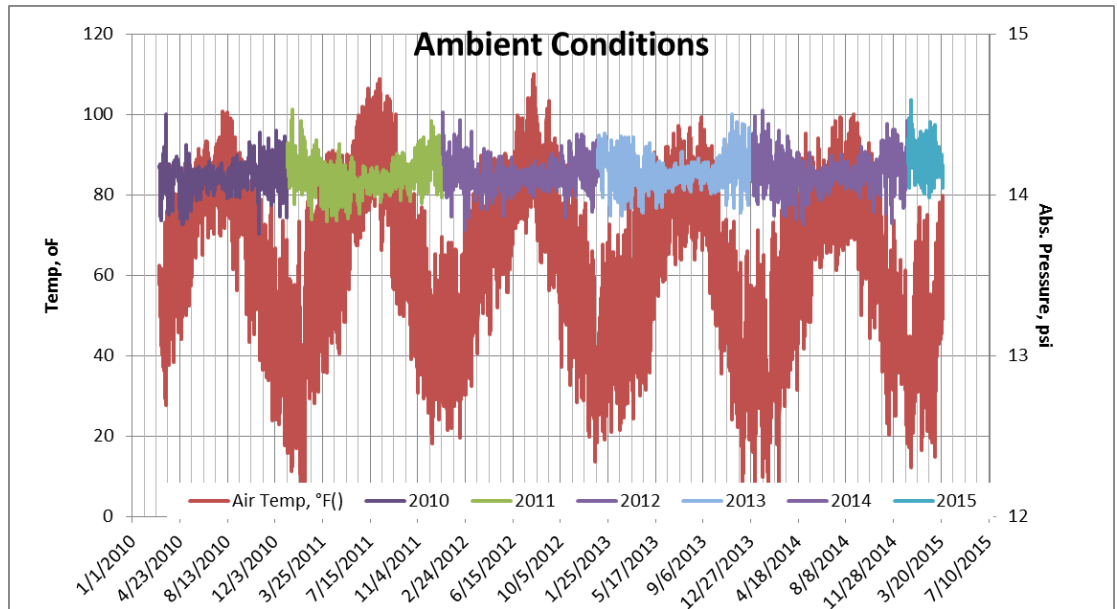


Figure 16: HOBO temperature and pressure plots for the Ambient Conditions site.

Figure 17 shows the temperature and pressure plots for the Little River at 60th Ave NE site. Once again diurnal and seasonal variation in temperature may be observed. The seasonal variation exhibits the same sinusoidal pattern observed at the Ambient Conditions site, but, with one exception, the diurnal variation is less than at the Ambient Conditions site. The exception occurs in July, 2011, when OCC employees inexplicably removed the staff gauge and the piping for the auto-sampler that the HOBO was attached to, and left the HOBO laying on the bank. As a result the HOBO was measuring the ambient temperature rather than water temperature.

The pressure plot for the Little River at 60th Ave NE site, unlike in the Ambient Conditions site plot, shows large spikes. These spikes are the result of deeper water associated with high flow events. Plots for all of the sites show similar trends in pressure.

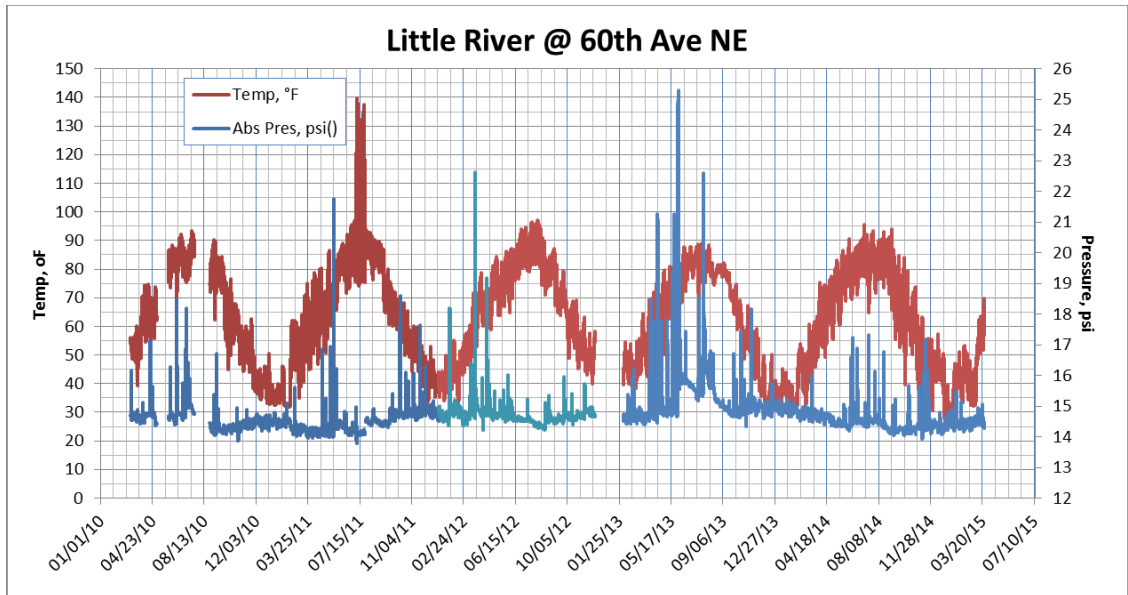


Figure 17: Temperature and pressure plots for the Little River at 60<sup>th</sup> Ave NE site.

Subtracting the ambient pressure, as recorded at the ambient conditions site, from the pressure recorded at each stream site, at the same date and time, produced a record of the hydrostatic pressure at each site. The hydrostatic pressure was then used to calculate the water depth, or stage, at each time step, for each monitoring site. Figure 18 shows the stage plot for the Little River at 60<sup>th</sup> Ave NE site. Stage plots for all of the sites are provided in Appendix C.

For the most part, data recording and collection during the study went well. However, there were a few exceptions, resulting in some anomalies, and thus gaps in the data, as may be seen in the Little River at 60<sup>th</sup> Ave NE site data plot shown in Figure 17. The first two anomalies occurred in the first six months of the study, apparently for the same reason; the HOBOS did not get restarted after downloading, and thus did not record any data until the next data download session, when the mistake was discovered. These mistakes resulted in gaps of data extending from May 2, 2010 to May 22, 2010,

and from July 22, 2010 to August 25, 2010. Incidents such as this are the primary reason data downloading is conducted every 30 to 60 days, because it minimizes the amount of lost data should unforeseen events such as this occur.

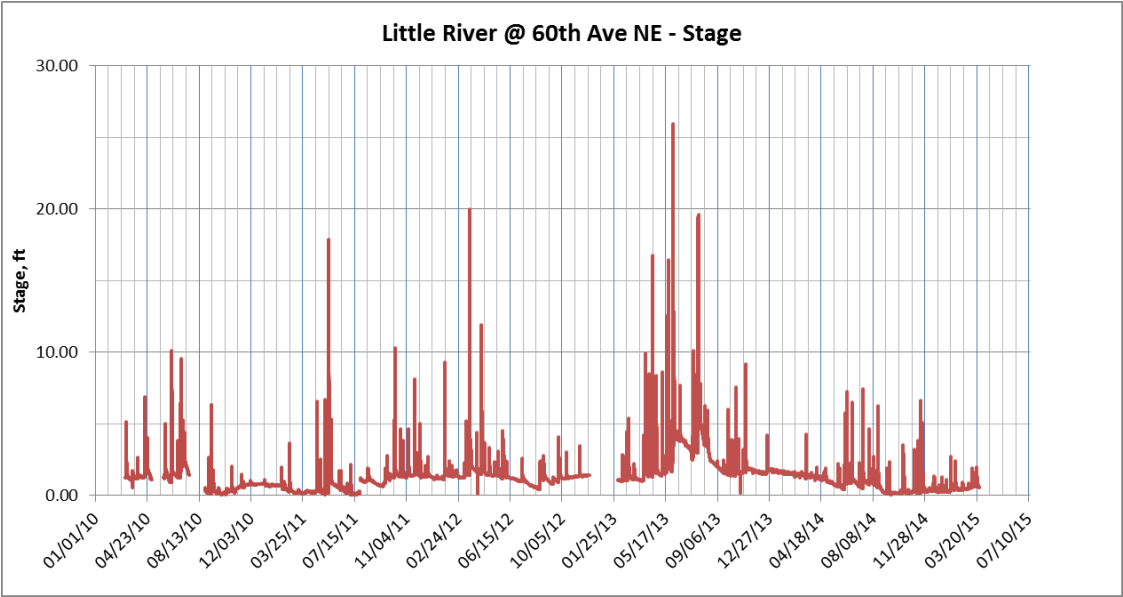


Figure 18: Stage plot for the Little River at 60<sup>th</sup> Ave NE site.

The next anomaly in the data occurred in July, 2011 when OCC employees left the HOBO laying on the bank as previously mentioned. The removal was not detected until July 26, 2011, when the next data download session took place. The HOBO was initially assumed lost, but was found the next day, lying on the bank, still in the housing, when a replacement HOBO was being installed. The replacement HOBO and housing were moved downstream slightly and were attached to gabion baskets along the right bank. After the re-installation was completed, the elevation of the replacement HOBO was surveyed to establish a new datum elevation for the site.

Even though the HOBO had been removed from the channel resulting in a gap of data from July 7, 2011 to July 26, 2011, it continued to collect data, as may be seen by the large temperature variations in the plot in Figure 17. It is this temperature data that allowed identification of the removal date as July 7.

The third and final data anomaly for the Little River at 60th Ave NE site occurred on December 3, 2012, when the HOBO stopped working the day after a data download session, as a result of a weak battery. Unfortunately, the problem was not discovered until February 2, 2013, when the next download session was conducted, resulting in a 2 month gap in data. Fortunately, a spare HOBO had been acquired for just such an occurrence, allowing for immediate replacement, or the data gap could have been larger. The spare was deployed at the site, and the inoperable one was returned for service.

Weak batteries resulted in other data anomalies, and resulting gaps in data, at other sites as well. On March 2, 2012, the HOBO at the North Fork site stopped recording and was not replaced until April 3, 2012 (App. C, Figure C.7.1). Then, on September 6, 2013, the HOBO at the Dave Blue Creek site stopped working and was not replaced until October 25, 2013 (App. C, Figure C.8.1). On both occasions, having a spare HOBO allowed for immediate replacement, reducing the amount of data lost.

Another anomaly in the data occurred in December, 2012 and January, 2013 at the North Fork site. When the data were downloaded on February 2, 2013, and examined, there were large unexpected fluctuations in pressure. Further investigation revealed the problem to be a result of the installation. Because the HOBO in its housing, at this site, was suspended horizontally under a rock, and the water level was extremely

low, the housing was hanging in the air right at water level. When the temperature dipped below freezing, water within the housing froze, applying pressure on the HOBO's sensor. This resulted in the observed pressure fluctuations not attributable to the discharge. To avoid or minimize the chances of this reoccurring, slits were cut into the housing sides to allow water to drain out of the housing.

The greatest loss of data occurred sometime after April 25, 2013, probably on June 1, 2013, when a significant rain event occurred in the watershed, and the OCC staff gauge at the Hog Creek site, to which the HOBO was attached (Figure 9), was washed away. The HOBO was lost, and was not replaced, so data for the Hog Creek site stopped being collected after April 25, 2013.

In the process of determining the source of the data anomaly at the North Fork site in December, 2012 and January, 2013, the decision was made to deploy two HOBOs at the site, as closely to each other as possible. On February 5, 2013 an additional HOBO was hung under the rock next to the HOBO that had previously been installed. The two HOBOs were run concurrently until April 25, 2013. Figures 19 – 21 show the pressure, temperature, and stage plots, respectively, for the two side-by-side HOBO measurements.

Visually there appears to be good agreement between the measured and calculated values from the two HOBOs, but it is difficult to tell how well the values agree due to the scale. Figures 22-24 show the difference in the pressures, temperatures and stages, respectively between the two HOBOs. These plots clearly show the similarity in values from the two HOBOs.

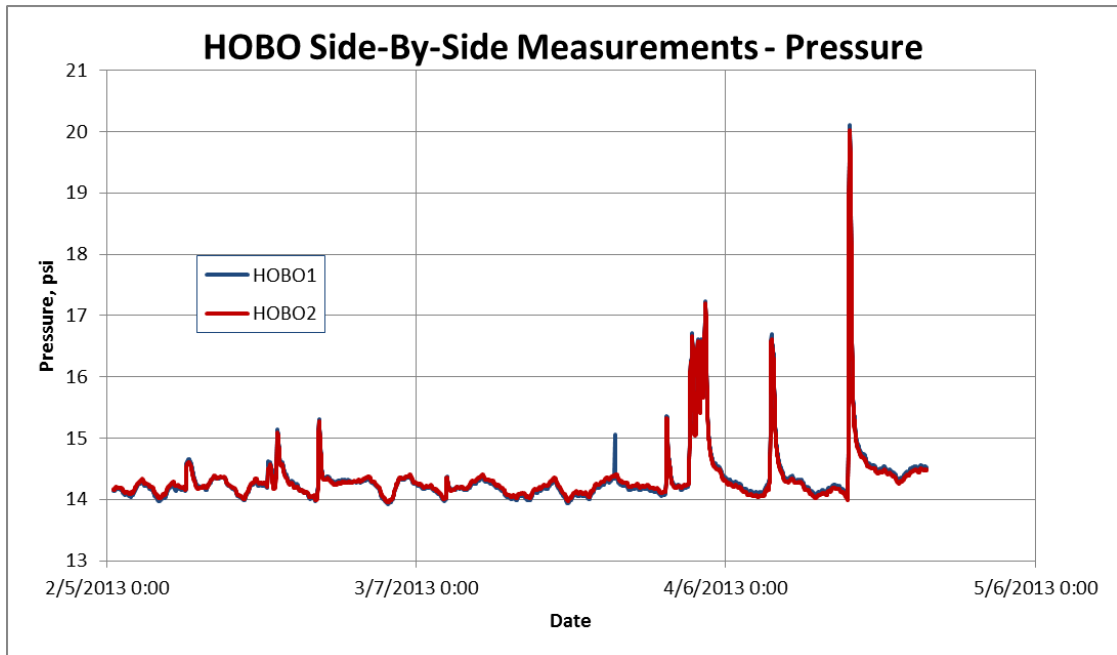


Figure 19: HOBO Side-By-Side Pressure Measurement Plots.

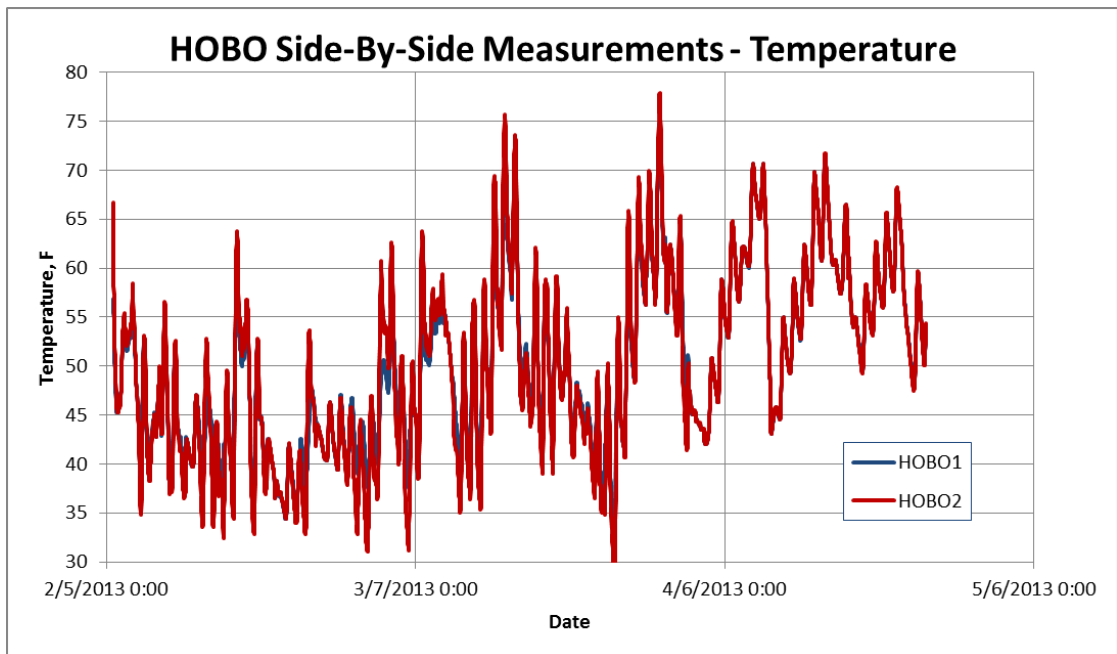


Figure 20: HOBO Side-By-Side Temperature Measurement Plots.

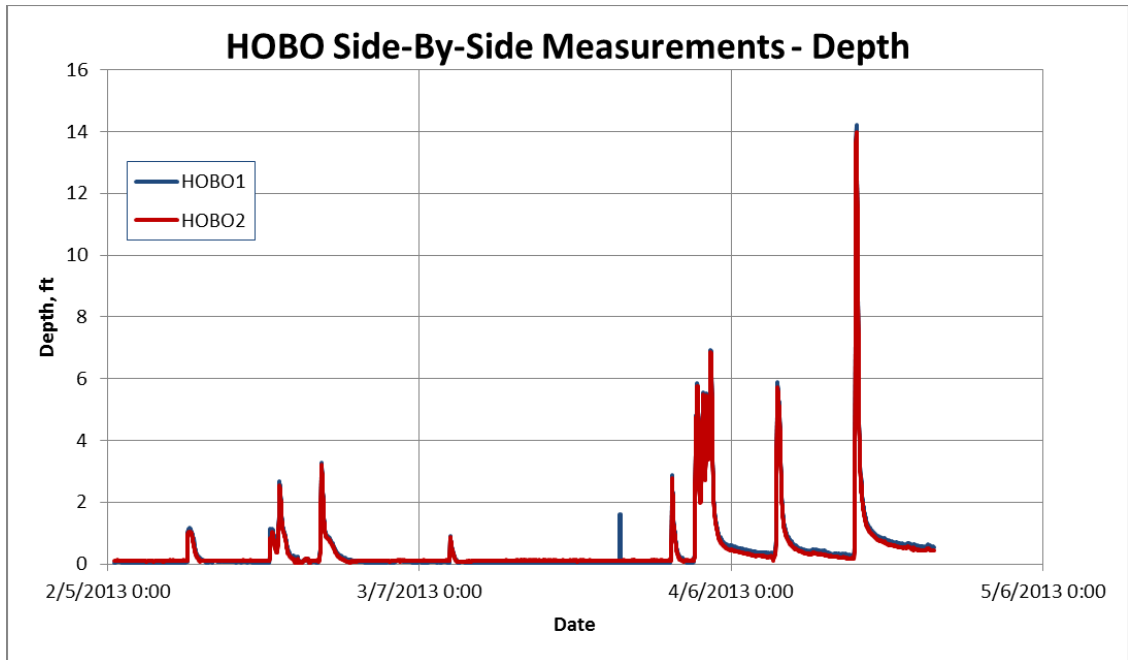


Figure 21: HOBO Side-By-Side Calculated Depth (Stage) Plots.

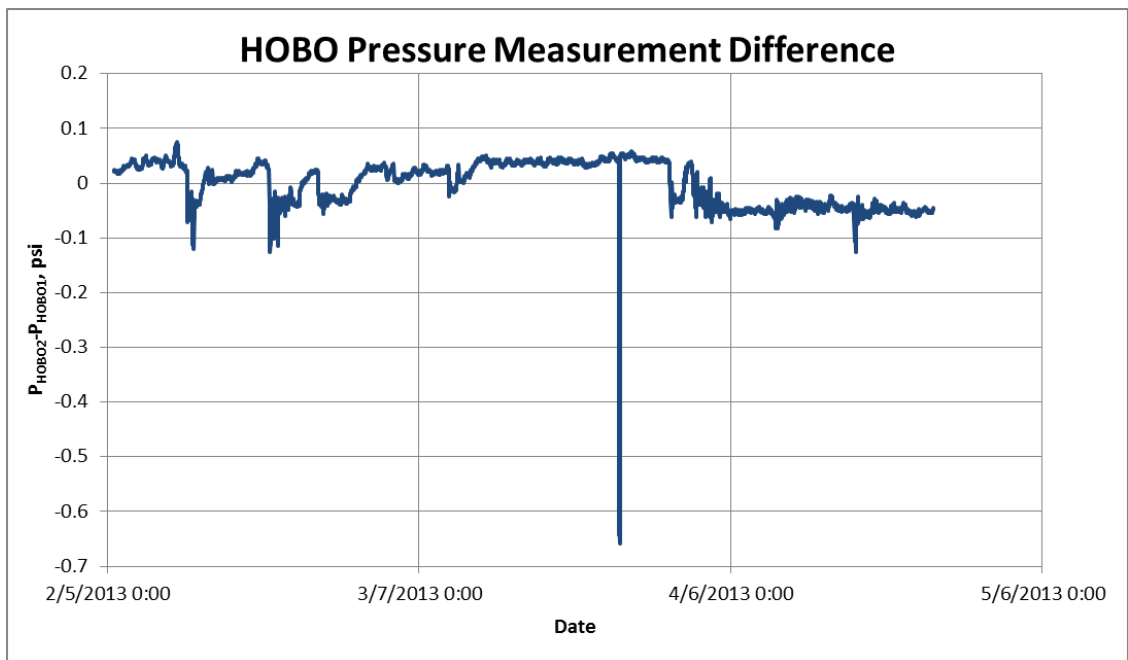


Figure 22: HOBO Side-By-Side Pressure Measurement Difference Plot.



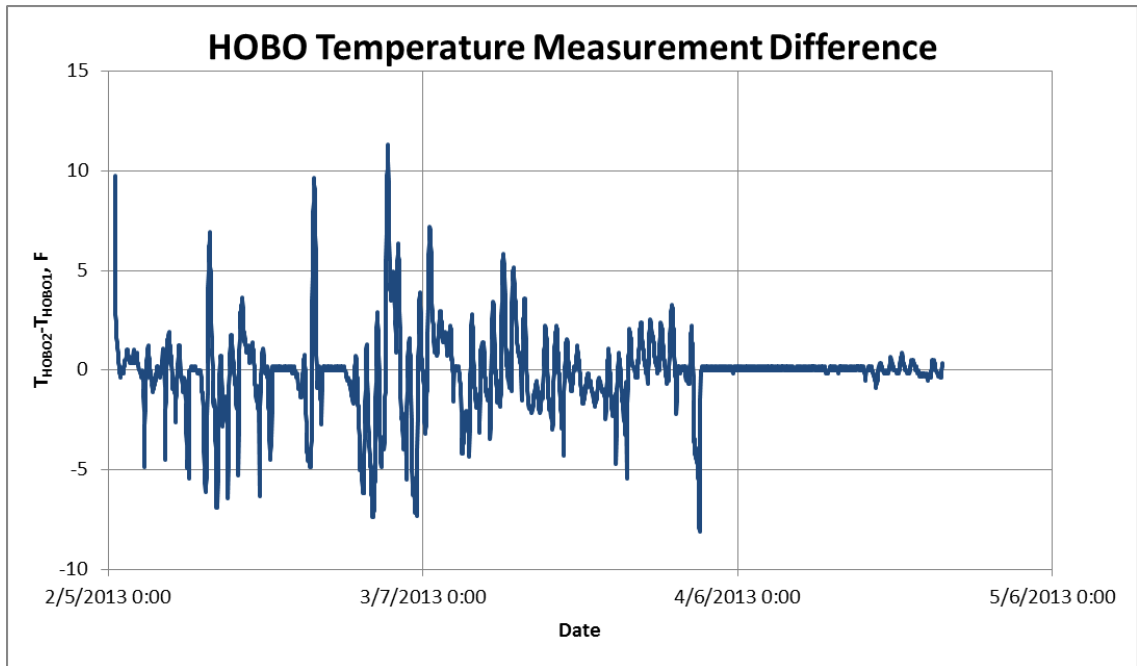


Figure 23: HOBO Side-By-Side Temperature Measurement Difference Plot.

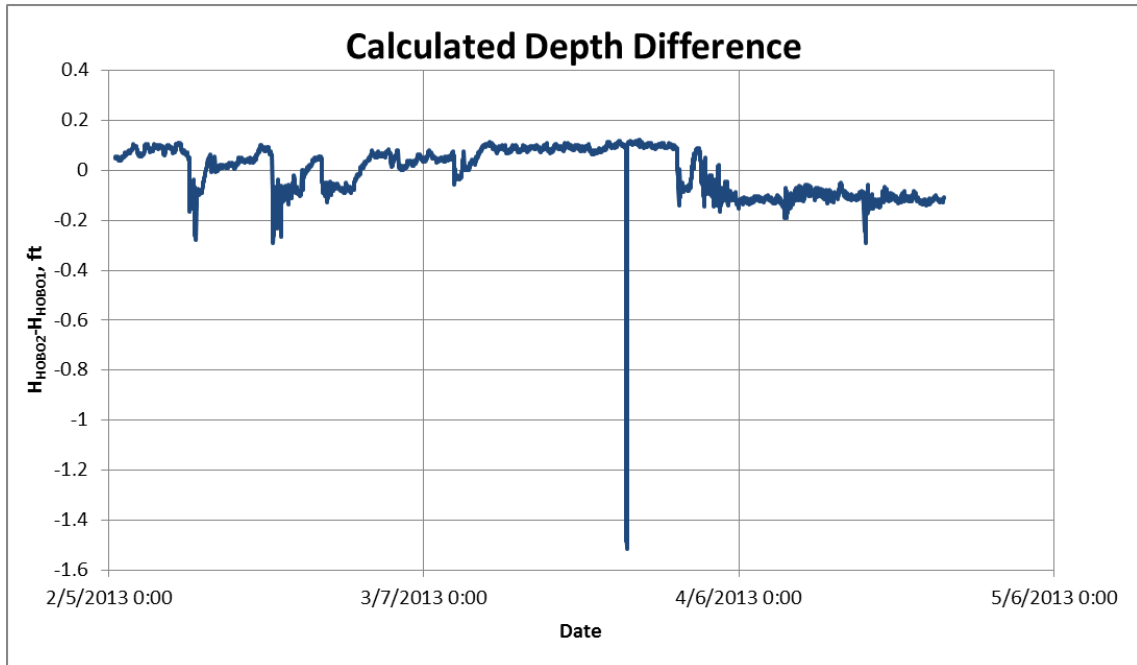


Figure 24: HOBO Side-By-Side Depth (stage) Measurement Difference Plot.

In Figure 22, it may be seen that, with one exception, the difference in pressure recorded by the two HOBOS is generally within +/- 0.1 psi, and typically within +/- 0.05 psi. The cause of this deviation may be a result of ice forming in one of the housings. Figure 23 shows that the temperature recorded by the two HOBOS was more variable, with the difference between them often reaching 10 °F. More typically though the difference was within +/- 5 °F, and often the difference between the values was essentially zero. With a few exceptions, the difference in the depth calculated for each HOBOS was typically between +/- 0.2 feet, as shown in Figure 24.

Figure 25 shows the pressure (left) and temperature (right) recorded by the two HOBOS plotted on the same graphs. If the HOBOS were recording exactly the same results, the slope of the regression line of the data would be 1.0, the intercept would be 0.0, and the coefficient of determination ( $R^2$ ) would be 1.0. It may be seen in the pressure plot on the left that the slope of the regression line is 0.966, the intercept is 0.49 psi, and the  $R^2$  is 0.9926, indicating that the two HOBOS measurements are very nearly identical. It may be seen in the temperature plot on the right that the slope of the regression line is 1.0886, the intercept is -4.578 °F, and the  $R^2$  is 0.9628, again indicating excellent agreement between the two HOBOS.

Figure 26 shows a plot of the water depths calculated for each HOBOS, plotted on the same graph, in the same manner as was shown for the pressure and temperature. Because the primary objective of the HOBOS measurements is to provide a means of determining water depth at the monitoring sites, it is perhaps more important that the two HOBOS provide similar records for the depth, than for the pressure and temperature. Note that the slope of the regression line in Figure 26 is 0.9625, the

intercept is 0.014 feet, and the  $R^2$  is 0.9928, indicating that the two HOBOS are providing essentially the same record of the water depth at the site.

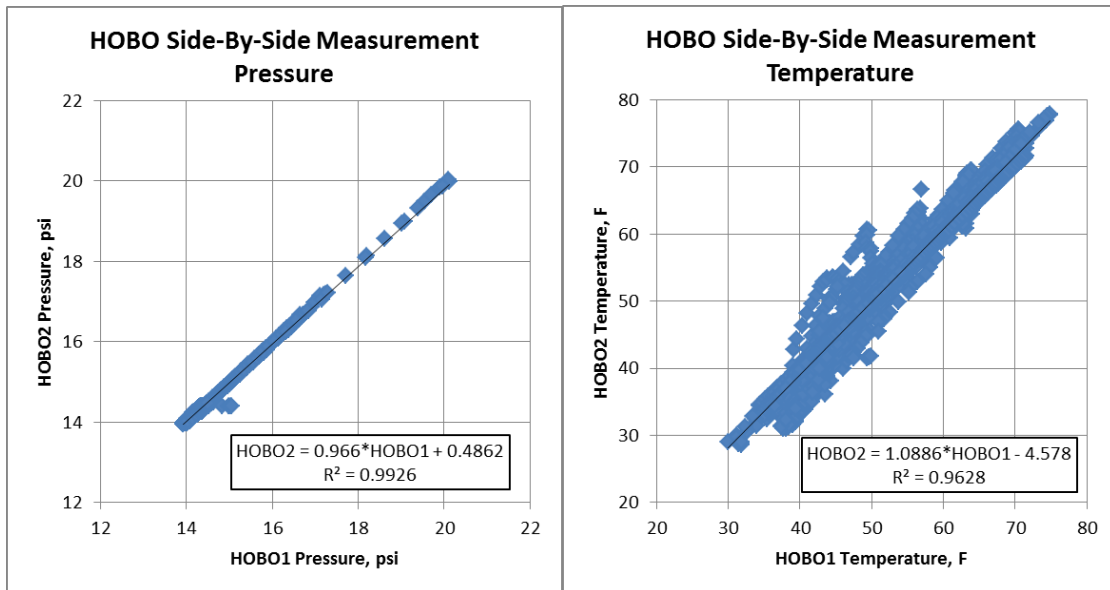


Figure 25: HOBOS Side-By-Side Measurement Plots; Left-Pressure, Right- Temperature.

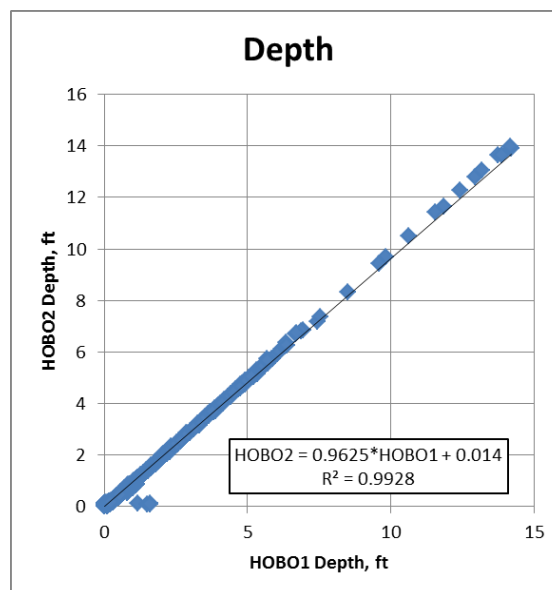


Figure 26: HOBOS Side-By-Side Measurement Depth Plot.

Much of this study was conducted when central and western Oklahoma were experiencing drought conditions. Table 9 shows the monthly rainfall at the Norman Mesonet station (No. 121), which is located less than a mile southwest of the watershed, for the months extending from January 2010 to March 2015. The average monthly precipitation for the years 1971-2000 is also provided. Note that in 2010, Norman received only 29.23 inches, or 78% of the normal annual rainfall. In 2011, only 27.56 inches, or 74% of the normal annual rainfall was received, and in 2012 only 22.80 inches, or 61%, was received. 2013 was a wet year with 47.17 inches, or 126% of the normal annual rainfall, but 2014 was the driest year of the study, with only 22.49 inches, or 60.1% of the normal annual rainfall. The rainfall over the 5 year period from 1010-2015 was 149.25 inches, or 79.8% of the normal rainfall for the five year period.

*Table 9: Monthly Rainfall Data for Norman, Oklahoma; Jan2010 – Mar2015. (OCS, 2015)*

Year	Monthly Rainfall (in) for the Norman Mesonet Station (Sta. No. 121)												Total
	Jan	Feb	Mar	Apr	May	Jun	Jul	Aug	Sep	Oct	Nov	Dec	
2010	1.32	3.74	1.21	3.03	3.30	4.03	5.55	0.72	4.05	1.40	0.71	0.17	29.23
2011	0.06	1.00	0.09	2.28	6.99	2.35	0.34	2.06	2.03	4.92	3.87	1.57	27.56
2012	1.58	0.91	5.95	2.88	2.57	0.82	0.02	3.14	2.79	0.44	0.94	0.76	22.80
2013	1.00	3.64	1.11	8.27	7.69	4.16	9.56	2.73	2.39	3.84	2.52	0.26*	47.17
2014	0.10	0.26	2.05	1.01	0.96	4.58	3.76	1.34	0.96	2.98	3.52	0.97	22.49
2015	1.64	0.17	2.42										
1971-2000 Normal	1.44	1.84	3.16	3.25	5.36	4.70	2.83	2.51	3.95	3.75	2.51	2.08	37.39

\*-Unavailable on Mesonet; Calculated from daily data for the month.

The presence of the drought was revealed in the HOBO data as well. Figure 27 shows the HOBO pressure and temperature plots for the Rock Creek site. Note the periods of large fluctuations in temperature, similar to the fluctuations observed in

Figure 17 for the Little River at 60<sup>th</sup> NE site, indicating exposure to the air. At the Rock Creek site, the exposure did not occur because the HOBO was moved. It occurred because the creek went dry.

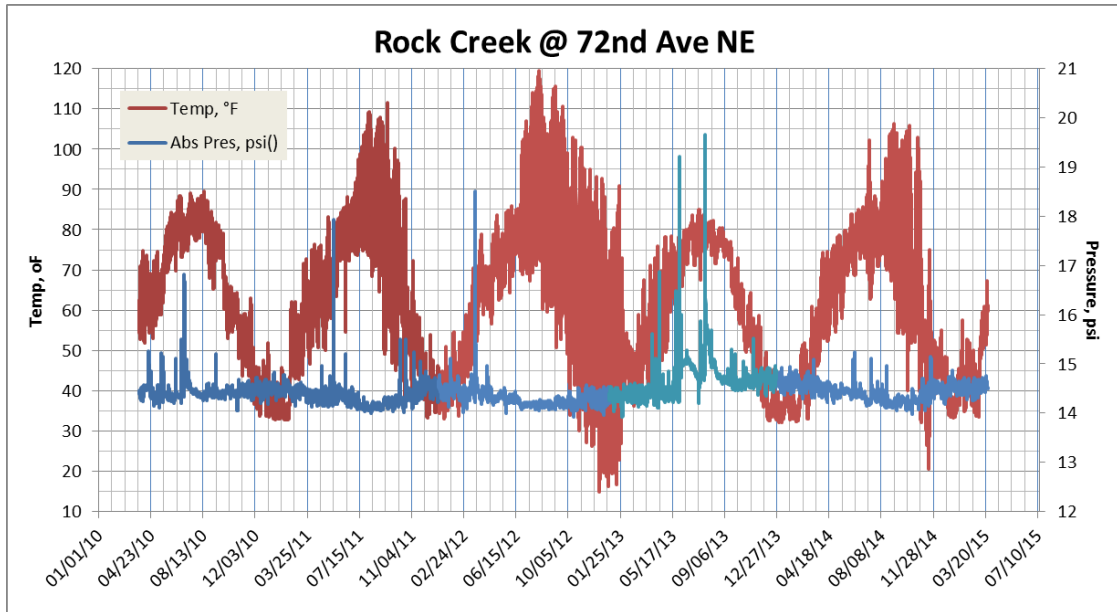


Figure 27: Temperature and pressure plots for the Rock Creek at 72<sup>nd</sup> Ave NE site.

The Rock Creek site is not the only site that went dry during the study. The North Fork site, the Dave Blue Creek site, and the Little River at Porter site all went dry at some point during the study. The only reason that the Little River at 60<sup>th</sup> site did not go dry was because the HOBO is located in a deep pool, and the Elm Creek site did not go dry because it is downstream of Lake Draper and seems to receive a constant supply of seepage from the dam.

Using the HOBO temperature data together with the calculated depth data, the number of days that the channel at each site was dry was estimated. The results are shown below in Table 10. Note that in the first year of the study, none of the sites went

dry. Four sites went dry in 2011 and the consecutive years of below normal rainfall resulted in an increase in the number of days the channels were dry in 2012, with Dave Blue Creek being dry 241 days.

The above normal rainfall in April (8.27 inches) and August (9.56 inches), 2013, provided some relief, especially for the Little River, which did not go dry at all in 2013, but in 2014 all four sites again went dry with Little River at Porter only being dry for 10 days, but Dave Blue Creek being dry for 162 days.

*Table 10: Number of days that the study sites went dry, by year.*

Number of Days Dry				
Year	North Fork	Rock Creek	Dave Blue Creek	Little River at Porter
2010	0	0	0	0
2011	23	91	115	51
2012	132	148	241	97
2013	59	15	81	0
2014	144	77	162	10

***iii. Discharge Measurements and Rating Curves***

The HOBO stage data provides a 5-year record of the water depth in the tributaries of Lake Thunderbird. For these data to be more useful, from a water resources perspective, however, it was necessary to develop discharge rating curves for the sites. This required performing discharge measurements at each of the seven sites, over a range of discharges, which was more effectively accomplished at some sites than at others.

The Marsh McBirney flow meter was used to measure low and medium discharges at all sites in 2010, with a few additional measurements being recorded in 2012. Use of the ADCP for measuring large discharge events was limited to three of the sites, Little River at 60<sup>th</sup>, Little River at Porter, and Rock Creek. Reasons for using the ADCP at only three of the seven sites include the relative difficulty in deploying the trimaran from bridges on incised channels, the relatively small size of the channels in the study, and the infrequent occurrence of measurable flows due to the drought conditions.

Initially, it was thought that measurements could easily be taken at multiple sites, when the infrequent storms, large enough to create significant measurable discharge, occurred. In fact, during one event, on May 20, 2011, discharge measurements were taken at the Little River at 60<sup>th</sup> and Rock Creek sites. Moving from site to site however proved more difficult than initially thought. The set-up for taking ADCP measurements, with GPS-RTK, is both fairly difficult and time consuming, especially for neophyte users, with very little, to no, experience operating ADCPs. Although valuable data were collected during this event, it was inefficient due to the time required to set-up.

Since valuable measurement time was lost in moving to, and setting up at, multiple sites, and the window for measuring the high flows associated with rainfall events is limited due to short lag and recession times, it was decided that for future events, measurements would be taken at just one site, and the different sites could be measured during separate events. The drought, which reduced the number of measurable events, was not anticipated. With the total number of significant discharge

events reduced, combined with the need for sediment data to complete Part II of the study, this resulted in data collection efforts using the ADCP being focused primarily at the Little River at 60<sup>th</sup> site.

The Little River site was selected as the primary site for sediment measurements over the other sites in the study, because it has the largest drainage area, and thus the biggest channel in the study. The initial presence of the OCC staff gauge, and monitoring site, as well as the remoteness of the site, with little traffic (making for a safe site), contributed to the decision.

Table 11 shows the total number of discharge measurements taken at each site. A total of 90 discharge measurements were taken at the sites using the Marsh McBirney flow meter and 47 measurements were taken using the ADCP. Of the 137 discharge measurements taken during the study, 61 of them (45%) and 38 of the 47 ADCP measurements (80%) were taken at the Little River at 60<sup>th</sup> Ave NE site.

*Table 11: Number of discharge measurements taken at each site.*

Site	ADCP	MMB
Little River @ 60th	38	23
Little River @ Porter	7	15
Hog Creek	0	8
Rock Creek	2	10
Elm Creek	0	11
North Fork	0	13
Dave Blue Creek	0	10
Total	47	90

ADCP-Acoustic Doppler Current Profiler  
MMB-Marsh McBirney Flow Meter



Note that seven discharge measurements were taken using the ADCP at the Little River at Porter site. Porter was at one time a state highway, and it is a fairly high traffic road, but utilities and road repair work south of the site resulted in the road being closed for a period of time. Fortunately, a number of measurable events occurred during the road closure, allowing for safe collection of the required data at the site.

As with the HOBO raw data, the raw discharge data is too extensive to include in this dissertation, even as an Appendix, but may be obtained from the author, Dr. Kolar, or Dr. Nairn upon request. Summaries of the data, including the stage-discharge measurements (Table D.1.1) and estimates of the discharge using the site geometry and Manning's equation (Table D.1.2) are included in Appendix D.

Figure 28 shows the stage-discharge rating curve for the Little River at 60<sup>th</sup> Ave NE site. The plot is typical of the plots for which ADCP data were collected, showing the measurements made with the Marsh McBirney flow meter as blue diamonds, measurements made with the ADCP as red squares, and discharge estimated using Manning's equation as purple x's. Discharges measured with the Marsh McBirney flow meter ranged from 2.8 cfs to 123 cfs, and discharges measured with the ADCP ranged from 31.5 cfs to 3,580 cfs. Notice that in regions of overlap, the discharges measured with the ADCP seem to agree very well with the discharges measured using the Marsh McBirney flow meter.

A regression line through all of the measured data, including measurements taken using the Marsh McBirney and the ADCP, has a coefficient of determination ( $R^2$ ) value of 0.915, showing excellent fit of the data. Because of the strong relationship, and

the wide range of discharges that were measured, the regression line was deemed to be acceptable as a rating curve for the site.

The discharge estimates using Manning’s equation were obtained using the channel geometry recorded in the site surveys and varying “n” at each stage until the estimated discharge matched the discharge given by the regression line. That is why the purple x’s lie directly on the regression line. Matching the regression line required adjusting Manning’s “n” from 0.5 at the lower discharges, and rapidly falling to 0.05 and then to 0.04 (Appendix D, Table D.1.2).

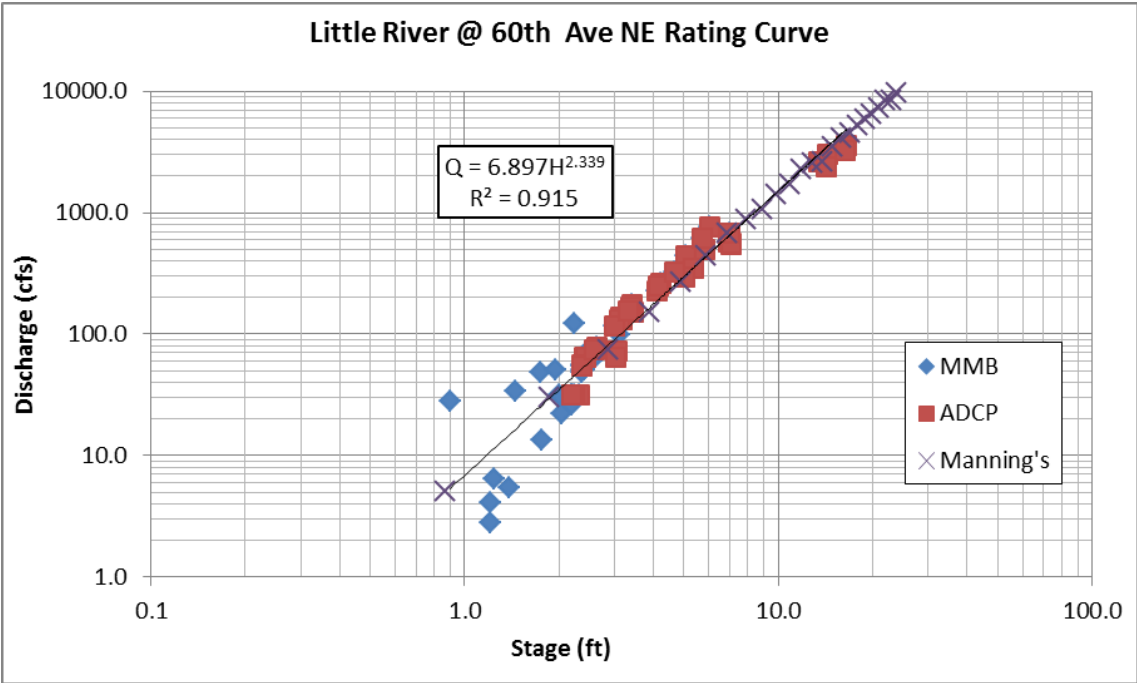


Figure 28: Little River at 60<sup>th</sup> Ave NE stage-discharge rating curve.

Figure 29 shows a plot of the Manning’s “n” values obtained in this matter versus the hydraulic radius of the channel cross section at the corresponding stage. The dashed lines on the plot show the Manning’s “n” for various classes of grass lined

channels, as presented in Strum (2001), using the following equation developed by Kouwen et al.(1969):

$$n = \frac{R^{1/6}}{a_0 + 16.4 \log(R^{1.4} S^{0.4})} \quad (4)$$

where

n = Manning's coefficient

R = Hydraulic radius (m)

S = Slope

$a_0$  = Vegetal Retardance Class dependent constant

= 24.7 for Class A

= 30.7 for Class B

= 36.4 for Class C

= 40.0 for Class D

= 42.7 for Class E

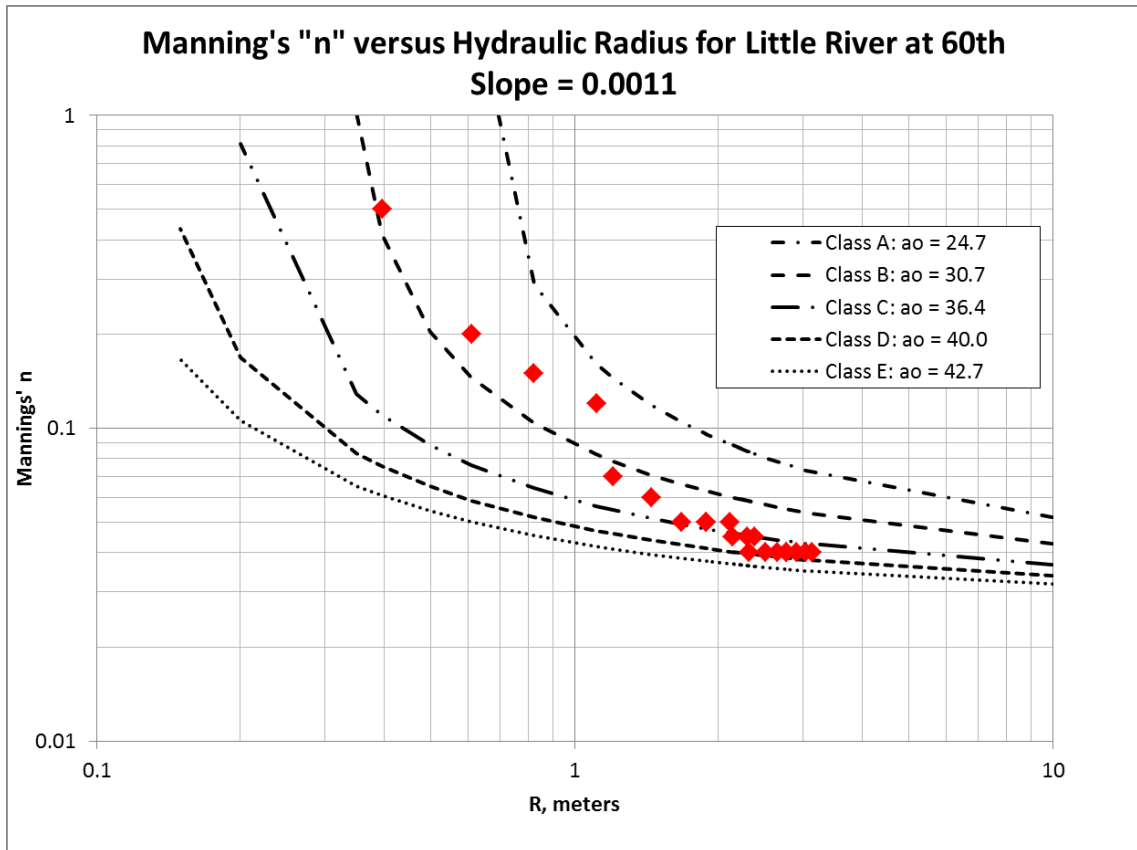


Figure 29: Manning's "n" versus hydraulic radius at Little River at 60<sup>th</sup> Ave NE.

It may be seen that, even though the Little River is not a grass lined channel, Manning's "n" shows a similar response to increasing hydraulic radius, although it appears to drop off more quickly and approach an asymptote of 0.04 at lower R-values. This difference may perhaps be explained by the lack of grass in the main channel reducing the depth at which the bed roughness is significant. In any case, the asymptotic 0.04 value agrees well with Rosgen's (1996) reported bankfull "n" value of 0.038 for Type G5 channels like Little River, and with 0.046 estimated using Cowan's (1956) procedure, as presented by Chow (1959).

Figure 30 shows the stage-discharge rating curve for the Little River at Porter site, the second site at which the ADCP was used to measure discharges at higher

stages. Once again, the measurements made with the Marsh McBirney flow meter are shown as blue diamonds, measurements made with the ADCP as red squares, and discharge estimated using Manning's equation as purple x's.

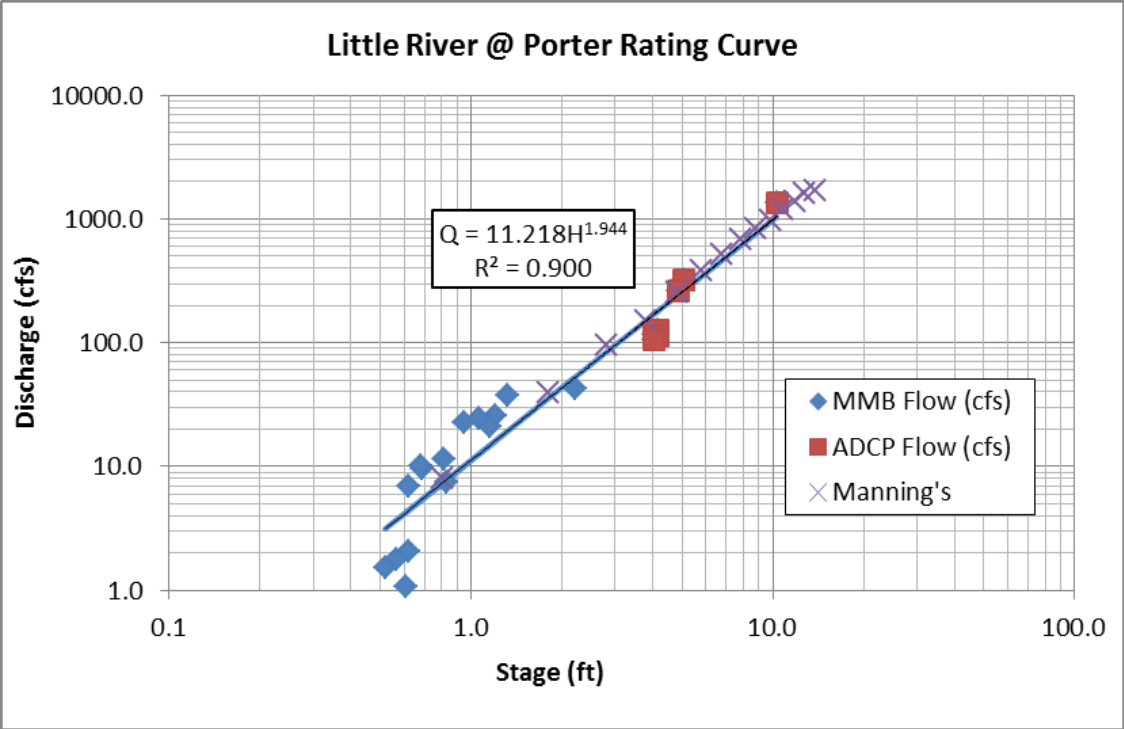


Figure 30: Little River at Porter stage-discharge rating curve.

The discharge measured using the Marsh McBirney flow meter varied from 1.1 cfs to 43 cfs, and the discharge measured using the ADCP varied from 106 cfs to 1,340 cfs. Although there was no overlap of measurements between discharges measured with the Marsh McBirney and discharges measured with the ADCP, a regression line through the data has a coefficient of determination ( $R^2$ ) value of 0.900, once again showing good fit of the data. As with the Little River at 60th site, because a wide range of discharges were measured at the Little River at Porter site, the regression line was considered acceptable as a rating curve for the site.

The discharge estimated using Manning's equation was once again "calibrated" to the regression line, by varying "n" at each stage until the estimated discharge at the stage matched the discharge given by the regression line. Matching the regression line at the Little River at Porter site required adjusting Manning's "n" to 0.12 at the lower discharges, with the value dropping rapidly to 0.08 (Appendix D, Table D2.2), which is double the lowest value observed at the Little River at 60<sup>th</sup> site. It is also typical of values for G5 channels reported by Rosgen (1996). This may perhaps be explained by the channel geometry at the site, as there is a sharp bend in the channel just downstream of the cross-section. There is also a small amount of rip-rap in the channel and on one bank. Accounting for these features in Cowan's (1956) procedure results in an estimated "n" value of 0.078.

Figure 31 shows a plot of the Manning's "n" values obtained in this matter versus the hydraulic radius of the channel cross section at the corresponding stage, with the dashed lines on the plot again showing the Manning's "n" for various classes of grass-lined channels, as presented in Strum (2001), and the equation developed by Kouwen et al. (1969). Note that the estimated "n" values fall within the bounds of the grass-lined plots, but the trend is different, i.e., it appears to be shifted up and to the left of the grass-lined channel plots.

The last site for which the ADCP was used to measure higher stage discharges was the Rock Creek at 72nd site. The stage-discharge rating curve for the site is shown in Figure 32. As with the previous plots, the measurements made with the Marsh McBirney flow meter are shown as blue diamonds and measurements made with the ADCP are shown as red squares. However, unlike in the other plots, estimates are

provided for two values of “n”, and two regression lines are shown, for reasons discussed below.

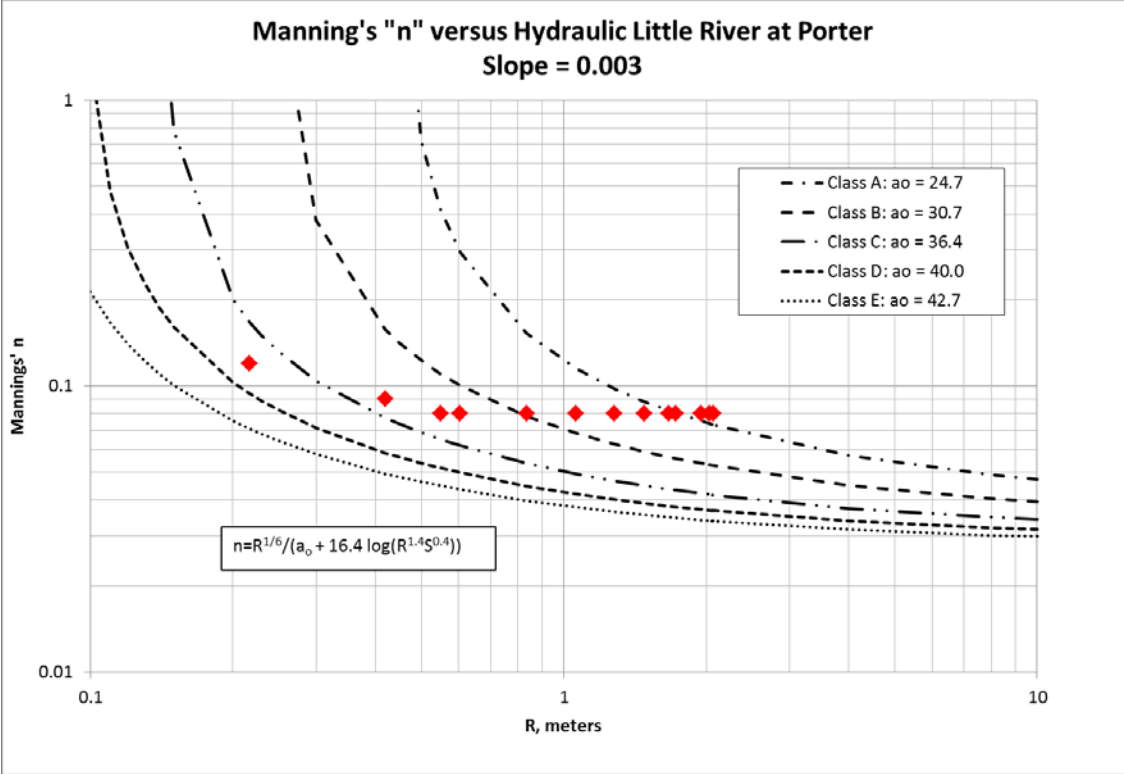


Figure 31: Manning’s “n” versus hydraulic radius at Little River at Porter.

Discharges measured at Rock Creek using the Marsh McBirney flow meter varied from 0.37 cfs to 19.9 cfs, and the two discharges measured using the ADCP, were 106 and 107 cfs. Once again there is no overlap in the measured data, but the regression line through the data (the solid black line in Figure 32) has a coefficient of determination ( $R^2$ ) of 0.911, showing very good correlation of the data. However, at the Rock Creek site, unlike at the Little River sites, the ADCP measurements were limited to a relatively moderate high-flow stage, with the maximum measured discharge occurring at a stage of 4.7 feet (1.4 meters).

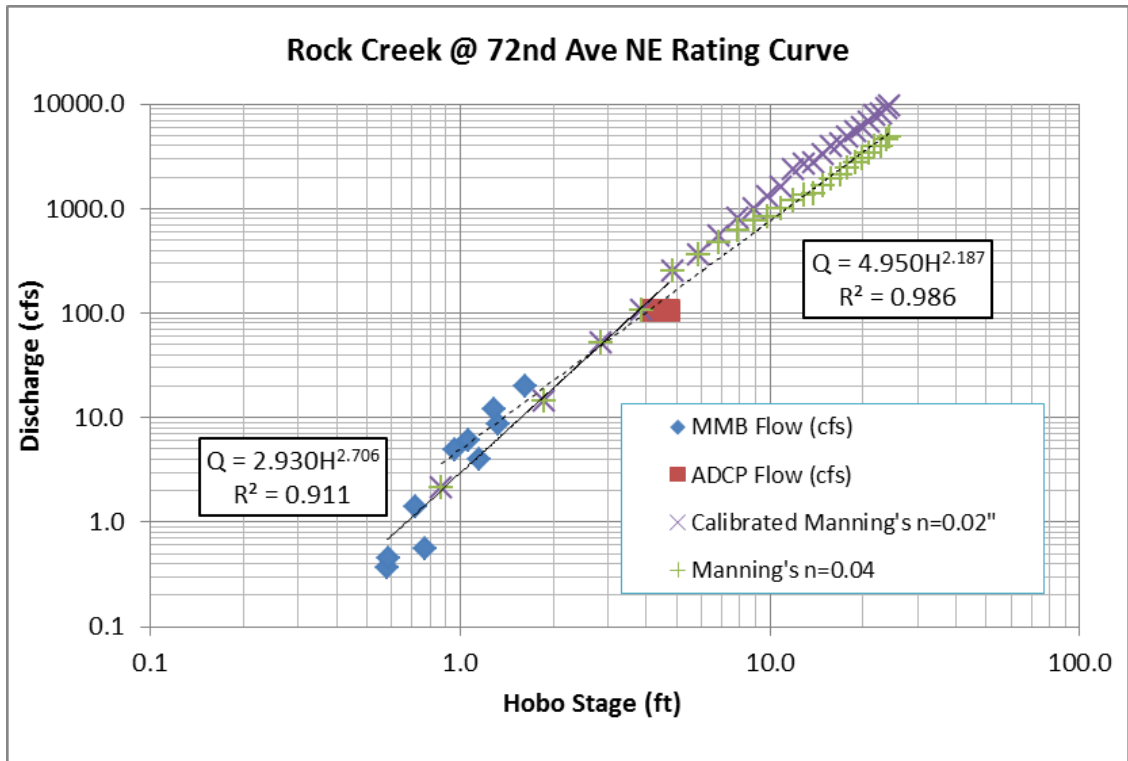


Figure 32: Rock Creek at 72<sup>nd</sup> stage-discharge rating curve.

The discharge estimated using Manning’s equation was once again “calibrated” to the regression line, by varying “n” at each stage until the estimated discharge at the stage matched the discharge given by the regression line, shown as purple x’s in Figure 32. Up to the stage of the largest measured discharge, the “n” required to achieve the calibration ranged from an initial value of 0.55, dropping to 0.04 at the higher stages (Appendix D, Table D.3.2). However, at stages above the measured data, calibration to the straight-line extrapolated regression curve required reducing “n” to 0.02, a value that is significantly lower than would be expected for a G5 channel such as Rock Creek. Estimates of the discharge greater than 4.7 feet (1.4 meters) were therefore obtained using a Manning’s “n” value of 0.04, typical of G5 channels, as shown by the green + signs in Figure 32.



The regression line through these data (dashed black line) has a coefficient of determination ( $R^2$ ) of 0.986, again showing very good correlation of the data, but this is not surprising, given that the upper end of the data used to define the line was calculated using the same equation. Note however, that the slope of the “modified” regression line determined in this manner is slightly less than the slope of the regression line of the measured data, resulting in a significant difference in the estimated discharges. This flattening of the slope at higher stages is a common characteristic of stage-discharge relationships. So, based on experience and judgment (as supplemented by the literature), and acknowledging that there is inherent uncertainty in estimating discharge outside of the measured data range, the modified regression line was used as the rating curve in this study to estimate discharges at the Rock Creek site.

As mentioned previously, the ADCP was not used to measure high stage discharges at four of the study sites - Hog Creek, Elm Creek, North Fork and Dave Blue Creek - and thus required development of rating curves beyond the data range. The rating curve for the first of these sites, Hog Creek at SE119<sup>th</sup> is shown in Figure 33.

The measured discharges are again shown by blue diamonds, and range from 2.93 cfs to 49.9 cfs. With an  $R^2$  of 0.919, the regression line for the measured data (solid black line) shows very good correlation with the data. Calibrating “n” to the regression line required varying it from 0.07, to 0.06, and to 0.05 for stages greater than 2 feet (Appendix D, Table D..2). Although this is slightly higher than reported for G5 channels, Rosgen (1996) reports “n” values of 0.048 for B3 channels, and even though Hog Creek is a sand and silt dominated channel, the cross section for the site is located downstream of a bridge, where rip-rap is present in the channel, so 0.05 is a reasonable

estimate of “n” for the site. Because of this, the regression line generated using the data was considered acceptable for use as the rating curve for the Hog Creek site.

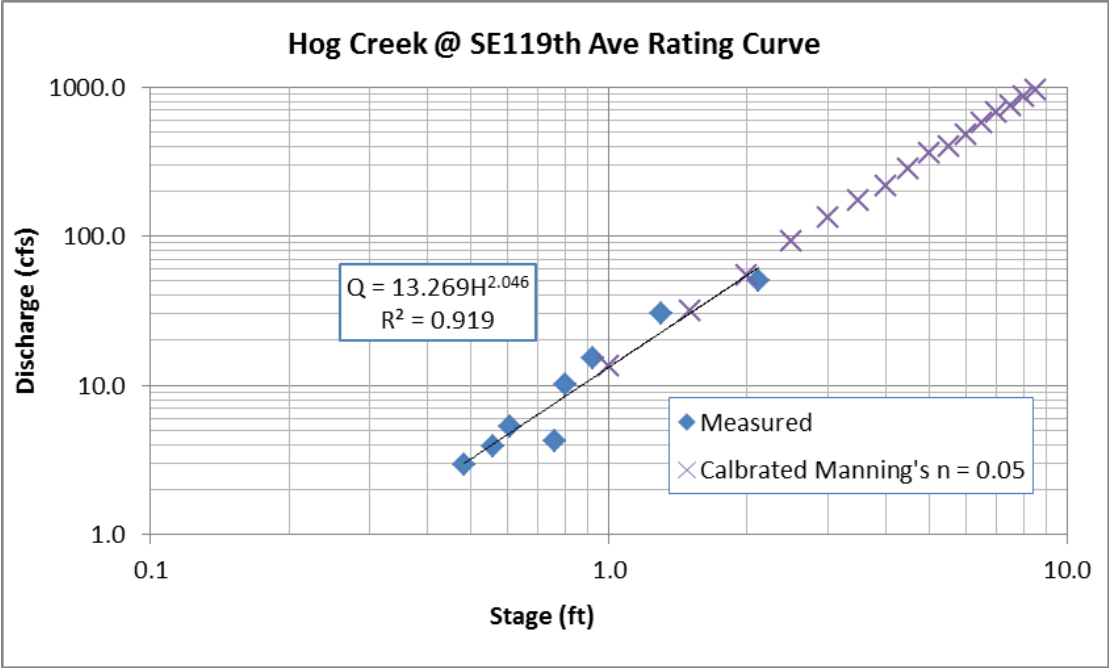


Figure 33: Hog Creek at SE119<sup>th</sup> stage-discharge rating curve.

Figure 34 shows the stage-discharge rating curve for the Elm Creek at Indian Hills site, the second site at which the ADCP was not used to measure high stage discharges. Again, the measured data are shown as blue diamonds. Discharge measurements ranged from 1.44 cfs to 25.64 cfs. The  $R^2$  value of the regression line from the measured data (solid line) is 0.8945, showing a fairly good relationship of the data. However, when calibration of “n” to the regression line was attempted, the “n” values required to match the extrapolated line dropped rapidly to less than 0.01, which is unrealistic, so that the extrapolated regression line of the data was deemed insufficient for use as a rating curve.

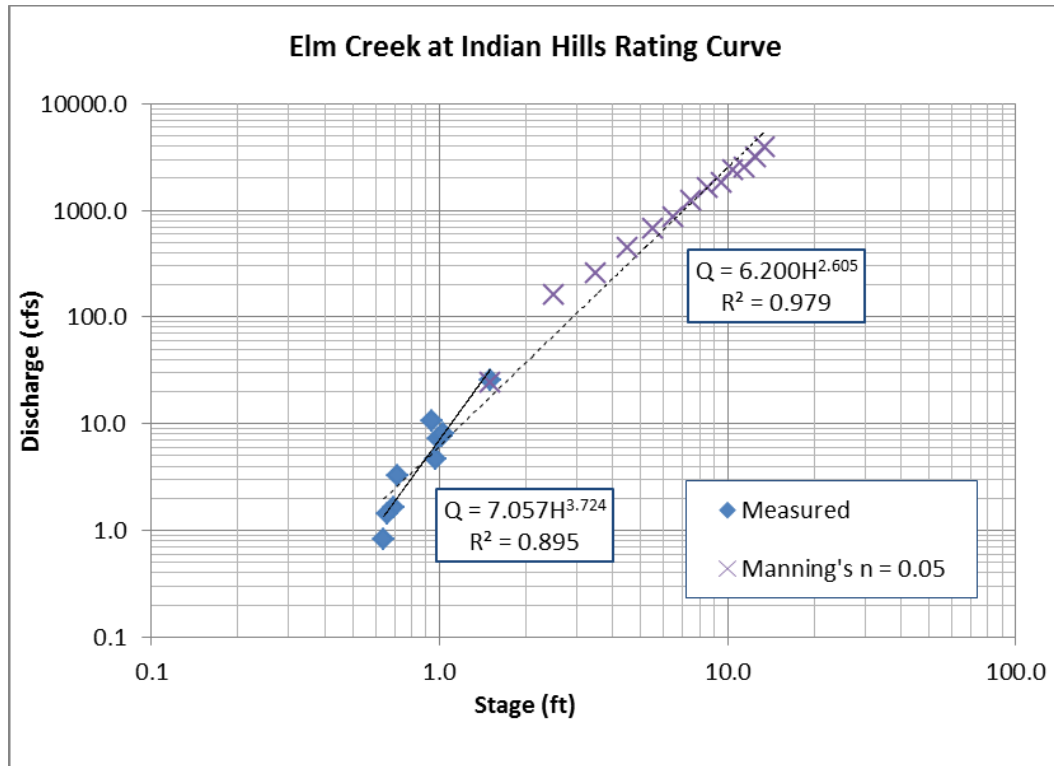


Figure 34: Elm Creek at Indian Hills stage-discharge rating curve.

The cross section for the Elm Creek site, like at the Hog Creek site, is located downstream of a bridge, and the channel is lined with rip-rap, so 0.05 is considered a reasonable estimate of “n” for the site, which was used to estimate the discharge, as shown by the purple x’s (Appendix D, Table D.5.2). Note that there is a flattening of the slope, similar to the one observed at the Rock Creek site.

Figure 35 shows the rating curve for the North Fork at Franklin site, the third site where the ADCP was not used to measure high stage discharges. Once again the measured discharges are represented by blue diamonds, and they range from 0.74 cfs to 46.90 cfs. The  $R^2$  value of the regression line from the measure data (solid black line), at 0.763, is not as good as the  $R^2$  observed previously at the other sites. Nevertheless, calibration of Manning’s “n” to the regression line was conducted as before and

required that “n” be set at 0.08, as shown by the purple x’s (Appendix D, Table D.6.2). The North Fork site is again located downstream of a bridge, but the channel bed is dominated by large irregular concrete slabs, so a Manning’s “n” of 0.08 is not unreasonable. Therefore, as with the Hog Creek site, the regression line generated using the data was considered acceptable for use as the rating curve at the North Fork site.

The final site where the ADCP was not used to measure high stage discharges was the Dave Blue Creek at 72<sup>nd</sup> Ave SE site. The stage-discharge rating curve for the site is shown in Figure 36. Measured discharges, shown as blue diamonds, range from 0.15 cfs to 19 cfs. The R<sup>2</sup> of the regression line of the measured data, at 0.6886, is the lowest observed in the study. This may be due to the extremely low discharges measured and possible error in measurement.

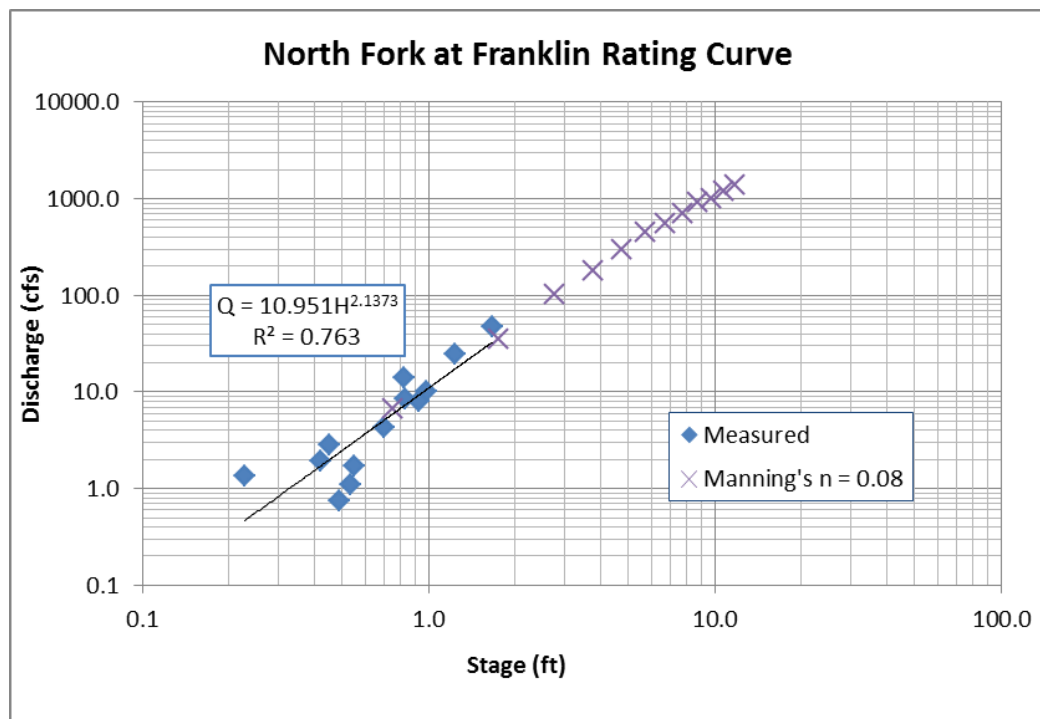


Figure 35: North Fork at Franklin stage-discharge rating curve.

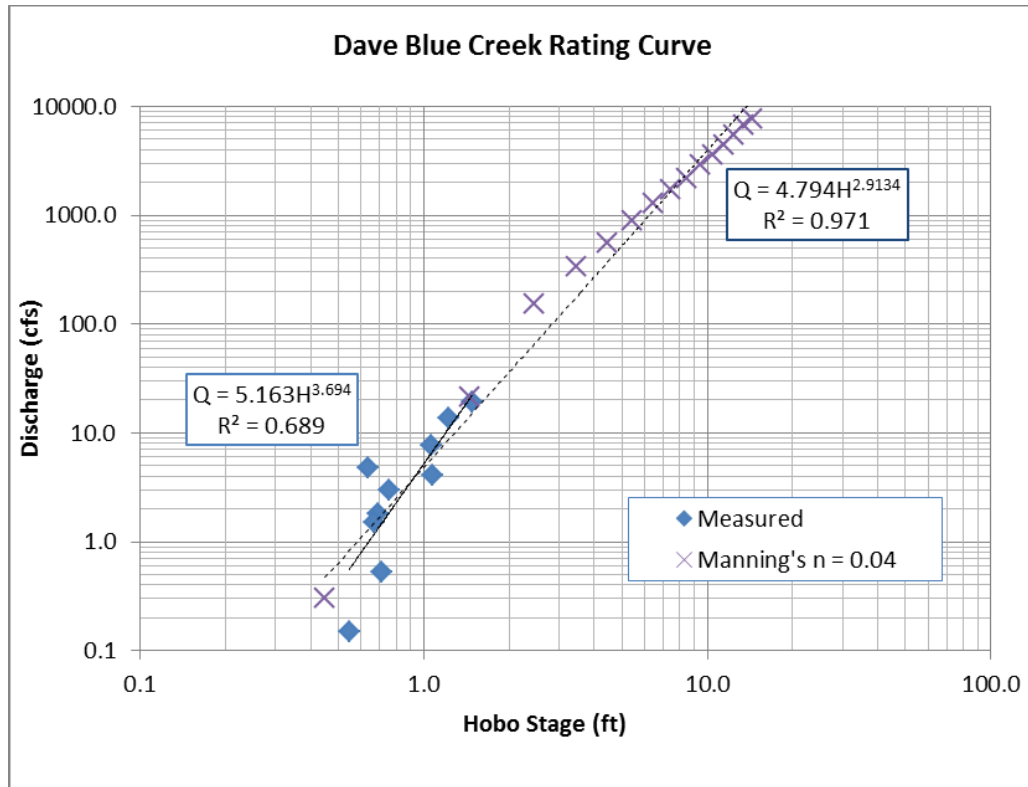


Figure 36: Dave Blue Creek at 72nd stage-discharge rating curve.

As with the Elm Creek site, attempts to calibrate “n” to the extrapolated regression line required setting “n” to unrealistically low values. Thus, the discharge estimates using Manning’s equation, shown by the purple x’s, assumed an “n” value of 0.04, as presented by Rosgen for B5 channels like Dave Blue Creek (Appendix D, Table D.7.2). As observed previously at other sites, the regression line through the measured and estimated data (dashed line), with an  $R^2$  of 0.971, has a flatter slope than the regression line through the measured data only. Again, noting the uncertainty of using rating curves for estimating discharges outside the measured range, the modified regression line was used as the rating curve at the Dave Blue Creek site.

Table 12 shows the coefficients and exponents of the stage-discharge rating curves developed for the study sites, and the coefficient of variation ( $R^2$ ) for the various

relationships. The values on the left are for the measured discharge regression lines, and the values on the right are for the modified regression lines developed using discharges estimated with Manning's equation and measured discharges. The values used in the current study are shown in bold. Using these values and the stage data collected by the HOBOS, continuous discharge plots were developed for each site. These discharge plots are provided below in Figures 37-43.

The maximum stage at four sites, Little River at 60<sup>th</sup>, Little River at Porter, Elm Creek, and North Fork, occurred on June 1, 2013. The peak stage observed at the Little River at 60<sup>th</sup> site was 26.86 feet, for an estimated discharge of 13,970 cfs (Figure 37). The peak stage observed at the Little River at Porter site was 15.64 feet, for an estimated discharge of 2,349 cfs (Figure 38). The peak stage observed at the Elm Creek site was 18.28 feet, for an estimated discharge of 12,018 cfs (Figure 41). And the peak stage observed at the North Fork site was 19.75 feet, for an estimated discharge of 6,431 cfs (Figure 42).

The maximum stage at the Rock Creek and Dave Blue Creek sites occurred on July 26, 2013. The peak stage observed at the Rock Creek site was 12.80 feet, for an estimated discharge of 1,307 cfs (Figure 39) and the peak stage observed at the Dave Blue Creek site was 16.15 feet, for an estimated discharge of 15,847 cfs (Figure 43). The maximum stage observed at the Hog Creek site was 8.14 feet on May 20, 2011, for an estimated discharge of 968 cfs (Figure 40), due to the fact that it was washed away sometime after April 25, 2013, probably on June 1, 2013. The large discharges observed at the Elm Creek and Dave Blue Creek sites appear to be unusually high, and highlight the need for validating the rating curves at larger discharges.

Table 12: Stage-Discharge rating curve coefficients and exponents.

Stage-Discharge Rating Curve Coefficients and Exponents; $Q = aH^b$						
Site	Measured			Modified		
	a	b	R <sup>2</sup>	a	b	R <sup>2</sup>
Little River @ 60th Ave NE	<b>6.8967</b>	<b>2.3388</b>	0.9148	---	---	---
Little River @ Porter	<b>11.2179</b>	<b>1.9435</b>	0.9004	---	---	---
Hog Creek @ SE 119th	<b>13.2690</b>	<b>2.0457</b>	0.9185	---	---	---
Rock Creek @ 72nd Ave NE	2.9304	2.7055	0.9105	<b>4.950</b>	<b>2.187</b>	0.986
Elm Creek @ Indian Hills	7.057	3.7236	0.8945	<b>6.200</b>	<b>2.605</b>	0.979
North Fork @ Franklin	<b>10.951</b>	<b>2.1373</b>	0.763	---	---	---
Dave Blue Creek @ 72nd Ave SE	5.163	3.6938	0.6886	<b>4.794</b>	<b>2.913</b>	0.971

Values in bold text were used for discharge estimates in the current study.

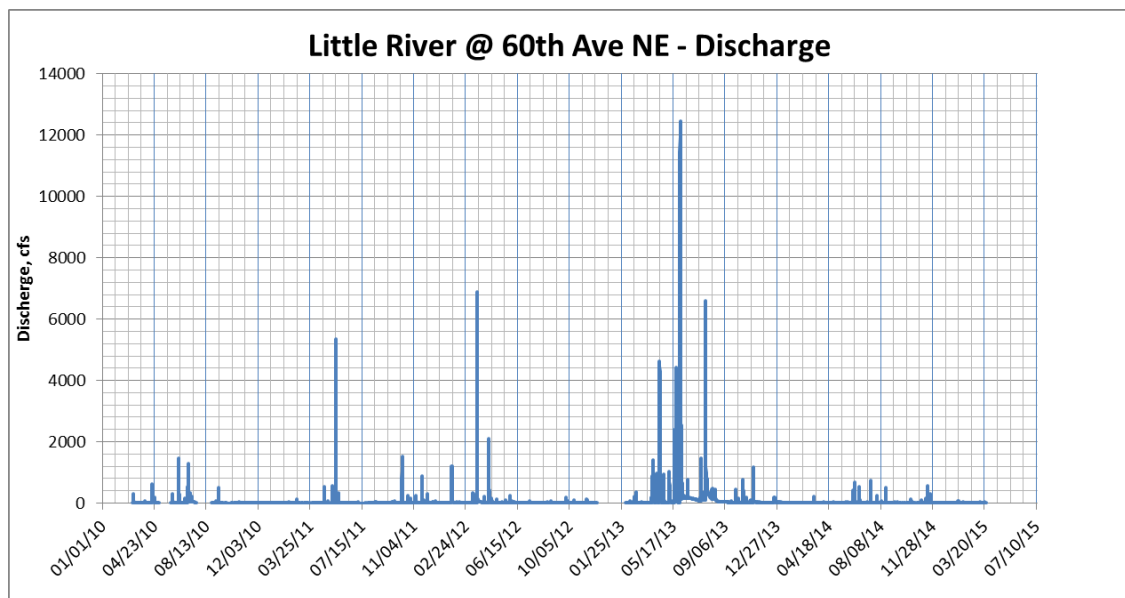


Figure 37: Little River at 60th Ave NE site discharge plot.

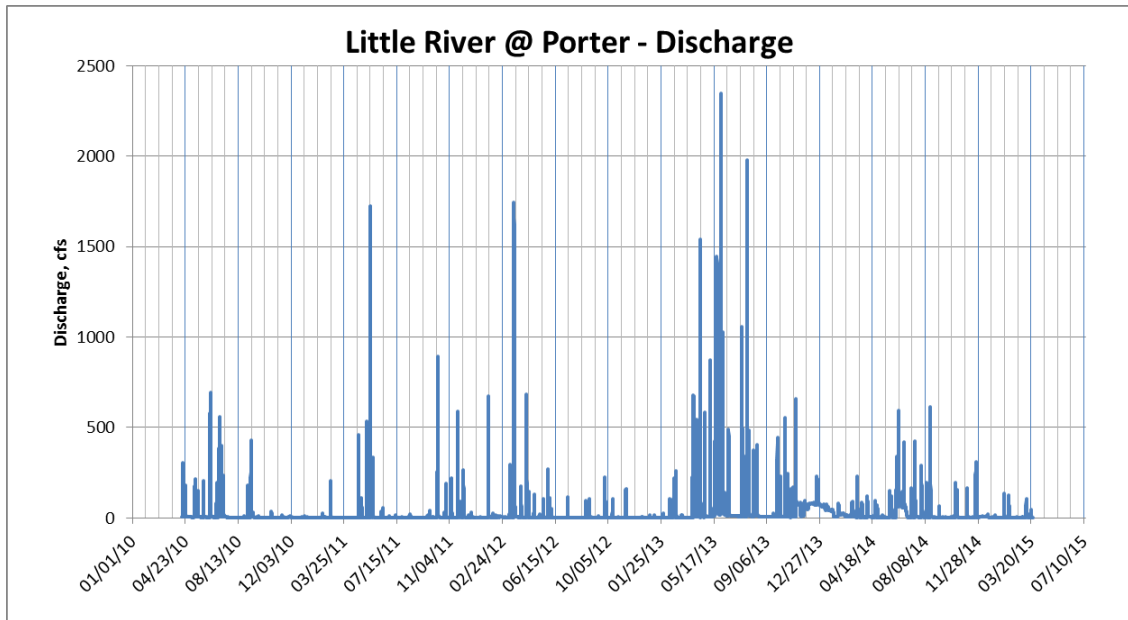


Figure 38: Little River at Porter site discharge plot.

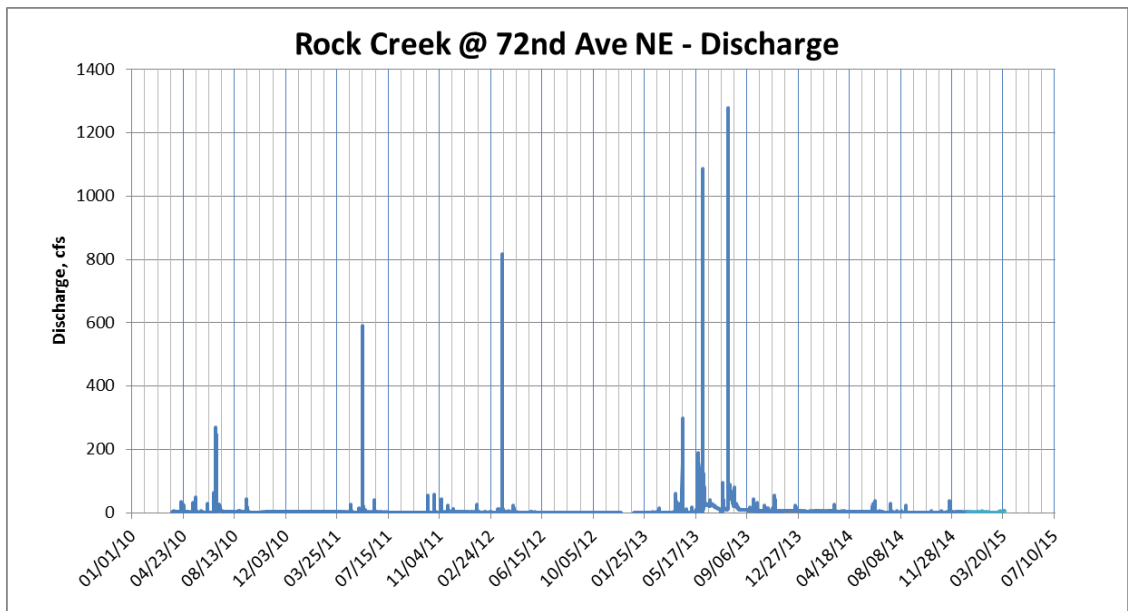


Figure 39: Rock Creek at 72nd Ave NE site discharge plot.



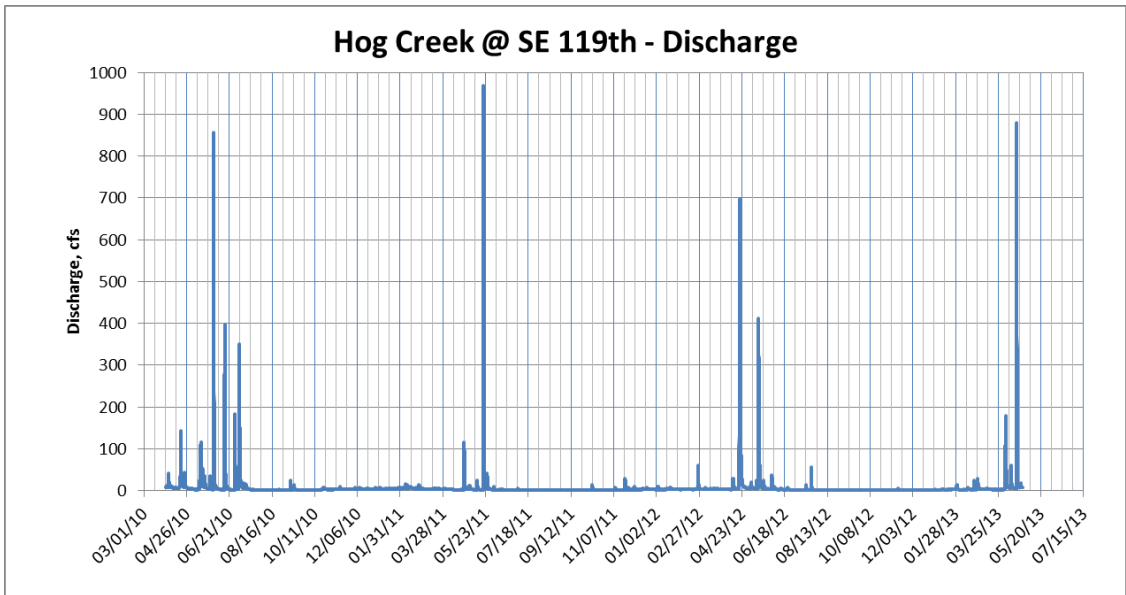


Figure 40: Hog Creek at SE 119th Ave site discharge plot.

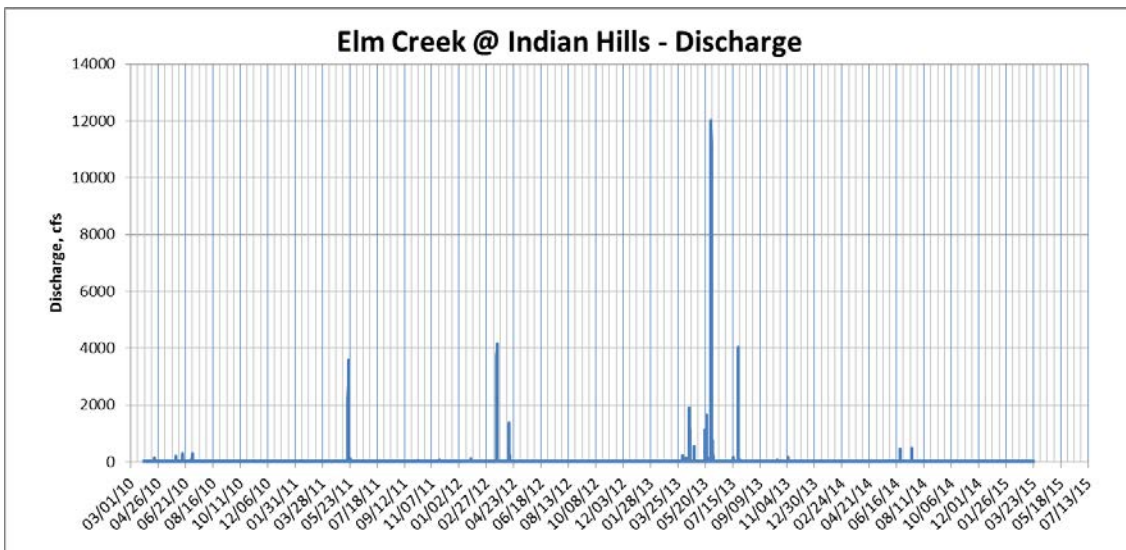


Figure 41: Elm Creek at Indian Hills site discharge plot.

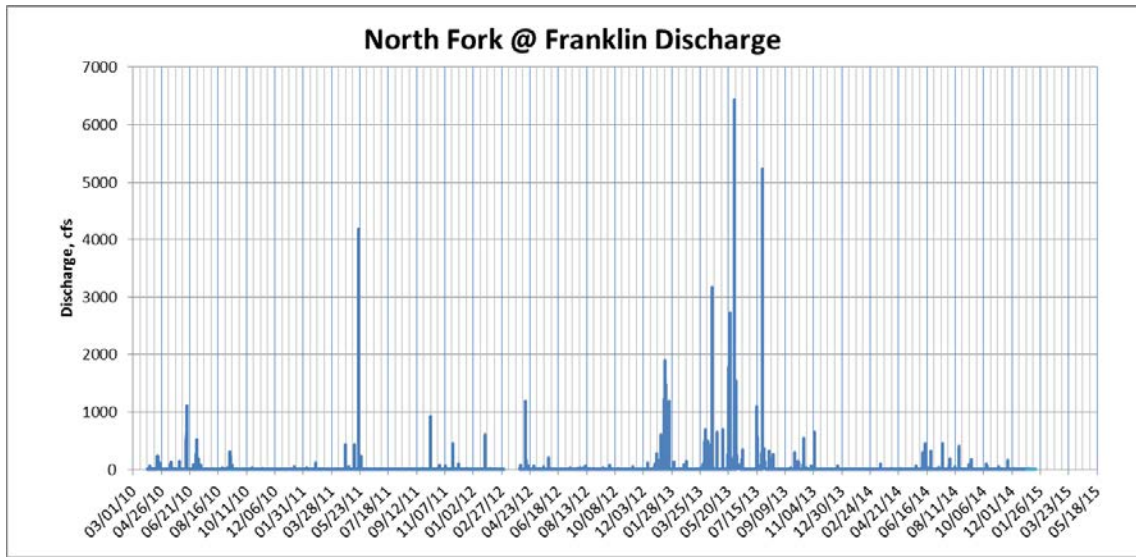


Figure 42: North Fork at Franklin site discharge plot.

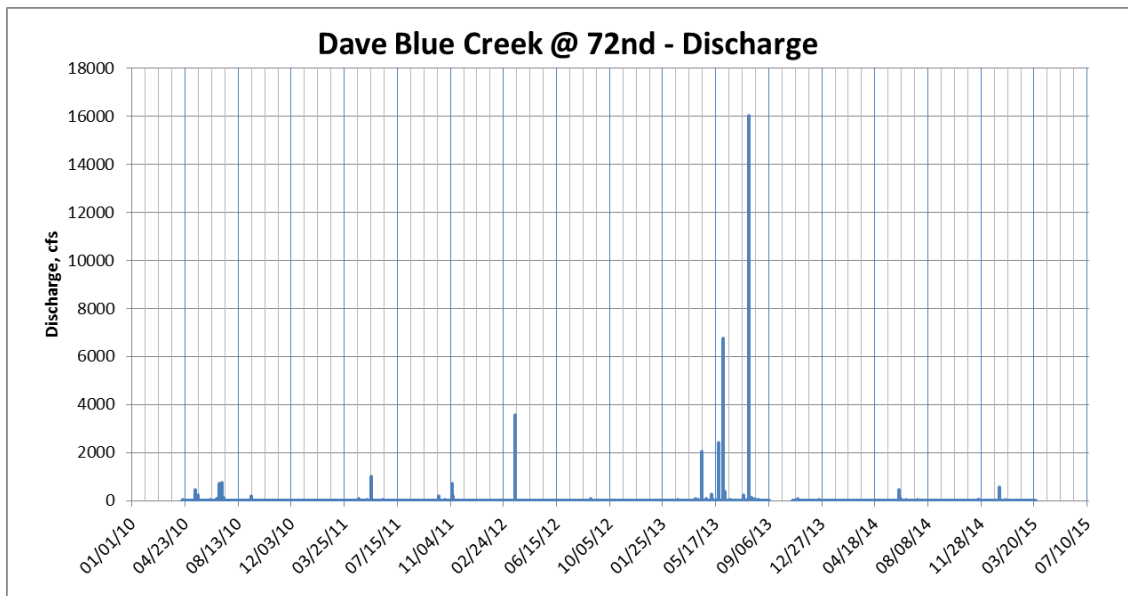


Figure 43: Dave Blue Creek at 72nd Ave SE site discharge plot.

*iv. Application of the Rating Curves*

Using the rating curves to estimate discharge, cumulative runoff was estimated for each site for the period March, or April, 2010 to March 2015 (except for the Hog Creek site, which was lost in April, 2013), as shown in Figures 44 to 50. It may be seen that the cumulative runoff at the sites was significantly larger in 2013, the only “wet” year during the study, than in any of the other four years.

At the Little River at 60th (Figure 44) and Rock Creek (Figure 45) sites, two of the three sites for which rating curves were developed using discharge data, the trends are similar, with the cumulative runoff for 2013 being approximately 5 times larger than the other years. The same trend is observed at North Fork at Franklin (Figure 46) and Dave Blue Creek (Figure 47), with the cumulative runoff for 2013 being roughly 6 times larger than other years at the North Fork site and 8 times larger at the Dave Blue Creek site. Note the relatively steep slopes following the storm events in early May and late June in 2013 at the Little River at 60th and Rock Creek sites. These increased slopes could potentially be a result of backwater from the lake. The increased slope is not observed at the North Fork at Franklin and Dave Blue Creek sites.

At the Little River at Porter (Figure 48) and Elm Creek (Figure 49) sites, the difference is not as pronounced. At the Little River at Porter site, the cumulative runoff in 2013 is 5 times larger than in 2010-2012, but only two and a half times the runoff in 2014. However, the steep slope observed in May, 2014 is not a result of increased discharge in the channel, but rather is suspected to be a result of backwater, due to activity occurring downstream, resulting in an increase in stage for the same discharge. If the slope in May were reduced to match the slopes seen in April and June, the cumulative runoff would be similar to that of 2010-2012. Because the HOB0 at Hog

Creek (Figure 50) disappeared in March 2013, and was not replaced, it was not possible to estimate the cumulative runoff in 2013 or 2014.

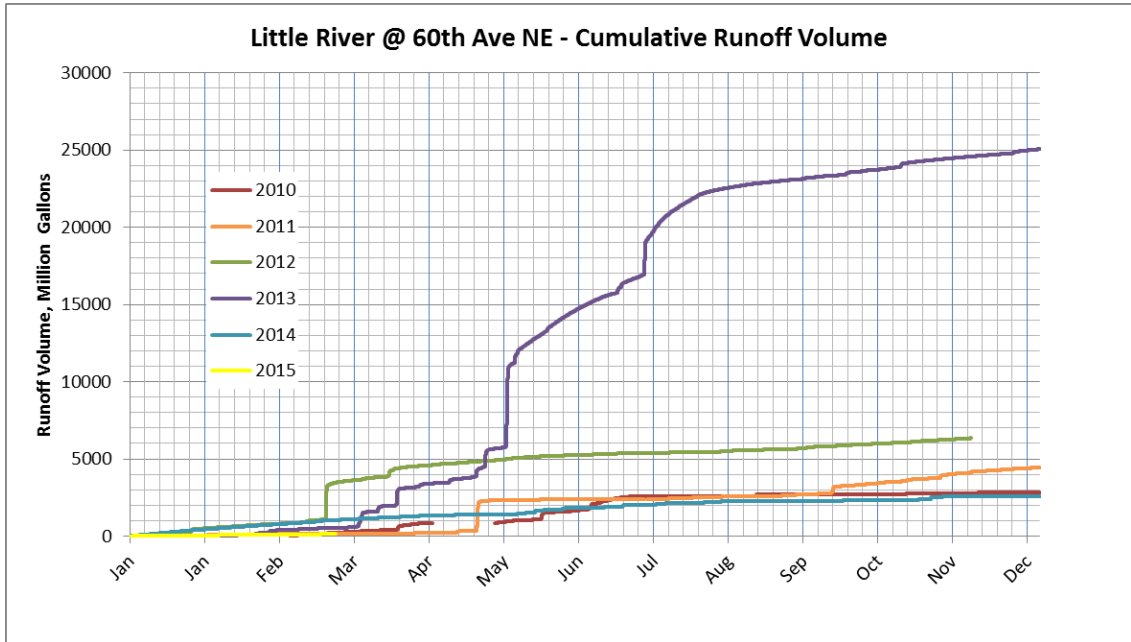


Figure 44: Cumulative Runoff Volume - Little River at 60<sup>th</sup> Ave, 2010-2014.

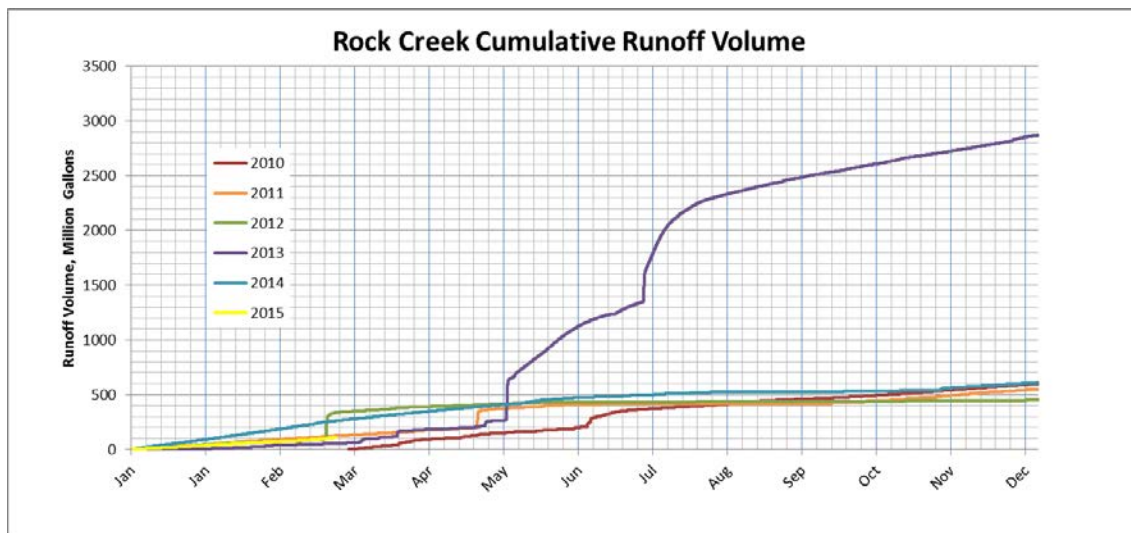


Figure 45: Cumulative Runoff Volume - Rock Creek, 2010-2014.

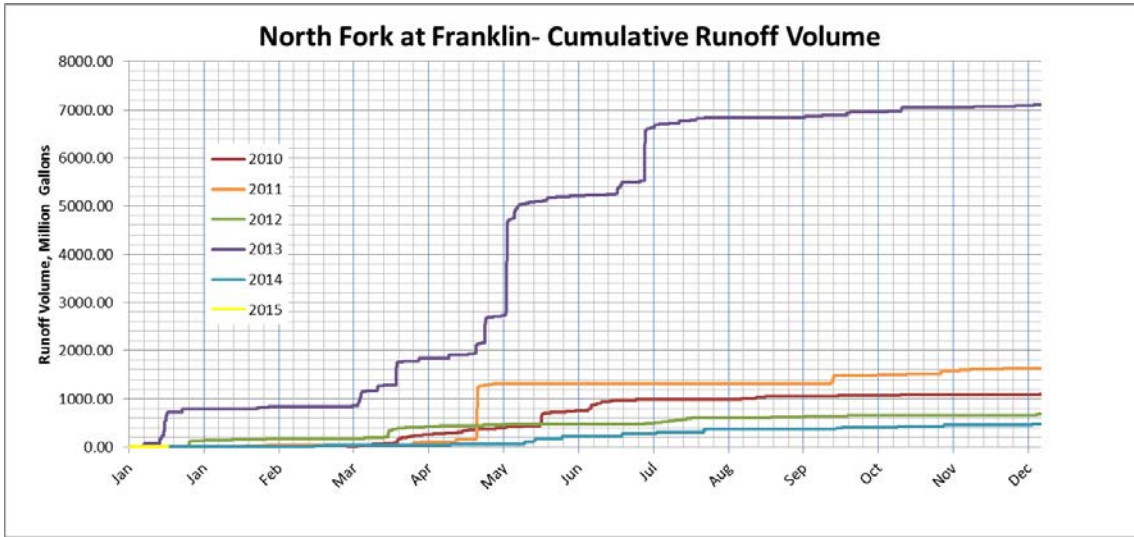


Figure 46: Cumulative Runoff Volume – North Fork at Franklin, 2010-2014.

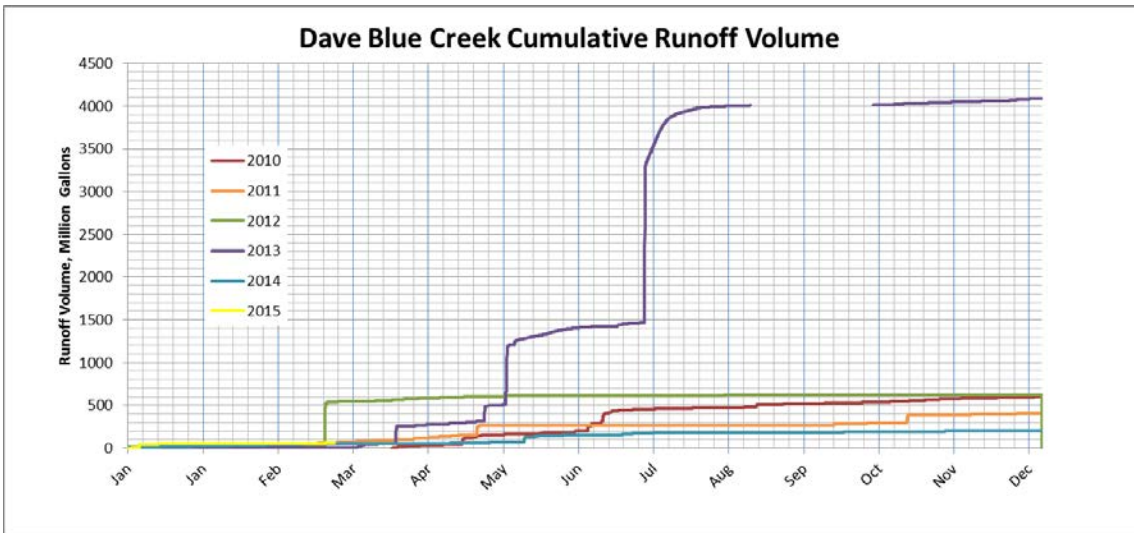


Figure 47: Cumulative Runoff Volume – Dave Blue Creek, 2010-2014.

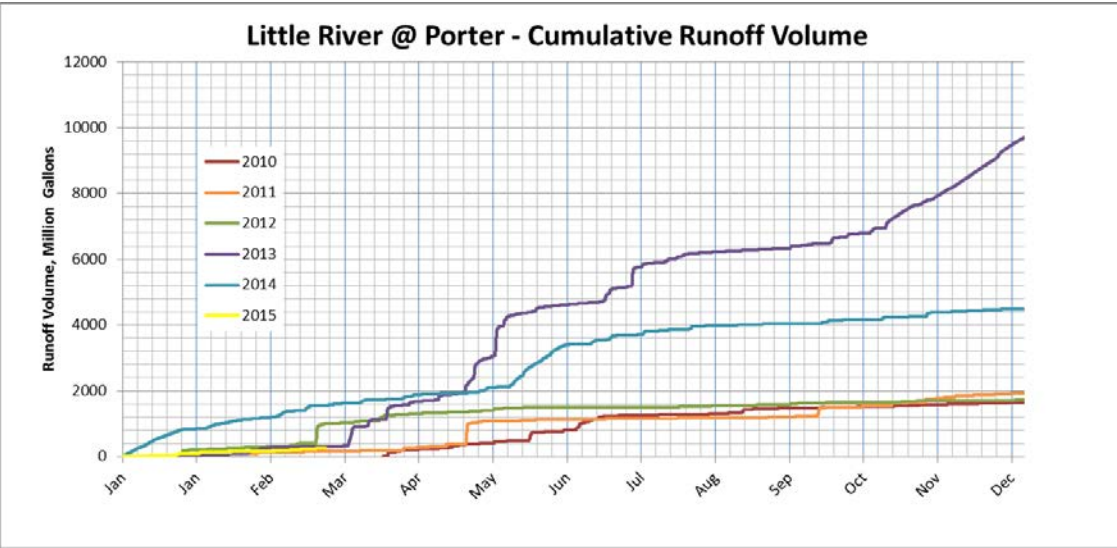


Figure 48: Cumulative Runoff Volume – Little River at Porter, 2010-2014.

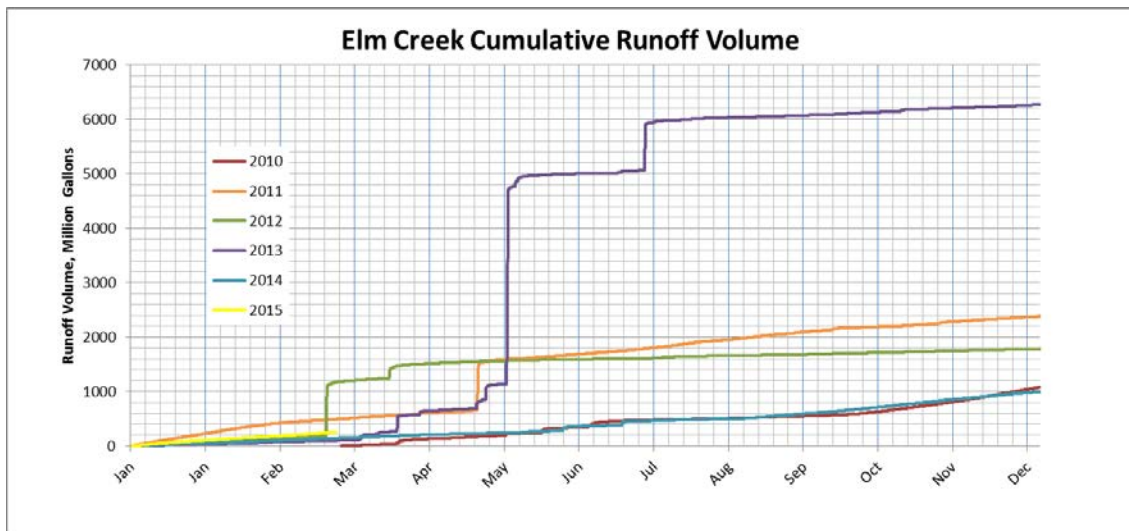


Figure 49: Cumulative Runoff Volume - Elm Creek, 2010-2014.

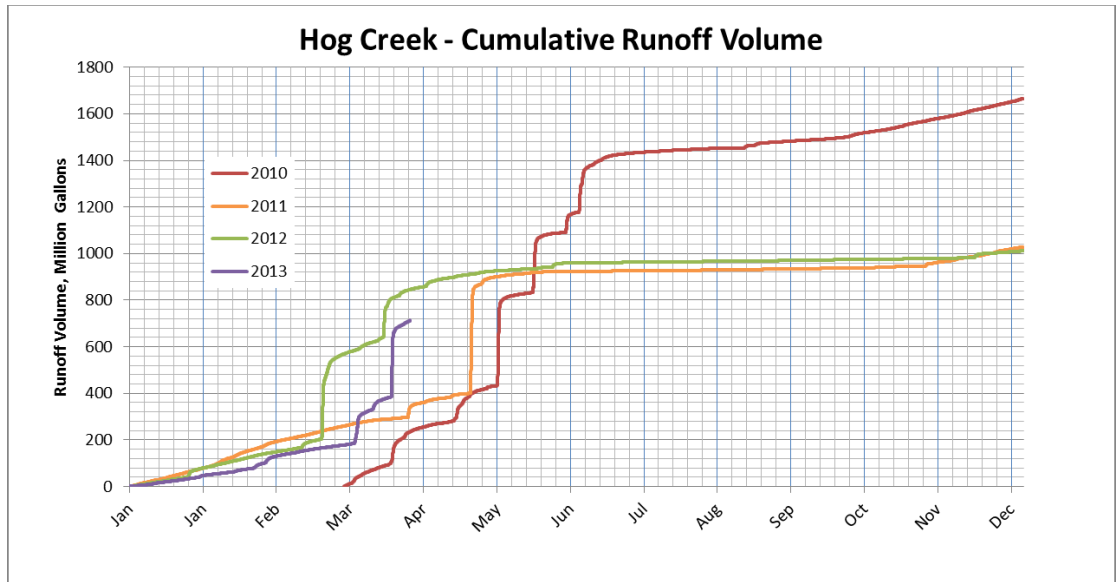


Figure 50: Cumulative Runoff Volume – Hog Creek, 2010-2013.

To further explore the data, to see if it may indicate the impacts that an extended drought could have on the runoff volume to Lake Thunderbird, the effects of antecedent conditions on runoff volume was evaluated. This was accomplished by looking at the volume of runoff at the Little River at 60<sup>th</sup> site generated by various storm events and investigating the effects of preceding rainfall on the results.

Figure 51 shows the 30 minute rainfall data recorded at the Norman Mesonet station (NRMN – Site No. 121) for the period of the study. It may be seen that the largest rainfall event during the study was nearly 5”, 9 events exceeded 2”, 15 exceeded 1.5”, 43 exceeded 1”, and 89 exceeded 0.5”. Only storms producing 1.5” or more were considered for this assessment.

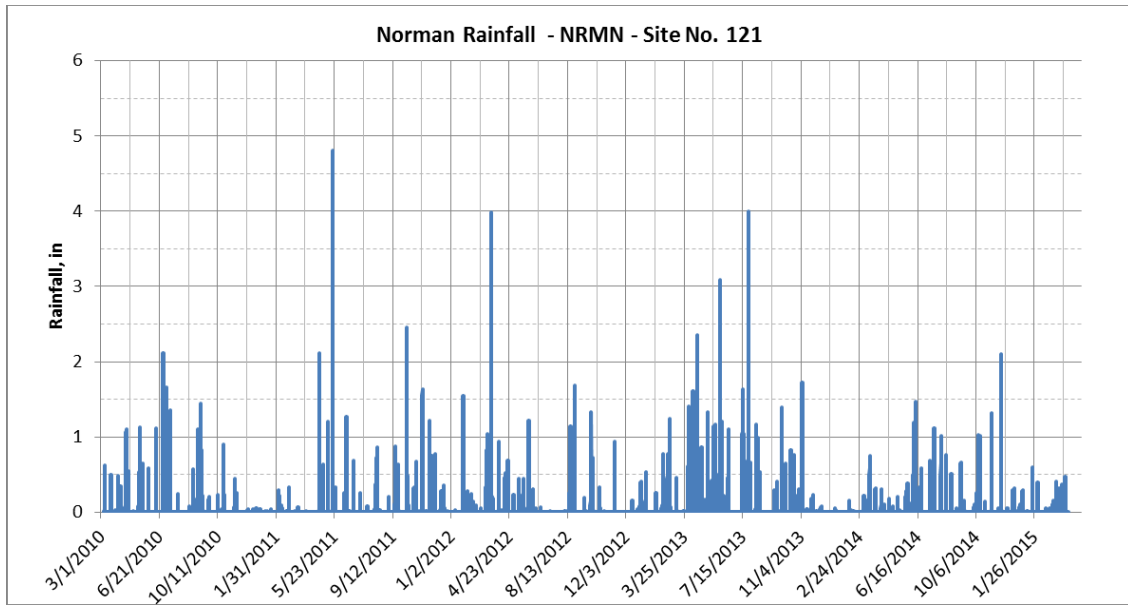


Figure 51: 30-Minute Rainfall Data for Norman, Oklahoma; Mar 2010 - Mar 2015.

Figure 52 shows a plot of the volume of storm water runoff (million gallons) at the Little River at 60<sup>th</sup> site associated with the 15 storm events exceeding 1.5". The data are color-coded based on the amount of rainfall received in the previous 10 days.

Events that had no rainfall occurring in the 10 days preceding the event are colored red, events that had less than 1" of rain in the preceding 10 days are colored orange, events that had 1-1.5" of rain in the preceding 10 days are colored yellow, events that had 1.5-2.5" of rain in the preceding 10 days are colored green, and events that had more than 2.5" are colored blue. A regression line through the data, though not particularly representative of the data ( $R^2 = 0.53$ ), is provided for reference.

Similar color-coded plots, based on rainfall received in the previous 30 days, and 60 days, are shown in Figures 53 and 54, respectively. In Figure 53, events that had less than 1" of rain in the preceding 10 days are colored red, events that had 1-2" are colored orange, events that had 2-3" of rain in the preceding 10 days are colored yellow,



events that had 3-4.5” of rain in the preceding 10 days are colored green, and events that had more than 4.5” are colored blue. In Figure 54, events that had less than 2” of rain in the preceding 10 days are colored red, events that had 2-4.5” are colored orange, events that had 4.5-6” of rain in the preceding 10 days are colored yellow, events that had 6-8” of rain in the preceding 10 days are colored green, and events that had more than 8” are colored blue.

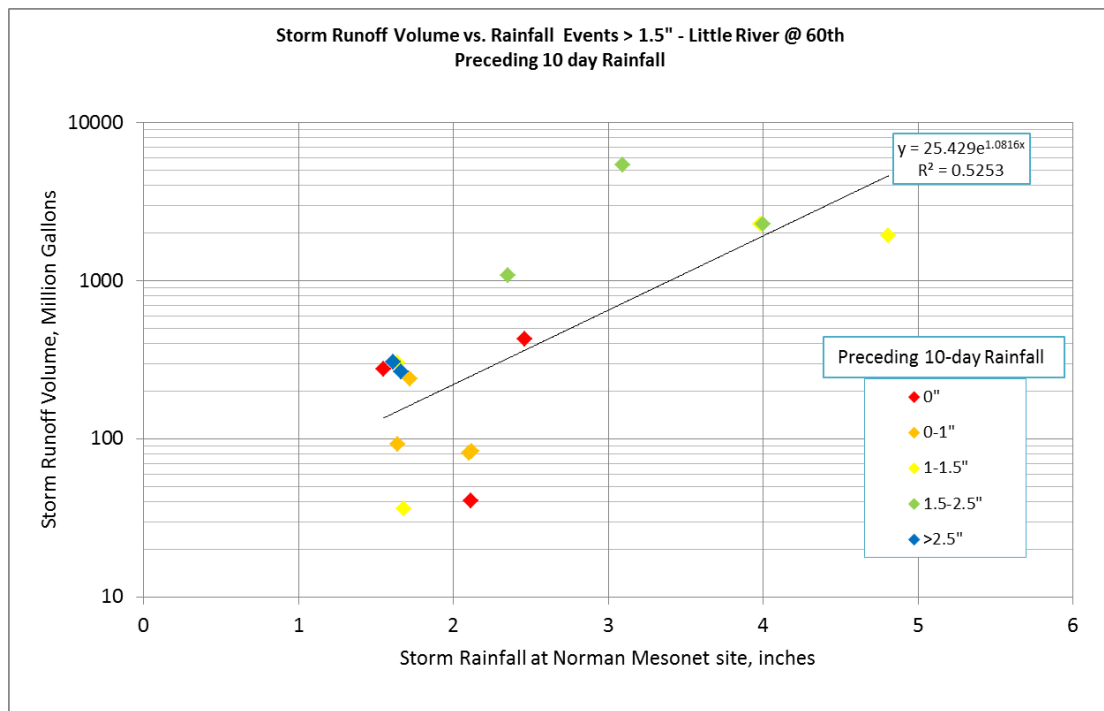


Figure 52: Storm Runoff Volume at Little River @ 60th vs. Rainfall Events > 1.5”; Preceding 10-day rainfall.

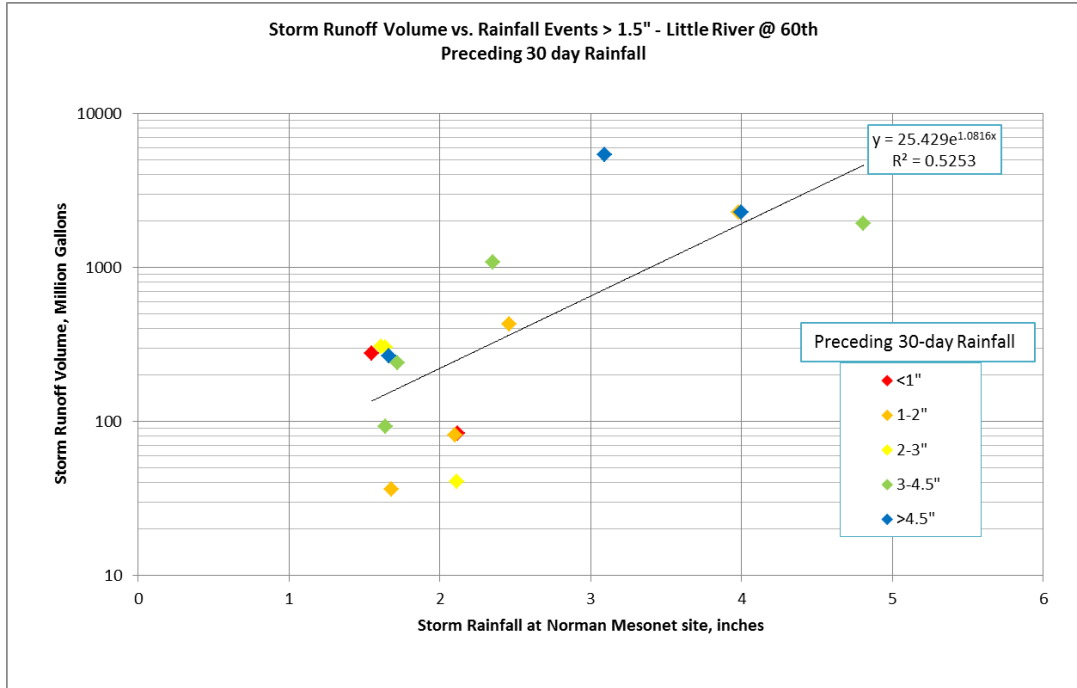


Figure 53: Storm Runoff Volume at Little River @ 60th vs. Rainfall Events > 1.5";  
Preceding 30-day rainfall.

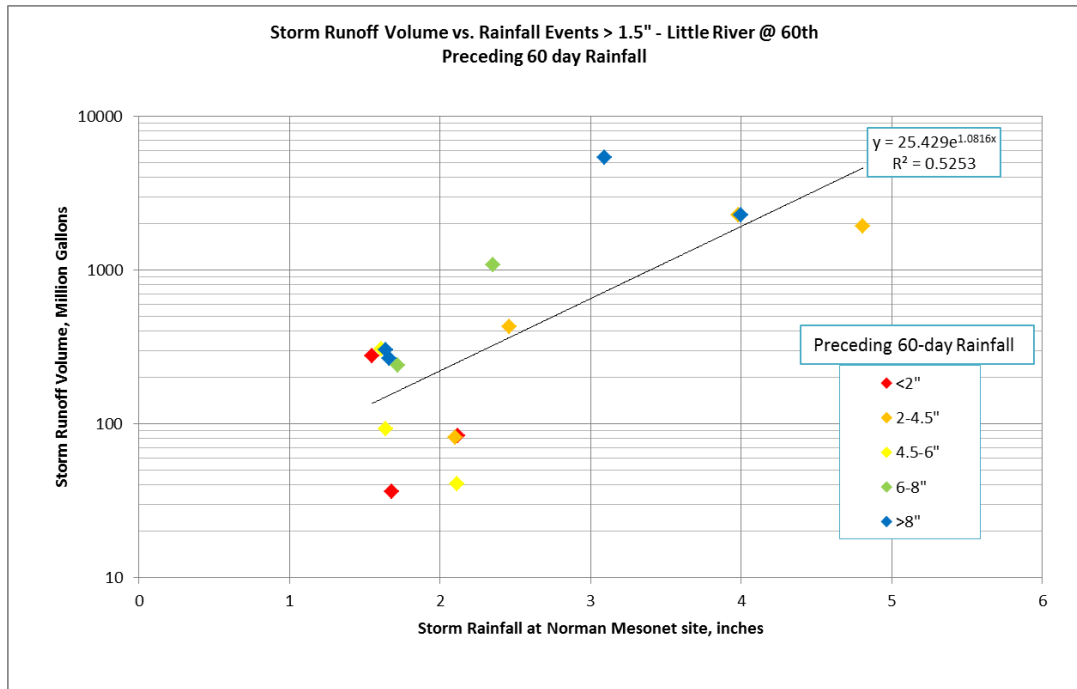


Figure 54: Storm Runoff Volume at Little River @ 60th vs. Rainfall Events > 1.5";  
Preceding 60-day rainfall.

If the runoff volume for a given storm is strongly dependent on the amount of rainfall received in the days preceding the event, one would expect to see the colors of the data points transition from blue, above the regression line, down to red, below the regression line. This trend is not consistent in the plots however, so the data do not show a strong relationship between runoff and preceding rainfall. However, it is apparent from the plots that there is a general trend that very wet antecedent conditions (green and blue dots) resulted in the largest runoff volumes, most likely due to less infiltration in the already-wet soils. At lower precipitation amounts, the trend is not as consistent, which implies that other factors besides soil moisture have a strong influence on runoff volumes, such as season, vegetation, and storm intensity.

Another possible explanation for this observed behavior could be that the rainfall is recorded at a point that, although nearby, is not located in the watershed. Because peak runoff events are generated by severe thunderstorms, which are localized in intensity, it is possible, and in fact likely, that the amount of rain falling on the watershed and generating the peaks used in this assessment was different than the amount of rain falling at the Mesonet site. A future assessment of this relationship could perhaps use radar data to better estimate the actual rainfall generating the runoff, and also include smaller rainfall events.

An example of how radar data, and the hydrology data obtained from this study, may be used to better assess the hydrology of the Lake Thunderbird watershed is demonstrated in a study conducted by Sagbohan (2010). Sagbohan used radar data as hydrologic input to Vflo, a physics-based distributed hydrologic model developed by Vieux & Associates, Inc. (2010), for simulating distributed runoff. Then, using

discharge data from the Little River at Rock Creek site, she calibrated the Vflo determined hydrograph to the site data for the July 4, 2010 runoff event (Figure 55). The rainfall reportedly had to be increased to match the hydrograph. It was conjectured that, because the site is located fairly near the radar and impacted by clutter suppression that the NWS introduces to their data, the quality of the radar may have been impacted. Another possibility is that the rating curve used for the site over estimates the discharge.

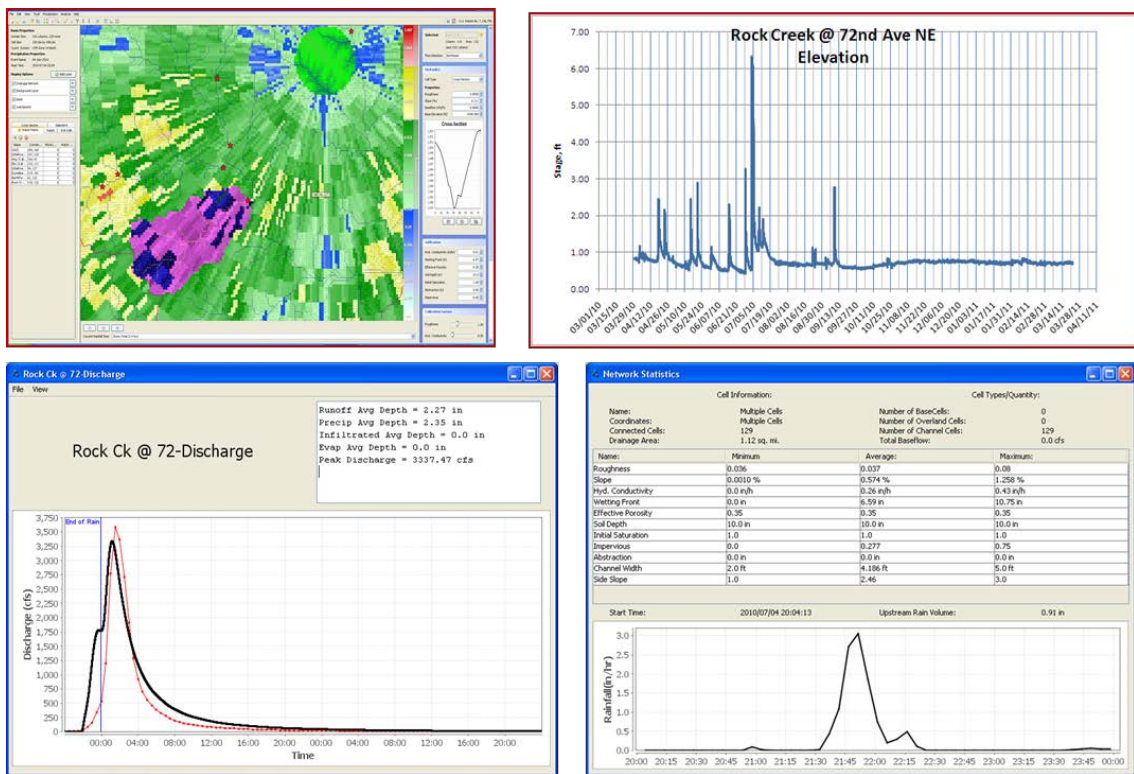


Figure 55: Rock Creek data used to calibrate Vflo hydrologic distributed runoff model (Sabohan, 2010)

Figure 56 shows a plot of the discharge at the Little River at 60<sup>th</sup> site and the rainfall recorded at the Norman Mesonet site for May, 2011. It may be seen that four rainfall events were recorded at the Mesonet station during the month, three of which produced noticeable runoff events as recorded at the Little River at 60<sup>th</sup> site. The fact that no significant runoff was recorded following the rain event observed on May 2 could be an example of the rainfall recorded at the Mesonet station not always being representative of the rain actually falling on the watershed.

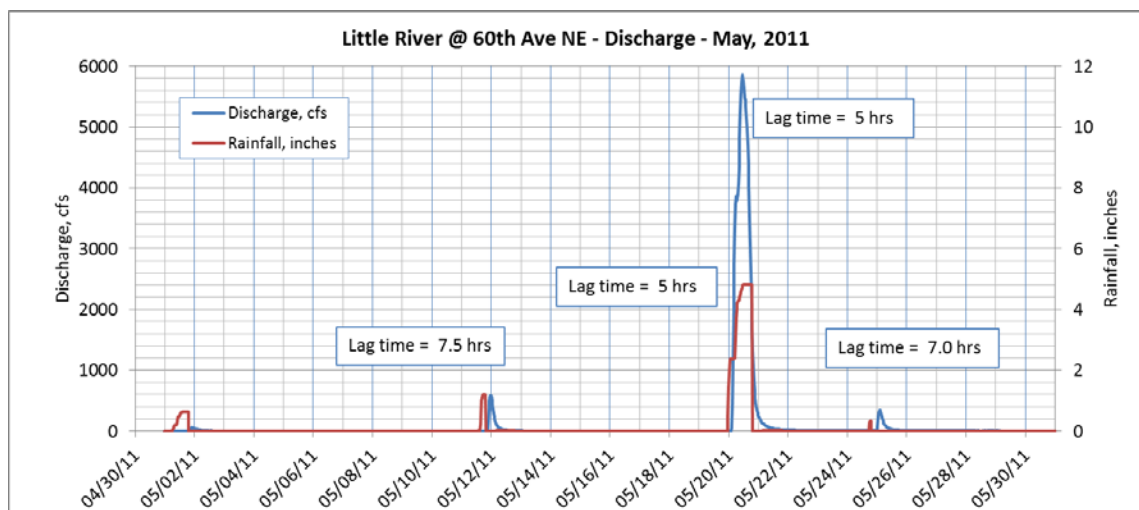


Figure 56: Discharge at Little River at 60<sup>th</sup> and rainfall at the Norman Mesonet station for May, 2011.

The three events that did produce runoff, showed lag times ranging from 5 to 7.5 hours. The rain event on May 20 was actually two separate events, and each of the events showed lag times between the peaks of 5 hours. Because both the discharge and rainfall data show this double peak, and because the lag times for these peaks are the same and shorter than the lag times for the smaller events as one might expect, the

rainfall recorded at the Mesonet site seems to provide a reasonable estimate of the actual rain falling in the watershed for three of the four storms shown.

The response times shown in Figure 56 also highlight the previously mentioned fact that the short lag and recession times of the runoff events complicated data collection efforts in this study. With the lag time ranging from 5 to 7 hours, there was little lead time to prepare for the sampling event, and the window of opportunity to measure the peak discharge was small.

As described above, the discharge estimates presented here were generated using rating curves developed for each site that relate discharge as a function of depth. Using rating curves to estimate discharge requires that the channel cross-section, and bed elevation be stable in order for the relationship between discharge and depth to be unique. It is also dependent on the sections remaining free flowing and not influenced by temporally-variable backwater effects.

Figure 57 shows plots of multiple cross-section surveys of the Little River at 60<sup>th</sup> site. Two of the four surveys were conducted as part of course activities at the University of Oklahoma, with the survey on April 12, 2012 being performed by students of Dr. Randall Kolar's Open Channel Flow class in the School of Civil Engineering and Environmental Science, and the survey on April 26, 2014 being surveyed by students in a Hydrology class taught by Dr. Aondover Tarhule in the Department of Geography and Environmental Sustainability. Note that there has not been much change in the cross-section over this time frame, although the bed on the right side of the channel appears to have degraded somewhat. The effect that this slight change in bed profile may, or may not, have had on the rating curve is uncertain, but it

is thought to be negligible. It is possible that the channels at some sites may have undergone more significant change than observed at the Little River at 60<sup>th</sup> site, but this is unknown. Extended studies in the watershed should include re-surveys of the HOBO sites on a periodic basis to evaluate the stability of the cross-section.

Figure 56 also shows the peak water surface elevation that was recorded during the study period (1,063.56 feet) and the highest measured water surface elevation (1054.06 feet). The largest discharge measured was 3,600 cfs, but the estimate from the rating curve at this stage is 4,200 cfs. Note that the channel was overflowing the right bank at the peak stage observed during the study, which had an estimated discharge of 12,500 cfs.

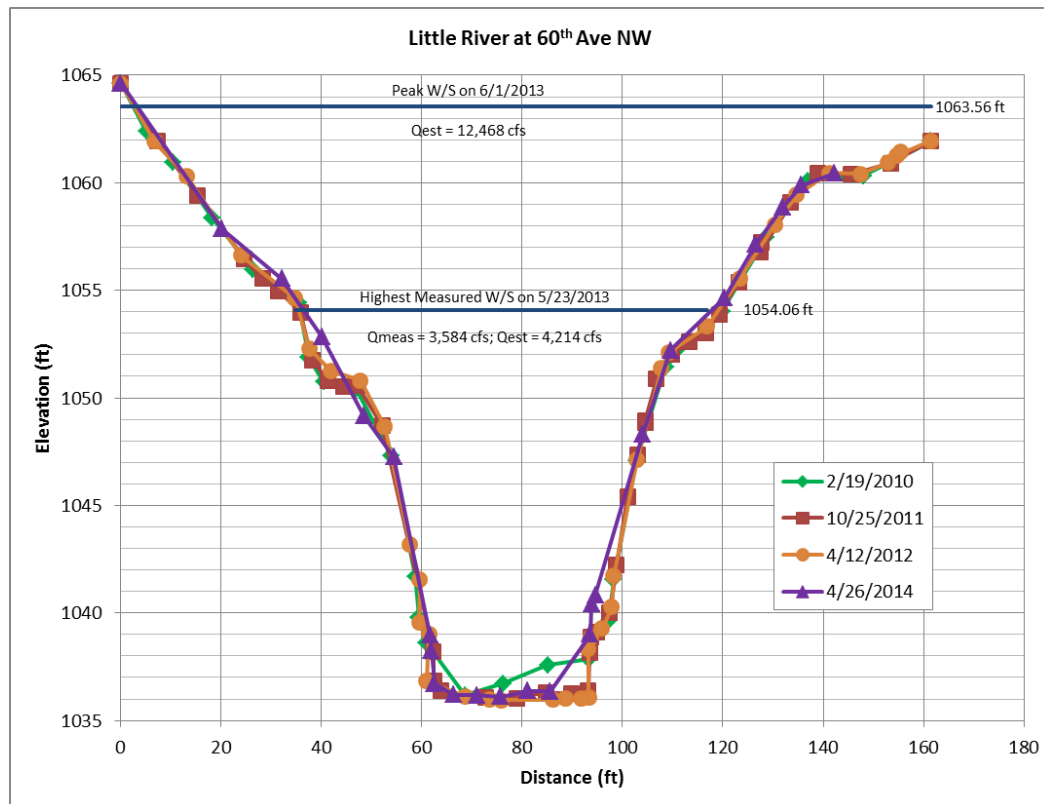


Figure 57: Cross-section Change at the Little River at 60<sup>th</sup> site.

## **2. Fluvial Geomorphology (FGM)**

In the next phase of the study, a morphological investigation of the Lake Thunderbird watershed was undertaken by conducting FGM surveys at 25 sites on the various tributaries within the watershed. The FGM surveys included land surveys, FGM assessments, and development of bank erosion indices for the sites. A summary of the FGM Assessment results is provided in Table 13. The raw data files and spreadsheets used in the study may be obtained from the author, Dr. Kolar, or Dr. Nairn upon request. Summaries of the FGM surveys for each of the FGM sites are provided in Appendix E. These summaries include the location of the site, a site description, a site survey map, cross-section and profile plots, and tables summarizing the channel morphology and stream channel stability indices.

It may be seen in Table 13 that nine sites were surveyed on the Little River, four sites were surveyed on both the North Fork and Dave Blue Creek, three sites were surveyed on Elm Creek and Rock Creek and two sites were surveyed on Hog Creek. The drainage area of the sites ranges from 2.5 to 93.4 square miles.

The bankfull width ranges from 9.2 feet to 84.9 feet, the bankfull depth ranges from 1.4 feet to 8.1 feet, and the bankfull cross-sectional area ranges from 26.7 square feet to 457.5 square feet. The width to depth ratios vary from 3.0 to 16.9, the entrenchment ratio, the width of the flood prone area to the bankfull width, where the width of the flood prone area is the width of the channel cross section at a depth that is twice the maximum bankfull depth, varies from 1.11 to 2.43, and the slopes range from -0.0031 to 0.0067. The -0.0031 slope was measured at site DBC-04 on Dave Blue Creek, and is a result of a bedrock outcrop at the site and short survey length.



Table 13: FGM Assessment Results Summary.

Site No.	Drainage Area (mi <sup>2</sup> )	Bankfull Area (ft <sup>2</sup> )	Bankfull Width (ft)	Bankfull Depth (ft)	Width-Depth Ratio	Entr. Ratio	Sinuosity	Slope	Bed Material	Rosgen Stream Type	Simon Evolution Stage	Comments
LR-01	93.4	302.3	84.9	5.0	16.9	1.41	1.92	0.0011	Sand	F5	IV	
LR-02	53.9	457.5	56.5	8.1	7.0	1.64	1.92	0.0011	Sand	G5c	IV	*Bankfull not identifiable.
LR-03	47.4	358.0	54.0	6.6	8.2	1.81	1.70	0.0009	Sand	G5c	IV	
LR-04	43.9	295.4	45.3	6.5	6.9	1.39	1.12	0.0039	Sand	G5c	IV	
LR-05	41.3	135.8	41.3	3.3	12.5	1.31	1.92	0.0009	Sand	G5c	IV	
LR-06	24.4	81.7	35.8	2.3	15.7	1.61	1.20	0.0030	Sand	B5c	IV	
LR-07	18.0	174.2	38.4	4.5	8.4	1.41	1.44	0.0018	Sand	G5c	IV	
LR-08	11.9	80.1	26.4	3.0	8.7	1.14	1.01	0.0012	Sand	G5c	IV	*Bankfull difficult to identify.
LR-09	11.0	61.3	21.4	2.9	7.4	1.61	1.44	0.0015	Sand	G5c	IV	
NF-01	16.6	183.7	31.8	5.8	5.5	1.11	1.05	0.0033	Sand	G5c	IV	
NF-02	14.9	98.8	24.1	4.1	5.9	1.22	1.05	0.0004	Sand	G5c	IV	*Bankfull not identifiable.
NF-03	11.8	67.3	21.7	3.1	7.0	2.00	1.63	0.0002	Sand	G5c	III	
NF-04	2.5	28.8	16.4	1.8	9.4	1.44	1.63	0.0050	Sand	G5c	III	
EC-01	18.6	123.4	32.1	3.8	8.3	1.17	1.05	0.0022	Sand	G5c	III	
EC-02	17.1	108.3	28.7	3.8	7.6	1.41	1.06	0.0011	Gravel	G4c	V	
EC-03	14.6	133.0	37.6	3.5	10.6	1.57	1.08	0.0003	Gravel	G4c	V	
RC-01	11.6	51.0	21.1	2.4	8.8	1.41	1.10	0.0010	Sand	G5c	IV	
RC-02	11.0	26.7	18.4	1.5	12.7	1.47	1.04	0.0026	Sand	B5c	IV	
RC-04	5.9	18.3	13.0	1.4	9.3	1.18	1.04	0.0019	Sand	G5c	III	
DBC-01	19.9	133.1	43.0	3.1	13.9	1.24	1.01	0.0016	Sand	G5c	IV	
DBC-02	18.7	114.2	32.3	3.5	9.2	1.49	1.00	0.0010	Sand	G5c	III	
DBC-03	13.2	69.1	25.4	2.7	9.3	1.75	1.05	0.0067	Sand	G5c	III	
DBC-04	10.7	71.3	25.4	2.8	9.0	1.50	1.05	-0.0031	BR/Sand	G1c/G5c	III	*Site at bedrock outcrop
HC-01	39.3	62.5	30.2	2.1	14.6	1.32	1.01	0.0002	Sand	F5	II	*Channelized
HC-02	38.6	28.1	9.2	3.1	3.0	2.43	1.00	0.0014	Clay	E6	III	*Channelized

Six different Rosgen stream types were represented in the assessment, with 17 sites being classified as G5c, two sites being classified as B5c, two sites being classified as G4c, two sites being classified as F5, one site being classified as E6, and one site being classified as G1c/G5c. The Simon channel evolution stage varied from Stage II to Stage V. The two sites on Hog Creek show fairly recent man-made alterations to the channels and are thus at Stage II. The channels at seven of the sites are at Stage III, fourteen of the channels are at Stage IV, and the two gravel bed sites on Elm Creek are at Stage V.

It should be noted that at three sites - LR-02, LR-08 and NF-02, all classified as G5c at Stage IV - the bankfull level was difficult if not impossible to determine. This difficulty in correctly identifying the bankfull level at these sites is attributable to the relatively rapid change in morphology occurring at the sites due to channel instability. At these sites, the bankfull level was estimated using best professional judgment.

Figures 58- 60 show the regional curve plots for the tributaries in the Lake Thunderbird watershed. Figure 58 shows the bankfull area (ft<sup>2</sup>) versus drainage area (mi<sup>2</sup>) plot, Figure 59 shows the bankfull width (ft<sup>2</sup>) versus drainage area (mi<sup>2</sup>) plot, and Figure 60 shows the bankfull depth (ft) versus drainage area (mi<sup>2</sup>) plot. On each of these plots, data from sites on the North Fork are shown as light blue diamonds, Little River sites are shown as red rectangles, Elm Creek sites are shown as green triangles, Rock Creek sites are shown as yellow circles with a red outline, Dave Blue sites are shown as dark blue diamonds and Hog Creek sites are shown as purple squares. Regression lines, color coded to the creeks, are shown for all creeks, except Hog Creek.

For his Master’s thesis, Dutnell (2000) surveyed 48 stream sites in Oklahoma, Missouri, Kansas and Texas with USGS gauge stations, evaluated the morphology and hydrology data at the sites, and developed “Regional Curves” for Oklahoma that relate bankfull channel dimensions and bankfull discharge versus drainage area. Sites were located in 7 of the Oklahoma’s 11 ecoregions, including the Central Great Plains and Central Oklahoma/Texas Plains ecoregions, where the Lake Thunderbird watershed is located, and had drainage areas ranging from 5.45 mi<sup>2</sup> to 23,151 mi<sup>2</sup>. Data from sites presented by Dutnell located within the Central Great Plains and Central Oklahoma/Texas Plains ecoregions and with drainage areas less than 100 mi<sup>2</sup> are included and are also shown as “+” signs on the plots. The regression line for these data is shown as a gray dashed line.

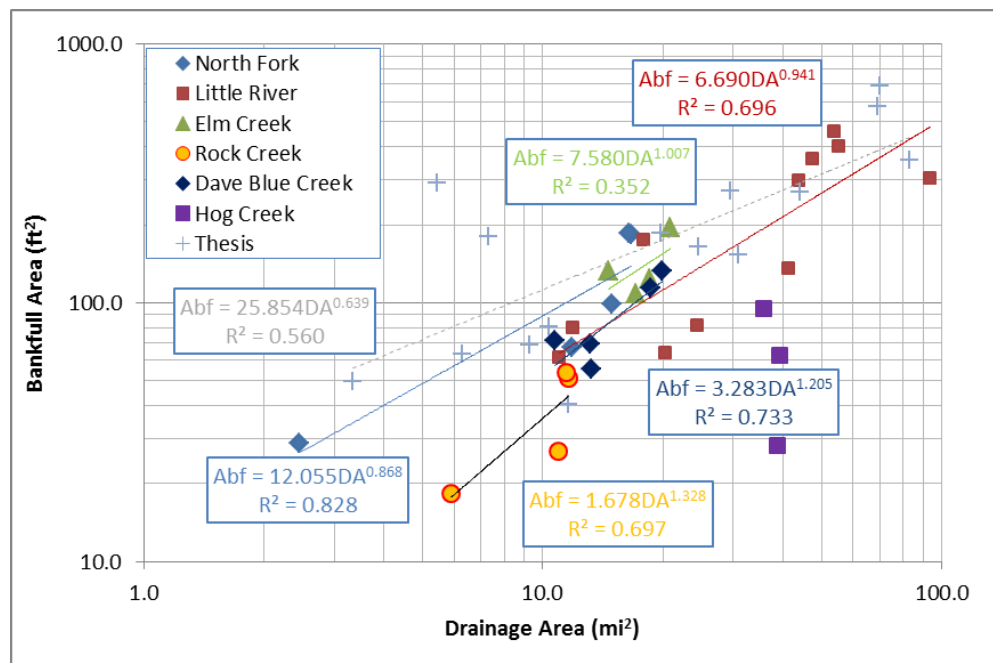


Figure 58: Bankfull Area (ft<sup>2</sup>) versus Drainage Area (mi<sup>2</sup>) Regional Curve for Lake Thunderbird watershed.

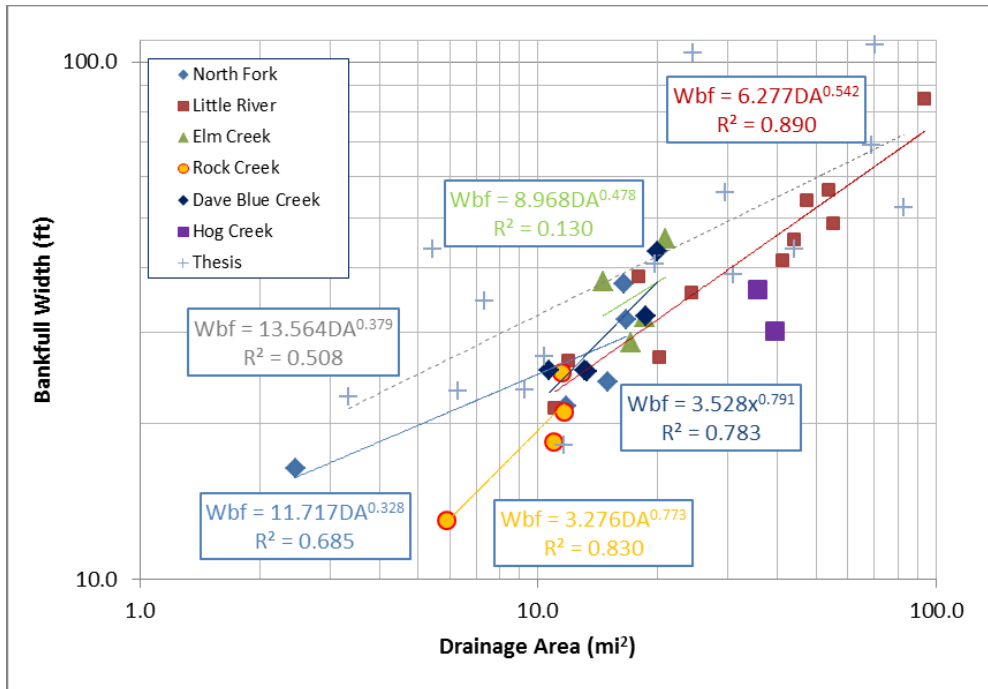


Figure 59: Bankfull Width (ft) versus Drainage Area (mi<sup>2</sup>) Regional Curve for Lake Thunderbird watershed.

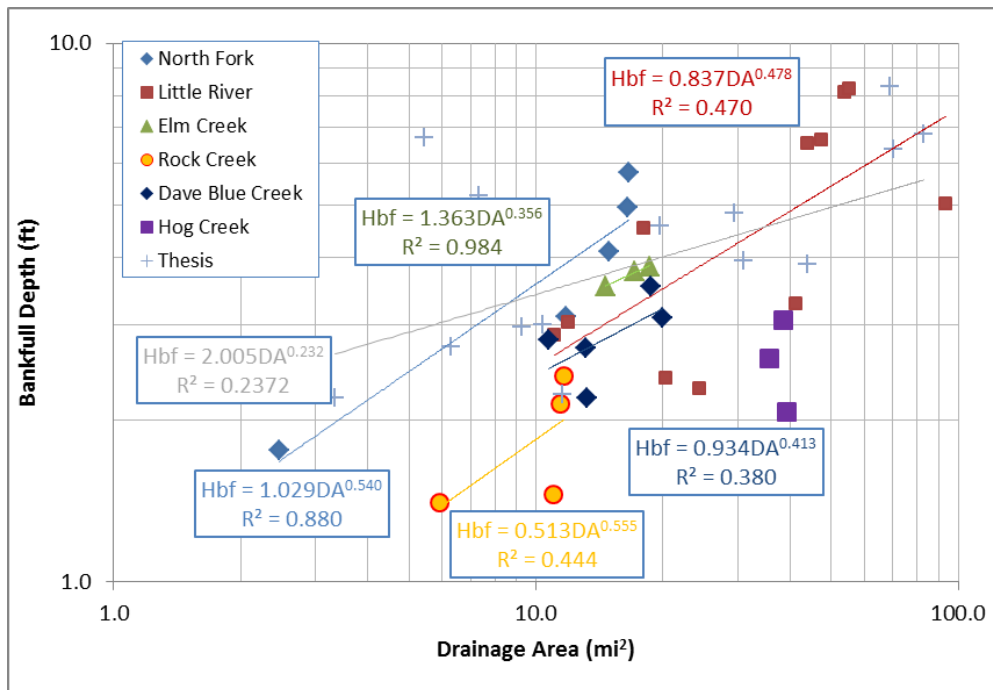


Figure 60: Bankfull Depth (ft) versus Drainage Area (mi<sup>2</sup>) Regional Curve for Lake Thunderbird watershed.

For the most part, the bankfull area versus drainage area data collected in the present study follows the same trend as reported in Dutnell's thesis, as may be seen in Figure 58. The main exception to the trend is observed at the Hog Creek sites. This anomaly is more evidence of the altered morphology of Hog Creek due to channel modification. Data at the upper end of Rock Creek shows a similar, though less pronounced, departure from the trend as well, possibly due to channel modification that appears to have occurred in the past.

In Figure 59, the bankfull width versus drainage area data collected in the present study again follows a trend similar to the trend reported by Dutnell, but appears to show that, for a given drainage area, the bankfull width is less in the Lake Thunderbird watershed than at other sites in central Oklahoma. The difference is less at sites with larger drainage area and could potentially be an indication of urbanization in the watershed. The bankfull depth versus drainage area data collected in the present study also follows a trend similar to the trend reported by Dutnell, as shown in Figure 60, with the exception being data from the Hog Creek sites.

Table 14 shows a summary of the bank erosion indices developed for the FGM sites. At 8 of the 9 sites located on the main stem of the Little River, assessments were conducted on the four banks nearest to the surveyed cross section. At site LR-01, which is located in the flood pool of the lake, the water was too deep to wade, so at this site, and the remaining sites, only one assessment was conducted at the bank nearest the cross section thought to be experiencing the most erosion. A total of 49 banks were assessed in the study.

Table 14: Bank Erosion Indices Results Summary

Waterbody	SiteNo	BankNo	Bank Location		CSI		BEHI		NBS		Pfunkuch		OEBSI	
			Lat	Long	Score	Stability	Score	Hazard	Score	Stress	Score	Stability	Score	Stability
Dave Blue Creek	DBC-01	1	35.2046	97.3176	24	Highly Unstable	41	Very High	***	Low	79	Fair-Mod. Unstable	35	Stable
Dave Blue Creek	DBC-02	1	35.1964	97.3308	19	Moderately Unstable	55	Extreme	***	Low	71	Good - Stable	37	Stable
Dave Blue Creek	DBC-03	1	35.1939	97.3389	23	Highly Unstable	47	Extreme	***	Moderate	85	Good - Stable	39.5	Stable
Dave Blue Creek	DBC-04	1	35.1867	97.3503	21	Highly Unstable	56	Extreme	***	Very High	83	Poor-Unstable	57	Highly Unstable
Elm Creek	EC-01	1	35.2820	97.3503	20.5	Highly Unstable	41	Very High	***	High	101	Poor-Unstable	59.5	Highly Unstable
Elm Creek	EC-02	1	35.3039	97.3571	20	Moderately Unstable	51	Extreme	***	High	67	Good - Stable	42	Unstable
Elm Creek	EC-03	1	35.3229	97.3763	20.5	Highly Unstable	50	Extreme	***	Low	79	Fair-Mod. Unstable	57	Highly Unstable
Hog Creek	HC-01	1	35.3209	97.2503	17	Moderately Unstable	40	Very High	***	Low	71	Fair-Mod. Unstable	37	Stable
Hog Creek	HC-02	1	35.3371	97.2548	18	Moderately Unstable	61	Extreme	***	Very Low	87	Fair-Mod. Unstable	52.5	Unstable
North Fork	NF-01	1	35.2750	97.4293	25.5	Highly Unstable	56	Extreme	***	Extreme	139	Poor-Unstable	62	Highly Unstable
North Fork	NF-02	1	35.2912	97.4345	28	Highly Unstable	57	Extreme	***	Low	125	Poor-Unstable	62	Highly Unstable
North Fork	NF-03	1	35.3065	97.4442	23	Highly Unstable	45	Very High	***	Extreme	103	Poor-Unstable	62	Highly Unstable
North Fork	NF-04	1	35.3399	97.4537	20.5	Highly Unstable	37	High	***	Extreme	102	Poor-Unstable	54.5	Unstable
Rock Creek	RC-01	1	35.2629	97.3321	28	Highly Unstable	46.5	Extreme	***	Low	117	Poor-Unstable	49.5	Unstable
Rock Creek	RC-02	1	35.2597	97.3391	25	Highly Unstable	41	Very High	***	Extreme	108	Poor-Unstable	37	Stable
Rock Creek	RC-04	1	35.2412	97.3755	27	Highly Unstable	63	Extreme	***	Low	117	Poor-Unstable	60	Highly Unstable
Little River	LR-01	1	35.2688	97.3320	24.5	Highly Unstable	41	Very High	***	High	86	Fair-Mod. Unstable	44.5	Unstable
Little River	LR-02	1	35.2801	97.3674	22.5	Highly Unstable	44	Very High	***	Extreme	116	Poor-Unstable	62	Highly Unstable
Little River	LR-02	2	35.2801	97.3674	22.5	Highly Unstable	43	Very High	***	Extreme	114	Poor-Unstable	62	Highly Unstable
Little River	LR-02	3	35.2797	97.3649	24	Highly Unstable	41	Very High	***	Low	122	Poor-Unstable	67	Highly Unstable
Little River	LR-02	4	35.2785	97.3645	25	Highly Unstable	46	Extreme	***	Extreme	118	Poor-Unstable	69	Highly Unstable
Little River	LR-03	1	35.2760	97.3955	22.5	Highly Unstable	41	Very High	***	High	113	Poor-Unstable	54.5	Unstable
Little River	LR-03	2	35.2747	97.3939	27	Highly Unstable	44	Very High	***	Moderate	99	Poor-Unstable	77	Highly Unstable
Little River	LR-03	3	35.2754	97.3933	25	Highly Unstable	44	Very High	***	High	109	Poor-Unstable	52	Unstable
Little River	LR-03	4	35.2750	97.3914	20.5	Highly Unstable	37	High	***	High	99	Poor-Unstable	57	Highly Unstable

CSI - Channel Stability Index; BEHI - Bank Erosion Hazard Index; NBS - Near Bank Stress; OEBSI - Ozark Eco-Region Bank Stability Index

Table 14 (Continued): Bank Erosion Indices Results Summary

Waterbody	SiteNo	BankNo	Bank Location		CSI		BEHI		NBS		Pfrankuch		OEBSI	
			Lat	Long	Score	Stability	Score	Hazard	Score	Stress	Score	Stability	Score	Stability
Little River	LR-04	1	35.27489	97.41092	25	Highly Unstable	36	High	***	Extreme	99	Poor-Unstable	42	Unstable
Little River	LR-04	2	35.27495	97.41042	21	Highly Unstable	48	Extreme	***	Low	100	Poor-Unstable	62	Highly Unstable
Little River	LR-04	3	35.27536	97.4085	19.5	Moderately Unstable	44	Very High	***	Moderate	97	Poor-Unstable	44.5	Unstable
Little River	LR-04	4	35.27491	97.40694	22	Highly Unstable	40	Very High	***	Extreme	88	Fair-Mod. Unstable	54.5	Unstable
Little River	LR-05	1	35.27438	97.42243	28.5	Highly Unstable	56	Extreme	***	Extreme	103	Poor-Unstable	62	Highly Unstable
Little River	LR-05	2	35.27518	97.42227	23	Highly Unstable	46	Extreme	***	Extreme	117	Poor-Unstable	67	Highly Unstable
Little River	LR-05	3	35.27436	97.42141	26	Highly Unstable	58	Extreme	***	Very High	121	Poor-Unstable	67	Highly Unstable
Little River	LR-05	4	35.27529	97.42133	25	Highly Unstable	40	Very High	***	Extreme	125	Poor-Unstable	59.5	Highly Unstable
Little River	LR-06	1	35.273128	97.428772	22.5	Highly Unstable	45	Very High	***	Extreme	106	Poor-Unstable	47	Unstable
Little River	LR-06	2	35.273842	97.428186	26	Highly Unstable	45.5	Very High	***	Very High	123	Poor-Unstable	47	Unstable
Little River	LR-06	3	35.274231	97.426919	21.5	Highly Unstable	41.5	Very High	***	Extreme	110	Poor-Unstable	44.5	Unstable
Little River	LR-06	4	35.273781	97.426458	25	Highly Unstable	53	Extreme	***	Extreme	113	Poor-Unstable	54.5	Unstable
Little River	LR-07	1	35.270061	97.454528	25	Highly Unstable	60	Extreme	***	Extreme	111	Poor-Unstable	67.5	Highly Unstable
Little River	LR-07	2	35.269253	97.454272	25	Highly Unstable	48	Extreme	***	Extreme	124	Poor-Unstable	59.5	Highly Unstable
Little River	LR-07	3	35.2692	97.453036	28	Highly Unstable	47	Extreme	***	Extreme	121	Poor-Unstable	59.5	Highly Unstable
Little River	LR-07	4	35.269642	97.453078	26	Highly Unstable	58	Extreme	***	Extreme	131	Poor-Unstable	59.5	Highly Unstable
Little River	LR-08	1	35.276806	97.466364	28	Highly Unstable	51.5	Extreme	***	Low	121	Poor-Unstable	59.5	Highly Unstable
Little River	LR-08	2	35.277517	97.466731	27	Highly Unstable	44	Very High	***	Moderate	119	Poor-Unstable	47	Unstable
Little River	LR-08	3	35.2784	97.466664	28	Highly Unstable	43	Very High	***	Low	110	Poor-Unstable	49.5	Unstable
Little River	LR-08	4	35.279431	97.466286	26.5	Highly Unstable	49.5	Extreme	***	High	123	Poor-Unstable	56.5	Highly Unstable
Little River	LR-09	1	35.286944	97.47235	27	Highly Unstable	54	Extreme	***	Very High	125	Poor-Unstable	54.5	Unstable
Little River	LR-09	2	35.287125	97.471556	26.5	Highly Unstable	54	Extreme	***	Very High	123	Poor-Unstable	57	Highly Unstable
Little River	LR-09	3	35.28655	97.471506	25.5	Highly Unstable	62	Extreme	***	Moderate	121	Poor-Unstable	65	Highly Unstable
Little River	LR-09	4	35.286328	97.472942	28	Highly Unstable	54	Extreme	***	Extreme	127	Poor-Unstable	59.5	Highly Unstable

CSI - Channel Stability Index; BEHI - Bank Erosion Hazard Index; NBS - Near Bank Stress; OEBSI - Ozark Eco-Region Bank Stability Index

The Channel Stability Indices (CSI's) ranged from 17, moderately stable, at HC-01, to 27, highly unstable, at LR-03 Bank 1. The majority of banks, 44 of the 49 assessed, were classified as highly unstable. A map of the study area showing color-coded CSI ratings for the sites, with green being stable, yellow being moderately stable and red being unstable, is shown in Figure 61. It may be seen that none of the banks assessed using the CSI were determined to be stable, and only five banks were found to be moderately unstable. Two of these moderately unstable banks are located on Hog Creek, which has been channelized and is currently at Stage II in the evolutionary cycle. The evolutionary stage of the channel is one of the metrics in the CSI, and is lower for Stage II channels than for Stage III or IV channels. If these channels were classified as Stage IV channels, they too would be considered unstable.

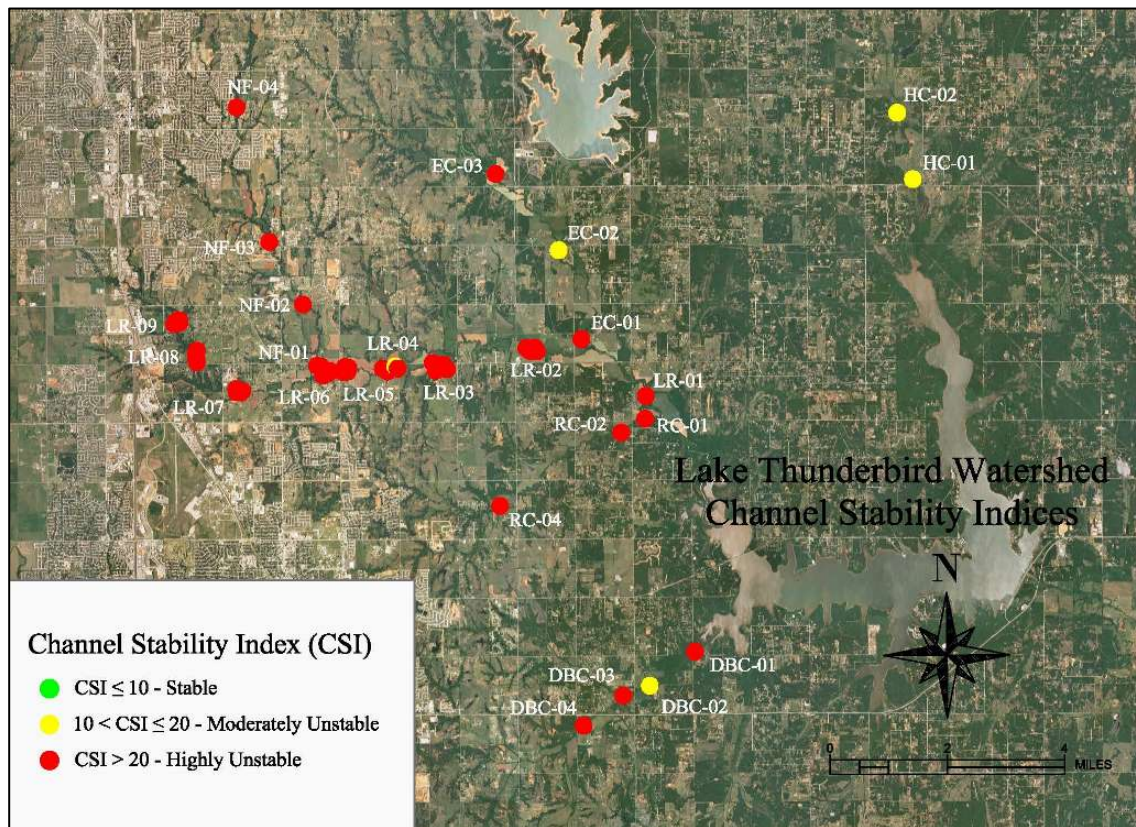


Figure 61: Channel Stability Indices (CSI's) in the Lake Thunderbird watershed.



The Bank Erosion Hazard Indices (BEHI's) ranged from 36, high hazard, at LR-04, Bank 1, to 63, extreme hazard, at RC-04. Figure 62 shows a map of the study area with color-coded BEHI's for the banks, with blue being very low hazard, green being low hazard, yellow being moderate hazard, orange being high hazard, red being very high hazard, and dark red being extreme hazard. Twenty-six sites were found to have an extreme erosion hazard, twenty were found to have a very high hazard and three were found to have a high hazard. Not a single bank was considered to have a very low or low hazard.

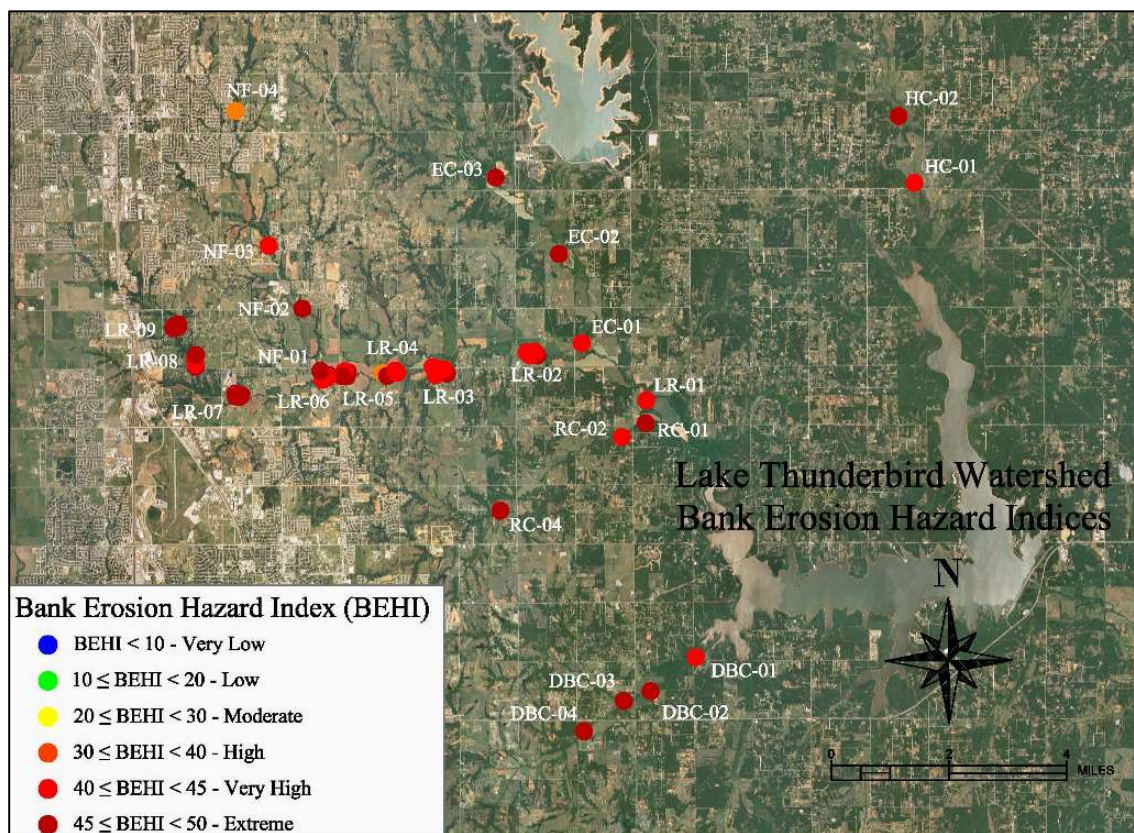


Figure 62: Bank Erosion Hazard Indices (BEHI's) in the Lake Thunderbird watershed.

The BEHI provides an index of a bank's susceptibility to erosion based on characteristics of the bank. In order for a bank to erode, however, shear stress must be applied to the bank, and for a given flow, or stage, the shear stress a bank is subjected to is dependent on the channel morphology. Stress on a bank on the outside of a sharp bend is much greater than on a straight reach, or on the inside of a bend. Near Bank Stress (NBS) ratings provide a qualitative prediction of stresses near the bank based on the radius of curvature of the bend, the bankfull width, the mean bankfull depth, and the near-bank maximum depth.

Figure 63 shows a map of the study area with color-coded Near Bank Stress (NBS) ratings for the banks, with blue being very low stress, green being low stress, yellow being moderate stress, orange being high stress, red being very high stress, and dark red being extreme stress. NBS ratings ranged from very low, at HC-02, to extreme for 20 banks. The wide range of the ratings is primarily an indication of the variation in channel alignment at the sites. The sites on Hog Creek and the lower sites of Dave Blue Creek, for example, have very low or low NBS because the channels are essentially straight at the sites.

Because the BEHI provides an index of a bank's susceptibility to erosion, should stress be applied to it, and NBS provides a prediction of near-bank stress on the bank, the NBS rating and BEHI may be used together to predict the erosion potential of the bank. As an example, consider the HC-02 and DBC-04 sites. The BEHI's at both sites are considered extreme, but the NBS is very low at HC-02, and very high at DBC-04. The potential for bank erosion is therefore greater at DBC-04 than it is at HC-02. In some cases, however, it is not so clear cut. Consider sites HC-01 and HC-02. HC-01 has

a very high BEHI, and a low NBS rating, whereas HC-02 has an extreme BEHI and a very low NBS rating. Which bank has the greater potential for erosion? Without additional data this question cannot be answered, but given the limitations associated with qualitative predictors, some predictions may still be made. For the most part, for example, the sites on the Little River have BEHI's and NBS ratings on the upper end of their spectrums so that the potential for future bank erosion on the Little River is likely to be high.

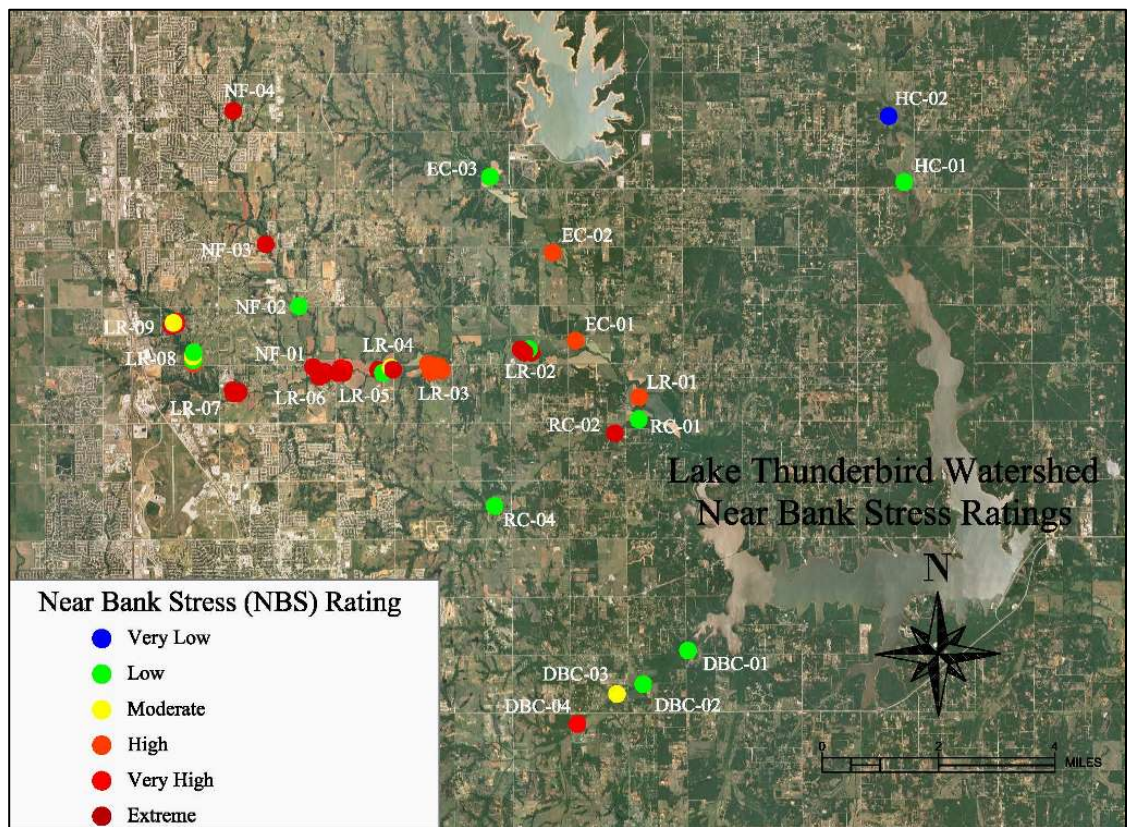


Figure 63: Near Bank Stress (NBS) Ratings in the Lake Thunderbird watershed.

Pfankuch stream stability ratings ranged from 67, good-stable, at EC-02 to 127, poor-unstable, at LR-09 Bank 4, with 40 of the sites rated as poor-unstable, and an

additional 6 sites rated as fair, moderately unstable. Only 3 banks were rated as good-stable. Figure 64 shows a map of the study area with color-coded Pfankuch stream stability ratings for the banks, with green as good-stable, yellow as fair-moderately unstable and red as unstable. It may be seen that the Pfankuch stability ratings at the sites are similar to the CSI's, which is not surprising because both indices use similar channel and bank features to generate the metrics used in their development.

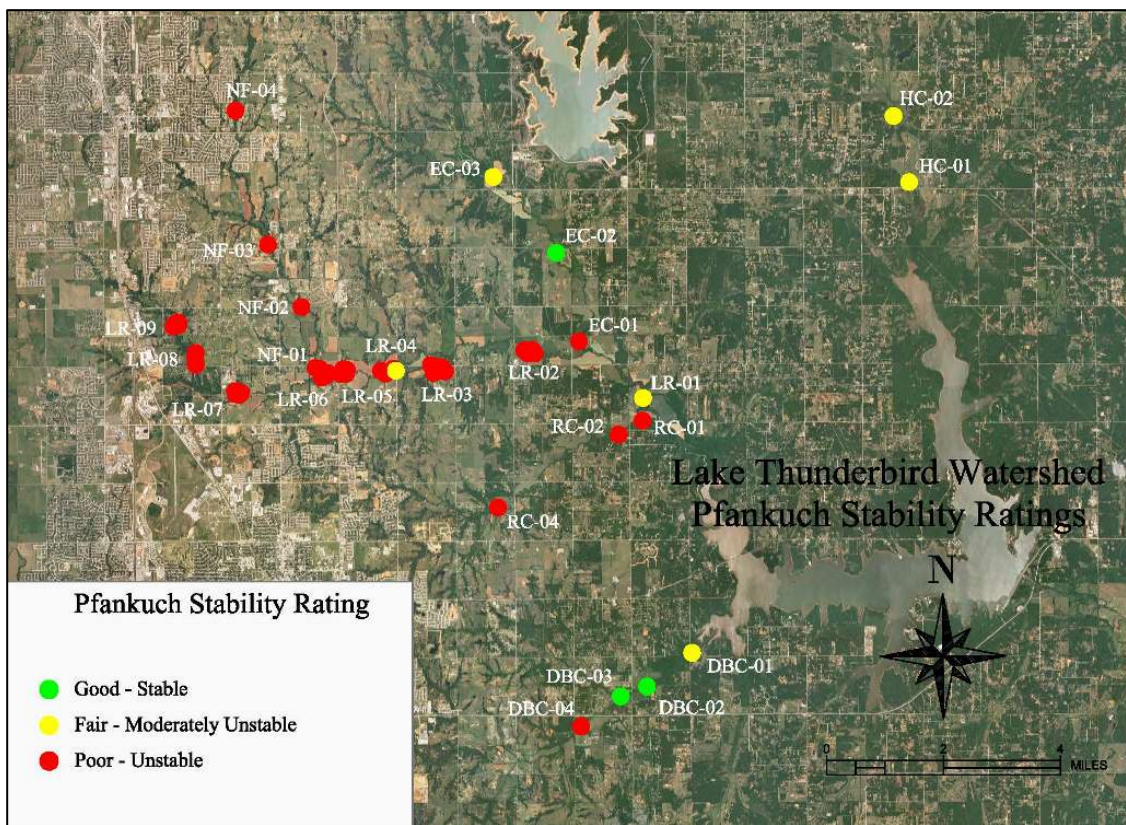


Figure 64: Pfankuch Ratings in the Lake Thunderbird watershed.

Finally, the Ozark Eco-region Bank Stability Indices (OEBSI's) ranged from 35, stable, at DBC-01, to 77, highly unstable, at LR-03 Bank 2, and of the 49 banks assessed, 17 were classified as unstable, and 27 as highly unstable. Only 5 were

considered stable and none were considered highly stable. Figure 65 shows a map of the study area with color-coded OEBSI's. Highly stable banks are shown as blue, stable banks as green, unstable banks as yellow, and highly unstable banks as red. Comparing the OESBI results with the CSI and Pfankuch results, it may be seen that the results are again similar. The OESBI shows more variability than the CSI or Pfankuch ratings, because it incorporates slightly different channel parameters, but still indicates that very few of the 49 banks assessed in this study are stable.

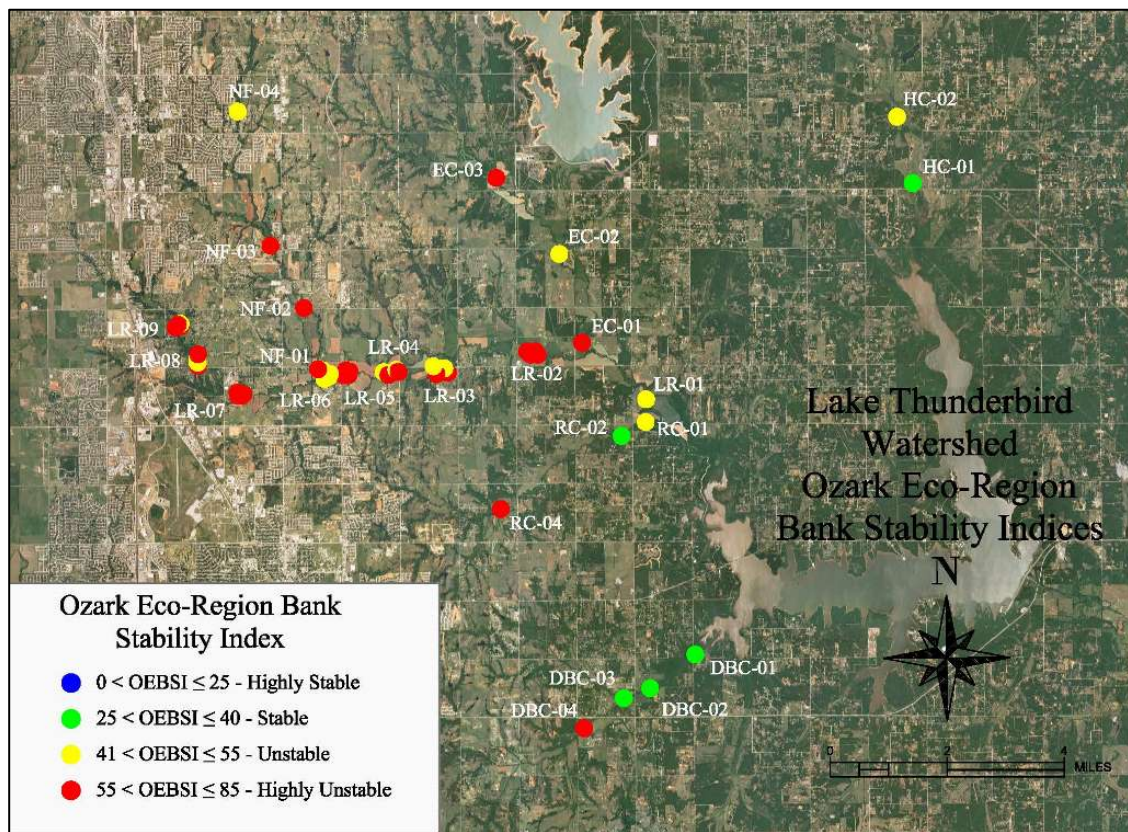


Figure 65: Ozark Eco-Region Bank Stability Indices (OEBSI's) in the Lake Thunderbird watershed.

## **E. Comments and Conclusions**

The results of the hydrological study presented above provide a record of the discharge in the main tributaries of Lake Thunderbird covering nearly a five year period from March (or April) 2010 to March 2015. It is the only long-term continuous record available for the watershed, and may provide useful information for water resource managers, and valuable input for future hydrological models. As fate would have it, the study documents the response of the watershed to drought conditions, and could perhaps provide a glimpse of what a “worst-case” scenario of the amount of water available from stream flow into the lake might look like, and may even portend the future hydrology in the watershed as a result of climate change.

Table 9 shows that the rainfall in the years 2010, 2011, 2012 and 2014 was roughly half that in 2013, yet the cumulative runoff to the lake, estimated in this study, was reduced by roughly 80%. Because impoundment of this runoff is a major component of the City of Norman’s water supply, the possibility of climate change resulting in a drier climate in Oklahoma could have profound implications on the available water supply.

Unfortunately, there are some gaps in the data due to various reasons, including operating error, dead batteries, and ice. All of these issues could be alleviated with redundancy. Having two HOBOS at each site would provide a backup should one of them be inoperable. The problem with this, though, is that it doubles the cost to monitor each site. In lieu of that, loss of data may be prevented with more diligence in deploying the HOBOS by making sure to restart it after downloads, using only fully charged HOBOS, and installing them so that ice cannot form in the housing. Deploying only

fully charged HOBOS is not practical, as it too would be expensive. An alternative is to monitor the battery level more carefully and download the data more frequently, which reduces the likelihood of data loss from a low battery. Having a spare reduces the amount of data loss should it occur.

Another regrettable deficiency in the study is the lack of high stage discharge measurements at several of the sites, necessitating the need for “synthetic” rating curves generated using Manning’s equation. Due to the limited number of opportunities available to measure high discharge rates, the relative difficulty of moving the ADCP set up from site to site, and the narrow window of opportunity available for measuring the peak flow after each storm, a decision was made to focus the high discharge measurements on fewer sites in order to assure that these sites had sufficient measurements to develop reliable rating curves at these sites. Although using Manning’s “n” is not the preferred method for determining the discharges, the discharges presented above provide a reasonable estimate of the discharge at the sites using the best available techniques.

The data obtained in this study were also analyzed to see if antecedent conditions, in the form of rainfall in the days preceding a storm event, affected the runoff volume from that event. Although a definitive trend was not observed in the limited data set used in this study, rainfall events with very wet antecedent conditions resulted in the largest runoff volumes. An analysis using radar data to better estimate the rainfall in the watershed, similar to work done by Sabohan (2010) could include smaller rainfall events and possibly provide a more effective means of assessing this relationship.

The results of the fluvial geomorphological study document the channel morphology at 25 sites on the main tributaries of Lake Thunderbird. The surveys provided the data necessary to classify the channels and to determine their state of evolution. The assessments provided the data required to compute various bank erosion indices at each site. Analysis of the data reveals a system in flux, with the majority of sites showing signs of active incision.

The Little River is at Stage IV of the Simon Evolution Model and is both incising and widening. The lower reaches of North Fork, Rock Creek and Dave Blue Creek are also at Stage IV and are down cutting and widening. Further upstream in these channels, they are at Stage III and are only incising at this point. The lower reaches of Elm Creek are also at Stage III, but the sites on the upper reaches are at Stage V. The banks are still retreating, but there are signs of deposition in the channel. This may be a response to a previous, perhaps localized channel alteration. The sites on Hog Creek are both on “improved” channels that have been dredged and straightened and at the time of the assessment were clearly at Stage II. The individuals who did this, though perhaps well intended, have initiated the process of stream evolution the consequences of which will result in incising, widening, loss of stream bank (with subsequent deposition in Lake Thunderbird), which will also cause further headcuts in side channels - all negative responses due to stream alteration.

The bank erosion indices (BEI's) estimated in this study provide a predictive tool for qualitatively estimating the potential for a given bank to erode. The results are consistent with what would be expected in the channels based on their stream types and stage of evolution. Repeated measurements at the sites, over an extended period of time



are needed to validate the various indices and determine which, if any, is more applicable to the Lake Thunderbird, and perhaps provide data for developing an index specifically for the watershed. Repeated measurements may possibly even allow for development of quantitative predictors that could determine not just the potential that a given bank has to erode, but the amount that it is likely to erode.

### **III. Part 2: Evaluation of an Acoustic Doppler Current Profiler (ADCP) for use in Measuring Sediment Transport in the Lake Thunderbird Watershed in Central Oklahoma**

#### **A. Basics of ADCP Operation**

ADCPs use acoustic transducers operating at megahertz frequencies to transmit sound pulses on the order of microseconds into the water column. As the pulse propagates through the water column, sediments in suspension backscatter a proportion of the sound to the transducer. Because of the Doppler effect, the frequency of the return signal is altered, depending on the relative velocity of the particles to the ADCP. By using multiple beams, the ADCP can determine the magnitude and direction of particles suspended in the water column. Further, the backscatter intensity, i.e., the strength of the return signal, is a function of the concentration and size of the sediment in suspension. As stated in the introduction, numerous researchers are using this property of sound to estimate suspended sediment concentration or flux in rivers and estuaries (Derrow II et al., 1998; Holdaway et al., 1999; Kim and Voulgaris, 2003; Filizola and Guyot, 2004; Kostaschuk et al., 2004; Stephens, 2005; Kostaschuk, 2005; Wall et al., 2006). However a study comparing the results obtained from ADCPs and results obtained by traditional methods has yet to be conducted on small streams like those found in this study.

#### **B. Hypothesis**

The hypothesis evaluated in Part 2 of the proposed study is that a Teledyne RDI 600 kHz Workhorse Rio Grande may be used to accurately measure sediment transport in small rivers and streams. The accuracy of the ADCP was evaluated by comparing the

sediment flux determined using the ADCP versus the sediment flux determined using traditional sediment sampling methods. Because it was not possible to collect the traditional samples and conduct the ADCP measurements at precisely the same moment in time, accuracy was assumed to be confirmed if the sediment flux rating curves developed using the ADCP were found to be statistically insignificant from sediment flux rating curves developed using traditional sampling results.

### **C. Objectives**

The primary objective of Part 2 of the study was to evaluate the use of ADCPs for measuring sediment transport in small rivers. A secondary objective of the study was to develop sediment rating curves at the test sites that could be used to estimate sediment loadings to Lake Thunderbird. The “laboratory” for this evaluation was the tributaries of the lake, including the Little River.

### **D. Methodology**

The tasks performed to accomplish the objectives of Part 2 of the proposed study included deployment of the ADCP, sampling using “traditional” suspended sediment sampling methods, and analysis of the data. The methods used in performing these tasks are described below.

#### **1. ADCP Deployment Methods**

The ADCP used in this study was the Teledyne RDI 600 kHz Workhorse Rio Grande. The 600 kHz Rio Grande was selected over other models for a couple of reasons. The primary reason was that commercial software is available from Aqua Vision (Aqua Vision, 2013) that does the required computations and iterations

necessary to convert the backscatter data from the ADCP to suspended sediment concentration and flux. The software was designed to work specifically with the Rio Grande ADCPs. The reason for selecting the 600 kHz ADCP over the 1200 kHz was a tradeoff. 1200 kHz ADCPs work in shallower water, but they do not have the penetration power needed to get through highly turbid water. Reasoning that the majority of the sediment in the streams would be moving when the stage was high, and that the water would be highly turbid at these higher stages, the 600 kHz instrument was selected. The ADCP is mounted in an OceanScience Riverboat equipped with RTK GPS, as shown in Figure 66.



*Figure 66: Teledyne RDI 600 kHz Workhorse Rio Grande OceanScience Riverboat with RTK GPS.*

The ADCP was deployed from bridges at the location of the HOBOS due to safety factors related to taking high discharge measurements. Using the WinRiver II firmware that came with the ADCP, the stream discharge was measured by traversing the channel with the RiverBoat, following methods developed by the USGS (Oberg et

al., 2005; Mueller et al., 2009) and explained in Section II.C.1. A discharge was determined for each crossing and a typical measurement consisted of 10 crossings, although in some instances, due to various circumstances, such as the current flipping the trimaran upside down, or power related problems, fewer crossings were made. The reported discharges were then averaged to determine the stream discharge for the measurement.

Because the backscatter equation is a function of both particle size and concentration, suspended sediment samples were collected to calibrate the Aqua Vision software that is used to convert the backscatter to concentration. The procedure followed in the study, as recommended by personal communication with Jeroen Aardoom from Aqua Vision, is as follows:

1. The channel was divided into three sections;
2. The boat was held stationary in the center of the left section and ADCP data were collected for 1-2 minutes;
3. As soon as the ADCP recording was turned off, a grab sample was collected at two-thirds depth;
4. The process was repeated for the center and center right sections;
5. The samples were analyzed for particle size distribution and concentration;
6. The ADCP data were reprocessed in Aqua Vision's ViSea Plume Detection Toolbox (PDT) using the averaging option;
7. Calibration iteration was conducted using data from step 5;
8. WinRiver discharge data were reprocessed with ViSea and the new coefficients obtained in step 7.

## 2. Traditional Suspended Sediment Sampling Methods

Either immediately before, or after measuring the discharge with the ADCP and collecting the final sample in step 4, above, samples were collected using traditional sediment sampling methods. As soon as the traditional samples were collected, another flow measurement was taken, so that each complete sampling event generated seven samples for analysis and two flow measurements. The traditional sediment sampling methods used in the study included grab sampling and depth-integrated sampling. A single grab sample was collected in the middle of the channel at mid-depth, and three depth-integrated samples were collected, one each at center-left, middle and center-right of the channel. All samples were collected using a FISP DH-76 isokinetic depth-integrated sampler, shown in Figure 67 below, and poured into 500mL Nalgene plastic bottles. Special care or preservation is not required for sediment samples as it is for many chemical analyses, and the samples were stored at room temperature until the samples could be analyzed for particle size distribution and concentration.



*Figure 67: FISP DH-76 isokinetic depth integrated sampler.*

### **3. Data Analysis**

#### *i. Analysis of Total Suspended Material*

The suspended sediment analysis was conducted using standard filtration/drying methods for Total Suspended Material (TSM). The procedure followed in this study is the same procedure used by the U.S. Army Engineer Research and Development Center (ERDC), in Vicksburg, Mississippi, as provided by Dave Perkey. The procedure, provided in Appendix G, involved filtering a known volume of sample through pre-weighed 90 mm glass fiber filters (0.7 $\mu$ m pore size), drying the filter in an oven set to 50°-60°C (120°F-140°F) for 24 hours, and reweighing the filter. Dividing the weight difference by the sample volume yielded the concentration, which was recorded and entered into a spreadsheet.

#### *ii. Particle Size Distribution*

Particle size distributions were determined using laser diffraction particle size analyzers. Initial sample analyses were conducted at the U.S. Army Engineer Research and Development Center (ERDC) in Vicksburg, Mississippi, due to the fact that a laser diffraction particle size analyzer was not available locally. Later analyses were conducted in the Center for Restoration of Ecosystems and Watersheds (CREW) laboratories in Carson Engineering Center at the University of Oklahoma (OU) in Norman, Oklahoma. The particle size analyses conducted at ERDC used a Malvern Mastersizer 2000 particle size analyzer. A Laser In Situ Scattering and Transmissometry (LISST) Portable XR particle size analyzer from Sequoia Scientific, Inc. was used at OU.

Laser diffraction particle size analyzers are sophisticated instruments that use light scattering to determine the size distribution and volume concentration of particles in a sample. There are numerous papers published about them in the literature (Agrawal et al., 2008; Pedocchi and Garcia, 2006; Gartner et al., 2001; Traykovski et al., 1999; McCave et al., 1986). A brief description of the principles of their operation is provided below.

Due to the properties of light, when a ray of light strikes a particle that is much larger than the wavelength of the light ( $> 20$  times), the majority of the light is diffracted around the particle at small angles in the forward direction, with the angle increasing with decreasing size. LISSTs, and other laser diffraction particle size analyzers, exploit this property and measure the particle size distribution by measuring the angular distribution of forward scattered light energy. The LISST Portable XR instruments measure the scattered light with 32 logarithmically spaced, ring-shaped detectors. These scattering data are inverted to produce size distribution using a so-called kernel matrix.

The LISST-Portable|XR and the Malvern Mastersizer 2000 allow the user to choose between two different optical models for inverting the scattering pattern into a size distribution; the Fraunhofer diffraction model and the Mie scattering model. The difference between the models is that the Fraunhofer model assumes that all of the detected light is generated by diffraction only, whereas the Mie model accounts for refraction, reflection and absorption, which become increasingly significant for transparent materials and for very small particles. The Mie model is more complete, but its proper application requires that the refractive index of the particles and suspension



fluid, and the absorption coefficient of the particles, be known. It is also only applicable to single property particles, not for mixtures (Wolfgang, 2012).

The LISST-Portable|XR includes the optical properties of a wide range of materials for applying the Mie model, but the User's Manual (Sequoia, 2013) says, "If you have absolutely no knowledge about the material in your sample, you should choose the Fraunhofer model." It goes on to say that, "if you have just some information, it might often be better to choose the Mie model, and then select the optical model that best fits your knowledge of your sample." However, in phone and e-mail correspondence with technical representatives at Sequoia, who manufactured the instrument, it was suggested that the Fraunhofer model be used for the current study due to the fact that the exact properties of the particles was unknown, and it was a mixture of materials.

Based on this advice, the decision was made to use the Fraunhofer model for the LISST analyses. The optical model used for the analyses performed using the Malvern Mastersizer 2000 was set by ERDC lab personnel and was not recorded at the time. Later, when the significance of the settings was realized, they were contacted and it was learned that the Mie theory was used, and that for unknown sediments ERDC typically uses the density and refractive index of quartz ( $2.65 \text{ g/cm}^3$  and 1.55, respectively).

The procedure followed for both instruments was essentially the same. A clean mixing chamber was first filled with DI water, and a blanking procedure was performed to obtain background measurements. A small sample was then squirted into the mixing chamber, and the measurement was taken. The small samples were taken from the sample bottle using a small plastic suction pipette. In an effort to obtain representative

samples, the sample was first well mixed by shaking the bottle vigorously to suspend all of the material. The lid was then immediately removed from the bottle and the pipette was swiped through the bottle in a swirling motion, while gradually releasing pressure on the pipette. The results of the measurements were recorded and entered into a spreadsheet.

### **iii. Sediment Flux**

With the concentrations and particle size distributions of the samples determined, the sediment flux associated with the samples could be calculated. For the grab samples, calculating the flux was simply a matter of multiplying the sample concentration by the discharge associated with the sample. Calculating the flux from the depth-integrated samples was also fairly straight forward, but required first averaging the concentrations from the three samples, before multiplying the resultant concentration by the discharge associated with the sample. Calculating the flux from the ADCP samples was not as straight forward, and required post-processing the ADCP data using the ViSea PDT software.

The underlying principle of the PDT software is the sonar equation, which was developed to detect targets (literally) in the water. At the point of detection, the signal level coming from the target is just barely greater than the background masking level. Urick (1967) presented the fundamental active-sonar equation in terms of the sonar parameters as:

$$SL - 2TL + TS = NL - DI + DT \quad (5)$$

Where  $SL$  is the projector source level (equipment dependent),  $TL$  is the transmission loss (medium dependent),  $TS$  is the target strength (target dependent),  $NL$  is the ambient

noise level (equipment and medium dependent),  $DI$  is the receiving directivity index (equipment dependent), and  $DT$  is the detection threshold (equipment dependent).

The parameters are shown graphically in Figure 68. The signal level coming from the target is the signal level of the projector ( $SL$ ) minus transmission losses to and from the target ( $2TL$ ) plus the target strength ( $TS$ ). The background masking level is equal to the ambient noise level ( $NL$ ) minus the receiving directivity index ( $DI$ ), as a result of the transducer acting as a receiver or hydrophone, plus the detection threshold ( $DT$ ).

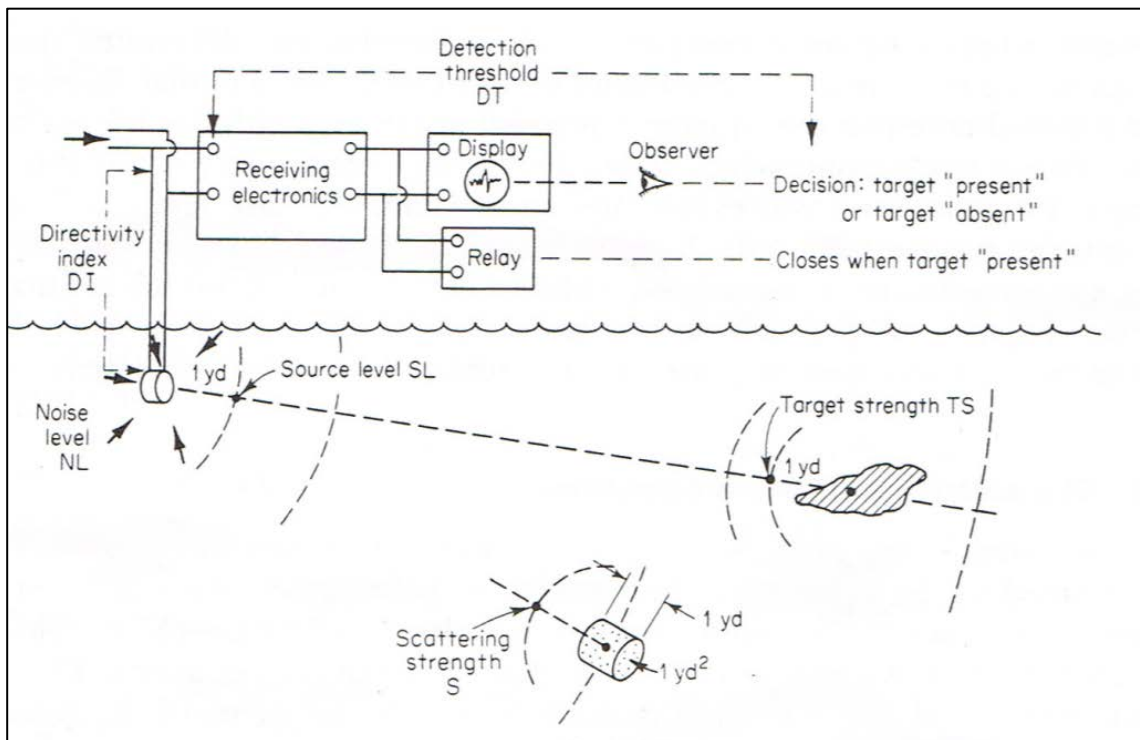


Figure 68: Diagrammatic view of the sonar parameters; from Urick (1967).

The source level ( $SL$ ), directivity index ( $DI$ ) and the detection threshold ( $DT$ ) are equipment dependent. They are typically determined by the manufacturer of the acoustic transducer and may be regarded as constants for a specific instrument. The transmission loss ( $TL$ ), the target strength ( $TS$ ) and ambient noise level ( $NL$ ) are all medium dependent and influenced by the amount of backscatter in the water. Transmission losses ( $TL$ ) include attenuation due to water absorption and the sediment particles, and the target strength ( $TS$ ) of suspended sediment is a function of particle shape, size, rigidity, and acoustic wavelength.

Deines (1999) developed a working version of the sonar equation for the broadband RDI ADCP, rearranged to solve for the backscatter coefficient ( $S_v$ ) in decibels:

$$S_v = C + 10\log_{10}((T_x + 273.16)R^2) - L_{DBM} - P_{DBW} + 2\alpha R + K_c(E - E_r) \quad (6)$$

where  $S_v$  is the backscattering strength in dB,  $C$  is a constant,  $T_x$  is the temperature of the transducer ( $^{\circ}C$ ),  $L_{DBM}$  is  $10\log_{10}$  (transmit pulse length, meters),  $P_{DBW}$  is  $10\log_{10}$  (transmit power, Watts),  $\alpha$  is the absorption coefficient of water (dB/m),  $R$  is range along the beam (slant range) to the scatterers (m),  $K_c$  is the received signal strength indicator scale factor,  $E$  is the echo strength (in counts), and  $E_r$  is the received noise (in counts).

Noting that the parameters  $L_{DBM}$ ,  $P_{DBW}$  and  $E_r$  can also be regarded as constants for specific ADCP instruments and constant power supply, Kim and Voulgaris (2003) simplified equation 6 to:

$$10\log_{10}(SSC) = C_k + 10\log_{10}(R^2) + 2\alpha R + K_c E \quad (7)$$

where  $SSC$  is suspended sediment concentration (in  $\text{kg/m}^3$ ),  $C_k$  is a combined constant, and the remaining parameters are as defined above. The attenuation coefficient,  $\alpha$ , depends primarily on the frequency of the transmitted pulse and partially on the temperature, salinity, density and depth of the water column.  $C_k$  and  $K_c$  cannot be measured directly. Instead they must be estimated through calibration with acoustic data backscattered by sedimentary particles of known concentration.

The ViSea PDT software follows an approach similar to Kim and Voulgaris (2003), with a slight difference. ADCPs derive backscatter ( $E$ ) from the Received Signal Strength Indicator ( $RSSI$ ) of the receivers. The  $RSSI$  value when there is no signal present is denoted  $E_r$ , and it is typically 40 counts. Because the  $RSSI$  output is measured in counts that are proportional to the logarithm of power, an  $RSSI$  scale factor is required to convert to dB units. The scale factor ranges from 0.35 to 0.55 dB/cnt and is typically 0.45 dB/cnt. The PDT allows the user to input the  $RSSI$  and  $E_r$  in the initial step of sediment processing, and this reduces equation 6 to:

$$10\log_{10}(SSC) = C_1 + C_2 I \quad (8)$$

where  $SSC$  is the suspended sediment concentration in  $\text{mg/L}$  and  $I$  is the absolute back scatter in dB. The absolute backscatter, and therefore  $SSC$ , is dependent on particle attenuation. However, particle attenuation is dependent on  $SSC$ , so that the  $SSC$  values have to be optimized using an iterative calculation procedure, as follows. The PDT software takes the absolute backscatter in the first ADCP bin and calculates  $SSC$  using a

standard calibration relationship. However, sediment attenuation is not accounted for in the absolute backscatter calculation in the first ADCP bin, and acoustic loss is based only on acoustic spreading and water absorption. The resulting SSC value is used to calculate particle attenuation. This particle attenuation is used to complete the range normalization and obtain a corrected absolute backscatter. This process is repeated until SSC is fully optimized. This optimized SSC value for the first ADCP bin is then used to calculate particle attenuation and an optimized SSC value in the second ADCP bin. This process is continued until all ADCP bins have optimized SSC values.

As described in Section II.C.1, ADCP measurements were collected using the Teledyne RDI WinRiver II software. Although the ViSea DAS software was designed to work with the Workhore Rio Grande ADCPs for data collection, it was not used to collect the data in this study, primarily due to the fact that WinRiver II was already being used to measure discharge before the ViSea DAS and PDT software was acquired. Rather than face another learning curve with new software, it was decided that the ADCP measurements would continue to be taken using the WinRiver II software. The resulting output files were then post-processed using ViSea DAS and PDT to do the sediment transport analysis.

Post-processing involved the following steps:

Step 1: Start the ViSea DAS (Ver. 4.02.80) program.

Step 2: Start the PDT program within DAS.

Step 3: Play back the WinRiver II output files in DAS.

This also plays the files back in PDT.

Step 4: Input environmental parameters into PDT (Figure 69).

The environmental parameters are required so that the acoustic loss terms can be added to the converted backscatter, which is necessary to perform the iterative calibration required to determine the suspended sediment concentration in the water column. The environmental parameters include:

Profile modes for temperature, salinity, conductivity and the speed of sound. - For this study, the profile modes were set to “Take value from ADCP for entire water column.”

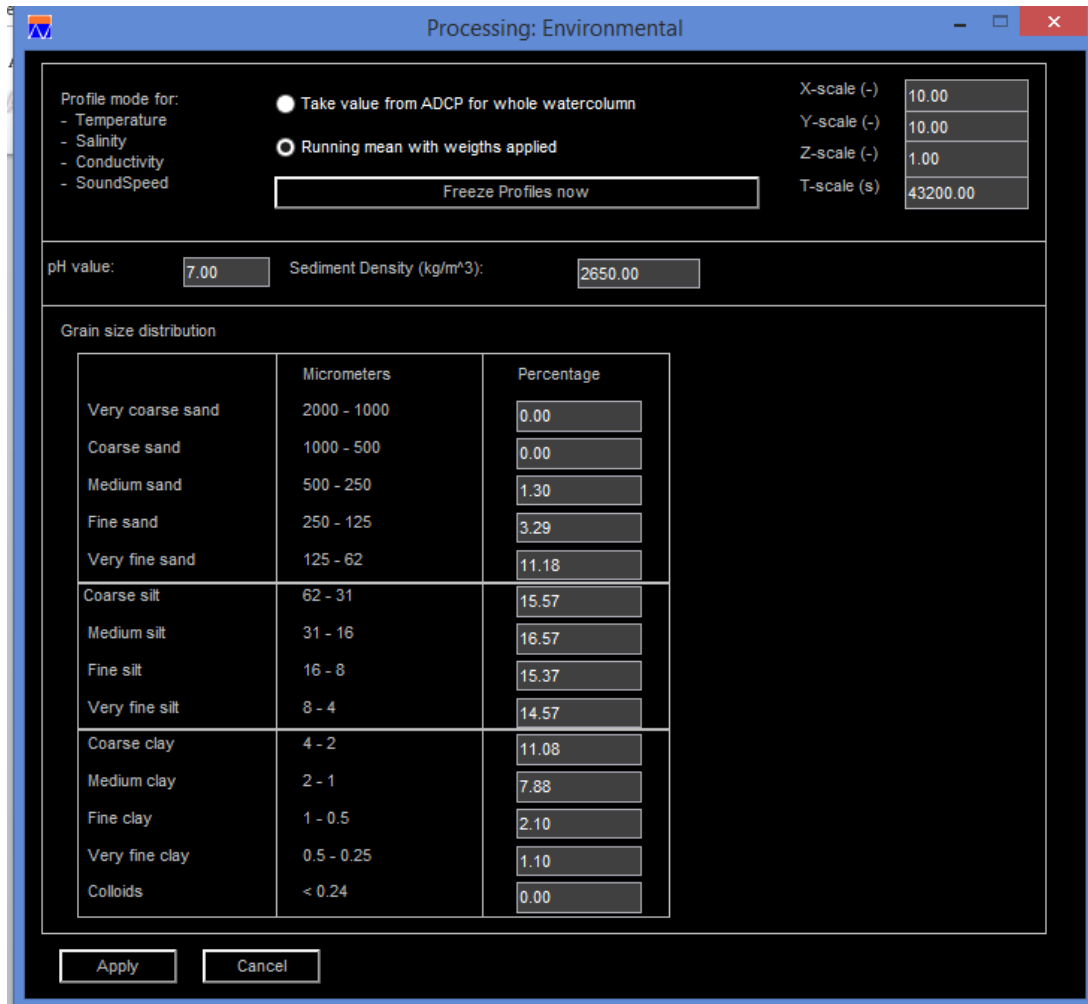


Figure 69: Environmental Processing screen in ViSea PDT.

pH of the water – 7

Sediment density - 2650.00 kg/m<sup>3</sup> (typical of quartz)

Suspended sediment particle size distribution.

Step 5: Enter water sample data in PDT (Figure 70).

For this study, as described previously, the water sample data consisted of grab samples collected at three locations across the channel, left-center, center and right-center. These grab samples were collected immediately after stationary ADCP data were collected at each location. The concentrations determined in the sample analysis were then entered into the PDT software at the proper depth and location on the corresponding transect. Figure 69 shows the sample data for the Little River at 60<sup>th</sup> site on April 15, 2012.

Nr	userID	TrackId	EnsNr	Date	X	Y	Depth	SSC
1	Lr1-1	LR-60_0_000	1	2012/04/15,11:04:39.240	-350470.91	127000.00	1.00	2105.05
2	Lr1-2	LR-60_0_000	3	2012/04/15,11:05:19.240	-350470.92	127000.00	1.00	2105.05
3	Lr1-3	LR-60_0_000	5	2012/04/15,11:05:59.240	-350470.92	127000.02	1.00	2105.05
4	Ctr1-1	LR-60_0_001	1	2012/04/15,11:09:24.840	-350470.88	126999.97	1.00	2397.70
5	Ctr1-2	LR-60_0_001	3	2012/04/15,11:10:04.840	-350470.88	126999.95	1.00	2397.70
6	Ctr1-3	LR-60_0_001	6	2012/04/15,11:11:04.840	-350470.88	126999.93	1.00	2397.70
7	Rt1-1	LR-60_0_002	1	2012/04/15,11:40:59.080	NaN	NaN	1.00	2394.43
8	Rt1-2	LR-60_0_002	2	2012/04/15,11:41:19.080	NaN	NaN	1.00	2394.43

0	-	LR-01_0_000	280	2012/04/15,11:48:50.170	-350470.89	127000.16	0.00	0
---	---	-------------	-----	-------------------------	------------	-----------	------	---

Add Remove Close

Figure 70: Sample Data screen in ViSea PDT.



Step 6: Input required iteration information in PDT (Figure 71).

In order to perform the iteration, PDT requires some additional information, including the following:

Backscatter Coefficients - Default values were used.

OBS (Optical Back Scatter) Coefficients - Not required.

Number of fixed bins – Used default value of 1.

Maximum iteration steps – Used default value of 1.

Iteration test value “until (mg/l)” – Set to 1.

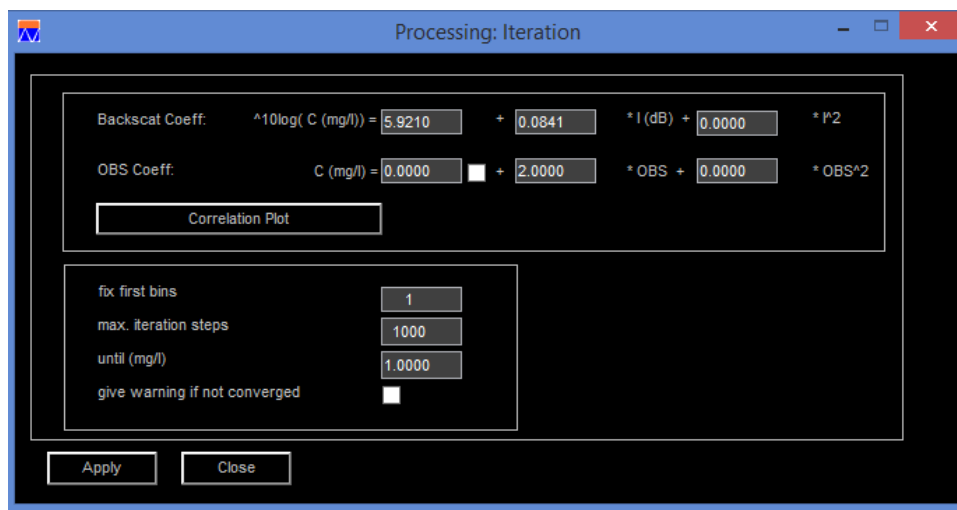


Figure 71: Iteration Processing screen in ViSea PDT.

Step 7: Open the Correlation Processing screen by selecting the “Correlation Plot” button. The correlation plot shows the concentration from absolute backscatter versus the concentration from the water samples in mg/l, as shown in Figure 72.

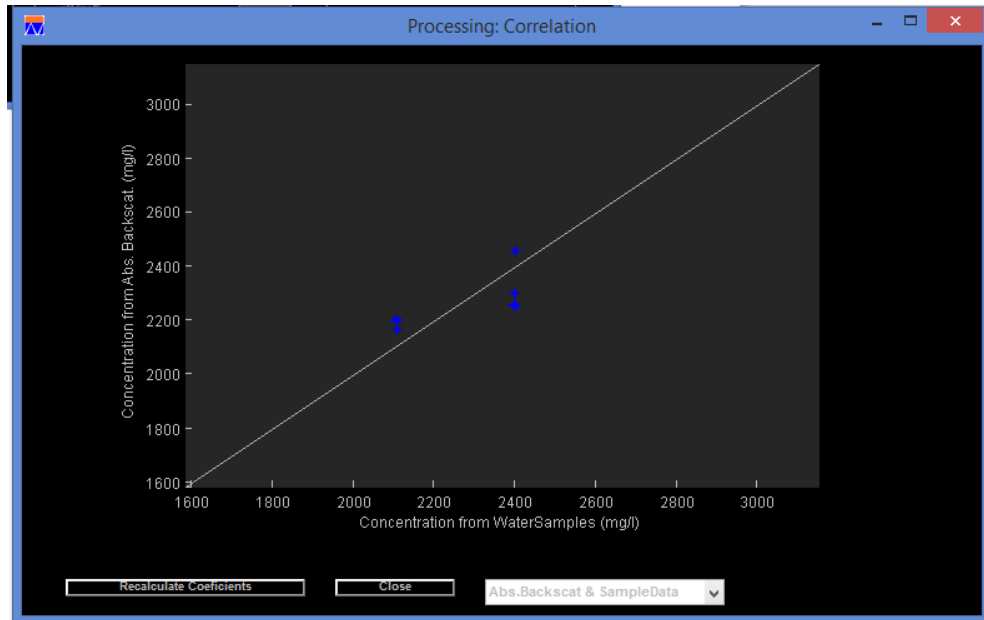


Figure 72: Correlation Processing screen in ViSea PDT.

Step 8: Recalculate the backscatter coefficients by selecting the “Recalculate Coefficients” button. A new set of backscatter coefficients is generated to calibrate the data to the samples.

Step 9: Return to the Iteration Processing screen and “Apply” the new coefficients. PDT reprocesses the data using the new coefficients.

Step 10: Repeat steps 7-9 until the backscatter coefficients remained constant.

Step 11: Reprocess transects in DAS. (This also reprocesses the data in PDT).

This final step reprocesses all of the transect data with the calibrated coefficients and generates estimates of both the discharge ( $\text{m}^3/\text{s}$ ) and sediment flux ( $\text{kg}/\text{s}$ ) for each transect. The PDT software displays the total flux for the transect, and allows the user to view the data distribution across the transect as shown in Figure 73, which is a plot from one of the transects at the Little River at 60<sup>th</sup> site on July 17, 2013.

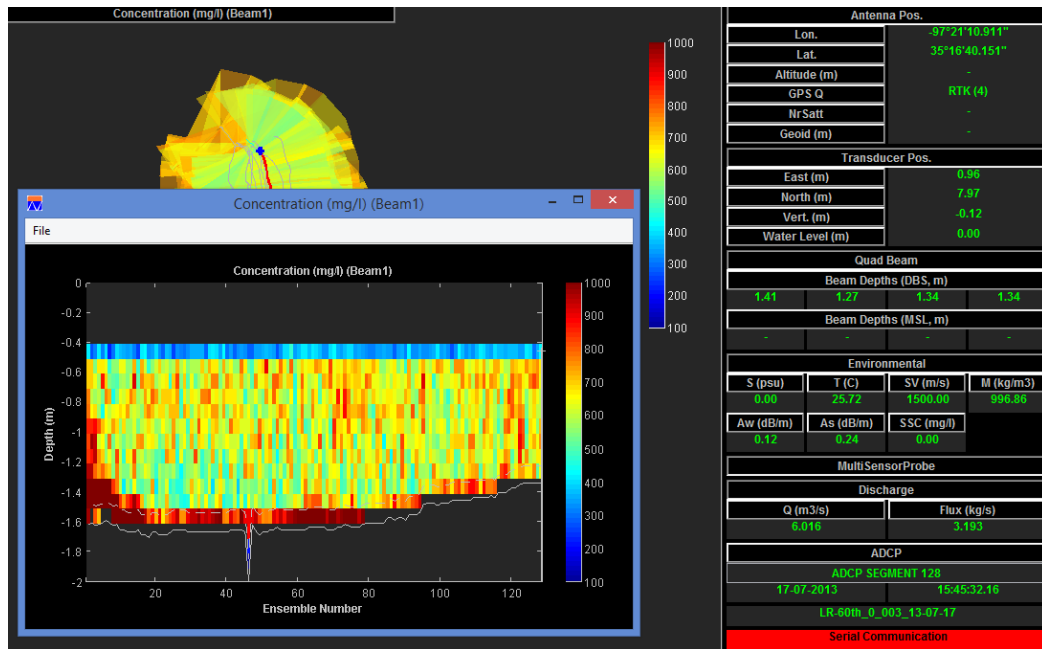


Figure 73: Typical ViSea PDT screen display; transect of the Little River at 60th site on July 17, 2013.

Discharge and flux results generated from the ADCP data with the ViSea PDT software were used to generate sediment flux curves. These curves were then compared statistically to the flux curves generated from grab samples and depth-integrated samples.

## E. Results

### 1. Sediment Analysis

Table 15 shows the dates and locations in the Lake Thunderbird watershed where the ADCP was deployed during this study. The table shows that the ADCP was deployed 23 separate days at 3 different sites. During these deployments, 49 distinct discharge measurements were made and data for 26 suspended sediment analyses were collected, which allowed for estimates of suspended sediment flux. In the earlier ADCP

deployments, no attempt was made to measure sediment as the researchers familiarized themselves with use of the ADCP for measuring discharge. In later deployments, due to various reasons, data for suspended sediment flux operations were either not collected or were somehow unsatisfactory.

The sediment sampling events generated over 166 samples that were analyzed for particle size and concentration. In addition, a dozen or so low flow samples, collected early in the study, were analyzed only for concentration. The results of the total suspended solids concentration analyses are summarized in Appendix H, and the results of the particle size analyses are summarized in Appendix I.

*Table 15: ADCP Deployments*

Date	Site	# of Q Meas	# of Sed Meas
7/10/2010	Little River at 60th	4	0
7/12/2010	Little River at 60th	1	0
7/13/2010	Little River at 60th	3	0
5/20/2011	Little River at 60th	2	2
5/20/2011	Rock Creek @ 72nd	2	2
3/20/2012	Little River at 60th	2	2
3/21/2012	Little River at 60th	2	1
3/22/2012	Little River at 60th	1	1
4/15/2012	Little River at 60th	2	2
4/4/2013	Little River at 60th	2	2
4/13/2013	Little River at 60th	1	0
4/18/2013	Little River at 60th	2	0
5/21/2013	Little River at Porter	4	3
5/22/2013	Little River at 60th	2	0
5/23/2013	Little River at 60th	2	1
5/24/2013	Little River at 60th	3	1
6/4/2013	Little River at Porter	2	2
6/5/2013	Little River at 60th	3	2
6/17/2013	Little River at 60th	3	2
7/15/2013	Little River at Porter	1	1
7/16/2013	Little River at 60th	2	1
7/17/2013	Little River at 60th	2	1
7/26/2013	Little River at 60th	1	0
	Total	49	26

As mentioned previously, initial sediment sample analysis was conducted at the ERDC, in Vicksburg, Mississippi, due to the fact that a LISST was not available locally at the beginning of the study. Two trips were made to Vicksburg. The first trip was in November 2011, but only a relatively few samples were analyzed, as this initial trip was used to become familiar with the laboratory and the procedures and to get a feel for how long it was going to take to perform the analyses. A second trip was taken in September 2013, and 80 samples were transported for analysis. Of these 80 samples, 60 were analyzed for particle size and concentration, and 20 were analyzed only for particle size. The reason for not doing the concentration analysis on these 20 samples was to allow a comparison of the particle size analysis results of the Mastersizer 2000 and the LISST Portable XR.

In November, 2013 the LISST Portable XR particle size analyzer arrived from Sequoia, but the instrument was not tested until March, 2014. Initial tests on the LISST were conducted using samples from the Little River, collected specifically for this purpose. The samples were collected at low flow, so the bottom sediments were stirred up and the sample was collected by swiping the sample bottle through the sediment “cloud” in the water. Initial results were not promising, as they were not repeatable, even when using only DI water for the sample. After discussion with technical representatives from Sequoia, the instrument was sent back for inspection and recalibration. When the instrument was returned, tests on a standard sample Sequoia sent confirmed that the instrument had been fixed and was operating properly.

At this point, one of the Little River test samples was again used to evaluate the repeatability of the instrument and sampling procedure. The test was conducted by

analyzing 20 sub-samples of the test sample. Figure 74 shows the size distribution plots for the 20 sub-samples. It may be seen that there is considerable variability among the samples, especially for larger particles, with the Coefficient of Variation (CV) increasing from less than 5% for the smaller sizes ( $\leq 1.37\mu\text{m}$ ) to over 24% for the larger sizes (between  $80.49$  and  $117.03\mu\text{m}$ ). The source of this variation is possibly due to the sub-sampling method used in the study being somewhat ineffective at collecting a representative sample. Using a churn splitter or cone splitter would likely have resulted in less scatter of the data, especially for the larger size particles.

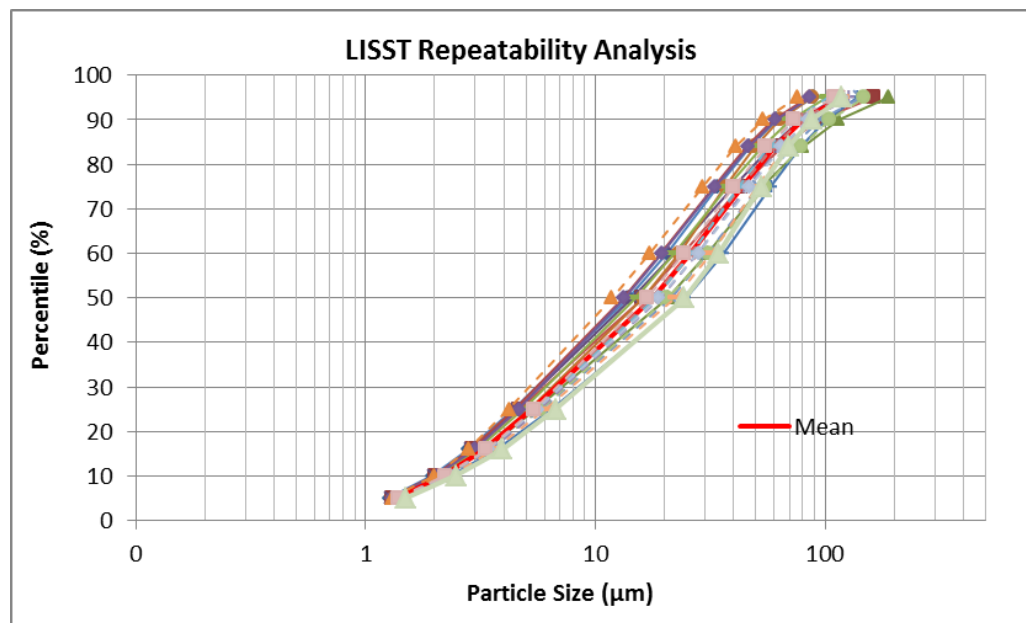


Figure 74: LISST Repeatability Analysis Particle Size Distribution Plot.

The variability between the particle size results obtained using the Mastersizer 2000 and the results obtained using the LISST Portable XR is also significant. Figure 75 shows the mean particle size (D50) of the 20 samples as determined by plotting the

LISST values against the values determined with the Mastersizer. The agreement between the two instruments is not good.

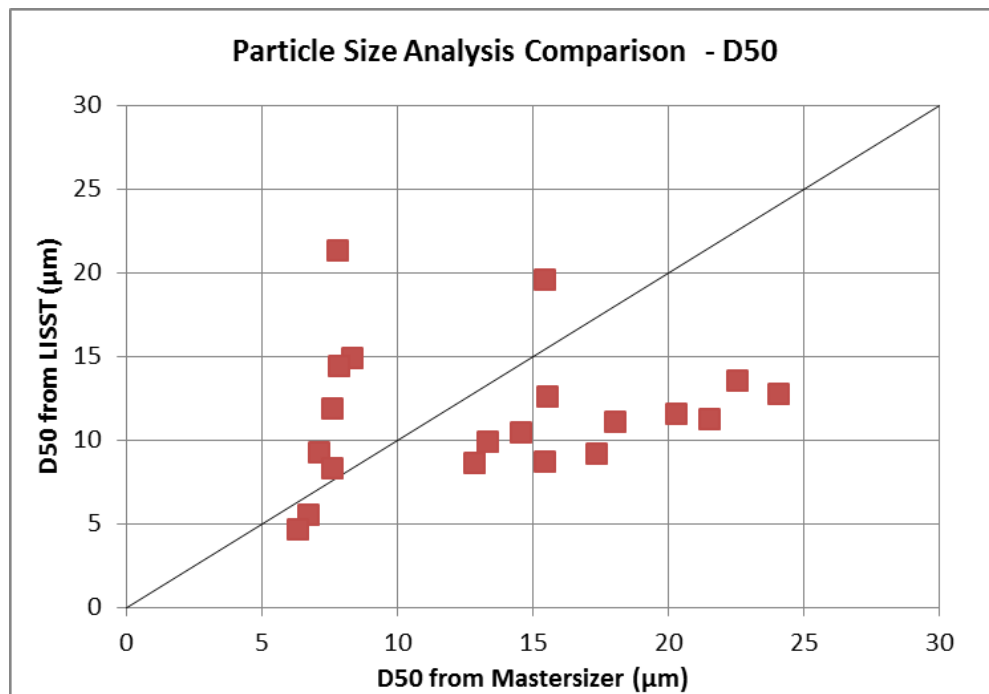


Figure 75: Mean Particle Size Value Comparison between the Sequoia LISST Portable|XR and the Malvern Mastersizer 2000.

However, according to the operator’s manual for the LISST Portable XR particle size analyzer (Sequoia, 2013), “it is extremely important that you only compare measurements analyzed using the same model” because “the same measurement of light scattering can give two very different size distributions if two different optical models are used.” As mentioned previously, the Mie theory model was used when taking measurements with the Malvern, using the density and refractive index of quartz (2.65 g/cm<sup>3</sup> and 1.55, respectively), and measurements taken with the LISST used the

Fraunhoffer model. The poor agreement in measurements between the two instruments is attributed to this model mismatch.

The variability between the results from the two instruments may also be seen in Figures 76-78, which show the particle size class distribution plots for three of the samples. Similar plots were developed for all 20 of the samples analyzed using both instruments, but only the first three are shown, due to space considerations. The data used to generate the plots are provided in Appendix I.

The three samples were selected for display because among the 20 samples, they are the only grab samples used to calibrate the ADCP conversion coefficients. The particle size classes shown in the plots are the class sizes used in the ViSea PDT program. The Mastersizer does not measure or report particle size classes less than 4  $\mu\text{m}$ , and instead reports them only as  $<4\mu\text{m}$ . As a result, for the three samples shown, the LISST measures a greater percentage of small particles ( $<4\mu\text{m}$ ) and a lower percentage of mid-range particles than does the Mastersizer.

The question then became: How much does the variability of the particle size distribution affect the sediment flux estimated using the ViSea PDT software? Initially, before the PDT software was acquired and used, it was thought that a particle size distribution was required for every sample. That turns out not to be the case, however, and only one distribution is entered for a given analysis. It may be seen that the particle size distributions varied between left (Fig. 76), center (Fig. 77) and right (Fig. 78) samples, as well as between instruments, which again begs the question of the sensitivity of the PDT software to particle size distribution.



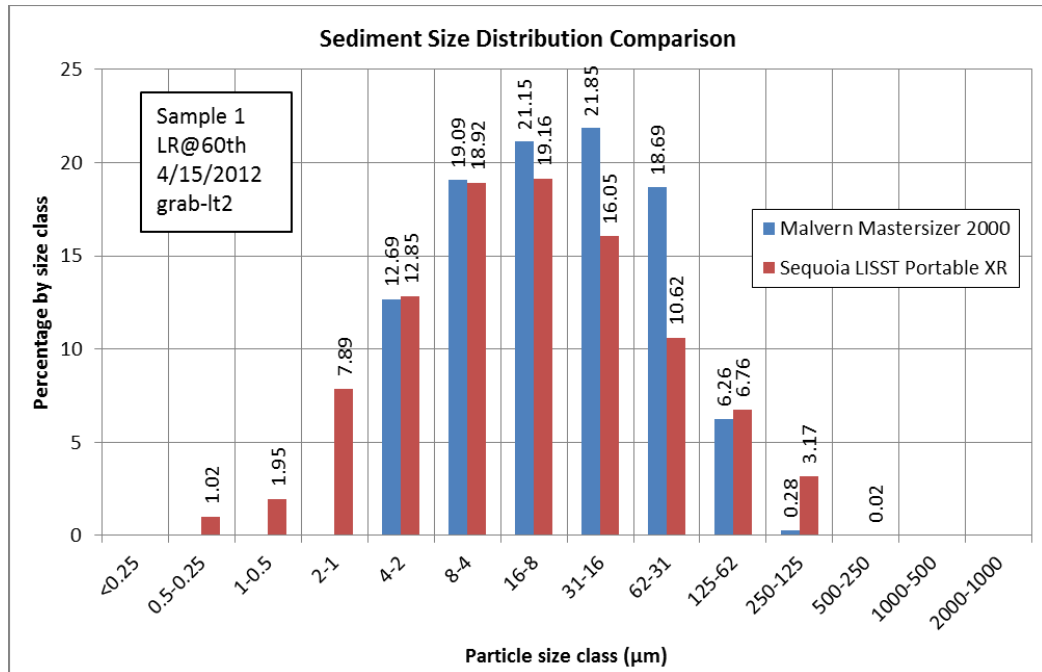


Figure 76: Particle Size Class Distribution of the Sequoia LISST Portable|XR and the Malvern Mastersizer 2000 – Sample 1 – LR@60th; 4-15-2012; grab-lt2.

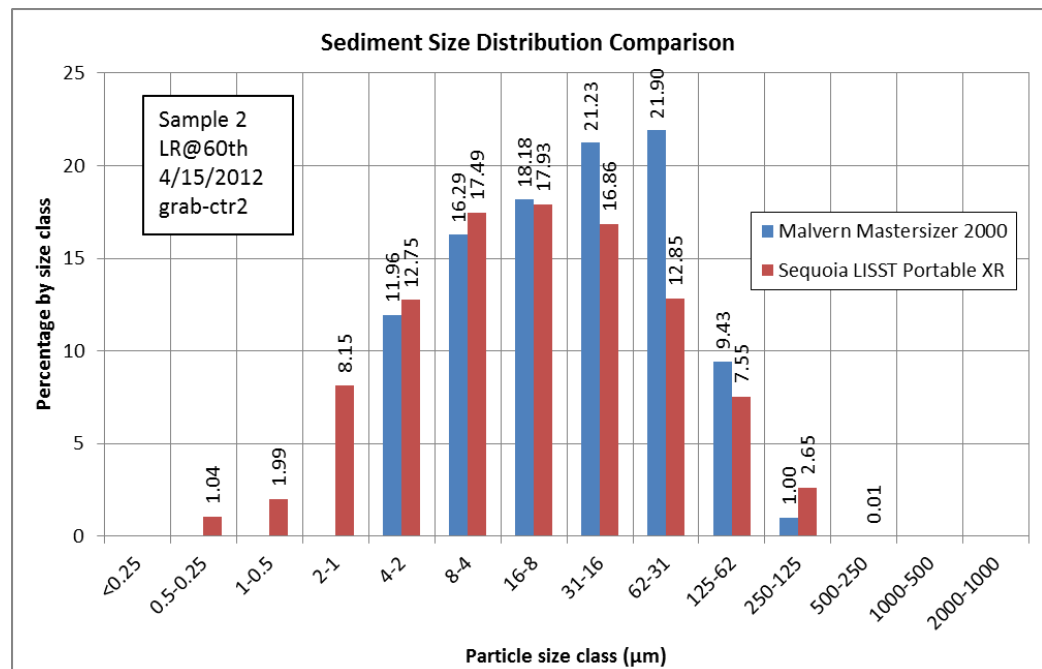


Figure 77: Particle Size Class Distribution of the Sequoia LISST Portable|XR and the Malvern Mastersizer 2000 – Sample 2 – LR@60th; 4-15-2012; grab-ctr2.

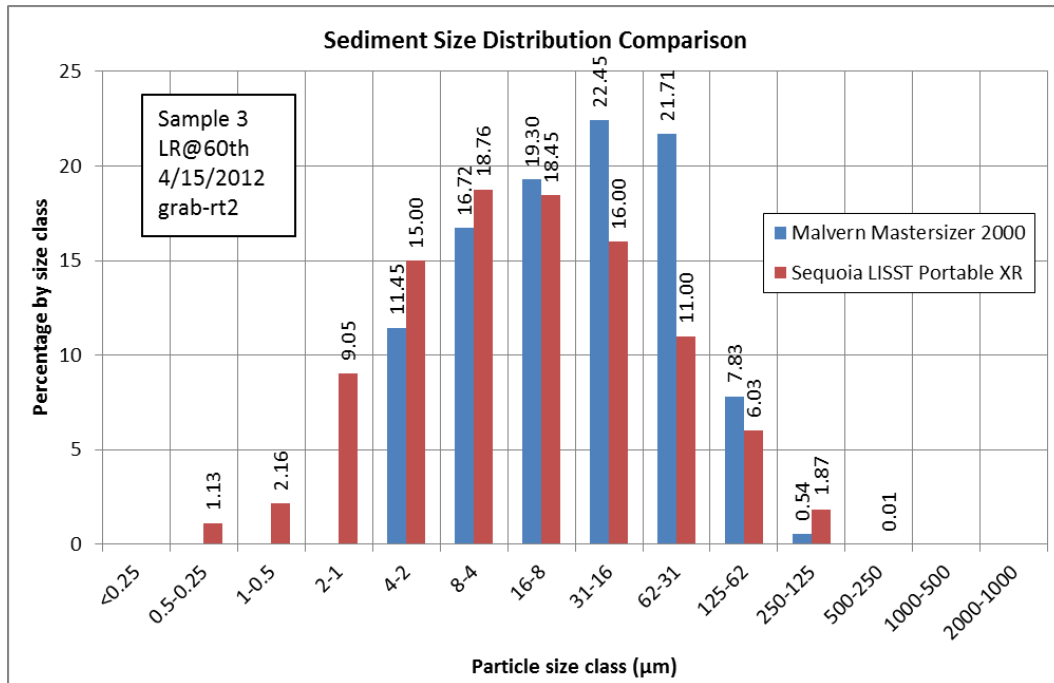


Figure 78: Particle Size Class Distribution of the Sequoia LISST Portable|XR and the Malvern Mastersizer 2000 – Sample 3 – LR@60th; 4-15-2012; grab-rt.

To evaluate the effect that varying particle size distribution has on the sediment flux estimate provided by ViSea PDT, consider the second set of data collected at the Little River at 60<sup>th</sup> site on April 15, 2012. This particular measurement consisted of eight transects, and the discharge, as estimated by the ViSea PDT software, averaged 13.70 cms (483.81 cfs), with a standard deviation of 0.97 cms (34.34 cfs) and a coefficient of variation of 0.07.

Table 16, below, shows the particle size distribution results, as determined by the Mastersizer and LISST for Samples 1-3, corresponding to samples collected on the left, center and right sides of the channel, respectively. Data from the table were used to generate the plots shown in Figures 76-78.

Table 16: Particle Size Distribution for Little River at 60<sup>th</sup>, April 15, 2012;

Sample 1 – Left; Sample 2 – Center; Sample 3 – Right.

Sample #	Instr.	Percentage by class size (µm)													
		2000-1000	1000-500	500-250	250-125	125-62	62-31	31-16	16-8	8-4	4-2	2-1	1-0.5	0.5-0.25	<0.25
M-1	Master sizer	0.00	0.00	0.00	0.28	6.26	18.69	21.85	21.15	19.09	12.69	***	***	***	***
M-2		0.00	0.00	0.00	1.00	9.43	21.90	21.23	18.18	16.29	11.96	***	***	***	***
M-3		0.00	0.00	0.00	0.54	7.83	21.71	22.45	19.30	16.72	11.45	***	***	***	***
L-1	LISST	0.00	0.00	0.02	3.17	6.76	10.62	16.05	19.16	18.92	12.85	7.89	1.95	1.02	0.00
L-2		0.00	0.00	0.01	2.65	7.55	12.85	16.86	17.93	17.49	12.75	8.15	1.99	1.04	0.00
L-3		0.00	0.00	0.01	1.87	6.03	11.00	16.00	18.45	18.76	15.00	9.05	2.16	1.13	0.00

Table 17 shows the conversion coefficients calculated by ViSea PDT, and the estimated sediment flux (kg/s) for each of the eight transects, using the particle size distributions shown in Table 16. Note that the average flux is similar for all sample runs, ranging from 30.86 kg/s - 31.20 kg/s. The standard deviations of the fluxes are also similar for all sample runs, ranging from 2.21-2.24 kg/s, and the coefficient of variation for all runs is 0.07.

Table 17: Sediment flux (kg/s) estimated by ViSea PDT for Little River at 60<sup>th</sup>, April 15, 2012; Sample 1 – Left; Sample 2 – Center; Sample 3 – Right.

Sample #	Conversion Coeff.		Sediment Flux (kg/s)										
	C1	C2	S0	S1	S2	S3	S4	S5	S6	S7	Savg	StDev	CV
M-1	4.6587	0.0429	32.99	28.57	32.51	26.69	33.59	30.92	32.22	30.32	30.98	2.22	0.07
M-2	4.7146	0.0446	32.92	28.51	32.43	26.63	33.51	30.85	32.14	30.25	30.91	2.21	0.07
M-3	4.7106	0.0445	32.87	28.46	32.38	26.59	33.45	30.80	32.09	30.20	30.86	2.21	0.07
L-1	4.5069	0.0383	33.14	28.71	32.65	26.81	33.78	31.07	32.38	30.46	31.13	2.23	0.07
L-2	4.5243	0.0388	33.18	28.74	32.69	26.84	33.81	31.11	32.42	30.50	31.16	2.24	0.07
L-3	4.4659	0.0371	33.22	28.78	32.73	26.87	33.86	31.15	32.47	30.54	31.20	2.24	0.07

Despite the difference in the particle size distributions, the mean sediment flux of the eight transects was found to be 30.92 kg/s, with a standard deviation of 0.05 kg/s and a coefficient of variation of 0.002, using the Mastersizer particle size results. Using

the particle size results from the LISST, the mean sediment flux of the eight transects was found to be 31.16 kg/s, with a standard deviation of 0.032 kg/s and a coefficient of variation of 0.001. Thus, it appears that the observed variability in the measured particle size distributions does not significantly affect the sediment flux estimates. In other words, the ViSea PDT software is not particularly sensitive to the observed variability of the particle size distributions, and thus the observed variability does not significantly affect the sediment flux estimates of the software.

To further investigate the sensitivity of the estimated sediment flux to the particle size, the particle size distributions on the Environmental Processing screen in ViSea PDT (Figure 69) were modified to look at four scenarios: uniform, uniform sand, uniform silt and uniform clay. For the uniform distribution scenario each, of the 14 categories was set to 7.14%. For the uniform sand distribution, each of the five categories of sand was set to 20%, and the silt and clay percentages were set to 0%. Similarly, for the uniform silt distribution scenario the four categories of silt were set to 25%, and the sand and clay percentages were set to 0, and finally for the uniform clay distribution scenario, the five categories of clay were set to 20%, and the sand and clay percentages were set to 0.

Table 18 shows the conversion coefficients calculated by ViSea PDT, and the estimated sediment flux (kg/s) for each of the eight transects under the four uniform distribution scenarios. Table 19 shows the difference between the conversion coefficient values and the estimated flux values, for each of the eight transects, using measured particle size data (Table 17) and the uniform distribution (Table 18). Table 20 shows the percentage difference in the estimates.

The tables show that, even though ViSea PDT was not found to be particularly sensitive to the variation in particle size distribution obtained from the various samples, it is sensitive to the distributions in the four scenarios. The average estimated flux for the eight transects varies from 27.11 kg/s for the uniform silt distribution, to 35.10 kg/s for the uniform sand distribution (Table 18). The average sediment flux estimated using the uniform distribution, 28.96 kg/s, most closely matches the fluxes observed using the measured distributions.

*Table 18: Effect of particle size distribution on sediment flux (kg/s) estimated by ViSea PDT for Little River at 60<sup>th</sup>, April 15, 2012.*

Distribution	Conversion Coeff.		Sediment Flux (kg/s)										
	C1	C2	S0	S1	S2	S3	S4	S5	S6	S7	Savg	StDev	CV
Uniform-All	5.5875	0.0761	27.75	29.46	30.62	27.51	29.77	27.00	29.18	30.40	28.96	1.28	0.04
Uniform Sand	5.1381	0.064	30.63	33.53	34.64	32.45	35.57	39.11	37.59	37.31	35.10	2.67	0.08
Uniform Silt	5.9179	0.083	26.85	27.61	28.84	25.75	27.78	24.95	27.02	28.08	27.11	1.18	0.04
Uniform Clay	5.7229	0.0796	27.41	28.96	30.14	27.03	29.23	26.44	28.60	29.77	28.45	1.26	0.04

*Table 19: Difference in flux (kg/s) estimated by ViSea PDT for Little River at 60<sup>th</sup>, April 15, 2012 using uniform distribution versus measured distribution.*

Sample #	Conversion Coeff.		Sediment Flux Estimate Comparson - Analyzed vs. Uniform - All (kg/s)										
	C1	C2	S0	S1	S2	S3	S4	S5	S6	S7	Savg	StDev	CV
M-1	-0.48	-0.02	5.24	-0.89	1.89	-0.82	3.82	3.92	3.04	-0.08	2.02	2.21	1.10
M-2	-0.42	-0.02	5.17	-0.95	1.81	-0.88	3.74	3.85	2.96	-0.15	1.94	2.21	1.14
M-3	-0.43	-0.02	5.12	-1.00	1.76	-0.92	3.68	3.80	2.91	-0.20	1.89	2.21	1.17
L-1	-0.63	-0.03	5.39	-0.75	2.03	-0.70	4.01	4.07	3.20	0.06	2.16	2.23	1.03
L-2	-0.61	-0.03	5.43	-0.72	2.07	-0.67	4.04	4.11	3.24	0.10	2.20	2.23	1.01
L-3	-0.67	-0.03	5.47	-0.68	2.11	-0.64	4.09	4.15	3.29	0.14	2.24	2.23	1.00

*Table 20: Percent difference in flux estimated by ViSea PDT for Little River at 60<sup>th</sup>, April 15, 2012 using uniform sand distribution versus measured distribution.*

Sample #	Conversion Coeff.		Sediment Flux Estimate Comparison - Analyzed vs. Uniform - All (% Difference)										
	C1	C2	S0	S1	S2	S3	S4	S5	S6	S7	Savg	StDev	CV
M-1	-10.3%	-49.2%	15.9%	-3.1%	5.8%	-3.1%	11.4%	12.7%	9.4%	-0.3%	6.1%	7.0%	1.14
M-2	-9.0%	-43.5%	15.7%	-3.3%	5.6%	-3.3%	11.2%	12.5%	9.2%	-0.5%	5.9%	7.0%	1.19
M-3	-9.1%	-43.8%	15.6%	-3.5%	5.4%	-3.5%	11.0%	12.3%	9.1%	-0.7%	5.7%	7.0%	1.22
L-1	-14.0%	-67.1%	16.3%	-2.6%	6.2%	-2.6%	11.9%	13.1%	9.9%	0.2%	6.5%	6.9%	1.06
L-2	-13.6%	-64.9%	16.4%	-2.5%	6.3%	-2.5%	11.9%	13.2%	10.0%	0.3%	6.6%	6.9%	1.04
L-3	-15.1%	-72.5%	16.5%	-2.4%	6.4%	-2.4%	12.1%	13.3%	10.1%	0.5%	6.8%	6.9%	1.02

The conversion coefficients for all four of the uniform distributions are smaller than for the measured distributions, with C1 being 9-15.1% less and C2 being 43.5-72.5% less. However, even though the calibration coefficients are significantly different, the difference in the average estimated flux is only around 6-7% larger when comparing the measured distribution to the uniform distribution, although there is a lot of variability in the data, with the difference ranging from -3.5% to 16.5%.

The implications of the results of this assessment are that rough estimates of the sediment flux at the Little River at 60<sup>th</sup> site may be obtained using the ADCP and ViSea PDT and a uniform distribution, if limited resources or time constraints preclude conducting particle size analyses. However, this analysis only looked at one event, and may or may not be repeatable for other events. Also, the calibration procedure would still be required using grab samples collected, as described previously, so it is still recommended that particle size analyses be conducted if possible.

## 2. Sediment Flux Methods Analysis

With the suspended sediment concentration and particle size analyses completed, estimates of sediment flux were determined for the various sampling events. Estimates of flux were made using grab samples, depth-integrated samples, and the ADCP with the ViSea PDT software. These flux estimates are reported in Appendix J.

As described previously, calculating the flux for the grab samples was simply a matter of multiplying the sample concentration by the discharge associated with the sample, and calculating the flux from the depth-integrated samples was only slightly more complicated in that the arithmetic mean of the three samples had to be calculated before multiplying the resultant concentration by the discharge associated with the sample. Calculating the flux from the ADCP samples was not so straight-forward, and required post-processing the WinRiver II ADCP data using Aqua Vision's ViSea Plume Detection Toolbox (PDT) with the ViSea Data Acquisition Software (DAS).

After playing back the ADCP data files in ViSea DAS, ViSea PDT provides an estimate for the discharge (cms) and sediment flux (kg/s) for each transect. It may be seen in Table J.5 in Appendix J that the discharge estimates from ViSea PDT are consistently less than the WinRiver II estimates. This discrepancy was pointed out to Aqua Vision, and the discrepancy has reportedly been corrected in the newest version of the software. For this study, the WinRiver II discharge estimates were used to determine the fluxes for the grab and depth-integrated sample methods, and the ADCP /ViSea PDT method used the discharge and sediment flux as reported by the ViSea PDT software.

Figure 79 shows the plots of suspended sediment flux (tons/day) versus discharge (cfs), as determined for the Little River at 60<sup>th</sup> site, using the three methods: grab, depth-integrated, and the ADCP with the ViSea PDT. The exponents and coefficients for the regression lines for the three data sets, as well as the R<sup>2</sup> values for the relationships, are provided in Table 21. It may be seen that the regression lines describe the relationship between the data well, with R<sup>2</sup> values of 0.8865, 0.8972, and 0.8740, for the grab, depth-integrated and ADCP/ViSea PDT data, respectively. The slopes of the regression lines are all similar too, with the slopes of the grab and ADCP/ViSea PDT lines being virtually indistinguishable.

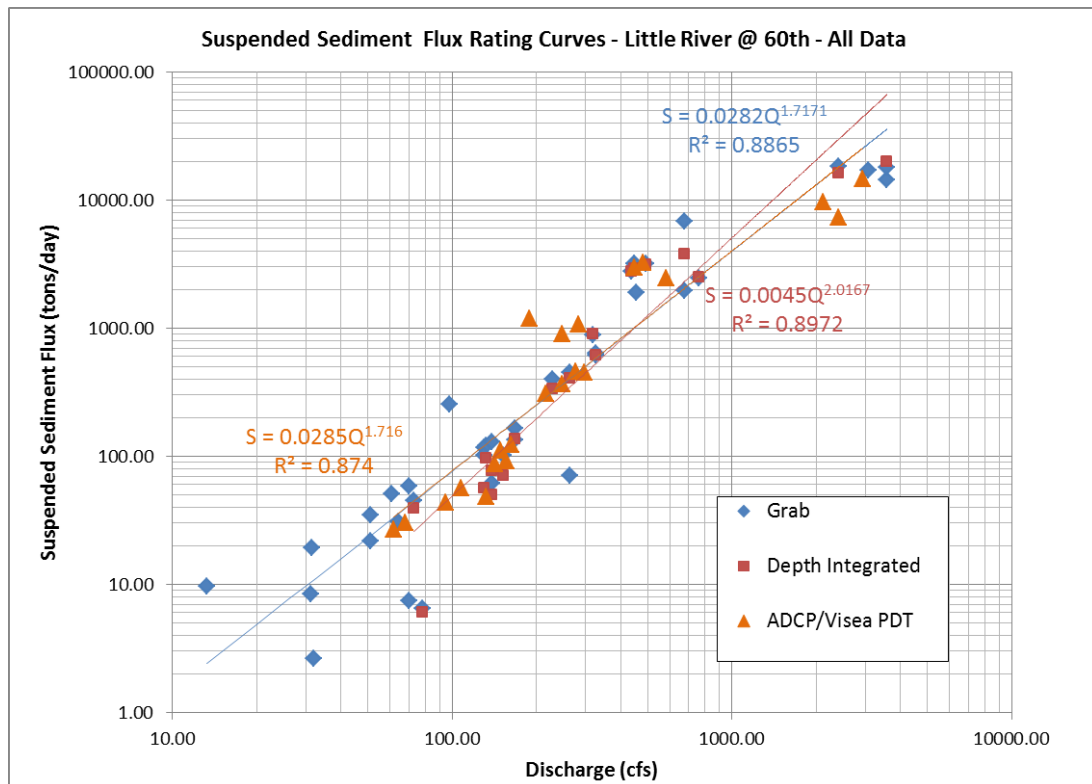


Figure 79: Suspended Sediment Rating Curves for Little River at 60<sup>th</sup>; All Data.



*Table 21: Sediment Flux Rating Curve Coefficients and Exponents for Little River at 60th; All Data.*

Sediment Flux rating curve coefficients and exponents for Little River at 60 <sup>th</sup> - All Data; $S = aQ^b$			
Sample Source	a	b	R <sup>2</sup>
Grab	0.0282	1.7171	0.8865
Depth Integrated	0.0045	2.0167	0.8972
ADCP with ViSea PDT	0.0285	1.7176	0.8740

However, in order to better compare the results of the three methods, only data within a common range of discharges were considered. Thus grab sample data at discharges below 60 cfs were removed from the data set, as they are outside the range of data from the depth-integrated and ADCP/ViSea PDT methods. Figure 80 shows the plots of suspended sediment flux (tons/day) versus discharge (cfs), as determined for the Little River at 60<sup>th</sup> site using the three methods, for discharges above 60 cfs. The exponents and coefficients for the regression lines for the three data sets, as well as the R<sup>2</sup> values for the relationships, are provided in Table 22. Again, it may be seen that the regression lines describe the relationship between the data well, with R<sup>2</sup> values of 0.8653 for the grab sample data, and the values for depth integrated and ADCP/ViSea PDT data remaining at 0.8972, and 0.8740, respectively. The slopes of the regression lines are all similar as well.

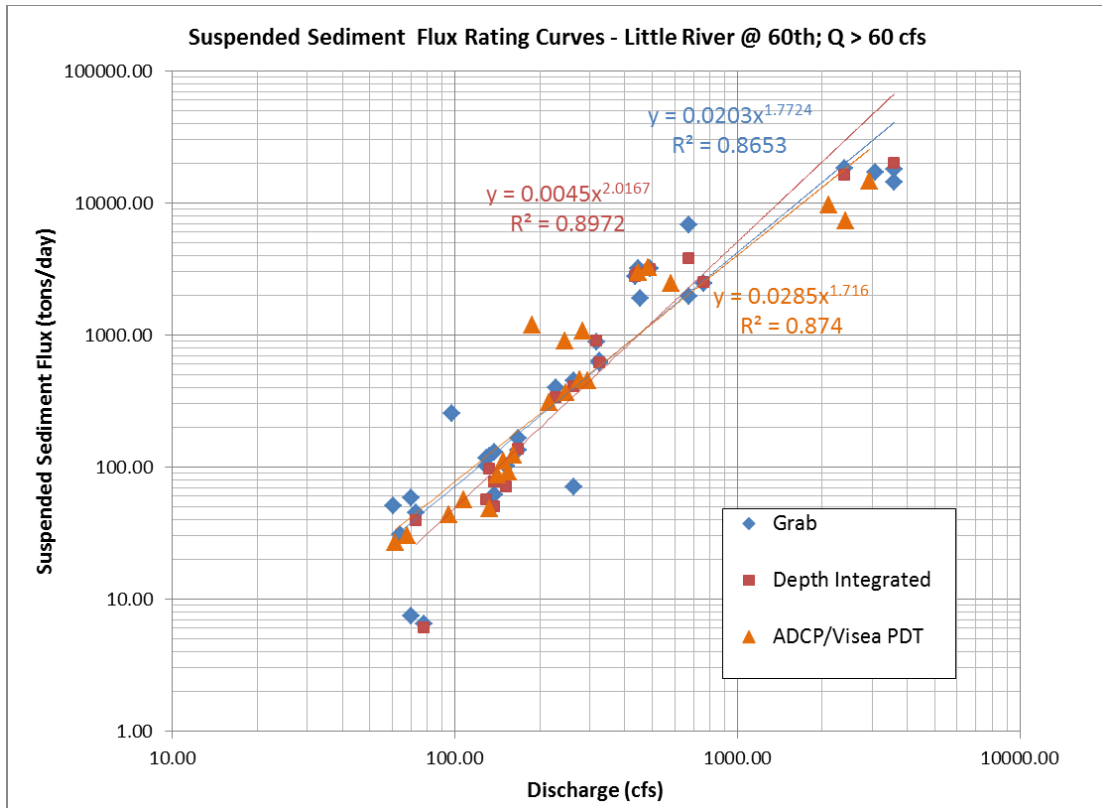


Figure 80: Suspended Sediment Rating Curves for Little River at 60<sup>th</sup>;  $Q > 60$  cfs.

Table 22: Sediment Flux Rating Curve Coefficients and Exponents for Little River at 60<sup>th</sup>;  $Q > 60$  cfs.

Sediment Flux rating curve coefficients and exponents for Little River at 60 <sup>th</sup> ; $S = aQ^b$			
Sample Source	a	b	R <sup>2</sup>
Grab	0.0203	1.7724	0.8653
Depth Integrated	0.0045	2.0167	0.8972
ADCP with ViSea PDT	0.0285	1.7176	0.8740

Although the slopes of the regression lines appear to be similar, it was necessary to determine if the differences between the lines are statistically significant. To accomplish this, hypothesis tests of the slope and intercept were performed. Procedures for performing the required tests are provided by Blank (1980), Kleinbaum et al. (1998)

and Howell (2010). The slope was tested first using the null hypothesis that the two slopes are equal, which may be expressed as:

$$H_0: \beta_1 = \beta_2 \text{ i.e. } \beta_1 - \beta_2 = 0$$

The test statistic is given by:

$$t = \frac{b_1 - b_2}{S_{b_1 - b_2}} \quad (9)$$

with  $(n_1 + n_2 - 4)$  degrees of freedom, and where  $b_1$  and  $b_2$  are the slopes of the regression lines being compared, and where:

$$S_{b_1 - b_2} = \sqrt{S_{b_1}^2 + S_{b_2}^2} \quad (10)$$

$S_{b_1}$  and  $S_{b_2}$ , are the standard error of the slopes of the regression lines being compared and are given by:

$$S_{b_1} = S_{y_1, x_1} / (S_{x_1} * \sqrt{n_1 - 1}) \quad (11)$$

and

$$S_{b_2} = S_{y_2, x_2} / (S_{x_2} * \sqrt{n_2 - 1}) \quad (12)$$

where

$S_{y_1, x_1}$  = the standard error of the predicted  $y_1$ -value for each  $x_1$  in the regression

$S_{y_2, x_2}$  = the standard error of the predicted  $y_2$ -value for each  $x_2$  in the regression

$n_1$  = number of samples in data set 1

$n_2$  = number of samples in data set 2

Table 23 shows the results of this assessment. The top five lines of data in the table give the number of samples (n), the slope of the regression line (b), the standard

error of the predicted y-value for each x in the regression ( $S_{y,x}$ ), the standard deviation of the x-values ( $S_x$ ), and the standard error of the slopes of the regression line ( $S_b$ ) for each of the three methods.

In the lower part of the table the values needed to compare the slopes are presented. In the first column, the grab sample method is compared to the depth-integrated sample method; in the second column the grab sample method is compared to the ADCP ViSea PDT method, and in the third column the depth-integrated sampling method is compared to the ADCP ViSea PDT method. The first row shows the  $S_{b_1-b_2}$  values needed to calculate the test statistic (t) for each comparison, shown on the second row. The third row shows the degrees of freedom (df) for each comparison, given by  $n_1+n_2-4$ , the fourth row gives the desired significance level ( $\alpha$ ), and the fifth row gives the p-value derived from the test statistic for each comparison. The last row shows if the difference between the slopes of the compared regression lines is significant.

Table 23: Suspended Sediment Flux Curve Slope Comparison – Little River at 60th;  $Q > 60$  cfs.

Suspended Sediment Flux Rating Curve Statistics				
	Grab	DI	ADCP	
n	33	19	22	=count(logQ)
b	1.7724	2.0167	1.7160	=slope(logS,logQ)
$S_{y-x}$	0.360634	0.319991	0.309791	=steyx(logS,logQ)
$S_x$	0.507522	0.45556	0.463937	=stdev(logQ)
$S_b$	0.125614	0.16556	0.145713	= $S_{y,x}/(S_x * \text{SQRT}(n-1))$
Comparison of Two Slopes				
	Grab-DI	Grab-ADCP	DI-ADCP	
$S_{b1-b2}$	0.20782	0.192383	0.220551	= $\text{SQRT}(S_{b1}^2+S_{b2}^2)$
t	-1.1756	0.29313	1.363429	= $(b_1-b_2)/(S_{b1-b2})$
df	48	51	37	= $(n_1+n_2-4)$
$\alpha$	0.05	0.05	0.05	
p-value	0.245555	0.770612	0.180986	=TDIST( t , df,2)
sig	No	No	No	=yes if p-value< $\alpha$

If the two error variances are equal, which is the case here, the estimates of the error variances can be pooled to test for the differences in the means, weighing each by their degrees of freedom, so that:

$$S_{Res}^2 = \frac{(n_1-2)S_{Res1}^2 + (n_2-2)S_{Res2}^2}{(n_1-2) + (n_2-2)} \quad (13)$$

Since,

$$S_{b_1}^2 = \frac{S_{Res1}^2}{S_{x_1}^2(n_1-1)} \quad (14)$$

and

$$S_{b_2}^2 = \frac{S_{Res2}^2}{S_{x_2}^2(n_2-1)} \quad (15)$$

The numerators can be replaced by the pooled value  $S_{Res}^2$  to yield:

$$S_{b_1-b_2} = S_{Res} \sqrt{\frac{1}{S_{x_1}^2(n_1-1)} + \frac{1}{S_{x_2}^2(n_2-1)}} \quad (16)$$

Table 24 shows the results of this assessment. The first row shows the pooled error variance, squared ( $S_{Res}^2$ ) for each comparison, the second row shows the  $S_{b_1-b_2}$  values needed to calculate the test statistic (t) for each comparison, shown on the third row. The remaining rows are the same as before, with the fourth row showing the degrees of freedom (df) for each comparison, given by  $n_1+n_2-4$ , the fifth row giving the desired significance level ( $\alpha$ ), and the sixth row giving the p-value derived from the test statistic for each comparison. The last row shows if the difference between the slopes of the compared regression lines is significant.

Table 24: Suspended Sediment Flux Curve Slope Comparison Using Pooled Error Variance – Little River at 60<sup>th</sup>; Q > 60 cfs.

Comparison of Two Slopes Using Pooled Error Variance				
	Grab-DI	Grab-ADCP	DI-ADCP	
$s_{Res}^2$	0.12026	0.11669	0.098922	$=((n_1-2)s_{y-x1}^2+(n_2-2)s_{y-x2}^2)/(n_1+n_2-4)$
$s_{b1-b2}$	0.216294	0.199934	0.219923	$=s_{Res} * \text{SQRT}(1/s_{x1}^2(n_1-1)+1/(s_{x2}^2(n_2-1)))$
t	-1.12954	0.28206	1.367322	$=(b_1-b_2)/(s_{b1-b2})$
df	48	51	37	$=(n_1+n_2-4)$
$\alpha$	0.05	0.05	0.05	
p-value	0.264284	0.779039	0.179774	$=\text{TDIST}( t , df, 2)$
sig	No	No	No	$=\text{yes if } p\text{-value} < \alpha$

Using both pooled and unpooled values, the null hypothesis ( $H_0$ : the slopes are equal) cannot be rejected for any of the comparisons made. Therefore, it can be concluded that there is no statistically significant difference between the slopes of the regression lines of the data obtained from the different methods.

With the slopes of the lines found to be statistically the same, the intercept was tested using the null hypothesis:

$$H_0: \alpha_1 = \alpha_2 \text{ i.e. } \alpha_1 - \alpha_2 = 0$$

The test statistic is given by:

$$t = \frac{a_1 - a_2}{s_{a_1 - a_2}} \quad (17)$$

with  $(n_1 + n_2 - 4)$  degrees of freedom, and where  $a_1$  and  $a_2$  are the intercepts of the regression lines being compared, and where:

:

$$s_{a_1 - a_2} = s_{res} \sqrt{\frac{1}{n_1} + \frac{1}{n_2} + \frac{Q_{1avg}^2}{(n_1-1)S_{a_1}^2} + \frac{Q_{2avg}^2}{(n_2-1)S_{a_2}^2}} \quad (18)$$

$S_{a_1}$  and  $S_{a_2}$ , are the standard error of the intercepts of the regression lines being compared, and  $Q_{1avg}$  and  $Q_{2avg}$  are the means of the predictor variable.

As before, Excel was used to perform the required computation.

Table 25 shows the results of this assessment. The first row shows the means on the predictor variable, M and the second row shows the intercepts of the regression lines, a.

The lower part of the table shows the values needed to compare the intercepts of the lines. As before, in the first column the grab sample method is compared to the depth-integrated sample method, in the second column the grab sample method is compared to the ADCP ViSea PDT method, and in the third column the depth-integrated sampling method is compared to the ADCP ViSea PDT method. The first row shows the  $S_{a_1-a_2}$  values needed to calculate the test statistic (t) for each comparison, shown on the second row. The third row shows the degrees of freedom (df) for each comparison, given by  $n_1+n_2-4$ , the fourth row gives the desired significance level ( $\alpha$ ), and the fifth row gives the p-value derived from the test statistic for each comparison. The last row shows if the difference between the slopes of the compared regression lines is significant.

Based on this assessment, the null hypothesis ( $H_0$ : the intercepts are equal) cannot be rejected for any of the comparisons made. Therefore, it can be concluded that there is no statistically significant difference between the intercepts of the regression lines of the data obtained from the different methods, so that, using the ADCP with the ViSea PDT to estimate suspended sediment flux curves provided results that are

statistically insignificant from results using the traditional grab and depth-integrated sampling methods.

Table 25: Suspended Sediment Flux Curve Intercept Comparison – Little River at 60th;  $Q > 60$  cfs.

Comparison of two intersects				
	Grab	DI	ADCP	
M	2.460379	2.544326	2.540503	=avg(x)
a	-1.91931	-2.0819	-1.22736	=intercept(y,x)
	Grab-DI	Grab-ADCP	DI-ADCP	
$s_{a1-a2}$	1.392607	1.17181	1.07077	$=s_{Res}^2(1/n_1+1/n_2+M_1^2/(s_{x1}(n_1-1))+M_2^2/(s_{x2}(n_2-1)))$
t	0.116758	-0.59049	-0.79806	$=(a_1-a_2)/s_{a1-a2}$
df	43	40	35	$=(n_1+n_2-4)$
$\alpha$	0.05	0.05	0.05	
p-value	0.907595	0.558184	0.430216	$=TDIST( t , df, 2)$
sig	No	No	No	$=yes\ if\ p-value < \alpha$

The only other site where a comparison was done between the three methods was at the Little River at Porter site, although the number of data points was limited to 13 for the grab sample method, and four each for the depth-integrated and ADCP ViSea PDT methods. If the data are reduced, as was done for the Little River at 60<sup>th</sup> data, to include only data from the same discharge range, then this reduces to five data points for the grab sample method, four points for the ADCP ViSea PDT method, and only three points for the depth-integrated method. Figure 81 shows the plots of suspended sediment flux (tons/day) versus discharge (cfs) as determined for the Little River at Porter site using three methods: grab, depth-integrated, and the ADCP with the ViSea PDT. The exponents and coefficients for the regression lines for the three data sets, as well as the  $R^2$  values for the relationships, are provided in Table 26. Figure 82 shows the plots for the Little River at Porter site for discharges between 60 cfs and 1,000 cfs, and the exponents and coefficients for the regression lines for the three data sets, as well



as the  $R^2$  values for the relationships, are provided in Table 27. The  $R^2$  value of almost 1 for the ADCP/ViSea PDT data is due to the fact that the data are lumped so that a line is essentially being fit between two points.

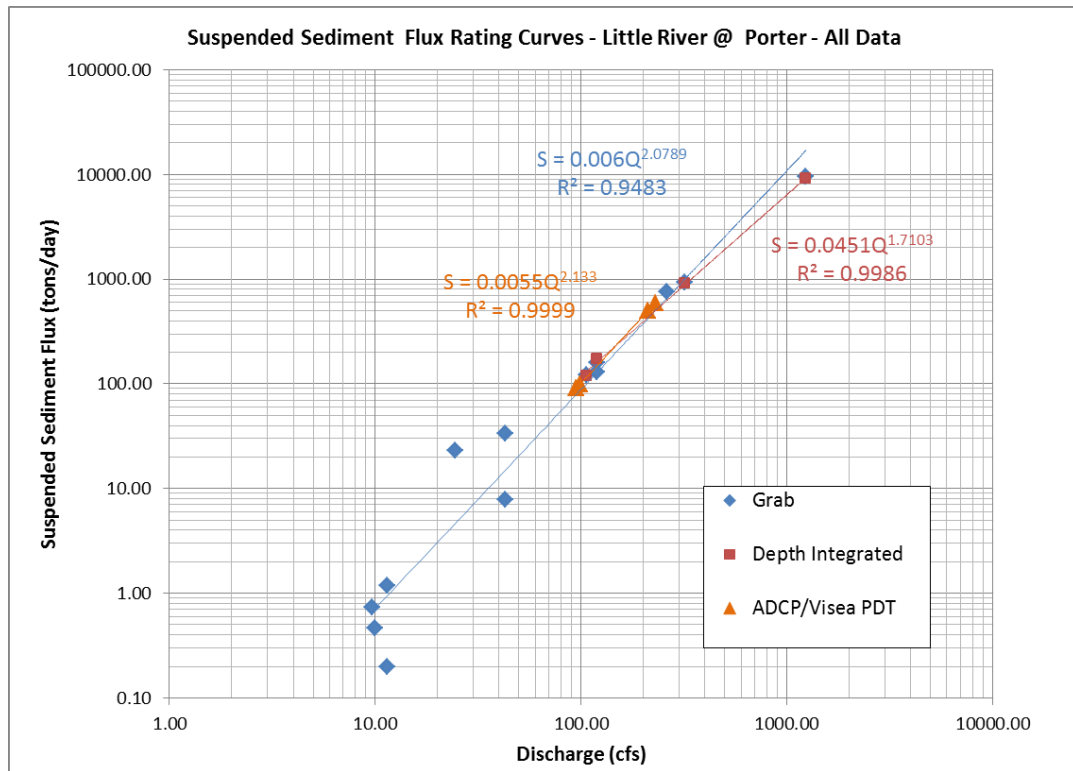


Figure 81: Suspended Sediment Rating Curves for Little River at Porter; All Data

Table 26: Sediment Flux Rating Curve Coefficients and Exponents for Little River at Porter; All Data.

Sediment Flux rating curve coefficients and exponents for Little River at Porter - All Data; $S = aQ^b$			
Sample Source	a	b	$R^2$
Grab	0.0006	2.0789	0.9483
Depth Integrated	0.0451	1.7103	0.9986
ADCP with ViSea PDT	0.0055	2.133	0.9999

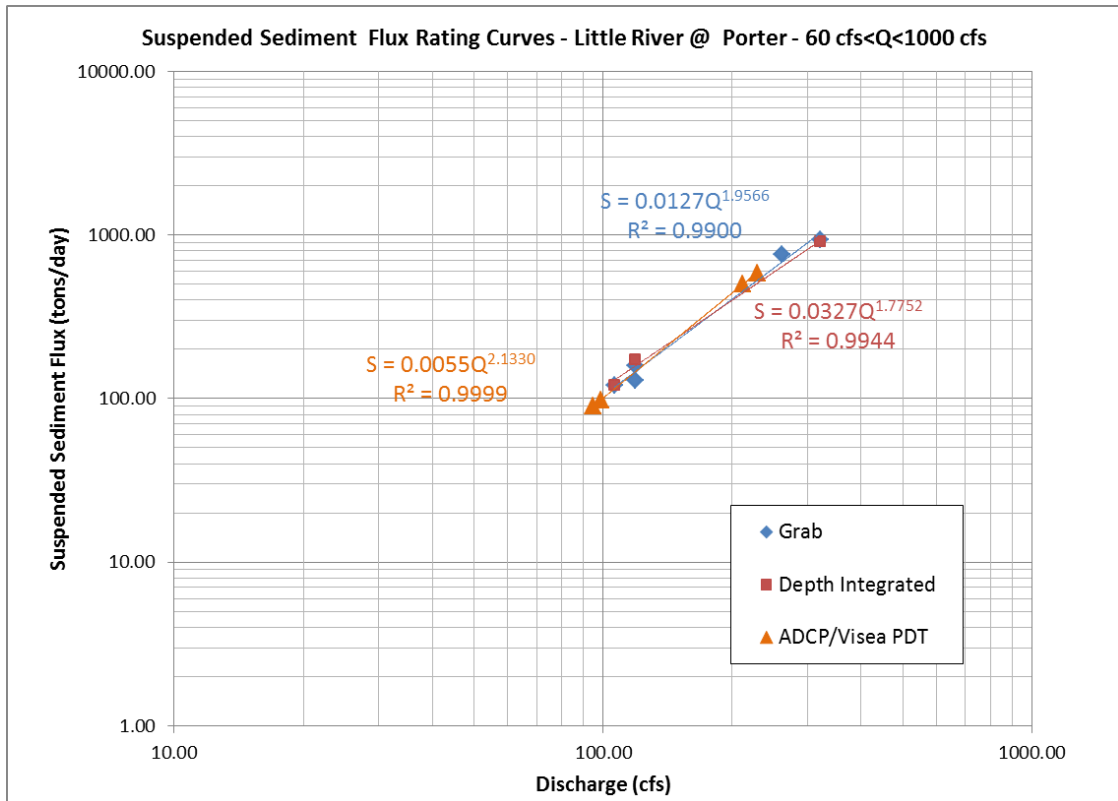


Figure 82: Suspended Sediment Rating Curves for Little River at Porter; 60 cfs < Q < 1000 cfs.

Table 27: Sediment Flux Rating Curve Coefficients and Exponents for Little River at Porter; 60 cfs < Q < 1000 cfs.

Sediment Flux rating curve coefficients and exponents for Little River at Porter - All Data; $S = aQ^b$			
Sample Source	a	b	R <sup>2</sup>
Grab	0.0127	1.9566	0.9900
Depth Integrated	0.0327	1.7752	0.9944
ADCP with ViSea PDT	0.0055	2.1330	0.9999

Even though the number of data points is limited, the difference in the slopes of the regression lines were still evaluated for statistical significance. Tables 28 and 29 show the comparison of the slopes for unpooled and pooled variances, respectively, for Little River at Porter, using only data for discharges between 60 cfs and 1,000 cfs.

Table 28: Suspended Sediment Flux Curve Slope Comparison – Little River at Porter;  $60 \text{ cfs} < Q < 1,000 \text{ cfs}$ .

Comparison of two slopes				
	Grab	DI	ADCP	
n	4	3	5	=count(x)
b	1.8885	1.9549	2.1029	=slope(y,x)
$s_{y-x}$	0.045288	0.047567	0.014071	=steyx(y,x)
$s_x$	0.242024	0.214206	0.201248	=stdev(x)
$s_b$	0.108036	0.157021	0.03496	= $s_{y-x}/(s_x * \text{SQRT}(n-1))$
		Grab-ADCP		
	Grab-DI	ADCP	DI-ADCP	
$s_{b1-b2}$	0.190597	0.113552	0.160865	= $\text{SQRT}(s_{b1}^2 + s_{b2}^2)$
t	-0.34822	-1.88774	-0.91994	=( $b_1 - b_2$ )/( $s_{b1-b2}$ )
df	3	5	4	=( $n_1 + n_2 - 4$ )
$\alpha$	0.05	0.05	0.05	
p-value	0.750679	0.117701	0.409661	=TDIST( t , df,2)
t-crit	3.182446	2.570582	2.776445	=TINV(alpha, df)
sig	No	No	No	=yes if p-value< $\alpha$

Table 29: Suspended Sediment Flux Curve Slope Comparison Using Pooled Error Variance – Little River at Porter;  $60 \text{ cfs} < Q < 1,000 \text{ cfs}$ .

Using pooled error variance				
	Grab-DI	Grab-ADCP	DI-ADCP	
$s_{Res}^2$	0.002122	0.000939	0.000714	=( $(n_1-2)s_{y-x1}^2 + (n_2-2)s_{y-x2}^2$ )/( $n_1+n_2-4$ )
$s_{b1-b2}$	0.187595	0.105557	0.11041	= $s_{Res} * \text{SQRT}(1/s_{x1}^2(n_1-1) + 1/(s_{x2}^2(n_2-1)))$
t	-0.35379	-2.03071	-1.34034	=( $b_1 - b_2$ )/( $s_{b1-b2}$ )
df	3	5	4	=( $n_1 + n_2 - 4$ )
$\alpha$	0.05	0.05	0.05	
p-value	0.746899	0.098022	0.2512	=TDIST( t , df,2)
t-crit	3.182446	2.570582	2.776445	=TINV(alpha, df)
sig	No	No	No	=yes if p-value< $\alpha$

Once again, it may be seen that using both pooled and unpooled values, the null hypothesis ( $H_0$ : the slopes are equal) cannot be rejected for any of the comparisons made. Therefore, it can be concluded that there is no statistically significant difference

between the slopes of the regression lines of the data obtained from the different methods.

Table 30 shows the comparison of the intercepts for Little River at Porter, using only data for discharges between 60 cfs and 1,000 cfs. It may once again be seen that the null hypothesis ( $H_0$ : the intercepts are equal) cannot be rejected for any of the comparisons made. Therefore, it can be concluded that there is no statistically significant difference between the intercepts of the regression lines of the data obtained from the different methods. However, the limited number of samples in the analysis diminishes the results findings, and more data are needed to get meaningful relationships between the methods for this site.

*Table 30: Suspended Sediment Flux Curve Intercept Comparison – Little River at Porter; 60 cfs < Q < 1,000 cfs.*

Comparison of two intersects				
	Grab	DI	ADCP	
M	2.254981	2.171336	2.123858	=avg(x)
a	-1.72617	-1.85101	-2.19364	=intercept(y,x)
	Grab-DI	Grab-ADCP	DI-ADCP	
$s_{a_1-a_2}$	1.435001	0.810464	0.675268	$=s_{Res}^2(1/n_1+1/n_2+M_1^2/(s_{x1}(n_1-1))+M_2^2/(s_{x2}(n_2-1)))$
t	0.086994	0.576794	0.507406	$=(a_1-a_2)/s_{a_1-a_2}$
df	3	5	4	$=(n_1+n_2-4)$
$\alpha$	0.05	0.05	0.05	
p-value	0.936158	0.589073	0.638567	=TDIST( t , df,2)
sig	No	No	No	=yes if p-value< $\alpha$

### 3. Suspended Sediment Load to Lake Thunderbird

The suspended sediment flux rating curves developed in this study were used to estimate the suspended sediment load delivered to Lake Thunderbird during the period

of the study. Using the rating curve developed using the ADCP shown in Figure 81 ( $a=0.0055$ ;  $b=2.133$ ), the annual cumulative sediment loads at the Little River at 60<sup>th</sup> site were estimated for the time period extending from March, 2010 through 2014. The results are shown graphically in Figure 83 and a summary is provided in Table 31. Because the Little River at 60<sup>th</sup> site is located less than a mile from the pool elevation of the lake these loads are representative of the loading to Lake Thunderbird from the Little River watershed.

It may be seen in Figure 83 that the majority of suspended sediment loading to the lake occurs during runoff events associated with severe thunderstorms that typically occur in the spring. The extreme year-to-year variability observed in the plots reflects the ongoing drought in the region, which received less than 80 % of the normal rainfall during the five-year period of the study.

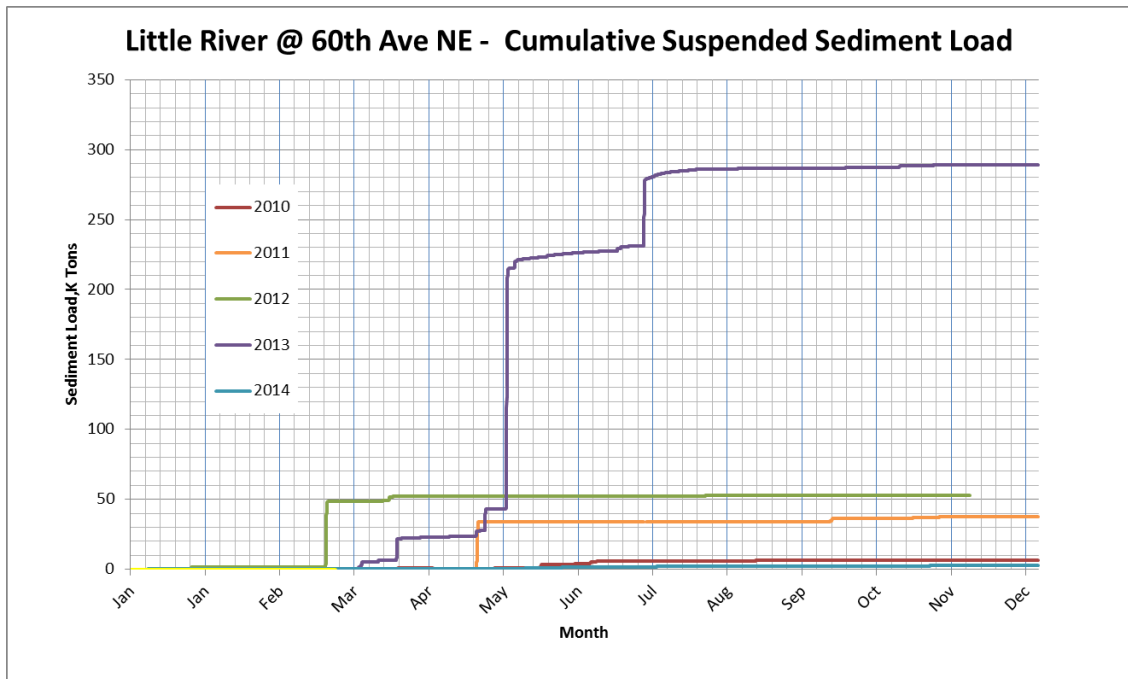


Figure 83: Annual Cumulative Sediment Loads to Lake Thunderbird from the Little River Watershed; 2010-2014.

*Table 31: Total Annual Sediment Loads to Lake Thunderbird from the Little River Watershed (DA=55.4 mi<sup>2</sup>); 2010-2014.*

Total Annual Sediment Load			
Year	ktons	acre-ft	acre-ft/mi <sup>2</sup>
2010*	6.2	1.7	0.03
2011	37.6	10.4	0.19
2012	52.9	14.7	0.26
2013	289	80.2	1.45
2014	2.6	0.7	0.01
Avg	77.7	21.6	0.39
*3/6/2010-12/31/2010			

In the driest years, 2012 and 2014, the rainfall received was just over 60% of normal. The lack of rainfall shows up in the plots, with the curves for these years being mostly flat, indicating little, or no sediment loading; without rainfall, there is no runoff, and without runoff, there is no flow in the channel to move the sediment. The most striking feature of the two plots for 2012 and 2014 is that even though the annual rainfall for the two years was practically the same, the difference in suspended sediment loads is considerably different. The primary difference between the plots is due to a single storm event that occurred on March 19, 2012, that resulted in a peak discharge of 6,900 cfs, at a stage of 20 feet. During this peak, the calculations showed that 1,300 tons (1 acre-ft) of sediment was transported past the site and to the lake in a 30 minute period.

The annual suspended sediment loading shown for 2010, 6.2 ktons (1.7 acre-feet), is the second lowest observed in the study, however data collection at the site did not begin until March 6, so the data do not include data from January, February and the

first week of March. Because at least 5 of the 29 inches of annual rain fell in that time period, the annual loading shown is significantly lower than it actually was for the year.

In 2011, the annual rainfall was roughly 20% higher than in 2012 and 2014, but the estimated sediment load, at 37.6 ktons was significantly higher than 2.6 ktons, as estimated for 2014, and somewhat less than 52.9 ktons estimated for 2012. Again, a significant amount of the annual loading occurred during one event, this one occurring on May 20, 2011, with a peak discharge of 5,400 cfs at a stage of 17.9 feet.

The only wet year of the study was 2013 with Norman receiving 126% of the normal annual rainfall, including intense thunderstorms in early May and late July, which accounts for the observed spikes in suspended sediment loading. The runoff event on June 1, 2013 was the largest event experienced during the study, with an estimated discharge of 12,500 cfs at a stage of 25.9 feet. The river overflowed its banks, forcing numerous road closings along the river. Access to the site was cut off. A second peak on July 26, 2013, was the third highest observed in the study, with an estimated discharge of 6,600 cfs at a stage of 19.5 feet. A series of smaller storms between these two events resulted in a larger than normal sediment loading rate for this period, as indicated by the steeper slope seen on the plot. As a result, the suspended sediment load to Lake Thunderbird was considerably higher in 2013 than any other year at 289 ktons or 80.2 acre-ft.

It should be kept in mind while evaluating these data that both the discharge and suspended sediment flux estimates were determined using rating curves based on stage (actually pressure) and that the largest stage in the data set used to develop the rating curves was 16.4 feet, with an estimated discharge of 3,600 cfs. Thus, estimates of

discharge and flux above these values, as were all of the events creating the sediment loading spikes, are extrapolations of the rating curves, and therefore contain a lot of uncertainty.

Acknowledging that there is considerable uncertainty in the high flow data, the mean annual suspended sediment loading to the lake for the nearly five year period was found to be 77.7 ktons/year, or 21.6 acre-feet/year. The drainage area at the Little River at 60<sup>th</sup> site is 55.4 mi<sup>2</sup>, so the mean sedimentation rate was found to be 0.39 acre-ft/mi<sup>2</sup>/year, varying from 0.01 to 1.45 acre-ft/mi<sup>2</sup>/year over the five year period.

A recent study conducted by the Grand River Dam Authority (GRDA) reported sedimentation rates of reservoirs in the Tulsa District of the U.S. Army Corps of Engineers (COE) including Grand Lake, Oologah Lake, Tenkiller Lake, Kaw Lake and John Redmond Lake (GRDA, 2015). They found sedimentation rates ranging from 0.0268 acre-ft/mi<sup>2</sup>/year in Grand Lake, for the period from 1940 to 2010, to 0.5995 acre-ft/mi<sup>2</sup>/year in Oologah Lake for the period 1977 to 2010. The sedimentation rate of John Redmond Lake, located in the Central Irregular Plains eco-region, in southeast Kansas for the period between 1963 and 2007 is reported to be 0.3973 acre-ft/mi<sup>2</sup>/year. With the exception of 2013, the wet year, the results of this study show good agreement with the GRDA study.

The drainage area of Lake Thunderbird is 257 mi<sup>2</sup> so Little River drains 21.6% of the lake's watershed. If, for sake of argument, it is assumed that similar loading rates are experienced throughout the watershed, the average sediment loading rate for the five year period would be 100 acre-feet/year. This is less than the 393 acre-feet/year measured by OWRB (2002) and the 350 acre-feet/year estimated by BOR in 1965



(Flaigg, 1959). However in 2013, a wet year, the loading was 372 acre-feet/year, which splits these values. Therefore, because these values agree with the OWRB measured, and BOR estimated, values and compare favorably to the sedimentation rates found by OWRB (2002), the estimated fluxes found in this study seem to be reasonable. It should be kept in mind however, that the suspended sediment loading estimates presented here do not include bed load, which could be significant.

Figure 84 shows plots of the annual cumulative sediment loads estimated at the Little River at Porter site for the time period extending from April 2010 through 2014, and Table 32 shows a summary of the total annual suspended sediment loads at the site. Although sediment loadings at the site do not represent loadings to Lake Thunderbird, the estimates are provided for comparison.

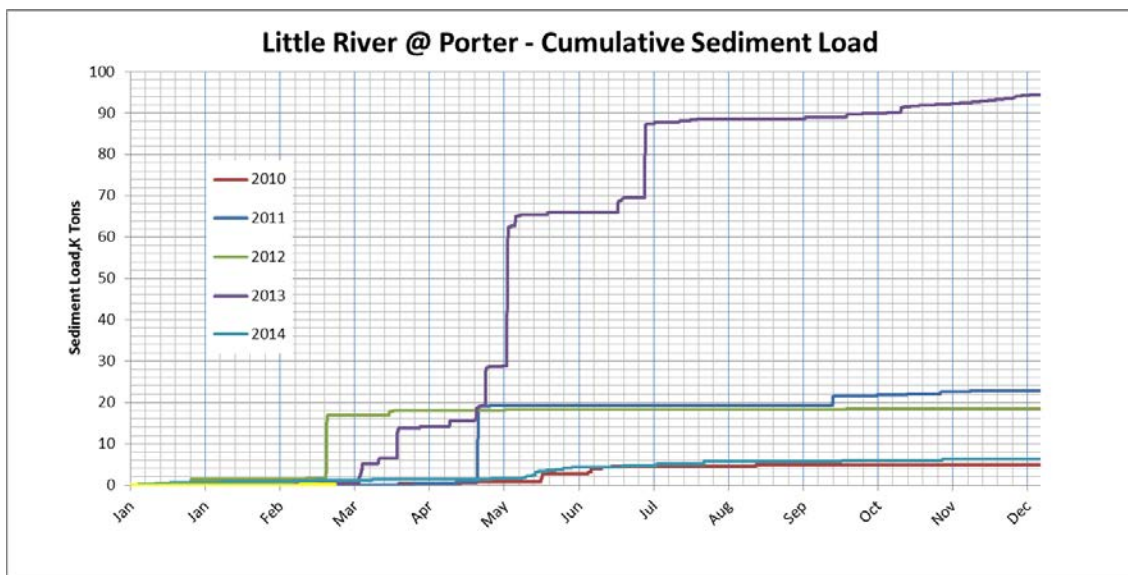


Figure 84: Annual Cumulative Sediment Loads at the Little River at Porter site; 2010-2014.

Table 32: Total Annual Sediment Loads at the Little River at Porter site (DA=20.26 mi<sup>2</sup>); 2010-2014.

Total Annual Sediment Load			
Year	ktons	acre-ft	acre-ft/mi <sup>2</sup>
2010*	5.0	1.4	0.07
2011	22.7	6.3	0.31
2012	18.4	5.1	0.25
2013	94.5	26.2	1.29
2014	6.3	1.8	0.09
Avg	29.4	8.2	0.40
*4/16/2010-12/31/2010			

The majority of sediment load is again due to severe thunderstorms, and the wet year of 2013 produced a significantly larger sediment load (94.5 ktons, 26.2 acre-feet) than was observed in the other years of the study. As observed at the Little River at 60<sup>th</sup> site, the lowest annual suspended sediment loading, 5.0 ktons (1.4 acre-feet) occurred in 2010 due to the fact that the data collection at the site did not begin until April 16. The mean annual loading for the five year period was found to be 29.4 ktons (8.2 acre-feet).

The drainage area of the watershed above the Little River at Porter site is 20.26 mi<sup>2</sup>, resulting in an average annual aerial loading rate of 0.40 acre-ft/mi<sup>2</sup>. This agrees very well with the 0.39 acre-ft/mi<sup>2</sup>/year rate observed at the Little River at 60<sup>th</sup> site, although there is a lot of variability in the data. Comparing the loading rates for the Little River at Porter site shown in Table 32 with the rates for the Little River at 60<sup>th</sup> site shown in Table 31, it may be seen that the annual loading rates are generally lower at the Porter site than at the 60<sup>th</sup> site.

An exception to this trend occurs in 2014, where the total sediment loading at the Porter site (6.3 ktons) is almost three times the loading at the site at 60<sup>th</sup> (2.6 ktons). Although the reason for this anomaly is uncertain, it is suspected to be due to discharge

estimate issues at the site as a result of construction activity observed to be occurring nearby. Prior to November 6, 2013, the base stage level at the site was around 0.7 feet. After that time it was 2.7 feet, until November 17, 2013, when it went back down to 0.7 feet before climbing back to 2.7 feet on November 22. It remained above 2 feet until January 23, 2014, and returned to 0.7 feet on January 25. Similar rises were observed in February and June. This artificial raising of the stage resulted in over estimation of the discharge for the effected periods, which in turn resulted in over estimation of the sediment load.

## **F. Discussion**

Although the ADCP/ViSea PDT method produced acceptable results that are statistically the same as traditional methods, it does not mean that it is necessarily the preferred method. ADCPs are increasingly being used for measuring the discharge of creeks and rivers throughout the world. For large runoff events that are too deep to be measured safely using wading methods, ADCPs are the best viable option at the time.

It was reasoned, before this study was initiated, that since ADCPs were being used to measure discharge, they could, at the same time, be used to measure flux with fewer samples and less effort. This would be true on larger rivers where there are large variations in sediment concentration across the channel, requiring numerous depth-integrated samples. However, on smaller rivers like the Little River, which are uniformly mixed at high flows, this study shows that simply collecting and analyzing single grab samples for concentration produces the same results as using the ADCP/ViSea method, which requires a minimum of three samples that must be

analyzed for concentration and particle size analyzes of at least one sample. Using the ADCP/ViSea method therefore increases the amount of effort required and potentially introduces another level of complexity in determining particle size.

The ADCP/ViSea method does offer one big advantage over traditional methods due to the fact that the ADCP measures discharge and backscatter in discrete bins throughout the channel. Processing the ADCP data in ViSea PDT allows one to see the distribution of the sediment in the water column, as may be seen in the suspended sediment concentration and flux profile plots generated by the software shown in Figures 84 and 85.

The plots in Figure 84 were generated using data from the Little River at Porter sampling event of May 21, 2013, with a measured discharge of 3.26 cms (115 cfs) and a measured flux of 1.33 kg/s (127 tons/day). They are typical of the majority of the plots generated in the study, with the concentration plot (on the left) showing a band of higher concentration near the bed, and a fairly well-mixed zone of lower concentration higher in the water column. The flux plot (on the right) is also typical of many of the plots, as cores of higher fluxes were often seen in the central part of the channel, although the cores were sometimes shifted more to one side of the channel than the other.

The plots in Figure 85 were generated using data from the Little River at 60th sampling event of May 23, 2013, with a measured discharge of 73.4 cms (2,590 cfs) and a measured flux of 123.9 kg/s (11,800 tons/day). The concentration plot (on the left), once again, shows a band of higher concentrations near the bed, except that the band does not follow the bed on the right side of the channel and instead angles up. The

reason for this is unknown, but it is suspected to be due to submerged tree branches in the vicinity of the transect effecting the backscatter return signal.

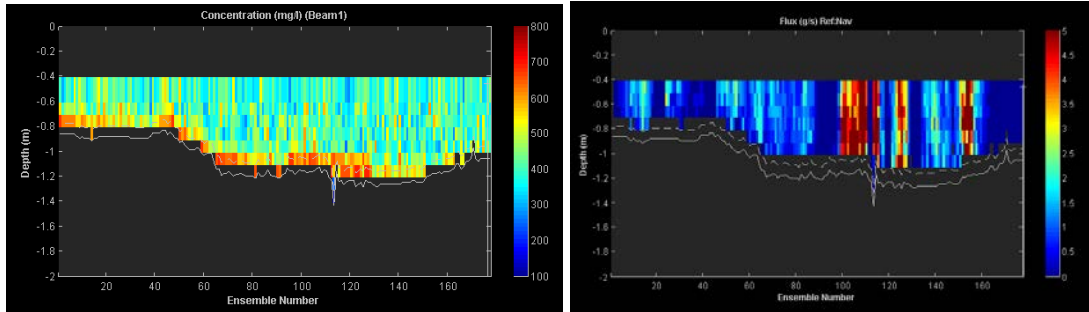


Figure 84: Aqua Vision ViSea PDT Suspended Sediment Concentration (Lt) and Flux (Rt) Profile Plots; Little River at Porter; May 21, 2013; Transect 5;  $Q = 3.26$  cms (115 cfs); Flux = 1.33 kg/s (127 tons/day)

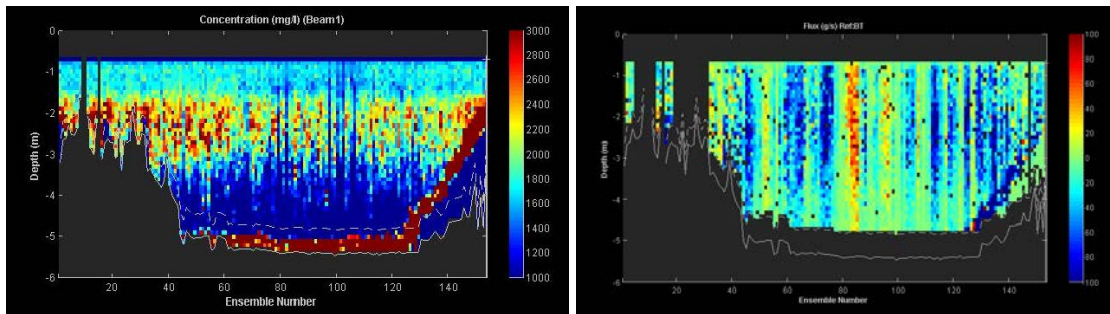


Figure 85: Aqua Vision ViSea PDT Suspended Sediment Concentration (Lt) and Flux (Rt) Profile Plots; Little River at 60<sup>th</sup>; May 23, 2013; Transect 6;  $Q = 73.43$  cms (2.593.2 cfs); Flux = 123.9 kg/s (11,800.2 tons/day).

The plot also appears to show a zone of lower concentration in the lower third of the channel, with a band of higher concentration in the middle third of the channel that was not present in the majority of other plots observed in this study. This does not make sense from a physical standpoint, and the reason for it is not completely understood. It is possible, perhaps, that the high suspended sediment concentration in the water

column resulted in a shadowing effect that reduced the backscatter at lower depths. Despite the anomalies in the concentration plot, the suspended sediment flux profile plot (on the right), displays the same cores of higher flux observed in other plots.

Whatever the underlying cause of the observed distributions may be, the point is that because the ADCP/ViSea PDT method provides discrete estimates of concentration at numerous bins throughout the water column, using the method allows for evaluation and study of phenomena that cannot be addressed with the concentration data aggregated as a single value. Future modeling efforts could benefit from this extra level of detail in the data, which in the author's opinion justifies the minimum additional effort required.

## **G. Conclusion**

The results From Part 2 of this study appear to support the stated hypothesis that a Teledyne RDI 600 kHz Workhorse Rio Grande may be used to accurately measure sediment transport in small rivers. Suspended sediment flux curves generated using a Teledyne RDI 600 kHz Workhorse Rio Grande ADCP and Aqua Vision's ViSea DAS and ViSea PDT software were found to be statistically the same as curves generated using traditional grab sampling and depth-integrated sampling methods.

However, even though the results of this study seem to support the stated hypothesis, which also allows for sediment flux estimates in the Little River watershed, the sample set was collected from only one river, at only two sites, one of which had relatively few samples. Much more data are needed from the existing sites and from several other small rivers for the method to be validated for use on all small rivers.

#### **IV. Summary of Hydrologic, Geomorphologic, and Sediment Transport Findings**

In Part 1 of this study, the hydrology and fluvial geomorphology (FGM) of the Lake Thunderbird watershed were investigated. The hydrological investigation was conducted using HOBO pressure transducers installed and set to record pressure at 30 minute intervals at seven monitoring sites in the watershed, including the Little River at 60<sup>th</sup>, Little River at Porter, Hog Creek at SE 119<sup>th</sup>, Rock Creek at 72<sup>nd</sup>, Elm Creek at Indian Hills, North Fork at Franklin and Dave Blue Creek at 72<sup>nd</sup>.

These data, together with discharge measurements collected using a Marsh McBirney flow meter with a wading rod, and a Teledyne RDI 600kHz Workhorse Rio Grande ADCP, were used to generate discharge rating curves for each site. These rating curves were used to generate hydrographs that provide a record of discharge in the tributaries of Lake Thunderbird extending over a five year period from March 2010 to March 2015. The data are mostly continuous, although there are a few gaps in the data that occurred for various reasons, e.g. the HOBO data at the Hog Creek site stops on April 25, 2013, because the HOBO, and OCC's staff gauge, were washed away due to a storm event on June 1, 2013, and were not replaced.

Monthly rainfall data from OCS (2014) for Norman shows below normal rainfall over the five-year period of study, as the region was (and still is) experiencing a drought. Data from this study show the effects of the drought on the surface hydrology in the watershed. During the first year of the study, none of the sites went dry, but with successive dry years, four of the sites went dry for an increasing number of days, until the rains in the spring and summer of 2013 spelled some temporary relief.

To complete the morphological investigation, fluvial geomorphological (FGM) surveys were conducted, and bank stability indices were developed at 25 sites within the Lake Thunderbird watershed. The results show that almost all of the channels in the watershed are down cutting and most are both down cutting and widening, and are thus at Stage III and Stage IV of Simon's Channel Evolution Model. At a majority of sites the channels are classified as G5c, according to the Rosgen stream classification system.

Bank stability indices developed at the sites included the Channel Stability Index (CSI), the Bank Erosion Hazard Index (BEHI), the Near Bank Stress (NBS), the Pfankuch Stream Stability Index, and the Ozark Eco-region Bank Stability Index (OESBI). The banks at the majority of sites were deemed unstable regardless of what index was used, and show that the Little River and other tributaries of Lake Thunderbird are unstable. Validation of the indices requires that follow up surveys be conducted to measure erosion rates, but the fact that all of the indices indicate that the assessed banks are unstable is good evidence that the indices may be used as qualitative indicators of channel stability, even without validation. Future work is required to validate the indices, and potentially allow them to be used as quantitative indices. This study provides a baseline for that work.

In Part 2 of the study, the hypothesis that a Teledyne RDI 600 kHz Workhorse Rio Grande may be used to accurately measure sediment transport in small rivers was tested. The accuracy of the ADCP was evaluated by comparing the sediment flux determined using the ADCP with Aqua Vision's PDT software to the sediment flux determined using traditional grab and depth-integrated sampling methods. Data were collected and evaluated at two sites, Little River at 60<sup>th</sup> and Little River at Porter,



although data for the latter were limited. The results support the hypothesis because no statistical significance was found between any of the sediment flux curves generated using the three methods. However, the data set was limited to just two sites on one river, so validating the method for use on all small rivers would require more study.

The suspended sediment flux rating curve for the Little River at 60<sup>th</sup> site was used, in combination with the hydrographs developed in Part 1 of the study, to estimate the suspended sediment loadings to Lake Thunderbird from the Little River watershed. The estimated loading rate of suspended sediment varied from 0.01 to 1.45 acre-ft/mi<sup>2</sup>/year over the five-year study period, with a mean of 0.39 acre-ft/mi<sup>2</sup>/year. With the exception of 2013, the wet year, the results of this study compare favorably to sedimentation rates recently reported by GRDA (2015) for reservoirs operated by the Tulsa District of the Corps, including Grand Lake, Oolagah Lake, Tenkiller Lake, Kaw Lake and John Redmond Lake, which ranged from 0.0268 acre-ft/mi<sup>2</sup>/year in Grand Lake to 0.5995 acre-ft/mi<sup>2</sup>/year in Oolagah Lake. Estimated suspended sediment loading rates for the watershed are less than the 393 acre-feet/year measured by OWRB (OWRB, 2002), and the 350 acre-feet/year estimated by BOR in 1965 (Flaigg, 1959), for four of the five years of the study, but in 2013, the wet year, the sediment loading was estimated to be 372 acre-feet/year.

The suspended sediment flux rating curve for the Little River at Porter site was used, in combination with the hydrographs developed in Part 1 of the study, to estimate the suspended sediment loadings for the site. Although sediment loadings at the site do not represent loadings to Lake Thunderbird, the estimates were made for comparison

purposes. The average annual sediment was determined to be 0.40 acre-ft/mi<sup>2</sup>, which shows good agreement with the estimated loadings at the Little River at 60<sup>th</sup> site.

## **V. Future Work**

Prior to this study there had been very little documentation of the hydrology within the Lake Thunderbird watershed, and no documentation of the fluvial geomorphological characteristics of the Little River or the other tributaries of the lake. The data presented here provide a baseline for continuing research in the watershed, but it should be augmented with other information that resource managers are going to need to comprehensively address sedimentation in reservoirs.

The hydrological investigation of the watershed is ongoing and the HOBOS are still deployed and recording data. The author intends to continue downloading and maintaining the data for as long as he is physically capable of getting up and down the banks, and for as long as he can find somebody to pay for battery replacement when it is needed. Additional discharge measurements are required to continue development of rating curves for the sites, and it will be necessary at some point to re-survey the sites to check for channel adjustments that could affect the rating curves.

The FGM surveys and assessments conducted in this study lay a foundation for future study in the watershed. At some point in the future the 25 sites presented here should be re-visited and the cross-sections resurveyed. These data could be used to validate the various bank erosion indices evaluated in this study, and determine which, if any, are most applicable to the banks in the Lake Thunderbird watershed. The data

could also be used to estimate the amount of sediment loading to the lake that is attributable to stream bed and bank erosion.

Although this study showed that ADCPs may be used to estimate sediment transport in the Little River, more research is needed to validate their results for application to a wider range of small rivers. Further investigation of the effects of particle size distribution on the sediment flux estimated in ViSea PDT is warranted, as the brief assessment conducted in this study appears to show that the program is not particularly sensitive to it. If a single distribution could be developed for use at a given site, the need for particle size analysis could be eliminated.

Another option, worthy of investigation, is the use of an optical backscatter probe in conjunction with the ADCP to collect real time optical backscatter simultaneously with ADCP backscatter, a feature that is supported by the Aqua Vision ViSea PDT software. Instead of calibrating to grab samples, as was done in this study, the coefficients are calibrated to the OBS data. This requires calibrating the OBS to the suspended concentration signal, which still requires sample collection and analysis, but if the optical backscatter signal can be calibrated for a specific site, the need to collect samples for calibration would be greatly reduced. It is not known if this approach would work, but it is worthy of further exploration.

Investigation of bed load transport in the watershed is also recommended. This study examined only the suspended fraction of the sediment load moving in the channels and did not address the bed load, which is potentially significant. Initially, it was hoped that the ADCP could also be used to evaluate the bed load transport, as other researchers are doing (Rennie et al., 2002; Gaeuman and Jacobson, 2007; Abraham and

Pratt, 2011), but it was decided to focus the study on suspended sediment. A study focusing on bed load movement could supplement the data from this study and would help provide a greater understanding of the sediment flux in the tributaries of Lake Thunderbird, thus allowing a better estimate of the total sediment loading to the lake.

## VI. References

Abraham, D.D. and Pratt, T.C., (2011), Data Report: Bed-load Computations at 3 Sites on the Missouri River, From time sequenced bathymetric data collected at Barney, Hamburg and Nebraska City Sites, ERDC-CHL Data Report, USACE, Engineer Research and Development Center, Vicksburg, MS, Mar, 2011.

Agrawal, Y.C., A. Whitmire, O.A. Mikkelsen, and H.C. Pottsmith, (2008), Light scattering by random shaped particles and consequences on measuring suspended sediments by laser diffraction, *Journal of Geophysical Research*, Vol. 113, C04023, doi:10.1029/2007JC004403.

Aquatec, (2009), Aquascat 1000, accessed March 2, 2009, at <http://www.aquatecgroup.com/aquascat.html>.

Aqua Vision, (2013), [http://www.AquaVision.nl/plume\\_detection\\_toolbox.html](http://www.AquaVision.nl/plume_detection_toolbox.html)

Barclay, J.S., (1980), Impact of Stream Alterations on Riparian Communities in Southcentral Oklahoma, Fish and Wildlife Service Contract 14-16-0008-2039, Fish and Wildlife Service, U.S. Department of the Interior, FWS/OBS-80/17, August, 1980.

Barnes, Jr., H.H. (1967), Roughness Characteristics of Natural Channels, U.S. Geological Survey Water Supply Paper 1849, United States Government Printing Office, Washington, D.C.

Blank, L.T., (1980), *Statistical Procedures for Engineering, Management, and Science*, McGraw Hill, ISBN: 0070058512.

Cowan, W.L., (1956), Estimating hydraulic roughness coefficients, *Agricultural Engineering*, vol. 37, no. 7, pp. 473-475, July, 1956.

Deines, K. L., (1999), Backscatter estimation using broadband acoustic Doppler current profilers, Proceedings IEEE 6th Working Conference on Current Measurements, 249-253, San Diego, CA.

Derrow II, R.W., R.A. Kuhnle, and I.P. Jones, (1998), Acoustically Measuring Suspended Sediment Concentration and Size Distribution, Proceedings, Federal Interagency Workshop, Sediment Technology for the 21'st Century, St. Petersburg, FL, February 17-19, 1998.

Dutnell, Russell, (2000), Development of Bankfull Discharge and Channel Geometry Relationships for Natural Channel Design in Oklahoma Using a Fluvial Geomorphic Approach, Master's Thesis, Univ.of Oklahoma, Norman, OK., 317pp.

Edwards, T.K. and G.D.Glysson, (1999), Field Methods for Measurement of Fluvial Sediment: U. S. Geological Survey Techniques of Water-Resources Investigations, book 3, chapter 2, 89 p., accessed March, 1, 2009, at <http://water.usgs.gov/osw/techniques/Edwards-TWRI.pdf>.

FWPCA, (2009), Federal Water Pollution Control Act, 33 U.S.C. §§1251-1387.

Filizola, N. and J.L. Guyot, (2004), The use of Doppler technology for suspended sediment discharge determination in the River Amazon, Hydrological Sciences Journal, 49(1), pp143-153.

Flaigg, Norman G., (1959), Acting Area Engineer, US Dept. of the Interior, Bureau of Reclamation. Correspondence to Mr. Frank Raab, Executive Director, Oklahoma Water Resources Board June 12, 1959. Oklahoma Water Resources Board Project Files, Oklahoma City.

Fox, G.A., A. Sheshukov, R. Cruse, R.L. Kolar, K.R. Gesch and R.C. Dutnell (2015), Reservoir Sedimentation and Upstream Sediment Sources: Perspectives and Future Research Needs on Streambank and Gully Erosion, Environmental Management, In Review, Submitted March, 2015.

Gaeuman, D. and R.B. Jacobson, (2007), Field Assessment of Alternative Bed-Load Transport Estimators, Journal of Hydraulic Engineering, Vol. 133, No. 12, December 1, 2007. ©ASCE, ISSN 0733-9429/2007/12-1319–1328/.

Gartner, J.W., R.T. Cheng, P-F Wang, and K. Richter, (2001), Laboratory and field evaluations of the LISST-100 instrument for suspended particle size determinations, Marine Geology 175 (2001) 199-219, Elsevier, www.elsevier.nl.

Graf, W. L., E. Wohl, T. Sinha, and J. L. Sabo (2010), Sedimentation and sustainability of western American reservoirs, Water Resour. Res., 46, W12535, doi:10.1029/2009WR008836.

**GRDA, (2015),**

Gray, J.R., Laronne, J.B., Marr, J.D.G., (2010), Bedload-surrogate monitoring technologies: U.S. Geological Survey Scientific Investigations Report 2010–5091, 37p.; also available at <http://pubs.usgs.gov/sir/2010/5091>.

Harrelson, C.C., C.L. Rawlins, and J.P. Potyondy, (1994), Stream Channel Reference Sites: An Illustrated Field Guide to Field Technique. USDA Forest Service, General Technical Report RM-245, April 1994. URL: <http://www.stream.fs.fed.us/publications/PDFs/RM245E.PDF>.

Henson, H., (2011), Partial Bathymetry Study of Lake Thunderbird and the Lower Arm of the Little River, A Non-Thesis Project Submitted To The CEES

Graduate Studies Committee in Partial Fulfillment of the Requirements for the Degree of Master of Civil Engineering, University of Oklahoma, Norman, OK.

Hicks, D.M. and P.D. Mason, (1991), *Roughness Characteristics of New Zealand Rivers*, National Institute of Water and Atmospheric Research Ltd, Water Resources Publications, Christchurch, New Zealand, ISBN 0-477-02608-7, 329pp.

Holdaway, G.P., P.D. Thorne, D. Flatt, S.E. Jones and D. Prandle, (1999), Comparison between ADCP and transmissometer measurements of suspended sediment concentration, *Continental Shelf Research* 19 (1999) 421-441, PII: S0278-4343(98)00097-1, Elsevier Science Ltd.

Howell, D.C. (2010), *Statistical Methods for Psychology*, Wadsworth CENGAGE Learning, Belmont, CA, ISBN: 1-111-83548-9.

Kim, Y. H., & Voulgaris, G., (2003). Estimation of suspended sediment concentration in estuarine environments using acoustic backscatter from an ADCP. In *Proc. Fifth Int. Conf. on Coastal Sediments*.

Kleinbaum, D., L. Kupper, A. Nizam, and E.S. Rosenberg, (1998), *Applied Regression Analysis and Other Multivariable Methods*, CENGAGE Learning, Boston, MA, ISBN: 1-285-05308-4.

Knighton, D., (1998), *Fluvial Forms and Processes: A New Perspective*, Arnold, London, England, ISBN0 340 66318 8.

Kostaschuk, R., J. Best, P. Villard, J. Peakall, and M. Franklin, (2004), Measuring flow velocity and sediment transport with an acoustic Doppler current profiler, *Geomorphology* 68 (2005) 25–37.



Kouwen, N., Unny, T. E., & Hill, H. M. (1969), Flow retardance in vegetated channels, *Journal of the Irrigation and Drainage Division*, Vol. 95, No. 2, June 1969, pp. 329-344.

Kuhnle, R.A. and D.G. Wren, (2006), Proceedings of the Eighth Federal Interagency Sedimentation Conference (8thFISC), Breakout Session I, Suspended-Sediment Measurement: Data Needs, Uncertainty, and New Technologies, April 2--6, 2006, Reno, NV, USA.

Lane, E.W., (1955), "Design of stable channels," in *American Society of Civil Engineers Transactions*, Vol. 120, pp-1234-1279.

McCave, I.N., R.J. Bryant, H.F. Cook, and C.A. Coughanowr, (1986), Evaluation of a laser-diffraction-size analyzer for use with natural sediments, *Journal of Sedimentary Research*, v. 56 no. 4 p561-564.

Mueller, D.S., and Wagner, C.R., (2009), Measuring discharge with acoustic Doppler current profilers from a moving boat: U.S. Geological Survey Techniques and Methods 3A–22, 72 p. (available online at <http://pubs.water.usgs.gov/tm3a22>).

Mueller, D.S., Wagner, C.R., Rehmel, M.S., Oberg, K.A., and Rainville, Francois, (2013), Measuring discharge with acoustic Doppler current profilers from a moving boat (ver. 2.0, December 2013): U.S. Geological Survey Techniques and Methods, book 3, chap. <http://dx.doi.org/10.3133/tm3A22>.

Nortek AS, (2009), Aquadopp Profiler 400 kHz - 600 kHz - 1MHz - 2 MHz, accessed March, 2, 2009, at: <http://www.nortekusa.com/hardware/AquadoppProfiler.html>.

Oberg, K.A., S.E. Morlock and W.S. Caldwell, (2005), Quality-Assurance Plan for Discharge Measurements Using Acoustic Doppler Current Profilers, Scientific Investigations Report 2005-5183, U.S. Department of the Interior, U.S. Geological Survey.

OCS, (2015), Oklahoma Climatological Survey and the Oklahoma Mesonet Web site: [https://www.mesonet.org/index.php/weather/monthly\\_rainfall\\_table](https://www.mesonet.org/index.php/weather/monthly_rainfall_table).

OKMaps, (2010), OK Maps - Oklahoma GIS Data Clearinghouse Search, Web site accessed at: <http://ogi.state.ok.us/ogi/Search.aspx?LAYERS=55e019d1-d752-42dc-99f7-fbd7289c6519>.

OWRB, (2002), Lake Thunderbird Capacity and Water Quality for the Central Oklahoma Master Conservancy District. Final Report. June 2002. Published by the Oklahoma Water Resources Board.

OWRB, (2004). Lake Thunderbird Water Quality 2003 for the Central Oklahoma Master Conservancy District. Final Report. May 2004. Published by the Oklahoma Water Resources Board.

OWRB, (2005), Report of the Oklahoma Beneficial Use Monitoring Program Lakes Report. Lakes Sampling 2004-2005. Published by the Oklahoma Water Resources Board.

OWRB, (2007) Oklahoma Water Atlas, 2007, Published by the Oklahoma Water Resources Board – Out of print.

Pedocchi, F and M.H. Garcia, (2006), Evaluation of the LISST-ST instrument for suspended particle size distribution and settling velocity measurements, Continental Shelf Research 26 (2006) 943–958, Elsevier, [www.elsevier.com](http://www.elsevier.com).

Pfankuch, D.J., (1975), Stream reach inventory and channel stability evaluation (USDAFS No. R1-75-002, GPO No. 696-260/200), Washington, D.C., U.S.

Government Printing Office.

Qinghua, Z. and Wenhao, Z (1989), Soil Erosion in the Yellow River basin and its impacts on reservoir sedimentation and the lower Yellow River, Sediment and the Environment (Proceedings of the Baltimore Symposium, May 1989), IAHS Publ. no. 184, 1989.

RD Instruments USA, (2009), Teledyne RD Instruments, Water Resources: Precision Flow Measurement for Every Environment, ChannelMaster H-ADCP, accessed March, 2, 2009, at <http://www.rdinstruments.com/channelmaster.html>.

Rennie, C.D., Millar, R.G., and Church, M.A., (2002), Measurement of bed load velocity using an acoustic Doppler current profiler: Journal of Hydraulic Engineering, v. 128, no. 5, p. 473-483.

Rosgen, D.L., (1994), A Classification of Natural Rivers, Catena, Vol. 22, pp 169-99.

Rosgen, D.L., (1996), Applied River Morphology, Wildland Hydrology, Pagosa Springs, CO, ISBN 0-9653289-0-2.

Rosgen, D.L., (2001), A practical method of computing streambank erosion rate, In Proceedings of the seventh Federal Interagency Sedimentation Conference: Vol. 1, (pp. II-9-II-15), Reno, NV: Subcommittee on Sedimentation.

Ryan, S.E., K. Blunte and J.P. Potyondy, (2006), Proceedings of the Eighth Federal Interagency Sedimentation Conference (8thFISC), Breakout Session II,

Breakout Session II, Bed load-Transport Measurement: Data Needs, Uncertainty, and New Technologies, April 2--6, 2006, Reno, NV, USA.

Sabo, J. L., Sinha, T., Bowling, L. C., Schoups, G. H., Wallender, W. W., Campana, M. E., ... & Wohl, E. E. (2010). Reclaiming freshwater sustainability in the Cadillac Desert. *Proceedings of the National Academy of Sciences*, 107(50), 21263-21269.

Sagbohan, F.M., (2010), Semi - Report model implementation for Rock Creek basin, A Non-Thesis Project Submitted To The CEES Graduate Studies Committee in Partial Fulfillment of the Requirements for the Degree of Master of Civil Engineering, University of Oklahoma, Norman, OK.

Schumm, S.A., Harvey, M.D. and Watson, C.C., (1984), *Incised Channels: Morphology, Dynamics, and Control*. Water Resources Publications, Littleton, CO, 200 pp.

Sequoia, (2009), *Sequoia: Research and Products for Environmental Science*, Sequoia Scientific, Inc. accessed March, 2, 2009, at <http://www.sequoiasci.com/products/Suspended.aspx>

Sequoia, (2013), *LISST-Portable|XR Manual, Version 1.00*, May, 2013, Sequoia Scientific, Inc., Bellevue, WA .

Simon, A., (1989), A model of channel response in disturbed alluvial channels, *Earth Surface Processes and Landforms* 14, 11-16.

Simon, A., (1994), *Gradation Processes and Channel Evolution in Modified West Tennessee Streams: Process, Response, and Form*, USGS Professional Paper 1470, United States Government Printing Office, Washington, D.C., pp 44 – 58.

Simon, A., and P.W. Downs, (1995), An interdisciplinary approach to evaluation of potential instability in alluvial channels. *Geomorphology*. 12: 215-232.

Sontek/YSI, Inc., (2009), Hydrology Applications and Products, accessed March, 2, 2009, at <http://www.sontek.com/hydrology.html>.

Stephens, D.P., (2005), Proceedings of the 2005 Georgia Water Resources Conference, held April 25–27, 2005, at the University of Georgia. Kathryn J. Hatcher, editor, Institute of Ecology, The University of Georgia, Athens, Georgia.

Strum, T.W., (2001), *Open Channel Hydraulics*, McGraw-Hill, 2001, 493 pp.

Teledyne RDI, (1999a), When to Use Differential GPS in Place of Bottom Track, Application Note, August, 1999, FSA-006, Teledyne RD Instruments, 14020 Stowe Dr., Poway, CA 92064, <http://www.rdinstruments.com/>.

Teledyne RDI, (1999b), Measuring River Discharge in High Flow (Flood) or High Sediment Concentration Conditions, Application Note, August, 1999, FSA-007, Teledyne RD Instruments, 14020 Stowe Dr., Poway, CA 92064, <http://www.rdinstruments.com/>.

Teledyne RDI, (2002a), High Resolution Water Profiling Water Mode 11, Application Note, March, 2002, FSA-013, Teledyne RD Instruments, 14020 Stowe Dr., Poway, CA 92064, <http://www.rdinstruments.com/>.

Teledyne RDI, (2002b), Shallow Water Bottom Tracking Bottom Mode 7, Application Note, March, 2002, FSA-015, Teledyne RD Instruments, 14020 Stowe Dr., Poway, CA 92064, <http://www.rdinstruments.com/>.

Teledyne RDI, (2007a), Workhorse Rio Grande ADCP User's Guide, Teledyne RD Instruments, P/N 957-6167-00 (November, 2007), 14020 Stowe Dr., Poway, CA 92064, <http://www.rdinstruments.com/>.

Teledyne RDI, (2007b), Work Horse Rio Grande Acoustic Doppler Current Profiler Technical Manual, Teledyne RD Instruments, P/N 957-6241-00 (November, 2007), 14020 Stowe Dr., Poway, CA 92064, <http://www.rdinstruments.com/>.

Traykovski, P., R.J. Latter, and J.D. Irish, (1999), A laboratory evaluation of the laser in situ scattering and transmissometry instrument using natural sediments, *Marine Geology* 159 (1999), 355-367, Elsevier, [www.elsevier.nl](http://www.elsevier.nl).

Urlick, R.J., (1967), "Principles of Underwater Sound for Engineers", Peninsula Publishing, Los Altos Hills, CA.

U.S. Army Corps of Engineers (2013), Dam Safety Program Activities web site: <http://www.usace.army.mil/Missions/CivilWorks/DamSafetyProgram/ProgramActivities.aspx>.

U.S. Army Corps of Engineers - National Inventory of Dams (2013), <http://nid.usace.army.mil>, U.S. Army Corps of Engineers, 7701 Telegraph Road, Alexandria, VA 22315-3864.

U.S. Census Bureau, (2015), U.S. Census Bureau website, <http://www.census.gov/>.

U.S. Environmental Protection Agency, (2013), Watershed Assessment, Tracking & Environmental Results Web site, [http://ofmpub.epa.gov/waters10/attains\\_nation\\_cy.control](http://ofmpub.epa.gov/waters10/attains_nation_cy.control).

U.S. Geological Survey (1977), National handbook of recommended methods for water data acquisition. U.S. Govt. Printing Office, Washington, DC.

Vieux & Associates, Inc, (2007), Lake Thunderbird Watershed Analysis and Water Quality Evaluation, Prepared for the Oklahoma Conservation Commission, Final Report, June 30, 2007.

Vieux & Associates, Inc, (2010), Vflo (Version 4.0), 350 David L. Boren Blvd, Suite 2500, Norman, OK 73072-7267.

Wall, G.R., E.A Nystrom, and S. Litten,(2006), Use of an ADCP to compute suspended-sediment discharge in the tidal Hudson River, New York: U.S. Geological Survey Scientific Investigations Report 2006-5055, 16 pp.

Water Survey of Canada, (2004), Procedures for Conducting ADCP Discharge Measurements, First Edition, qSOP-NA001-01-2004, Meteorological Service of Canada, Environment Canada, Ottawa, Canada, 2004.

World Commission on Dams (2000), “Dams and Development: A New Framework for Decision Making”, Earthscan Publications Ltd, 22883 Quicksilver Drive, Sterling, VA 20166-2012, USA, 1-85383-797-0.

Wolfgang, L., (2012), Particle Size and Counting Analysis, LinkedIn Discussion, <https://www.linkedin.com/groups/Mie-Theory-Fraunhofer-diffraction-in-147418.S.134764466>, Accessed on February 18, 2015.

## **VII. APPENDICES**



## A. Appendix A – Monitoring Sites Summary

### A.1 Little River at 60th Ave NE

HOBO Deployment Date: March 6, 2010

HOBO start time: 1430 (GMT-0600)

HOBO Elevation: 1037.63 feet above MSL (1036.97' after July 26, 2011)

Control Pin Locations (NAD83 State Plane, feet)

	Easting	Northing	Elevation
Left	2161614.23	708336.74	1064.62
Right	2161616.37	708175.26	1061.93



Figure A.1.1: Little River at 60<sup>th</sup> Ave NE site location map.



*Figure A.1.2: Little River at 60<sup>th</sup> Ave NE HOBOT initial installation.*



*Figure A.1.3: Little River at 60<sup>th</sup> Ave NE HOBOT replaced installation.*

Table A.1.1: Little River at 60<sup>th</sup> Ave NE Cross-section survey data.

Cross-Section Survey Coordinates				
(NAD83 State Plane, feet)				
No	Easting	Northing	Elev.	Desc.
111	2161616.371	708175.26	1061.93	RtPin
112	2161616.192	708188.71	1060.32	SS
113	2161616.047	708199.66	1060.10	SS
114	2161615.936	708208.03	1057.47	SS
115	2161615.819	708216.89	1054.01	SS
116	2161615.67	708228.13	1051.43	SS
117	2161615.593	708233.95	1047.10	SS
118	2161615.532	708238.55	1041.55	SS
119	2161615.52	708239.41	1039.66	SS
143	2161615.473	708242.97	1038.78	WS
144	2161615.468	708243.37	1037.86	SS
145	2161615.357	708251.69	1037.57	SS
146	2161615.239	708260.61	1036.72	SS
147	2161615.14	708268.12	1036.18	SS
148	2161615.038	708275.83	1038.60	SS
149	2161615.017	708277.38	1039.81	SS
150	2161615.008	708278.07	1041.70	SS
151	2161614.945	708282.77	1047.30	SS
152	2161614.852	708289.82	1050.38	SS
153	2161614.766	708296.31	1050.74	SS
154	2161614.727	708299.27	1051.88	SS
155	2161614.699	708301.35	1054.44	SS
156	2161614.58	708310.31	1055.96	SS
157	2161614.471	708318.55	1058.35	SS
158	2161614.368	708326.30	1060.96	SS
159	2161614.308	708331.59	1062.39	SS
160	2161614.23	708336.74	1064.62	LtPin

Table A.1.2: Little River at 60<sup>th</sup> Ave NE initial HOBO elevation Survey data.

HOBO Elevation Survey				
(feet above MSL)				
BS(+)	HI	FS(-)	Elev.	Comment
6.99	1071.61		1064.62	Lt. Pin
		32.75	1038.86	W/S Elev @ HOBO

HOBO Depth at time of survey: 1.23 feet

Table A.1.3: Little River at 60th Ave NE HOBO replacement elevation Survey data (after July 27, 2011).

HOBO Elevation Survey				
(feet above MSL)				
BS(+)	HI	FS(-)	Elev.	Comment
5.83	1070.45		1064.62	Lt. Pin
		32.45	1038.00	W/S Elev @ HOBO

HOBO Depth at time of survey: 1.03 feet

Staff Gauge Information

Initially the Oklahoma Conservation Commission (OCC) had a staff gauge installed at the site. Information on the staff gauge is as follows:

Staff Gauge Reading at time of survey: 2.16 feet

Staff Gauge 0-Datum Elev.: 1036.70 feet

The staff gauge was removed by OCC on July 7, 2011.

Cross-Section Plot

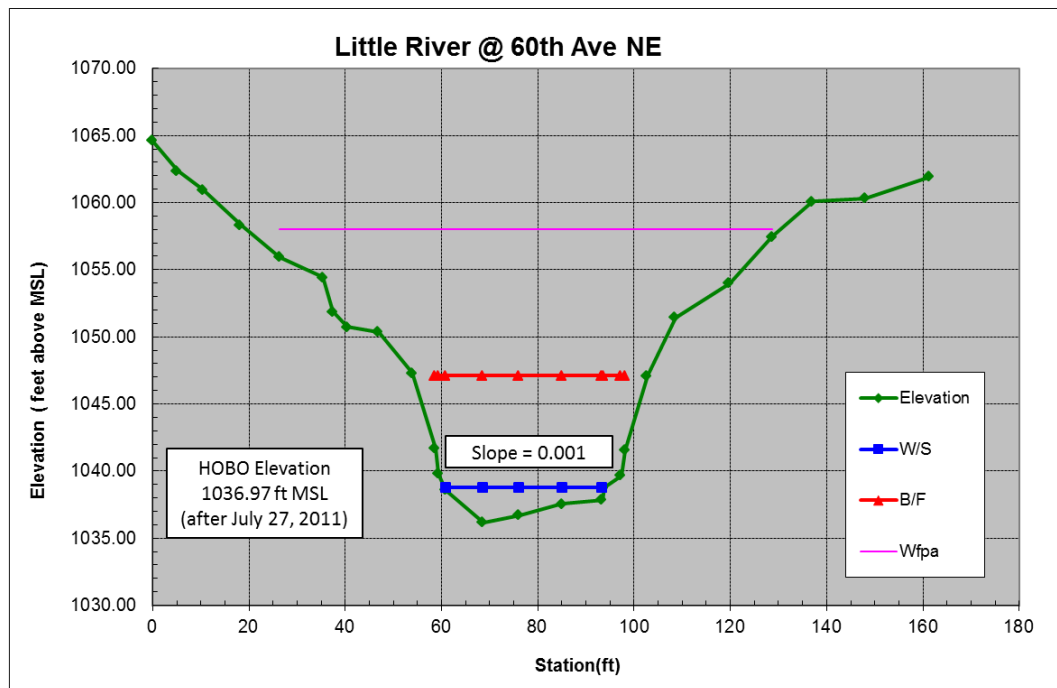


Figure A.1.4: Little River at 60<sup>th</sup> Ave NE - Site cross-section plot.

## A.2 Little River at Porter

HOBO Deployment Date: April 16, 2010

HOBO start time: 1130 (GMT-0600)

HOBO Elevation: 1094.20 feet above MSL

Control Pin Locations (NAD83 State Plane, feet)

	Easting	Northing	Elevation
Left	2135303.82	704871.89	1108.38
Right	2135303.82	704934.01	1108.46

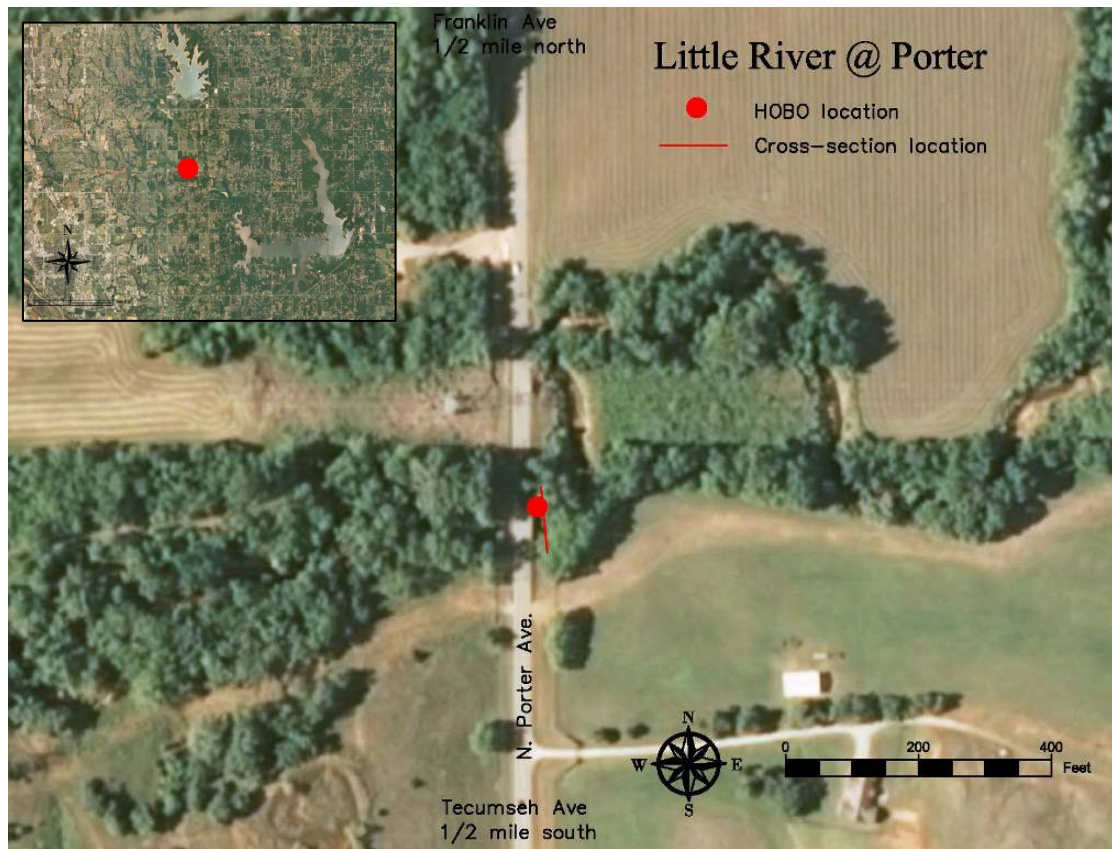


Figure A.2.1: Little River at Porter Ave site location map.



Figure A.2.2: Little River at Porter Ave HOB0 installation.

Table A.2.1: Little River at Porter Ave Cross-section survey data.

Cross-Section Survey Coordinates				
(NAD83 State Plane, feet)				
No	Easting	Northing	Elev.	Desc.
1	2135303.82	704871.89	1108.38	Lt Pin
2	2135303.82	704934.01	1108.46	Rt Pin
3	2135303.82	704925.46	1107.57	SS
4	2135303.82	704917.02	1097.14	SS
5	2135303.82	704915.20	1094.34	SS
6	2135303.82	704911.94	1094.04	SS
7	2135303.82	704909.25	1093.94	SS
8	2135303.82	704905.51	1093.89	SS
9	2135303.82	704902.71	1094.27	SS
10	2135303.82	704899.14	1094.79	ws
11	2135303.82	704894.25	1095.73	SS
12	2135303.82	704890.56	1096.80	SS
13	2135303.82	704883.30	1103.40	SS
14	2135303.82	704880.87	1105.81	SS
15	2135303.82	704877.96	1107.16	SS

Table A.2.2: Little River at Porter Ave HOB0 elevation Survey data,

HOB0 Elevation Survey				
(feet above MSL)				
BS(+)	HI	FS(-)	Elev.	Comment
4.36	1112.75		1108.39	Lt. Pin
		17.85	1094.90	W/S Elev @ HOB0

HOB0 Depth at time of survey: 0.70 feet

Staff Gauge Information

Not Applicable

Cross-Section Plot

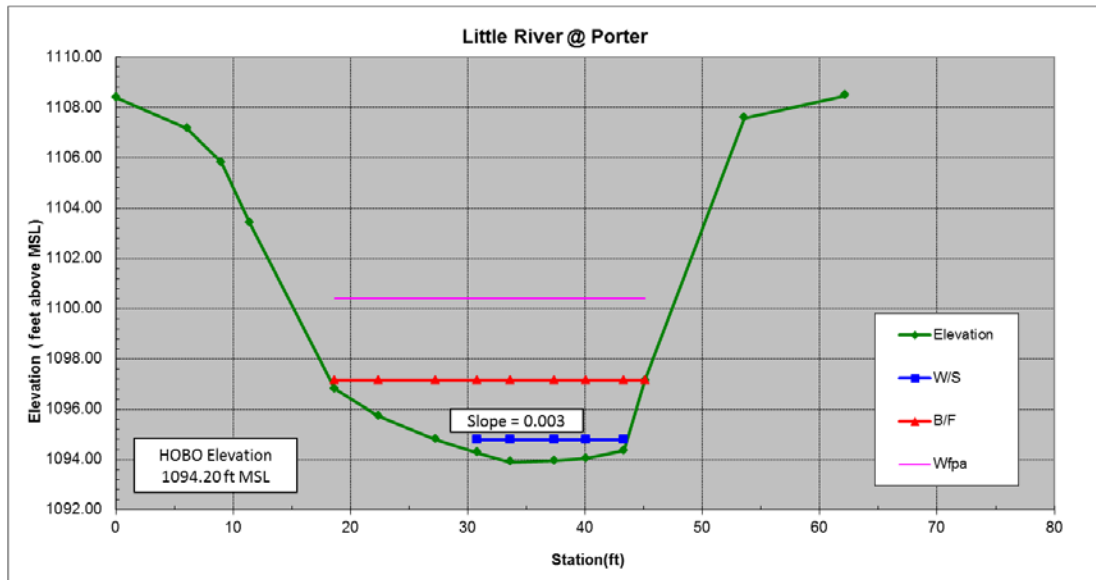


Figure A.2.3: Cross-section plot for the Little River at Porter monitoring site.

### A.3 Hog Creek at SE 119<sup>th</sup> Ave.

HOBO Deployment Date: March 29, 2010

HOBO start time: 1330 (GMT-0500)

HOBO Elevation: 91.79 feet (reference)

Control Pin Locations (NAD83 State Plane, feet)

	Easting	Northing	Elevation (reference)
Left	2189755.72	734115.3887	100.00
Right	2189688.10	734120.14	98.50



Figure A.3.1: Hog Creek at SE 119<sup>th</sup> Ave site location map.





Figure A.3.2: Hog Creek at SE119th Ave site HOBOT installation.

Table A.3.1: Hog Creek at SE 119<sup>th</sup> Ave cross-section survey data.

Cross-Section Survey Coordinates (NAD83 State Plane, feet)				
No	Easting	Northing	Ref. Elev.	Desc.
1	2189755.72	734115.39	100.00	Lt Pin
2	2189688.10	734120.14	98.50	Rt Pin
3	2189696.69	734119.53	96.10	ss
4	2189697.34	734119.49	95.22	ss
5	2189700.59	734119.26	93.49	ss
6	2189701.76	734119.18	92.14	ss
7	2189707.29	734118.79	91.01	ss
8	2189712.67	734118.41	91.01	ss
9	2189717.49	734118.07	91.25	ss
10	2189721.38	734117.80	91.00	ss
12	2189725.85	734117.49	90.92	ss
13	2189729.20	734117.25	92.52	ss
14	2189735.22	734116.83	94.36	ss
15	2189739.82	734116.51	94.95	ss
16	2189743.22	734116.27	96.58	ss
17	2189745.97	734116.07	97.90	ss
18	2189746.35	734116.05	98.64	ss
19	2189750.29	734115.77	99.81	ss

Table A.3.2: Hog Creek at SE 119<sup>th</sup> Ave SE HOBO elevation Survey data.

HOBO Elevation Survey				
(feet above MSL)				
BS(+)	HI	FS(-)	Elev.	Comment
9.88	109.88		100.00	Lt. Pin
		17.31	92.57	W/S Elev @ HOBO

HOBO Depth at time of survey: 0.78 feet

### Staff Gauge Information

Initially the Oklahoma Conservation Commission (OCC) had a staff gauge installed at the site. Information on the staff gauge is as follows:

Staff Gauge Reading at time of survey: 1.02 feet

Staff Gauge 0-Datum Elev.: 91.55 feet (reference)

The staff gauge with the HOBO attached was knocked out by a storm on April 25, 2013.

### Cross-Section Plot

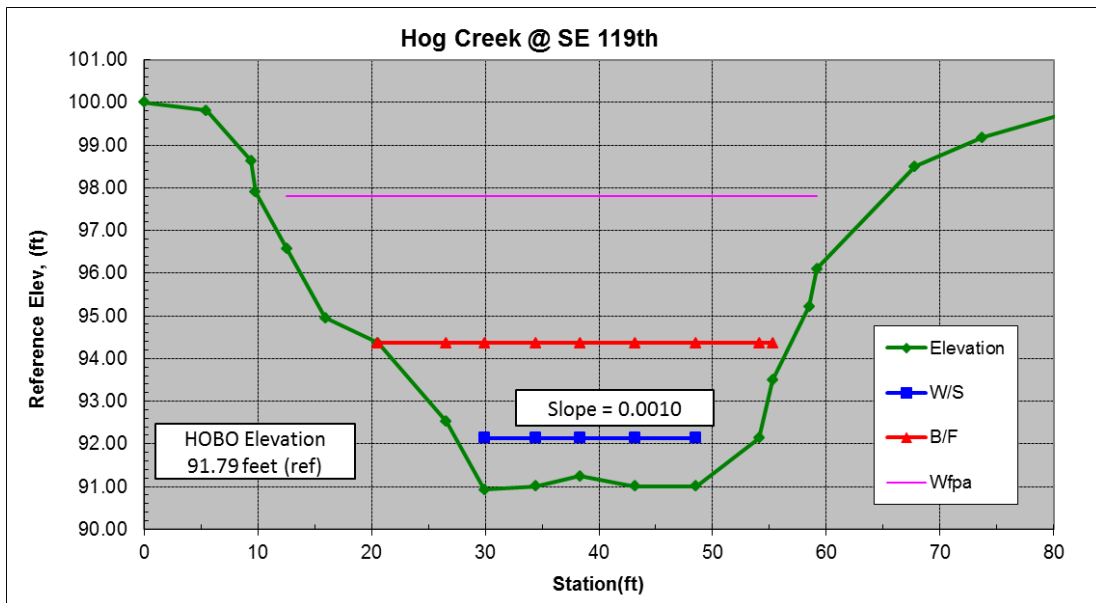


Figure A.3.3: Cross-section plot for the Hog Creek at SE 119<sup>th</sup> Ave monitoring site.

#### A.4 Rock Creek at 72<sup>nd</sup> Ave NE

HOBO Deployment Date: March 29, 2010

HOBO Start Time: 1430 (GMT-0500)

HOBO Elevation: 1039.85 feet above MSL

Control Pin Locations (NAD83 State Plane, feet)

	Easting	Northing	Elevation (reference)
Left	2166872.43	702295.69	1050.97
Right	2166878.93	702221.90	1053.24

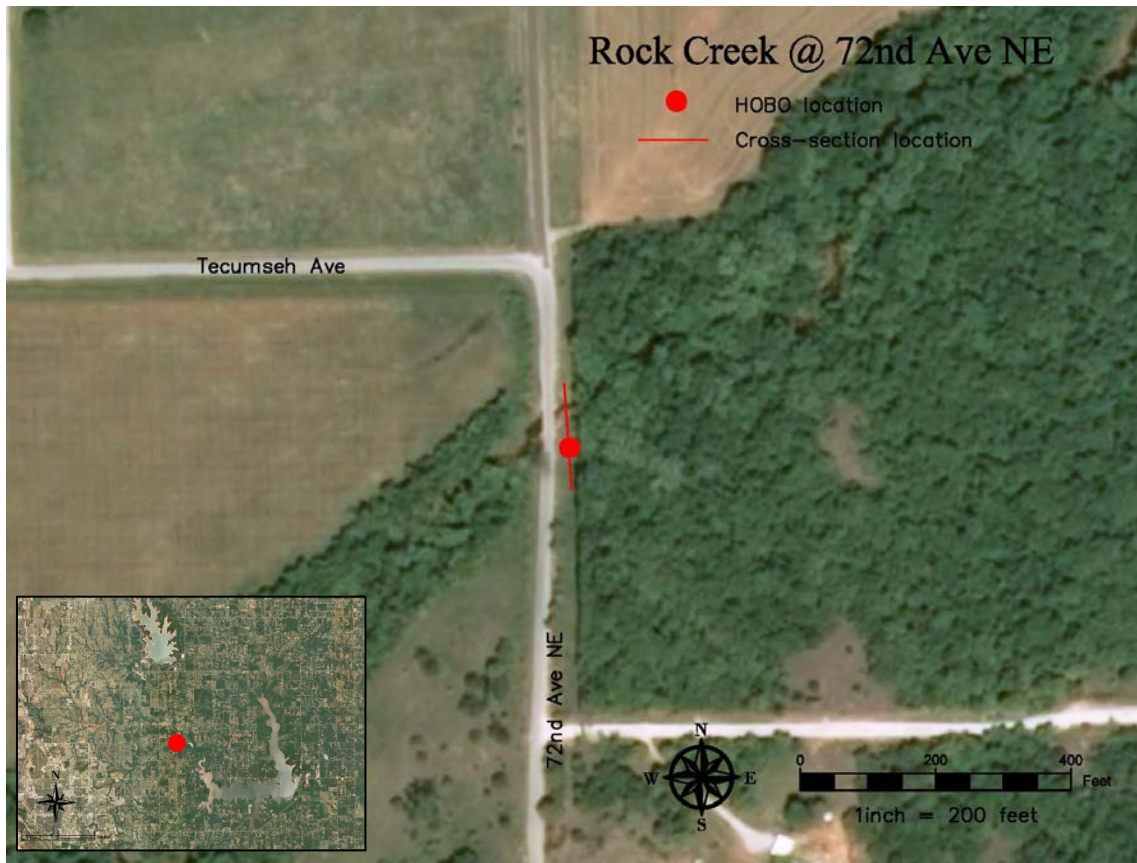


Figure A.4.1: Rock Creek at 72<sup>nd</sup> Ave NE site location map.



Figure A.4.2: Rock Creek at 72<sup>nd</sup> Ave NE site HOBO installation.

Table A.4.1: Rock Creek at 72nd Ave NE Cross-section survey data.

Cross-Section Survey Coordinates				
(NAD83 State Plane, feet)				
No	Easting	Northing	Elevation	Desc.
99	2166878.93	702221.90	1053.24	Rtpin
100	2166878.46	702227.23	1052.80	ss
101	2166878.09	702231.44	1051.43	ss
102	2166877.78	702234.93	1049.44	ss
103	2166877.57	702237.33	1048.40	ss
104	2166877.18	702241.78	1046.68	ss
105	2166876.81	702245.98	1044.66	ss
106	2166876.55	702248.92	1043.43	ss
107	2166876.14	702253.58	1041.07	ss
108	2166875.73	702258.19	1041.31	ss
109	2166875.62	702259.46	1040.75	ws
110	2166875.47	702261.12	1039.83	ss
111	2166875.26	702263.49	1039.03	th
112	2166875.11	702265.28	1038.95	ss
113	2166874.89	702267.78	1040.87	ss
114	2166874.57	702271.37	1042.74	ss
115	2166874.32	702274.24	1043.26	ss
116	2166874.00	702277.86	1045.28	ss
117	2166873.58	702282.60	1047.80	ss
118	2166873.15	702287.54	1049.54	ss
119	2166872.78	702291.70	1050.37	ss
97	2166872.43	702295.69	1050.97	Ltpin

Table A.4.2: Rock Creek at 72nd Ave NE HOBO elevation Survey data.

HOBO Elevation Survey				
(feet above MSL)				
BS(+)	HI	FS(-)	Elev.	Comment
4.52	1055.49		1050.97	Lt. Pin
		14.81	1040.68	W/S Elev @ HOBO

HOBO Depth at time of survey: 0.83 feet

Staff Gauge Information

Not Applicable

Cross-Section Plot

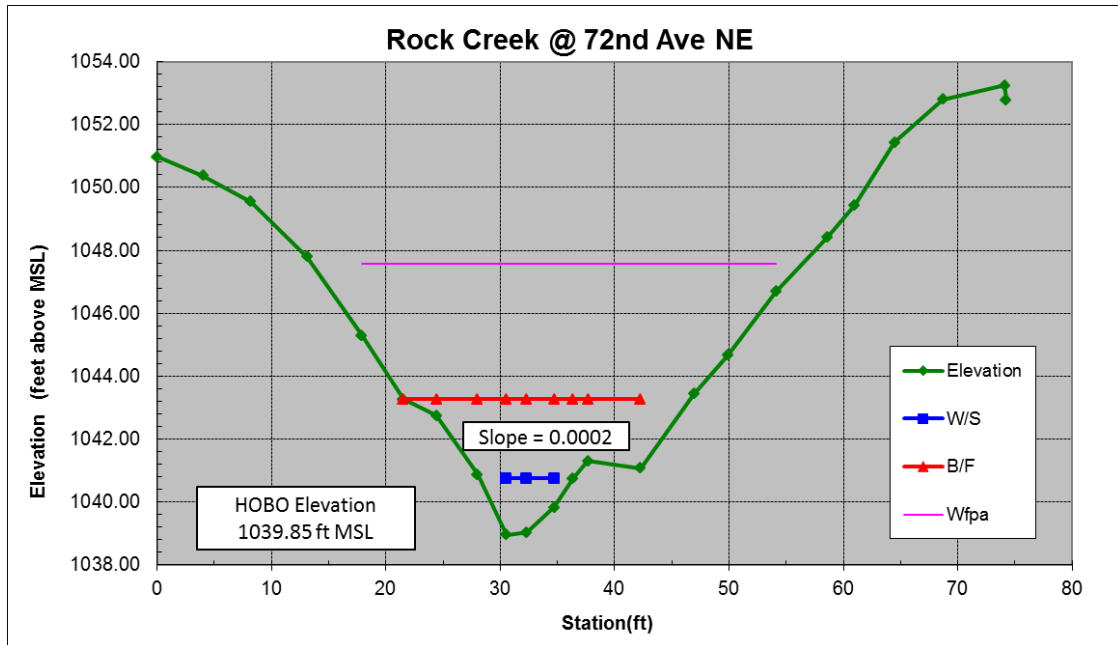


Figure A.4.3: Cross-section plot for the Rock Creek at 72nd Ave NE monitoring site.

## A.5 Elm Creek at Indian Hills

HOBO Deployment Date: March 26, 2010

HOBO start time: 1400 (GMT-0500)

HOBO Elevation: 1050.39 feet above MSL

Control Pin Locations (NAD83 State Plane, feet)

	Easting	Northing	Elevation (reference)
Left	2162925.46	712973.24	1064.56
Right	2162801.54	712971.16	1061.22

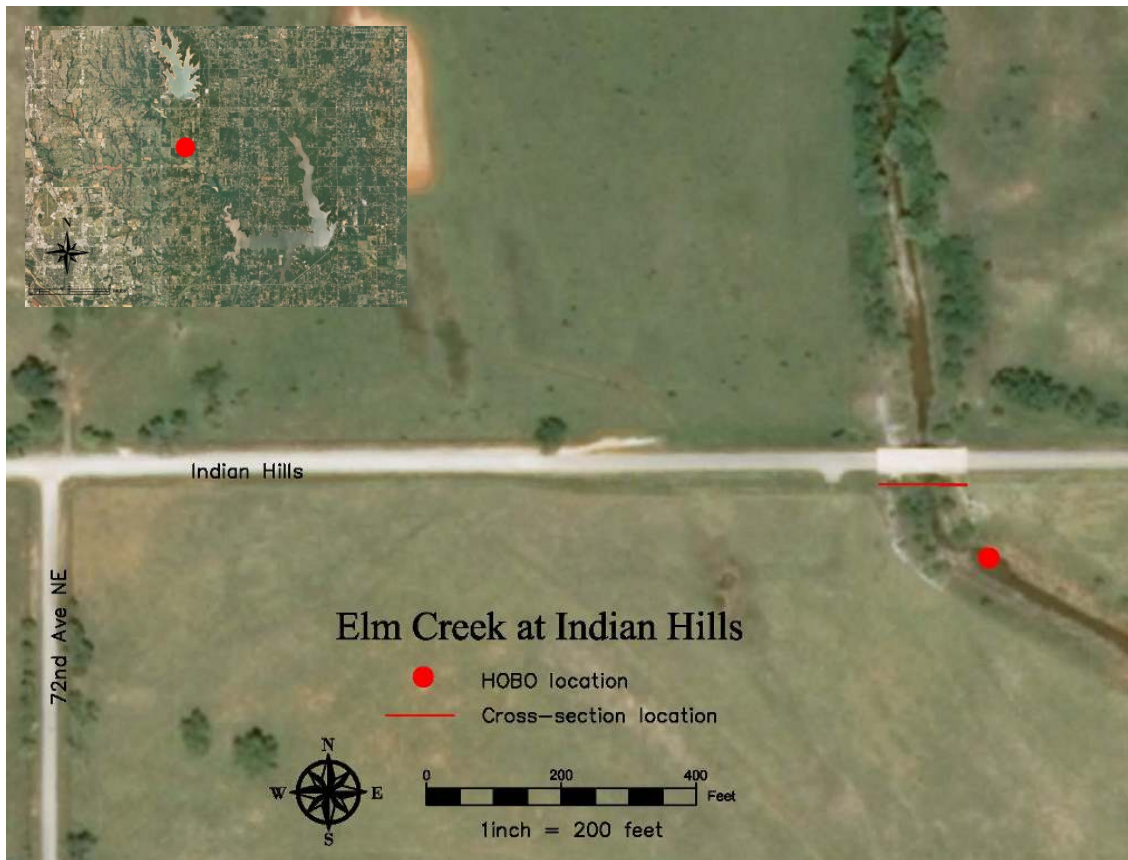


Figure A.5.1: Elm Creek at Indian Hills (SE 179<sup>th</sup>) monitoring site location map.



Figure A.5.2: Elm Creek at Indian Hills (SE 179<sup>th</sup>) monitoring site HOBO installation.

Table A.5.1: Elm Creek at Indian Hills (SE179<sup>th</sup>) cross-section survey data.

Cross-Section Survey Coordinates				
(NAD83 State Plane, feet)				
No	Easting	Northing	Elevation	Desc.
1	2162925.46	712973.24	1064.56	LtPin
2	2162801.54	712971.16	1061.22	RtPin
3	2162823.47	712971.53	1055.62	ss
4	2162833.16	712971.69	1053.41	ss
5	2162840.68	712971.82	1050.57	ss
6	2162847.59	712971.93	1047.7	ss
7	2162855.97	712972.07	1044.98	ss
8	2162858.17	712972.11	1044.78	ws
9	2162858.51	712972.12	1044.37	ss
10	2162866.37	712972.25	1044.14	ss
11	2162873.48	712972.37	1044.47	ss
12	2162880.48	712972.49	1047.5	ss
13	2162885.43	712972.57	1050.11	ss
14	2162890.85	712972.66	1053.82	ss
15	2162898.87	712972.79	1056.29	ss
16	2162904.25	712972.89	1057.44	ss
17	2162911.55	712973.01	1060.41	ss
18	2162918.04	712973.12	1062.48	ss

Table A.5.2: Elm Creek at Indian Hills HOB0 elevation Survey data.

HOB0 Elevation Survey				
(feet above MSL)				
BS(+)	HI	FS(-)	Elev.	Comment
4.36	1068.92		1064.56	Lt. Pin
		17.85	1051.07	W/S Elev @ HOB0

HOB0 Depth at time of survey: 0.68 feet

Staff Gauge Information

Not Applicable

Cross-Section Plot

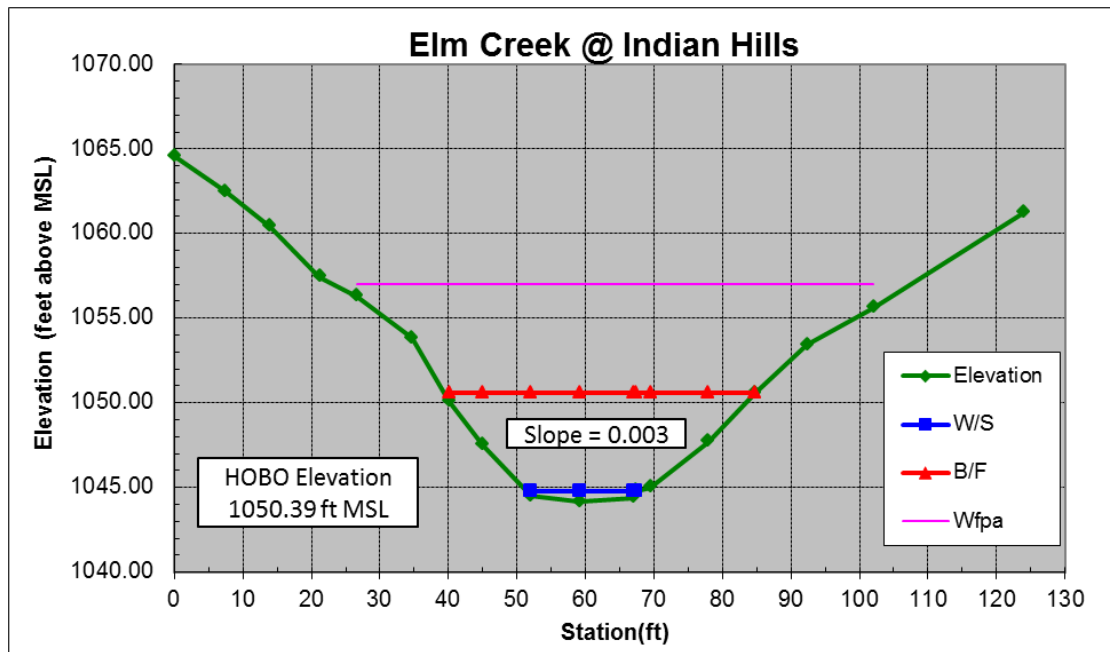


Figure A.5.3: Cross-section plot for the Elm Creek at Indian Hills monitoring site.



## A.6 North Fork at Franklin

HOBO Deployment Date: March 29, 2010

HOBO start time: 1200 (GMT-0500)

HOBO Elevation: 1082.76 feet above MSL

Control Pin Locations (NAD83 State Plane, feet)

	Easting	Northing	Elevation (reference)
Left	2138671.53	707556.97	1099.79
Right	2138586.21	707556.93	1098.54

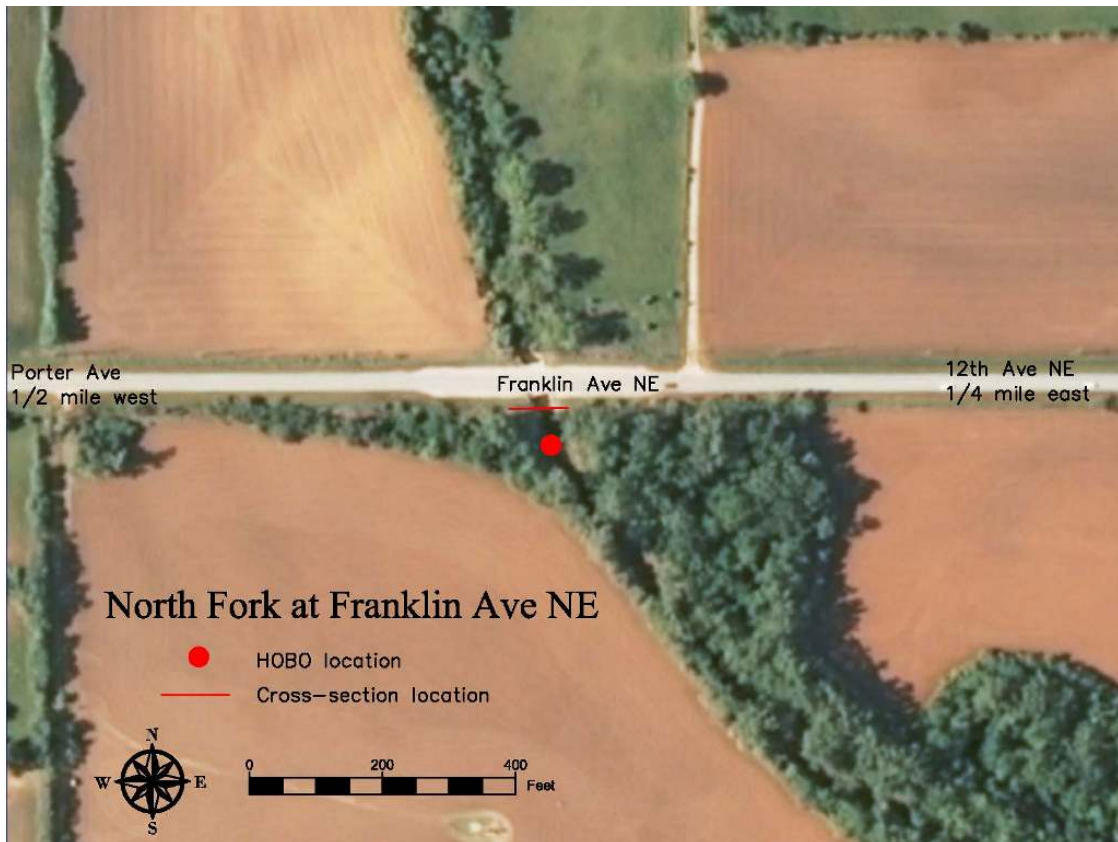


Figure A.6.1: North Fork at Franklin monitoring site location map.



Figure A.6.2: North Fork at Franklin monitoring site HOB0 installation.

Table A.6.1: North Fork at Franklin Cross-section survey data.

Cross-Section Survey Coordinates				
(NAD83 State Plane, feet)				
No	Easting	Northing	Elevation	Desc.
1	2138671.53	707556.97	1099.79	LtPin
2	2138586.21	707556.93	1098.54	RtPin
3	2138599.80	707556.94	1097.36	ss
4	2138611.60	707556.94	1095.87	ss
5	2138616.27	707556.94	1092.18	ss
6	2138617.55	707556.94	1095.26	wing wall
7	2138617.07	707556.94	1095.26	wing wall
8	2138617.70	707556.94	1087.26	ss
9	2138623.89	707556.95	1087.12	ss
10	2138631.52	707556.95	1087.05	ss
11	2138632.03	707556.95	1086.53	ledge
12	2138636.32	707556.95	1086.25	ss
14	2138640.34	707556.96	1086.25	ss
15	2138644.17	707556.96	1086.54	ss
16	2138648.34	707556.96	1087.67	ss
17	2138653.34	707556.96	1089.79	ss
18	2138656.06	707556.96	1093.79	ss
19	2138659.20	707556.96	1096.95	ss
20	2138662.80	707556.97	1098.78	ss

Table A.6.2: North Fork at Franklin HOBO elevation Survey data.

HOBO Elevation Survey				
(feet above MSL)				
BS(+)	HI	FS(-)	Elev.	Comment
2.47	1102.26		1099.79	Lt. Pin
		18.73	1083.53	W/S Elev @ HOBO

HOBO Depth at time of survey: 0.77 feet

Staff Gauge Information

Not Applicable

Cross-Section Plot

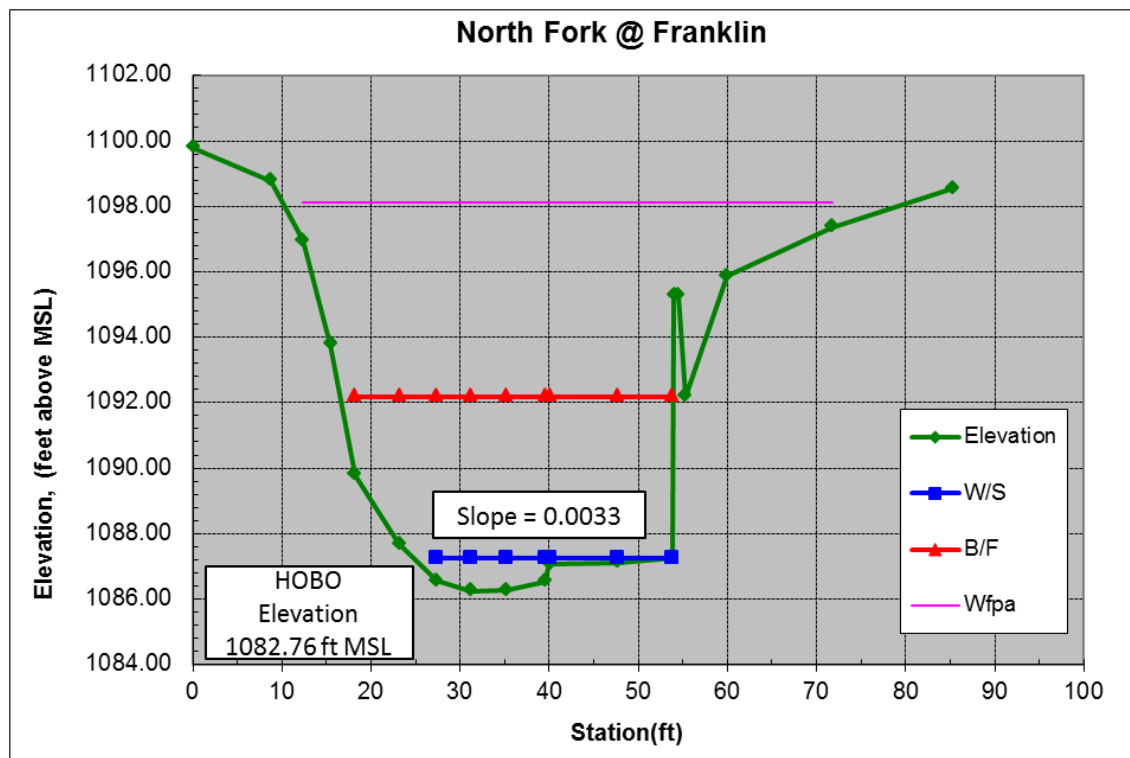


Figure A.6.3: Cross-section plot for the North Fork at Franklin monitoring site.

## A.7 Dave Blue Creek at 72<sup>nd</sup> Ave SE

HOBO Deployment Date: March 16, 2010

HOBO start time: 1200 (GMT-0500)

HOBO Elevation: 1034.85 feet above MSL

Control Pin Locations (NAD83 State Plane, feet)

	Easting	Northing	Elevation (reference)
Left	2167085.35	678217.79	1049.74
Right	2167090.94	678107.49	1053.30



Figure A.7.1: Dave Blue Creek at 72<sup>nd</sup> Ave SE monitoring site location map.



*Figure A.7.2: Dave Blue Creek at 72<sup>nd</sup> Ave SE monitoring site HOB0 installation.*

Table A.7.1: Dave Blue Creek at 72nd Ave SE Cross-section survey data.

Cross-Section Survey Coordinates				
(NAD83 State Plane, feet)				
No	Easting	Northing	Elevation	Desc.
1	2167085.35	678217.79	1049.74	left pin
2	2167090.94	678107.49	1053.30	right pin
3	2167090.61	678114.03	1053.11	SS
4	2167090.32	678119.78	1052.29	SS
5	2167090.10	678124.12	1051.83	SS
6	2167089.86	678128.79	1050.18	SS
7	2167089.67	678132.65	1048.42	SS
8	2167089.52	678135.60	1046.50	SS
9	2167089.28	678140.21	1044.35	SS
10	2167089.00	678145.84	1042.78	SS
11	2167088.71	678151.51	1041.47	SS
12	2167088.39	678157.74	1038.34	SS
13	2167088.32	678159.09	1037.72	BF
14	2167088.30	678159.47	1036.92	SS
15	2167088.27	678160.19	1036.27	SS
16	2167088.25	678160.54	1034.36	SS
17	2167088.08	678163.81	1034.05	SS
18	2167087.91	678167.24	1034.77	SS
19	2167087.87	678168.13	1035.35	WS
20	2167087.79	678169.63	1035.20	SS
21	2167087.63	678172.77	1034.98	SS
22	2167087.48	678175.68	1035.36	WS
23	2167087.32	678178.88	1036.50	SS
24	2167087.11	678182.98	1037.51	SS
25	2167086.93	678186.67	1038.08	SS
26	2167086.70	678191.17	1038.87	SS
27	2167086.50	678195.04	1040.96	SS
28	2167086.43	678196.34	1041.74	SS
29	2167086.39	678197.27	1042.84	SS
30	2167086.13	678202.29	1044.69	SS
31	2167085.93	678206.29	1046.24	SS
32	2167085.71	678210.53	1048.55	SS

Table A.7.2: Dave Blue Creek at 72nd Ave SE HOBO elevation Survey data.

HOBO Elevation Survey				
(feet above MSL)				
BS(+)	HI	FS(-)	Elev.	Comment
2.37	1052.11		1049.74	Lt. Pin
		16.63	1035.48	W/S Elev @ HOBO

HOBO Depth at time of survey: 0.63 feet

Staff Gauge Information

Not Applicable

Cross-Section Plot

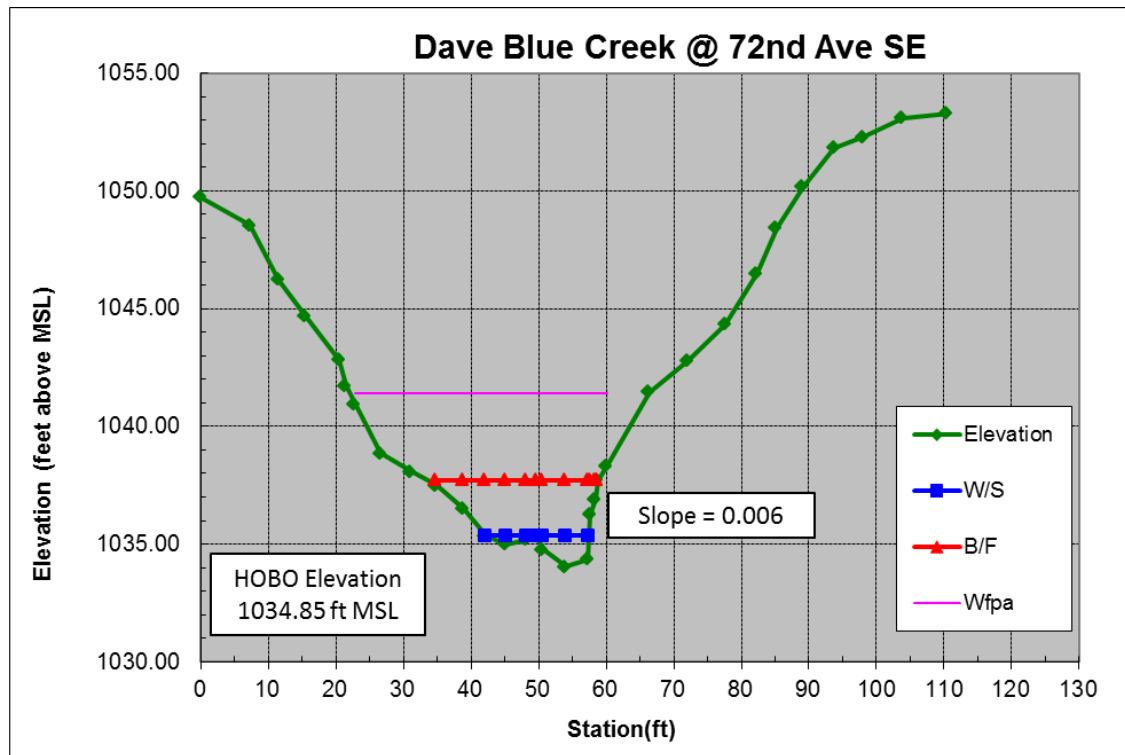
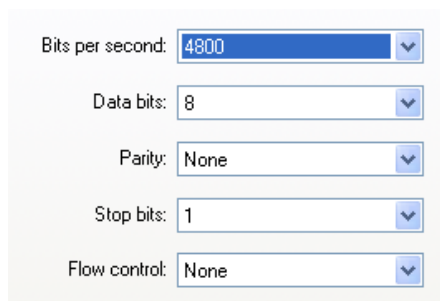


Figure A.7.3: Cross-section plot for the Dave Blue Creek at 72<sup>nd</sup> Ave SE monitoring site.

## B. Appendix B – ADCP Operating Procedure

- I. Base Communication connections (All are color-coded):
  - A. Connect GPS Antennae cable to GPS Antennae and to GPS unit (yellow).
  - B. Connect GPS Radio Antennae (blue).
  - C. Connect ADCP Antennae (orange).
  - D. Connect Battery.
  - E. Turn GPS unit on.
- II. Base Computer Connections:
  - A. Plug one of the 9-pin to USB cables into a USB port on the computer.
  - B. DO NOT ATTACH 9-PIN.
  - C. Check port configuration on computer.
    1. START; Control Panel; System; Hardware; Device Manager.
    2. Expand “Ports (COM & LPT).”
    3. The port should either be COM6 or COM7.
    4. If COM6:
      - a) Plug nine pin on cable into nine-pin on COM6 connector on base Station.
      - b) Check COM6 Port settings; Double click COM6; Settings should be:

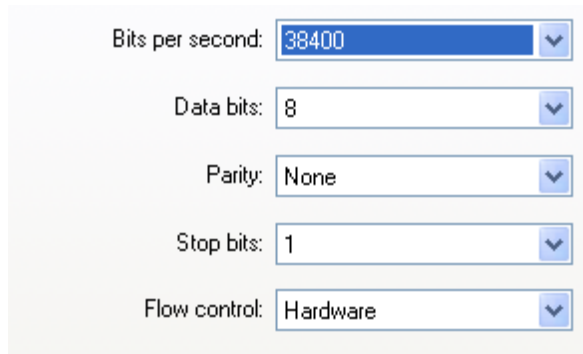


The image shows a screenshot of the COM6 Port settings dialog box. The settings are as follows:

Bits per second:	4800
Data bits:	8
Parity:	None
Stop bits:	1
Flow control:	None



- c) Plug other 9-pin to USB cable into another USB port on the computer.
- d) DO NOT ATTACH 9-PIN.
- e) Check port configuration on computer (See II.C.1.).
- f) Expand “Ports (COM & LPT)” (See II.C.2.).
- g) The Port should be COM7.
- h) Check COM7 Port settings; Double click COM7; Settings should be:



- i) Plug nine pin on cable into nine-pin on COM7 connector on base Station.

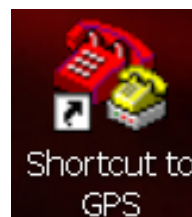
5. If COM7, reverse the order (II.C.4.g)-i), then II.C.4.a)-f)).

### III. Boat Preparation:

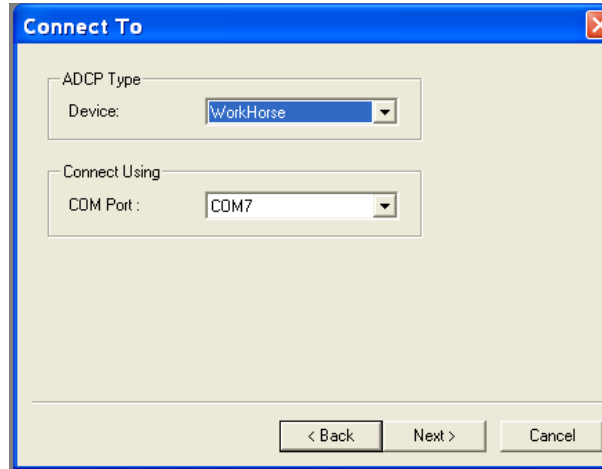
- A. Connect batteries.
- B. Turn on boat.
- C. Turn on GPS.
- D. Wait for solid green GPS lock on base unit and boat.

### IV. Check GPS communication.

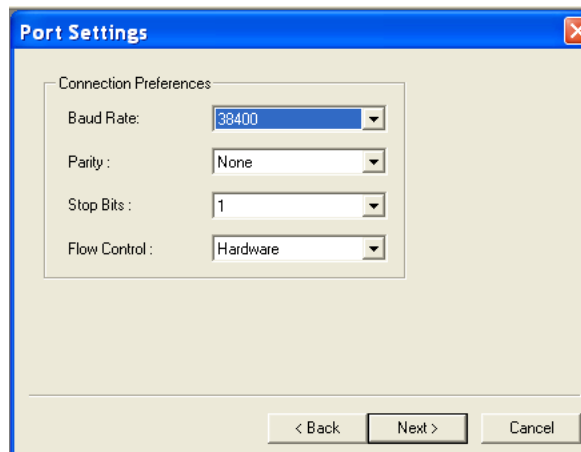
- A. Use hyperterminal link.



- B. Screen should start scrolling data.
  - C. Disconnect and close hyperterminal.
- V. Check ADCP Communication.
- A. Use BBTalk link.
  - B. You should see:

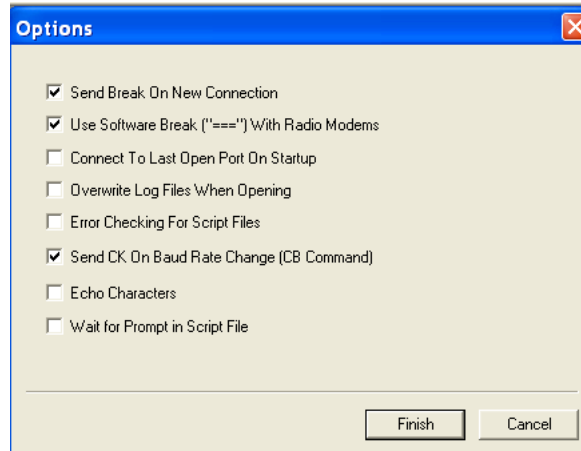


- C. Click on "Next>".
- D. You should see:



- E. Click on "Next>".

F. You should see:



G. Click “Finish.”

H. You should see a header and then a cursor, “>”.

I. Disconnect and close BBTalk.

VI. Prepare the ADCP for measurement.

A. Start “WinRiver II”.

B. Start new measurement (File; New Measurement...).

C. Should get Setup Dialog.

D. Enter Site Information as desired. Click “Next”.

E. Don’t need to change Rating Information so click “Next”.

F. On Configuration Dialog page do the following:

1. Confirm that the ADCP is recognized. The light will turn green and the ADCP Serial Number will be displayed.
2. Click on GPS. It will turn green.
3. Set transducer depth (0.3 ft).
4. Set Magnetic variation (In Norman, 4).

5. Enter estimated maximum water depth (ft), and secondary (minimum) depth (ft), max. water speed and max boat speed, and streambed material.
  6. Click on “Next.”
  - G. On the Output Filename Options screen, select a directory and name for the measurement. Click on “Next.”
  - H. On the Measurement Wizard screen type in any commands you want to send to the ADCP to override the Wizard in the “User:” column. Click on “Next.”
  - I. Review the Summary Page screen and Click on “Finish.”
- VII. Compass calibration.
- A. Select “Execute compass calibration” from the menu. REQUIRED if using GPS as reference or the loop method to detect and/or correct for a moving bed.
  - B. Press “Calibration” button and follow directions. Compass calibrations and evaluations involve rotating the ADCP 360 degrees, at a constant rate, while keeping pitch and roll to a minimum. The ADCP should be rotated as close to the measurement section as possible. This is done with the ADCP on the bank, away from electro-magnetic objects.
  - C. Press “Evaluate Compass”. An evaluation MUST always be completed after a calibration and the total error reported should be typically less than 1 degree. If the total error exceeds 1 degree, the calibration procedure should be repeated, and then reevaluated.
- VIII. Complete Loop moving bed tests. The loop moving bed test is preferred over the stationary method. The method presented here is for earlier versions of

WinRiver II. The procedure for the latest version, released April, 2014, is different than what is presented here.

- A. Start the instrument pinging (F4).
- B. Place the ADCP on the water. If lowering from a bridge, lower carefully so as to prevent shifting of the contents.
- C. Move the trimaran across the channel to ensure that the expected conditions entered in the measurement wizard are appropriate.
- D. Compass must be calibrated.
- E. Establish a marked starting point, on the left bank, where the ADCP can be returned to the exact location.
- F. Choose “Select Moving Bed test” (F6) from the Menu, then select “Loop Test” and press “Start”.
- G. Make a steady pass back and forth across the stream, but do not stop recording until the ADCP is returned to the starting location. The maximum boat speed should be less than 1.5 times the mean water speed, with a total duration of the loop no less than 3 minutes. The boat speed should be consistent for the entire loop, even near the edges.
- H. Stop the recording of the loop test (F6) when the ADCP arrives back at the starting location.
- I. Turn off pinging (F4).
- J. Toggle to Classic ASCII output from the Configure tab... ASCII Output... Classic ASCII Output. It does not matter if you select to output backscatter or intensity data.

- K. Reprocess Loop moving bed transect. This will create an ASCII file that can be read by the LC program.
  - L. Toggle off Classic ASCII output from the Configure tab... ASCII Ouput... Classic ASCII Ouput.
  - M. Run the USGS's Loop Correction (LC) program, press the select Loop file button and load the ASCII output file just created.
  - N. If LC recommends a correction, the moving bed was found to be significant.
- IX. Collecting Transect measurements.
- A. Start the instrument pinging. (F4)
  - B. Establish starting and ending locations.
  - C. Start at left bank.
  - D. Start logging data. (F5)
  - E. Enter distance from bank. Click on "O.K."
  - F. Remain at start point for 10 ensembles.
  - G. Cross the channel slowly. Go slower than the current.
  - H. At the right bank, wait for 10 ensembles.
  - I. Stop logging data. (F5)
  - J. Enter distance from bank. Click on "O.K."
  - K. To see Summary press F12.
  - L. For the return transect, start logging data. (F5)
  - M. Enter distance from bank. Click on "O.K."
  - N. Remain at start point for 10 ensembles.
  - O. Cross the channel slowly. Go slower than the current.

- P. At the left bank, wait for 10 ensembles.
- Q. Stop logging data. (F5)
- R. Enter distance from bank. Click on “O.K.”
- S. To see Summary press F12.
- T. Repeat steps VII.A.-R. as desired.
- U. Stop the instrument pinging. (F4)
- X. Shutting down.
  - A. Turn off GPS on boat.
  - B. Turn off boat.
  - C. Disconnect batteries on boat.
  - D. Turn off base station GPS.
  - E. Disconnect base station battery.

## C. Appendix C – HOBO Data Plots

### C.1 Ambient Conditions

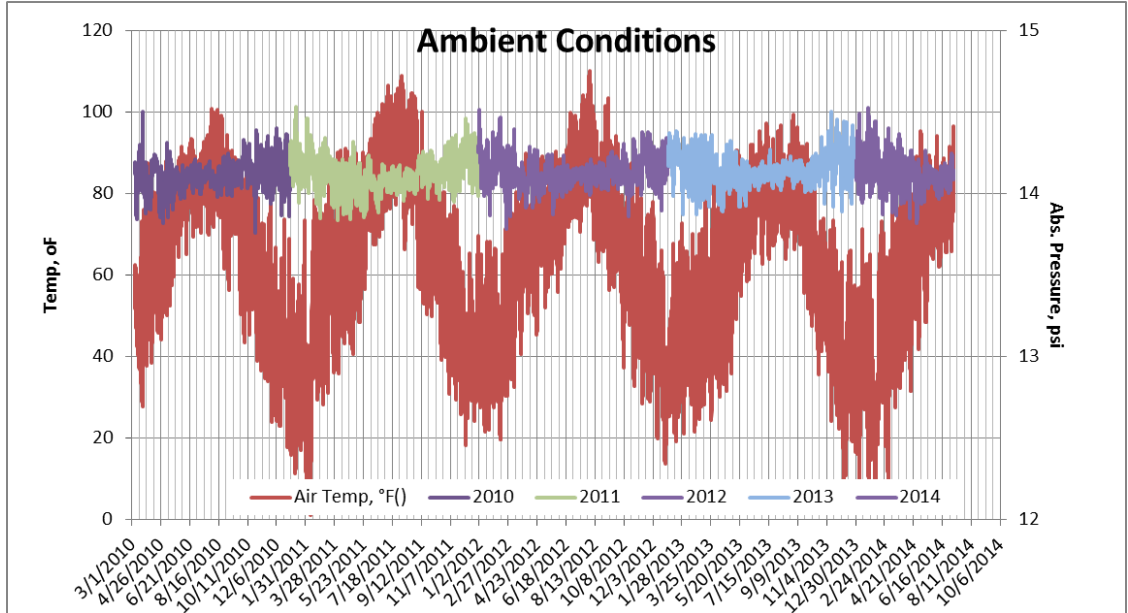


Figure C.1.1: Ambient Conditions site HOBO data plot.

### C.2 Little River @ 60th Ave NE

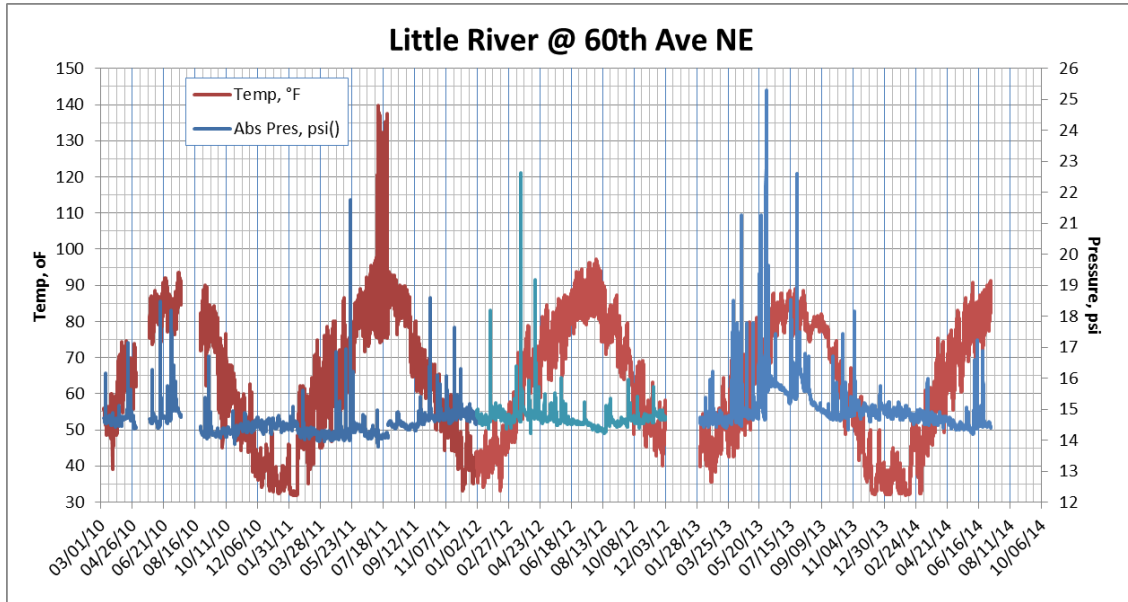


Figure C.2.1: Little River at 60<sup>th</sup> Ave NE site HOBO data plot.



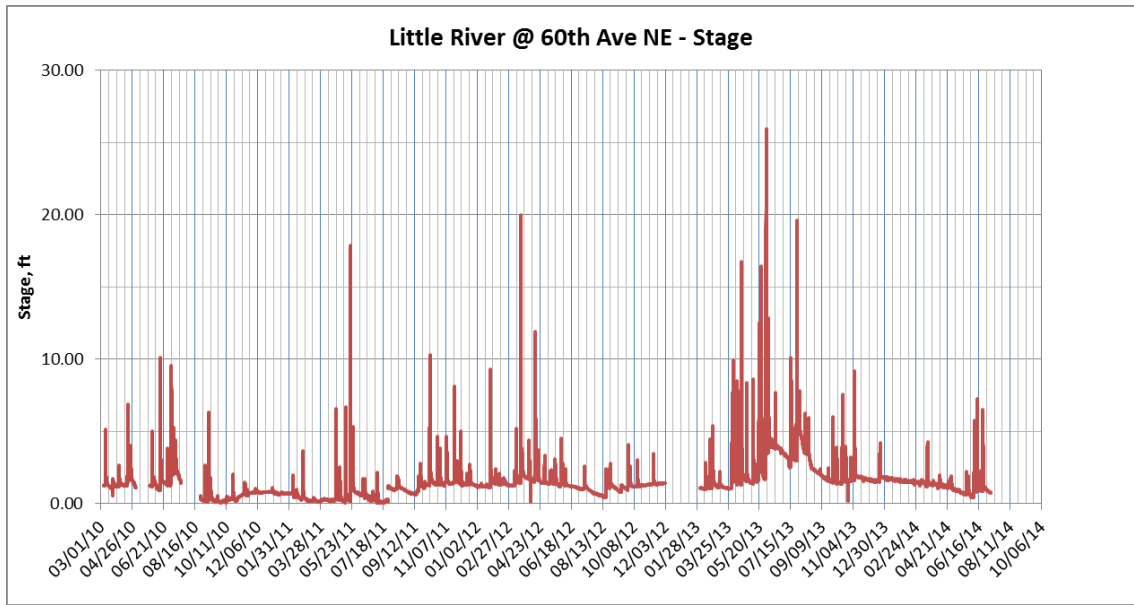


Figure C.2.2: Little River at 60<sup>th</sup> Ave NE site stage plot.

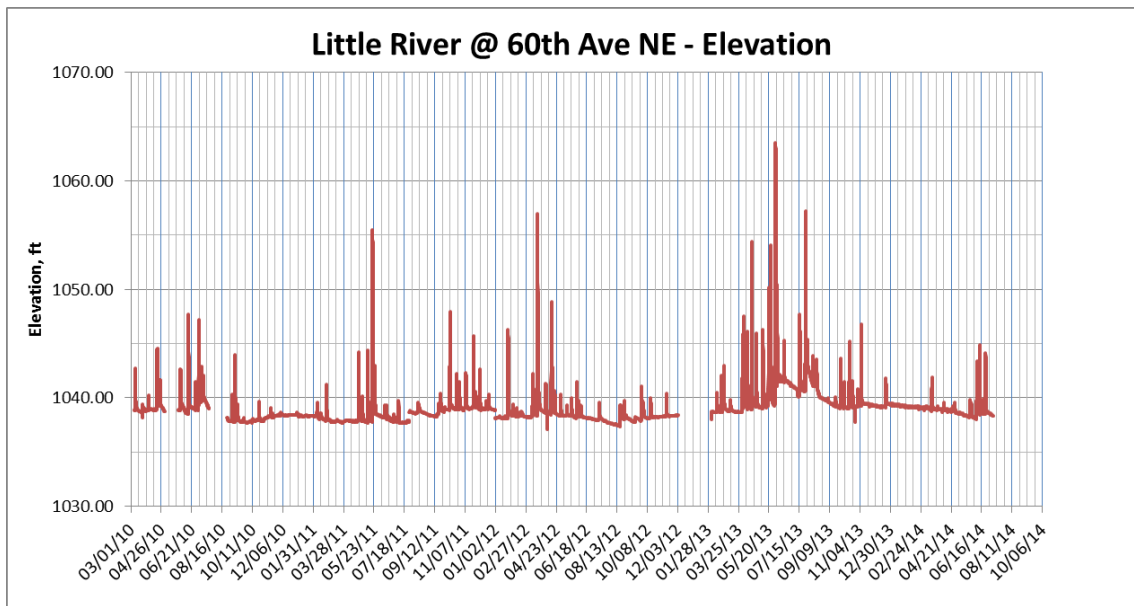


Figure C.2.3: Little River at 60<sup>th</sup> Ave NE site water surface elevation plot.

### C.3 Little River at Porter

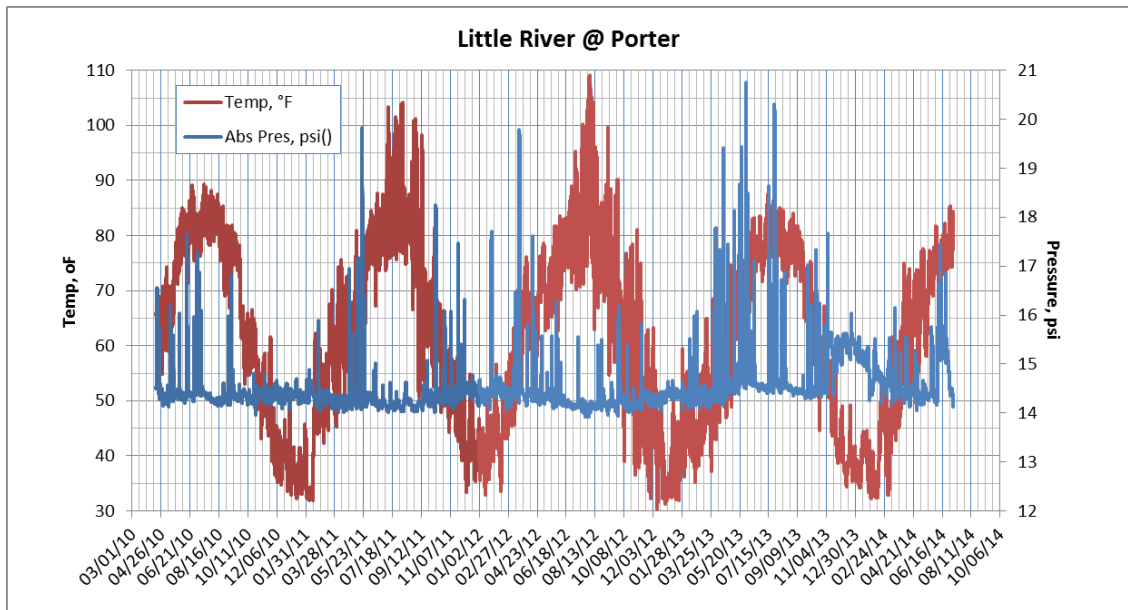


Figure C.3.1: Little River at Porter site HOBO data plot.

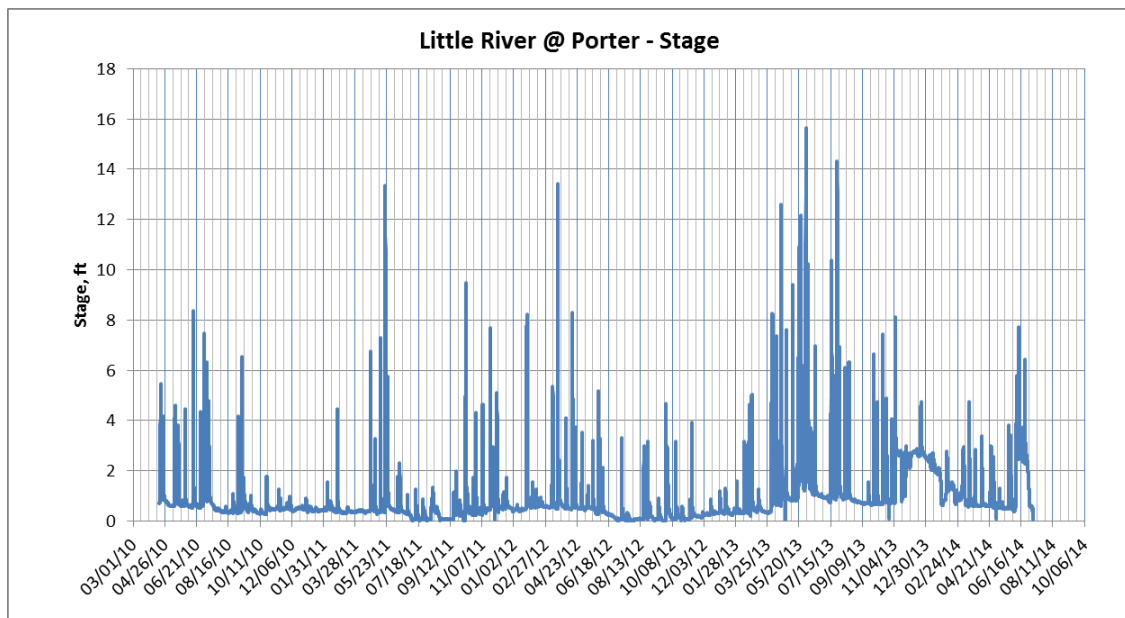


Figure C.3.2: Little River at Porter site stage plot.

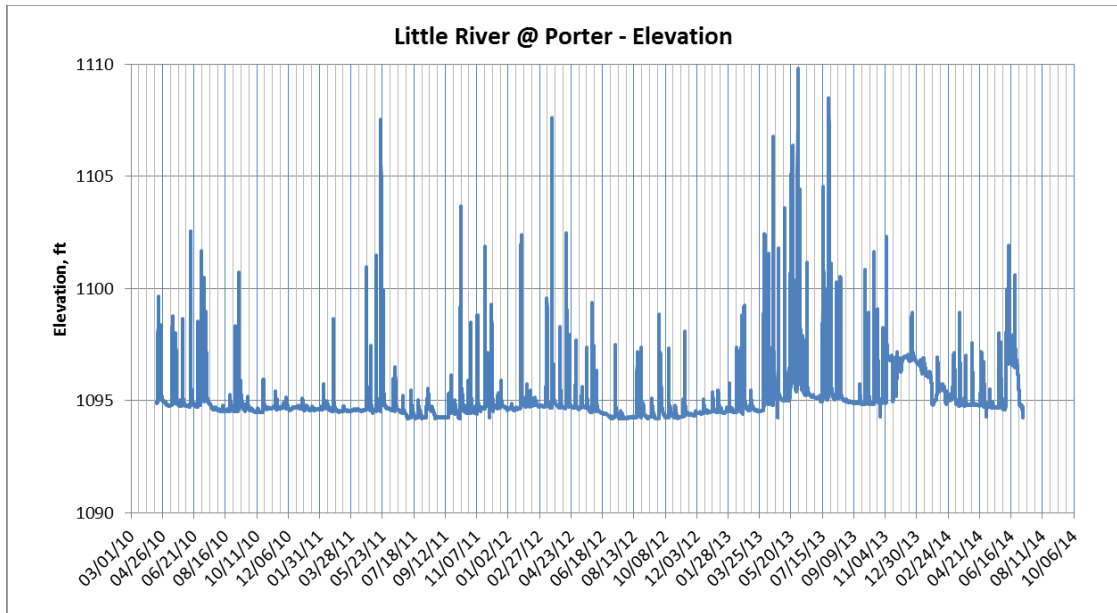


Figure C.3.3: Little River at Porter site water surface elevation plot.

#### C.4 Hog Creek at SE 119<sup>th</sup> Ave.

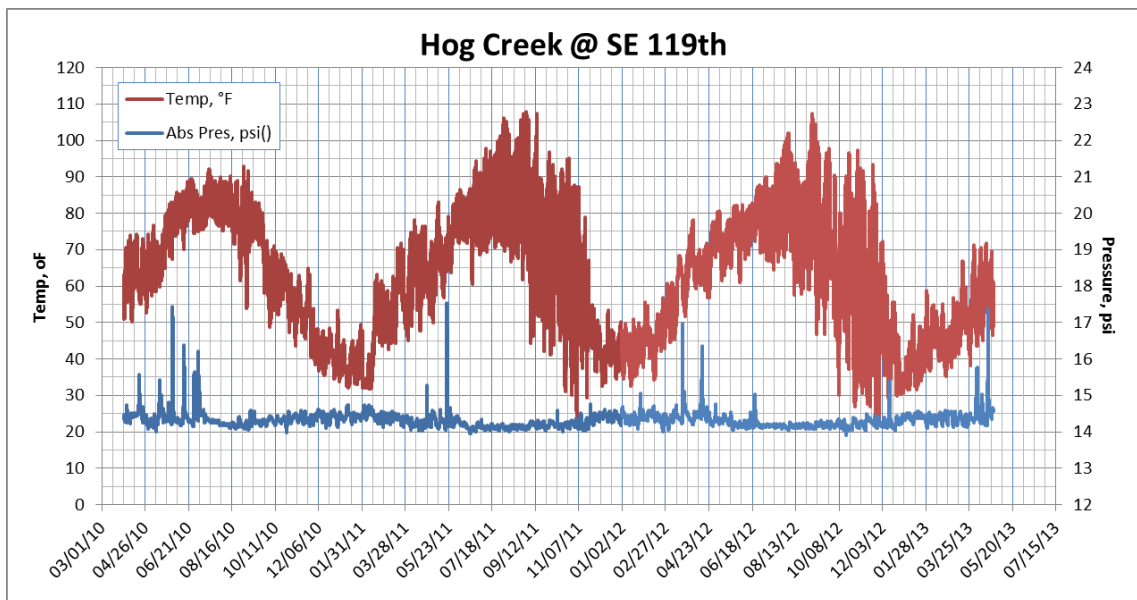


Figure C.4.1: Hog Creek at SE 119<sup>th</sup> Ave site HOBO data plot.

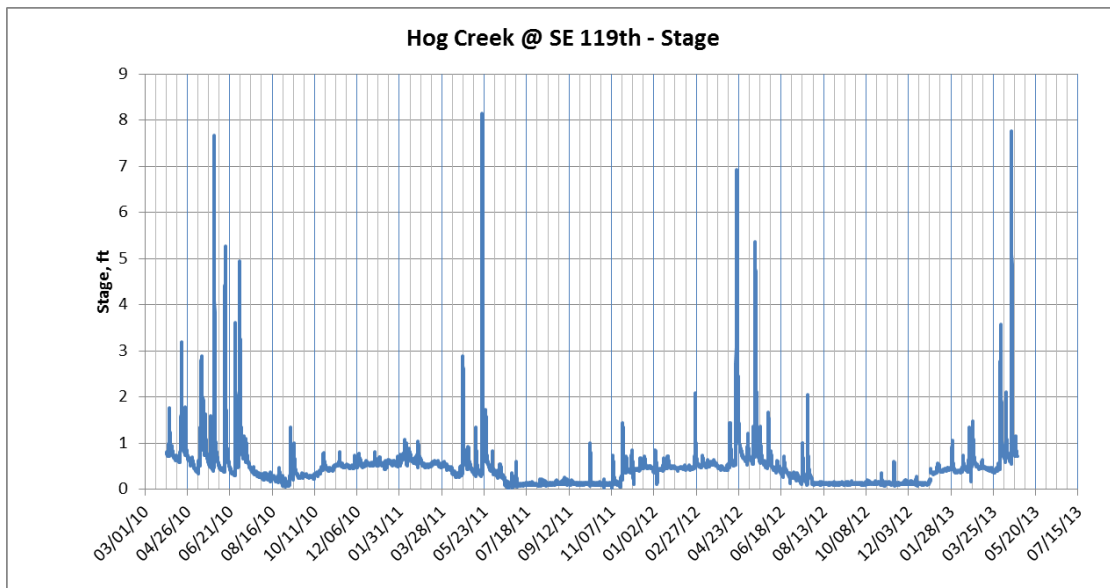


Figure C.4.2: Hog Creek at SE 119<sup>th</sup> Ave site stage plot.

### C.5 Rock Creek at 72<sup>nd</sup> Ave NE

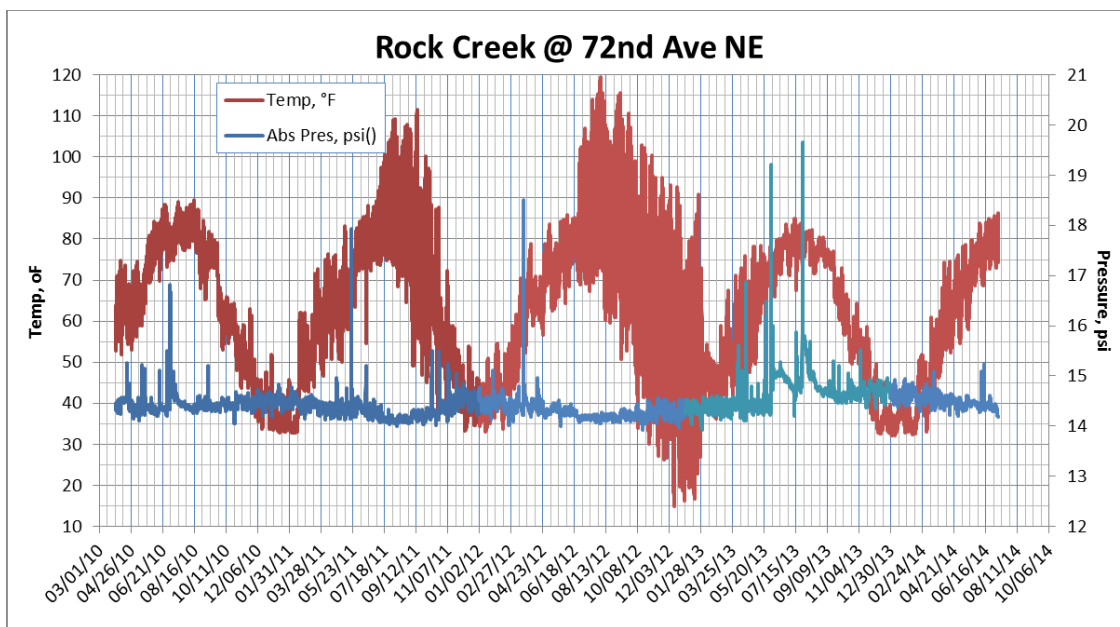


Figure C.5.1: Rock Creek at 72<sup>nd</sup> Ave NE site HOBO data plot.

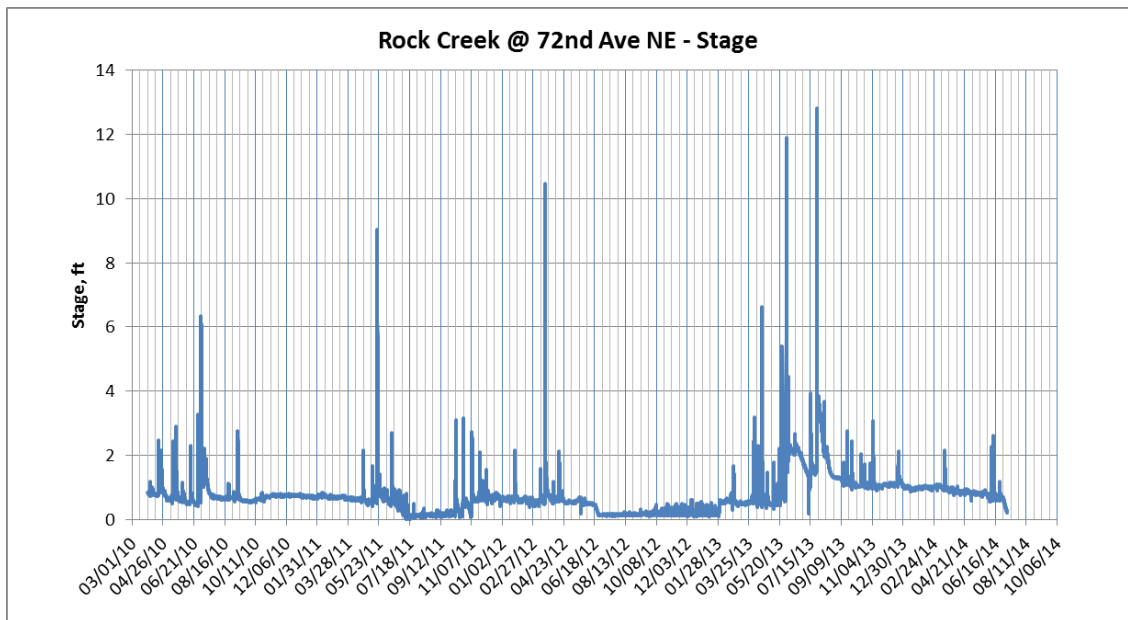


Figure C.5.2: Rock Creek at 72<sup>nd</sup> Ave NE site stage plot.

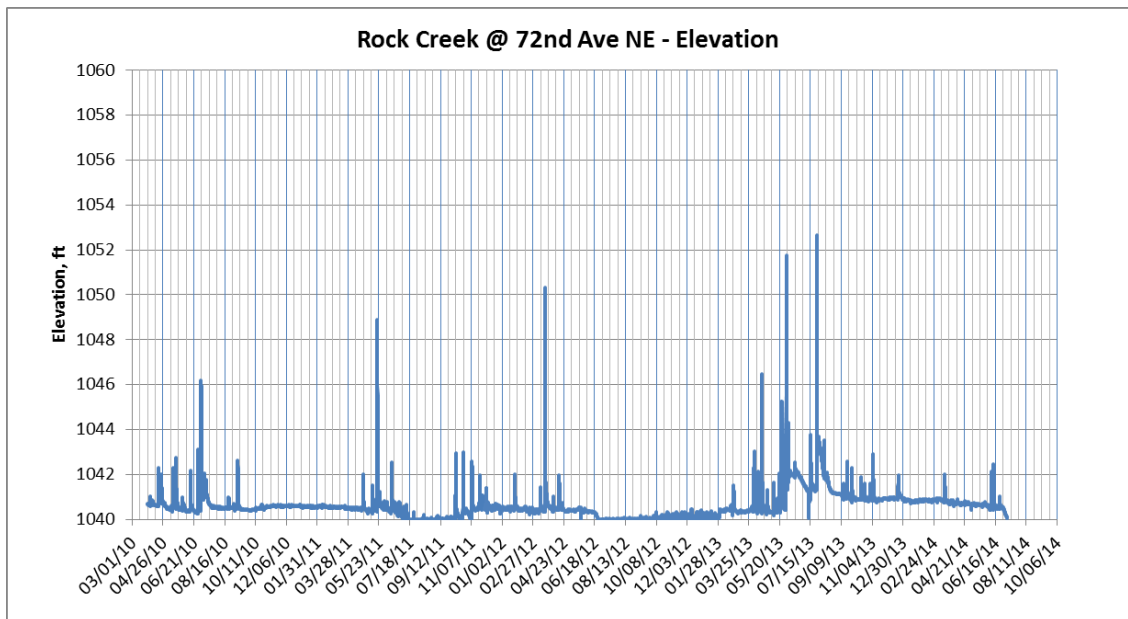


Figure C.5.3: Rock Creek at 72<sup>nd</sup> Ave NE site water surface elevation plot.

**C.6 Elm Creek at Indian Hills**

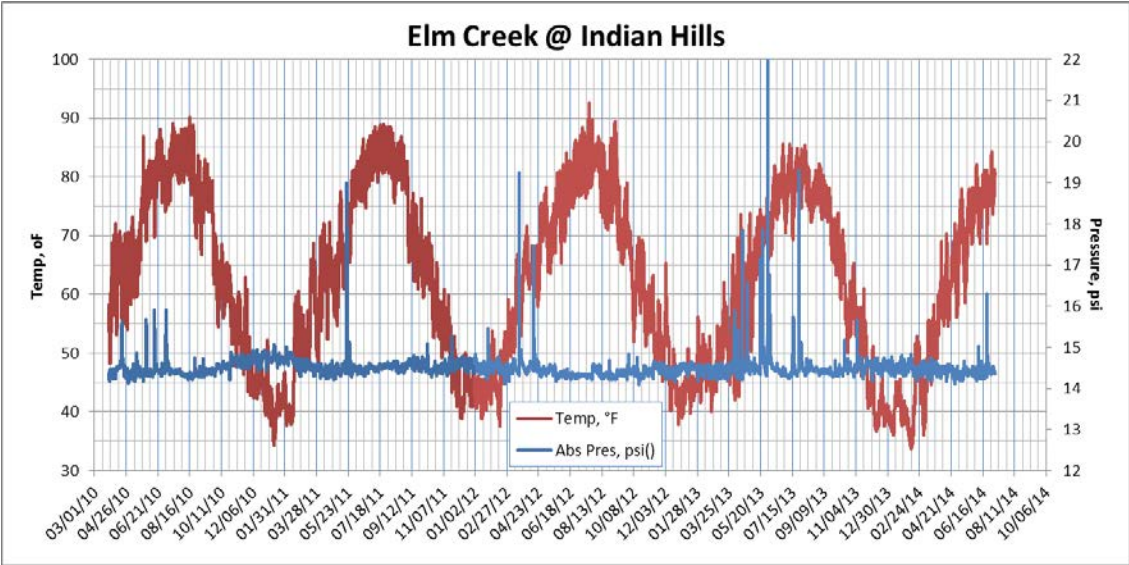


Figure C.6.1: Elm Creek at Indian Hills site HOBO data plot.

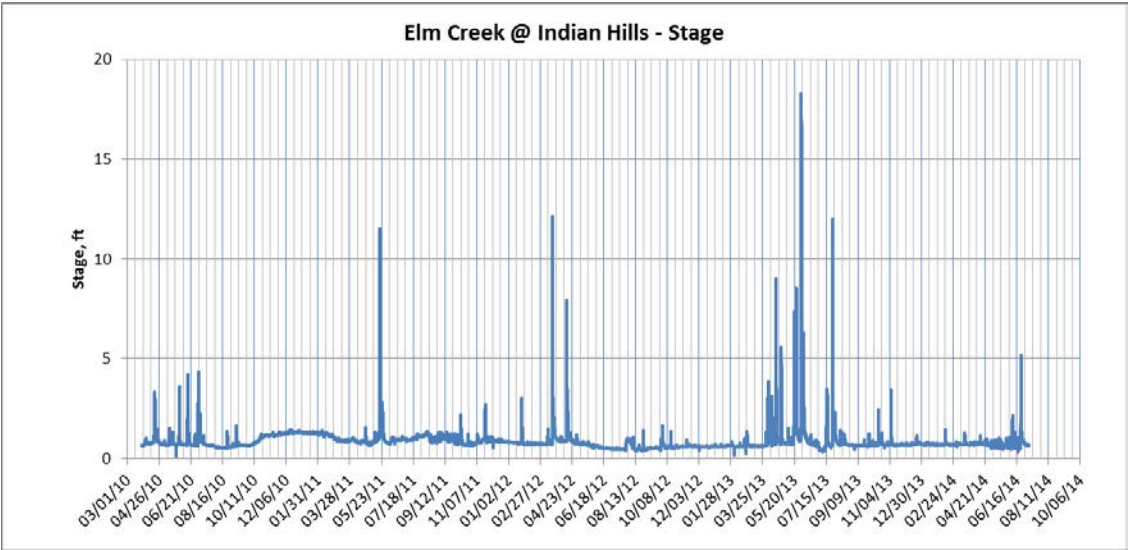


Figure C.6.2: Elm Creek at Indian Hills site stage plot.

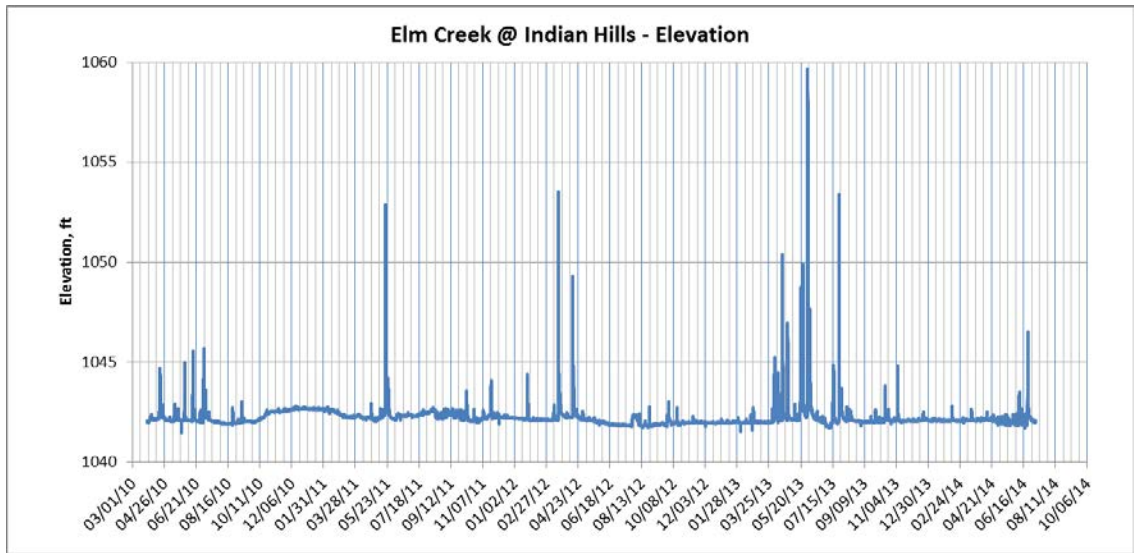


Figure C.6.3: Elm Creek at Indian Hills site water surface elevation plot.

### C.7 North Fork at Franklin

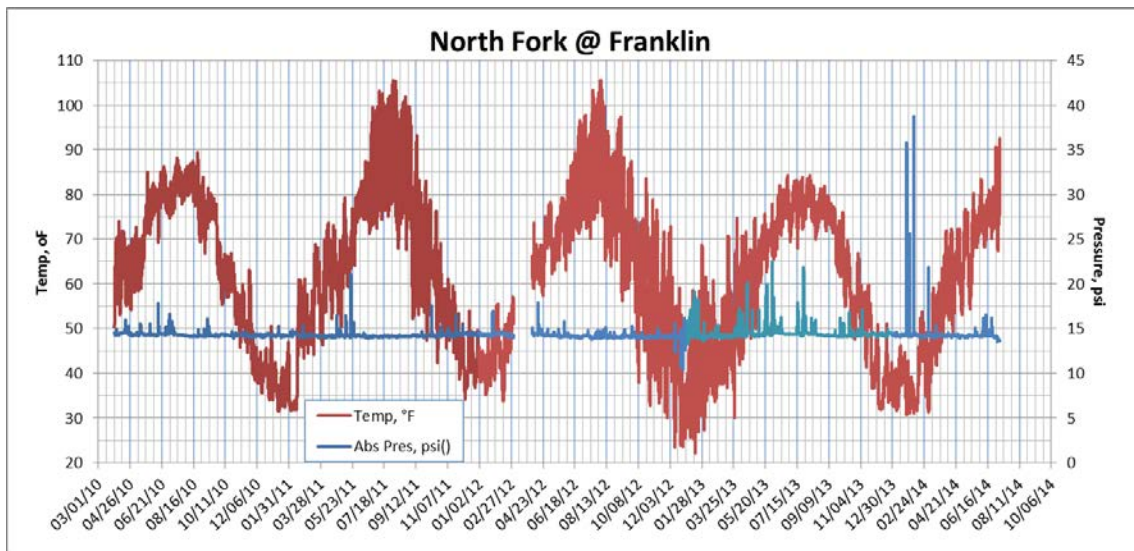


Figure C.7.1: North Fork at Franklin site HOBO data plot.

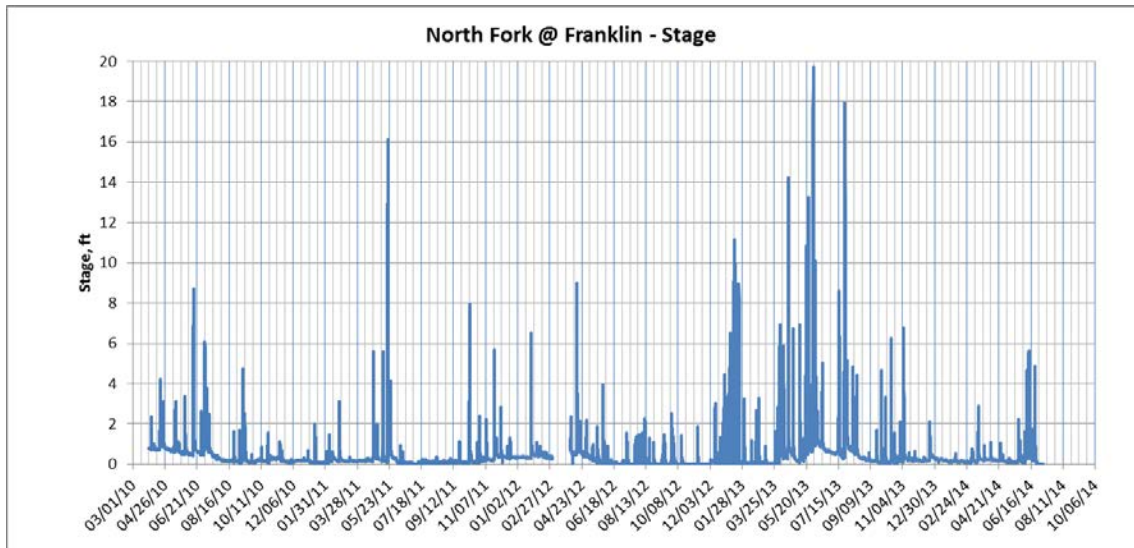


Figure C.7.2: North Fork at Franklin site stage plot.

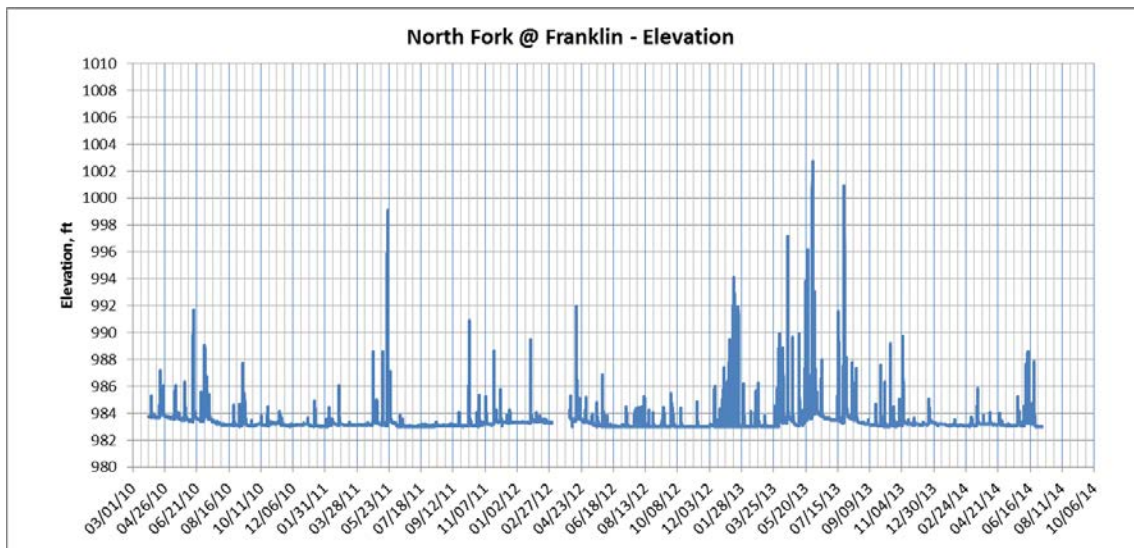


Figure C.7.3: North Fork at Franklin site water surface elevation plot.



## C.8 Dave Blue Creek at 72<sup>nd</sup> Ave SE

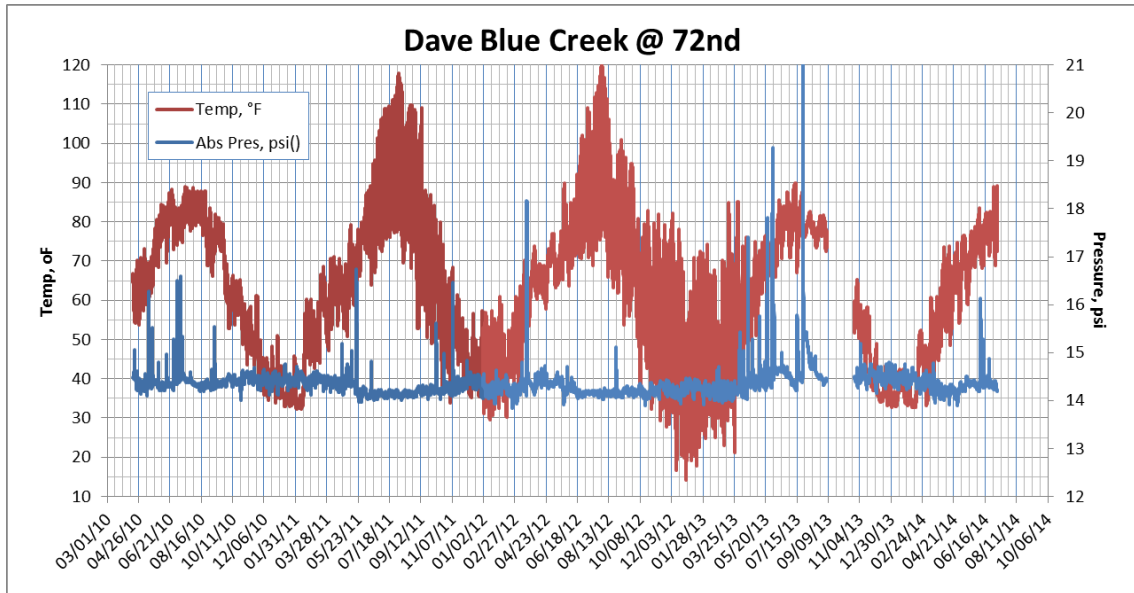


Figure C.8.1: Dave Blue Creek at 72<sup>nd</sup> Ave SE site HOBOTemp and Abs Pres plot.

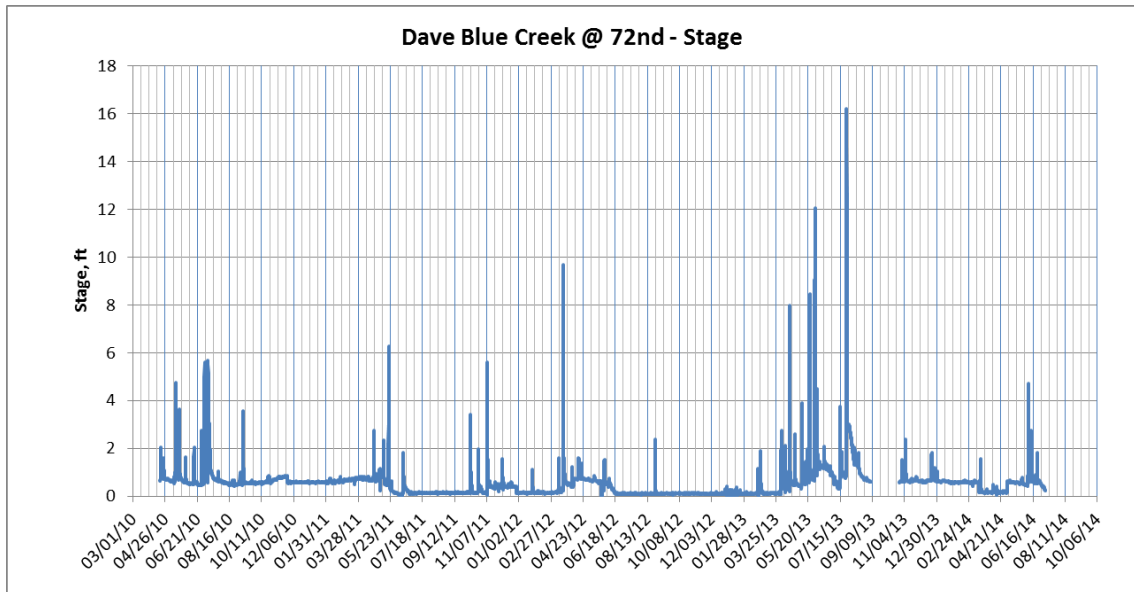


Figure C.8.2: Dave Blue Creek at 72<sup>nd</sup> Ave SE site stage plot.

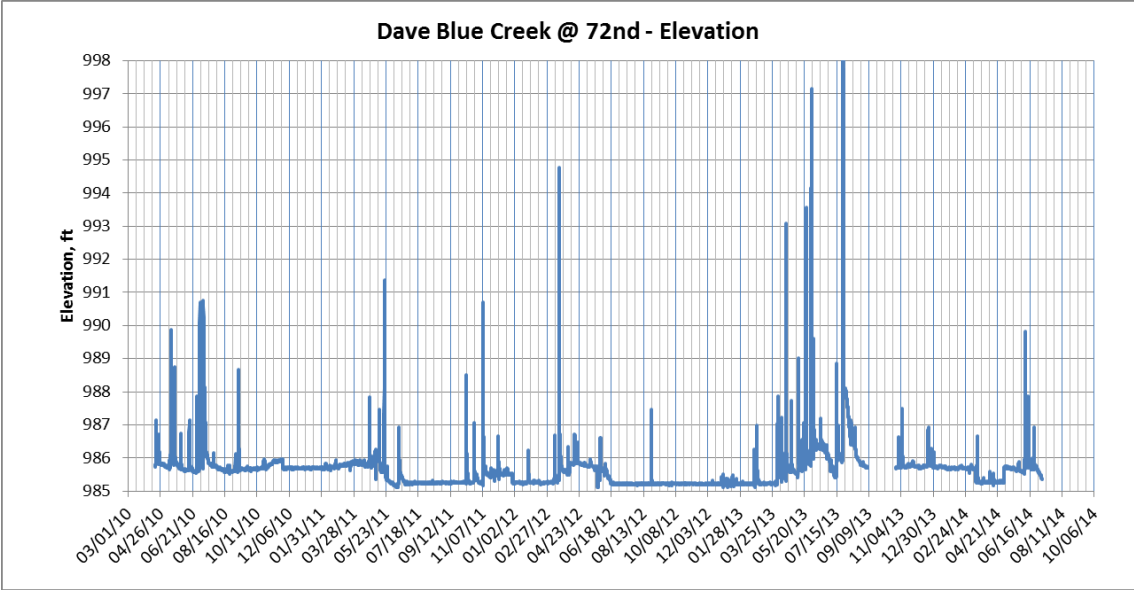


Figure C.8.3: Dave Blue Creek at 72<sup>nd</sup> Ave SE site water surface elevation plot.

## D. Appendix D – Stage-Discharge Data Summaries and Rating Curves

### D.1 Little River at 60<sup>th</sup> Ave NE

Table D.1.1: Stage-Discharge Measurements at Little River at 60<sup>th</sup> Ave NE.

Date	Time	Hobo Stage (ft)	Discharge (cfs)		Date	Time	Hobo Stage (ft)	Discharge (cfs)	
			ADCP	MMB				ADCP	MMB
5/15/2010	10:30	1.74		47.86	3/20/2012	13:45	4.23	264.23	
5/20/2010	16:45	1.45		33.66	3/20/2012	15:45	4.10	227.88	
5/23/2010	12:45	1.24		6.36	3/21/2012	11:00	3.18	130.06	
5/26/2010	13:45	1.21		4.12	3/21/2012	12:15	3.15	138.48	
5/28/2010	9:30	1.21		2.83	3/22/2012	12:00	3.44	152.69	
7/1/2010	14:40	1.39		5.40	9/27/2012	15:20	3.13		97.82
7/4/2010	10:30	1.94		50.56	9/28/2012	15:00	1.76		13.30
7/8/2010	9:30	2.04		22.35	4/4/2013	18:00	3.11	132.59	
7/9/2010	15:15	2.46		69.98	4/4/2013	19:00	3.00	115.22	
7/10/2010	9:00	2.33	31.94		4/13/2013	12:00	1.63	190.22	
7/10/2010	10:30	2.24	31.77		4/18/2013	12:00	6.02	759.98	
7/10/2010	10:30	2.24		28.48	4/18/2013	12:15	5.74	607.88	
7/10/2010	11:15	2.20	31.89		5/22/2013	12:45	2.65	78.22	
7/10/2010	11:30	2.20	31.50		5/22/2013	13:45	2.59	73.71	
7/10/2010	12:30	2.21		26.31	5/23/2013	15:00	16.43	3584.54	
7/12/2010	10:30	2.41	64.62		5/23/2013	16:00	16.34	3271.93	
7/12/2010	11:00	2.47		62.34	5/24/2013	11:00	3.43	174.33	
7/12/2010	11:40	2.49		60.77	5/24/2013	11:30	3.38	168.14	
7/12/2010	12:30	2.53		60.13	5/24/2013	12:30	3.31	156.80	
7/13/2010	11:30	2.42	63.79		6/5/2013	14:15	6.93	566.66	
7/13/2010	12:00	2.41		51.21	6/5/2013	14:45	7.05	539.90	
7/13/2010	12:30	2.38		51.69	6/5/2013	15:30	7.08	564.75	
7/13/2010	13:00	2.37	55.45		6/17/2013	13:30	6.97	675.61	
7/13/2010	13:30	2.36		51.04	6/17/2013	16:30	5.38	343.68	
7/13/2010	14:00	2.36		48.17	6/17/2013	17:30	5.05	291.42	
7/13/2010	14:30	2.35	54.20		7/16/2013	15:15	3.06	73.01	
9/3/2010	15:30	0.90		28.29	7/16/2013	17:15	3.02	64.31	
9/9/2010	13:00	2.25		123.40	7/17/2013	15:45	4.13	248.27	
5/20/2011	17:00	14.39	2992.87		7/17/2013	14:15	4.67	325.12	
5/20/2011	17:30	13.52	2615.08		7/26/2013	19:30	14.16	2401.20	
3/12/2012	14:30	2.01		31.27					

ADCP-Acoustic Doppler Current Profiler; MMB-Marsh McBirney Flow Meter

Table D.1.2: Estimated Discharges for Little River at 60<sup>th</sup> Ave NE.

Channel Slope =		0.0011	Q=(1.49/n)*A*R <sup>0.666667</sup> *S <sup>0.5</sup>			
Datum Elevation =		1037.63				
Elev	Stage	Area	P	R	n	Q
1061.9	24.30	1748.2	169.86	10.29	0.04	10217.8
1061.5	23.87	1685.0	168.42	10	0.04	9662.5
1060.5	22.87	1541.0	164.45	9.37	0.04	8461.8
1059.5	21.87	1416.4	137.26	10.32	0.04	8294.7
1058.5	20.87	1297.8	136.05	9.54	0.04	7212.3
1057.5	19.87	1186.1	130.34	9.1	0.04	6386.8
1056.5	18.87	1083.8	118.82	9.12	0.04	5844.8
1055.5	17.87	985.8	113.37	8.7	0.04	5151.8
1054.5	16.87	892.4	108.62	8.22	0.04	4490.7
1053.5	15.87	809.4	95.92	8.44	0.04	4145.2
1052.5	14.87	731.6	96.31	7.6	0.04	3493.8
1051.5	13.87	654.8	93.14	7.03	0.045	2638.7
1050.5	12.87	588.6	75.29	7.82	0.045	2546.5
1049.5	11.87	532.5	70.53	7.55	0.045	2250.5
1048.5	10.87	477.2	68.74	6.94	0.05	1716.1
1047.5	9.87	422.0	68.32	6.18	0.05	1404.5
1046.5	8.87	385.9	62.21	6.2	0.05	1287.3
1045.5	7.87	339.5	61.76	5.5	0.05	1045.4
1044.5	6.87	293.0	61.75	4.75	0.06	681.9
1043.5	5.87	246.5	62.18	3.96	0.07	435.6
1042.5	4.87	200.0	62.94	3.18	0.08	267.2
1041.5	3.87	154.4	42.26	3.65	0.12	150.7
1040.5	2.87	115.6	42.84	2.7	0.15	73.9
1039.5	1.87	77.6	38.77	2	0.2	30.4
1038.5	0.87	43.2	33.2	1.3	0.5	5.1

## D.2 Little River at Porter

Table D.2.1: Stage-Discharge Measurements at Little River at Porter.

Date	Time	Hobo Stage (ft)	Discharge (cfs)	
			ADCP	MMB
5/15/2010	13:30	0.95		22.53
5/23/2010	11:30	0.62		2.06
5/26/2010	12:00	0.62		6.92
7/1/2010	12:40	0.61		1.08
7/4/2010	8:30	1.21		25.99
7/7/2010	8:30	1.16		20.81
7/9/2010	8:45	2.22		43.03
8/25/2010	10:00	0.57		1.78
9/3/2010	13:30	0.83		7.47
9/9/2010	13:50	1.32		37.29
11/29/2011	13:30	0.52		1.54
3/12/2012	14:00	0.81		11.4
4/3/2012	11:00	0.69		9.7
9/27/2012	13:45	1.07		24.48
9/28/2012	13:30	0.68		10.02
5/21/2013	17:45	4.04	117.755	
5/21/2013	18:00	4.18	124.487	
5/21/2013	18:45	4.15	114.076	
5/21/2013	19:30	4.06	106.268	
6/4/2013	15:00	5.09	320.565	
6/4/2013	15:30	4.87	261.446	
7/15/2013	15:30	10.32	1342.26	

ADCP-Acoustic Doppler Current Profiler; MMB-Marsh McBirney Flow Meter

Table D.2.2: Estimated Discharges for Little River at Porter.

Channel Slope =		0.003	Q=(1.49/n)*A*R^0.666667*S^0.5			
Datum Elevation =		1094.20				
Elev	Stage	Area	P	R	n	Q
1108.0	13.81	472.4	70.9	6.7	0.08	1705.8
1107.0	12.81	423.2	57.5	7.4	0.08	1632.9
1106.0	11.81	381.4	56.2	6.8	0.08	1394.6
1105.0	10.81	341.7	53.3	6.4	0.08	1202.2
1104.0	9.81	302.5	53.4	5.7	0.08	980.3
1103.0	8.81	265.3	48.6	5.5	0.08	839.6
1102.0	7.81	231.0	47.6	4.9	0.08	675.3
1101.0	6.81	196.7	46.9	4.2	0.08	521.6
1100.0	5.81	162.4	46.6	3.5	0.08	380.6
1099.0	4.81	128.1	46.7	2.7	0.08	255.8
1098.0	3.81	93.8	47.3	2.0	0.08	150.9
1097.0	2.81	62.5	34.7	1.8	0.08	94.5
1096.0	1.81	35.4	25.7	1.4	0.09	39.7
1095.0	0.81	14.8	20.8	0.7	0.12	8.0

### D.3 Rock Creek at 72<sup>nd</sup> Ave NE

Table D.3.1: Stage-Discharge Measurements at Rock Creek at 72<sup>nd</sup> Ave NE.

Date	Time	Hobo Stage (ft)	Discharge (cfs)	
			ADCP	MMB
5/15/2010	12:30	0.97		4.91
5/23/2010	14:45	0.72		1.42
5/26/2010	16:30	0.58		0.37
7/1/2010	15:20	0.59		0.45
7/4/2010	11:00	1.62		19.88
7/7/2010	11:30	1.15		4.01
7/9/2010	11:00	1.33		8.55
9/3/2010	16:00	0.78		0.56
9/9/2010	12:20	1.29		12.14
5/20/2011	18:30	4.70	105.98	
5/20/2011	19:00	4.19	107.332	
3/23/2012	10:30	1.07		5.98

ADCP-Acoustic Doppler Current Profiler; MMB-Marsh McBirney Flow Meter

Table D.3.2: Estimated Discharges for Rock Creek at 72<sup>nd</sup> Ave NE.

Channel Slope =		0.00024				Q=(1.49/n)*A*R <sup>0.666667</sup> *S <sup>0.5</sup>		
Datum Elevation =		1037.63						
Elev	Stage	Area	P	R	n	Q	n	Q
1061.9	24.30	1748.2	169.86	10.29	0.02	9555.1	0.04	4777.56
1061.5	23.87	1685	168.42	10	0.02	9035.8	0.04	4517.91
1060.5	22.87	1541.04	164.45	9.37	0.02	7913.0	0.04	3956.50
1059.5	21.87	1416.42	137.26	10.32	0.02	7756.7	0.04	3878.37
1058.5	20.87	1297.83	136.05	9.54	0.02	6744.5	0.04	3372.26
1057.5	19.87	1186.05	130.34	9.1	0.02	5972.6	0.04	2986.31
1056.5	18.87	1083.8	118.82	9.12	0.02	5465.7	0.04	2732.86
1055.5	17.87	985.81	113.37	8.7	0.02	4817.7	0.04	2408.85
1054.5	16.87	892.43	108.62	8.22	0.02	4199.4	0.04	2099.71
1053.5	15.87	809.4	95.92	8.44	0.02	3876.4	0.04	1938.19
1052.5	14.87	731.59	96.31	7.6	0.02	3267.2	0.04	1633.61
1051.5	13.87	654.75	93.14	7.03	0.02	2776.0	0.04	1387.98
1050.5	12.87	588.58	75.29	7.82	0.02	2679.0	0.04	1339.52
1049.5	11.87	532.5	70.53	7.55	0.02	2367.7	0.04	1183.83
1048.5	10.87	477.22	68.74	6.94	0.025	1604.8	0.04	1002.99
1047.5	9.87	421.96	68.32	6.18	0.025	1313.4	0.04	820.86
1046.5	8.87	385.92	62.21	6.2	0.03	1003.2	0.04	752.37
1045.5	7.87	339.45	61.76	5.5	0.03	814.6	0.04	610.97
1044.5	6.87	292.98	61.75	4.75	0.035	546.6	0.04	478.23
1043.5	5.87	246.51	62.18	3.96	0.04	356.4	0.04	356.43
1042.5	4.87	200.04	62.94	3.18	0.04	249.9	0.04	249.88
1041.5	3.87	154.36	42.26	3.65	0.08	105.7	0.08	105.69
1040.5	2.87	115.62	42.84	2.7	0.1	51.8	0.1	51.80
1039.5	1.87	77.57	38.77	2	0.2	14.2	0.2	14.23
1038.5	0.87	43.18	33.2	1.3	0.55	2.2	0.55	2.16



#### D.4 Hog Creek at SE 119<sup>th</sup> Ave

Table D.4.1: Stage-Discharge Measurements at Hog Creek at SE 119<sup>th</sup> Ave.

Date	Time	Hobo Stage (ft)	Discharge (cfs)	
			ADCP	MMB
5/15/2010	11:30	1.30		30.39
5/23/2010	14:00	0.61		5.23
5/26/2010	15:45	0.48		2.93
7/1/2010	10:45	0.56		3.93
7/3/2010	13:15	2.12		49.89
7/7/2010	10:45	0.92		15.06
9/9/2010	10:45	0.80		10.17
4/3/2012	13:00	0.76		4.21

ADCP-Acoustic Doppler Current Profiler; MMB-Marsh McBirney Flow Meter

Table D.4.2: Estimated Discharges for Hog Creek at SE 119<sup>th</sup> Ave.

Channel Slope =	0.00104		$Q=(1.49/n)*A*R^{0.666667}*S^{0.5}$			
Datum Elevation =	91.00					
Elev	Stage	Area	P	R	n	Q
99.7	8.70	372.31	78.54	4.74	0.05	1009.6
99.5	8.50	358.37	77.88	4.6	0.05	952.6
99.0	8.00	324.64	69.56	4.67	0.05	871.7
98.5	7.50	293.27	67.6	4.34	0.05	749.9
98.0	7.00	266.29	61.94	4.3	0.05	676.7
97.5	6.50	239.97	60.2	3.99	0.05	580.1
97.0	6.00	213.81	59.5	3.59	0.05	481.8
96.5	5.50	187.89	57.7	3.26	0.05	397.0
96.0	5.00	163.73	47.8	3.43	0.05	357.9
95.5	4.50	141.42	47.1	3	0.05	282.7
95.0	4.00	119.55	46.02	2.6	0.05	217.2
94.5	3.50	100.02	40.97	2.44	0.05	174.2
94.0	3.00	82.61	38.34	2.16	0.05	132.7
93.5	2.50	65.94	36.8	1.79	0.05	93.4
93.0	2.00	50.37	31.87	1.58	0.06	54.7
92.5	1.50	34.9	29.39	1.19	0.06	31.4
92.0	1.00	22.17	26.6	0.83	0.07	13.4

**D.5 Elm Creek at Indian Hills**

*Table D.5.1: Stage-Discharge Measurements at Elm Creek at Indian Hills.*

Date	Time	Hobo Stage (ft)	Discharge (cfs)	
			ADCP	MMB
5/15/2010	13:30	0.94		10.65
5/23/2010	11:30	0.72		3.30
5/26/2010	11:45	0.70		1.66
7/1/2010	14:00	0.64		0.82
7/4/2010	10:00	1.00		7.14
7/7/2010	10:00	1.50		25.64
7/9/2000	10:15	1.02		7.66
9/3/2010	14:45	0.66		1.44
9/9/2010	12:45	1.04		8.00
3/12/2012	16:00	0.97		4.72
9/27/2012	15:45	0.78		1.39

ADCP-Acoustic Doppler Current Profiler; MMB-Marsh McBirney Flow Meter

*Table D.5.2: Estimated Discharges for Elm Creek at Indian Hills.*

Channel Slope =		0.003	$Q=(1.49/n)*A*R^{0.666667}*S^{0.5}$			
Datum Elevation =		1044.50				
Elev	Stage	Area	P	R	n	Q
1058.0	13.5	697.1	111.1	6.3	0.05	3870.7
1057.0	12.5	604.4	106.2	5.7	0.05	3145.5
1056.0	11.5	517.3	101.5	5.1	0.05	2500.5
1055.0	10.5	444.7	75.8	5.9	0.05	2360.5
1054.0	9.5	378.2	74.2	5.1	0.05	1828.8
1053.0	8.5	320.6	59.6	5.4	0.05	1607.2
1052.0	7.5	269.4	58.6	4.6	0.05	1216.1
1051.0	6.5	218.2	58.4	3.7	0.05	857.7
1050.0	5.5	171.6	46.4	3.7	0.05	670.1
1049.0	4.5	132.8	44.7	3.0	0.05	448.0
1048.0	3.5	94.0	43.9	2.1	0.05	254.6
1047.0	2.5	63.5	32.4	2.0	0.05	162.3
1046.0	1.5	38.3	30.4	1.3	0.15	24.3

## D.6 North Fork at Franklin

Table D.6.1: Stage-Discharge Measurements at North Fork at Franklin.

Date	Time	Hobo Stage (ft)	Discharge (cfs)	
			ADCP	MMB
5/15/2010	9:45	0.98		10.21
5/23/2010	12:00	0.55		1.72
5/26/2010	13:00	0.53		1.10
7/1/2010	13:20	0.49		0.74
7/4/2010	9:00	0.93		8.01
7/7/2010	9:00	1.67		46.90
7/9/2000	9:30	1.24		24.88
7/22/2010	12:30	0.42		1.95
9/3/2010	14:15	0.45		2.82
9/9/2010	13:30	0.83		8.55
4/3/2012	12:00	0.70		4.27
9/27/2012	14:30	0.82		13.97
9/28/2012	14:30	0.23		1.34

Table D.6.2: Estimated Discharges for North Fork at Franklin.

Channel Slope =		0.003	$Q=(1.49/n)*A*R^{0.666667}*S^{0.5}$			
Datum Elevation =		1086.25				
Elev	Stage	Area	P	R	n	Q
1098.0	11.75	461.2	91.1	5.1	0.08	1386.9
1097.0	10.75	397.8	77.0	5.2	0.08	1212.3
1096.0	9.75	345.7	73.2	4.7	0.08	992.6
1095.0	8.75	301.1	58.3	5.2	0.08	917.7
1094.0	7.75	258.4	59.5	4.3	0.08	701.2
1093.0	6.75	217.9	55.0	4.0	0.08	556.7
1092.0	5.75	178.6	46.8	3.8	0.08	445.1
1091.0	4.75	141.6	47.4	3.0	0.08	299.6
1090.0	3.75	104.5	48.3	2.2	0.08	178.4
1089.0	2.75	70.5	42.3	1.7	0.08	101.1
1088.0	1.75	37.3	41.0	0.9	0.08	35.7
1087.0	0.75	9.0	14.7	0.6	0.08	6.6

## D.7 Dave Blue Creek at 72<sup>nd</sup> Ave SE

Table D.7.1: Stage-Discharge Measurements at Dave Blue Creek at 72<sup>nd</sup> Ave.

Date	Time	Hobo Stage (ft)	Discharge (cfs)	
			ADCP	MMB
5/15/2010	13:00	1.23		13.51
5/23/2010	15:30	0.75		2.98
5/26/2010	17:15	0.69		1.83
7/1/2010	16:00	0.55		0.15
7/4/2010	11:30	1.07		7.62
7/7/2010	12:00	0.67		1.52
7/9/2000	11:30	1.48		19.04
9/3/2010	16:30	0.71		0.53
9/9/2010	12:00	1.08		4.07
3/23/2012	9:30	0.64		4.74

Table D.7.2: Estimated Discharges for Dave Blue Creek at 72<sup>nd</sup> Ave.

Slope =		0.0059	$Q=(1.49/n)*A*R^{0.666667}*S^{0.5}$			
Datum Elevation =		1034.55				
Elev	Stage	Area	P	R	n	Q
1049.0	14.45	702.54	94.66	7.42	0.04	7647.0
1048.0	13.45	620.85	84.77	7.32	0.04	6697.0
1047.0	12.45	546.47	83.29	6.56	0.04	5479.3
1046.0	11.45	472.84	79.7	5.93	0.04	4432.4
1045.0	10.45	406.13	74.993	5.42	0.04	3585.5
1044.0	9.45	341.67	66.69	5.12	0.04	2904.1
1043.0	8.45	284.84	64.58	4.41	0.04	2191.7
1042.0	7.45	232.34	56.14	4.13	0.04	1711.2
1041.0	6.45	185.65	48.79	3.8	0.04	1293.5
1040.0	5.45	146.23	46.4	3.15	0.04	899.1
1039.0	4.45	107.7	45.51	2.37	0.04	547.8
1038.0	3.45	71.72	33.49	2.14	0.04	340.8
1037.0	2.45	45.56	25.92	1.76	0.05	152.0
1036.0	1.45	24.95	21.02	1.19	0.15	21.4
1035.0	0.45	8.25	16.67	0.5	1.5	0.3

## **E. Appendix E – FGM Survey Summaries**

## E.1 FGM Site LR-01

Site Name: LR-01

Drainage Area: 93.4 mi<sup>2</sup>

Site Legal Description: SW 1/4, Sect. 8, T9N-R1W, Cleveland Co.

FGM Survey Date: January 9-10, 2012

Stability Assessment: January 27, 2015

Figure E.1.1: FGM Site LR-01 Site Map with Survey Points.

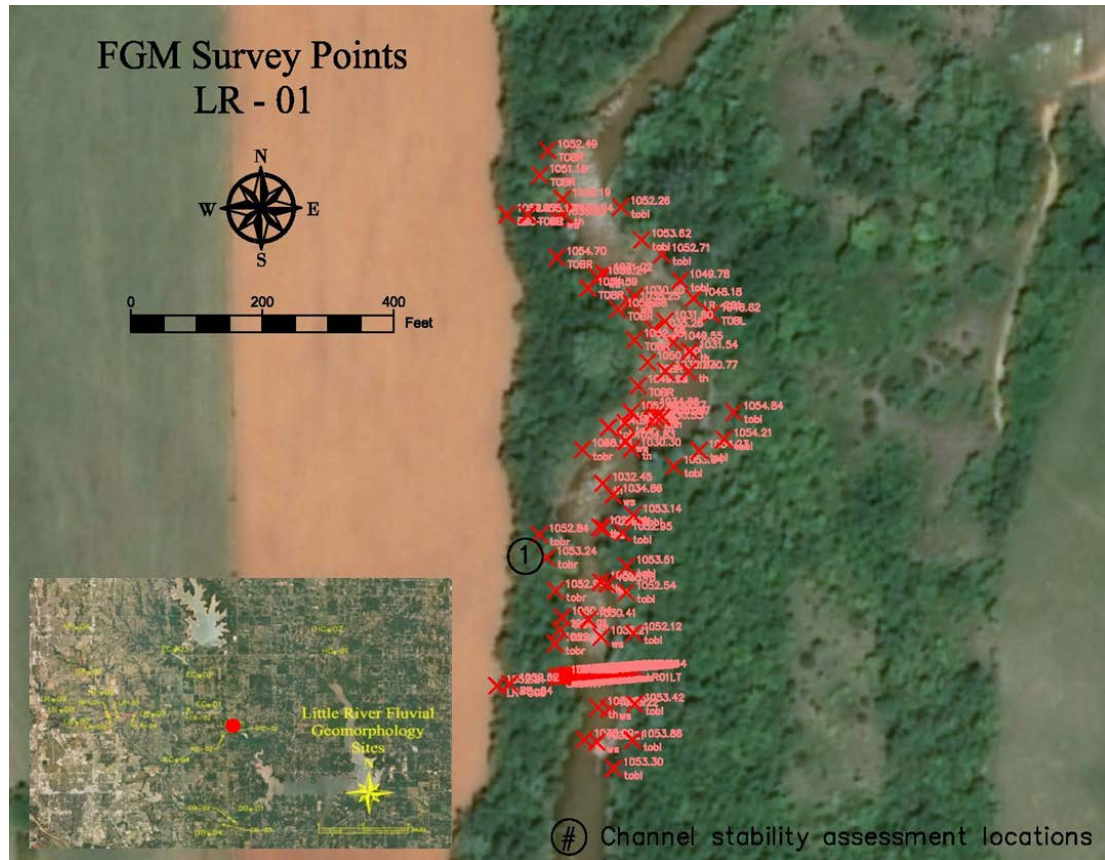


Table E.1.1: FGM Site LR-01 Survey Control.

OK State Plane NAD83, South Zone (U.S. Ft); NAVD88 (U.S. Ft)			
Left Pin		Right Pin	
<b>Name:</b>	LR01LT	<b>Name:</b>	LR01RT
<b>Easting:</b>	2168074.80	<b>Easting:</b>	2167951.82
<b>Northing:</b>	704362.00	<b>Northing:</b>	704352.63
<b>Elevation:</b>	1052.64	<b>Elevation:</b>	1052.56
Geodetic Coordinates (Decimal Degrees)			
Left Pin		Right Pin	
<b>Lat. (N):</b>	35.26693	<b>Lat. (N):</b>	35.26690
<b>Long. (W):</b>	97.33146	<b>Long. (W):</b>	97.33188

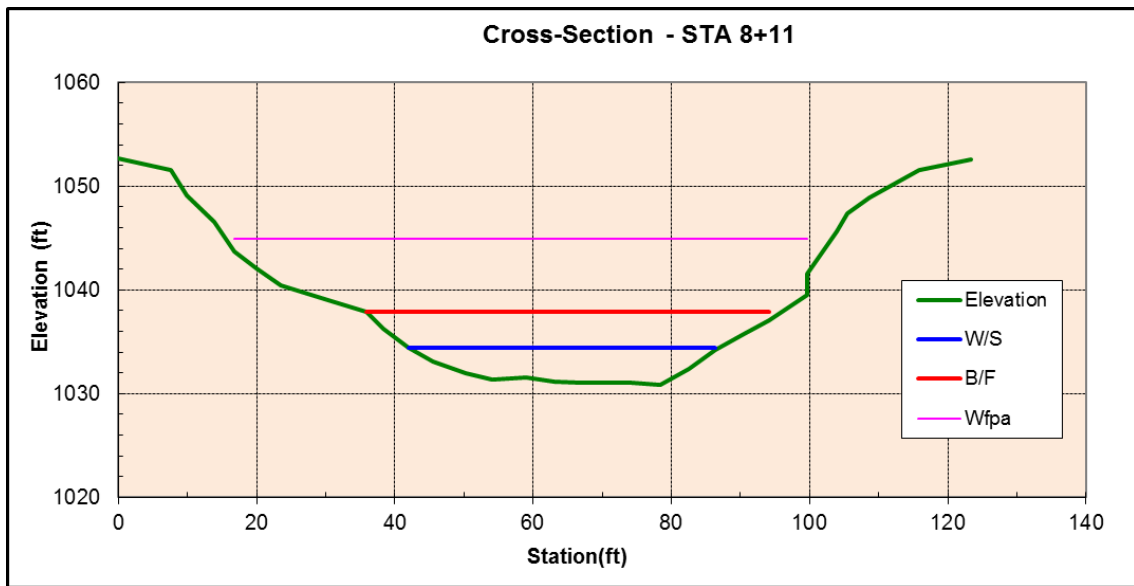


Figure E.1.2: FGM Site LR-01 Cross-section Survey Plot.

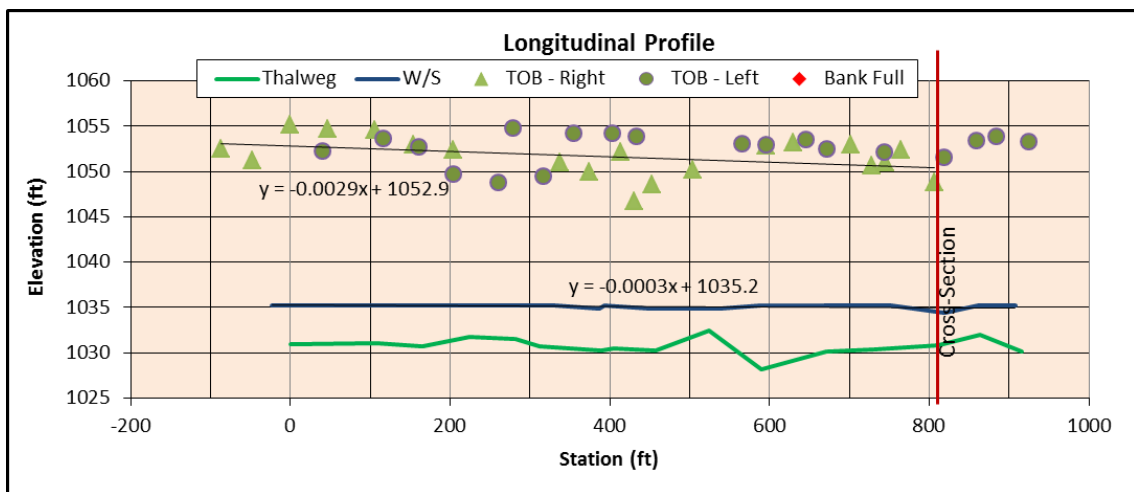


Figure E.1.3: FGM Site LR-01 Longitudinal Profile Survey Plot.

*Table E.1.2: FGM Site LR-01 Channel Morphology Summary.*

Bankfull Width (ft):	60.14
Mean Bankfull Depth (ft):	5.03
Maximum Bankfull Depth (ft):	7.03
Flood Prone Area Width (ft):	84.91
Bankfull Area (ft <sup>2</sup> ):	302.34
Entrenchment Ratio:	1.41
Width/Depth Ratio:	12.0
Sinuosity:	1.9
Slope:	0.0011
Bed Material:	Sand
Rosgen Stream Type:	F5
Channel Evolution Stage:	IV

*Table E.1.3: FGM Site LR-01 Stream Channel Stability Summary.*

Bank No.	1
CSI Score:	24.5
Rating:	Highly Unstable
Pfankuch Score:	86
Rating:	Fair-Mod. Unstable
BEHI Score:	21
Rating:	Moderate
NBS Score:	***
Rating:	High
OEBSI Score:	44.5
Rating:	Unstable





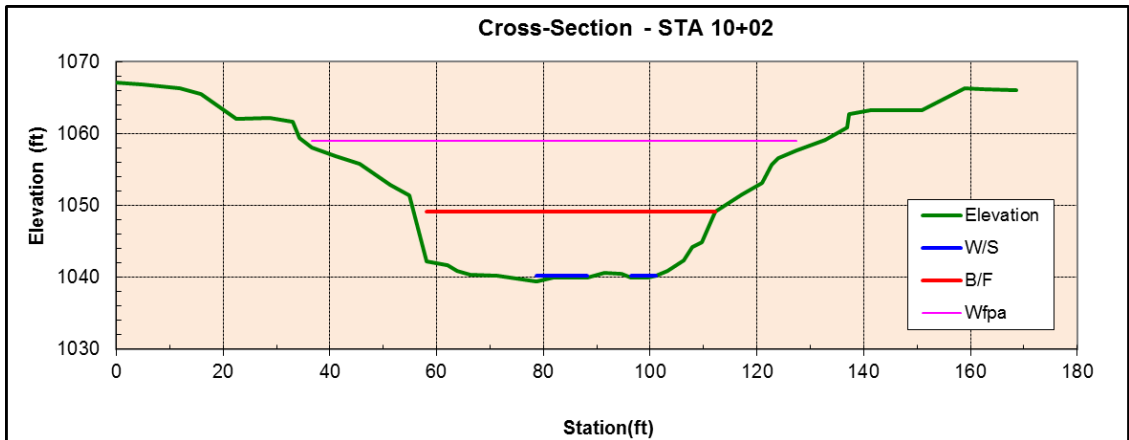


Figure E.2.2: FGM Site LR-02 Cross-section Survey Plot.

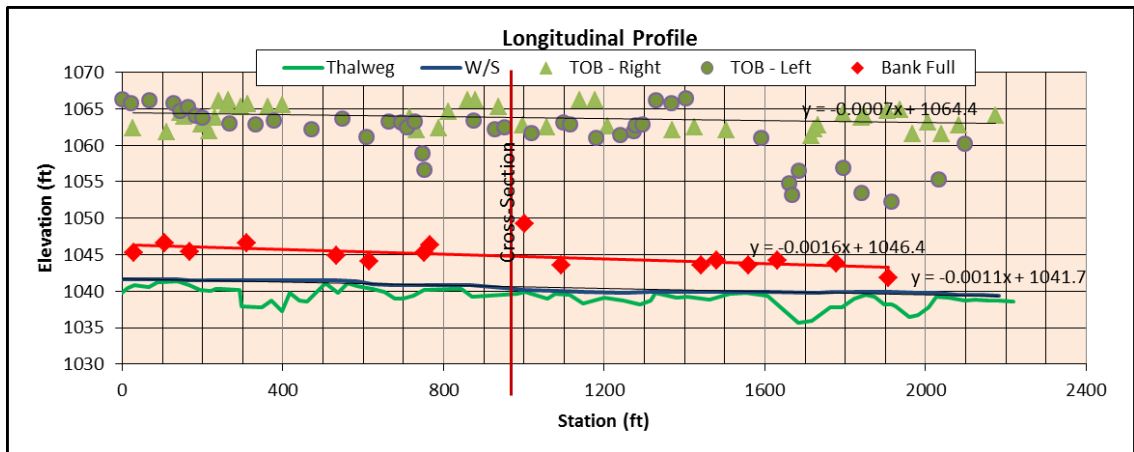


Figure E.2.3: FGM Site LR-02 Longitudinal Profile Survey Plot.

Table E.2.2: FGM Site LR-02 Channel Morphology Summary.

Bankfull Width (ft):	56.52
Mean Bankfull Depth (ft):	8.09
Maximum Bankfull Depth (ft):	9.78
Flood Prone Area Width (ft):	92.83
Bankfull Area (ft <sup>2</sup> ):	457.52
Entrenchment Ratio:	1.64
Width/Depth Ratio:	7.0
Sinuosity:	1.9
Slope:	0.0011
Bed Material:	Sand
Rosgen Stream Type:	G5c
Channel Evolution Stage:	IV

Table E.2.3: FGM Site LR-02 Stream Channel Stability Summary.

Bank No.	1	2	3	4
CSI Score:	22.5	22.5	24	25
Rating:	HIGHLY UNSTABLE	HIGHLY UNSTABLE	HIGHLY UNSTABLE	HIGHLY UNSTABLE
Pfankuch Score:	116	114	122	118
Rating:	Poor- Unstable	Poor- Unstable	Poor- Unstable	Poor- Unstable
BEHI Score:	41	34.5	34	37.5
Rating:	Very High	High	High	High
NBS Score:	***	***	***	***
Rating:	Extreme	Extreme	Low	Extreme
OEBSI Score:	62	62	65	69
Rating:	Highly Unstable	Highly Unstable	Highly Unstable	Highly Unstable

### E.3 FGM Site LR-03

Site Name: LR-03

Drainage Area: 47.4 mi<sup>2</sup>

Site Legal Description: NW 1/4, Sect. 10, T9N-R2W, Cleveland Co.

FGM Survey Date: January 11-13, 2011

Stability Assessment: January 21, 2015

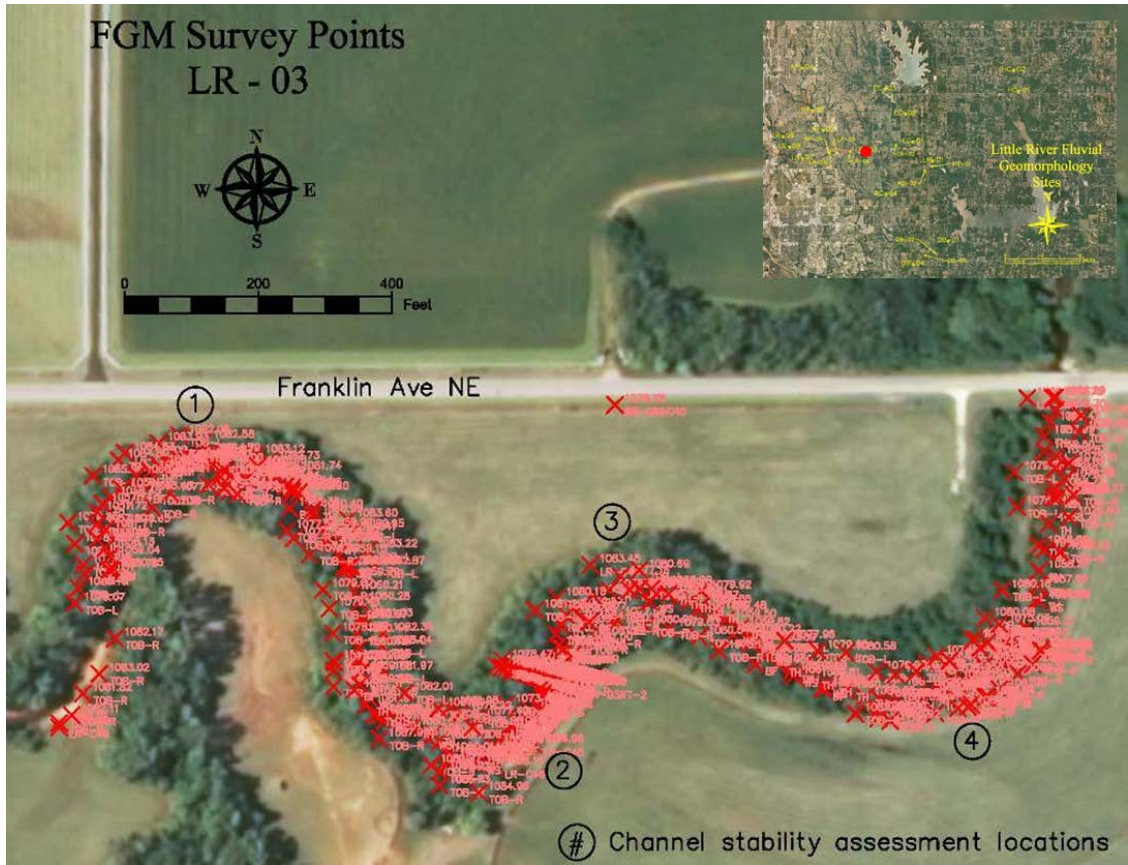


Figure E.3.1: FGM Site LR-03 Site Map with Survey Points.

Table E.3.1: FGM Site LR-03 Survey Control.

OK State Plane NAD83, South Zone (U.S. Ft); NAVD88 (U.S. Ft)			
Left Pin		Right Pin	
Name:	LR-03LT	Name:	LR-03RT
Easting:	2149376.87	Easting:	2149495.76
Northing:	707217.57	Northing:	707184.95
Elevation:	1081.02	Elevation:	1083.55
Geodetic Coordinates (Decimal Degrees)			
Left Pin		Right Pin	
Lat. (N):	35.2751	Lat. (N):	35.2750
Long. (W):	97.3940	Long. (W):	97.3936

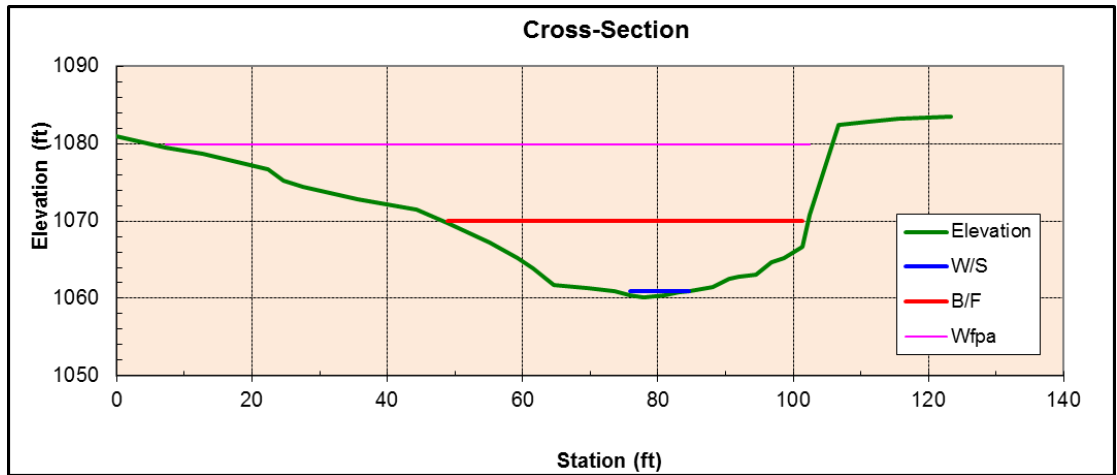


Figure E.3.2: FGM Site LR-03 Cross-section Survey Plot.

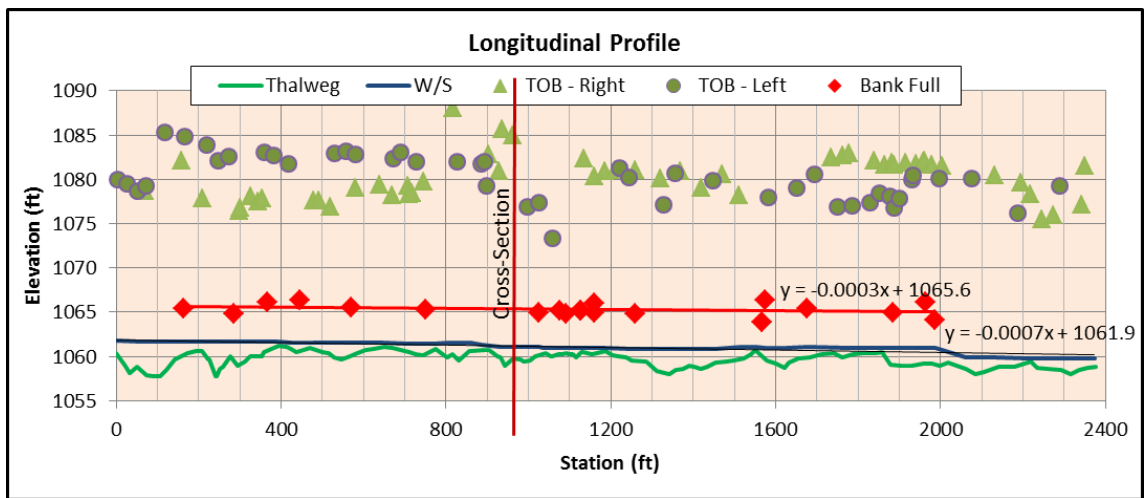


Figure E.3.3: FGM Site LR-03 Longitudinal Profile Survey Plot.

*Table E.3.2: FGM Site LR-03 Channel Morphology Summary.*

Bankfull Width (ft):	54.03
Mean Bankfull Depth (ft):	6.63
Maximum Bankfull Depth (ft):	9.87
Flood Prone Area Width (ft):	98.02
Bankfull Area (ft <sup>2</sup> ):	358.00
Entrenchment Ratio:	1.81
Width/Depth Ratio:	8.2
Sinuosity:	1.7
Slope:	0.0009
Bed Material:	Sand
Rosgen Stream Type:	G5c
Channel Evolution Stage:	IV

*Table E.3.3: FGM Site LR-03 Stream Channel Stability Summary.*

Bank No.	1	2	3	4
CSI Score:	22.5	27	25	20.5
Rating:	Highly unstable	Highly unstable	Highly unstable	Highly unstable
Pfankuch Score:	116	99	109	99
Rating:	Poor-Unstable	Poor-Unstable	Poor-Unstable	Poor-Unstable
BEHI Score:	41	35.5	35.5	28.5
Rating:	Very High	High	High	Moderate
NBS Score:	***	***	***	***
Rating:	Extreme	Moderate	High	High
OEBSI Score:	62	77	52	57
Rating:	Highly unstable	Highly unstable	Unstable	Highly unstable

### E.4 FGM Site LR-04

Site Name: LR-04

Drainage Area: 43.9 mi<sup>2</sup>

Site Legal Description: NE 1/4, Sect. 9, T9N-R2W, Cleveland Co.

FGM Survey Date: March 14-15, 2011

Stability Assessment: January 21, 2015

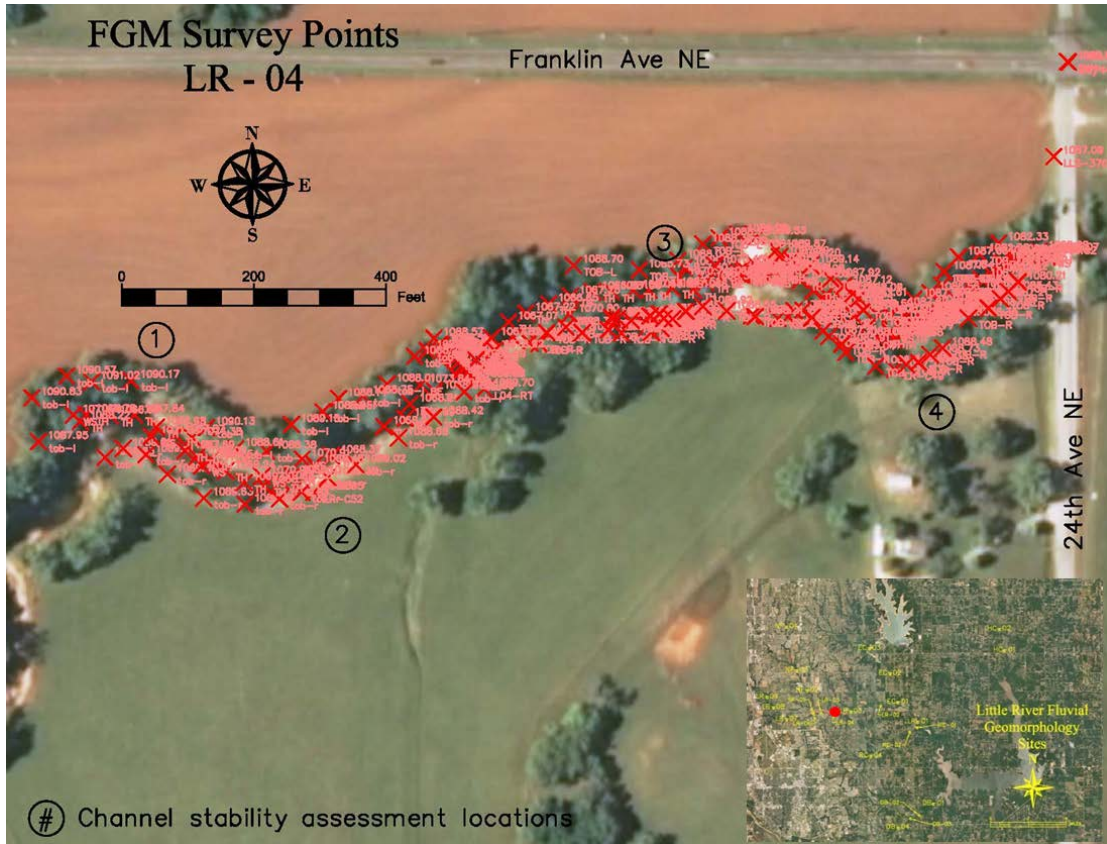


Figure E.4.1: FGM Site LR-04 Site Map with Survey Points.

Table E.4.1: FGM Site LR-04 Survey Control.

OK State Plane NAD83, South Zone (U.S. Ft); NAVD88 (U.S. Ft)			
Left Pin		Right Pin	
Name:	LR-04LT	Name:	L04-RT
Easting:	2144852.40	Easting:	2144919.81
Northing:	707170.28	Northing:	707102.34
Elevation:	1088.56	Elevation:	1089.70
Geodetic Coordinates (Decimal Degrees)			
Left Pin		Right Pin	
Lat. (N):	35.2750	Lat. (N):	35.2749
Long. (W):	97.4092	Long. (W):	97.4090

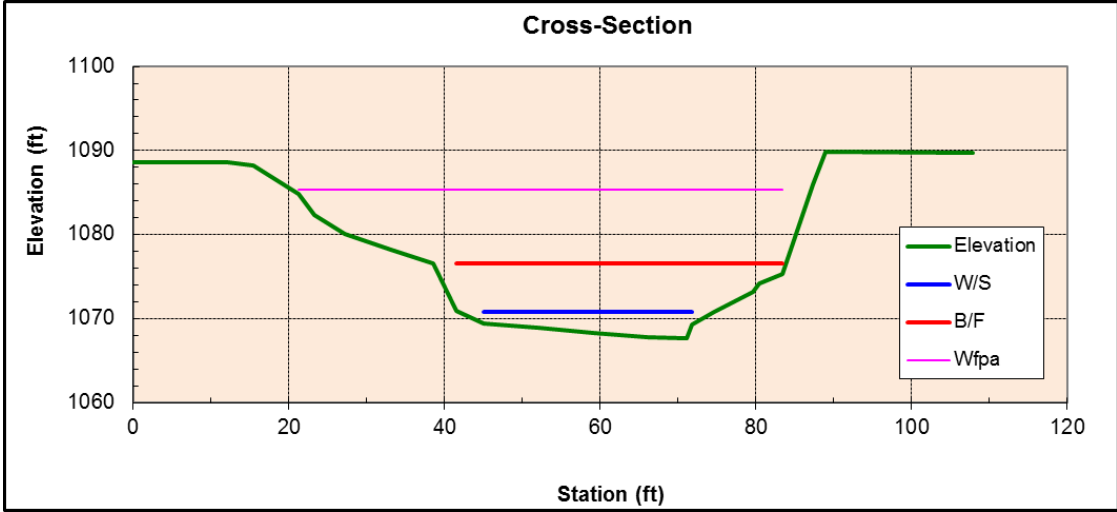


Figure E.4.2: FGM Site LR-04 Cross-section Survey Plot.

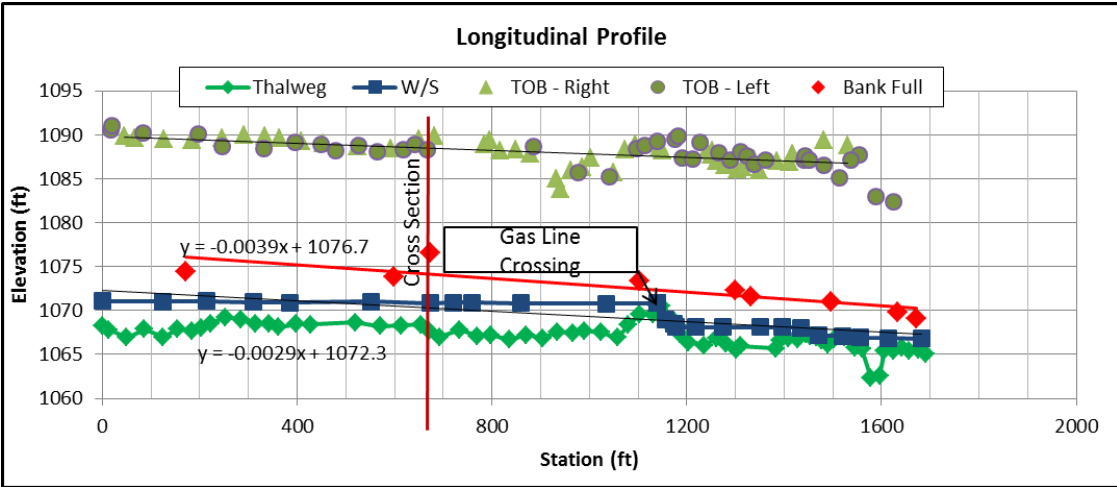


Figure E.4.3: FGM Site LR-04 Longitudinal Profile Survey Plot.



*Table E.4.2: FGM Site LR-04 Channel Morphology Summary.*

Bankfull Width (ft):	45.30
Mean Bankfull Depth (ft):	6.52
Maximum Bankfull Depth (ft):	8.81
Flood Prone Area Width (ft):	63.18
Bankfull Area (ft <sup>2</sup> ):	295.41
Entrenchment Ratio:	1.39
Width/Depth Ratio:	6.9
Sinuosity:	1.1
Slope:	0.0039
Bed Material:	Sand
Rosgen Stream Type:	G5c
Channel Evolution Stage:	IV

*Table E.4.3: FGM Site LR-04 Stream Channel Stability Summary.*

Bank No.	1	2	3	4
CSI Score:	25	21	19.5	22
Rating:	Highly Unstable	Highly Unstable	Moderately Stable	Highly Unstable
Pfankuch Score:	99	100	97	88
Rating:	Poor-Unstable	Poor-Unstable	Poor-Unstable	Fair-Mod. Unstable
BEHI Score:	27.5	39.5	15.5	31.5
Rating:	Moderate	High	Low	High
NBS Score:	***	***	***	***
Rating:	Extreme	Low	Moderate	Extreme
OEBSI Score:	42	62	44.5	54.5
Rating:	Unstable	Highly Unstable	Unstable	Unstable

## E.5 FGM Site LR-05

Site Name: LR-05

Drainage Area: 41.3 mi<sup>2</sup>

Site Legal Description: NW 1/4, Sect. 9, T9N-R2W, Cleveland Co.

FGM Survey Date: March 15-16, 2011

Stability Assessment: January 28, 2015

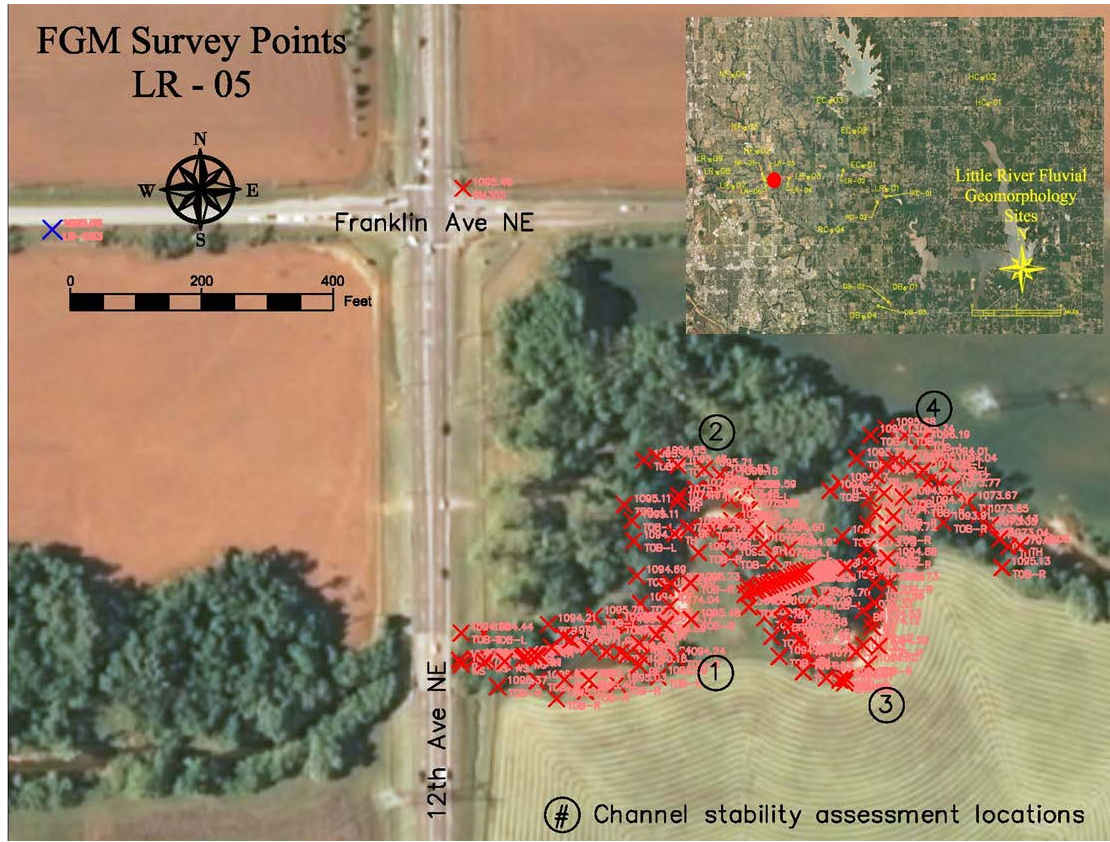


Figure E.5.1: FGM Site LR-05 Site Map with Survey Points.

Table E.5.1: FGM Site LR-05 Survey Control.

<b>Left Pin</b>		<b>Right Pin</b>	
<b>Name:</b>	LR-05LT	<b>Name:</b>	LR-05RT
<b>Easting:</b>	2141102.63	<b>Easting:</b>	2141005.26
<b>Northing:</b>	707052.02	<b>Northing:</b>	707015.02
<b>Elevation:</b>	1095.46	<b>Elevation:</b>	1095.46
<b>Geodetic Coordinates (Decimal Degrees)</b>			
<b>Left Pin</b>		<b>Right Pin</b>	
<b>Lat. (N):</b>	35.2748	<b>Lat. (N):</b>	35.2747
<b>Long. (W):</b>	97.4218	<b>Long. (W):</b>	97.4221

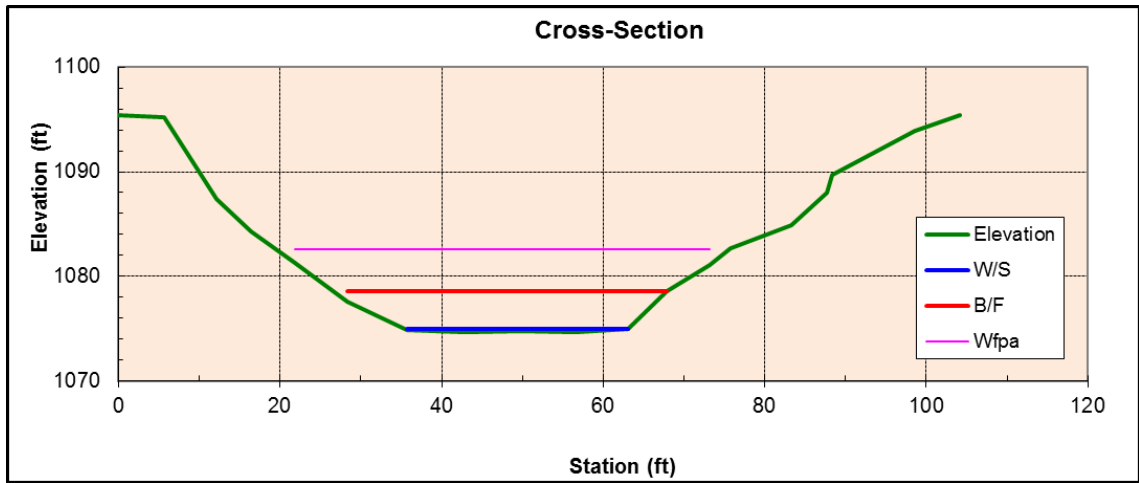


Figure E.5.2: FGM Site LR-05 Cross-section Survey Plot.

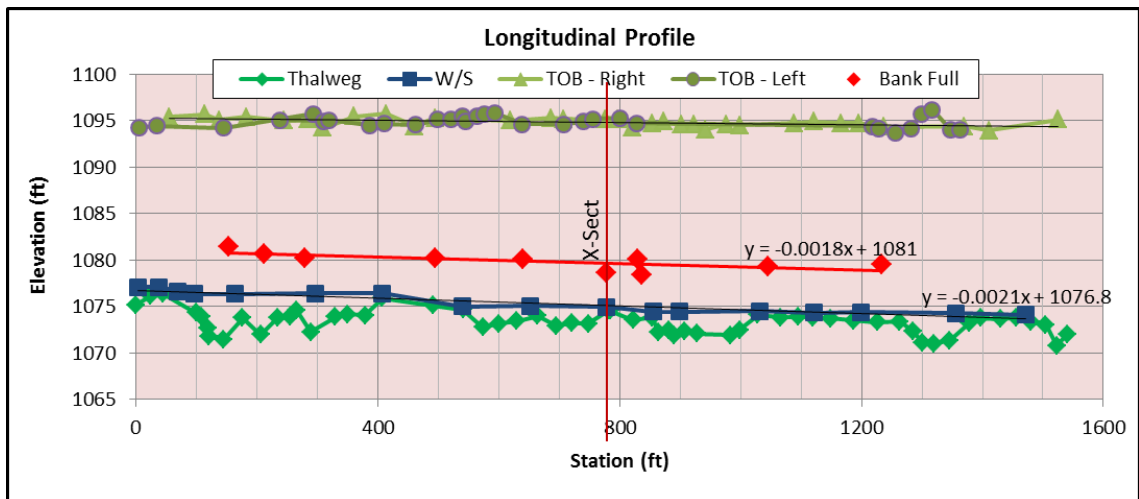


Figure E.5.3: FGM Site LR-05 Longitudinal Profile Survey Plot.

*Table E.5.2: FGM Site LR-05 Channel Morphology Summary.*

Bankfull Width (ft):	41.27
Mean Bankfull Depth (ft):	3.29
Maximum Bankfull Depth (ft):	3.98
Flood Prone Area Width (ft):	53.87
Bankfull Area (ft <sup>2</sup> ):	135.76
Entrenchment Ratio:	1.31
Width/Depth Ratio:	12.5
Sinuosity:	1.9
Slope:	0.0009
Bed Material:	Sand
Rosgen Stream Type:	G5c
Channel Evolution Stage:	IV

*Table E.5.3: FGM Site LR-05 Stream Channel Stability Summary.*

Bank No.	1	2	3	4
CSI Score:	28.5	23	26	25
Rating:	Highly Unstable	Highly Unstable	Highly Unstable	Highly Unstable
Pfankuch Score:	103	117	121	125
Rating:	Poor-Unstable	Poor-Unstable	Poor-Unstable	Poor-Unstable
BEHI Score:	36	46	38	40
Rating:	High	Extreme	High	Very High
NBS Score:	***	***	***	***
Rating:	Extreme	Extreme	Very High	Extreme
OEBSI Score:	62	67	67	59.5
Rating:	Highly Unstable	Highly Unstable	Highly Unstable	Highly Unstable

## E.6 FGM Site LR-06

Site Name: LR-06

Drainage Area: 24.4 mi<sup>2</sup>

Site Legal Description: NE 1/4, Sect. 8, T9N-R2W, Cleveland Co.

FGM Survey Date: January 17, 2012

Stability Assessment: January 28, 2015

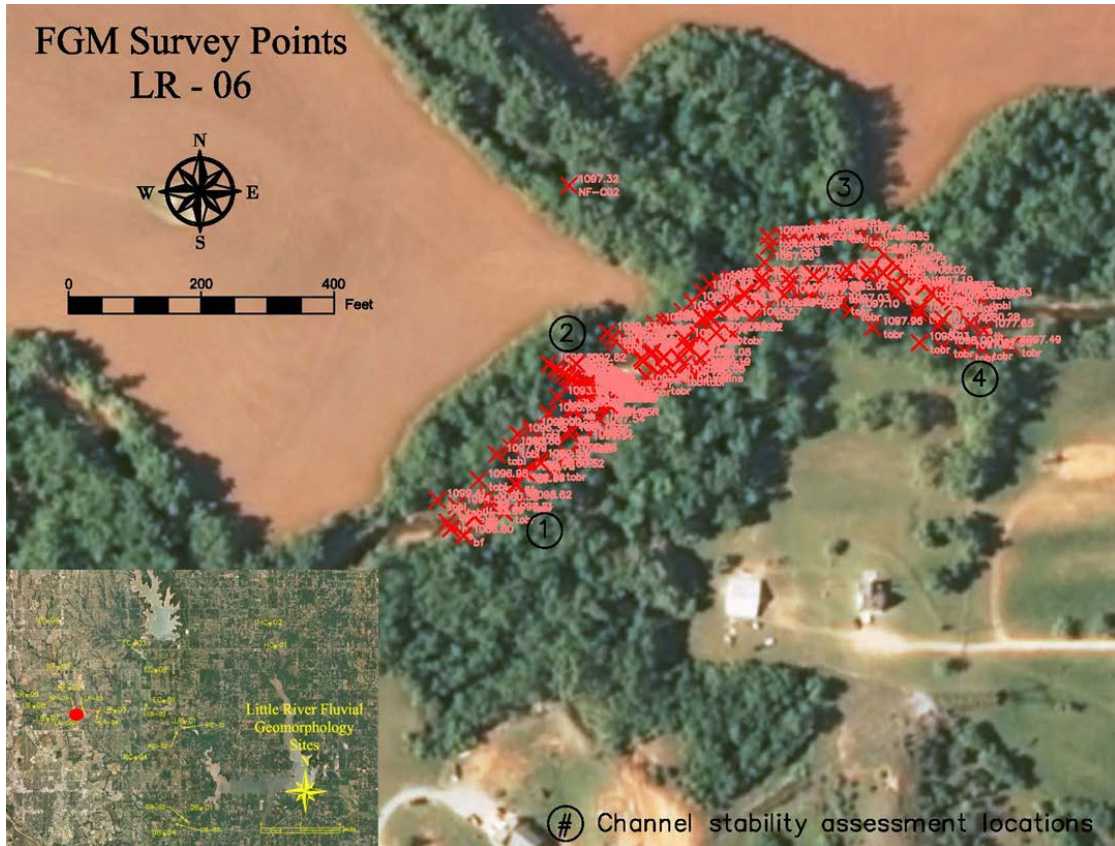


Figure E.6.1: FGM Site LR-06 Site Map with Survey Points.

Table E.6.1: FGM Site LR-06 Survey Control.

OK State Plane NAD83, South Zone (U.S. Ft); NAVD88 (U.S. Ft)			
Left Pin		Right Pin	
Name:	LR-06LT	Name:	LR-06RT
Easting:	2139100.11	Easting:	2139191.43
Northing:	706677.06	Northing:	706615.21
Elevation:	1098.20	Elevation:	1095.19
Geodetic Coordinates (Decimal Degrees)			
Left Pin		Right Pin	
Lat. (N):	35.2738	Lat. (N):	35.2736
Long. (W):	97.4285	Long. (W):	97.4282

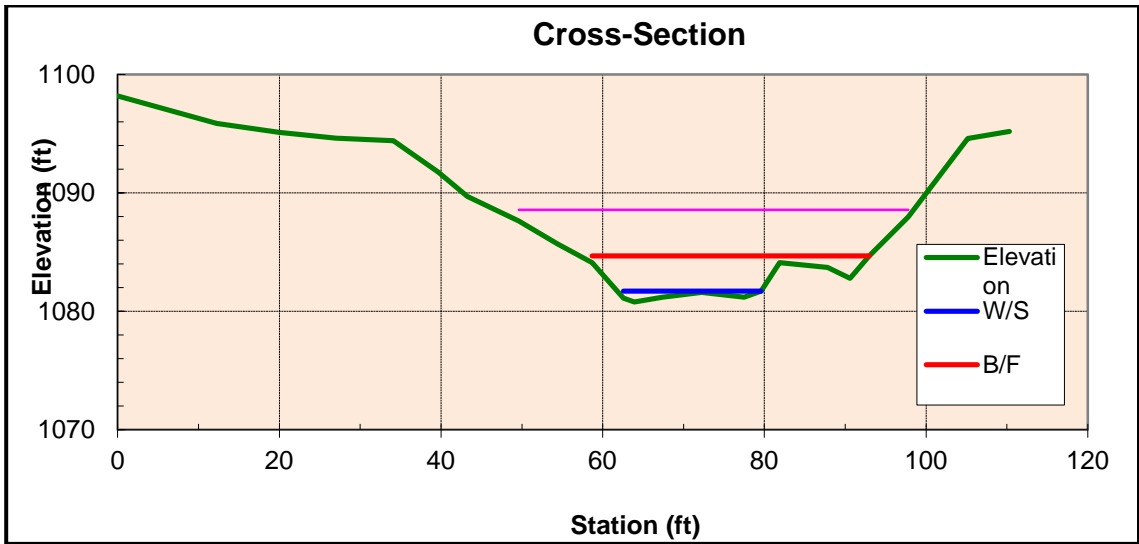


Figure E.6.2: FGM Site LR-06 Cross-section Survey Plot.

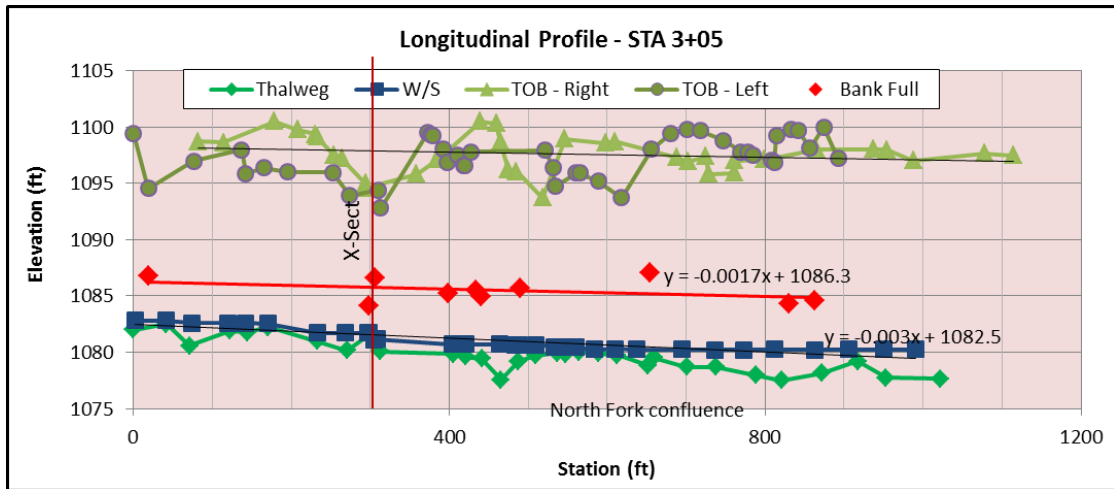


Figure E.6.3: FGM Site LR-06 Longitudinal Profile Survey Plot.

*Table E.6.2: FGM Site LR-06 Channel Morphology Summary.*

Bankfull Width (ft):	35.80
Mean Bankfull Depth (ft):	2.28
Maximum Bankfull Depth (ft):	3.89
Flood Prone Area Width (ft):	57.77
Bankfull Area (ft <sup>2</sup> ):	81.69
Entrenchment Ratio:	1.61
Width/Depth Ratio:	15.7
Sinuosity:	1.2
Slope:	0.003
Bed Material:	Sand
Rosgen Stream Type:	B5c
Channel Evolution Stage:	IV

*Table E.6.3: FGM Site LR-06 Stream Channel Stability Summary.*

Bank No.	1	2	3	4
CSI Score:	22.5	26	21.5	25
Rating:	Highly Unstable	Highly Unstable	Highly Unstable	Highly Unstable
Pfankuch Score:	106	123	110	113
Rating:	Poor-Unstable	Poor-Unstable	Poor-Unstable	Poor-Unstable
BEHI Score:	25	30.5	26.5	33
Rating:	Moderate	High	Moderate	High
NBS Score:	***	***	***	***
Rating:	Extreme	Very High	Extreme	Extreme
OEBSI Score:	47	47	44.5	54.5
Rating:	Unstable	Unstable	Unstable	Unstable

## E.7 FGM Site LR-07

Site Name: LR-07

Drainage Area: 18.0 mi<sup>2</sup>

Site Legal Description: NE 1/4, Sect. 8, T9N-R2W, Cleveland Co.

FGM Survey Date: January 30, 2012

Stability Assessment: February 6, 2015

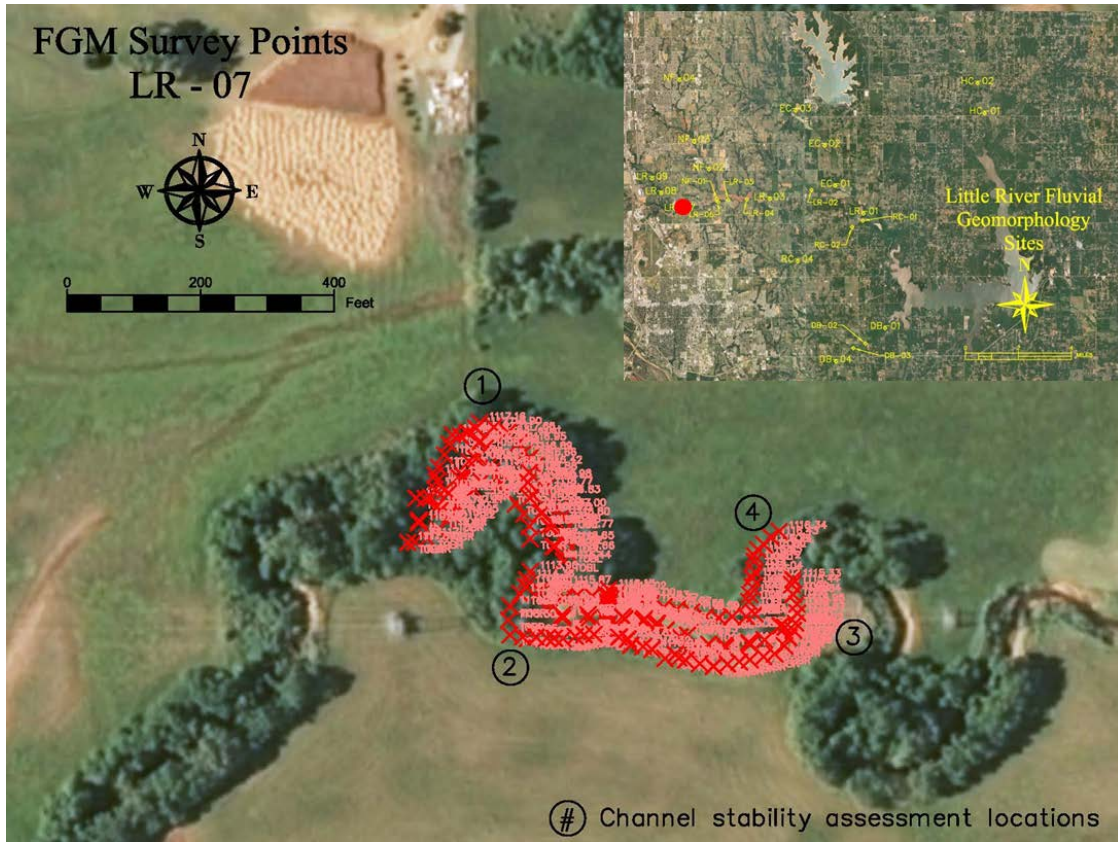


Figure E.7.1: FGM Site LR-07 Site Map with Survey Points.

Table E.7.1: FGM Site LR-07 Survey Control.

OK State Plane NAD83, South Zone (U.S. Ft); NAVD88 (U.S. Ft)			
Left Pin		Right Pin	
<b>Name:</b>	LR-07LT	<b>Name:</b>	LR-07RT
<b>Easting:</b>	2131514.32	<b>Easting:</b>	2131510.35
<b>Northing:</b>	705053.57	<b>Northing:</b>	704978.24
<b>Elevation:</b>	1116.15	<b>Elevation:</b>	1116.04
Geodetic Coordinates (Decimal Degrees)			
Left Pin		Right Pin	
<b>Lat. (N):</b>	35.2694	<b>Lat. (N):</b>	35.2692
<b>Long. (W):</b>	97.4539	<b>Long. (W):</b>	97.4539



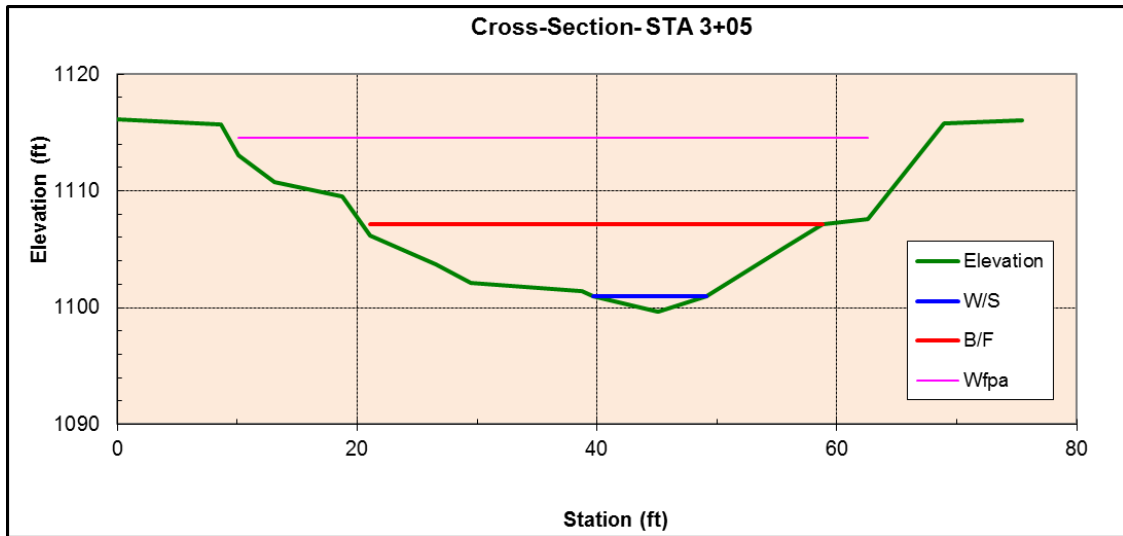


Figure E.7.2: FGM Site LR-07 Cross-section Survey Plot.

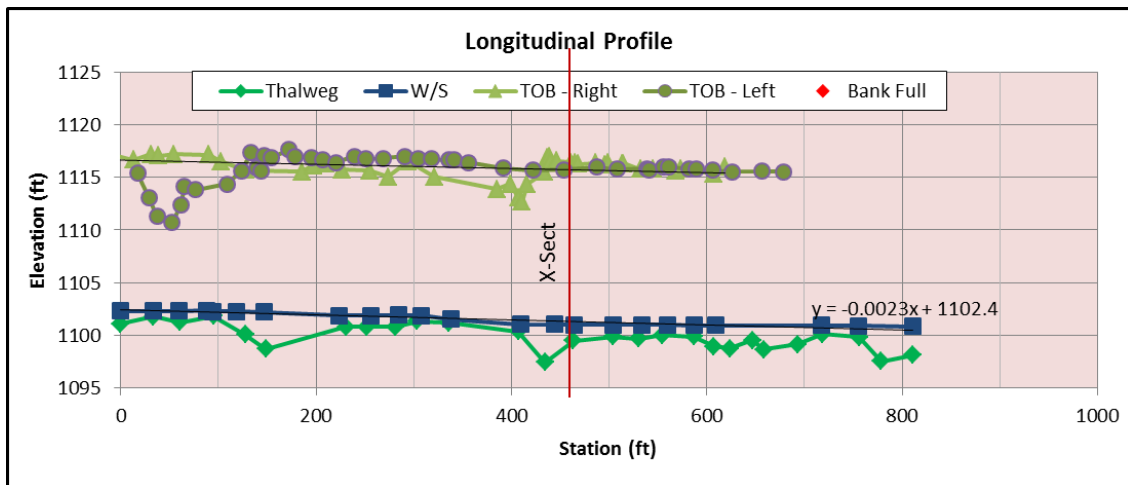


Figure E.7.3: FGM Site LR-07 Longitudinal Profile Survey Plot.

*Table E.7.2: FGM Site LR-07 Channel Morphology Summary.*

Bankfull Width (ft):	38.36
Mean Bankfull Depth (ft):	4.54
Maximum Bankfull Depth (ft):	7.46
Flood Prone Area Width (ft):	54.21
Bankfull Area (ft <sup>2</sup> ):	174.20
Entrenchment Ratio:	1.41
Width/Depth Ratio:	8.4
Sinuosity:	1.4
Slope:	0.0018
Bed Material:	Sand
Rosgen Stream Type:	G5c
Channel Evolution Stage:	IV

*Table E.7.3: FGM Site LR-07 Stream Channel Stability Summary.*

Bank No.	1	2	3	4
CSI Score:	25	25	28	26
Rating:	Highly Unstable	Highly Unstable	Highly Unstable	Highly Unstable
Pfankuch Score:	111	124	121	131
Rating:	Poor-Unstable	Poor-Unstable	Poor-Unstable	Poor-Unstable
BEHI Score:	45	48	47	38
Rating:	Very High	Extreme	Extreme	High
NBS Score:	***	***	***	***
Rating:	Extreme	Extreme	Extreme	Extreme
OEBSI Score:	67.5	59.5	59.5	59.5
Rating:	Highly Unstable	Highly Unstable	Highly Unstable	Highly Unstable

## E.8 FGM Site LR-08

Site Name: LR-08

Drainage Area: 11.9 mi<sup>2</sup>

Site Legal Description: SE 1/4, Sect. 1, T9N-R3W, Cleveland Co.

FGM Survey Date: February 6-8, 2012

Stability Assessment: February 7, 2015

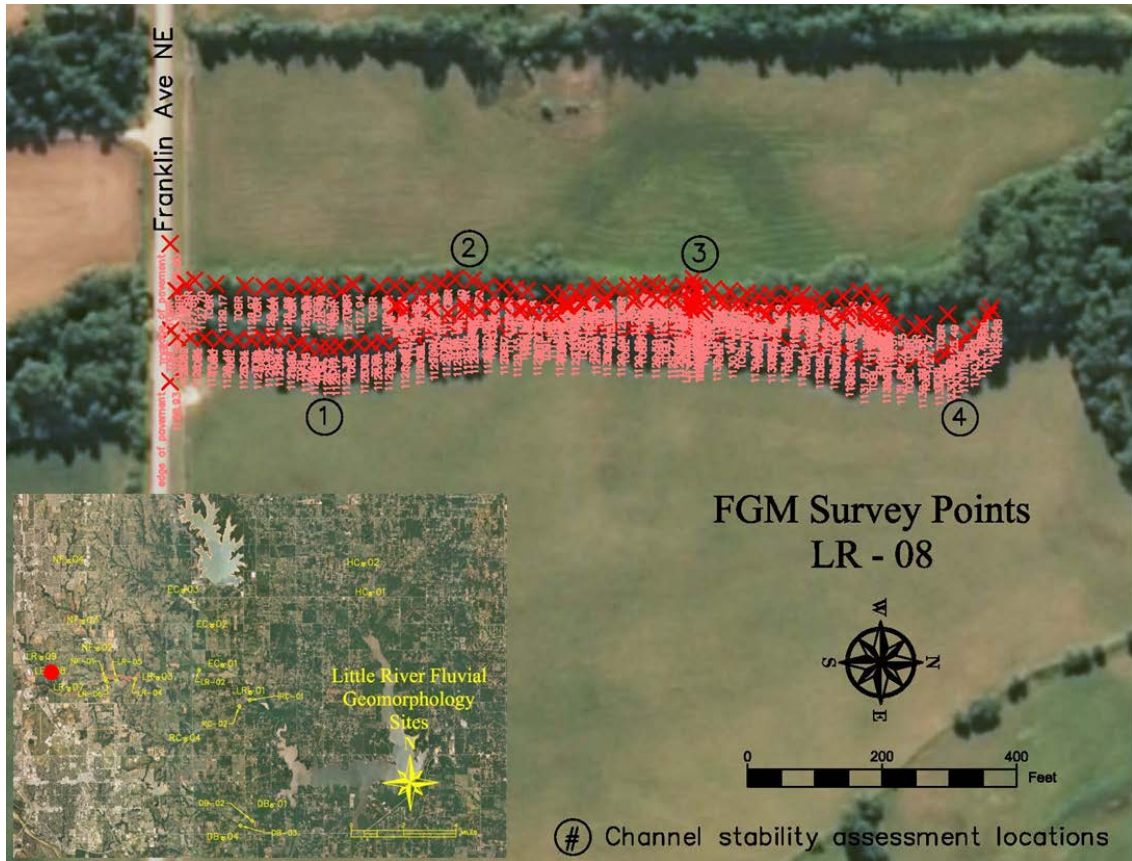


Figure E.8.1: FGM Site LR-08 Site Map with Survey Points.

Table E.8.1: FGM Site LR-08 Survey Control.

OK State Plane NAD83, South Zone (U.S. Ft); NAVD88 (U.S. Ft)			
Left Pin		Right Pin	
<b>Name:</b>	LR-08LT	<b>Name:</b>	LR-08RT
<b>Easting:</b>	2127775.27	<b>Easting:</b>	2127695.18
<b>Northing:</b>	708354.70	<b>Northing:</b>	708354.92
<b>Elevation:</b>	1130.48	<b>Elevation:</b>	1129.39
Geodetic Coordinates (Decimal Degrees)			
Left Pin		Right Pin	
<b>Lat. (N):</b>	35.2786	<b>Lat. (N):</b>	35.2786
<b>Long. (W):</b>	97.4664	<b>Long. (W):</b>	97.4667

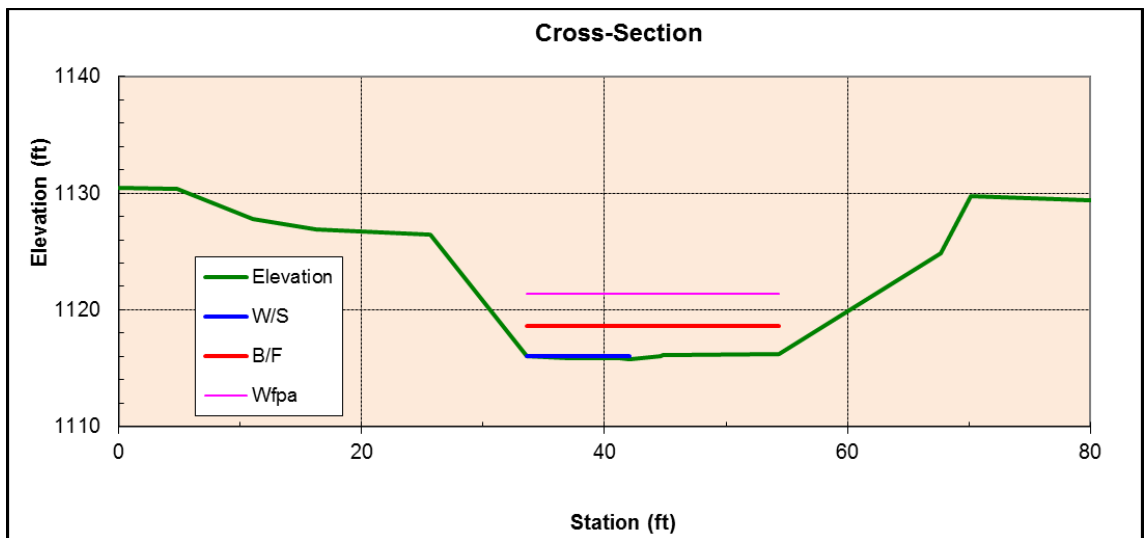


Figure E.8.2: FGM Site LR-08 Cross-section Survey Plot.

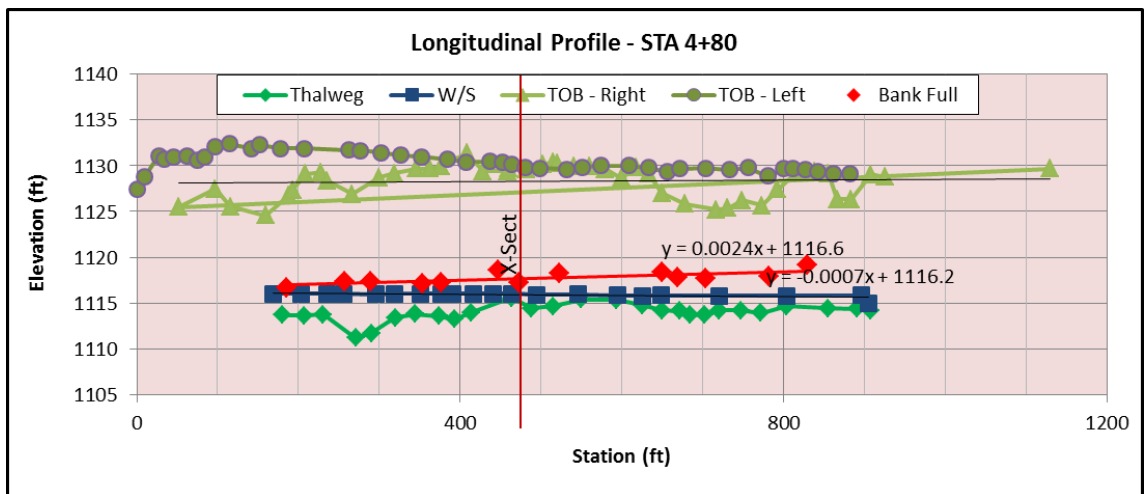


Figure E.8.3: FGM Site LR-08 Longitudinal Profile Survey Plot.

*Table E.8.2: FGM Site LR-08 Channel Morphology Summary.*

Bankfull Width (ft):	26.38
Mean Bankfull Depth (ft):	3.03
Maximum Bankfull Depth (ft):	2.80
Flood Prone Area Width (ft):	30.15
Bankfull Area (ft <sup>2</sup> ):	80.05
Entrenchment Ratio:	1.14
Width/Depth Ratio:	8.7
Sinuosity:	1.0
Slope:	0.0012
Bed Material:	Sand
Rosgen Stream Type:	G5c
Channel Evolution Stage:	IV

*Table E.8.3: Site LR-08 Stream Channel Stability Summary.*

Bank No.	1	2	3	4
CSI Score:	28	27	28	26.5
Rating:	Highly Unstable	Highly Unstable	Highly Unstable	Highly Unstable
Pfankuch Score:	121	119	110	123
Rating:	Poor-Unstable	Poor-Unstable	Poor-Unstable	Poor-Unstable
BEHI Score:	36.5	24	23	34.5
Rating:	High	Moderate	Moderate	High
NBS Score:	***	***	***	***
Rating:	Low	Moderate	Low	High
OEBSI Score:	59.5	47	49.5	56.5
Rating:	Highly Unstable	Unstable	Unstable	Highly Unstable

**E.9 FGM Site LR-09**

Site Name: LR-09

Drainage Area: 11.0 mi<sup>2</sup>

Site Legal Description: NE 1/4, Sect. 8, T9N-R2W, Cleveland Co.

FGM Survey Date: March 5, 2012

Stability Assessment: February 9, 2015

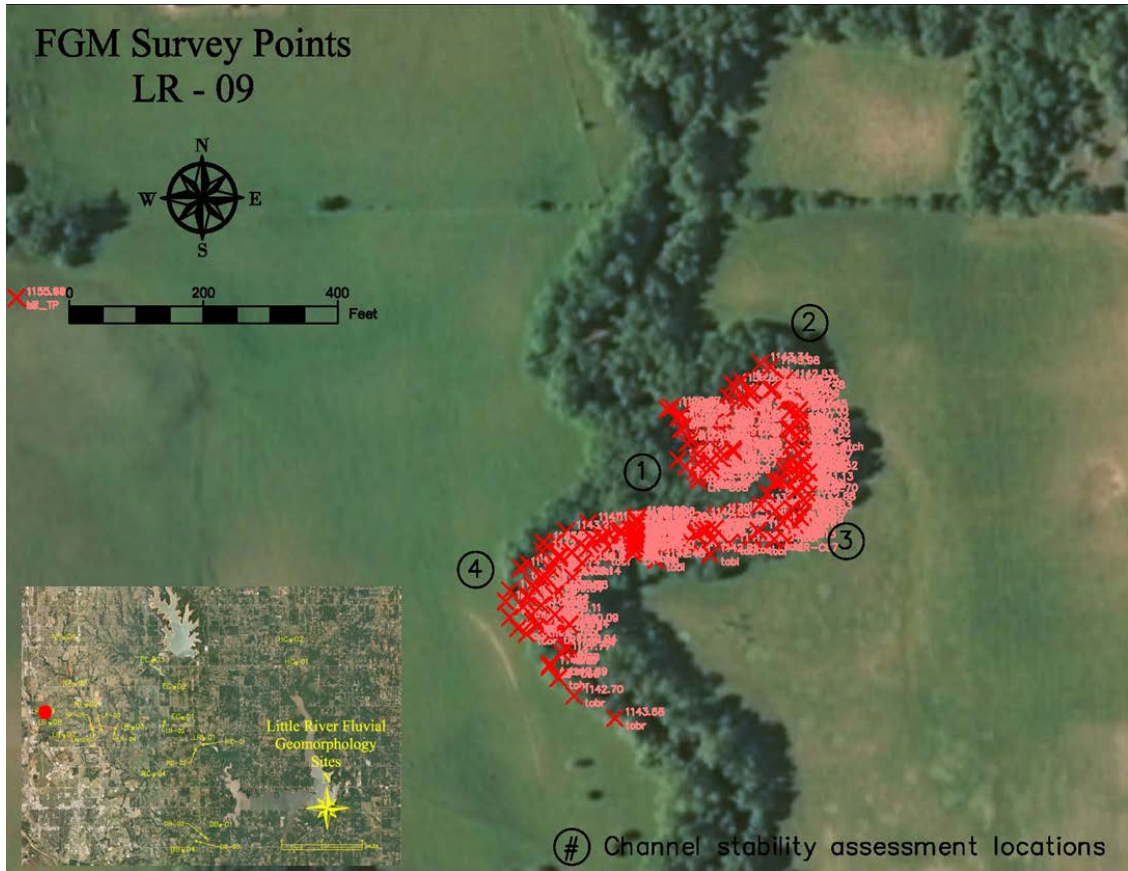


Figure E.9.1: FGM Site LR-09 Site Map with Survey Points.

Table E.9.1: FGM Site LR-09 Survey Control.

OK State Plane NAD83, South Zone (U.S. Ft); NAVD88 (U.S. Ft)			
Left Pin		Right Pin	
Name:	LR-09LT	Name:	LR-09RT
Easting:	2125981.52	Easting:	2125987.08
Northing:	711242.91	Northing:	711297.07
Elevation:	1139.73	Elevation:	1140.02
Geodetic Coordinates (Decimal Degrees)			
Left Pin		Right Pin	
Lat. (N):	35.2865	Lat. (N):	35.2867
Long. (W):	97.4723	Long. (W):	97.4723

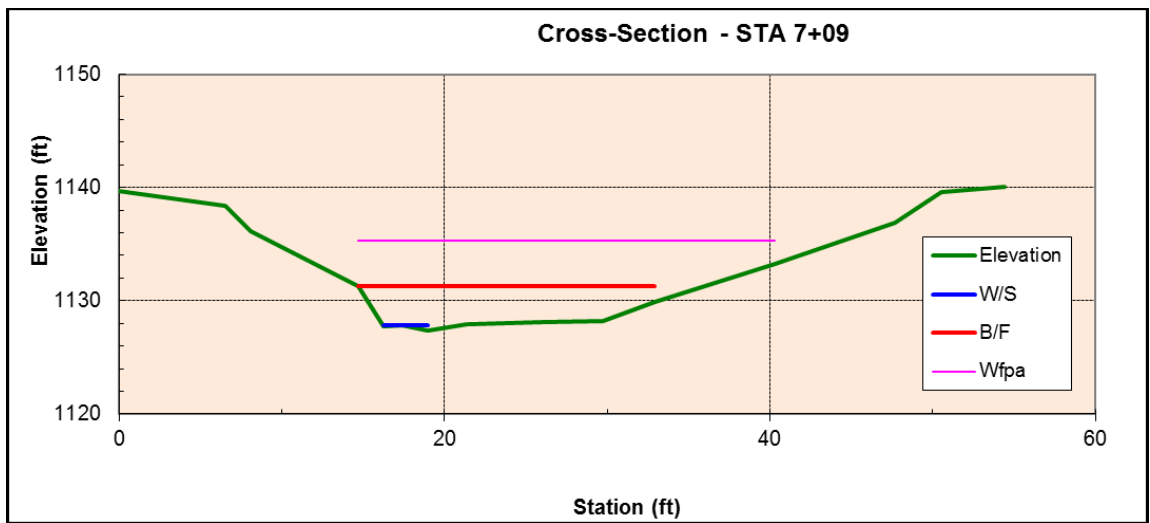


Figure E.9.2: FGM Site LR-09 Cross-section Survey Plot.

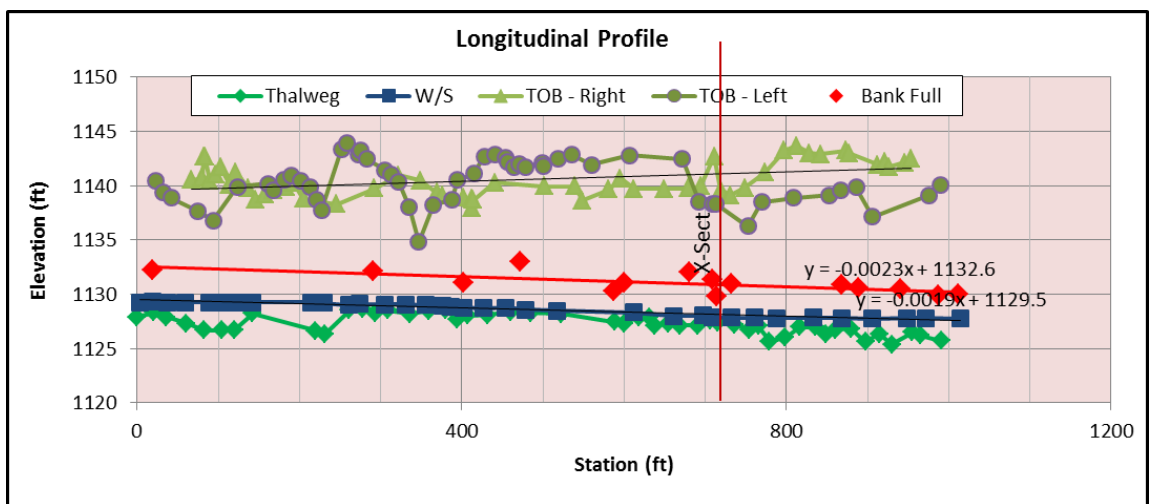


Figure E.9.3: FGM Site LR-09 Longitudinal Profile Survey Plot.

Table E.9.2: FGM Site LR-09 Channel Morphology Summary.

Bankfull Width (ft):	21.37
Mean Bankfull Depth (ft):	2.87
Maximum Bankfull Depth (ft):	3.94
Flood Prone Area Width (ft):	34.37
Bankfull Area (ft <sup>2</sup> ):	61.32
Entrenchment Ratio:	1.61
Width/Depth Ratio:	7.4
Sinuosity:	1.4
Slope:	0.0015
Bed Material:	Sand
Rosgen Stream Type:	G5c
Channel Evolution Stage:	IV

Table E.9.3: Site LR-09 Stream Channel Stability Summary.

Bank No.	1	2	3	4
CSI Score:	27	26.5	25.5	28
Rating:	Highly Unstable	Highly Unstable	Highly Unstable	Highly Unstable
Pfankuch Score:	125	123	121	127
Rating:	Poor-Unstable	Poor-Unstable	Poor-Unstable	Poor-Unstable
BEHI Score:	34	34	42	34
Rating:	High	High	Very High	High
NBS Score:	***	***	***	***
Rating:	Very High	Very High	Moderate	Extreme
OEBSI Score:	54.5	57	65	59.5
Rating:	Unstable	Highly Unstable	Highly Unstable	Highly Unstable



**E.10 FGM Site NF-01**

Site Name: NF-01

Drainage Area: 16.6 mi<sup>2</sup>

Site Legal Description: NE 1/4, Sect. 8, T9N-R2W, Cleveland Co.

FGM Survey Date: January 17, 2012 Stability Assessment: February 10, 2015

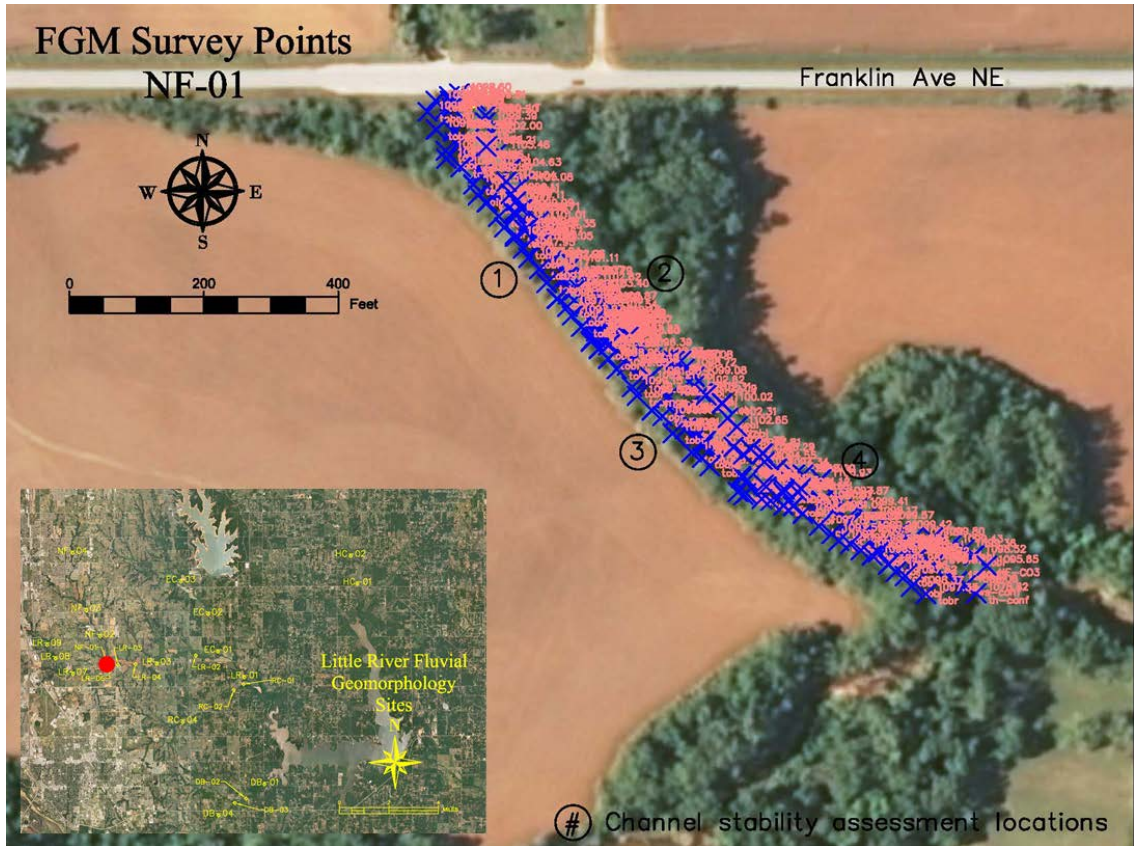


Figure E.10.1: FGM Site NF-01 Site Map with Survey Points.

Table E.10.1: FGM Site NF-01 Survey Control.

OK State Plane NAD83, South Zone (U.S. Ft); NAVD88 (U.S. Ft)			
<b>Left Pin</b>		<b>Right Pin</b>	
<b>Name:</b>	NF-01L	<b>Name:</b>	NF-01R
<b>Easting:</b>	2138877.36	<b>Easting:</b>	2138843.14
<b>Northing:</b>	707227.65	<b>Northing:</b>	707194.10
<b>Elevation:</b>	1099.69	<b>Elevation:</b>	1098.82
Geodetic Coordinates (Decimal Degrees)			
<b>Left Pin</b>		<b>Right Pin</b>	
<b>Lat. (N):</b>	35.2753	<b>Lat. (N):</b>	35.2752
<b>Long. (W):</b>	97.4292	<b>Long. (W):</b>	97.4293

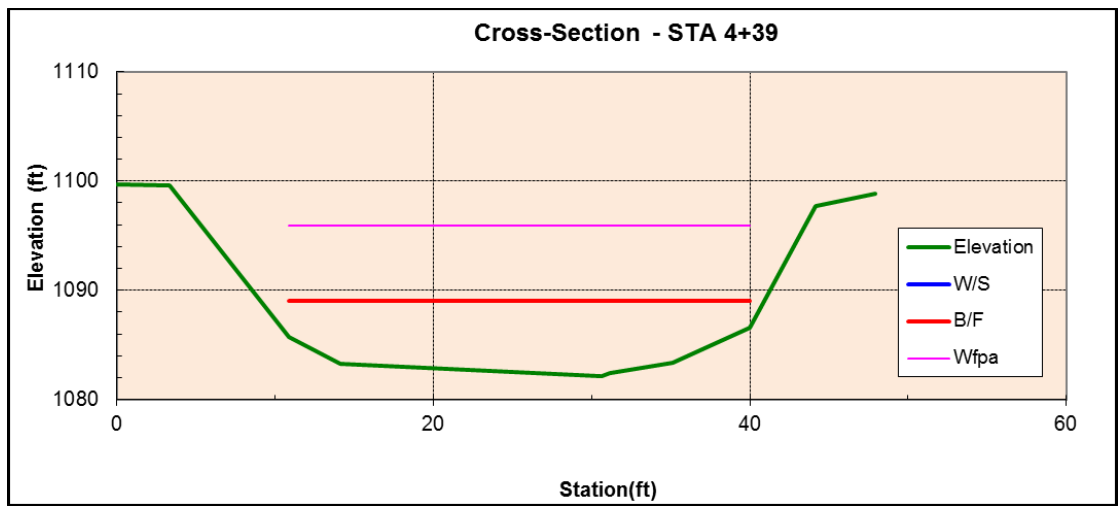


Figure E.10.2: FGM Site NF-01 Cross-section Survey Plot.

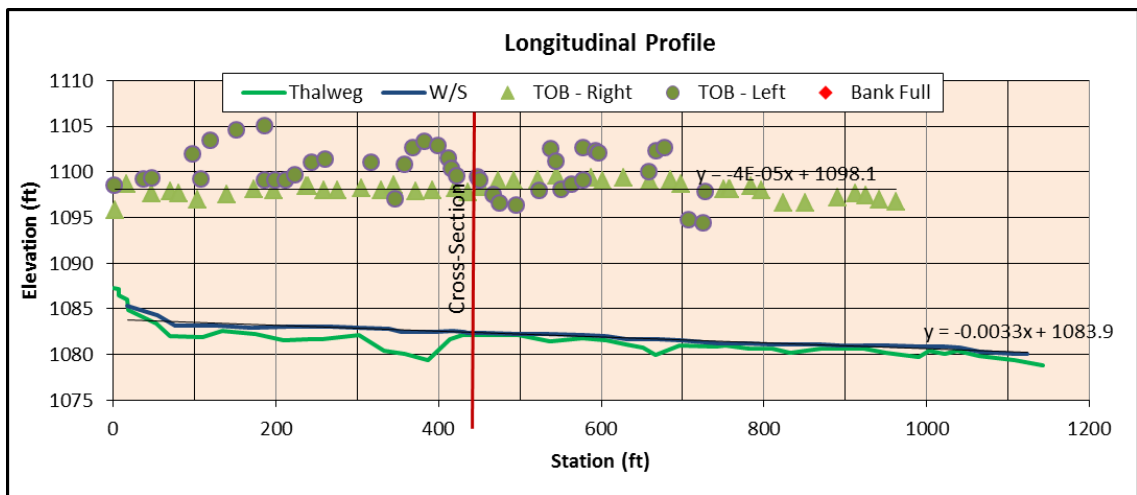


Figure E.10.3: FGM Site NF-01 Longitudinal Profile Survey Plot.

*Table E.10.2: FGM Site NF-01 Channel Morphology Summary.*

Bankfull Width (ft):	31.83
Mean Bankfull Depth (ft):	5.77
Maximum Bankfull Depth (ft):	6.90
Flood Prone Area Width (ft):	35.32
Bankfull Area (ft <sup>2</sup> ):	183.70
Entrenchment Ratio:	1.11
Width/Depth Ratio:	5.5
Sinuosity:	1.1
Slope:	0.0033
Bed Material:	Sand
Rosgen Stream Type:	G5c
Channel Evolution Stage:	IV

*Table E.10.3: Site NF-01 Stream Channel Stability Summary.*

Bank No.	1
CSI Score:	22.5
Rating:	Highly Unstable
Pfankuch Score:	116
Rating:	Poor - Unstable
BEHI Score:	41
Rating:	Very High
NBS Score:	***
Rating:	Extreme
OEBSI Score:	62
Rating:	Highly Unstable

**E.11 FGM Site NF-02**

Site Name: NF-02

Drainage Area: 14.9 mi<sup>2</sup>

Site Legal Description: SW 1/4, Sect. 32, T10N-R2W, Cleveland Co.

FGM Survey Date: May 22, 2012

Stability Assessment: February 10, 2015

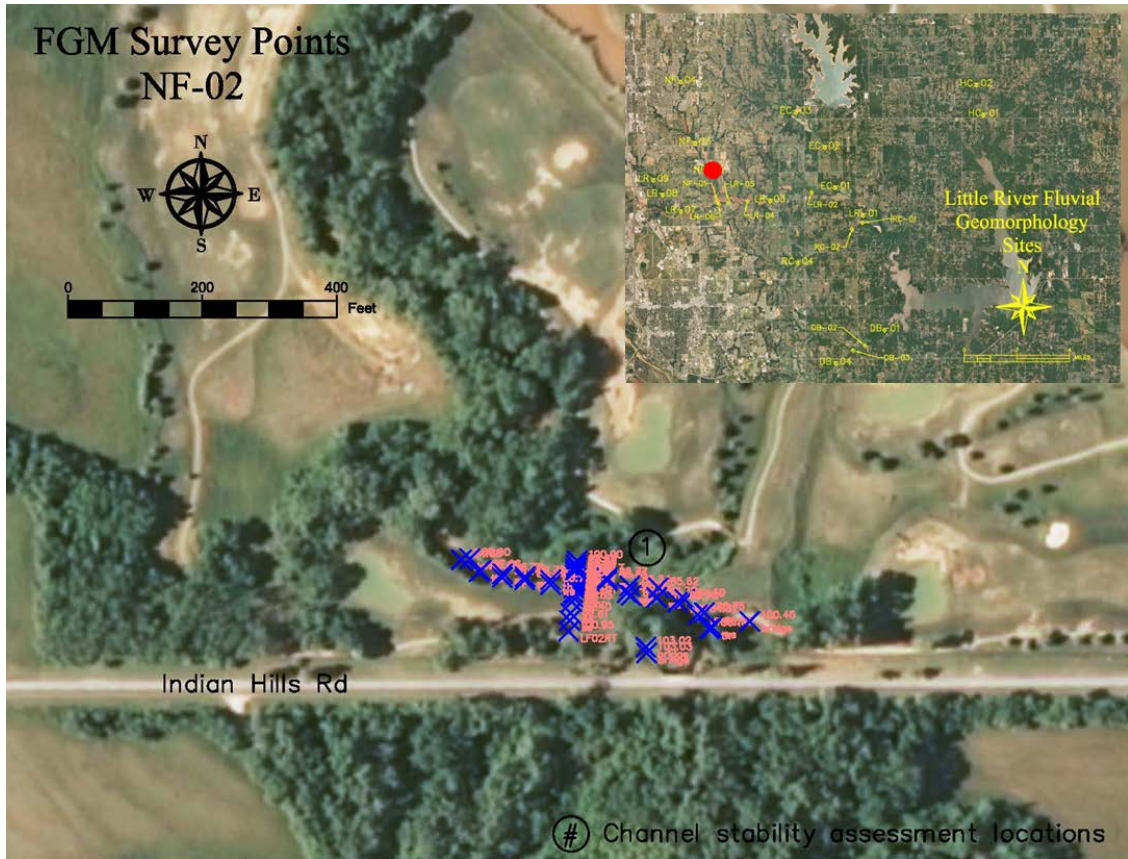


Figure E.11.1: FGM Site NF-02 Site Map with Survey Points.

Table E.11.1: FGM Site NF-02 Survey Control.

OK State Plane NAD83, South Zone (U.S. Ft); Ref. Elev. (U.S. Ft)			
<b>Left Pin</b>		<b>Right Pin</b>	
<b>Name:</b>	NF02LT	<b>Name:</b>	NF02RT
<b>Easting:</b>	2137285.64	<b>Easting:</b>	2137273.11
<b>Northing:</b>	713050.13	<b>Northing:</b>	712945.40
<b>Ref. Elev.:</b>	100.00	<b>Ref. Elev.:</b>	100.95
Geodetic Coordinates (Decimal Degrees)			
<b>Left Pin</b>		<b>Right Pin</b>	
<b>Lat. (N):</b>	35.2913	<b>Lat. (N):</b>	35.2910
<b>Long. (W):</b>	97.4344	<b>Long. (W):</b>	97.4345

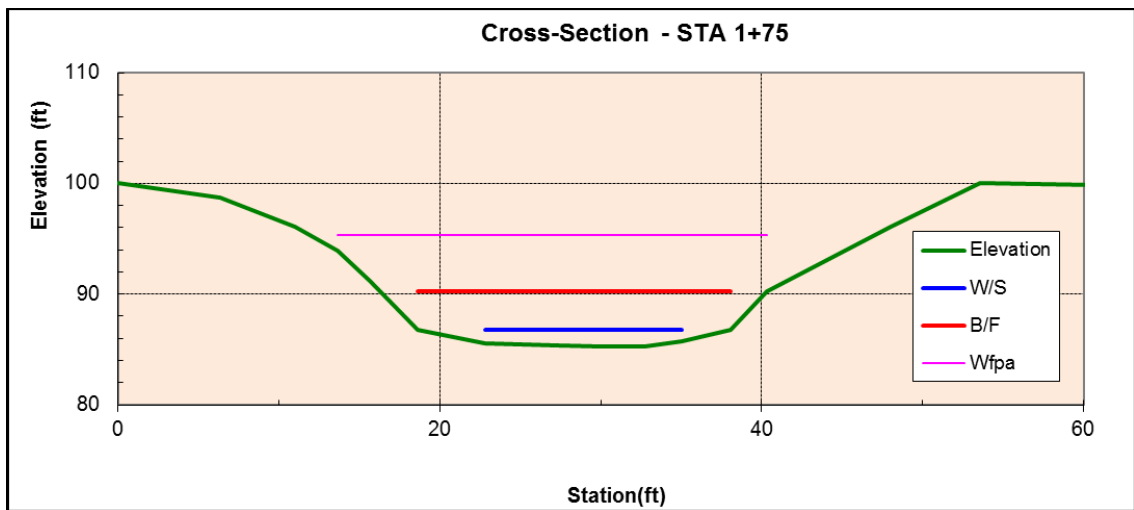


Figure E.11.2: FGM Site NF-02 Cross-section Survey Plot.

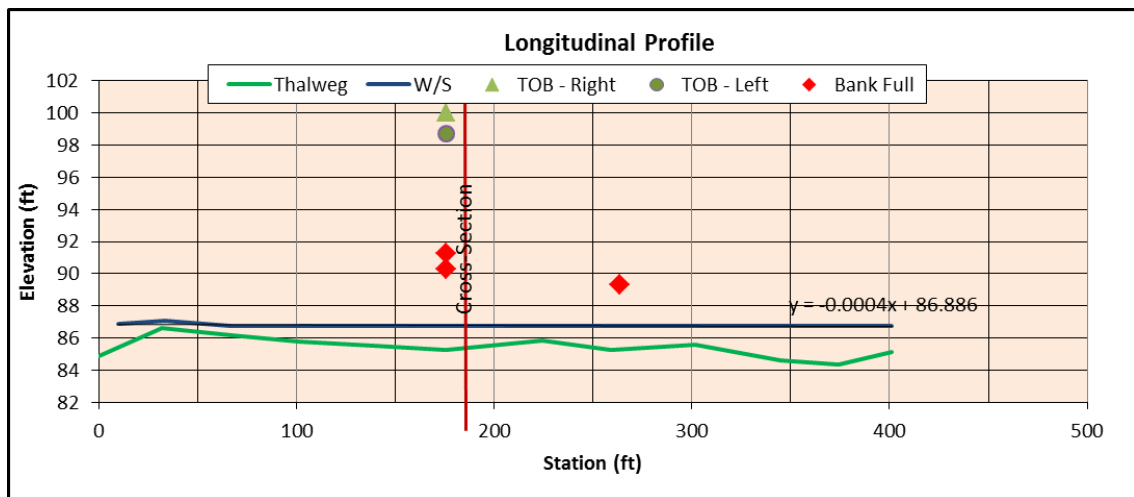


Figure E.11.3: FGM Site NF-02 Longitudinal Profile Survey Plot.

*Table E.11.2: FGM Site NF-02 Channel Morphology Summary.*

Bankfull Width (ft):	24.07
Mean Bankfull Depth (ft):	4.10
Maximum Bankfull Depth (ft):	5.07
Flood Prone Area Width (ft):	29.43
Bankfull Area (ft <sup>2</sup> ):	98.77
Entrenchment Ratio:	1.22
Width/Depth Ratio:	5.9
Sinuosity:	1.1
Slope:	0.0004
Bed Material:	Sand
Rosgen Stream Type:	G5c
Channel Evolution Stage:	IV

*Table E.11.3: Site NF-02 Stream Channel Stability Summary.*

Bank No.	1
CSI Score:	28
Rating:	Highly Unstable
Pfankuch Score:	125
Rating:	Poor-Unstable
BEHI Score:	37
Rating:	High
NBS Score:	***
Rating:	Low
OEBSI Score:	62
Rating:	Highly Unstable

**E.12 FGM Site NF-03**

Site Name: NF-03

Drainage Area: 11.8 mi<sup>2</sup>

Site Legal Description: SW 1/4, Sect. 19, T10N-R2W, Cleveland Co.

FGM Survey Date: May 29, 2012

Stability Assessment: May 29, 2012

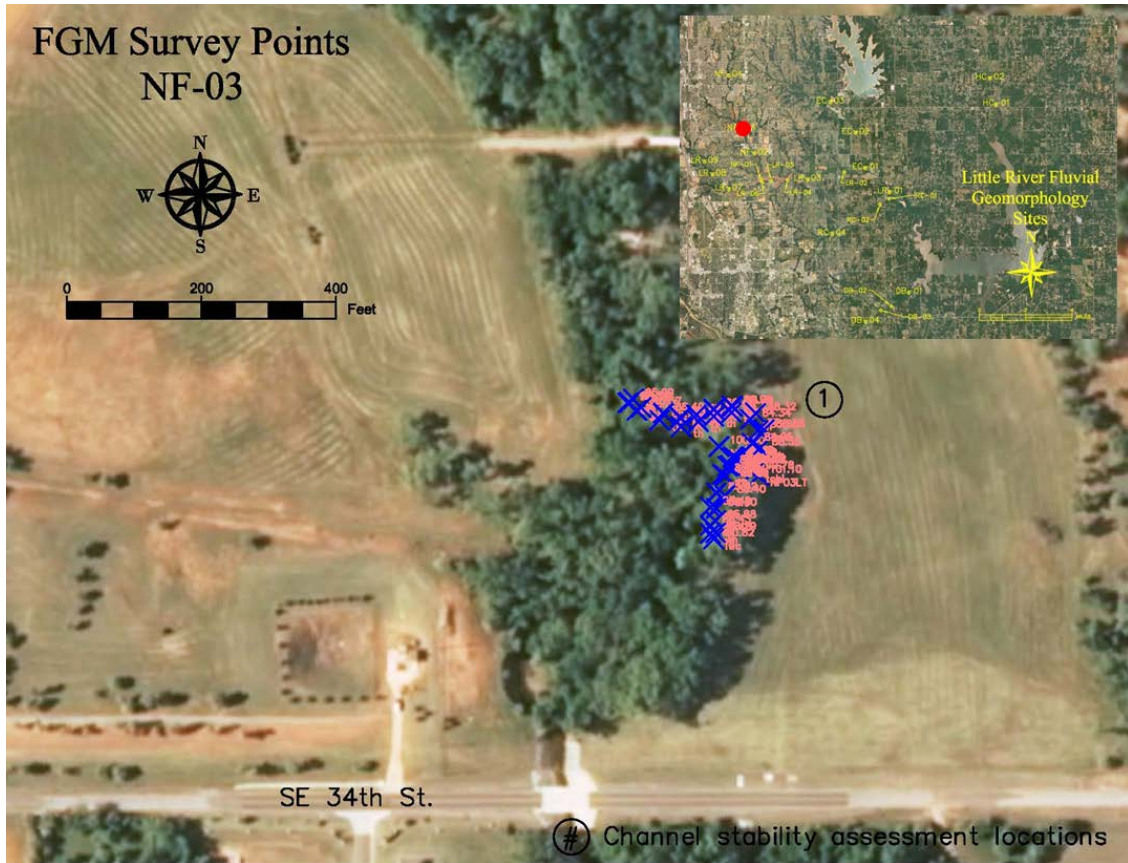


Figure E.12.1: FGM Site NF-03 Site Map with Survey Points.

Table E.12.1: FGM Site NF-03 Survey Control.

OK State Plane NAD83, South Zone (U.S. Ft); Ref. Elev. (U.S. Ft)			
Left Pin		Right Pin	
Name:	NF03LT	Name:	NF03RT
Easting:	2134336.54	Easting:	2134277.60
Northing:	718572.15	Northing:	718615.31
Ref. Elev.:	101.10	Ref. Elev.:	100.00
Geodetic Coordinates (Decimal Degrees)			
Left Pin		Right Pin	
Lat. (N):	35.3065	Lat. (N):	35.3066
Long. (W):	97.4442	Long. (W):	97.4444

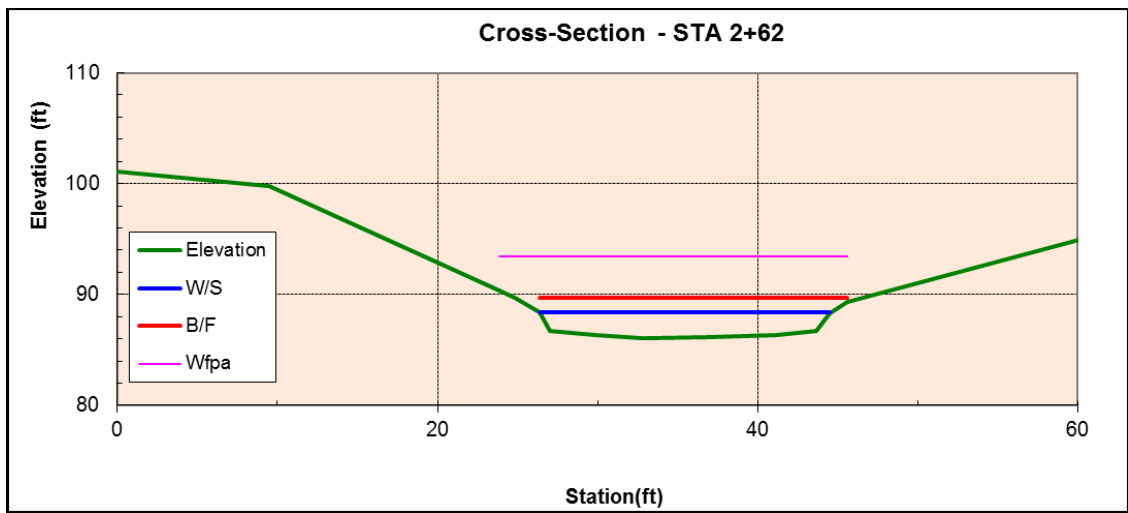


Figure E.12.2: FGM Site NF-03 Cross-section Survey Plot.

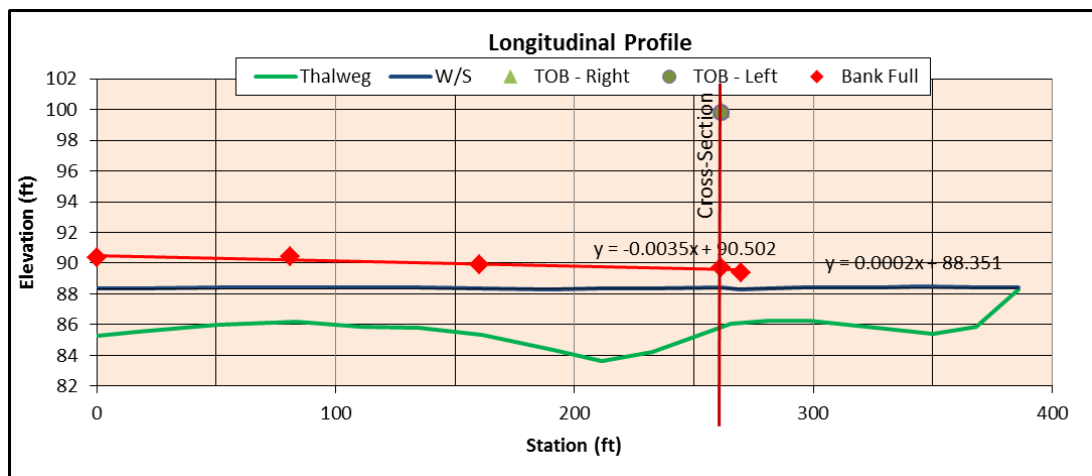


Figure E.12.3: FGM Site NF-03 Longitudinal Profile Survey Plot.



Table E.12.2: FGM Site NF-03 Channel Morphology Summary.

Bankfull Width (ft):	21.66
Mean Bankfull Depth (ft):	3.11
Maximum Bankfull Depth (ft):	3.68
Flood Prone Area Width (ft):	43.41
Bankfull Area (ft <sup>2</sup> ):	67.31
Entrenchment Ratio:	2.00
Width/Depth Ratio:	7.0
Sinuosity:	1.6
Slope:	0.0002
Bed Material:	Sand
Rosgen Stream Type:	G5c
Channel Evolution Stage:	III

Table E.12.3: FGM Site NF-03 Stream Channel Stability Summary.

Bank No.	1
CSI Score:	23
Rating:	HIGHLY UNSTABLE
Pfankuch Score:	103
Rating:	Poor- Unstable
BEHI Score:	36.5
Rating:	High
NBS Score:	***
Rating:	Extreme
OEBSI Score:	62
Rating:	Highly Unstable

**E.13 FGM Site NF-04**

Site Name: NF-04

Drainage Area: 2.5 mi<sup>2</sup>

Site Legal Description: SW 1/4, Sect. 18, T10N-R2W, Cleveland Co.

FGM Survey Date: June 1, 2012

Stability Assessment: June 1, 2012

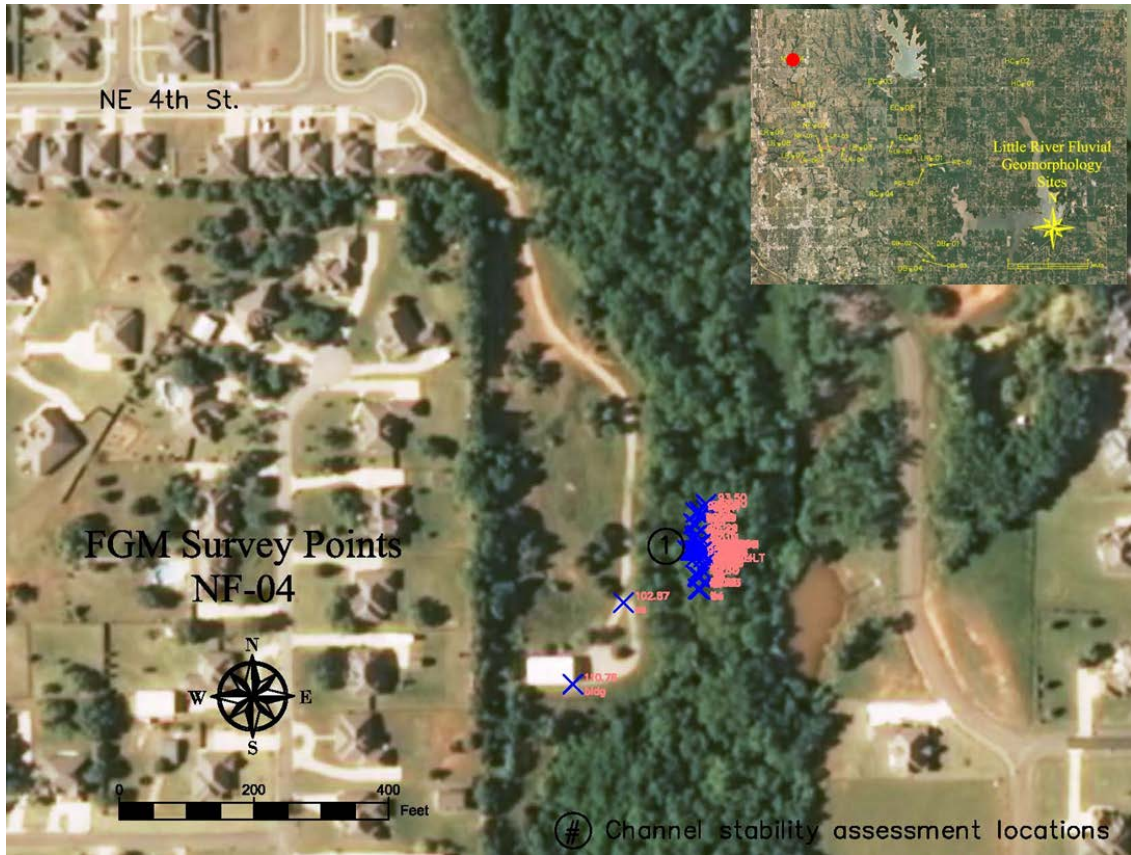


Figure E.13.1: FGM Site NF-04 Site Map with Survey Points.

Table E.13.1: FGM Site NF-04 Survey Control.

OK State Plane NAD83, South Zone (U.S. Ft); Ref. Elev. (U.S. Ft)			
<b>Left Pin</b>		<b>Right Pin</b>	
<b>Name:</b>	NF04LT	<b>Name:</b>	NF04RT
<b>Easting:</b>	2131449.30	<b>Easting:</b>	2131407.54
<b>Northing:</b>	730712.50	<b>Northing:</b>	730713.26
<b>Ref. Elev.:</b>	100.41	<b>Ref. Elev.:</b>	100.00
Geodetic Coordinates (Decimal Degrees)			
<b>Left Pin</b>		<b>Right Pin</b>	
<b>Lat. (N):</b>	35.3399	<b>Lat. (N):</b>	35.339926
<b>Long. (W):</b>	97.4537	<b>Long. (W):</b>	97.453812

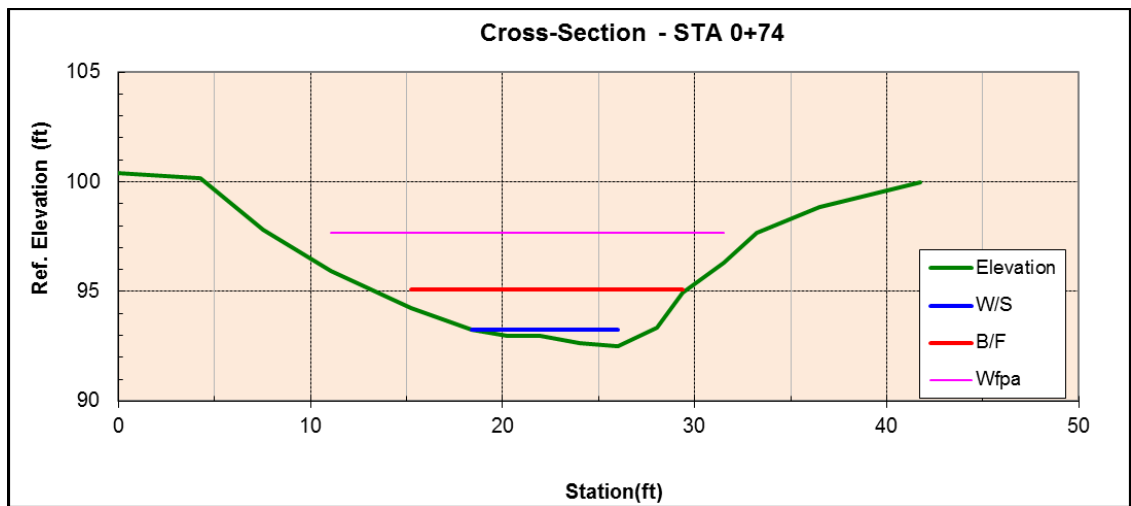


Figure E.13.2: FGM Site NF-04 Cross-section Survey Plot.

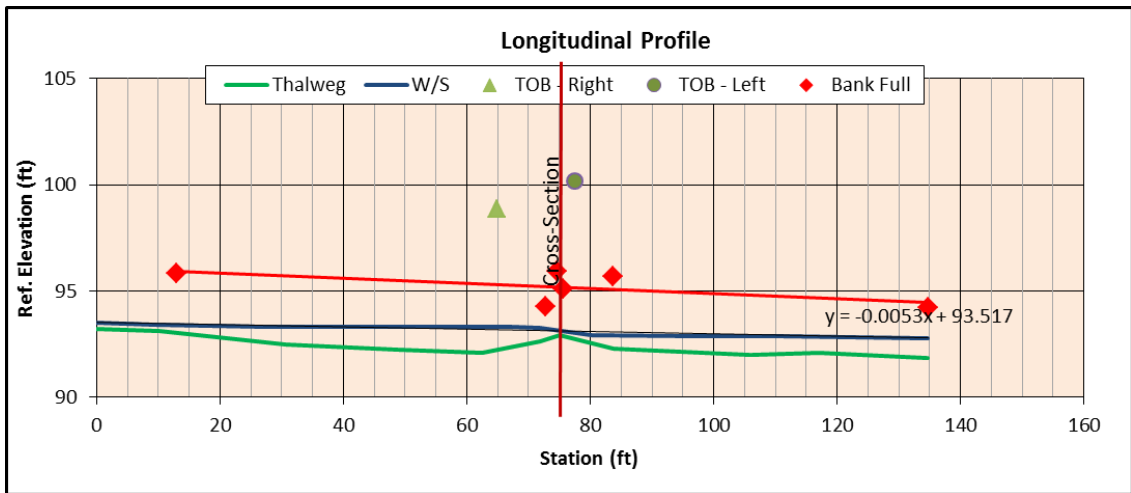


Figure E.13.3: FGM Site NF-04 Longitudinal Profile Survey Plot.

*Table E.13.2: FGM Site NF-04 Channel Morphology Summary.*

Bankfull Width (ft):	16.43
Mean Bankfull Depth (ft):	1.75
Maximum Bankfull Depth (ft):	2.58
Flood Prone Area Width (ft):	23.70
Bankfull Area (ft <sup>2</sup> ):	28.78
Entrenchment Ratio:	1.44
Width/Depth Ratio:	9.4
Sinuosity:	1.6
Slope:	0.005
Bed Material:	Sand
Rosgen Stream Type:	G5c
Channel Evolution Stage:	III

*Table E.13.3: FGM Site NF-04 Stream Channel Stability Summary.*

Bank No.	1
CSI Score:	20.5
Rating:	HIGHLY UNSTABLE
Pfankuch Score:	102
Rating:	Poor-Unstable
BEHI Score:	28.5
Rating:	Moderate
NBS Score:	***
Rating:	Extreme
OEBSI Score:	54.8
Rating:	Unstable

**E.14 FGM Site EC-01**

Site Name: EC-01

Drainage Area: 18.6 mi<sup>2</sup>

Site Legal Description: SW 1/4, Sect. 6, T9N-R1W, Cleveland Co.

FGM Survey Date: June 8, 2012

Stability Assessment: June 8, 2012

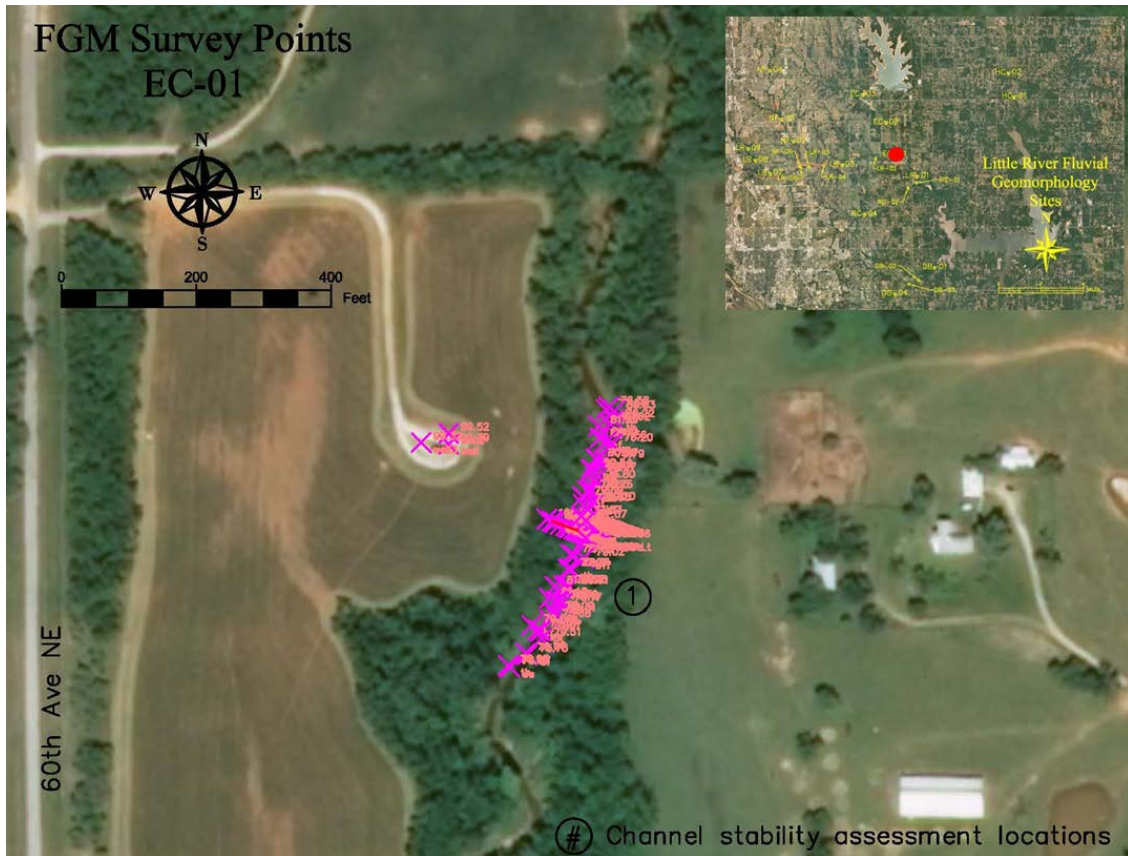


Figure E.14.1: FGM Site EC-01 Site Map with Survey Points.

Table E.14.1: FGM Site EC-01 Survey Control.

OK State Plane NAD83, South Zone (U.S. Ft); Ref. Elev. (U.S. Ft)			
Left Pin		Right Pin	
Name:	EC01LT	Name:	EC01RT
Easting:	2162417.90	Easting:	2162331.78
Northing:	709814.33	Northing:	709845.40
Ref. Elev.:	100.06	Ref. Elev.:	100.00
Geodetic Coordinates (Decimal Degrees)			
Left Pin		Right Pin	
Lat. (N):	35.2820	Lat. (N):	35.2821
Long. (W):	97.3503	Long. (W):	97.3506

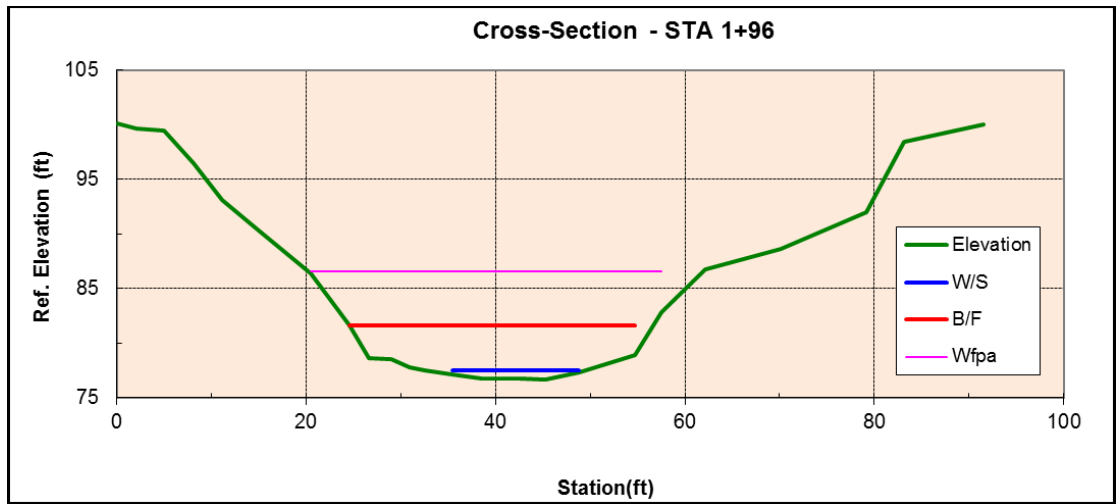


Figure E.14.2: FGM Site EC-01 Cross-section Survey Plot.

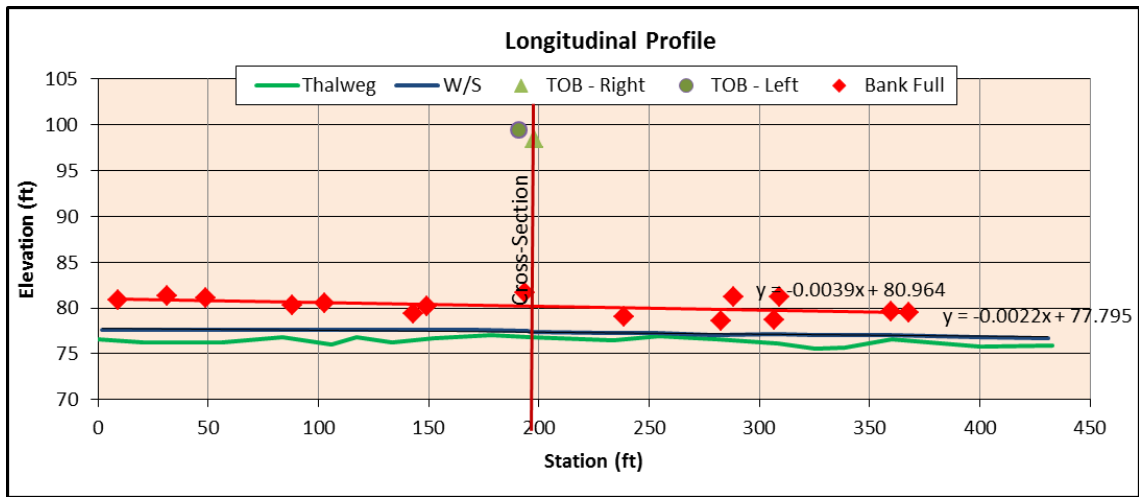


Figure E.14.3: FGM Site EC-01 Longitudinal Profile Survey Plot.

Table E.14.2: FGM Site EC-01 Channel Morphology Summary.

Bankfull Width (ft):	32.10
Mean Bankfull Depth (ft):	3.85
Maximum Bankfull Depth (ft):	4.92
Flood Prone Area Width (ft):	37.51
Bankfull Area (ft <sup>2</sup> ):	123.43
Entrenchment Ratio:	1.17
Width/Depth Ratio:	8.3
Sinuosity:	1.1
Slope:	0.0022
Bed Material:	Sand
Rosgen Stream Type:	G5c
Channel Evolution Stage:	III

Table E.14.3: FGM Site EC-01 Stream Channel Stability Summary.

Bank No.	1
CSI Score:	20.5
Rating:	HIGHLY UNSTABLE
Pfankuch Score:	101
Rating:	Poor-Unstable
BEHI Score:	32.5
Rating:	High
NBS Score:	***
Rating:	High
OEBSI Score:	59.5
Rating:	Highly Unstable

**E.15 FGM Site EC-02**

Site Name: EC-02

Drainage Area: 17.1 mi<sup>2</sup>

Site Legal Description: NW 1/4, Sect. 25, T10N-R2W, Cleveland Co.

FGM Survey Date: June 13, 2012

Stability Assessment: June 13, 2012

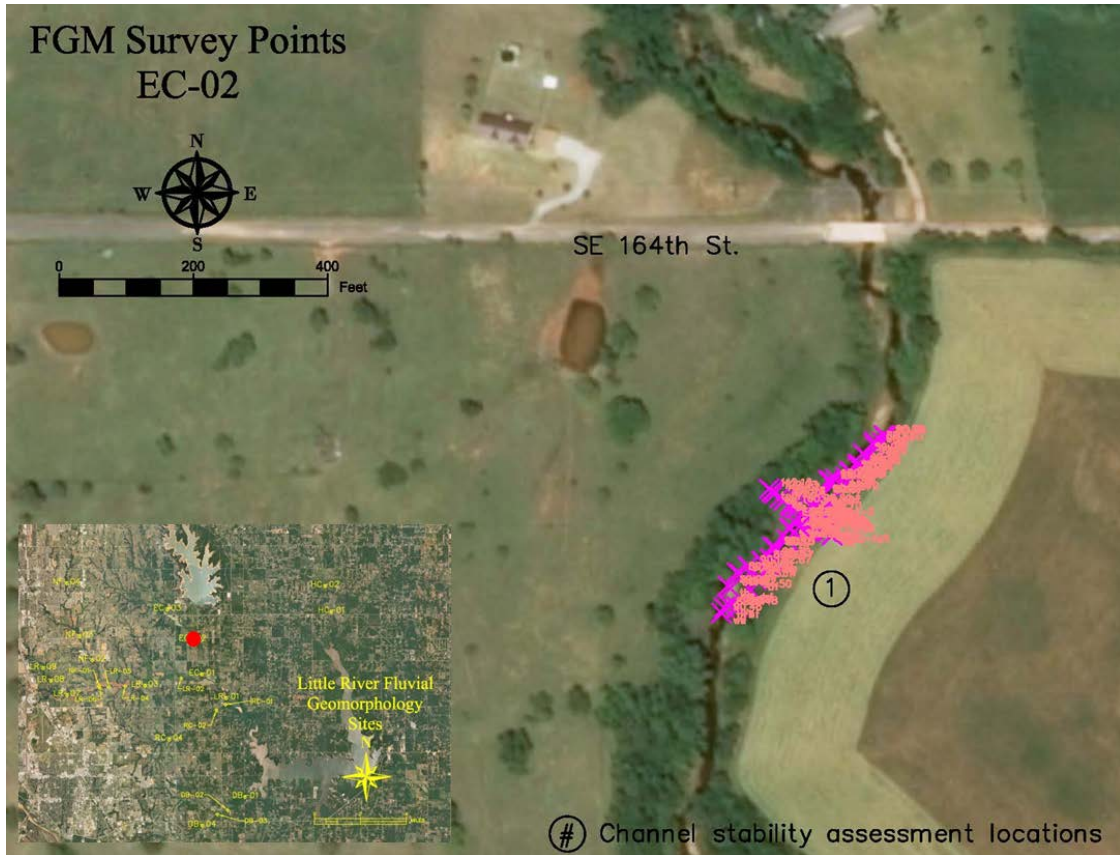


Figure E.15.1: FGM Site EC-02 Site Map with Survey Points.

Table E.15.1: FGM Site EC-02 Survey Control.

OK State Plane NAD83, South Zone (U.S. Ft); Ref. Elev. (U.S. Ft)			
<b>Left Pin</b>		<b>Right Pin</b>	
<b>Name:</b>	EC02-left	<b>Name:</b>	EC02-right
<b>Easting:</b>	2160336.35	<b>Easting:</b>	2160281.02
<b>Northing:</b>	717758.75	<b>Northing:</b>	717798.95
<b>Ref. Elev.:</b>	111.38	<b>Ref. Elev.:</b>	100.00
Geodetic Coordinates (Decimal Degrees)			
<b>Left Pin</b>		<b>Right Pin</b>	
<b>Lat. (N):</b>	35.3039	<b>Lat. (N):</b>	35.3040
<b>Long. (W):</b>	97.3571	<b>Long. (W):</b>	97.3573



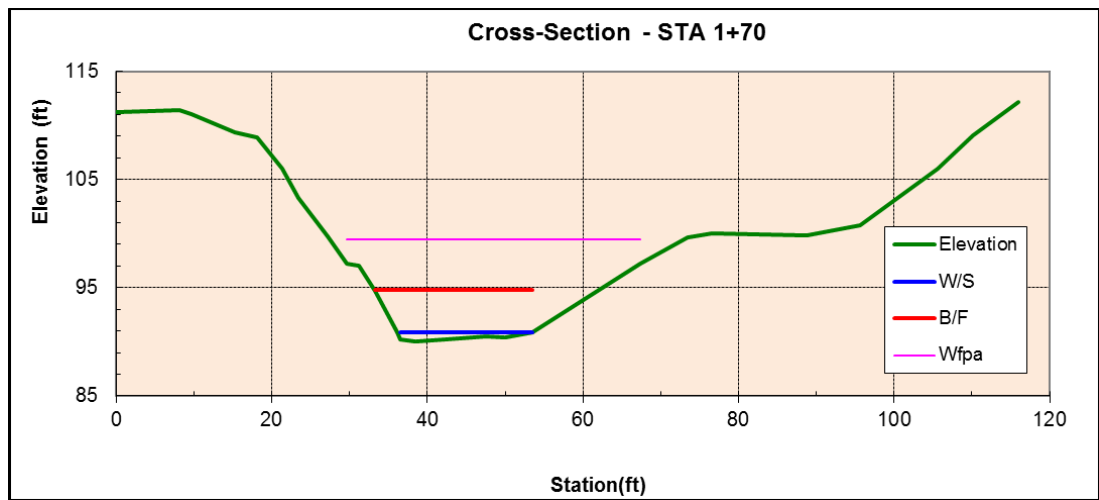


Figure E.15.2: FGM Site EC-02 Cross-section Survey Plot.

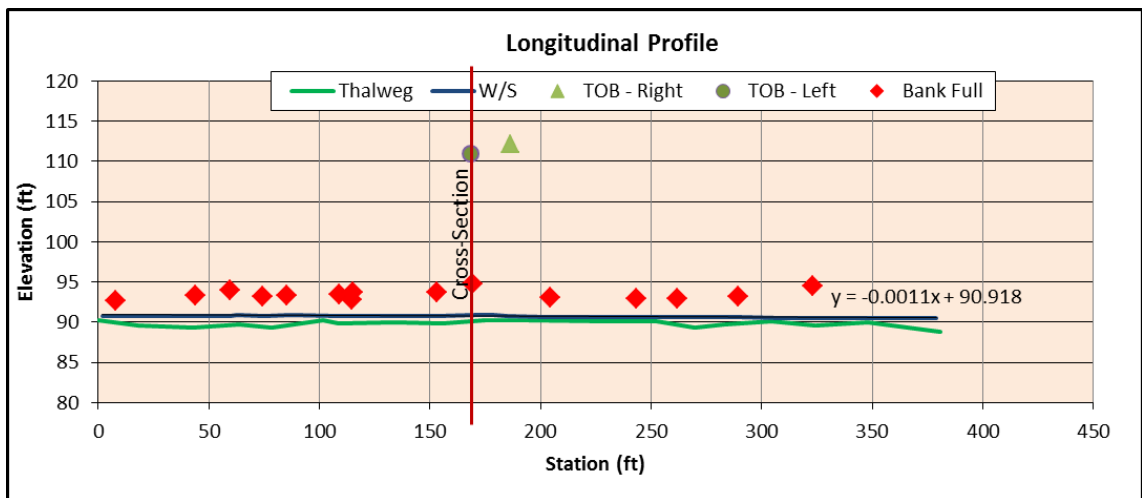


Figure E.15.3: FGM Site EC-02 Longitudinal Profile Survey Plot.

Table E.15.2: FGM Site EC-02 Channel Morphology Summary.

Bankfull Width (ft):	28.69
Mean Bankfull Depth (ft):	3.78
Maximum Bankfull Depth (ft):	4.68
Flood Prone Area Width (ft):	40.48
Bankfull Area (ft <sup>2</sup> ):	108.33
Entrenchment Ratio:	1.41
Width/Depth Ratio:	7.6
Sinuosity:	1.1
Slope:	0.0011
Bed Material:	Gravel
Rosgen Stream Type:	G4c
Channel Evolution Stage:	V

Table E.15.3: FGM Site EC-02 Stream Channel Stability Summary.

Bank No.	1
CSI Score:	20.5
Rating:	HIGHLY UNSTABLE
Pfankuch Score:	101
Rating:	Poor-Unstable
BEHI Score:	32.5
Rating:	High
NBS Score:	***
Rating:	High
OEBSI Score:	59.5
Rating:	Highly Unstable

**E.16 FGM Site EC-03**

Site Name: EC-03

Drainage Area: 14.6 mi<sup>2</sup>

Site Legal Description: SE 1/4, Sect. 23, T10N-R2W, Cleveland Co.

FGM Survey Date: June 15, 2012

Stability Assessment: June 15, 2012

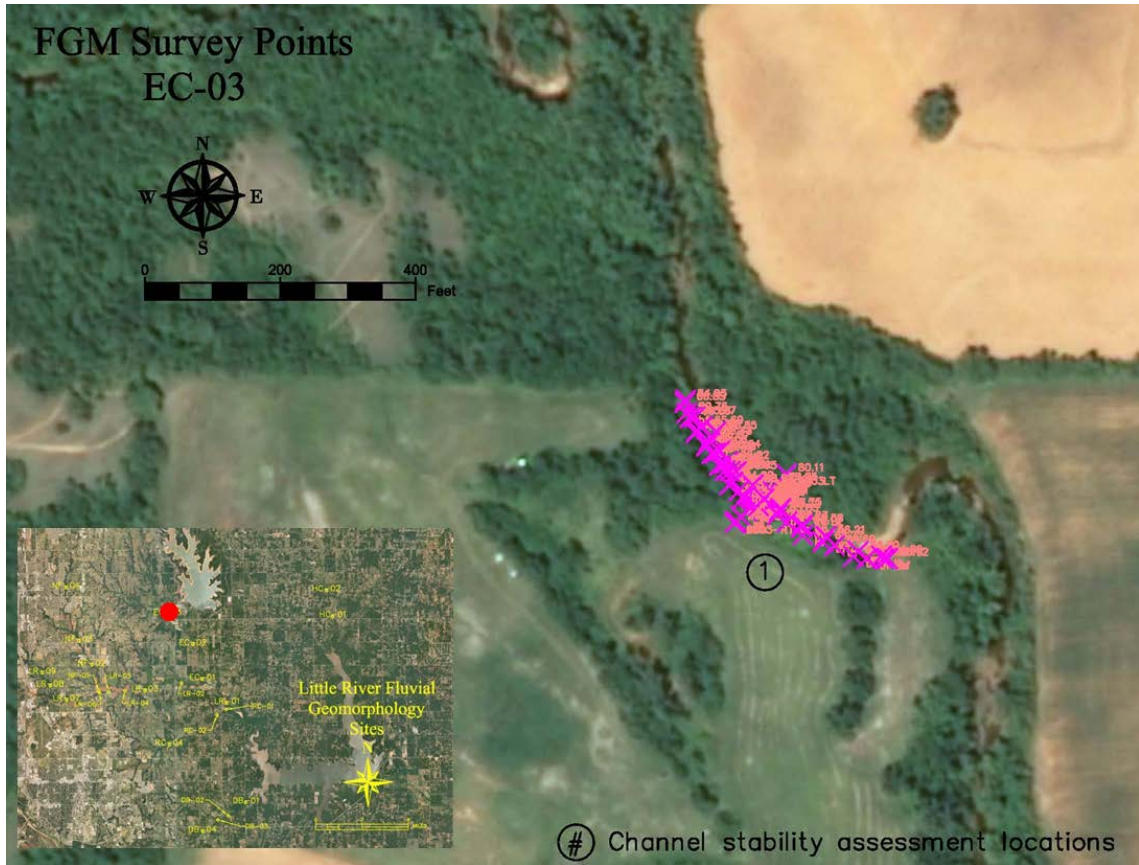


Figure E.16.1: FGM Site EC-03 Site Map with Survey Points.

Table E.16.1: FGM Site EC-03 Survey Control.

OK State Plane NAD83, South Zone (U.S. Ft); Ref. Elev. (U.S. Ft)			
Left Pin		Right Pin	
<b>Name:</b>	EC03-LT	<b>Name:</b>	EC03-RT
<b>Easting:</b>	2154552.43	<b>Easting:</b>	2154476.33
<b>Northing:</b>	724662.96	<b>Northing:</b>	724591.13
<b>Ref. Elev.:</b>	80.11	<b>Ref. Elev.:</b>	100.00
Geodetic Coordinates (Decimal Degrees)			
Left Pin		Right Pin	
<b>Lat. (N):</b>	35.3229	<b>Lat. (N):</b>	35.3227
<b>Long. (W):</b>	97.3763	<b>Long. (W):</b>	97.3766

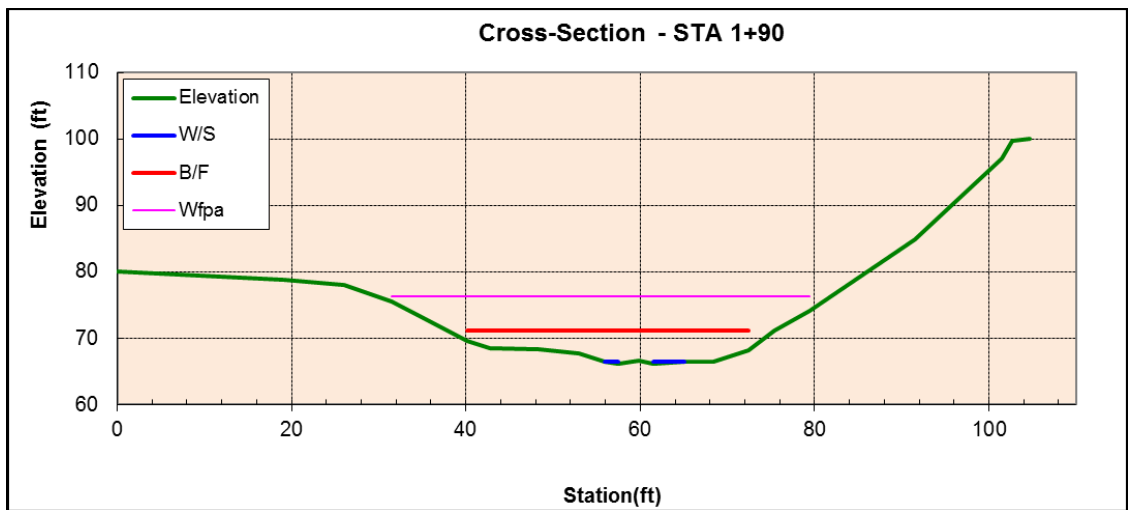


Figure E.16.2: FGM Site EC-03 Cross-section Survey Plot.

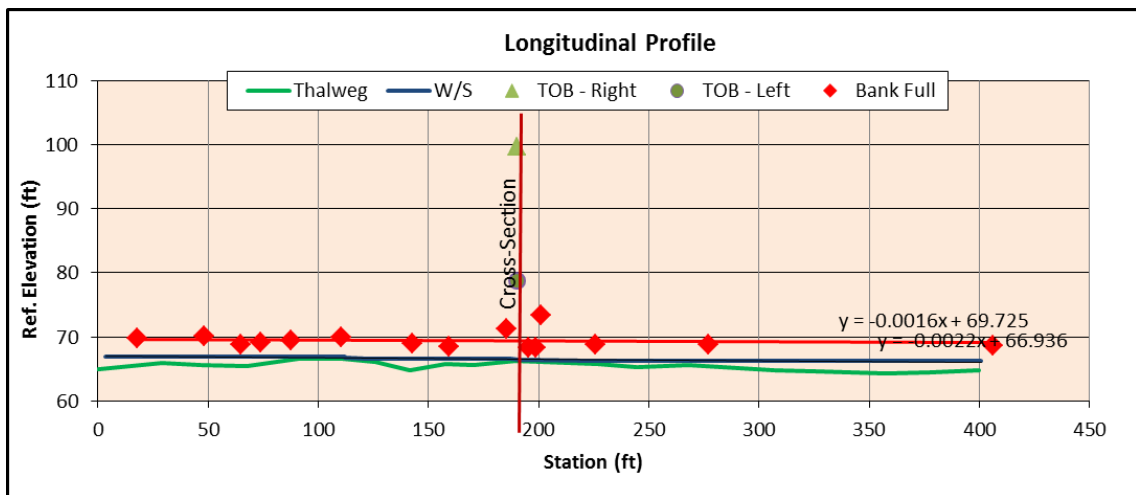


Figure E.16.3: FGM Site EC-03 Longitudinal Profile Survey Plot.

Table E.16.2: FGM Site EC-03 Channel Morphology Summary.

Bankfull Width (ft):	37.59
Mean Bankfull Depth (ft):	3.54
Maximum Bankfull Depth (ft):	5.09
Flood Prone Area Width (ft):	59.16
Bankfull Area (ft <sup>2</sup> ):	133.00
Entrenchment Ratio:	1.57
Width/Depth Ratio:	10.6
Sinuosity:	1.1
Slope:	0.0003
Bed Material:	Gravel
Rosgen Stream Type:	G4c
Channel Evolution Stage:	V

Table E.16.3: FGM Site EC-03 Stream Channel Stability Summary.

Bank No.	1
CSI Score:	20.5
Rating:	HIGHLY UNSTABLE
Pfankuch Score:	79
Rating:	Fair-Mod. Unstable
BEHI Score:	21.5
Rating:	Moderate
NBS Score:	***
Rating:	Low
OEBSI Score:	57
Rating:	Highly Unstable

**E.17 FGM Site RC-01**

Site Name: RC-01

Drainage Area: 11.6 mi<sup>2</sup>

Site Legal Description: SW 1/4, Sect. 8, T9N-R1W, Cleveland Co.

FGM Survey Date: November 19, 2010

Stability Assessment: January 27, 2015

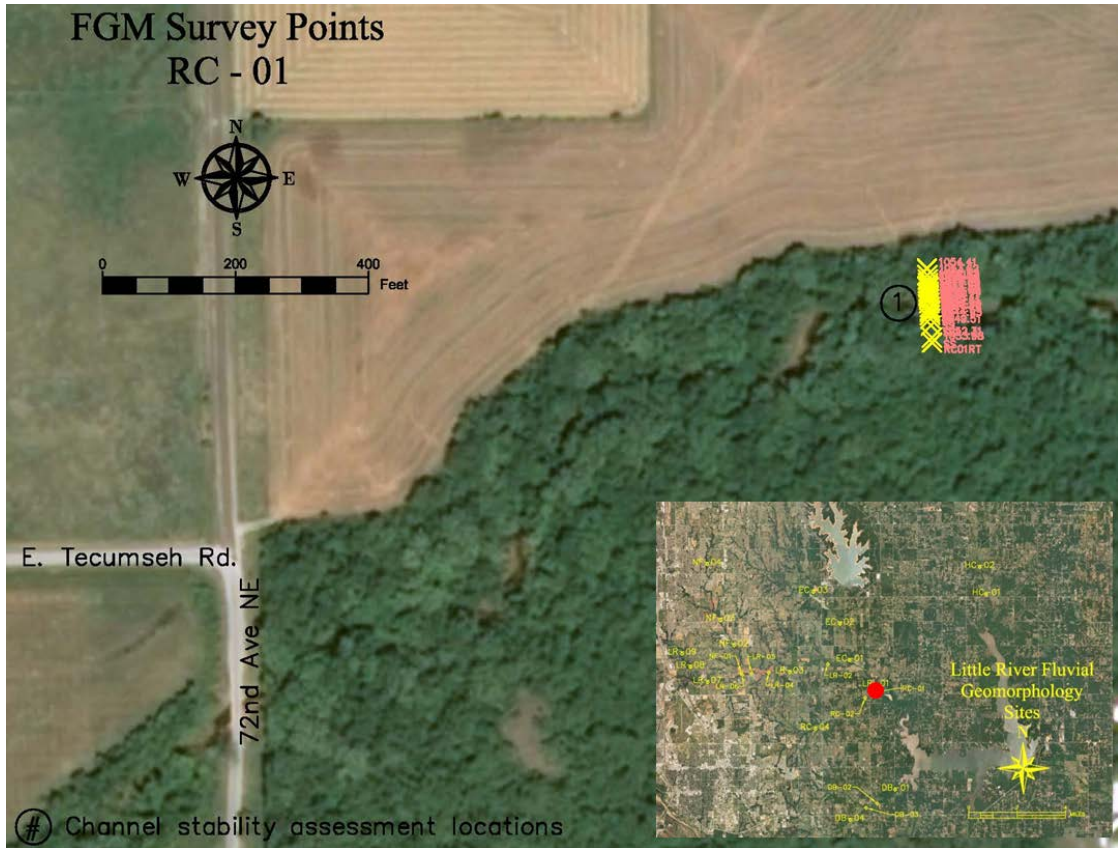


Figure E.17.1: FGM Site RC-01 Site Map with Survey Points.

Table E.17.1: FGM Site RC-01 Survey Control.

OK State Plane NAD83, South Zone (U.S. Ft); Ref. Elev. (U.S. Ft)			
Left Pin		Right Pin	
Name:	RC01LT	Name:	RC01RT
Easting:	702906.88	Easting:	702795.92
Northing:	2167887.00	Northing:	2167894.90
Ref. Elev.:	1054.41	Ref. Elev.:	1053.98
Geodetic Coordinates (Decimal Degrees)			
Left Pin		Right Pin	
Lat. (N):	35.2629	Lat. (N):	35.2626
Long. (W):	97.3321	Long. (W):	97.3321

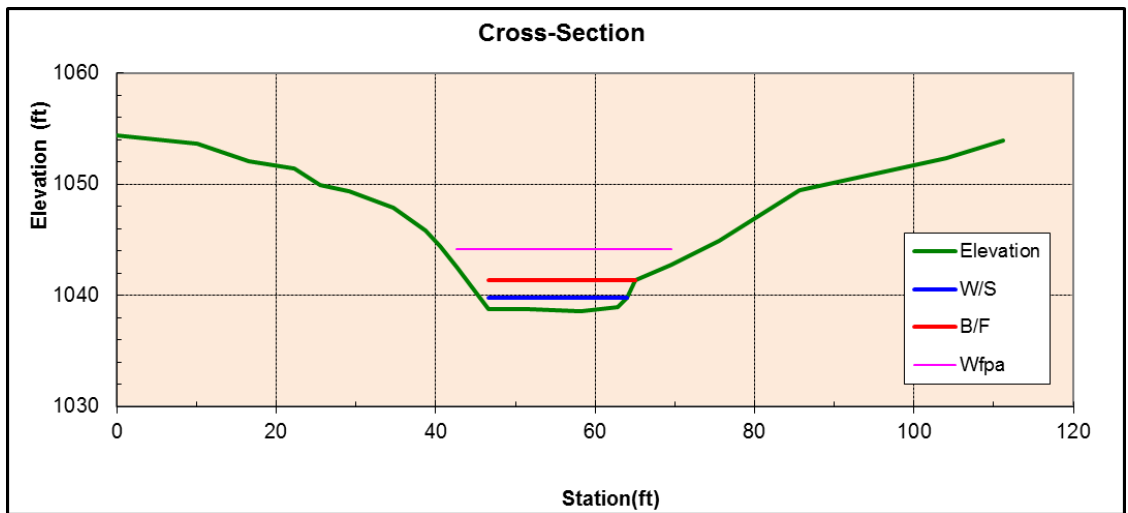


Figure E.17.2: FGM Site RC-01 Cross-section Survey Plot.

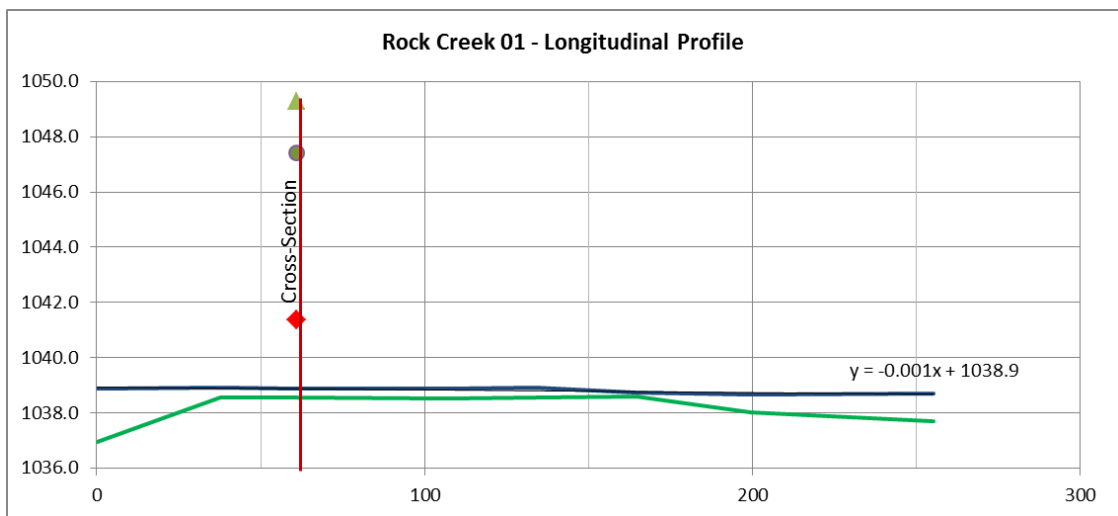


Figure E.17.3: FGM Site RC-01 Longitudinal Profile Survey Plot.

*Table E.17.2: FGM Site RC-01 Channel Morphology Summary.*

Bankfull Width (ft):	21.13
Mean Bankfull Depth (ft):	2.41
Maximum Bankfull Depth (ft):	2.76
Flood Prone Area Width (ft):	30.82
Bankfull Area (ft <sup>2</sup> ):	50.96
Entrenchment Ratio:	1.57
Width/Depth Ratio:	10.6
Sinuosity:	1.1
Slope:	0.001
Bed Material:	Sand
Rosgen Stream Type:	G5c
Channel Evolution Stage:	IV

*Table E.17.3: FGM Site RC-01 Stream Channel Stability Summary.*

Bank No.	1
CSI Score:	28
Rating:	Highly Unstable
Pfankuch Score:	117
Rating:	Poor-Unstable
BEHI Score:	31.5
Rating:	High
NBS Score:	***
Rating:	Low
OEBSI Score:	49.5
Rating:	Unstable



**E.18 FGM Site RC-02**

Site Name: RC-02

Drainage Area: 11.0 mi<sup>2</sup>

Site Legal Description: NE 1/4, Sect. 18, T9N-R1W, Cleveland Co.

FGM Survey Date: October 18, 2012 Stability Assessment: October 18, 2012

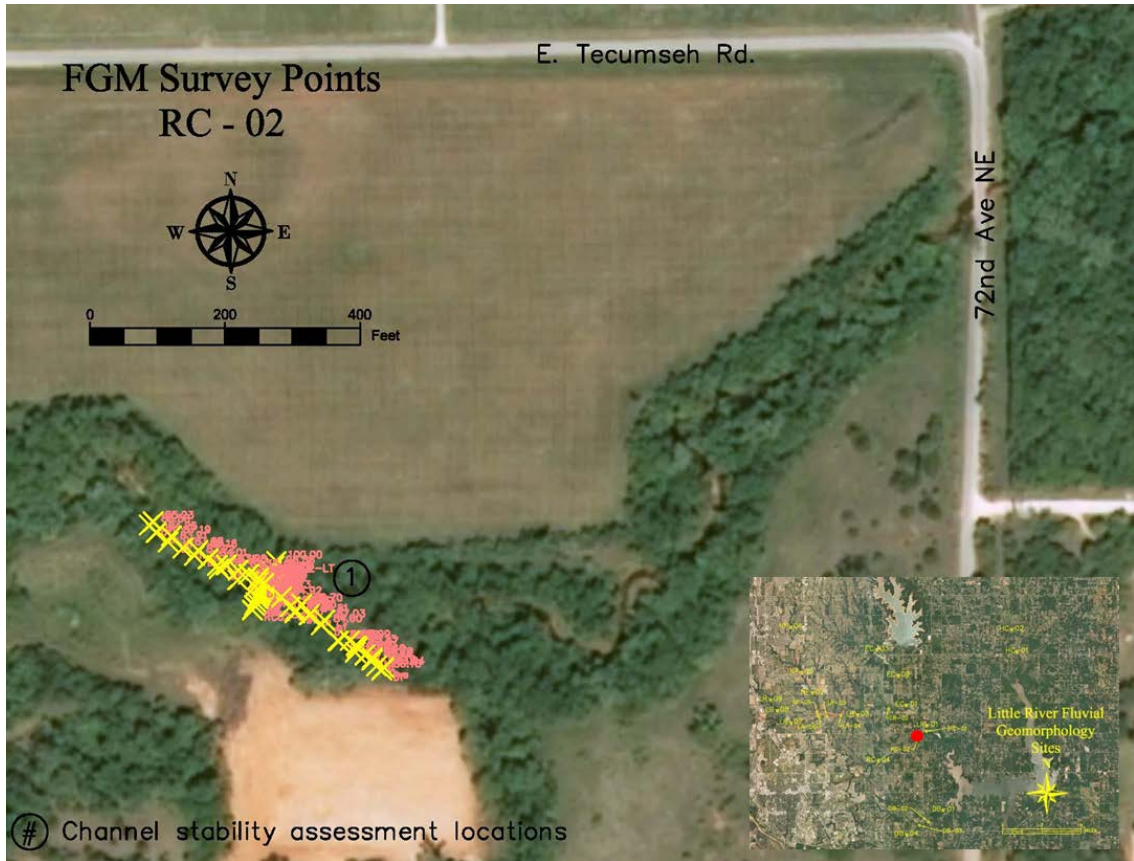


Figure E.18.1: FGM Site RC-02 Site Map with Survey Points.

Table E.18.1: FGM Site RC-02 Survey Control.

OK State Plane NAD83, South Zone (U.S. Ft); Ref. Elev. (U.S. Ft)			
Left Pin		Right Pin	
<b>Name:</b>	RC02-LT	<b>Name:</b>	RC02-RT
<b>Easting:</b>	2165806.70	<b>Easting:</b>	2165770.83
<b>Northing:</b>	701705.02	<b>Northing:</b>	701632.75
<b>Ref. Elev.:</b>	100.00	<b>Ref. Elev.:</b>	99.48
Geodetic Coordinates (Decimal Degrees)			
Left Pin		Right Pin	
<b>Lat. (N):</b>	35.2597	<b>Lat. (N):</b>	35.2595
<b>Long. (W):</b>	97.3391	<b>Long. (W):</b>	97.3392

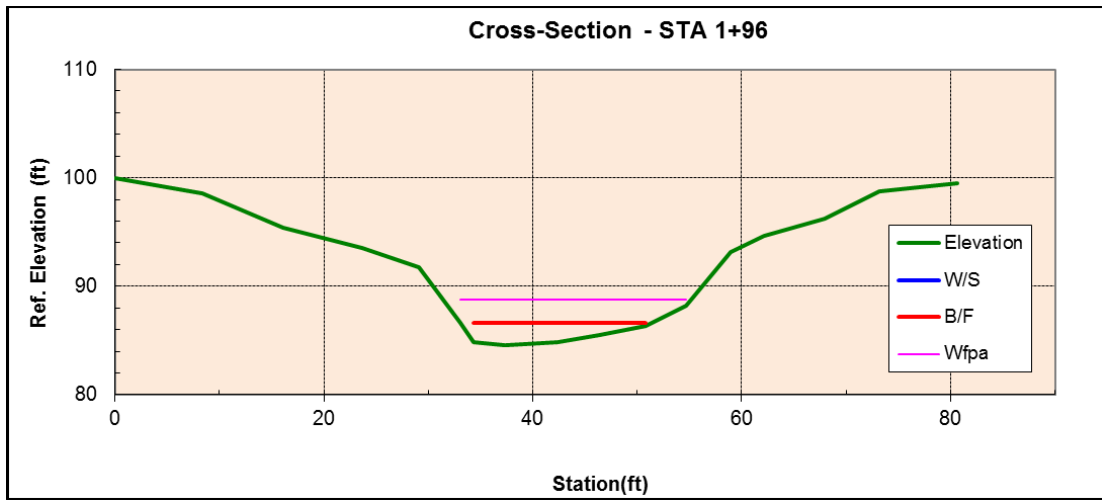


Figure E.18.2: FGM Site RC-02 Cross-section Survey Plot.

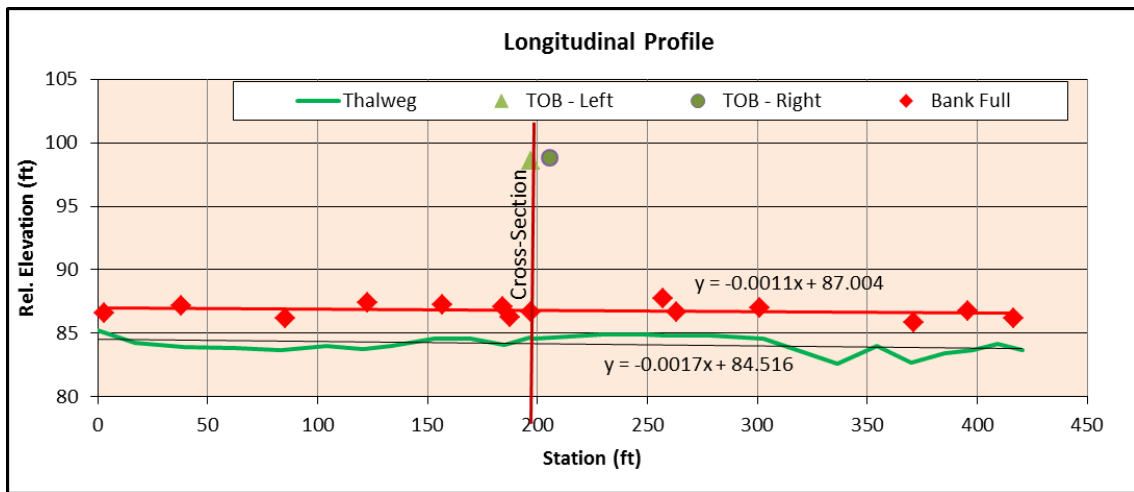


Figure E.18.3: FGM Site RC-02 Longitudinal Profile Survey Plot.

*Table E.18.2: FGM Site RC-02 Channel Morphology Summary.*

Bankfull Width (ft):	18.42
Mean Bankfull Depth (ft):	1.45
Maximum Bankfull Depth (ft):	2.10
Flood Prone Area Width (ft):	27.05
Bankfull Area (ft <sup>2</sup> ):	26.74
Entrenchment Ratio:	1.47
Width/Depth Ratio:	12.7
Sinuosity:	1.0
Slope:	0.0026
Bed Material:	Sand
Rosgen Stream Type:	B5c
Channel Evolution Stage:	IV

*Table E.18.3: FGM Site RC-02 Stream Channel Stability Summary.*

Bank No.	1
CSI Score:	25
Rating:	HIGHLY UNSTABLE
Pfankuch Score:	108
Rating:	Poor-Unstable
BEHI Score:	12.5
Rating:	Low
NBS Score:	***
Rating:	Extreme
OEBSI Score:	37
Rating:	Stable

**E.19 FGM Site RC-04**

Site Name: RC-04

Drainage Area: 5.9 mi<sup>2</sup>

Site Legal Description: NE 1/4, Sect. 23, T9N-R2W, Cleveland Co.

FGM Survey Date: March 21, 2013

Stability Assessment: February 13, 2015

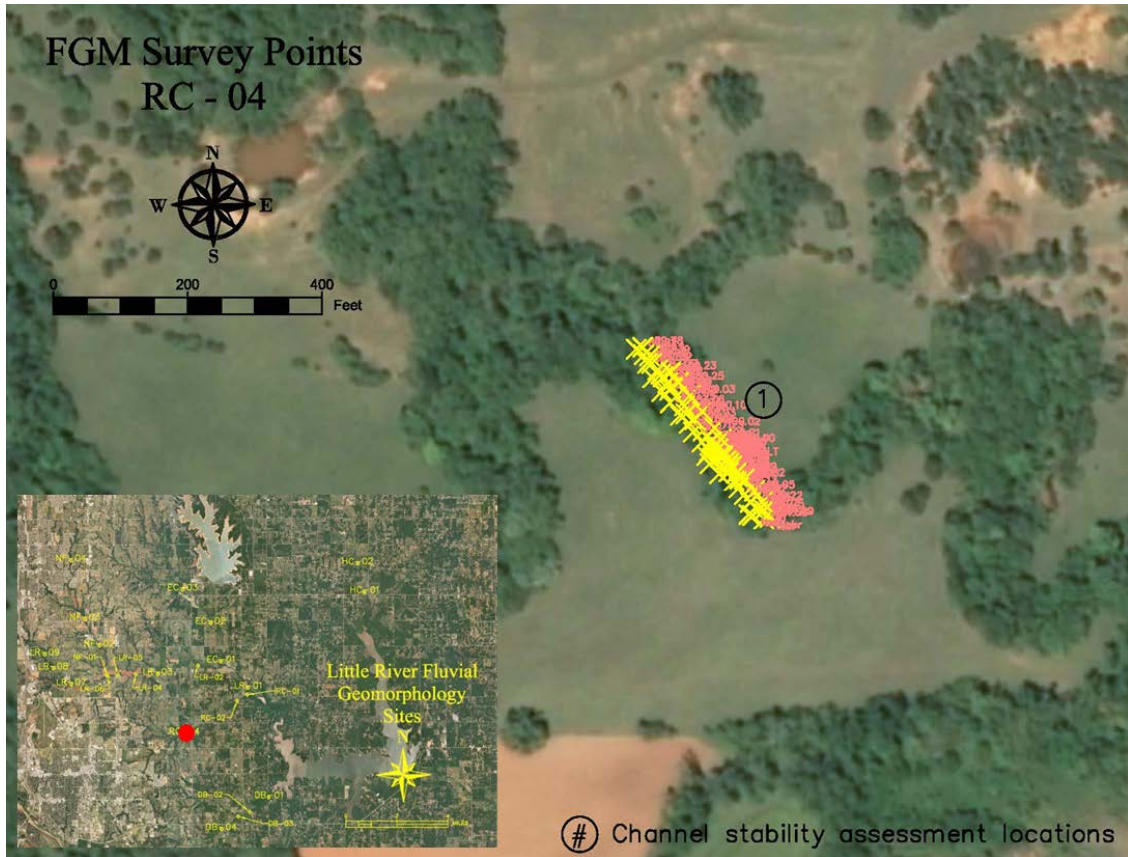


Figure E.19.1: FGM Site RC-04 Site Map with Survey Points.

Table E.19.1: FGM Site RC-04 Survey Control.

OK State Plane NAD83, South Zone (U.S. Ft); Ref. Elev. (U.S. Ft)			
Left Pin		Right Pin	
<b>Name:</b>	RC04LT	<b>Name:</b>	RC04RT
<b>Easting:</b>	2154975.31	<b>Easting:</b>	2154946.31
<b>Northing:</b>	694894.76	<b>Northing:</b>	694866.55
<b>Ref. Elev.:</b>	100.00	<b>Ref. Elev.:</b>	99.52
Geodetic Coordinates (Decimal Degrees)			
Left Pin		Right Pin	
<b>Lat. (N):</b>	35.2412	<b>Lat. (N):</b>	35.2411
<b>Long. (W):</b>	97.3755	<b>Long. (W):</b>	97.3756

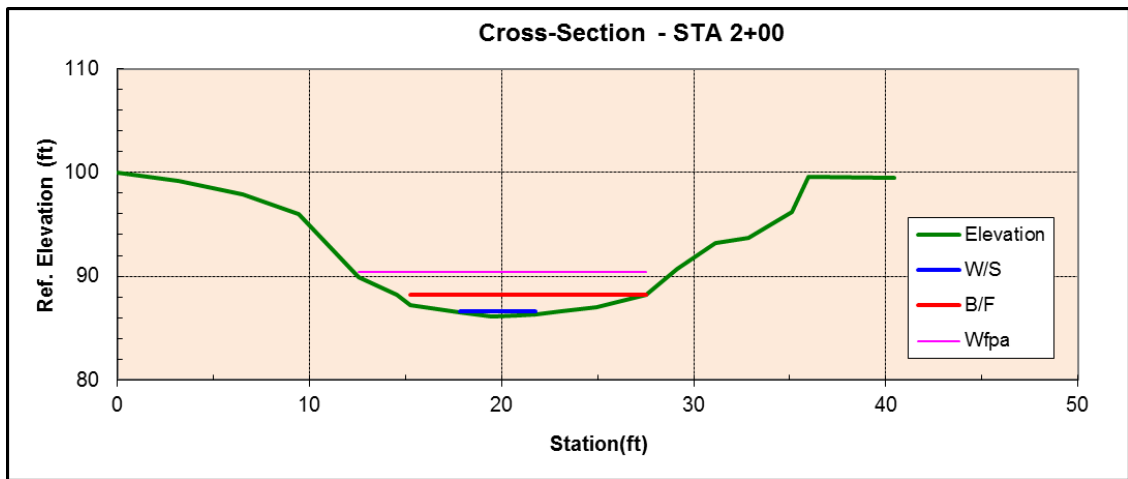


Figure E.19.2: FGM Site RC-04 Cross-section Survey Plot.

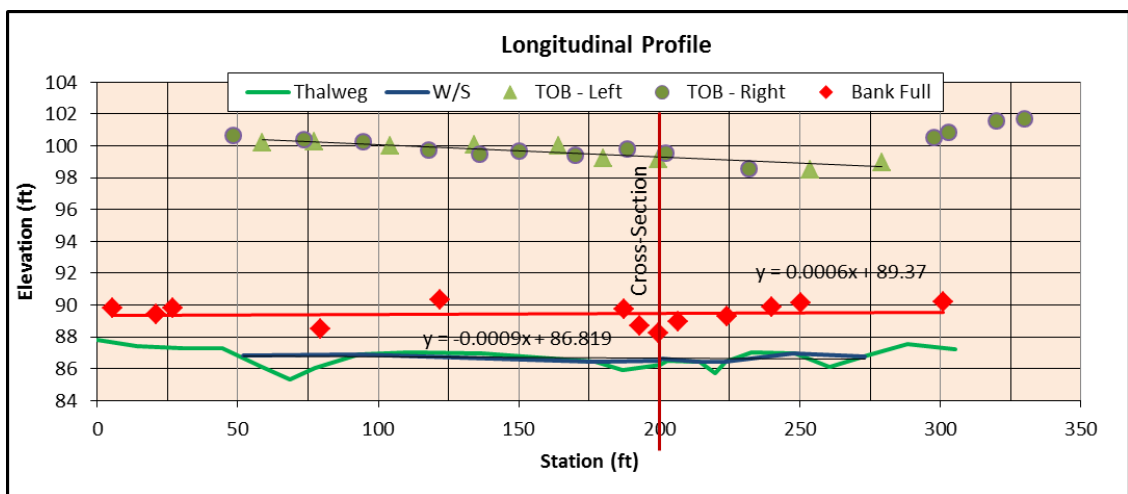


Figure E.19.3: FGM Site RC-04 Longitudinal Profile Survey Plot.

Table E.19.2: FGM Site RC-04 Channel Morphology Summary.

Bankfull Width (ft):	13.02
Mean Bankfull Depth (ft):	1.40
Maximum Bankfull Depth (ft):	2.14
Flood Prone Area Width (ft):	15.39
Bankfull Area (ft <sup>2</sup> ):	18.28
Entrenchment Ratio:	1.18
Width/Depth Ratio:	9.3
Sinuosity:	1.04
Slope:	0.0019
Bed Material:	Sand
Rosgen Stream Type:	G5c
Channel Evolution Stage:	III

Table E.19.3: FGM Site RC-04 Stream Channel Stability Summary.

Bank No.	1
CSI Score:	27
Rating:	Highly Unstable
Pfankuch Score:	117
Rating:	Poor-Unstable
BEHI Score:	48
Rating:	Extreme
NBS Score:	***
Rating:	Low
OEBSI Score:	60
Rating:	Highly Unstable



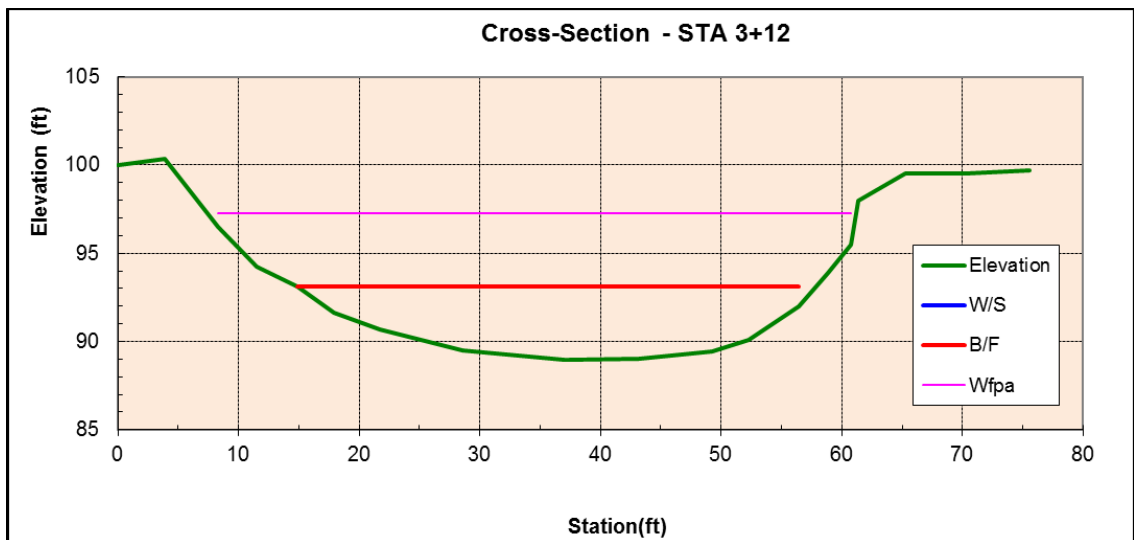


Figure E.20.2: FGM Site DBC-01 Cross-section Survey Plot.

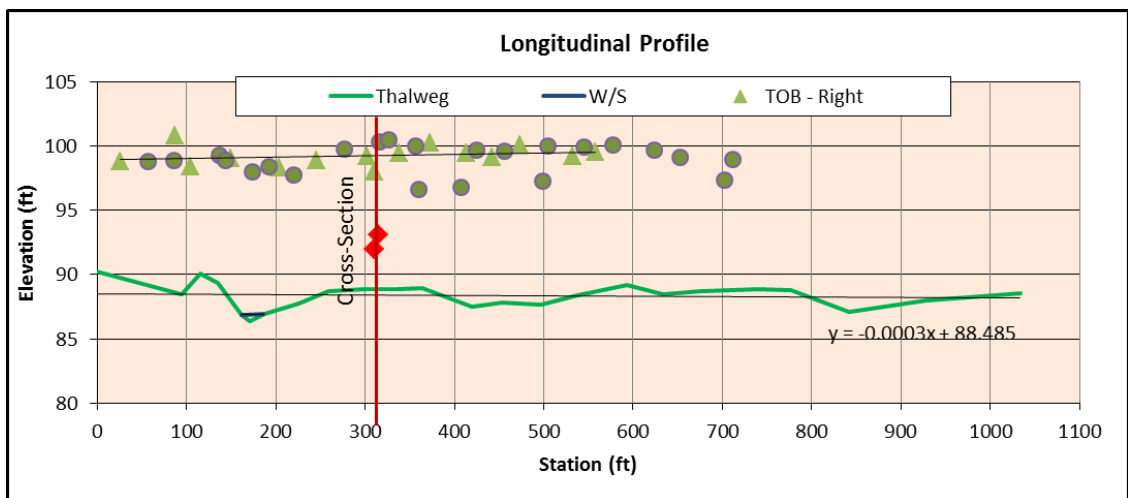


Figure E.20.3: FGM Site DBC-01 Longitudinal Profile Survey Plot.



Table E.20.2: FGM Site DBC-01 Channel Morphology Summary.

Bankfull Width (ft):	42.98
Mean Bankfull Depth (ft):	3.10
Maximum Bankfull Depth (ft):	4.17
Flood Prone Area Width (ft):	53.50
Bankfull Area (ft <sup>2</sup> ):	133.09
Entrenchment Ratio:	1.24
Width/Depth Ratio:	13.9
Sinuosity:	1.0
Slope:	0.0016
Bed Material:	Sand
Rosgen Stream Type:	B5c
Channel Evolution Stage:	IV

Table E.20.3: FGM Site DBC-01 Stream Channel Stability Summary.

Bank No.	1
CSI Score:	19
Rating:	MODERATELY STABLE
Pfankuch Score:	71
Rating:	Good - Stable
BEHI Score:	26.5
Rating:	Moderate
NBS Score:	***
Rating:	Low
OEBSI Score:	37
Rating:	Stable

**E.21 FGM Site DBC-02**

Site Name: DBC-02

Drainage Area: 18.7 mi<sup>2</sup>

Site Legal Description: SW 1/4, Sect. 5, T8N-R1W, Cleveland Co.

FGM Survey Date: September 4, 2012

Stability Assessment: September 4, 2012

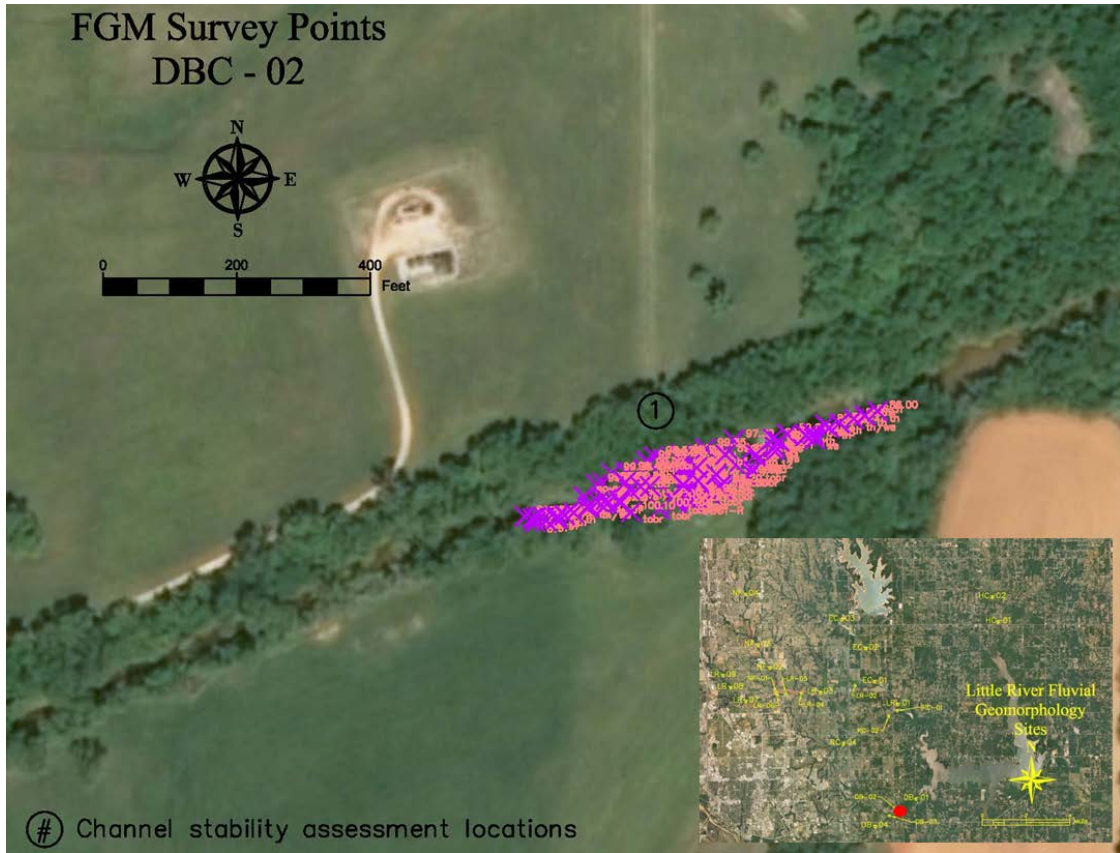


Figure E.21.1: FGM Site DBC-02 Site Map with Survey Points.

Table E.21.1: FGM Site DBC-02 Survey Control.

OK State Plane NAD83, South Zone (U.S. Ft); Ref. Elev. (U.S. Ft)			
<b>Left Pin</b>		<b>Right Pin</b>	
<b>Name:</b>	DBC02-LT	<b>Name:</b>	DBC02-RT
<b>Easting:</b>	2168434.38	<b>Easting:</b>	2168449.33
<b>Northing:</b>	678684.85	<b>Northing:</b>	678611.78
<b>Ref. Elev.:</b>	100.00	<b>Ref. Elev.:</b>	101.12
Geodetic Coordinates (Decimal Degrees)			
<b>Left Pin</b>		<b>Right Pin</b>	
<b>Lat. (N):</b>	35.1964	<b>Lat. (N):</b>	35.1962
<b>Long. (W):</b>	97.3308	<b>Long. (W):</b>	97.3308

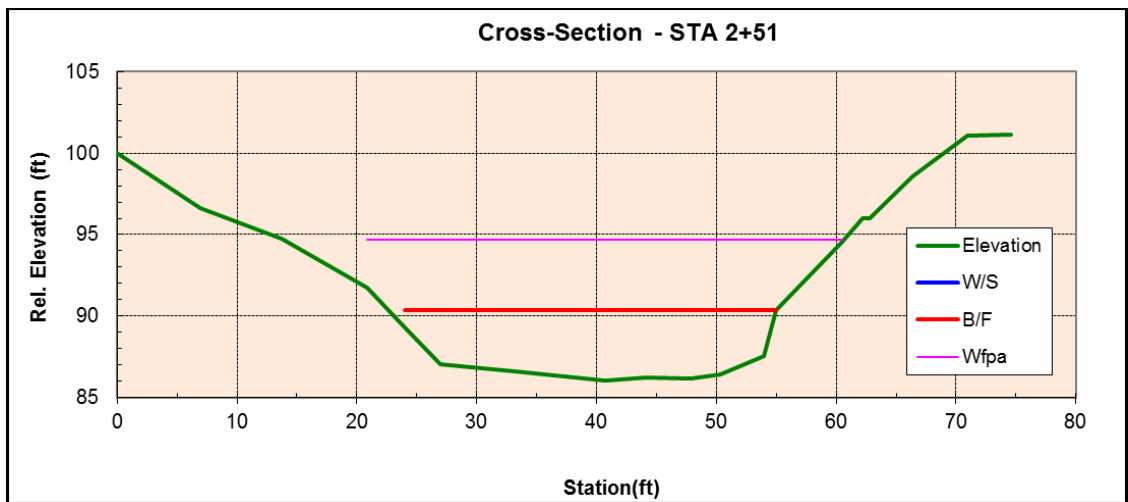


Figure E.21.2: FGM Site DBC-02 Cross-section Survey Plot.

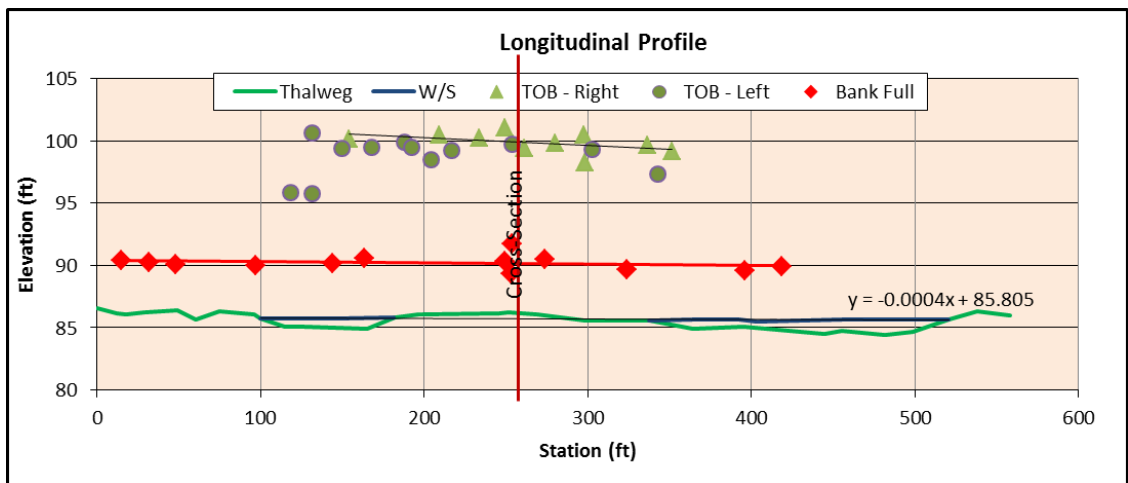


Figure E.21.3: FGM Site DBC-02 Longitudinal Profile Survey Plot.

*Table E.21.2: FGM Site DBC-02 Channel Morphology Summary.*

Bankfull Width (ft):	32.34
Mean Bankfull Depth (ft):	3.53
Maximum Bankfull Depth (ft):	4.30
Flood Prone Area Width (ft):	48.09
Bankfull Area (ft <sup>2</sup> ):	114.24
Entrenchment Ratio:	1.49
Width/Depth Ratio:	9.2
Sinuosity:	1.00
Slope:	0.0010
Bed Material:	Sand
Rosgen Stream Type:	G5c
Channel Evolution Stage:	III

*Table E.21.3: FGM Site DBC-02 Stream Channel Stability Summary.*

Bank No.	1
CSI Score:	19
Rating:	Moderately Stable
Pfankuch Score:	71
Rating:	Good - Stable
BEHI Score:	26.5
Rating:	Moderate
NBS Score:	***
Rating:	Low
OEBSI Score:	37
Rating:	Stable

**E.22 FGM Site DBC-03**

Site Name: DBC-03

Drainage Area: 13.2 mi<sup>2</sup>

Site Legal Description: SE 1/4, Sect. 6, T8N-R1W, Cleveland Co.

FGM Survey Date: January 23, 2013

Stability Assessment: January 23, 2013

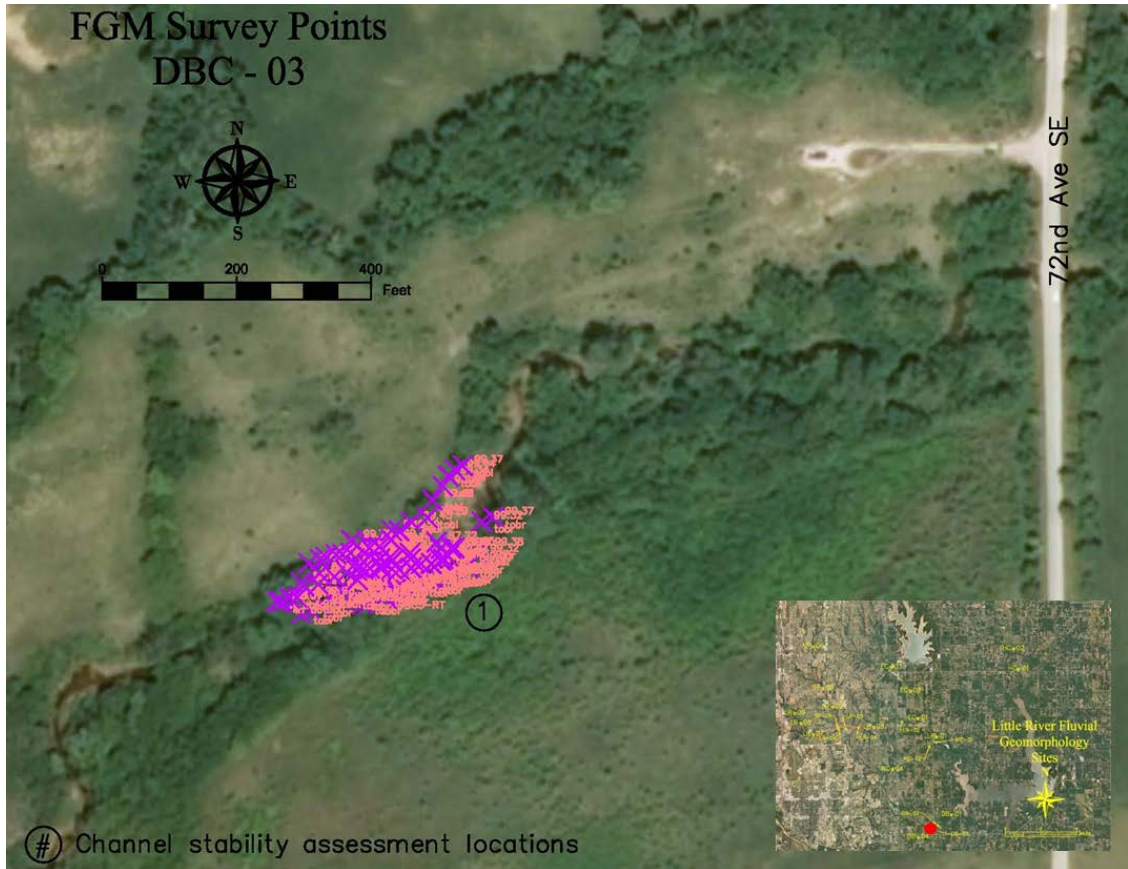


Figure E.22.1: FGM Site DBC-03 Site Map with Survey Points.

Table E.22.1: FGM Site DBC-03 Survey Control.

OK State Plane NAD83, South Zone (U.S. Ft); Ref. Elev. (U.S. Ft)			
<b>Left Pin</b>		<b>Right Pin</b>	
<b>Name:</b>	DBC3-LT	<b>Name:</b>	DBC3-RT
<b>Easting:</b>	2166029.15	<b>Easting:</b>	2166049.70
<b>Northing:</b>	677769.94	<b>Northing:</b>	677691.63
<b>Ref. Elev.:</b>	100.00	<b>Ref. Elev.:</b>	99.40
Geodetic Coordinates (Decimal Degrees)			
<b>Left Pin</b>		<b>Right Pin</b>	
<b>Lat. (N):</b>	35.1939	<b>Lat. (N):</b>	35.1937
<b>Long. (W):</b>	97.3389	<b>Long. (W):</b>	97.3388

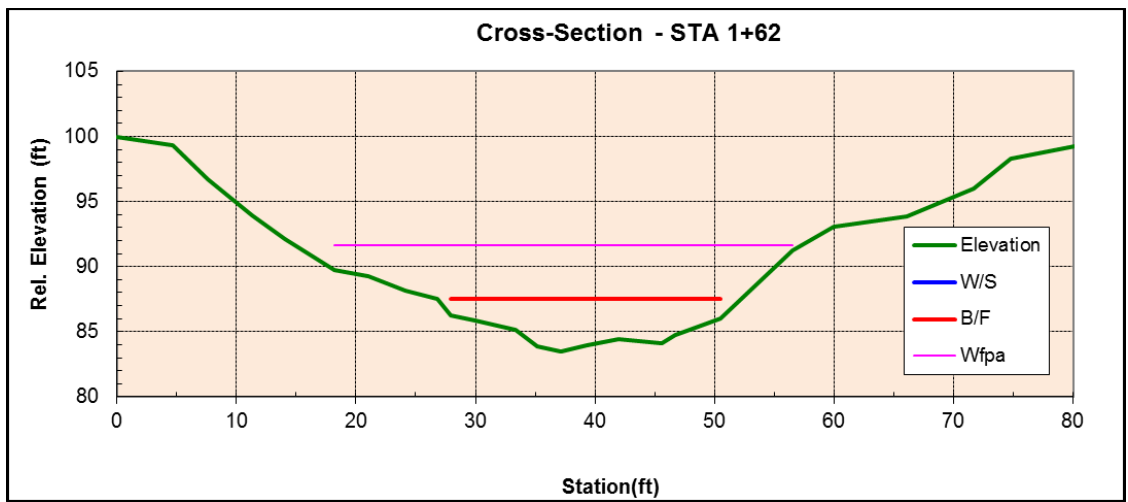


Figure E.22.2: FGM Site DBC-03 Cross-section Survey Plot.

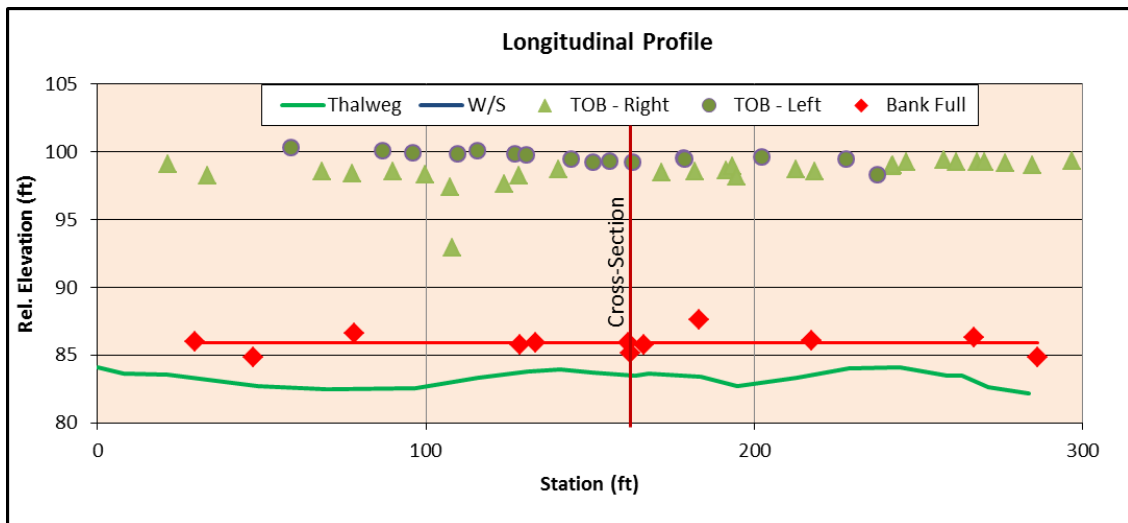


Figure E.22.3: FGM Site DBC-03 Longitudinal Profile Survey Plot.

*Table E.22.2: FGM Site DBC-03 Channel Morphology Summary.*

Bankfull Width (ft):	25.40
Mean Bankfull Depth (ft):	2.72
Maximum Bankfull Depth (ft):	4.06
Flood Prone Area Width (ft):	44.47
Bankfull Area (ft <sup>2</sup> ):	69.14
Entrenchment Ratio:	1.75
Width/Depth Ratio:	9.3
Sinuosity:	1.05
Slope:	0.0067
Bed Material:	Sand
Rosgen Stream Type:	G5c
Channel Evolution Stage:	III

*Table E.22.3: FGM Site DBC-03 Stream Channel Stability Summary.*

Bank No.	1
CSI Score:	23
Rating:	Highly Unstable
Pfankuch Score:	85
Rating:	Good - Stable
BEHI Score:	18.5
Rating:	Low
NBS Score:	***
Rating:	Moderate
OEBSI Score:	39.5
Rating:	Stable

**E.23 FGM Site DBC-04**

Site Name: DBC-04

Drainage Area: 10.7 mi<sup>2</sup>

Site Legal Description: NW 1/4, Sect. 7, T8N-R1W, Cleveland Co.

FGM Survey Date: March 18, 2013

Stability Assessment: March 18, 2013

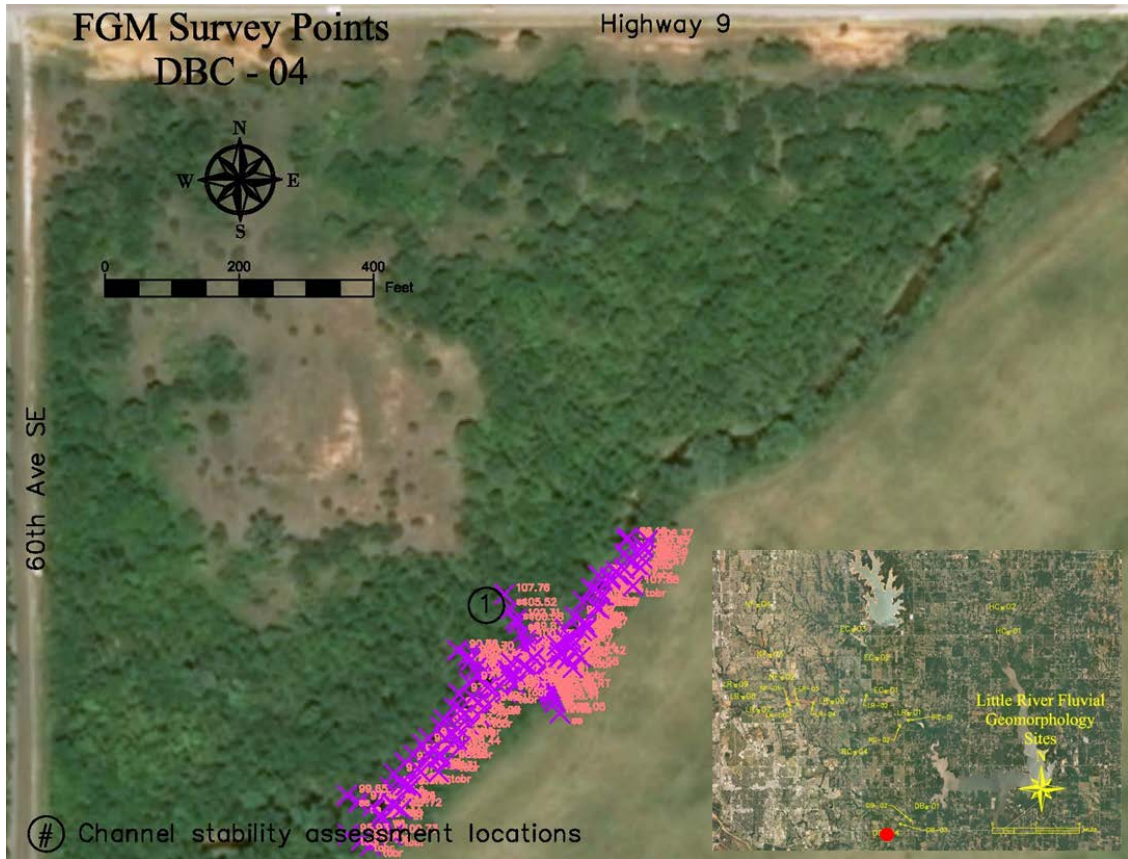


Figure E.23.1: FGM Site DBC-04 Site Map with Survey Points.

Table E.23.1: FGM Site DBC-04 Survey Control.

OK State Plane NAD83, South Zone (U.S. Ft); Ref. Elev. (U.S. Ft)			
Left Pin		Right Pin	
Name:	DBC-4-LT	Name:	DBC-4-RT
Easting:	2162574.17	Easting:	2162599.44
Northing:	675115.81	Northing:	675061.56
Ref. Elev.:	100.00	Ref. Elev.:	98.22
Geodetic Coordinates (Decimal Degrees)			
Left Pin		Right Pin	
Lat. (N):	35.1867	Lat. (N):	35.1865
Long. (W):	97.3505	Long. (W):	97.3504



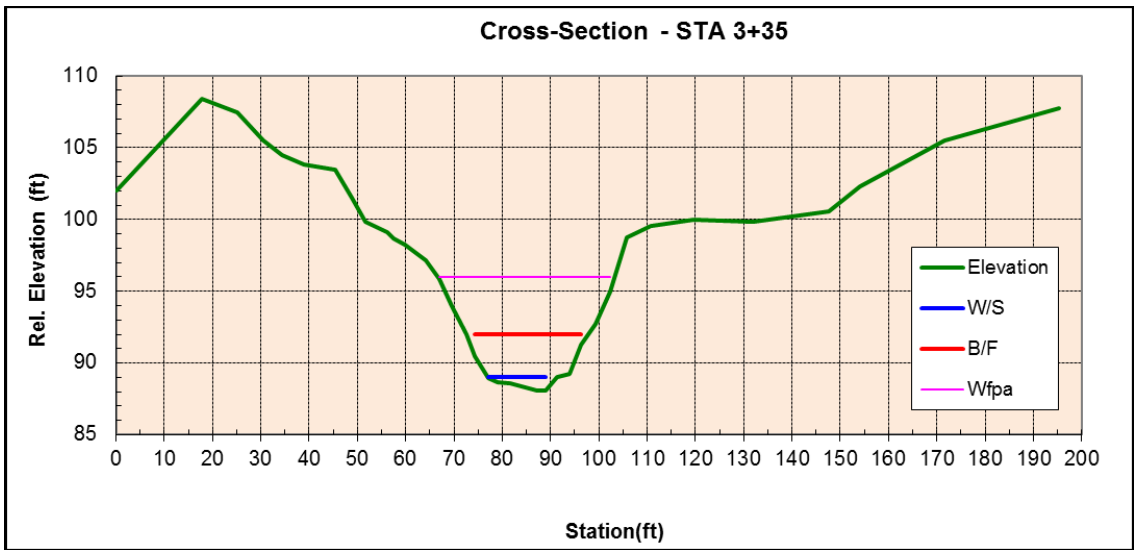


Figure E.23.2: FGM Site DBC-04 Cross-section Survey Plot.

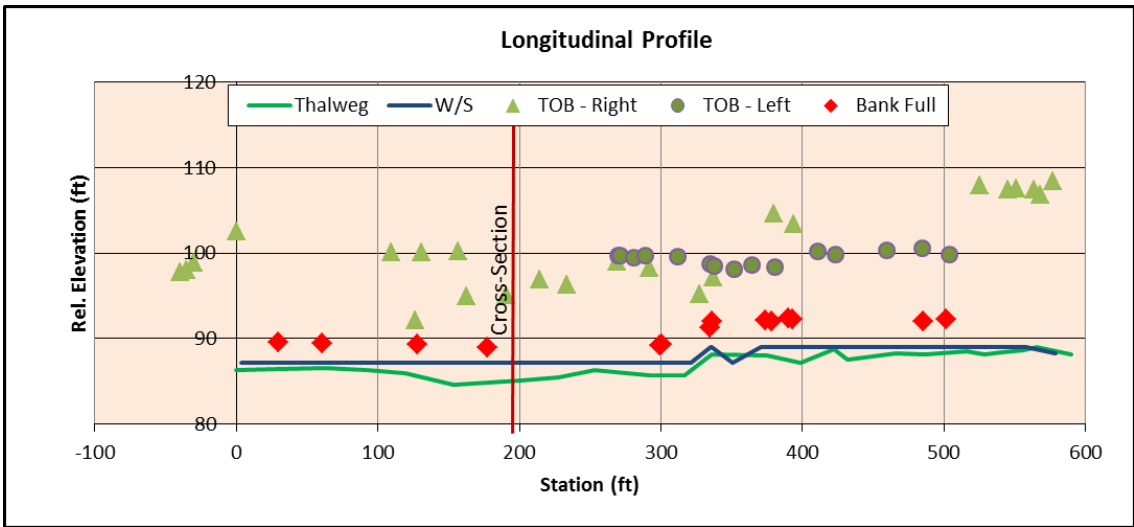


Figure E.23.3: FGM Site DBC-04 Longitudinal Profile Survey Plot.

*Table E.23.2: FGM Site DBC-04 Channel Morphology Summary.*

Bankfull Width (ft):	25.40
Mean Bankfull Depth (ft):	2.81
Maximum Bankfull Depth (ft):	3.93
Flood Prone Area Width (ft):	38.12
Bankfull Area (ft <sup>2</sup> ):	71.31
Entrenchment Ratio:	1.50
Width/Depth Ratio:	9.0
Sinuosity:	1.05
Slope:	-0.0031
Bed Material:	Bedrock/Sand
Rosgen Stream Type:	G1c/G5c
Channel Evolution Stage:	III

*Table E.23.3: FGM Site DBC-04 Stream Channel Stability Summary.*

Bank No.	1
CSI Score:	21
Rating:	Highly Unstable
Pfankuch Score:	83
Rating:	Poor- Unstable
BEHI Score:	27.5
Rating:	Moderate
NBS Score:	***
Rating:	Very High
OEBSI Score:	57
Rating:	Highly Unstable



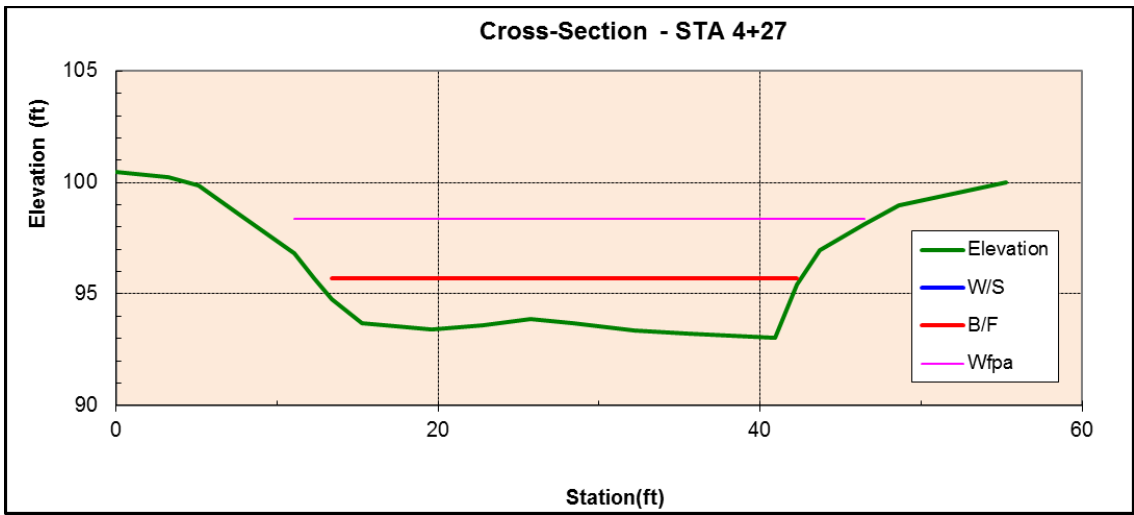


Figure E.24.2: FGM Site HC-01 Cross-section Survey Plot.

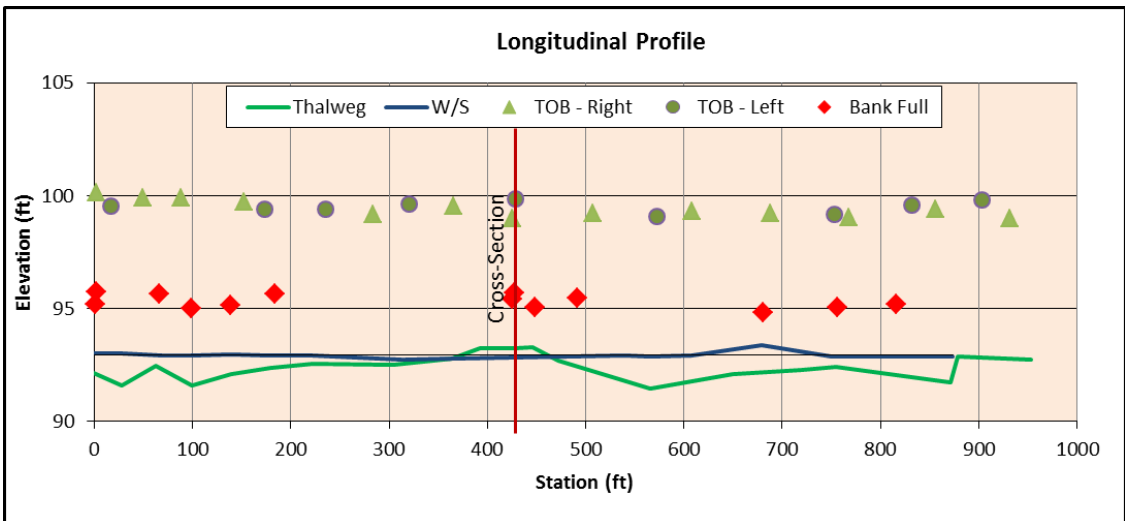


Figure E.24.3: FGM Site HC-01 Longitudinal Profile Survey Plot.

Table E.24.2: FGM Site HC-01 Channel Morphology Summary.

Bankfull Width (ft):	30.22
Mean Bankfull Depth (ft):	2.07
Maximum Bankfull Depth (ft):	2.65
Flood Prone Area Width (ft):	39.97
Bankfull Area (ft <sup>2</sup> ):	62.52
Entrenchment Ratio:	1.32
Width/Depth Ratio:	14.6
Sinuosity:	1.01
Slope:	0.0002
Bed Material:	Sand
Rosgen Stream Type:	FU5
Channel Evolution Stage:	II

Table E.24.3: FGM Site HC-01 Stream Channel Stability Summary.

Bank No.	1
CSI Score:	16
Rating:	MODERATELY STABLE
Pfankuch Score:	71
Rating:	Good - Stable
BEHI Score:	11.5
Rating:	Low
NBS Score:	***
Rating:	Low
OEBSI Score:	37
Rating:	Stable

**E.25 FGM Site HC-02**

Site Name: HC-02

Drainage Area: 38.6 mi<sup>2</sup>

Site Legal Description: SE 1/4, Sect. 13, T10N-R1W, Cleveland Co.

FGM Survey Date: August 28, 2012

Stability Assessment: August 28, 2012

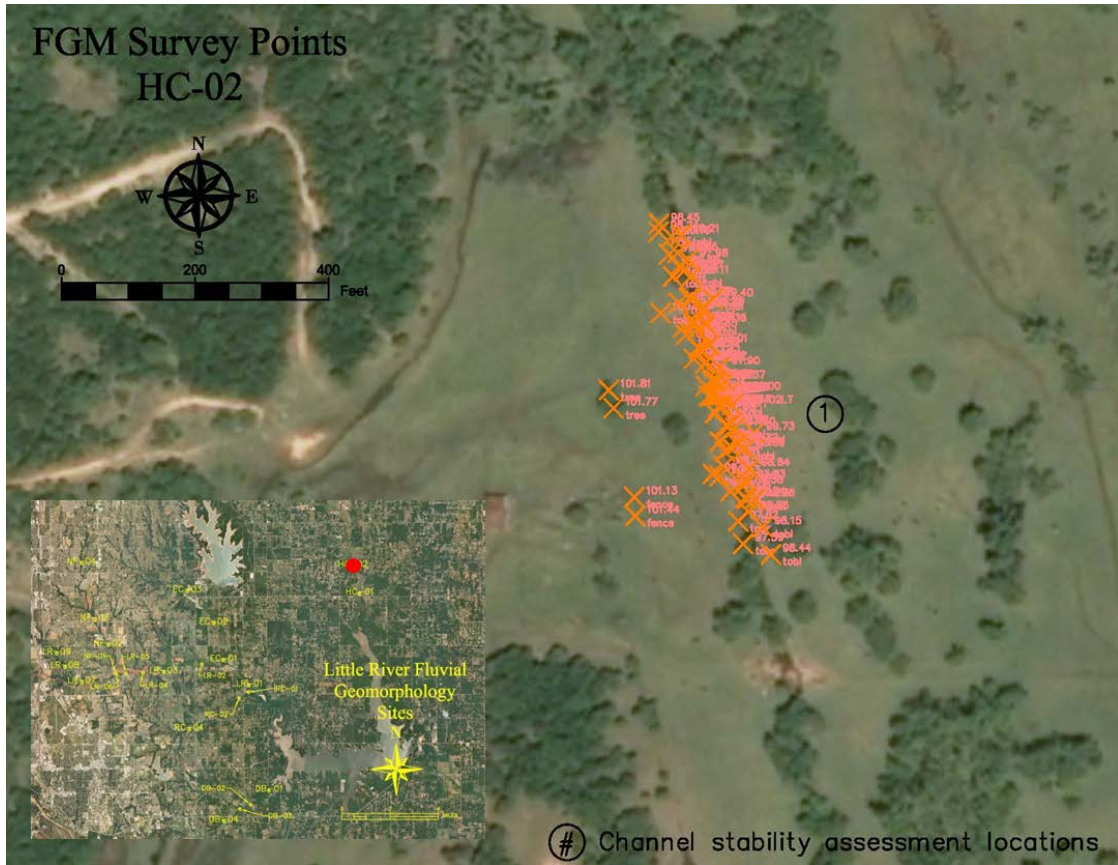


Figure E.25.1: FGM Site HC-02 Site Map with Survey Points.

Table E.25.1: FGM Site HC-02 Survey Control.

OK State Plane NAD83, South Zone (U.S. Ft); Ref. Elev. (U.S. Ft)			
Left Pin		Right Pin	
Name:	HC-02LT	Name:	HC-02RT
Easting:	2190784.11	Easting:	2190744.25
Northing:	730074.62	Northing:	730069.03
Ref. Elev.:	100.00	Ref. Elev.:	98.25
Geodetic Coordinates (Decimal Degrees)			
Left Pin		Right Pin	
Lat. (N):	35.3371	Lat. (N):	35.3371
Long. (W):	97.2548	Long. (W):	97.2549

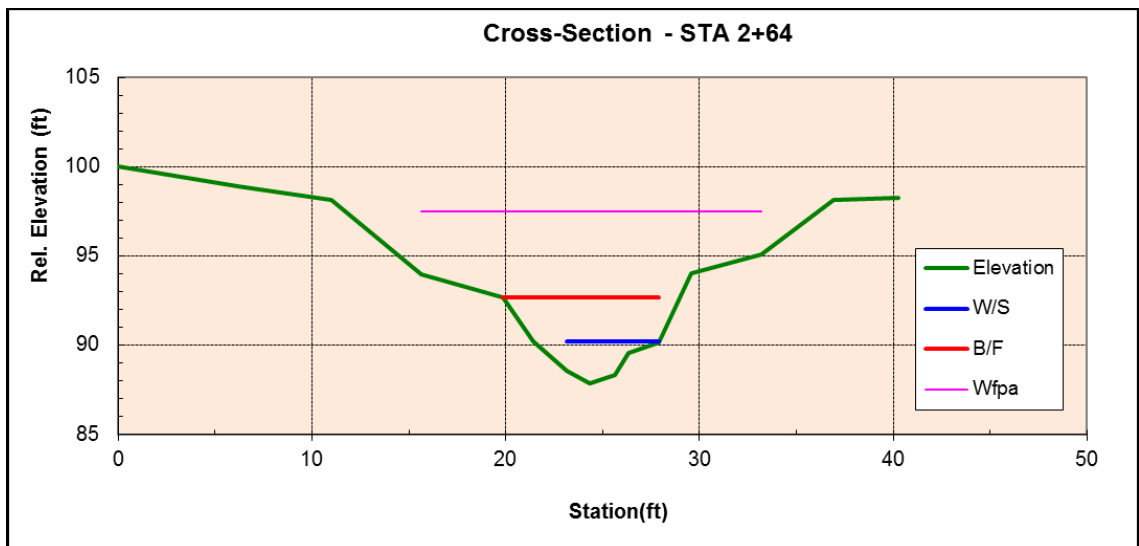


Figure E.25.2: FGM Site HC-02 Cross-section Survey Plot.

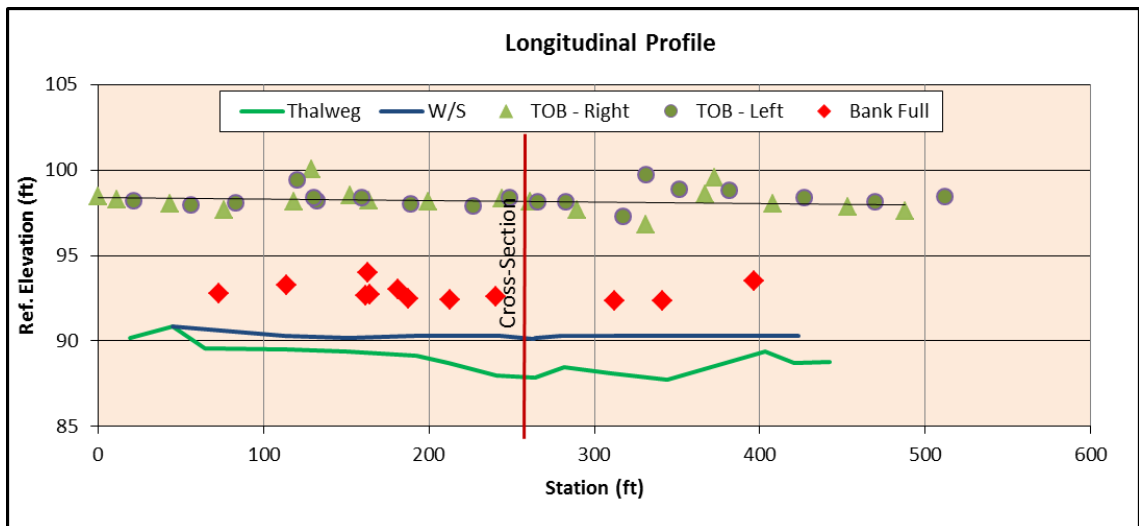


Figure E.25.3: FGM Site HC-02 Longitudinal Profile Survey Plot.

*Table E.25.2: FGM Site HC-02 Channel Morphology Summary.*

Bankfull Width (ft):	9.16
Mean Bankfull Depth (ft):	3.06
Maximum Bankfull Depth (ft):	4.81
Flood Prone Area Width (ft):	22.29
Bankfull Area (ft <sup>2</sup> ):	28.07
Entrenchment Ratio:	2.43
Width/Depth Ratio:	3.0
Sinuosity:	1.00
Slope:	0.0014
Bed Material:	Clay
Rosgen Stream Type:	E6
Channel Evolution Stage:	III

*Table E.25.3: FGM Site HC-02 Stream Channel Stability Summary.*

Bank No.	1
CSI Score:	18
Rating:	MODERATELY STABLE
Pfankuch Score:	87
Rating:	Fair-Mod. Unstable
BEHI Score:	32.5
Rating:	High
NBS Score:	***
Rating:	Very Low
OEBSI Score:	52.5
Rating:	Unstable



## F. Appendix F – FGM Site Photographs

### F.1 FGM Site LR-01



*Figure F.1.1: FGM Site LR-01 – Looking upstream (lt); Looking downstream (rt).*



*Figure F.1.2: FGM Site LR-01 – Right Bank.*

## F.2 FGM Site LR-02



*Figure F.2.1: FGM Site LR-02 – Cross Section - Looking upstream (lt); Looking downstream (rt).*



*Figure F.2.2: FGM Site LR-02 – Cross Section - Left Bank (lt) – Right bank (rt).*



*Figure F.2.3: FGM Site LR-02 – Bank 1 - Bank (lt) – Looking upstream (rt).*



*Figure F.2.4: FGM Site LR-02 – Bank 1 - Facing downstream (lt); Bank 2 - Bank (rt).*



*Figure F.2.5: FGM Site LR-02 – Bank 2 - Facing upstream (lt); Facing downstream (rt).*



*Figure F.2.6: FGM Site LR-02 – Bank 3 - Bank (lt); Facing upstream (rt).*



*Figure F.2.7: FGM Site LR-02 – Bank 3 – Facing downstream (lt); Bank 4 - Bank (rt).*



*Figure F.2.8: FGM Site LR-02 – Bank 4 – Facing upstream (lt); Facing downstream (rt).*

### F.3 FGM Site LR-03



*Figure F.3.1: FGM Site LR-03 – Cross Section - Looking upstream (lt); Looking downstream (rt).*



*Figure F.3.2: FGM Site LR-03 – Cross Section - Left Bank (lt) – Right bank (rt).*



*Figure F.3.3: FGM Site LR-03 – Bank 1 - Bank (lt) – Looking upstream (rt).*



*Figure F.3.4: FGM Site LR-03 – Bank 1-Facing downstream (lt); Bank 2-Bank (rt).*



*Figure F.3.5: FGM Site LR-03 – Bank 2-Facing upstream (lt); Facing downstream (rt).*



*Figure F.3.6: FGM Site LR-03 – Bank 3 - Bank (lt); Facing upstream (rt).*



*Figure F.3.7: FGM Site LR-03 – Bank 3–Facing downstream (lt); Bank 4-Bank (rt).*



*Figure F.3.8: FGM Site LR-03 – Bank 4–Facing upstream (lt); Facing downstream (rt).*

#### F.4 FGM Site LR-04



*Figure F.4.1: FGM Site LR-04 – Cross Section - Looking upstream (lt); Looking downstream (rt).*



*Figure F.4.2: FGM Site LR-04 – Cross Section - Left Bank (lt) – Right bank (rt).*



*Figure F.4.3: FGM Site LR-04 – Bank 1 - Bank (lt) – Looking upstream (rt).*





*Figure F.4.4: FGM Site LR-04 – Bank 1-Facing downstream (lt); Bank 2-Bank (rt).*



*Figure F.4.5: FGM Site LR-04–Bank 2-Facing upstream (lt);Facing downstream (rt).*



*Figure F.4.6: FGM Site LR-04 – Bank 3 - Bank (lt); Facing upstream (rt).*



*Figure F.4.7: FGM Site LR-04 – Bank 3–Facing downstream (lt); Bank 4-Bank (rt).*



*Figure F.4.8: FGM Site LR-04-Bank 4–Facing upstream (lt);Facing downstream (rt).*

## F.5 FGM Site LR-05



*Figure F.5.1: FGM Site LR-05 – Cross Section - Looking upstream (lt); Looking downstream (rt).*



*Figure F.5.2: FGM Site LR-05 – Cross Section - Left Bank (lt) – Right bank (rt).*



*Figure F.5.3: FGM Site LR-05 – Bank 1 - Bank (lt) – Looking upstream (rt).*



*Figure F.5.4: FGM Site LR-05 – Bank 1-Facing downstream (lt); Bank 2-Bank (rt).*



*Figure F.5.5: FGM Site LR-05–Bank 2-Facing upstream (lt);Facing downstream (rt).*



*Figure F.5.6: FGM Site LR-05 – Bank 3 - Bank (lt); Facing upstream (rt).*



*Figure F.5.7: FGM Site LR-05 – Bank 3–Facing downstream (lt); Bank 4-Bank (rt).*



*Figure F.5.8: FGM Site LR-05-Bank 4–Facing upstream (lt);Facing downstream (rt).*

## F.6 FGM Site LR-06



*Figure F.6.1: FGM Site LR-06 – Cross Section - Looking upstream (lt); Looking downstream (rt).*



*Figure F.6.2: FGM Site LR-06 – Cross Section - Left Bank (lt) – Right bank (rt).*



*Figure F.6.3: FGM Site LR-06 – Bank 1 - Bank (lt) – Looking upstream (rt).*



*Figure F.6.4: FGM Site LR-06 – Bank 1-Facing downstream (lt); Bank 2-Bank (rt).*



*Figure F.6.5: FGM Site LR-06–Bank 2-Facing upstream (lt);Facing downstream (rt).*



*Figure F.6.6: FGM Site LR-06 – Bank 3 - Bank (lt); Facing upstream (rt).*



*Figure F.6.7: FGM Site LR-06 – Bank 3–Facing downstream (lt); Bank 4-Bank (rt).*



*Figure F.6.8: FGM Site LR-06-Bank 4–Facing upstream (lt);Facing downstream (rt).*



**F.7 FGM Site LR-07**



*Figure F.7.1: FGM Site LR-07 – Cross Section - Looking upstream (lt); Looking downstream (rt).*



*Figure F.7.2: FGM Site LR-07 – Cross Section - Left Bank (lt) – Right bank (rt).*



*Figure F.7.3: FGM Site LR-07 – Bank 1 - Bank (lt) – Looking upstream (rt).*



*Figure F.7.4: FGM Site LR-07 – Bank 1-Facing downstream (lt); Bank 2-Bank (rt).*



*Figure F.7.5: FGM Site LR-07–Bank 2-Facing upstream (lt);Facing downstream (rt).*



*Figure F.7.6: FGM Site LR-07 – Bank 3 - Bank (lt); Facing upstream (rt).*



*Figure F.7.7: FGM Site LR-07 – Bank 3–Facing downstream (lt); Bank 4-Bank (rt).*



*Figure F.7.8: FGM Site LR-07-Bank 4–Facing upstream.*

## F.8 FGM Site LR-08



*Figure F.8.1: FGM Site LR-08 – Cross Section - Looking upstream (lt); Looking downstream (rt).*



*Figure F.8.2: FGM Site LR-08 – Cross Section - Left Bank (lt) – Right bank (rt).*



*Figure F.8.3: FGM Site LR-08 – Bank 1 - Bank (lt) – Looking upstream (rt).*



*Figure F.8.4: FGM Site LR-08 – Bank 1-Facing downstream (lt); Bank 2-Bank (rt).*



*Figure F.8.5: FGM Site LR-08–Bank 2-Facing upstream (lt);Facing downstream (rt).*



*Figure F.8.6: FGM Site LR-08 – Bank 3 - Bank (lt); Facing upstream (rt).*



*Figure F.8.7: FGM Site LR-08 – Bank 3–Facing downstream (lt); Bank 4-Bank (rt).*



*Figure F.8.8: FGM Site LR-08-Bank 4–Facing upstream (lt);Facing downstream (rt).*



*Figure F.8.9: FGM Site LR-08 – Debris jam (lt); Large Oak tree (rt).*

**F.9 FGM Site LR-08**



*Figure F.9.1: FGM Site LR-09 – Cross Section - Looking upstream (lt); Looking downstream (rt).*



*Figure F.9.2: FGM Site LR-09 – Cross Section - Left Bank (lt) – Right bank (rt).*



*Figure F.9.3: FGM Site LR-09 – Bank 1 - Bank (lt) – Looking upstream (rt).*



Figure F.9.4: FGM Site LR-09 – Bank 1-Facing downstream (lt); Bank 2-Bank (rt).



Figure F.9.5: FGM Site LR-09–Bank 2-Facing upstream (lt);Facing downstream (rt).



Figure F.9.6: FGM Site LR-09 – Bank 3 - Bank (lt); Facing upstream (rt).





*Figure F.9.7: FGM Site LR-09 – Bank 3–Facing downstream (lt); Bank 4-Bank (rt).*



*Figure F.9.8: FGM Site LR-09-Bank 4–Facing upstream (lt);Facing downstream (rt).*

**F.10 FGM Site NF-01**



*Figure F.10.1: FGM Site NF-01 – Cross Section - Looking upstream (lt); Looking downstream (rt).*



*Figure F.10.2: FGM Site NF-01 – Cross Section - Left Bank (lt) – Right bank (rt).*

**F.11 FGM Site NF-02**



*Figure F.11.1: FGM Site NF-02 – Cross Section - Looking upstream (lt); Looking downstream (rt).*



*Figure F.11.2: FGM Site NF-02 – Cross Section - Left Bank (lt) – Right bank (rt).*



*Figure F.11.3: FGM Site NF-02 – Bank 1 - Bank (lt) – Looking upstream (rt).*



*Figure F.11.4: FGM Site NF-02 – Bank 1 - Looking downstream (rt).*

**F.12 FGM Site NF-03**



*Figure F.12.1: FGM Site NF-03 – Cross Section - Looking upstream (lt); Looking downstream (rt).*



*Figure F.12.2: FGM Site NF-03 – Cross Section - Left Bank (lt) – Right bank (rt).*

**F.13 FGM Site NF-04**



*Figure F.13.1: FGM Site NF-04 – Cross Section - Looking upstream (lt); Looking downstream (rt).*



*Figure F.13.2: FGM Site NF-04 – Cross Section - Left Bank (lt) – Right bank (rt).*

**F.14 FGM Site EC-01**



*Figure F.14.1: FGM Site EC-01 – Cross Section - Looking upstream (lt); Looking downstream (rt).*



*Figure F.14.2: FGM Site EC-01 – Cross Section - Left Bank (lt) – Right bank (rt).*

**F.15 FGM Site EC-02**



*Figure F.15.1: FGM Site EC-02 – Cross Section - Looking upstream (lt); Looking downstream (rt).*



*Figure F.15.2: FGM Site EC-02 – Cross Section - Left Bank (lt) – Right bank (rt).*



**F.16 FGM Site EC-03**



*Figure F.16.1: FGM Site EC-03 – Cross Section - Looking upstream (lt); Looking downstream (rt).*



*Figure F.16.2: FGM Site EC-03 – Cross Section - Left Bank (lt) – Right bank (rt).*

**F.17 FGM Site RC-01**



*Figure F.17.1: FGM Site RC-01 – Cross Section - Looking upstream (lt); Looking downstream (rt).*



*Figure F.17.2: FGM Site RC-01 – Cross Section - Left Bank (lt) – Right bank (rt).*

**F.18 FGM Site RC-02**



*Figure F.18.1: FGM Site RC-02 – Cross Section - Looking upstream (lt); Looking downstream (rt).*



*Figure F.18.2: FGM Site RC-02 – Cross Section - Left Bank (lt) – Right bank (rt).*

**F.19 FGM Site RC-04**



*Figure F.19.1: FGM Site RC-04 – Cross Section - Looking upstream (lt); Looking downstream (rt).*



*Figure F.19.2: FGM Site RC-04 – Cross Section - Left Bank (lt) – Right bank (rt).*

**F.20 FGM Site DBC-01**



*Figure F.20.1: FGM Site DBC-01 – Cross Section - Looking upstream (lt); Looking downstream (rt).*



*Figure F.20.2: FGM Site DBC-01 – Cross Section - Left Bank (lt) – Right bank (rt).*

**F.21 FGM Site DBC-02**



*Figure F.21.1: FGM Site DBC-02 – Cross Section - Looking upstream (lt); Looking downstream (rt).*



*Figure F.21.2: FGM Site DBC-02 – Cross Section - Left Bank (lt) – Right bank (rt).*

## F.22 FGM Site DBC-03



*Figure F.22.1: FGM Site DBC-03 – Cross Section - Looking upstream (lt); Looking downstream (rt).*



*Figure F.22.2: FGM Site DBC-03 – Cross Section - Left Bank (lt) – Right bank (rt).*

**F.23 FGM Site DBC-04**



*Figure F.23.1: FGM Site DBC-04 – Cross Section - Looking upstream (lt); Looking downstream (rt).*



*Figure F.23.2: FGM Site DBC-04 – Cross Section - Left Bank (lt) – Right bank (rt).*



**F.24 FGM Site HC-01**



*Figure F.24.1: FGM Site HC-01 – Cross Section - Looking upstream (lt); Looking downstream (rt).*



*Figure F.24.2: FGM Site HC-01 – Cross Section - Left Bank (lt) – Right bank (rt).*

**F.25 FGM Site HC-02**



*Figure F.25.1: FGM Site HC-02 – Cross Section - Looking upstream (lt); Looking downstream (rt).*



*Figure F.25.2: FGM Site HC-02 – Cross Section - Left Bank (lt) – Right bank (rt).*

## **G. Appendix G: Total Suspended Material (TSM) SOP**

- 1) Obtain a Suspended Sediment Sample analysis form and legibly record the project name, analyst name, and samples being processed on this form. These forms are log sheets for the TSM samples and are kept as records to show which samples have been run.
- 2) Set up the filter towers and clean the funnels, flasks, and filter holders with distilled water and kim wipes.
- 3) Place a 90mm glass fiber filter (0.7 $\mu$ m pore size) on a large, tin weighing boat and place them in the analytical balance. Record the tray number. The resulting weight is recorded as the tare weight on log sheet. Before recording weight, make sure that the balance is level by checking the bubble level at the front right corner of the balance.
- 4) Place filter in the center of the ground glass filter holder and wet it down with distilled water to make sure it stays in place. Place the glass funnel over the filter and clamp into place with the large alligator clamp.
- 5) Shake up the contents of the sample bottle and pour into a clean, 1L graduated cylinder. Record volume on log sheet. \*(If the volume of the bottle is greater than 1L a second cylinder can be used to obtain the total sample volume. If a second cylinder is not available, fill the cylinder to the 900ml line. Then transfer the contents of the cylinder to the filter funnel and pour the remaining sample into the empty cylinder. The total volume of the sample should be recorded and a note should be made that an extra transfer was required.)

- 6) Pour contents of graduated cylinder into funnel of filter tower. Use distilled water to carefully rinse all the sediment in the cylinder(s) and sample bottle into the filter funnel.
- 7) Connect the vacuum pump to the filtration system with tubing and open the valves to the vacuum flasks. Turn on the vacuum pump.
- 8) Rinse the sides of filter funnel with distilled water to make sure are particles are washed onto the filter. \*(If the samples are ocean samples the filters should be rinsed with 25-50ml of distilled water to make sure salt is rinsed from the filter before drying.)
- 9) Turn off vacuum pump and remove filter funnel from the top of the filter. Place the funnel on the bench top with the ground glass surface facing up. Check the ground glass surface for sample residue. Rinse any residue into the corresponding tin weighing pan.
- 10) Fold filter into quarters and place in tin weighing pan.
- 11) Place weighing pan with filter in oven set to 50-60°C. Allow filters to dry overnight.
- 12) Remove filters and pans from the oven and place in desiccators until they are allowed to reach room temperature. Reweigh drying pans with folded filters, record as gross weight
- 13) Calculate sediment concentration in mg/L.

**H. Appendix H – Suspended Sediment Concentration Analyses  
Summary Tables**

Table H.1: Suspended Sediment Concentration Analyses Summary (1 of 4).

Sample #	Sample Name	Date	Time	Type	Conc (mg/L)
WES-1	LR-Porter	5/21/2013	1830	Grab	495.11
WES-2	LR-Porter	5/21/2013	1830	di-lt	525.19
WES-3	LR-Porter	5/21/2013	1830	di-ctr	541.90
WES-4	LR-Porter	5/21/2013	1830	di-rt	545.67
WES-5	LR-Porter	5/21/2013	1900	adcp-ctr	401.32
WES-6	LR-Porter	5/21/2013	1900	adcp-rt	451.35
WES-7	LR-Porter	5/21/2013	1900	adcp-lt	406.54
WES-8	LR-Porter	5/21/2013	1930	di-lt	424.36
WES-9	LR-Porter	5/21/2013	1930	di-rt	415.00
WES-10	LR-Porter	5/21/2013	1930	di-ctr	416.11
WES-11	LR-Porter	5/21/2013	1930	grab	420.65
WES-12	LR-Porter	6/4/2013	1600	grab	1088.04
WES-13	LR-Porter	6/4/2013	1600	di-lt	1069.82
WES-14	LR-Porter	6/4/2013	1600	di-ctr	1075.53
WES-15	LR-Porter	6/4/2013	1600	di-rt	1014.43
WES-16	LR-Porter	6/4/2013	1545	adcp-lt	1053.80
WES-17	LR-Porter	6/4/2013	1545	adcp-ctr	1074.37
WES-18	LR-Porter	6/4/2013	1545	adcp-rt	999.32
WES-19	LR-Porter	7/15/2013	1545	grab	2872.12
WES-20	LR-Porter	7/15/2013	1545	di-lt	2875.88
WES-21	LR-Porter	7/15/2013	1545	di-ctr	2591.67
WES-22	LR-Porter	7/15/2013	1545	di-rt	2710.99
WES-23	LR-Porter	9/27/2012	1345	grab	347.65
WES-24	LR-60	4/4/2013	1830	adcp-lt	238.37
WES-25	LR-60	4/4/2013	1830	adcp-ctr	340.24
WES-26	LR-60	4/4/2013	1830	adcp-rt	267.76
WES-27	LR-60	4/4/2013	1830	di-lt	240.29
WES-28	LR-60	4/4/2013	1830	di-ctr	273.47
WES-29	LR-60	4/4/2013	1830	di-rt	302.25
WES-30	LR-60	6/5/2013	1500	grab	2624.31
WES-31	LR-60	6/5/2013	1500	di-lt	2307.91
WES-32	LR-60	6/5/2013	1500	di-ctr	2378.33
WES-33	LR-60	6/5/2013	1500	di-rt	2532.14
WES-34	LR-60	6/5/2013	1500	adcp-lt	2274.67
WES-35	LR-60	6/5/2013	1500	adcp-ctr	2643.33
WES-36	LR-60	6/5/2013	1500	adcp-rt	2298.89
WES-37	Elm Creek	9/27/2012	1430	grab	43.88
WES-38	LR-60	9/28/2012	1500	grab	266.92
WES-39	NF	9/28/2012	1500	grab	517.45
WES-40	LR-60	6/17/2013	1700	grab	1026.60
WES-41	LR-60	6/17/2013	1700	di-lt	1076.99
WES-42	LR-60	6/17/2013	1700	di-ctr	1033.90
WES-43	LR-60	6/17/2013	1700	di-rt	1034.19
WES-44	LR-60	6/17/2013	1530	adcp-lt	1460.00
WES-45	LR-60	6/17/2013	1530	adcp-ctr	1547.09
WES-46	LR-60	6/17/2013	1530	adcp-rt	1715.47

Table H.2: Suspended Sediment Concentration Analyses Summary (2 of 4).

Sample #	Sample Name	Date	Time	Type	Conc (mg/L)
WES-47	LR-60	6/17/2013	1400	grab	3776.05
WES-48	LR-60	6/17/2013	1400	di-lt	2120.88
WES-49	LR-60	6/17/2013	1400	di-ctr	2199.39
WES-50	LR-60	6/17/2013	1400	di-rt	1940.34
WES-51	LR-60	6/17/2013	1400	adcp-lt	1032.41
WES-52	LR-60	6/17/2013	1400	adcp-ctr	1078.30
WES-53	LR-60	6/17/2013	1400	adcp-rt	1012.28
WES-54	LR-60	5/23/2013	1515	grab	1476.70
WES-55	LR-60	5/23/2013	1515	di-lt	1956.90
WES-56	LR-60	5/23/2013	1515	di-ctr	2072.60
WES-57	LR-60	5/23/2013	1515	di-rt	2153.40
WES-58	LR-60	5/23/2013	1515	adcp-lt	2564.67
WES-59	LR-60	5/23/2013	1515	adcp-ctr	1868.60
WES-60	LR-60	5/23/2013	1515	adcp-rt	2174.38
WES-61	LR-60	5/24/2013	1130	grab	363.60
WES-62	LR-60	5/24/2013	1130	di-lt	368.93
WES-63	LR-60	5/24/2013	1130	di-ctr	270.98
WES-64	LR-60	5/24/2013	1130	di-rt	269.06
WES-65	LR-60	5/24/2013	1130	adcp-lt	307.50
WES-66	LR-60	5/24/2013	1130	adcp-ctr	296.14
WES-67	LR-60	5/24/2013	1130	adcp-rt	296.29
WES-68	LR-60	7/17/2013	1430	Grab	698.33
WES-69	LR-60	7/17/2013	1430	di-lt	782.18
WES-70	LR-60	7/17/2013	1430	di-ctr	673.85
WES-71	LR-60	7/17/2013	1430	di-rt	636.94
WES-72	LR-60	7/17/2013	1430	adcp-lt	665.77
WES-73	LR-60	7/17/2013	1430	adcp-ctr	720.00
WES-74	LR-60	7/17/2013	1430	adcp-rt	734.15
WES-75	LR-60	7/16/2013	1530	grab	227.02
WES-76	LR-60	7/16/2013	1530	di-lt	220.93
WES-77	LR-60	7/16/2013	1530	di-ctr	178.60
WES-78	LR-60	7/16/2013	1700	adcp-lt	177.63
WES-79	LR-60	7/16/2013	1700	adcp-ctr	175.96
WES-80	LR-60	7/16/2013	1700	adcp-rt	168.47
OU-1	LR-60	4/15/2012	1230	grab-lt2	2105.05
OU-2	LR-60	4/15/2012	1230	grab-ctr2	2397.70
OU-3	LR-60	4/15/2012	1230	grab-rt2	2394.43
OU-4	LR-60	4/15/2012	1230	di-lt2	2400.00
OU-5	LR-60	4/15/2012	1230	di-ctr2	2513.45
OU-6	LR-60	4/15/2012	1230	di-rt2	2124.54
OU-7	LR-60	5/22/2013	1300	Grab	30.45
OU-8	LR-60	5/22/2013	1300	di-lt	38.43
OU-9	LR-60	5/22/2013	1300	di-ctr	13.33
OU-10	LR-60	5/22/2013	1300	di-rt	34.80
OU-11	LR-60	5/22/2013	1300	grab-lt	1.25
OU-12	LR-60	7/26/2013	2000	grab	2826.29

Table H.3: Suspended Sediment Concentration Analyses Summary (3 of 4).

Sample #	Sample Name	Date	Time	Type	Conc (mg/L)
OU-13	LR-60	7/26/2013	2000	di-lt	2682.27
OU-14	LR-60	7/26/2013	2000	di-ctr	2789.17
OU-15	LR-60	7/26/2013	2000	di-rt	2051.25
OU-16	LR-Porter	4/3/2012	1100	grab	28.21
OU-17	Hog	4/3/2012	1300	grab	304.84
OU-18	LR-60	9/27/2012	1530	grab	968.79
OU-19	NFork	9/27/2012	1500	grab	413.27
OU-20	LR-Porter	9/28/2012	1400	grab	17.08
OU-21	LR-60	3/22/2012	1200	grab-lt	230.42
OU-22	LR-60	3/22/2012	1200	grab-ctr	247.57
OU-23	LR-60	3/22/2012	1200	grab-rt	219.44
OU-24	LR-60	3/22/2012	1200	di-lt	180.95
OU-25	LR-60	3/22/2012	1200	di-ctr	166.92
OU-26	LR-60	3/22/2012	1200	di-rt	163.51
OU-27	Rock Cr	3/23/2012	1030	grab	21.39
OU-28	Dave Blue Cr	3/23/2012	930	grab	9.63
OU-29	LR-60	3/21/2012	1100	grab-lt	233.18
OU-30	LR-60	3/21/2012	1100	grab-ctr	331.65
OU-31	LR-60	3/21/2012	1100	grab-rt	173.33
OU-32	LR-60	3/21/2012	1100	di-lt	126.09
OU-33	LR-60	3/21/2012	1100	di-ctr	219.79
OU-34	LR-60	3/21/2012	1100	di-rt	140.38
OU-35	LR-60	3/21/2012	1215	di-lt	132.67
OU-36	LR-60	3/21/2012	1215	di-ctr	173.95
OU-37	LR-60	3/21/2012	1215	di-rt	96.29
OU-38	LR-60	3/21/2012	1215	di-lt2	241.17
OU-39	LR-60	3/21/2012	1215	di-ctr2	173.39
OU-40	LR-60	3/21/2012	1215	di-rt2	202.44
OU-41	LR-60	3/21/2012	1215	Grab	165.69
OU-42	LR-60	4/15/2012	1130	di-lt	2121.33
OU-43	LR-60	4/15/2012	1130	di-ctr	2554.19
OU-44	LR-60	4/15/2012	1130	di-rt	2377.31
OU-45	LR-60	4/15/2012	1130	grab-lt	1931.07
OU-46	LR-60	4/15/2012	1130	grab-ctr	2332.77
OU-47	LR-60	4/15/2012	1130	grab-rt	2509.36
OU-48	LR-60	4/18/2013	1430	di-lt	1260.53
OU-49	LR-60	4/18/2013	1430	di-ctr	1210.69
OU-50	LR-60	4/18/2013	1430	di-rt	1169.27
OU-51	LR-60	4/18/2013	1430	grab	1201.57
OU-52	Nfork	4/3/2012	1145	grab	20.70
OU-53	LR-Porter	7/9/2010	850	grab	67.23
OU-54	Rock Cr	7/9/2010	1100	grab	46.35
OU-55	Dave Blue Cr	7/9/2010	1130	grab	8.06
OU-56	LR-60	7/9/2010	1700	grab	39.13
OU-57	Elm Cr	7/9/2010	1030	grab	0.27
OU-58	LR-60	7/10/2010	1200	grab	1.97



Table H.4: Suspended Sediment Concentration Analyses Summary (4 of 4).

Sample #	Sample Name	Date	Time	Type	Conc (mg/L)
OU-59	LR-60	7/12/2010	1100	grab	2.50
OU-60	LR-60	7/13/2010	1200	grab	30.43
OU-61	LR-60	7/13/2010	1330	grab	2.15
OU-62	LR-Porter	3/12/2012	1330	grab	6.47
OU-63	LR-Porter	3/12/2012	1430	grab	38.46
OU-64	NFork	3/12/2012	1445	grab	4.31
OU-65	NFork	3/12/2012	1515	grab	27.25
OU-66	Elm Cr	3/12/2012	1530	grab	19.42
OU-67	Elm Cr	3/12/2012	1615	grab	26.41
OU-68	LR-60	3/12/2012	1430	grab	99.21
OU-69	LR-60	3/20/2012	1345	grab	98.82
OU-70	LR-60	3/20/2012	1345	di-lt	544.68
OU-71	LR-60	3/20/2012	1345	di-ctr	564.32
OU-72	LR-60	3/20/2012	1345	di-rt	592.91
OU-73	LR-60	3/20/2012	1545	di-lt2	546.51
OU-74	LR-60	3/20/2012	1545	di-ctr2	539.18
OU-75	LR-60	3/20/2012	1345	grab-lt	505.38
OU-76	LR-60	3/20/2012	1345	grab-ctr	628.40
OU-77	LR-60	3/20/2012	1345	grab-rt	602.02
OU-78	LR-60	3/20/2012	1345	grab-rt	704.36
OU-79	LR-60	3/20/2012	1545	grab-lt2	707.52
OU-80	LR-60	3/20/2012	1545	grab-ctr2	649.57
OU-81	LR-60	3/20/2012	1545	grab-rt2	608.89
OU-82	LR-60	3/21/2012	1100	grab-lt1	323.04
OU-83	LR-60	3/21/2012	1100	grab-ctr1	290.00
OU-84	LR-60	3/21/2012	1100	grab-rt1	260.64
OU-85	LR-60	3/21/2012	1215	grab-lt2	362.34
OU-86	LR-60	3/21/2012	1215	grab-ctr2	347.96
NA	North Fork	7/9/2010	930	grab	142.30
NA	Rock Creek	7/9/2010	1100	grab	339.00
NA	Elm Creek	7/9/2010	1030	grab	249.00
NA	Dave Blue Cr	7/9/2010	1130	grab	200.00
NA	LR-Porter	7/9/2010	830	grab	288.00
NA	LR-60th	7/9/2010	1700	grab	308.00
NA	LR-60th	7/10/2010	1200	grab	227.00
NA	LR-60th	7/12/2010	1100	grab	310.30
NA	LR-60th	7/13/2010	1200	grab	251.30
NA	LR-60th	7/13/2010	1330	grab	158.00
NA	LR-60th	5/20/2011	1700	grab	2062.75
NA	Rock Creek	5/20/2011	1730	grab	946.15

**I. Appendix I - Suspended Particle Size Distribution Analyses Summary Tables**

Table I.1: Suspended Particle Size Distribution Analyses Summary (1 of 6).

Sample #	Sample Name	Date	Time	Sample Type	Percentage by class size (µm)														
					2000-1000-1000	500-250-125	125-62	62-31	31-16	16-8	8-4	4-2	2-1	1-0.5	0.5-0.25	<0.25			
WES-1	LR-Porter	5/21/2013	1830	Grab	0.00	0.00	0.64	0.54	3.71	14.66	19.01	21.35	22.17	17.93	***	***	***		
WES-2	LR-Porter	5/21/2013	1830	di-lt	0.00	0.00	0.00	0.00	2.37	11.99	19.35	25.40	24.96	15.92	***	***	***		
WES-3	LR-Porter	5/21/2013	1830	di-ctr	0.00	0.00	0.27	0.17	1.78	10.70	18.47	24.78	25.71	18.13	***	***	***		
WES-4	LR-Porter	5/21/2013	1830	di-r	0.00	0.00	0.08	0.30	3.59	14.44	19.19	23.21	23.49	15.69	***	***	***		
WES-5	LR-Porter	5/21/2013	1900	adcp-ctr	0.00	0.00	0.00	0.07	4.02	15.18	19.62	23.01	22.92	15.19	***	***	***		
WES-6	LR-Porter	5/21/2013	1900	adcp-r	0.00	0.00	0.00	0.28	2.50	8.04	13.81	23.96	28.71	22.71	***	***	***		
WES-7	LR-Porter	5/21/2013	1900	adcp-lt	0.00	0.00	0.13	0.64	1.67	6.02	11.12	21.42	30.13	28.86	***	***	***		
WES-8	LR-Porter	5/21/2013	1930	di-lt	0.00	0.00	0.00	0.44	1.78	6.32	10.27	20.89	32.13	28.18	***	***	***		
WES-9	LR-Porter	5/21/2013	1930	di-r	0.00	0.00	0.00	0.05	2.24	7.65	12.44	21.62	29.01	27.00	***	***	***		
WES-10	LR-Porter	5/21/2013	1930	di-ctr	0.00	0.00	0.00	0.06	1.88	7.43	12.39	21.14	29.07	28.03	***	***	***		
WES-11	LR-Porter	5/21/2013	1930	grab	0.00	0.00	0.05	0.22	1.99	7.34	12.50	21.52	29.35	27.03	***	***	***		
WES-12	LR-Porter	6/4/2013	1600	grab	1.06	11.14	16.02	11.98	11.45	14.44	13.38	10.20	6.40	3.94	***	***	***		
WES-13	LR-Porter	6/4/2013	1600	di-lt	0.00	0.93	6.44	6.20	9.53	20.70	23.64	18.20	9.82	4.53	***	***	***		
WES-14	LR-Porter	6/4/2013	1600	di-ctr	0.00	0.33	5.82	5.92	6.17	15.00	20.05	22.67	17.20	6.86	***	***	***		
WES-15	LR-Porter	6/4/2013	1600	di-r	6.81	17.87	18.46	11.61	8.44	9.70	9.56	8.37	5.75	3.44	***	***	***		
WES-16	LR-Porter	6/4/2013	1545	adcp-lt	0.08	4.39	7.58	8.04	11.07	17.19	17.75	15.11	10.97	7.82	***	***	***		
WES-17	LR-Porter	6/4/2013	1545	adcp-ctr	0.00	0.09	3.39	6.95	9.04	16.36	21.08	21.59	14.72	6.99	***	***	***		
WES-18	LR-Porter	6/4/2013	1545	adcp-r	0.00	1.06	3.96	5.35	11.18	20.68	21.75	17.47	11.47	7.09	***	***	***		
WES-19	LR-Porter	7/15/2013	1545	grab	0.00	0.00	0.00	0.11	6.85	22.40	22.31	18.33	16.83	13.17	***	***	***		
WES-20	LR-Porter	7/15/2013	1545	di-lt	0.00	0.00	0.00	0.22	9.00	23.69	21.77	17.90	15.85	11.57	***	***	***		
WES-21	LR-Porter	7/15/2013	1545	di-ctr	0.00	0.00	0.00	0.58	9.52	22.85	21.21	18.34	16.12	11.37	***	***	***		
WES-22	LR-Porter	7/15/2013	1545	di-r	0.00	0.00	0.00	0.07	5.36	19.50	22.29	20.61	18.65	13.53	***	***	***		
WES-23	LR-Porter	9/27/2012	1345	grab	0.00	0.00	0.29	0.31	1.23	5.32	11.84	23.19	30.27	27.55	***	***	***		
WES-24	LR-60	4/4/2013	1830	adcp-lt	0.00	0.08	0.77	0.64	1.51	7.28	15.55	24.86	27.49	21.84	***	***	***		
WES-25	LR-60	4/4/2013	1830	adcp-ctr	0.00	0.00	0.00	0.10	3.47	12.01	17.73	23.34	24.32	19.03	***	***	***		
WES-26	LR-60	4/4/2013	1830	adcp-r	0.00	0.00	0.26	0.68	1.46	6.95	15.51	25.71	27.98	21.45	***	***	***		
WES-27	LR-60	4/4/2013	1830	di-lt	0.00	0.06	0.85	0.89	2.13	7.59	16.00	25.33	26.59	20.57	***	***	***		
WES-28	LR-60	4/4/2013	1830	di-ctr	0.00	0.07	0.42	0.22	2.02	8.41	16.45	25.97	27.19	19.25	***	***	***		
WES-29	LR-60	4/4/2013	1830	di-r	0.00	0.00	0.00	0.00	1.02	6.46	14.43	24.87	29.76	23.46	***	***	***		
WES-30	LR-60	6/5/2013	1500	grab	0.00	0.30	3.31	3.98	7.43	17.35	23.13	22.83	14.44	7.23	***	***	***		
WES-31	LR-60	6/5/2013	1500	di-lt	10.30	18.03	13.29	7.65	7.21	11.08	11.45	9.29	6.73	4.97	***	***	***		
WES-32	LR-60	6/5/2013	1500	di-ctr	1.68	8.59	9.53	6.63	9.34	16.99	17.39	13.75	9.55	6.56	***	***	***		
WES-33	LR-60	6/5/2013	1500	di-r	0.00	0.11	0.74	0.27	1.78	16.31	29.38	25.48	15.69	10.26	***	***	***		
WES-34	LR-60	6/5/2013	1500	adcp-lt	0.42	5.65	7.34	5.16	8.28	18.09	20.64	16.66	10.83	6.94	***	***	***		
WES-35	LR-60	6/5/2013	1500	adcp-ctr	0.00	0.00	0.00	0.10	5.13	18.06	24.70	25.28	17.86	8.87	***	***	***		

Table I.2: Suspended Particle Size Distribution Analyses Summary (2 of 6).

Sample #	Sample Name	Date	Time	Sample Type	Percentage by class size (µm)														
					2000-1000	1000-500	500-250	250-125	125-62	62-31	31-16	16-8	8-4	4-2	2-1	1-0.5	0.5-0.25	<0.25	
WES-36	LR-60	6/5/2013	1500	adcp-rt	0.00	0.08	0.88	1.13	7.33	24.02	28.44	20.84	11.48	5.80	***	***	***		
WES-37	Elm Creek	9/27/2012	1430	grab	0.00	0.00	0.00	0.25	1.15	3.99	14.71	32.06	31.62	16.23	***	***	***		
WES-38	LR-60	9/28/2012	1500	grab	0.00	0.17	1.16	1.33	3.79	11.94	17.78	20.89	22.09	20.85	***	***	***		
WES-39	NF	9/28/2012	1500	grab	0.00	0.00	0.00	0.06	3.13	14.20	20.63	22.24	21.41	18.33	***	***	***		
WES-40	LR-60	6/17/2013	1700	grab	0.00	0.00	0.00	0.06	2.88	14.71	21.31	22.98	22.06	16.00	***	***	***		
WES-41	LR-60	6/17/2013	1700	di-ft	0.00	0.00	0.00	0.00	0.99	9.36	20.31	27.18	25.60	16.56	***	***	***		
WES-42	LR-60	6/17/2013	1700	di-ctr	0.00	0.00	0.12	0.19	2.83	13.79	21.02	24.46	22.82	14.77	***	***	***		
WES-43	LR-60	6/17/2013	1700	di-rt	0.00	0.00	0.11	0.28	2.28	12.80	20.72	23.75	23.00	17.06	***	***	***		
WES-44	LR-60	6/17/2013	1530	adcp-lt	0.00	0.00	0.05	0.08	2.85	14.80	21.97	23.39	21.65	15.22	***	***	***		
WES-45	LR-60	6/17/2013	1530	adcp-ctr	0.00	0.00	0.01	0.17	2.86	13.12	20.58	24.13	22.74	16.39	***	***	***		
WES-46	LR-60	6/17/2013	1530	adcp-rt	0.00	0.00	0.00	0.02	2.72	13.19	19.27	22.52	23.61	18.66	***	***	***		
WES-47	LR-60	6/17/2013	1400	grab	0.00	0.00	0.00	0.02	5.48	21.34	23.59	20.18	17.34	12.06	***	***	***		
WES-48	LR-60	6/17/2013	1400	di-ft	0.00	0.00	0.00	0.08	5.58	20.15	22.91	20.30	18.01	12.98	***	***	***		
WES-49	LR-60	6/17/2013	1400	di-ctr	0.00	0.00	0.00	0.07	3.70	17.41	22.82	21.81	19.74	14.45	***	***	***		
WES-50	LR-60	6/17/2013	1400	di-rt	0.00	0.00	0.00	0.00	2.48	15.44	22.93	23.00	20.93	15.23	***	***	***		
WES-51	LR-60	6/17/2013	1400	adcp-lt	0.00	0.00	0.05	0.08	2.62	13.07	20.45	23.64	22.68	17.40	***	***	***		
WES-52	LR-60	6/17/2013	1400	adcp-ctr	0.00	0.00	0.22	0.30	2.69	14.09	21.90	24.48	22.05	14.27	***	***	***		
WES-53	LR-60	6/17/2013	1400	adcp-rt	0.00	0.00	0.00	0.00	1.98	12.57	21.05	24.58	23.37	16.45	***	***	***		
WES-54	LR-60	5/23/2013	1515	grab	0.00	0.00	0.00	0.00	2.40	13.70	23.02	25.96	21.59	13.29	***	***	***		
WES-55	LR-60	5/23/2013	1515	di-ft	0.00	0.07	0.67	0.38	3.09	15.04	22.56	24.53	20.98	12.69	***	***	***		
WES-56	LR-60	5/23/2013	1515	di-ctr	0.00	0.08	0.66	0.85	7.26	18.87	21.39	21.67	18.37	10.87	***	***	***		
WES-57	LR-60	5/23/2013	1515	di-rt	0.00	0.09	0.58	0.95	8.53	20.32	20.24	19.26	17.83	12.21	***	***	***		
WES-58	LR-60	5/23/2013	1515	adcp-lt	0.00	0.00	0.00	0.32	6.52	18.73	20.48	20.95	19.78	13.22	***	***	***		
WES-59	LR-60	5/23/2013	1515	adcp-ctr	0.00	0.05	0.38	0.68	6.10	19.22	23.43	21.81	17.34	10.99	***	***	***		
WES-60	LR-60	5/23/2013	1515	adcp-rt	0.00	0.11	0.84	0.64	6.60	20.21	24.17	21.68	16.09	9.67	***	***	***		
WES-61	LR-60	5/24/2013	1130	grab	0.00	0.02	0.40	1.24	4.43	11.41	18.45	25.83	23.97	14.24	***	***	***		
WES-62	LR-60	5/24/2013	1130	di-ft	0.00	0.00	0.30	1.35	3.38	9.96	18.19	26.57	24.97	15.28	***	***	***		
WES-63	LR-60	5/24/2013	1130	di-ctr	0.00	0.01	1.02	1.04	2.73	10.31	16.85	23.61	25.58	18.86	***	***	***		
WES-64	LR-60	5/24/2013	1130	di-rt	0.00	0.00	0.13	0.58	1.71	9.44	20.94	30.37	25.38	11.44	***	***	***		
WES-65	LR-60	5/24/2013	1130	adcp-lt	0.00	0.10	1.09	1.16	5.05	16.17	24.94	26.74	17.68	7.06	***	***	***		
WES-66	LR-60	5/24/2013	1130	adcp-ctr	0.00	0.00	0.26	1.25	2.50	7.89	16.26	26.93	27.57	17.34	***	***	***		
WES-67	LR-60	5/24/2013	1130	adcp-rt	0.00	0.01	0.51	0.37	2.56	11.70	20.78	27.68	24.04	12.36	***	***	***		
WES-68	LR-60	7/17/2013	1430	Grab	0.00	0.00	0.01	0.08	2.15	12.67	20.91	24.25	23.45	16.49	***	***	***		
WES-69	LR-60	7/17/2013	1430	di-ft	0.00	0.00	0.05	0.39	3.30	14.25	21.34	23.97	22.07	14.64	***	***	***		
WES-70	LR-60	7/17/2013	1430	di-ctr	0.00	0.00	0.12	0.19	2.74	12.83	20.92	24.57	22.74	15.88	***	***	***		

Table I.3: Suspended Particle Size Distribution Analyses Summary (3 of 6).

Sample #	Sample Name	Date	Time	Sample Type	Percentage by class size (µm)													
					2000-1000	1000-500	500-250	250-125	125-62	62-31	31-16	16-8	8-4	4-2	2-1	1-0.5	0.5-0.25	<0.25
WES-71	LR-60	7/17/2013	1430	di-rt	0.00	0.00	0.36	0.49	2.79	12.97	20.44	24.42	23.11	15.42	***	***	***	
WES-72	LR-60	7/17/2013	1430	adcp-lt	0.00	0.00	0.09	0.20	2.72	14.16	21.78	24.06	22.18	14.81	***	***	***	
WES-73	LR-60	7/17/2013	1430	adcp-ctr	0.00	0.00	0.01	0.15	3.16	13.91	21.34	24.57	22.38	14.50	***	***	***	
WES-74	LR-60	7/17/2013	1430	adcp-rt	0.00	0.02	0.25	0.26	4.46	17.05	20.94	20.52	15.97	***	***	***		
WES-75	LR-60	7/16/2013	1530	grab	0.00	0.06	0.45	0.64	2.55	7.58	14.28	24.25	27.80	22.38	***	***	***	
WES-76	LR-60	7/16/2013	1530	di-lt	0.00	0.00	0.00	0.44	2.48	6.58	13.67	25.30	29.05	22.48	***	***	***	
WES-77	LR-60	7/16/2013	1530	di-ctr	0.00	0.00	0.00	0.12	1.09	3.48	12.66	29.29	32.55	20.81	***	***	***	
WES-78	LR-60	7/16/2013	1700	adcp-lt	0.00	0.00	0.28	0.78	1.59	4.93	12.81	26.11	30.82	22.68	***	***	***	
WES-79	LR-60	7/16/2013	1700	adcp-ctr	0.02	0.65	0.91	0.77	1.97	5.35	13.74	27.32	29.33	20.23	***	***	***	
WES-80	LR-60	7/16/2013	1700	adcp-rt	0.00	0.00	0.00	0.73	1.24	4.34	13.06	27.32	31.25	22.07	***	***	***	
WES-81	LR-60	4/15/2012	1230	grab-lt2	0.00	0.00	0.00	0.28	6.26	18.69	21.85	21.15	19.09	12.69	***	***	***	
WES-82	LR-60	4/15/2012	1230	grab-ctr2	0.00	0.00	0.00	1.00	9.43	21.90	21.23	18.18	16.29	11.96	***	***	***	
WES-83	LR-60	4/15/2012	1230	grab-rt2	0.00	0.00	0.00	0.54	7.83	21.71	22.45	19.30	16.72	11.45	***	***	***	
WES-84	LR-60	4/15/2012	1230	di-lt2	0.00	0.00	0.00	0.74	7.83	19.81	20.59	19.22	17.99	13.81	***	***	***	
WES-85	LR-60	4/15/2012	1230	di-ctr2	0.00	0.00	0.00	0.70	6.78	17.29	18.98	20.45	20.84	14.95	***	***	***	
WES-86	LR-60	4/15/2012	1230	di-rt2	0.00	0.00	0.00	0.25	5.45	17.49	21.13	21.41	20.03	14.24	***	***	***	
WES-87	LR-60	5/22/2013	1300	grab	0.00	0.00	0.38	1.00	1.99	5.47	11.99	24.15	30.49	24.54	***	***	***	
WES-88	LR-60	5/22/2013	1300	di-lt	0.00	0.00	1.18	2.17	2.00	4.30	13.49	28.98	30.30	17.59	***	***	***	
WES-89	LR-60	5/22/2013	1300	di-ctr	0.00	0.15	0.90	0.97	1.90	4.60	12.94	27.63	30.73	20.19	***	***	***	
WES-90	LR-60	5/22/2013	1300	di-rt	0.00	0.00	0.09	0.74	1.77	4.61	12.31	28.01	32.18	20.29	***	***	***	
WES-91	LR-60	5/22/2013	1300	adcp-lt	0.00	0.37	1.15	1.27	1.75	4.61	12.44	26.13	30.79	21.49	***	***	***	
WES-92	LR-60	7/26/2013	2000	grab	0.00	0.00	0.00	0.61	10.60	26.73	22.76	15.94	13.35	10.02	***	***	***	
WES-93	LR-60	7/26/2013	2000	di-lt	0.00	0.00	0.00	1.35	13.24	26.47	20.74	14.83	12.90	10.48	***	***	***	
WES-94	LR-60	7/26/2013	2000	di-ctr	0.00	0.00	0.00	0.42	9.55	26.10	23.36	16.88	13.87	9.83	***	***	***	
WES-95	LR-60	7/26/2013	2000	di-rt	0.00	0.00	0.00	0.52	8.41	24.85	23.95	17.70	14.35	10.21	***	***	***	
WES-96	LR-Porter	4/3/2012	1100	grab	0.00	0.00	0.20	0.46	2.42	14.68	30.52	29.76	15.85	6.12	***	***	***	
WES-97	Hog	4/3/2012	1300	grab	0.00	0.42	0.86	1.86	7.50	17.15	21.28	22.49	18.15	10.31	***	***	***	
WES-98	LR-60	9/27/2012	1530	grab	0.00	0.00	0.00	0.00	0.14	2.89	12.36	26.59	31.73	26.28	***	***	***	
WES-99	NF	9/27/2012	1500	grab	0.19	1.09	2.43	1.26	2.42	7.09	11.26	16.73	25.37	32.17	***	***	***	
WES-100	LR-Porter	9/28/2012	1400	grab	0.00	0.00	0.08	0.99	1.99	5.37	13.27	27.12	30.57	20.60	***	***	***	
OU-1	LR-60	4/15/2012	1230	grab-lt2	0.00	0.00	0.02	0.03	0.07	0.11	0.16	0.19	0.19	0.13	0.08	0.02	0.01	
OU-2	LR-60	4/15/2012	1230	grab-ctr2	0.00	0.00	0.01	0.03	0.08	0.13	0.17	0.18	0.17	0.13	0.08	0.02	0.01	
OU-3	LR-60	4/15/2012	1230	grab-rt2	0.00	0.00	0.01	0.02	0.06	0.11	0.16	0.18	0.19	0.15	0.09	0.02	0.01	
OU-4	LR-60	4/15/2012	1230	di-lt2	0.00	0.00	0.00	0.01	0.06	0.11	0.15	0.18	0.19	0.16	0.09	0.02	0.01	
OU-5	LR-60	4/15/2012	1230	di-ctr2	0.00	0.00	0.00	0.01	0.07	0.12	0.15	0.17	0.19	0.15	0.10	0.02	0.01	

Table I.4: Suspended Particle Size Distribution Analyses Summary (4 of 6).

Sample #	Sample Name	Date	Time	Sample Type	Percentage by class size (µm)													
					2000-1000	1000-500	500-250	125-62	62-31	31-16	16-8	8-4	4-2	2-1	1-0.5	0.25	0.1	0.05
OU-6	LR-60	4/15/2012	1230	di-rt2	0.00	0.00	0.01	0.02	0.06	0.12	0.17	0.19	0.18	0.14	0.09	0.02	0.01	0.00
OU-7	LR-60	5/22/2013	1300	Grab	0.00	0.00	0.01	0.03	0.03	0.07	0.16	0.26	0.25	0.13	0.06	0.01	0.01	0.00
OU-8	LR-60	5/22/2013	1300	di-lt	0.00	0.00	0.13	0.09	0.05	0.07	0.15	0.20	0.17	0.09	0.05	0.01	0.01	0.00
OU-9	LR-60	5/22/2013	1300	di-ctr	0.00	0.00	0.15	0.09	0.06	0.07	0.12	0.16	0.17	0.11	0.06	0.01	0.01	0.00
OU-10	LR-60	5/22/2013	1300	di-rt	0.00	0.00	0.15	0.03	0.01	0.04	0.17	0.26	0.21	0.09	0.05	0.01	0.01	0.00
OU-11	LR-60	5/22/2013	1300	grab-lt	0.00	0.00	0.05	0.02	0.02	0.05	0.13	0.24	0.26	0.15	0.07	0.01	0.01	0.00
OU-12	LR-60	7/26/2013	2000	grab	0.00	0.00	0.01	0.03	0.11	0.15	0.16	0.15	0.15	0.12	0.08	0.02	0.01	0.00
OU-13	LR-60	7/26/2013	2000	di-lt	0.00	0.00	0.01	0.02	0.10	0.16	0.17	0.16	0.15	0.12	0.08	0.02	0.01	0.00
OU-14	LR-60	7/26/2013	2000	di-ctr	0.00	0.00	0.00	0.01	0.08	0.15	0.18	0.18	0.17	0.13	0.08	0.02	0.01	0.00
OU-15	LR-60	7/26/2013	2000	di-rt	0.00	0.00	0.00	0.01	0.07	0.15	0.18	0.17	0.16	0.13	0.09	0.02	0.01	0.00
OU-16	LR-Porter	4/3/2012	1100	grab	0.00	0.00	0.07	0.06	0.06	0.14	0.27	0.20	0.12	0.06	0.03	0.01	0.01	0.00
OU-17	Hog	4/3/2012	1300	grab	0.00	0.00	0.03	0.04	0.06	0.10	0.20	0.23	0.19	0.09	0.05	0.02	0.01	0.00
OU-18	LR-60	9/27/2012	1530	grab	0.00	0.00	0.02	0.01	0.01	0.03	0.09	0.20	0.24	0.20	0.13	0.03	0.02	0.00
OU-19	NFork	9/27/2012	1500	grab	0.00	0.00	0.01	0.02	0.03	0.05	0.09	0.14	0.18	0.22	0.17	0.04	0.02	0.00
OU-20	LR-Porter	9/28/2012	1400	grab	0.00	0.00	0.02	0.03	0.10	0.21	0.25	0.19	0.13	0.04	0.02	0.01	0.00	0.00
OU-21	LR-60	3/22/2012	1200	grab-lt	0.00	0.00	0.14	0.06	0.04	0.08	0.17	0.20	0.16	0.09	0.06	0.01	0.01	0.00
OU-22	LR-60	3/22/2012	1200	grab-ctr	0.00	0.00	0.03	0.02	0.02	0.08	0.19	0.24	0.21	0.12	0.08	0.02	0.01	0.00
OU-23	LR-60	3/22/2012	1200	grab-rt	0.00	0.00	0.05	0.04	0.05	0.12	0.22	0.22	0.17	0.08	0.05	0.01	0.01	0.00
OU-24	LR-60	3/22/2012	1200	di-lt	0.00	0.00	0.00	0.00	0.00	0.06	0.22	0.27	0.23	0.13	0.08	0.02	0.01	0.00
OU-25	LR-60	3/22/2012	1200	di-ctr	0.00	0.00	0.00	0.01	0.05	0.13	0.25	0.24	0.18	0.09	0.05	0.01	0.01	0.00
OU-26	LR-60	3/22/2012	1200	di-rt	0.00	0.00	0.01	0.01	0.03	0.08	0.18	0.23	0.22	0.14	0.09	0.02	0.01	0.00
OU-27	Rock Cr	3/23/2012	1030	grab	0.00	0.00	0.00	0.02	0.08	0.19	0.26	0.22	0.15	0.06	0.03	0.01	0.01	0.00
OU-28	Dave Blue Cr	3/23/2012	930	grab	0.00	0.00	0.02	0.04	0.09	0.20	0.28	0.20	0.12	0.04	0.02	0.01	0.01	0.00
OU-29	LR-60	3/21/2012	1100	grab-lt	0.00	0.00	0.05	0.12	0.24	0.18	0.16	0.13	0.08	0.04	0.02	0.01	0.01	0.00
OU-30	LR-60	3/21/2012	1100	grab-ctr	0.00	0.00	0.03	0.05	0.11	0.15	0.20	0.20	0.15	0.07	0.04	0.01	0.01	0.00
OU-31	LR-60	3/21/2012	1100	grab-rt	0.00	0.00	0.01	0.02	0.07	0.16	0.26	0.23	0.16	0.07	0.04	0.01	0.01	0.00
OU-32	LR-60	3/21/2012	1100	di-lt	0.00	0.00	0.04	0.05	0.08	0.15	0.22	0.20	0.15	0.07	0.04	0.01	0.01	0.00
OU-33	LR-60	3/21/2012	1100	di-ctr	0.00	0.00	0.11	0.15	0.16	0.12	0.14	0.13	0.10	0.05	0.03	0.01	0.00	0.00
OU-34	LR-60	3/21/2012	1100	di-rt	0.00	0.00	0.03	0.04	0.08	0.13	0.20	0.21	0.17	0.09	0.05	0.01	0.01	0.00
OU-35	LR-60	3/21/2012	1215	di-lt	0.00	0.00	0.01	0.03	0.07	0.13	0.23	0.23	0.18	0.08	0.04	0.01	0.01	0.00
OU-36	LR-60	3/21/2012	1215	di-ctr	0.00	0.00	0.01	0.03	0.12	0.23	0.25	0.16	0.11	0.05	0.03	0.01	0.00	0.00
OU-37	LR-60	3/21/2012	1215	di-rt	0.00	0.00	0.07	0.08	0.09	0.13	0.19	0.18	0.14	0.07	0.04	0.01	0.01	0.00
OU-38	LR-60	3/21/2012	1215	di-lt2	0.00	0.00	0.05	0.07	0.07	0.13	0.24	0.22	0.14	0.06	0.03	0.01	0.01	0.00
OU-39	LR-60	3/21/2012	1215	di-ctr2	0.00	0.00	0.02	0.03	0.05	0.11	0.21	0.23	0.19	0.10	0.05	0.01	0.01	0.00
OU-40	LR-60	3/21/2012	1215	di-rt2	0.00	0.00	0.15	0.09	0.06	0.11	0.18	0.17	0.13	0.07	0.04	0.01	0.01	0.00

Table I.5: Suspended Particle Size Distribution Analyses Summary (5 of 6).

Sample #	Sample Name	Date	Time	Sample Type	Percentage by class size (µm)																									
					2000-		1000-		500-		250-		125-		62-31		31-16		16-8		8-4		4-2		2-1		1-0.5		0.5-	
					1000	500	500	250	250	125	125	62-31	62-31	31-16	31-16	16-8	16-8	8-4	8-4	4-2	4-2	2-1	2-1	1-0.5	1-0.5	0.5-	0.5-	0.25	0.25	<0.25
OU-41	LR-60	3/21/2012	1215	Grab	0.00	0.00	0.01	0.04	0.13	0.19	0.25	0.20	0.13	0.05	0.02	0.01	0.00	0.00	0.00	0.00	0.01	0.01	0.00	0.00	0.00	0.00	0.00	0.00	0.00	
OU-41-2	LR-60	3/21/2012	1215	Grab	0.00	0.00	0.02	0.03	0.05	0.11	0.20	0.24	0.20	0.10	0.05	0.01	0.00	0.00	0.00	0.00	0.01	0.01	0.00	0.00	0.00	0.00	0.00	0.00	0.00	
OU-42	LR-60	4/15/2012	1130	di-lt	0.00	0.00	0.01	0.03	0.10	0.15	0.17	0.16	0.15	0.12	0.09	0.02	0.01	0.00	0.00	0.00	0.01	0.01	0.00	0.00	0.00	0.00	0.00	0.00	0.00	
OU-43	LR-60	4/15/2012	1130	di-ctr	0.00	0.00	0.01	0.03	0.11	0.16	0.17	0.15	0.15	0.11	0.08	0.02	0.01	0.00	0.00	0.00	0.01	0.01	0.00	0.00	0.00	0.00	0.00	0.00	0.00	
OU-44	LR-60	4/15/2012	1130	di-rt	0.00	0.00	0.01	0.03	0.09	0.15	0.17	0.17	0.16	0.12	0.08	0.02	0.01	0.00	0.00	0.00	0.01	0.01	0.00	0.00	0.00	0.00	0.00	0.00	0.00	
OU-45	LR-60	4/15/2012	1130	grab-lt	0.00	0.00	0.02	0.04	0.12	0.18	0.18	0.14	0.12	0.09	0.06	0.01	0.00	0.00	0.00	0.00	0.01	0.01	0.00	0.00	0.00	0.00	0.00	0.00	0.00	
OU-45-2	LR-60	4/15/2012	1130	grab-lt	0.00	0.00	0.01	0.03	0.13	0.20	0.18	0.14	0.12	0.09	0.06	0.02	0.01	0.00	0.00	0.00	0.01	0.01	0.00	0.00	0.00	0.00	0.00	0.00	0.00	
OU-46	LR-60	4/15/2012	1130	grab-ctr	0.00	0.00	0.00	0.03	0.16	0.21	0.18	0.14	0.12	0.08	0.06	0.02	0.01	0.00	0.00	0.00	0.01	0.01	0.00	0.00	0.00	0.00	0.00	0.00	0.00	
OU-47	LR-60	4/15/2012	1130	grab-rt	0.00	0.00	0.01	0.03	0.13	0.17	0.16	0.14	0.14	0.11	0.08	0.02	0.01	0.00	0.00	0.00	0.01	0.01	0.00	0.00	0.00	0.00	0.00	0.00	0.00	
OU-48	LR-60	4/18/2013	1430	di-lt	0.00	0.00	0.02	0.03	0.05	0.10	0.16	0.20	0.19	0.14	0.09	0.02	0.01	0.00	0.00	0.00	0.01	0.01	0.00	0.00	0.00	0.00	0.00	0.00	0.00	
OU-49	LR-60	4/18/2013	1430	di-ctr	0.00	0.00	0.04	0.03	0.07	0.11	0.16	0.18	0.12	0.08	0.02	0.01	0.00	0.00	0.00	0.00	0.01	0.01	0.00	0.00	0.00	0.00	0.00	0.00	0.00	
OU-50	LR-60	4/18/2013	1430	di-rt	0.00	0.00	0.01	0.02	0.06	0.12	0.16	0.19	0.19	0.13	0.09	0.02	0.01	0.00	0.00	0.00	0.01	0.01	0.00	0.00	0.00	0.00	0.00	0.00	0.00	
OU-51	LR-60	4/18/2013	1430	grab	0.00	0.00	0.00	0.02	0.06	0.12	0.18	0.19	0.19	0.14	0.09	0.02	0.01	0.00	0.00	0.00	0.01	0.01	0.00	0.00	0.00	0.00	0.00	0.00	0.00	
OU-52	Nfork	4/3/2012	1145	grab	0.00	0.00	0.07	0.13	0.28	0.24	0.15	0.07	0.04	0.02	0.01	0.00	0.00	0.00	0.00	0.01	0.01	0.00	0.00	0.00	0.00	0.00	0.00	0.00	0.00	
OU-53	LR-Porter	7/9/2010	850	grab	0.00	0.00	0.04	0.04	0.08	0.16	0.24	0.21	0.14	0.07	0.04	0.01	0.00	0.00	0.00	0.01	0.01	0.00	0.00	0.00	0.00	0.00	0.00	0.00	0.00	
OU-54	Rock Cr	7/9/2010	1100	grab	0.00	0.00	0.04	0.04	0.05	0.10	0.21	0.24	0.17	0.09	0.05	0.01	0.00	0.00	0.00	0.01	0.01	0.00	0.00	0.00	0.00	0.00	0.00	0.00	0.00	
OU-55	Dave Blue Cr	7/9/2010	1130	grab	0.00	0.00	0.12	0.06	0.04	0.06	0.16	0.23	0.17	0.09	0.06	0.01	0.00	0.00	0.00	0.01	0.01	0.00	0.00	0.00	0.00	0.00	0.00	0.00	0.00	
OU-56	LR-60	7/9/2010	1700	grab	0.00	0.00	0.03	0.03	0.07	0.19	0.29	0.19	0.11	0.05	0.03	0.01	0.00	0.00	0.00	0.01	0.01	0.00	0.00	0.00	0.00	0.00	0.00	0.00	0.00	
OU-57	Elm Cr	7/9/2010	1030	grab	0.00	0.00	0.06	0.04	0.07	0.24	0.28	0.16	0.09	0.04	0.02	0.01	0.00	0.00	0.00	0.01	0.01	0.00	0.00	0.00	0.00	0.00	0.00	0.00	0.00	
OU-58	LR-60	7/10/2010	1200	grab	0.00	0.00	0.07	0.05	0.03	0.05	0.14	0.23	0.23	0.13	0.05	0.01	0.00	0.00	0.00	0.01	0.01	0.00	0.00	0.00	0.00	0.00	0.00	0.00	0.00	
OU-59	LR-60	7/12/2010	1100	grab	0.00	0.00	0.14	0.07	0.08	0.13	0.21	0.17	0.11	0.06	0.03	0.01	0.00	0.00	0.00	0.01	0.01	0.00	0.00	0.00	0.00	0.00	0.00	0.00	0.00	
OU-60	LR-60	7/13/2010	1200	grab	0.00	0.00	0.02	0.04	0.08	0.14	0.23	0.22	0.16	0.07	0.04	0.01	0.00	0.00	0.00	0.01	0.01	0.00	0.00	0.00	0.00	0.00	0.00	0.00	0.00	
OU-61	LR-60	7/13/2010	1330	grab	0.00	0.00	0.07	0.06	0.09	0.18	0.25	0.17	0.10	0.06	0.03	0.01	0.00	0.00	0.00	0.01	0.01	0.00	0.00	0.00	0.00	0.00	0.00	0.00	0.00	
OU-62	LR-Porter	3/12/2012	1330	grab	0.00	0.00	0.11	0.16	0.33	0.19	0.10	0.06	0.04	0.01	0.00	0.00	0.00	0.00	0.00	0.01	0.01	0.00	0.00	0.00	0.00	0.00	0.00	0.00	0.00	
OU-62-2	LR-Porter	3/12/2012	1330	grab	0.00	0.00	0.04	0.11	0.36	0.24	0.12	0.07	0.04	0.02	0.01	0.00	0.00	0.00	0.00	0.01	0.01	0.00	0.00	0.00	0.00	0.00	0.00	0.00	0.00	
OU-63	LR-Porter	3/12/2012	1430	grab	0.00	0.00	0.05	0.20	0.40	0.18	0.09	0.04	0.03	0.01	0.00	0.00	0.00	0.00	0.00	0.01	0.01	0.00	0.00	0.00	0.00	0.00	0.00	0.00	0.00	
OU-64	NFork	3/12/2012	1445	grab	0.00	0.00	0.06	0.09	0.20	0.24	0.20	0.10	0.06	0.03	0.02	0.00	0.00	0.00	0.00	0.01	0.01	0.00	0.00	0.00	0.00	0.00	0.00	0.00	0.00	
OU-65	NFork	3/12/2012	1515	grab	0.00	0.00	0.05	0.17	0.36	0.18	0.10	0.06	0.04	0.02	0.01	0.00	0.00	0.00	0.00	0.01	0.01	0.00	0.00	0.00	0.00	0.00	0.00	0.00	0.00	
OU-66	Elm Cr	3/12/2012	1530	grab	0.00	0.00	0.03	0.04	0.07	0.16	0.26	0.21	0.14	0.07	0.04	0.01	0.00	0.00	0.00	0.01	0.01	0.00	0.00	0.00	0.00	0.00	0.00	0.00	0.00	
OU-67	Elm Cr	3/12/2012	1615	grab	0.00	0.00	0.07	0.08	0.18	0.22	0.18	0.12	0.08	0.04	0.02	0.01	0.00	0.00	0.00	0.01	0.01	0.00	0.00	0.00	0.00	0.00	0.00	0.00	0.00	
OU-68	LR-60	3/12/2012	1430	grab	0.00	0.00	0.08	0.07	0.09	0.19	0.23	0.15	0.11	0.05	0.03	0.01	0.00	0.00	0.00	0.01	0.01	0.00	0.00	0.00	0.00	0.00	0.00	0.00	0.00	
OU-69	LR-60	3/20/2012	1345	grab	0.00	0.00	0.03	0.07	0.19	0.23	0.21	0.14	0.09	0.04	0.02	0.01	0.00	0.00	0.00	0.01	0.01	0.00	0.00	0.00	0.00	0.00	0.00	0.00	0.00	
OU-70	LR-60	3/20/2012	1345	di-lt	0.00	0.00	0.01	0.04	0.13	0.19	0.23	0.19	0.13	0.06	0.03	0.01	0.00	0.00	0.00	0.01	0.01	0.00	0.00	0.00	0.00	0.00	0.00	0.00	0.00	
OU-71	LR-60	3/20/2012	1345	di-ctr	0.00	0.00	0.04	0.06	0.09	0.11	0.15	0.18	0.18	0.12	0.07	0.02	0.01	0.00	0.00	0.01	0.01	0.00	0.00	0.00	0.00	0.00	0.00	0.00	0.00	
OU-72	LR-60	3/20/2012	1345	di-rt	0.00	0.00	0.01	0.02	0.06	0.11	0.17	0.20	0.20	0.13	0.07	0.02	0.01	0.00	0.00	0.01	0.01	0.00	0.00	0.00	0.00	0.00	0.00	0.00	0.00	

Table I.6: Suspended Particle Size Distribution Analyses Summary (6 of 6).

Sample #	Sample Name	Date	Time	Sample Type	Percentage by class size (µm)														
					2000-1000	1000-500	500-250	250-125	125-62	62-31	31-16	16-8	8-4	4-2	2-1	1-0.5	0.5-0.25	<0.25	
OU-73	LR-60	3/20/2012	1545	di-ht2	0.00	0.00	0.02	0.04	0.09	0.15	0.21	0.19	0.16	0.09	0.05	0.01	0.00		
OU-74	LR-60	3/20/2012	1545	di-ctr2	0.00	0.00	0.05	0.04	0.05	0.09	0.17	0.20	0.18	0.13	0.07	0.02	0.01		
OU-75	LR-60	3/20/2012	1345	grab-ht	0.00	0.00	0.08	0.08	0.06	0.11	0.17	0.17	0.15	0.10	0.06	0.02	0.01		
OU-76	LR-60	3/20/2012	1345	grab-ctr	0.00	0.00	0.03	0.05	0.09	0.12	0.16	0.18	0.16	0.11	0.07	0.02	0.01		
OU-77	LR-60	3/20/2012	1345	grab-rt	0.00	0.00	0.01	0.03	0.06	0.10	0.16	0.21	0.21	0.13	0.07	0.02	0.01		
OU-78	LR-60	3/20/2012	1345	grab-rt	0.00	0.00	0.01	0.03	0.06	0.11	0.18	0.21	0.19	0.12	0.07	0.02	0.01		
OU-78-2	LR-60	3/20/2012	1345	grab-rt	0.00	0.00	0.01	0.03	0.06	0.11	0.18	0.21	0.19	0.12	0.07	0.02	0.01		
OU-79	LR-60	3/20/2012	1545	grab-ht2	0.00	0.00	0.01	0.03	0.08	0.13	0.20	0.21	0.18	0.10	0.06	0.01	0.00		
OU-80	LR-60	3/20/2012	1545	grab-ctr2	0.00	0.00	0.02	0.03	0.08	0.13	0.18	0.19	0.17	0.11	0.06	0.02	0.01		
OU-81	LR-60	3/20/2012	1545	grab-rt2	0.00	0.00	0.01	0.02	0.05	0.10	0.17	0.20	0.20	0.14	0.08	0.02	0.01		
OU-82	LR-60	3/21/2012	1100	grab-ht1	0.00	0.00	0.04	0.05	0.08	0.11	0.18	0.21	0.18	0.10	0.05	0.01	0.00		
OU-83	LR-60	3/21/2012	1100	grab-ctr1	0.00	0.00	0.02	0.04	0.08	0.12	0.18	0.21	0.18	0.10	0.06	0.01	0.00		
OU-84	LR-60	3/21/2012	1100	grab-rt1	0.00	0.00	0.03	0.04	0.09	0.14	0.20	0.21	0.16	0.08	0.05	0.01	0.00		
OU-85	LR-60	3/21/2012	1215	grab-ht2	0.00	0.00	0.04	0.03	0.06	0.11	0.18	0.21	0.19	0.11	0.06	0.01	0.00		
OU-86	LR-60	3/21/2012	1215	grab-ctr2	0.00	0.00	0.01	0.02	0.05	0.11	0.19	0.22	0.20	0.12	0.06	0.02	0.01		
NA	LR-60th	5/20/2011	1700	grab-ctr	0.00	0.01	0.65	2.45	9.89	18.51	19.53	21.95	18.09	8.94	0.00	0.00	0.00		
NA	Rock Creek	5/20/2011	1730	grab-ctr	0.00	0.01	0.61	0.35	2.76	11.02	20.07	29.19	24.88	11.11	0.00	0.00	0.00		



## **J. Appendix J – Sediment Flux Summary Tables**

Table J.1: Grab Sample Sediment Flux Summary (1 of 2).

Sample #	Sample Name	Date	Time	Discharge		Conc (mg/L)	Sediment Flux	
				(cfs)	(cms)		(kg/s)	(tons/day)
WES-01	LR-Porter	5/21/2013	1830	119.28	3.38	495.11	1.67	159.27
WES-05	LR-Porter	5/21/2013	1900	119.28	3.38	401.32	1.36	129.10
WES-11	LR-Porter	5/21/2013	1930	106.27	3.01	420.65	1.27	120.56
WES-12	LR-Porter	6/4/2013	1600	320.57	9.08	1088.04	9.88	940.64
WES-17	LR-Porter	6/4/2013	1545	261.45	7.40	1074.37	7.95	757.53
WES-19	LR-Porter	7/15/2013	1545	1342.26	38.01	2872.12	109.16	10396.84
WES-23	LR-Porter	9/27/2012	1345	24.48	0.69	347.65	0.24	22.95
WES-25	LR-60	4/4/2013	1830	132.59	3.75	340.24	1.28	121.66
WES-30	LR-60	6/5/2013	1500	564.75	15.99	2624.31	41.97	3997.02
WES-35	LR-60	6/5/2013	1500	564.75	15.99	2643.33	42.27	4026.00
WES-37	Elm Creek	9/27/2012	1430	1.39	0.04	43.88	0.00	0.16
WES-38	LR-60	9/28/2012	1500	13.30	0.38	266.92	0.10	9.57
WES-39	NF	9/28/2012	1500	1.34	0.04	517.45	0.02	1.87
WES-40	LR-60	6/17/2013	1700	317.55	8.99	1026.60	9.23	879.18
WES-45	LR-60	6/17/2013	1530	454.54	12.87	1547.09	19.91	1896.50
WES-47	LR-60	6/17/2013	1400	675.61	19.13	3776.05	72.24	6880.11
WES-52	LR-60	6/17/2013	1400	675.61	19.13	1078.30	20.63	1964.71
WES-54	LR-60	5/23/2013	1515	3584.54	101.50	1476.70	149.89	14275.38
WES-59	LR-60	5/23/2013	1515	3584.54	101.50	1868.60	189.67	18063.92
WES-61	LR-60	5/24/2013	1130	168.14	4.76	363.60	1.73	164.88
WES-66	LR-60	5/24/2013	1130	168.14	4.76	296.14	1.41	134.29
WES-68	LR-60	7/17/2013	1430	325.12	9.21	698.33	6.43	612.31
WES-73	LR-60	7/17/2013	1430	325.12	9.21	720.00	6.63	631.30
WES-75	LR-60	7/16/2013	1530	73.01	2.07	227.02	0.47	44.70
WES-79	LR-60	7/16/2013	1700	64.31	1.82	175.96	0.32	30.52
OU-02	LR-60	4/15/2012	1230	492.05	13.93	2397.70	33.41	3181.76
OU-07	LR-60	5/22/2013	1300	78.22	2.21	30.45	0.07	6.42
OU-12	LR-60	7/26/2013	2000	2401.20	67.99	2826.29	192.17	18302.37
OU-16	LR-Porter	4/3/2012	1100	9.70	0.27	28.21	0.01	0.74
OU-17	Hog	4/3/2012	1300	4.21	0.12	304.84	0.04	3.46
OU-18	LR-60	9/27/2012	1530	97.82	2.77	968.79	2.68	255.58
OU-19	NFork	9/27/2012	1500	13.97	0.40	413.27	0.16	15.57
OU-20	LR-Porter	9/28/2012	1400	10.02	0.28	17.08	0.00	0.46
OU-22	LR-60	3/22/2012	1200	152.69	4.32	247.57	1.07	101.95
OU-27	Rock Cr	3/23/2012	1030	5.98	0.17	21.39	0.00	0.34
OU-28	Dave Blue Cr	3/23/2012	930	4.74	0.13	9.63	0.00	0.12
OU-30	LR-60	3/21/2012	1100	130.06	3.68	331.65	1.22	116.33
OU-41	LR-60	3/21/2012	1215	138.48	3.92	165.69	0.65	61.88
OU-46	LR-60	4/15/2012	1130	437.49	12.39	2332.77	28.90	2752.35
OU-51	LR-60	4/18/2013	1430	759.98	21.52	1201.57	25.86	2462.70
OU-52	Nfork	4/3/2012	1145	4.54	0.13	20.70	0.00	0.25
OU-53	LR-Porter	7/9/2010	850	43.03	1.22	67.23	0.08	7.80
OU-54	Rock Cr	7/9/2010	1100	8.55	0.24	46.35	0.01	1.07
OU-55	Dave Blue Cr	7/9/2010	1130	19.04	0.54	8.06	0.00	0.41
OU-56	LR-60	7/9/2010	1700	69.98	1.98	39.13	0.08	7.39

Table J.2: Grab Sample Sediment Flux Summary (2 of 2).

Sample #	Sample Name	Date	Time	Discharge		Conc (mg/L)	Sediment Flux	
				(cfs)	(cms)		(kg/s)	(tons/day)
OU-57	Elm Cr	7/9/2010	1030	7.66	0.22	0.27	0.00	0.01
OU-58	LR-60	7/10/2010	1200	31.94	0.90	1.97	0.00	0.17
OU-59	LR-60	7/12/2010	1100	31.77	0.90	2.50	0.00	0.21
OU-60	LR-60	7/13/2010	1200	31.89	0.90	30.43	0.03	2.62
OU-61	LR-60	7/13/2010	1330	31.50	0.89	2.15	0.00	0.18
OU-62	LR-Porter	3/12/2012	1330	11.40	0.32	6.47	0.00	0.20
OU-63	LR-Porter	3/12/2012	1430	11.40	0.32	38.46	0.01	1.18
OU-64	NFork	3/12/2012	1445	8.84	0.25	4.31	0.00	0.10
OU-65	NFork	3/12/2012	1515	8.84	0.25	27.25	0.01	0.65
OU-66	Elm Cr	3/12/2012	1530	4.72	0.13	19.42	0.00	0.25
OU-67	Elm Cr	3/12/2012	1615	4.72	0.13	26.41	0.00	0.34
OU-68	LR-60	3/12/2012	1430	31.27	0.89	99.21	0.09	8.37
OU-69	LR-60	3/20/2012	1345	264.23	7.48	98.82	0.74	70.42
OU-76	LR-60	3/20/2012	1345	264.23	7.48	628.40	4.70	447.80
OU-80	LR-60	3/20/2012	1545	227.88	6.45	649.57	4.19	399.20
OU-83	LR-60	3/21/2012	1100	130.06	3.68	290.00	1.07	101.72
OU-86	LR-60	3/21/2012	1215	138.48	3.92	347.96	1.36	129.95
NA	North Fork	7/9/2010	930	24.88	0.70	142.30	0.10	9.55
NA	Rock Creek	7/9/2010	1100	8.55	0.24	339.00	0.08	7.82
NA	Elm Creek	7/9/2010	1030	7.66	0.22	249.00	0.05	5.14
NA	Dave Blue Cr	7/9/2010	1130	19.04	0.54	200.00	0.11	10.27
NA	LR-Porter	7/9/2010	830	43.03	1.22	288.00	0.35	33.42
NA	LR-60th	7/9/2010	1700	69.98	1.98	308.00	0.61	58.13
NA	LR-60th	7/10/2010	1200	31.50	0.89	227.00	0.20	19.28
NA	LR-60th	7/12/2010	1100	60.77	1.72	310.30	0.53	50.86
NA	LR-60th	7/13/2010	1200	51.21	1.45	251.30	0.36	34.71
NA	LR-60th	7/13/2010	1330	51.04	1.45	158.00	0.23	21.75
NA	LR-60th	5/20/2011	1700	3072.6	87.01	2062.75	179.47	17092.89
NA	Rock Creek	5/20/2011	1730	105.98	3.00	802.25	2.41	229.30
NA	Rock Creek	5/20/2011	1730	105.98	3.00	946.15	2.84	270.43

Table J.3: Depth-integrated Sample Sediment Flux Summary (1 of 2).

Sample #	Sample Name	Date	Time	Type	Conc (mg/L)	Avg Conc (mg/L)	Discharge (cfs)	Discharge (cms)	Sed Flux (kg/s)	Sed Flux (tons/day)
WES-02	LR-Porter	5/21/2013	1830	di-lt	525.19					
WES-03	LR-Porter	5/21/2013	1830	di-ctr	541.90	537.59	119.28	3.38	1.82	172.93
WES-04	LR-Porter	5/21/2013	1830	di-rt	545.67					
WES-08	LR-Porter	5/21/2013	1930	di-lt	424.36					
WES-09	LR-Porter	5/21/2013	1930	di-rt	415.00	418.49	106.27	3.01	1.26	119.94
WES-10	LR-Porter	5/21/2013	1930	di-ctr	416.11					
WES-13	LR-Porter	6/4/2013	1600	di-lt	1069.82					
WES-14	LR-Porter	6/4/2013	1600	di-ctr	1075.53	1053.26	320.57	9.08	9.56	910.57
WES-15	LR-Porter	6/4/2013	1600	di-rt	1014.43					
WES-20	LR-Porter	7/15/2013	1545	di-lt	2875.88					
WES-21	LR-Porter	7/15/2013	1545	di-ctr	2591.67	2726.18	1342.26	38.01	103.62	9868.57
WES-22	LR-Porter	7/15/2013	1545	di-rt	2710.99					
WES-27	LR-60	4/4/2013	1830	di-lt	240.29					
WES-28	LR-60	4/4/2013	1830	di-ctr	273.47	272.00	132.59	3.75	1.02	97.26
WES-29	LR-60	4/4/2013	1830	di-rt	302.25					
WES-31	LR-60	6/5/2013	1500	di-lt	2307.91					
WES-32	LR-60	6/5/2013	1500	di-ctr	2378.33	2406.13	564.75	15.99	38.48	3664.71
WES-33	LR-60	6/5/2013	1500	di-rt	2532.14					
WES-41	LR-60	6/17/2013	1700	di-lt	1076.99					
WES-42	LR-60	6/17/2013	1700	di-ctr	1033.90	1048.36	317.55	8.99	9.43	897.81
WES-43	LR-60	6/17/2013	1700	di-rt	1034.19					
WES-48	LR-60	6/17/2013	1400	di-lt	2120.88					
WES-49	LR-60	6/17/2013	1400	di-ctr	2199.39	2086.87	675.61	19.13	39.92	3802.36
WES-50	LR-60	6/17/2013	1400	di-rt	1940.34					
WES-55	LR-60	5/23/2013	1515	di-lt	1956.90					
WES-56	LR-60	5/23/2013	1515	di-ctr	2072.60	2060.96	3584.54	101.50	209.19	19923.55
WES-57	LR-60	5/23/2013	1515	di-rt	2153.40					
WES-62	LR-60	5/24/2013	1130	di-lt	368.93					
WES-63	LR-60	5/24/2013	1130	di-ctr	270.98	302.99	168.14	4.76	1.44	137.40
WES-64	LR-60	5/24/2013	1130	di-rt	269.06					
WES-69	LR-60	7/17/2013	1430	di-lt	782.18					
WES-70	LR-60	7/17/2013	1430	di-ctr	673.85	697.66	325.12	9.21	6.42	611.71
WES-71	LR-60	7/17/2013	1430	di-rt	636.94					
WES-76	LR-60	7/16/2013	1530	di-lt	220.93					
WES-77	LR-60	7/16/2013	1530	di-ctr	178.60	199.77	73.01	2.07	0.41	39.33
OU-04	LR-60	4/15/2012	1230	di-lt2	2400					
OU-05	LR-60	4/15/2012	1230	di-ctr2	2513.45	2346.00	492.05	13.93	32.69	3113.15
OU-06	LR-60	4/15/2012	1230	di-rt2	2124.54					
OU-08	LR-60	5/22/2013	1300	di-lt	38.4314					
OU-09	LR-60	5/22/2013	1300	di-ctr	13.3333	28.85	78.22	2.21	0.06	6.09
OU-10	LR-60	5/22/2013	1300	di-rt	34.8					
OU-13	LR-60	7/26/2013	2000	di-lt	2682.27					
OU-14	LR-60	7/26/2013	2000	di-ctr	2789.17	2507.56	2401.20	67.99	170.50	16238.40
OU-15	LR-60	7/26/2013	2000	di-rt	2051.25					

Table J.4: Depth-integrated Sample Sediment Flux Summary (2 of 2).

Sample #	Sample Name	Date	Time	Type	Conc (mg/L)	Avg Conc (mg/L)	Discharge (cfs)	Discharge (cms)	Sed Flux (kg/s)	Sed Flux (tons/day)
OU-24	LR-60	3/22/2012	1200	di-lt	180.952					
OU-25	LR-60	3/22/2012	1200	di-ctr	166.923	170.46	152.69	4.32	0.74	70.19
OU-26	LR-60	3/22/2012	1200	di-rt	163.505					
OU-32	LR-60	3/21/2012	1100	di-lt	126.087					
OU-33	LR-60	3/21/2012	1100	di-ctr	219.789	162.08	130.06	3.68	0.60	56.85
OU-34	LR-60	3/21/2012	1100	di-rt	140.377					
OU-35	LR-60	3/21/2012	1215	di-lt	132.667					
OU-36	LR-60	3/21/2012	1215	di-ctr	173.953	134.30	138.48	3.92	0.53	50.16
OU-37	LR-60	3/21/2012	1215	di-rt	96.2857					
OU-38	LR-60	3/21/2012	1215	di-lt2	241.165					
OU-39	LR-60	3/21/2012	1215	di-ctr2	173.388	205.67	138.48	3.92	0.81	76.81
OU-40	LR-60	3/21/2012	1215	di-rt2	202.444					
OU-42	LR-60	4/15/2012	1130	di-lt	2121.33					
OU-43	LR-60	4/15/2012	1130	di-ctr	2554.19	2350.94	437.49	12.39	29.12	2773.79
OU-44	LR-60	4/15/2012	1130	di-rt	2377.31					
OU-48	LR-60	4/18/2013	1430	di-lt	1260.53					
OU-49	LR-60	4/18/2013	1430	di-ctr	1210.69	1213.50	759.98	21.52	26.11	2487.16
OU-50	LR-60	4/18/2013	1430	di-rt	1169.27					
OU-70	LR-60	3/20/2012	1345	di-lt	544.681					
OU-71	LR-60	3/20/2012	1345	di-ctr	564.324	567.30	264.23	7.48	4.24	404.26
OU-72	LR-60	3/20/2012	1345	di-rt	592.909					
OU-73	LR-60	3/20/2012	1545	di-lt2	546.512					
OU-74	LR-60	3/20/2012	1545	di-ctr2	539.175	542.84	227.88	6.45	3.50	333.61

Table J.5: ADCP with ViSea PDT Sediment Flux Summary.

Sample Name	Date	Time	WinRiverII Discharge		Conversion Coefficients		ViSea Discharge		Sediment Flux	
			(cfs)	(cms)	C1	C2	(cms)	(cfs)	(kg/s)	(tons/day)
LR-Porter	5/21/2013	1730	117.75	3.33	?	?	2.80	98.88	1.03	97.81
LR-Porter	5/21/2013	1900	114.08	3.23	?	?	2.69	95.00	0.95	90.38
LR-Porter	6/4/2013	1545	320.57	9.08	?	?	6.00	211.89	5.29	503.82
LR-Porter	6/4/2013	1600	261.45	7.40	?	?	6.50	229.55	6.16	586.68
LR-60	4/4/2013	1800	132.59	3.75	8.36	0.17	3.04	107.29	0.59	55.96
LR-60	4/4/2013	1900	115.16	3.26	8.36	0.17	2.69	95.00	0.46	43.71
LR-60	6/5/2013	1500	564.75	15.99	4.44	0.03	5.34	188.46	12.41	1181.92
LR-60	6/17/2013	1630	347.67	9.84	4.23	0.03	8.04	283.93	11.27	1073.35
LR-60	6/17/2013	1330	675.98	19.14	4.23	0.03	16.45	580.93	25.70	2447.66
LR-60	6/17/2013	1730	291.42	8.25	4.23	0.03	6.98	246.50	9.37	892.40
LR-60	5/23/2013	1515	3584.54	101.50	5.87	0.07	82.86	2926.17	154.45	14709.77
LR-60	5/24/2013	1130	168.14	4.76	2.94	0.01	4.58	161.74	1.29	122.86
LR-60	5/24/2013	1230	143.17	4.05	2.94	0.01	4.21	148.67	1.16	110.48
LR-60	7/17/2013	1430	325.12	9.21	4.28	0.04	7.82	276.16	4.77	454.29
LR-60	7/17/2013	1545	248.27	7.03	4.28	0.04	6.12	216.13	3.23	307.62
LR-60	7/16/2013	1515	73.01	2.07	2.68	0.01	1.92	67.80	0.32	30.48
LR-60	7/16/2013	1715	64.29	1.82	2.68	0.01	1.75	61.80	0.28	26.86
LR-60	4/15/2012	1200	321.58	9.11	5.92	0.08	12.69	448.14	31.20	2971.48
LR-60	4/15/2012	1230	492.05	13.93	5.92	0.08	13.66	482.40	33.86	3224.82
LR-60	3/22/2012	1200	158.38	4.48	3.66	0.04	4.40	155.47	0.96	91.43
LR-60	3/21/2012	1100	130.06	3.68	3.54	0.03	4.01	141.61	0.92	87.62
LR-60	3/20/2012	1345	227.88	6.45	3.42	0.02	6.99	246.85	3.87	368.58
LR-60	3/20/2012	1345	264.23	7.48	3.42	0.02	8.40	296.64	4.70	447.63
LR-60	3/21/2012	1215	138.48	3.92	3.37	0.03	3.75	132.43	0.51	48.57
LR-60th	5/20/2011	1700	2992.87	84.75	4.81	0.05	68.30	2411.99	76.43	7279.17
LR-60th	5/20/2011	1730	2615.08	74.05	3.74	0.01	59.78	2111.11	102.15	9728.74
Rock Creek	5/20/2011	1730	105.98	3.00	3.30	0.01	2.32	81.93	1.59	151.43

## **K. Appendix K – Personal Reflections on the Study**

In this appendix, I would like to offer some of my personal reflections on the study in a less formal manner, starting with how it all began.

I was a horrible student as an undergraduate. Soccer and partying were more important than studying, and even though I put myself through, and earned my BS in Mechanical Engineering in May 1983, working first as an engineering tech at the City of Norman, and then as the only draftsman for the College of Engineering, I did not apply myself and my grades were poor. I learned engineering though, and how to take a methodological approach to solving problems.

Years later, life's path led me to rivers. In 1998, I started working at the Oklahoma State Department of Health (OSDH) that became the Oklahoma Department of Environmental Quality (DEQ), when Quang Pham hired me as an Environmental Engineer I, to do waste load allocation (WLA) modeling and NPDES permit writing. This is where I got my first exposure to data collection in creeks and rivers, and had the privilege to meet and work with Rocke Amonette, Jay Wright, and Randy Parham. We shared many memorable adventures doing WLA studies, collecting data at all hours of the night and day. I was also fortunate to have met, and had some interesting discussions with Jimmy Pigg, who was a prominent aquatic biologist and a remarkable man by any standard, as anyone who knew him can attest to. I never had the opportunity to work with Jimmy, but he was an inspiration for anybody doing stream data collection of any kind.

And I was doing a lot of stream work at the time, because I was doing time of travel surveys below waste water treatment plants to validate the velocity dependent

reaeration rate in the Streeter-Phelps equation. They had been assuming 10 miles/day, which I knew to be high (it's more like 0.5-1 miles/day) and convinced EPA that we should validate it. I spent a lot of time alone on creeks and rivers all across Oklahoma and really grew to love it. In today's climate, they would probably fire me, because the difference in velocity required better waste water treatment, which cost more money, but at the time some decisions were still based on science, and I worked my way up to Senior Environmental Engineer. While at DEQ, I took night classes at OU, mostly in CEES. Unlike when I was an undergrad, I did well, and enjoyed taking classes. It was also during this time that I met Troy Hill, then a newly higher engineer at EPA Region 6 in Dallas, and was exposed to the concepts of Fluvial Geomorphology (FGM), when he gave me a copy of the famous "Catena Paper" by Dave Rosgen. I began conducting FGM surveys at the time of travel sites.

In 1994, I went to work for the Oklahoma Conservation Commission (OCC) when John Hassell, the Director of the Water Quality Division at the time, hired me to do a TMDL study of Grand Lake, among other things. It was perhaps the most enjoyable time of my life. Dan Butler, Kendra Edelman, Jim Leach, and then later Geoff Canty and Chris Hise among others; we all worked together as a family in a highly informal and relaxed environment. We were all professionals and scientists that knew how to do our jobs and did them, even if we weren't PC. While at OCC I got to spend a lot of time walking and sampling creeks with Dan Butler, something I still get to do, as he helped me on some of the surveys conducted in this study and often goes with me on the HOBOT download runs. Dan is extremely knowledgeable, on any topic,



but especially on aquatic biology, and he has taught me most of what I know about aquatic insects, riparian vegetation, and stream ecology.

I was not at OCC long when Troy had Rosgen teach a class in Dallas, and Ed Fite, the director of the Oklahoma Scenic Rivers Commission (OSRC) and I went. It changed my life. Everything he said made sense, but it went against what I had been taught, so I went out to prove him wrong, or at least prove it to myself that he was not. With John's support I started doing surveys at USGS gauge stations across the state and also spearheaded a bank erosion study of the Illinois River that Darren Harmel and I conducted, and for which Darren received his PhD. Also with John's encouragement, I entered OU in pursuit of a master's degree. I was initially working with Baxter Vieux, but in the Fall of 1996 I enrolled in an Environmental Modeling class taught by a new professor, Dr. Randall (Randy) Kolar. When I told him about the work I was doing at OCC, he asked why I did not do my thesis on that. I told him that I wanted to do that, but that Baxter who was lukewarm to the idea at best. When he said he thought it would make a great topic, I switched advisors, wrote my thesis on Regional Curves for the state, and received my Master's Degree in Civil Engineering in 2000. Bob Nairn and Gerald Miller joined Randy on my committee.

While at OCC I also had the opportunity to implement the first FGM based stream restoration projects in the state, and as I said had some of the best times of my life, but all good things must end, and a shift in the political winds resulted in John resigning, and I was not far behind him. I had been doing some work in other parts of the country, so I formed Riverman Engineering PLC, and I have been working as a consultant since that time, doing both stream assessments and restoration projects. It's

been a fun journey. I like the technical aspects, and the traveling and getting to meet new people, but I don't like the business end. I am not a good businessman. I've been able to support my wife and I, but I'm never going to be rich.

In the fall of 2006, Dr. Reid Coffman a new professor in Landscape Architecture, who has since left and is now at Kent State University, asked me to co-teach a Park Design class with him, so we could introduce the students to the concepts of natural channel design. I thoroughly enjoyed the experience and Reid suggested that if I really like it I should look into getting a stipend. I went to Randy and told him that I was interested in pursuing an interdisciplinary master's degree in Environmental Engineering and Landscape Architecture that would incorporate the concepts of FGM and natural channel design to develop more sustainable and less damaging storm water management. When I asked him if there was any funding available, he said that there was. I was awarded a GAANN Fellowship and started taking classes in CEES and Landscape Architecture in Spring, 2007.

In Spring, 2009, I was taking Technical Communications (CEES5021) where you write your prospectus for your thesis or dissertation. It was then I learned that interdisciplinary degrees had to be approved before completing 12 hours towards the degree. I was in my 12<sup>th</sup> hour with no way to get the required signatures before the end of the semester, so I had missed the deadline. I talked it over with Randy and decided to pursue a PhD in environmental engineering instead. With no idea what I was going to do my dissertation on, I asked Dr. Bob Knox if what I wrote for the class locked me in on that topic. When he said no, I made up an FGM study I had wanted to do in the Little River watershed for years, and having recently read that ADCPs were being used for

estimating sediment transport, I added that into the mix as well. When I presented it to my committee, it was not received well, which was somewhat disheartening, to say the least. But then a proposal I had submitted to the Oklahoma Water Resource Research Institute (OWRRI) to do the work was selected for funding, and thus the adventure began.

At this point, I had never even seen an ADCP before, and with further reading I discovered that even though people were using ADCPs for estimating sediment transport rates, the method had yet to be validated. This meant that it needed to be validated, which meant having to use the sediment “bomb”, which is what I was trying to avoid by using the ADCP.

So, I knew very little about ADCPs when I went to San Diego in October 2009 for Teledyne RDI’s ADCP’s in Action Conference, and attended presentations on ADCP applications from the gurus in the field, including Dave Mueller and Kevin Oberg with USGS, Nick Everard with the UK Environment Agency, and David Williams with the Australian Institute of Marine Science, among others. More importantly, I got to spend an evening playing pool and drinking beer with them and the sales rep Dave Dalkin, and I was able to pick their brains about what I was trying to do and get their recommendations on what instrument to use. In the end everyone decided that the RioGrande 600kHz system would probably be the best, and so we bought one.

The system included the ADCP mounted on a trimaran Riverboat from Ocean Science that was outfitted with Hydrolink ML2 radios, antennas, and GPS-ready wiring for a GPS-RTK system, which were acquired directly from Hemisphere, and shipped to Ocean Science for installation, in order to receive the educational discount that they

offered only if purchased directly from them. Hollis Henson and I flew to Phoenix, Arizona for training on use of the GPS units and the software by Hemisphere.

Dave Dalkin from Teledyne RDI brought the instrument and set everything up with Hollis and me. Then we took it to the Little River at 60<sup>th</sup> site and he showed us how to use it. The depth of the river was barely sufficient to for us to get measurements, but we did. To set the instrument up for operation, the mobile GPS receiver, two radios and two batteries had to be arranged in a particular manner to fit inside the boat cavity. The base station included a laptop computer, a base GPS receiver, two radios, two antennas, and a battery.

Our first experiences operating the system by ourselves were not extremely promising. Due to the low flow at the monitoring sites we sought out alternative locations to practice on, and found two locations that were suitable, one below the dam on Lake Thunderbird, and the other on the Overholser Canal at Lake Hefner. Things were going well at first, but then during one measurement, one of the batteries on the boat died and when we replaced the battery and tried to restart the ADCP, we could not stop it from pinging. After a long diagnostic session with Dan Murphy a technical representative from Teledyne RDI, the problem could not be identified. We were told to ship the ADCP back for inspection and service because they had experienced this problem on a few occasions before. However, the problem had not been diagnosed because by the time the instruments get shipped back, the capacitors drain completely, and when power is applied the problem is gone. I let the ADCP sit a week, retried it, and it was still pinging, so we shipped it back. As Dan foretold, they could not identify a problem and the instrument was returned.

After that, we had some success measuring flow, but intermittent issues were experienced due to either power or communications problems. It was sometimes frustrating because we would seemingly do everything correctly but things wouldn't work right. At one point one of the batteries again died, and we were once again unable to get the instrument to stop pinging. This time we were advised to connect the cable that came with it straight to the computer, bypassing the radios, before sending the stop pinging signal, which solved the problem. This step had not been attempted during the previous incident, and having to send the instrument back probably could have been averted if it had been.

Another issue that complicated operating the system correctly for a short time was the fact that while the ADCP was gone, the GPS was disconnected and configured for point surveying as we had been taught by Hemisphere. This worked fine but when it was reconnected with the ADCP, the communication settings had been changed and we had a difficult time getting it to work properly again. Resolving this issue was complicated by the fact that since we bought the GPS units directly from Hemisphere, Ocean Science initially would not provide technical support on them, even though they sell the same unit. Hemisphere provided excellent support for the GPS, but couldn't provide support for the ADCP system interface.

On one occasion, in the process of lowering the boat to the water, the contents shifted and ripped the wire off of the fuse and switch, so to get the measurement, I perhaps unwisely, bypassed them. It worked, and we were able to complete the measurement, but bone headedly I did not wire it correctly as soon as I got home, and forgot about it until the next event several days later. Somehow, and I'm still not sure

what I did, I got a wire crossed and fried the wiring harness. Fortunately, it did no damage to the ADCP or GPS units, but the harnesses aren't cheap. I had missed another opportunity to get data, and I was without the instrument until we got a new harness. A good thing came out of this though, because after we received the harness, Teledyne sent Jeff Den Herder, one of their field techs out to help identify the intermittent issue we had been having. He swapped out an antenna on the boat, we took it to the Duck Pond, and I walked Jeff through the steps I had been following, which he said were correct and everything worked like a charm, and it has worked correctly since then.

It did not take me long to realize that some of my initial plans were naively over ambitious, bordering on ridiculous. One of the reasons for getting the RTK-GPS was because I was thinking that if I could float the river dragging the ADCP behind me, the GPS would provide position and elevation, and the ADCP would provide depth, so I could get a profile plot of the channel bed. I even bought an inflatable boat and an electric motor for this purpose, and surveyed control points to tie to. There were a few problems with this idea, the first being the fact that in order for the ADCP to work, the water needs to be at least 3 feet deep. At that depth it would not be safe to float the river. Even if it could be floated safely, the incised channels and overhanging canopy makes it difficult to get an accurate GPS signal, and even if an accurate GPS signal could be obtained, there is still another problem that we discovered: in tests we conducted on Cypress Lake in west Norman, and on bathymetric measurements we took on the Little River Arm of Lake Thunderbird as part of the research Hollis did for his Master's, the measured elevation would be constant and then jump up, or down a varying height, then stay flat again. On the lake studies, this is just an inconvenience

because the water surface elevation is constant and the results can easily be corrected. This correction would not be possible when doing a profile because the water surface would not be constant, so it would not be possible to determine the magnitude of the jumps.

Another thing I was initially thinking I could do as part of this study was evaluate the bed load transport, as well as the suspended sediment transport. It soon became clear though, that I would be biting off more than I could chew if I did that, so I decided to focus the study on the discharge and suspended sediment, and leave the bed load for another day.

While we were deciding what system to buy, and waited for its delivery, other aspects of the study were proceeding, but not without a hitch. The majority of stream studies I have conducted in my life have been as an employee of the state, as a contractor for the federal government, or in conjunction with projects I was doing with the landowner. Site access has never been an issue. Even if it was on private land I just went and did what I needed to do, and the few times I was even stopped, when I explained what I was doing, I was welcomed, and more than once invited in for dinner. Due to the litigious world we live in now, and the fact that I was doing the study as a student OU, this was not an option and I was required to get landowner permission before accessing the sites.

This was no easy task, and it required going to the Cleveland County website, identifying the land parcels that abut the creeks and rivers being studied, and then finding the name and address of the landowners of the 105 parcels identified. Access letters, approved by University attorneys, were sent to 72 landowners. Less than half

responded and a second letter was sent to 44 landowners. In the end, only about half responded and only a handful flatly denied access. One gentleman wrote his own letter, protecting himself, that OU attorneys had to approve. Another guy called me and said that he wouldn't sign anything, but that I was welcome to come anytime, and he would even open the gate for me, allowing me easier access to the creek. I took him up on his offer, and his was not the only land I accessed with verbal permission.

Installation of the HOBOS at the hydrology sites was done early in the study, and perhaps, the most surprising thing about the study is that only one HOBOS, the one at Hog creek, was lost. I was concerned that if the flow did not get them vandals might. The one at the Little River at 60<sup>th</sup> site was "semi-vandalized" by OCC when they removed their staff gauge, and left the HOBOS on the bank. Later, after I had replaced it, it was once saved by a single zip tie. Also, the t-post that the HOBOS is attached to at the Little River at Porter site got bent over a bit in one storm event, but was easily straightened. All in all, I think I got lucky not to have a higher attrition rate.

Downloading data every 30 to 60 days meant that data was downloaded in the summer when it was hot and muggy, and the ticks and mosquitos were in search of prey, and in the winter, when it was bitterly cold and ice had to be broken off of the water surface to retrieve the HOBOS. But it also meant that data was downloaded in the spring, when things were popping back to life, and the herons were out fishing, and in the fall when the cool breezes replace the oppressive heat of the summer and the trees were alive with color.

It is amazing how quickly 30 to 60 days seems to pass, and it seemed that no sooner had one download trip ended that it was time to do another. Reluctance to start



the download circuit each month, due to redundancy, was most always quickly replaced with enjoyment, because this phase of the study was often the most enjoyable. Many trips, I made solo, but numerous people joined me on one or more trips.

The FGM surveys were conducted at various times throughout the study as weather, time and available help allowed. The decision to include the bank stability indices (BSI) evaluation in the study was made after several surveys had been completed, so in some instances the BSI assessments were conducted on different dates than the classification surveys.

Anybody who has ever conducted research in creeks and rivers knows that there are good days in the field and there are bad days. Although the ADCP caused me some frustrating days, it did provide some good days, when it was working properly. Still, the best days and most enjoyable moments in this study occurred during the FGM surveys, and during the repeated trips to the sites to download the HOBO data.

One such memorable moment occurred when I was the rod man, surveying the Little River-04 site, with Steve Zawrotny running the instrument. This site is near a heron rookery that is active in spring, which was when the survey was conducted. I was in the channel surveying the thalweg profile and there was a partially submerged tree in the middle of the channel. As I neared the tree, a Great Blue Heron, apparently oblivious to my presence, floated in just over my head, and landed on a branch of the tree protruding from the water. He sat there for a short time before he noticed me and flew off upstream. On more than one occasion, I disturbed Blue Herons from doing what they do and was privileged to see these beautiful creatures take to the air.

Another time, when Steve and I were downloading the HOBO data from the Hog Creek site, before it got washed out, we were standing on the bank, when a flock of 8 geese flew low over our heads, honking as they flew, and you could hear the air being pushed by their wings. Still, another time, I was downloading the HOBO at the Elm Creek site by myself, and was walking down along the water, which is rocky and required me to watch my feet as I walked. At one point I looked up, and not two steps in front of me was a skunk. Not a dead skunk, but a live skunk, who was as surprised to see me as I was him. I just knew I was about to be sprayed, but I froze, then slowly took several steps back, before circling around him (or her) and proceeding on to the HOBO.

We had another encounter with a skunk while surveying the Rock Creek-04 site. We were part way through the survey and I had moved the instrument to the right side of the channel, to get better survey coverage, and was setting the instrument up to take a back site on the pin on the left side, where we started the survey. Steve had the prism, and I was preparing to take the shot when I looked on the bank, upstream of Steve, and saw a skunk doing a Pepe LePue imitation, making a beeline for Steve. For a split second I considered not saying anything, but yelled out to him to let him know. The skunk was not far from him when they both saw each other. The skunk shot into a shrub pile on the bank. Steve essentially threw himself off the bank grabbing the only tree nearby to control his descent. It was a Bois d' arc tree. Ouch! Fortunately he did not do too much damage, and only suffered a few scratches. The skunk circled around us and proceeded downstream, and we regrouped and completed the survey.

At the Dave Blue Creek-04 site, an interesting site, that happens to be just upstream of a bedrock outcropping, there were rose rocks all over the place, many quite

large and several of them in great shape. Steve collects rose rocks, so we returned to the van for a backpack and he added to his collection. I had a similar experience, only with golf balls, on the North Fork-03 site, which happens to be located on the Belmar Golf Club. While conducting the FGM assessment by myself, I loaded up my pack, collecting only the balls that I did not have to go out of my way to get. I asked the guys at the clubhouse if they wanted them, but they said I could have them.

The study also revealed how trashy some people are, because more than once I arrived at a site only to find it littered with new trash, from tires, to washing machines and old carpet, to dead deer carcasses that had been thrown off the bridge. A dead calf got washed into Dave Blue Creek at one point and made downloading the HOBOS very unpleasant until a storm finally washed it on downstream.

The time spent in the Little River and other tributaries of Lake Thunderbird revealed the extent to which the channels are eroding as they respond to past and present changes in the watershed. With the channels down cutting and widening like they are, numerous trees are falling into the channels. These fallen trees are themselves impacting the morphology of the channels, because they inevitably form log and debris jams across the channel. These jams back up the flow until eventually the water finds a weak spot on one of the banks, and cuts a gouge in the channel bank as it cuts around the jam. Active scallops and evidence of past scallops were observed in numerous locations throughout the watershed, and likely contribute significantly to the suspended sediment load to the lake, although quantifying it would be extremely difficult to do.

Although, I am not a biologist, and biological assessments were not conducted as part of this study, when I'm in a creek channel, I can't help but do cursory looks in

the substrate to identify the presence or absence of insects, and Dan Butler, who, as I said earlier, is a great biologist, was with me on many of my ventures. We discovered that the insect communities at the sites ranged from very good at the lower sites on the Little River and the upper reaches of Dave Blue Creek, and the North Fork, to extremely poor on the lower North Fork, and other sites on the Little River, as they were almost completely devoid of life of any kind. Future study in the watershed should include both habitat and biological assessments at the sites.

Lab work is not my favorite thing in the world to do, so it was not surprising to me that the lab work required to determine the particle sizes and suspended sediment concentrations was my least favorite part of this study. The concentration analyses was straight forward and went fairly smoothly, except that, on a couple of samples the graduated flask did not seat well on the filter, resulting in some leakage, which may have had a slight impact on the results. If it did, it was not readily identifiable. The set up and procedure that I used at OU was the same as that used at the ERDC lab in Vicksburg, Mississippi. Some of the samples analyzed at each location took a long time to pass through the filter due to the high suspended sediment concentrations of the samples, making for long wait times between samples.

The particle size analysis was new to me, and as I mentioned earlier, it was conducted on different instruments at OU and ERDC. The instrument used at ERDC was a Malvern Mastersizer 2000 using the Wie model for quartz. The instrument was set up by ERDC personnel and unfortunately I did not know enough about laser diffraction at the time to ask the right questions about its operation, so I did not learn what model was used until later.

The instrument used at OU was a Sequoia LISST Portable XR set up to use the Fraunhofer model. It is not surprising, as I have learned, that the two instruments produced different results. They were using different models, and even the same instrument will produce different results if different models are used. A few tests I conducted using the test samples that I had collected from the Little River, showed that even the Quartz A and Quartz B Mie models produced different results. Determining the best model for use in analyzing sediments in the Lake Thunderbird watershed would be worthy of a dissertation in its own right, but is outside the scope of this study. Fortunately, although it was somewhat disconcerting to me that the instruments did not give the same results, the equations used in the Aqua Vision ViSea PDT software do not appear to be overly sensitive to particle size distribution, so it is not thought that the differences observed significantly affected the results.

I learned a lot in this study about Doppler acoustics as it applies to ADCP operation, and laser diffraction as it applies to using the LISST particle size analyzer, but I feel that I now know enough to be dangerous. Prior to initiating this research I had no prior experience with ADCPs, and in fact had never seen one. Learning how to set it up and operate it properly was quite a learning experience, and at times was quite frustrating. Although I learned a lot during the course of this study, I make no pretense to being an expert in the operation of ADCPs for measuring discharge, much less sediment flux. Both the WinRiver II and ViSea PDT software were learned well enough to obtain the required results, but it is probable that experienced users of the ADCP and the software would produce better results than those presented here. There is so much more to know, and I am far from an expert on either. The same may be said about the

WinRiver II and ViSea PDT software. I learned how to use the software well enough to generate results, but I wouldn't consider myself a proficient user of either one. I think it was Einstein who said that "complex problems are infinitely more complex upon further inspection". I certainly found that to be the case in this study.

If nothing else, this has been a memorable and educational adventure. I learned a lot, and had some fun times along the way. Although it is not going to change the world, the data I collected provides at least some information about the morphology, flow, and sediment transport in the watershed, where previously none existed, and provides a base line for future research. The study shows that the Little River and other tributaries to Lake Thunderbird are incising and widening, contributing a significant amount of sediment to the lake. The study also seems to show that the ADCP can be effectively used to estimate sediment flux, because, at the two sites where it was used, it produced essentially the same results as traditional methods. However, the ADCP estimate requires measuring particle size as well as concentration, which requires more lab work, not less, as was hoped. Perhaps if an Optical Back Scatter (OBS) was used in conjunction with the ADCP, and a given site could be "calibrated", the sampling requirements would go down, but until that can be shown, it is simpler to use the ADCP just to measure discharge and collect grab samples for estimating flux.